JOURNAL OF THE MECHANICS AND PHYSICS OF SOLIDS

EDITORIAL ADVISORY BOARD

J. F. BAKER—Cambridge
E. BRANDENBERGER—Zürich
G. BUSCH—Zürich
A. H. COTTRELL—Birmingham
M. J. DRUYVESTEYN—Delft
A. KOCHENDÖRFER—Düsseldorf
N. F. MOTT—Bristol
A. NADAI—Pittsburgh, Pa.
G. SACHS—Syracuse, N.Y.
E. SIEBEL—Stuttgart
H. W. SWIFT—Sheffield

EDITORS

R. HILL
Bristol

W. M. BALDWIN
Cleveland

Volume 1
1952 — 53

PERGAMON PRESS LTD · LONDON

Vol.
1
1952/5

Contents of Volume 1

Number 1

Page

H. W. Swift : Plastic instability under plane stress 1

R. Hill : On discontinuous plastic states, with special reference to localized necking in thin sheets 19

A. P. Green and R. Hill : Calculations on the influence of friction and die geometry in sheet drawing 31

A. E. Johnson and N. E. Frost : Rheology of metals at elevated temperatures 37

A. H. Cottrell : The time laws of creep 53

W. M. Lomer : The yield phenomenon in polycrystalline mild steel .. 64

Book reviews 74

ol.
1
2/53

Number 2

E. T. Onat and W. Prager : Limit analysis of arches 77

A. R. Flint : The stability and strength of stocky beams 90

F. A. Gaydon : An analysis of the plastic bending of a thin strip in its plane 103

J. D. Campbell : An investigation of the plastic behaviour of metal rods subjected to longitudinal impact 113

D. G. B. Thomas : The autofrettage of thick tubes with free ends .. 124

A. K. Head : The mechanism of fatigue of metals 134

R. Hill : A note on the back-pull factor in strip-drawing 142

Book reviews 146

Number 3

J. F. Davidson : Flange buckling in a bent I-section beam 149

J. G. Wistreich : Die pressure in plane strain drawing : comparison of experiment with theory 164

A. J. Kennedy : On the generality of the cubic creep function 172

E. R. W. Jones and W. Munro : The " elastic hysteresis " of uranium .. 182

M. P. L. Siebel : The combined bending and twisting of thin cylinders in the plastic range 189

R. Hill and M. P. L. Siebel : On the plastic distortion of solid bars by combined bending and twisting 207

Book reviews 215

NUMBER 4

D. C. DRUCKER : Limit analysis of two and three dimensional soil mechanics problems 217

E. O. HALL : The brittle fracture of metals 227

N. LOIZOU and R. B. SIMS : The yield stress of pure lead in compression 234

O. G. FOLBERTH and A. KOCHENDÖRFER : Eine Theorie des Kriechens von Einkristallen 244

W. SYLWESTROWICZ : Experimental investigation of the behaviour of soil under a punch or footing 258

R. HILL : On the mechanics of cutting metal strips with knife-edged tools 265

R. HILL : A new method for determining the yield criterion and plastic potential of ductile metals 271

N. W. PURCHASE and S. J. TUPPER : Experiments with a laboratory extrusion apparatus under conditions of plane strain 277

H. LL. D. PUGH : A note on a test of the plastic isotropy of metals .. 284

Book reviews 287

Vol
1
1952/

Author Index

(B) denotes a book review

BALDWIN, W. M. pp. 215 (B), 216 (B), 287 (B).
BISHOP, J. F. W. p. 74 (B).
CAHN, R. W. p. 287 (B).
CAMPBELL, J. D. p. 113.
COTTRELL, A. H. p. 53.
DAVIDSON, J. F. p. 149.
DRUCKER, D. C. p. 217.
FLINT, A. R. p. 90.
FOLBERTH, O. G. p. 244.
FORD, H. p. 215.
FROST, N. E. p. 37.
GAYDON, F. A. p. 103.
GREEN, A. P. p. 31.
HALL, E. O. p. 227.
HEAD, A. K. p. 134.
HILL, R. pp. 19, 31, 74 (B), 142, 146 (B), 207, 265, 271.
JOHNSON, A. E. p. 37.
JONES, E. R. W. p. 182.
KENNEDY, A. J. p. 172.
KOCHENDÖRFER, A. p. 244.
LOIZOU, N. p. 234.
LOMER, W. M. p. 64.
MUNRO, W. p. 182.
NABARRO, F. R. N. p. 146 (B).
ONAT, E. T. p. 77.
PRAGER, W. p. 77.
PUGH, H. LL. D. pp. 284.
PURCHASE, N. W. p. 277.
QUARRELL, A. G. p. 75 (B).
SIEBEL, M. P. L. pp. 189, 207.
SIMS, R. B. p. 234.
SWIFT, H. p. 1.
SYLWESTROWICZ, W. p. 258.
THOMAS, D. G. B. p. 124.
TUPPER, S. J. p. 277.
WISTREICH, J. G. p. 164.

Journal of the Mechanics and Physics of Solids, 1952, Vol. 1, pp. 1 to 18. Pergamon Press Ltd., London.

PLASTIC INSTABILITY UNDER PLANE STRESS

By H. W. Swift
Department of Engineering, University of Sheffield

(*Received* 23*rd. May*, 1952)

Summary

This paper examines the conditions for instability of plastic strain under plane stress for a material conforming to the Mises-Hencky yield condition and strain-hardening according to a unique relationship between root-mean-square values of shear stress (q) and incremental strain ($\delta\psi$).

If, under fixed loading conditions, the material undergoes a strain increment which is consistent with the applied stress system, the conditions are stable or unstable according as the increment in representative yield stress is greater or less than the increment in representative induced stress.

The strain at which instability arises is found in terms of the biaxial stress ratio p_2/p_1 under different conditions of applied loading, and the effect is demonstrated of strain-hardening according to an empirical relation of the type $q = c\,(a + \psi)^n$.

The analysis is also applied to certain cases of non-uniform stress distribution. In the case of the hydrostatic bulge results are obtained showing a critical thinning ranging from 26 per cent for a non-hardening material to about 45 per cent for typical strain-hardening materials, values in general agreement with experimental data. Conditions over the punch head in the pressing of a cylindrical shell are discussed but computations are not attempted.

1. Introduction

When a bar of homogeneous ductile work-hardening material is subjected to a simple tensile load, the strain remains homogeneous until the stress reaches a value beyond which the proportional diminution in sectional area exceeds the corresponding proportional increment in yield stress. At this point the load reaches its maximum value, homogeneous strain becomes unstable and subsequent extension occurs by local necking under steadily diminishing load. The so-called " ultimate tensile strength " of the material is based on this maximum load, although actual fracture occurs subsequently under quite different conditions, and this " strength " is essentially a function of the strain-hardening characteristic of the material, and therefore of its plastic properties, and not in any sense of its intrinsic strength.

An instability giving rise to local necking may occur in a similar way in material subjected to biaxial or plane stress. This instability is of importance in deep-drawing operations because it determines the degree of thinning which the sheet metal can undergo in various parts of the pressing, and it has similar importance in stretch-forming and in the Erichsen, Guillery and other bulging tests. In all these cases the stress system is effectively biaxial, the third stress being insignificant.

The problem of necking under biaxial tension was encountered in America during the war, more particularly in connection with the hydraulic bulging of metal sheet, and a theoretical treatment was published by SACHS and LUBAHN (1946). For reasons of expediency they assumed as a representative stress-strain characteristic the relation between the larger principal stress p_1 and the numerically greatest principal strain, which is ϵ_1 or ϵ_3 according as the intermediate strain ϵ_2 is negative or positive. In fact this assumption is not particularly expedient, for it involves an element of discontinuity at $\epsilon_2 = 0$ and some difference of treatment in the two ranges, nor is it generally considered by plasticians so realistic as an assumption based on the Mises-Hencky hypothesis of yield. In the present paper conditions for the instability of plastic strain under plane or biaxial stress are developed, consistent with the Mises-Hencky hypothesis, on the assumption that the representative stress-strain characteristic is the relation between the root-mean-square shear stress and its natural strain analogue.

For biaxial tension the principal stresses can be written in descending order : p_1, $p_2 = xp_1$ and $p_3 = 0$, where x is a proper fraction. Corresponding increments of principal strain under this stress system will be e_1, e_2, e_3, where constancy of volume requires $e_1 + e_2 + e_3 = 0$, and the Lévy-Lode relationship implies similarity of the Mohr circle diagrams for strain and stress.

Adopting the Mises-Hencky criterion for yield, the elastic strength of the material can be measured by the representative r.m.s. shear stress when strain is imminent under principal stresses p_1, p_2, p_3. In the case of biaxial tension this stress may be written

$$q = p_1 \left(\frac{1 - x + x^2}{6} \right)^{\frac{1}{2}} . \tag{1}$$

The corresponding representative r.m.s angular strain increment $\delta\psi$ (half the shear strain) can be related to the individual strain increments :

$$\frac{\delta\psi}{\sqrt{\frac{3}{2}(1 - x + x^2)}} = \frac{e_1}{2 - x} = \frac{e_2}{2x - 1} = \frac{-e_3}{1 + x} . \tag{2}$$

Assume that under any given conditions of loading, which remains fixed, a small strain increment $\delta\psi$ occurs, consistent in its components e_1, e_2, e_3 with the applied loading, that is with the current stress system p_1, p_2, $p_3 = 0$. This strain increment will cause

(*a*) changes δp_1, δp_2 in the principal stresses depending on the impressed conditions of loading and straining, and a corresponding change in the representative stress :

$$\Delta q = \frac{(2 - x)\,\delta p_1 + (2x - 1)\,\delta p_2}{\sqrt{24\,(1 - x + x^2)}} \tag{3}$$

(*b*) a change δq in the intrinsic yield strength of the material, due to strain-hardening, if Δq is incremental ; but no change if Δq is decremental.

Plastic strain under the prescribed conditions will be stable provided that $\delta q_0 > \Delta q_0$, but it is unstable if $\delta q_0 < \Delta q_0$.

Vol
1
1952/

(*i*) *Tensile Forces.*

If the biaxial tension is applied through tensile forces, which remain unaffected by the assumed local strain increments e_1, e_2, then

$$\frac{\delta p_1}{p_1} = e_1, \text{ and } \frac{\delta p_2}{p_2} = e_2$$

and the condition for stability becomes

$$\delta p > p_1 e_2 \frac{\left\{2 - x + \frac{x(2x-1)^2}{2-x}\right\}}{\sqrt{24(1-x+x^2}}$$

which can be written : $$\frac{\delta q}{\delta \psi} > \frac{q}{z}$$

where $$z = \frac{\sqrt{6}(1-x+x^2)^{3/2}}{(1+x)(4-7x+4x^2)}. \quad (4)$$

If therefore the strain-hardening characteristic for the material is drawn as in Fig. 1 by plotting q against the integrated ψ, the condition of strain will be stable so long as the subtangent to the curve at the point of operation is less than the value of z appropriate to the stress ratio x, and necking will be imminent when this subtangent attains the value z. Values of z in terms of x are shown as z_1 in Fig. 2.

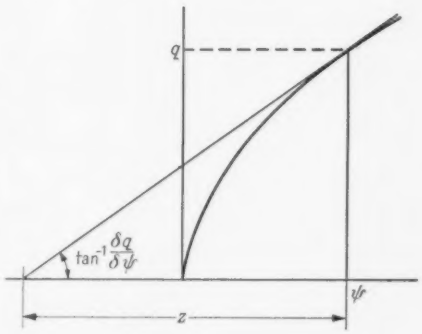

Fig. 1.

The case of biaxial stress in which one stress is compressive can be examined in a similar way, regard being paid to the fact that the intermediate stress p_2 is now zero and the intermediate strain e_2 represents the change in thickness of the material. It will be found that the stability condition is identical with (4), provided x is given the appropriate negative value. Fig. 2 shows, as would be expected, that the presence of a compressive stress defers the incidence of necking, and that when $x = -1$ and the stress system is equivalent to simple shear, the conditions of straining are always stable in a material which strain-hardens however little.

Values for the subtangent which would be obtained if SACHS and LUBAHN'S assumption were developed in a similar way are shown plotted in Fig. 2 as the broken curve SL, for comparison with values of z_1 according to the present treatment, over the range $0 < x < 1$. As it is uncertain what strain criterion SACHS and LUBAHN would apply under mixed biaxial stress ($x < 0$) the comparison has not been extended into that region.

(*ii*) *Thin Cylinder.*

In the case of a thin walled-cylinder of radius r under internal fluid pressure p and an independent axial tensile load $P > \pi r^2 p$, the principal stresses are

given by $p_1 2\pi rt = P + \pi r^2 p$ and $p_2 = \frac{pr}{t}$ where r, t are current values of the cylinder radius and wall thickness. In this case $e_2 = \frac{\delta r}{r}$ and $e_3 = \frac{\delta t}{t}$, so consequential changes of stress when P and p remain constant are given by

$$\delta p_1 = p_1 e_1 + p_2 e_2$$

$$\frac{\delta p_2}{p_2} = e_2 - e_3 = e_2 \cdot \frac{3x}{2x-1} = e_1 \cdot \frac{3x}{2-x}$$

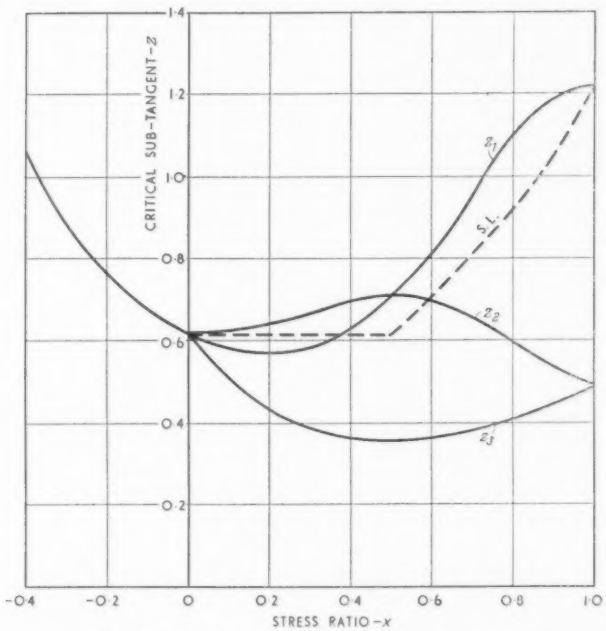

Fig. 2. Critical subtangents under biaxial stress.

The condition for stability from equation (3), making use of equations (2), can be written

$$\frac{\delta q}{\delta \psi} > q \frac{4 - 6x + 3x^2 + 4x^3}{\sqrt{6}\,(1 - x + x^2)^3}$$

so that the critical subtangent $z = \frac{\sqrt{6}\,(1 - x + x^2)^{3/2}}{4 - 6x + 3x^2 + 4x^3}$. This is plotted as z_2 in Fig. 2.

If $P < \pi r^2 p$, the hoop stress exceeds the longitudinal and becomes p_1, leading to a modified value for the critical subtangent :

$$z = \frac{\sqrt{6}\,(1 - x + x^2)^{3/2}}{4 + 3x - 6x^2 + 4x^3}$$

where $x = \frac{p_2}{p_1}$ = axial/hoop stress in this case. Values for z are plotted as z_3 in Fig. 2.

(*iii*) *Spherical Shell.*

In a thin-walled spherical shell without local restraint the diaphragm stress is $p_1 = p_2 = \frac{pr}{2t}$ and the corresponding strain increments are $e_1 = e_2 = -\frac{1}{2}e_3$. The condition for stability, with p remaining constant, is

$$\frac{\delta p_1}{p_1} > \frac{\delta r}{r} - \frac{\delta t}{t} = 3e_1$$

which gives $\frac{\delta q}{q} > \delta\psi\sqrt{6}$, so that the critical subtangent is $z = \frac{1}{\sqrt{6}} = 0{\cdot}41$. The stress ratio $x = \frac{p_2}{p_1}$ is of course unity.

2. Effect of Initial Overstrain

For any given value of the subtangent z, the point representing instability on the strain-hardening characteristic relating q to ψ is defined by the values of q and $\frac{dq}{d\psi}$ at this point, and the critical value of q is not otherwise affected by the form of the strain-hardening curve. In particular this critical value is not affected by any initial strain-hardening, the effect of which is merely to displace the origin along the ψ axis. In other words q does not depend on the strain history of the material, but ψ and consequently the elongation and thinning do.

A useful empirical formula for the strain-hardening characteristic is $q = c(a + \psi)^n$. In this expression c can be regarded as a general measure of the rate of hardening, n as a measure of the decrement of this rate and a as a measure of the initial state of the material, increasing with previous overstrain. For most metals of technical interest the value of n lies between 0·5 and 1·0, often approaching unity in the region of substantial overstrain. For a strain-hardening curve of this family it is easy to show that the sub-arc $a + \psi = nz$, as indicated diagrammatically in Fig. 3.

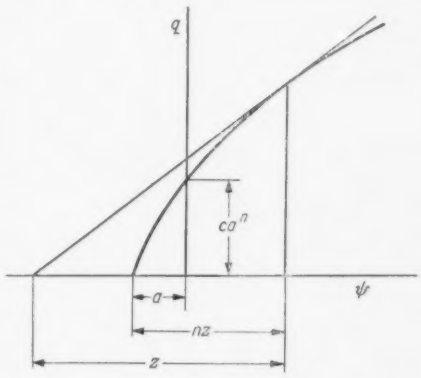

Fig. 3.

The relationship of ψ to the integrated strains $\epsilon_1 = \ln\frac{l_1}{l_0}$, etc., depends in general not only on the final stress ratio $\frac{p_2}{p_1} = x$ but also upon any changes in this ratio which may have occurred during the straining operation. In cases for which the ratio x has been constant during straining the total strains are given by simple integration of (2):

$$\frac{\epsilon_1}{c_1} = \frac{\epsilon_2}{c_2} = \frac{\epsilon_3}{c_3} = \psi, \text{ say, where}$$

$$c_1 = \frac{2 - x}{\sqrt{\frac{3}{2}(1 - x + x^2)}} \text{ and so on for } c_2,\ c_3.$$

For a strain-hardening characteristic of the type proposed above and shown in Fig. 3 the principal elongation strain $\epsilon_1 = c_1 \psi = c_1 (nz - a)$ while the thinning strain $\epsilon_3 = c_3 (nz - a)$, where z is the subtangent corresponding to the operative point on the strain-hardening characteristic. The critical elongation and thinning are obtained by giving z its appropriate critical value.

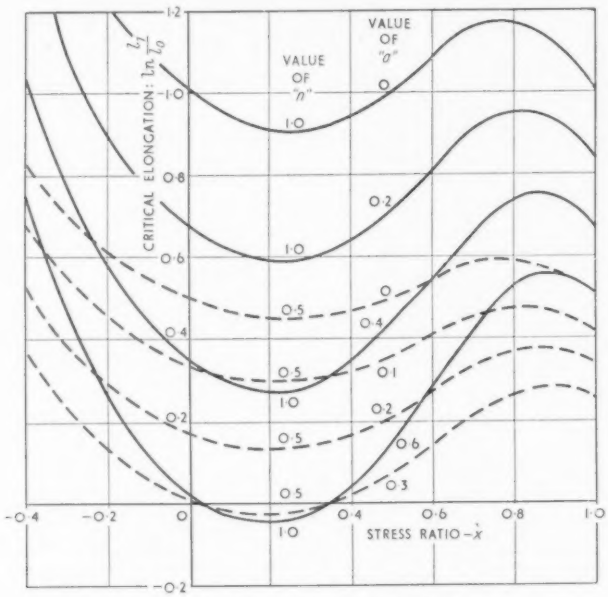

Fig. 4. Critical elongation under biaxial stress.

In order to show the effects of different strain-hardening characteristics and initial overstrain, critical values of the principal elongation have been plotted in Fig. 4 and the critical thinning in Fig. 5 for a case in which the impressed tensile forces are the controlling factor, so that $z = z_1$ in Fig. 2. Negative values of these critical strains have of course no special significance; they merely show that instability arises before any general elongation or thinning has occurred. The range of Figs. 4, 5 has been extended to small negative values of x, corresponding to biaxial combinations of tension and compression which are of practical interest in certain technological processes. The range of values of the initial overstrain a has been extended approximately to the point at which no elongation would occur before necking under simple tension; $a = 0{\cdot}6$ when $n = 1$, $a = 0{\cdot}3$ when $n = 0{\cdot}5$.

For material in the fully annealed condition ($a = 0$) it will be seen from Fig. 4 that the elongation at incipient instability is not greatly affected by the stress ratio x, but Fig. 5 shows that the critical thinning increases markedly with this ratio, particularly in the higher range of its values. Both the critical strains increase with the strain-hardening factor n for all values of the stress-ratio.

Work-hardening, or heat-treatment which produces an increase in the effective initial overstrain a, naturally leads to instability at smaller strains under all conditions, but Fig. 4 shows that the increase in criticial elongation with stress-

ratio is greater with greater overstrain, a trend which does not however extend to the critical thinning shewn in Fig. 5. It is notable that material which has been overstrained to such an extent that it has no general elongation in simple tension ($n = 1$, $a = 0{\cdot}6$ or $n = 0{\cdot}5$, $a = 0{\cdot}3$) may develop a considerable capacity for elongation, and more particularly for thinning, at higher values of the biaxial stress ratio. A higher value of the strain-hardening index n, with comparable initial overstrain, produces greater increments in both critical strains at higher stress ratios.

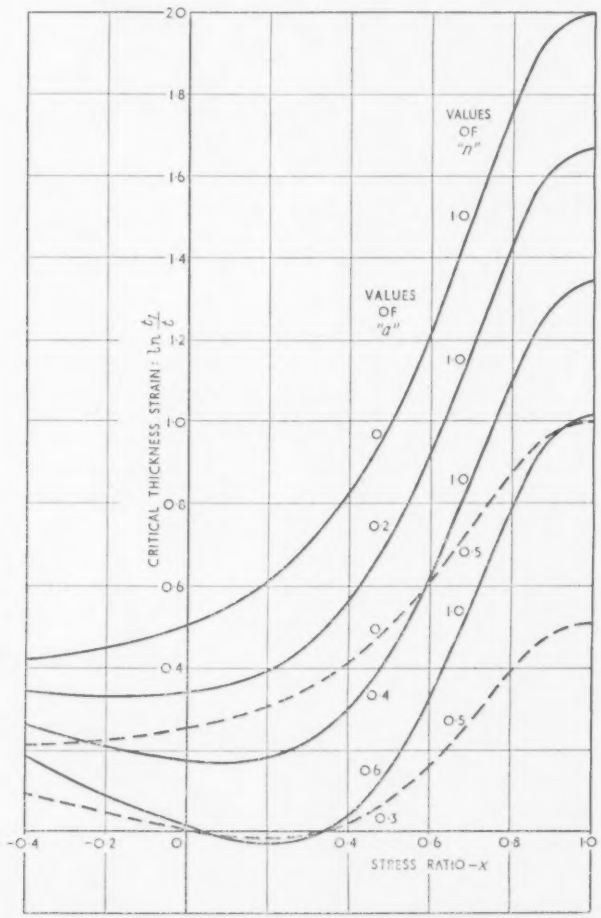

Fig. 5. Critical thinning under biaxial stress.

Fig. 5 shows that substantial thinning before instability, both with annealed and overstrained material, is chiefly associated with values of the stress ratio approaching unity, where it reflects the increased values of the sub-tangent z, in Fig. 2. The small degree of thinning indicated in the tension-compression range ($x < 0$) is of course due to the partial balancing of the longitudinal and lateral

strains, a balance which is complete when $x = -1$ and the conditions are those of simple shear. In this case no instability will arise in strain-hardening material.

The discussion above and its results affecting total strains have been based on the assumption that the stress ratio x has a constant value during the whole of the finite strain development. In cases where this ratio changes, the individual principal strains are not obtainable by simple integration from equations (2), although the values of q, $\frac{dq}{d\psi}$, z and consequently the effective value of ψ depend only on the value of x at the critical condition.

If the material were to remain isotropic during plastic strain the representative strain ψ could be visualised as half the line integral following the strains ϵ_1, ϵ_2, ϵ_3 in the curve relating these in a three-dimensional diagram, a curve which (since $\epsilon_1 + \epsilon_2 + \epsilon_3 \equiv 0$) will lie in the plane whose normal has direction ratios 1 : 1 : 1 in that diagram. In such a case, if the value of x were known at all stages of the strain development, this curve could be plotted and its integrated length used to correlate the actual strains with the q, ψ characteristic. The strains at the critical point on this characteristic could then be ascertained from the critical value of q corresponding to the value of x, and hence of z appropriate to the critical point.

Some idea of the effect of changing stress ratio on critical thinning in an extreme case, can be obtained by assuming that the material is strained in simple tension ($x = 0$) up to incipient necking and is then subjected to biaxial tension for which $x = 1$. If ψ_0, ψ_1 are the critical values of the representative strain for these ratios, the empirical strain-hardening formula gives

$$\psi_0 = \sqrt{\frac{3}{8}} \cdot n - a \qquad\qquad \psi_1 = \sqrt{\frac{3}{2}} \cdot n - a$$

and the appropriate equation (2) then gives the ultimate thinning :

$$-\ln \frac{t}{t_0} = \sqrt{\frac{2}{3}}\,\psi_0 + \sqrt{\frac{8}{3}}\,(\psi_1 - \psi_0) = \frac{3}{2}\,n - \sqrt{\frac{2}{3}}\,a.$$

If the material were subjected to biaxial tension ($x = 1$) throughout, the corresponding strain would be

$$-\ln \frac{t_1}{t_0} = 2n - \sqrt{\frac{8}{3}}\,a.$$

Hence the ultimate thicknesses according as the material is or is not subjected to initial simple tension are related by $\ln \frac{t}{t_1} = \frac{n}{2} - \sqrt{\frac{2}{3}}\,a$ which is the same value as the critical thinning ratio $\ln \frac{t_0}{t}$ under simple tension. According to this, a material which would give a general elongation of 10 per cent, say, and therefore a general thinnning of about 5 per cent under simple tension, will be up to 5 per cent thicker when instability occurs under biaxial tension ($x = 1$) if straining has commenced under simple tension.

Vol
1
1952/

In practice of course the assumption of continued isotropy cannot be fully sustained if the stress-ratio or the principal axes of stress become altered during the development of the strain. But insufficent is known at present of the Bauschinger and cognate effects to introduce them into the analysis.

3. Development of Unstable Strain

It is not the purpose of the present paper to follow the development of unstable strain beyond its inception, but since the evidences of instability in practice generally take the form of ruptured material which may have undergone considerable local – or even dispersed – strain after the inception of instability, some caution may be required in the interpretation of the ultimate conditions of rupture.

In the cases of instability discussed hitherto the distribution of stress and strain in the stable range has been uniform. Instability may therefore become imminent at any point or points. Before any unstable strain can actually occur however this imminence must extend to a band or zone which is capable of independent strain under the impressed or induced conditions. In the case of a strip under simple tension, for example, unstable strain might conceivably arise across a section perpendicular to the load line. If the band affected by this strain remained under simple tension its width (across the strip) would in isotropic material become reduced in the same proportion as its thickness. This reduction would induce lateral restraining stresses from the material adjacent to the incipient waist. On the other hand if the band of instability were to commence in a direction making an angle $\sin^{-1}(1/\sqrt{3})$ with the transverse plane the width of this band across the strip would remain unaltered by the existing system of strain, which could therefore continue indefinitely without restraint from or influence on adjacent material. Bijlaard (1940) has drawn attention to the fact that in strip metal in which necking commences while conditions are still fairly isotropic, the neck does in fact tend to follow the direction of zero lineal strain.

In the case of a thin cylinder under predominantly axial tension the boundary conditions inhibit oblique necking, so unstable strain develops round a transverse ring and induces secondary hoop stresses which spread the effect of the neck to some extent along the cylinder. When a thin cylinder is under predominantly hoop stress the development of instability follows a different course. The band of incipient unstable strain is naturally parallel to the axis and the first effect of the strain will be to cause a local swelling along this band. This swelling cannot however develop without substantial disturbance to the ambient stress distribution. For the local swelling produces a region of increased curvature, connected to the main, stable part of the cylinder periphery by a transition curve of reduced curvature. These changes automatically relieve the hoop stress at the initial swelling and increase it in the region of transition. Consequently unstable straining may develop over a considerable peripheral angle, as well as over a considerable axial length, and take the form of general thinning over a substantial area of swelling. For such unstable strain "necking" is little more than a courtesy title.

4. NON-UNIFORM STRESS DISTRIBUTION

In the press working of sheet metal cases frequently arise in which the impressed conditions of stress and strain are not uniform, but vary systematically from point to point. These cases differ from those of uniform stress in two ways.

In the first place it is necessary to ascertain not only the strain which gives rise to instability but also the zone in which it occurs. Every part of a sheet of metal under a stretch-forming operation in a press, for example, has its own stress ratio and restraints, and instability will occur in that zone which first reaches its own critical conditions having regard to the consequences of local strain. The fact that instability may be followed by local necking along a defined zone does not of course affect the conditions at the inception of instability, but only the way in which it develops.

In the second place the point of instability on the strain-hardening characteristic, as defined for example by the critical value of the subtangent z, is not an explicit function of the local stress-ratio and loading conditions as under uniformly distributed strain, but it depends on the way in which the stress and strain develop over the pressing as a whole, which in turn of course depends on the stress-strain characteristic of the particular sheet material. In so far as that there is at present no established theory of plastic strain covering the critical parts of even a simple pressing, any study of instability is therefore necessarily speculative. But if general lines of treatment can be laid down they may at least point the way for further inquiry and suggest trends to be checked by experiment.

Discussion in the present paper is confined to two relatively simple cases of the formation of a circular sheet of metal into a surface of revolution by lateral pressure. If this pressure is applied through a solid punch the form of the surface is prescribed but friction needs consideration for realistic treatment; if through fluid pressure as in the hydrostatic bulge, friction is negligible but the profile is a matter for investigation.

5. THE HYDROSTATIC BULGE

We shall discuss the conditions for stability in the case of a circular sheet clamped round the periphery, free of restraint on one side and subjected to fluid pressure on the other. Flexural stiffness of the sheet is assumed to be negligible, so that the clamp applies no restraining couple as the sheet bends from it during the development of the bulge. Instability of the bulge will arise if straining in any region is able to continue without further increment of the applied fluid pressure.

Preliminary physical considerations suggest that these critical conditions are likely to develop first at the central " pole," and that the form of the bulge near this pole is approximately spherical.

Adopting the notation of Fig. 6 and confining attention for the moment to the polar region, the divergence which develops between the radial or profile strain e_1 and the circumferential strain e_2 can be correlated with the common radius of curvature $\rho_1 = \rho_2 = \rho_0$ at the pole. For the difference between the arcual length $cr = s$ and the radial length $nr = r$ is $\rho_0(\theta - \sin\theta)$. And since

$s = (1 + e_1)\, r_0$ and $r = (1 + e_2)\, r_0$ where $\bar{e}_1$ is the mean radial (finite) strain over the arc, and e_2 the circumferential strain of the ring element defined by θ, we may write

$$\bar{e}_1 - e_2 = (1 + e_2)\,\frac{\theta^2}{6} \text{ nearly.}$$

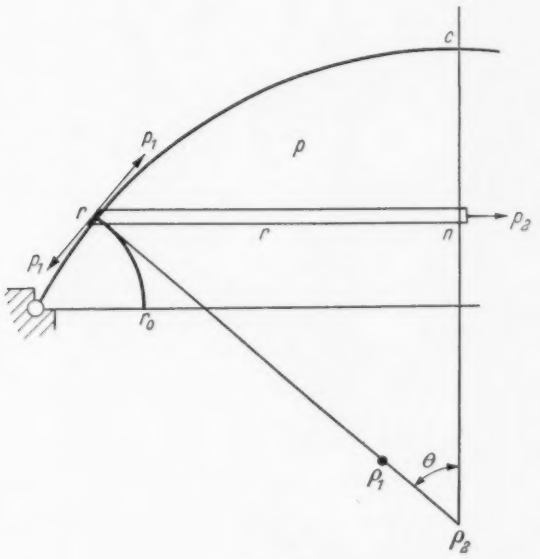

Fig. 6.

If the corresponding logarithmic strains are $\bar{\epsilon}_1 = \ln(1 + \bar{e}_1)$ and $\epsilon_2 = \ln(1 + e_2)$ it is easily shown that $\bar{\epsilon}_1 - \epsilon_2 = \dfrac{\theta^2}{6}$ nearly. For reasons of symmetry the strains are necessarily even functions of the angle θ, so that if θ^4 terms are neglected we may write

$$\epsilon_1 = \epsilon_0 - a_1\,\theta^2 \quad , \quad \epsilon_2 = \epsilon_0 - a_2\,\theta^2,$$

$$\text{where} \quad \bar{\epsilon}_1 = \epsilon_0 - \frac{a_1}{3}\,\theta^2 \quad \text{and} \quad -\frac{a_1}{3} + a_2 = \frac{1}{6}.$$

The stress ratio is nearly unity and it will be found that the difference

$$1 - x = \frac{\theta^2\,(-a_1 + a_2)}{3\epsilon_0 - \theta^2\,(2a_1 + a_2)}.$$

Provided the stress-ratio x is effectively constant during the strain development of an individual element, the thickness strain can be written

$$-\epsilon_3 = \psi.\frac{1 + x}{\sqrt{\frac{3}{2}\,(1 - x + x^2)}} = \psi\sqrt{\frac{8}{3}}\left\{1 - \frac{\theta^4}{24\epsilon_0^2}\,(a_1 - a_2)^2\right\}$$

$$= \psi\sqrt{\frac{8}{3}}, \text{ neglecting the } \theta^4 \text{ term.}$$

At the pole itself $\epsilon_0 = \psi_0 \sqrt{\frac{2}{3}}$, and in its region

$$\psi = \psi_0 - \sqrt{\frac{3}{8}}\,(a_1 + a_2)\,\theta^2.$$

The two curvatures are related

(*a*) geometrically : $\dfrac{d\rho_2}{d\theta} = -(\rho_2 - \rho_1)\cot\theta$

(*b*) statically : $x = \dfrac{p_2}{p_1} = 2 - \dfrac{\rho_2}{\rho_1}$.

Hence $\dfrac{\delta\rho_2}{\rho_0} = \dfrac{-\epsilon_1 + \epsilon_2}{3\epsilon_1}\cot\theta.\delta\theta$ and it will be found that

$$\ln\frac{\rho_2}{\rho_0} = \frac{(a_1 - a_2)}{6\epsilon_0}\,\theta^2, \text{ neglecting } \theta^4 \text{ terms, so that}$$

$$\frac{\rho_1}{\rho_0} = 1 + \frac{(a_1 - a_2)}{6\epsilon_0}\,\theta^2, \qquad \frac{\rho_2}{\rho_0} = 1 + \frac{(a_1 - a_2)}{2\epsilon_0}\,\theta^2.$$

Let us now assume that θ^4 terms are negligible over the whole range of the bulge $0 \leqslant \theta \leqslant \alpha$. Then we may write $\dfrac{\rho_1}{\rho_0} = 1 + b\theta^2$ where $b = \dfrac{a_1 - a_2}{6\epsilon_0}$ above. Typical arcual and radial dimensions are then

$$s = \rho_0\,\theta\,(1 + \frac{b}{3}\,\theta^2), \qquad r = \rho_0\,\theta\,(1 + \frac{b}{3} - \frac{1}{6}\,\theta^2),$$

so that $s - r = \rho_0 \cdot \dfrac{\theta^2}{6}$, as with the earlier assumption $b = 0$. Now at the clamped perimeter, where $\theta = \alpha$, the circumferential strain $\epsilon_2 \equiv 0$ while the radial strain ϵ_1 develops. Hence

$$x = \frac{1}{2} \text{ and } \frac{\rho_2}{\rho_1} = \frac{1 + \frac{1}{3}\,b\theta^2}{1 + b\theta^2} = \frac{3}{2}$$

when $\theta = \alpha$, so that $b = -\dfrac{3}{7\alpha^2}$. It immediately follows that

$$a_1 = \frac{1}{4} - \frac{9}{7}\frac{\epsilon_0}{\alpha^2} \quad , \quad a_2 = \frac{1}{4} - \frac{3}{7}\frac{\epsilon_0}{\alpha^2},$$

$$x = \frac{1 - \frac{1}{3}\frac{\theta^2}{\epsilon_0}\left(\frac{3}{4} - \frac{15}{7}\frac{\epsilon_0}{\alpha^2}\right)}{1 - \frac{1}{3}\frac{\theta^2}{\epsilon_0}\left(\frac{3}{4} - \frac{21}{7}\frac{\epsilon_0}{\alpha^2}\right)}.$$

And since $x - \dfrac{1}{2}$ when $\theta = \alpha$:

$$\frac{\alpha^2}{\epsilon_0} = \frac{40}{7},\ a_1 = \frac{1}{40},\ a_2 = \frac{7}{40},\ b = -\frac{3}{40\epsilon_0},$$

Vol. 1 1952/

$$\text{and } \frac{\rho_1}{\rho_0} = 1 - \frac{3}{40}\frac{\theta^2}{\epsilon_0}, \quad \frac{\rho_2}{\rho_0} = 1 - \frac{1}{40}\frac{\theta^2}{\epsilon_0}, \quad x = \frac{1 - \frac{1}{8}\frac{\theta^2}{\epsilon_0}}{1 - \frac{3}{40}\frac{\theta^2}{\epsilon_0}}.$$

Moreover, if x remains constant during strain for an individual fibre, it will be found that, if θ^4 terms are neglected,

$$-\epsilon_3 = \psi\sqrt{\frac{8}{3}} \quad \text{as before.}$$

In the immediate polar region : $p_1 t = \frac{1}{2} p \rho_0$. Hence the strain will become unstable when

$$\frac{\delta p_1}{p_1} + \frac{\delta t}{t} = \frac{\delta \rho_0}{\rho_0},$$

which is equivalent to $\frac{\delta q_0}{q_0} - 2\delta\epsilon_0 = -\frac{\delta\epsilon_0}{2\epsilon_0} - \frac{\delta\epsilon_0}{\frac{9}{10} - \epsilon_0}$.

Adopting the strain-hardening relation $q_0 = c\,(a + \psi_0)^n$, so that $\frac{\delta q_0}{q_0} = \frac{n.\delta\psi_0}{a + \psi_0}$, and noting that $\frac{\delta\epsilon_0}{\epsilon_0} = \frac{\delta\psi_0}{\psi_0}$ at the pole, it will be found that the polar strain ϵ_0 when instability occurs is given by

$$\epsilon_0^3 - \epsilon_0^2\left(\frac{33}{20} + \frac{n}{2} - a\sqrt{\frac{2}{3}}\right) + \epsilon_0\left(\frac{9}{40} + \frac{9}{20}\,n^{-a}\,.\,\frac{33}{20}\sqrt{\frac{2}{3}}\right) + a.\frac{9}{40}\sqrt{\frac{2}{3}} = 0.$$

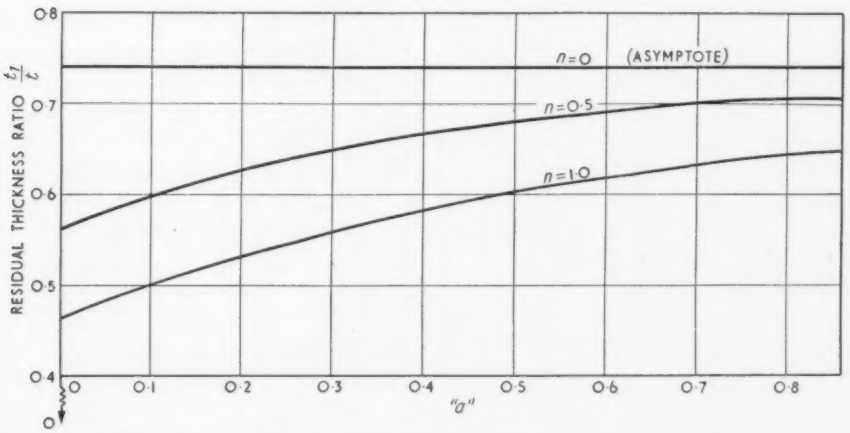

Fig. 7. Critical thinning of bulge as affected by strain-hardening.

The corresponding local reduction in thickness immediately follows : $\ln\frac{t}{t_1} = -2\epsilon_0$.

For practical purposes the useful range of n is from 0·5 to 1·0 and of a from 0 to 0·6, while a non-hardening material for which $n = 0$ has academic interest. Values of the residual thickness ratio t/t_1 covering these ranges are plotted in

Fig. 7. It will be seen from the table below that the thickness ratios are of an order consistent with general experimental evidence and that the curves in Fig. 7 follow expected trends; the higher the strain-hardening index n the greater the strain before instability, the greater the initial overstrain the less the subsequent thinning in the bulge.

Critical Thickness Ratios, $\frac{t}{t_1}$.

Metal		*Experimental Values*		
		B.S.	B.T.	M.
Copper	Soft	0·54	0·54	0·53
,,	Hard	0·57	0·56	0·57
Brass	Soft			0·53
	½ H			0·57
Aluminium	Soft			0·53
	¼ H			0·56
	½ H			0·69
Mild Steel	Soft		0·53	0·58
Stainless Steel	Soft		0·55	0·55
75 S–O			0·63	

B.S.—BROWN and SACHS (1948). B.T.—BROWN and THOMPSON (1949).
M.—P. B. MELLOR (unpub.)

The foregoing analysis is based on stress-strain relations which are only valid as long as the material at all parts of the bulge remains in a yielding condition. In other words it would cease to be valid if the representative stress q were to suffer a decrement in any zone at any stage of the straining. The possibility of this contingency can be settled quite simply by supposing that some elementary ring remains without further strain at a certain stage. Then in the statical equations $p_1 = \frac{p\rho_2}{2t}$, $p_2 = \frac{p\rho_2}{2t}(2 - \frac{\rho_2}{\rho_1})$, which are still valid for this ring, the values of t, ρ_1 and ρ_2 remain unchanged. Hence if the applied pressure p increases, so also must p_1 and p_2 and consequently the representative stress q. But an increment in q cannot occur without further incremental strain. Hence a local cessation of strain need not be contemplated before the pressure reaches its maximum value, and the analysis is not invalidated on this account so long as the conditions are stable.

The analysis above has been concerned with the conditions of instability at the pole. It remains to demonstrate that instability will in fact occur there and not elsewhere in the bulge. For this purpose it will suffice to show that when critical conditions have been reached at the pole, continued strain elsewhere requires an increment in applied pressure. In general, at any section :

$$\frac{\delta p}{p} = \frac{\delta p_1}{p_1} + \frac{\delta t}{t} - \frac{\delta \rho_2}{\rho_2}$$

$$= \frac{n\delta\psi}{a+\psi} - \delta\psi\sqrt{\frac{8}{3}} - \frac{\delta\rho_2}{\rho_2}$$

$$= \left(\frac{n\delta\psi_0}{a+\psi_0} - \delta\psi_0\sqrt{\frac{8}{3}} - \frac{\delta\rho_0}{\rho_0}\right) + \Delta, \text{ say.}$$

Vol 1 1952/

But since the conditions are critical at the pole the value of the group of terms in brackets in this expression is zero, so that the condition for stability elsewhere is that $\Delta > 0$. Substitution and algebraic manipulation give

$$\Delta = -\sqrt{\frac{3}{2}} \cdot \frac{n}{a+\psi} \cdot \frac{\delta\theta^2}{10} + \sqrt{\frac{3}{2}} \frac{n\theta^2}{(a+\psi)(a+\psi_0)} \cdot \frac{\delta\psi_0}{10} + \frac{\delta\theta^2}{5} + \frac{\delta\theta^2}{40\epsilon_0 - \theta^2}$$

where $\delta\theta^2$ relates to the change in profile slope of an elementary ring under strain increments $\delta\psi_0$, $\delta\epsilon_0$, at the pole. It would be tedious to attempt an examination of this expression for all values of θ, a, n, but the trend will be clear if we consider the conditions at the rim, where $\theta = \alpha$. Appropriate substitutions are then

$$\alpha^2 = \frac{40}{7}\epsilon_0, \qquad \psi_0 = \epsilon_0\sqrt{\frac{3}{2}}.$$

After manipulation, making occasional use of critical relations at the pole, the condition for stability at the rim of the bulge reduces for practical purposes to the form :

$$-\epsilon_0^3 + \frac{181}{240}\epsilon_0^2 + \frac{21}{160}\epsilon_0 - \frac{301}{144}\sqrt{\frac{2}{3}}a\epsilon_0 + \frac{133}{160}\sqrt{\frac{2}{3}}a > 0.$$

For values of a within the practical range 0 to 0·6 this condition is fulfilled for all positive values of ϵ_0 up to 0·5, and having regard to the useful range of a in relation to n and of ϵ_0 in relation to both, it will be seen that the conditions at the rim for all materials of practical interest are substantially more stable than those at the pole.

The conditions of instability in a hydrostatic bulge have been discussed by Hill (1950) using quite a different method of approach, and he has obtained formulae for numerical solutions for materials corresponding to $n = 0$ and $n = 1$ in the above analysis. For non-hardening materials his critical thickness ratio is 0·70 by one method and 0·76 by another, as compared with 0·74 in Fig. 7. For a strain-hardening material corresponding to $n = 1$ and $a = 1{\cdot}225$ his value is 0·69 as compared with 0·68 in Fig. 7. At lower values of a, Hill does not consider his formula valid up to instability.

6. Cylindrical Shell Pressing

When a sheet of metal is in process of being formed over the head of a cylindrical punch, the conditions of static equilibrium lead to the following relation between the " radial " stress p_1 and the circumferential stress p_2 :—

$$p_2 t\rho = \frac{\cos\phi}{\cos(\theta-\phi)}\frac{d}{d\theta}(p_1 tr) - \frac{\sin\phi}{\cos(\theta-\phi)}(p_1 tr) \qquad (5)$$

where t, ρ are local and current values of the metal thickness and (profile) radius of curvature, and ϕ is the angle of friction $\tan^{-1}\mu$ measured in the appropriate sense (notation analogous to Fig. 6). The complementary statical equation involves the local interfacial pressure as an additional variable and does not further clarify the relation between p_1, p_2, θ.

The geometrical consequences of strain lead to the following relationship between

the incremental radial (e_1) and circumferential (e_2) strains when the concomitant rotation $\delta\theta$ of an element defined by θ is known in terms of the conditions of strain :

$$e_1 = \tan\theta \,.\, \delta\theta + dr/d\,(re_2).$$

If the punch has a flat base of radius R merging into a toroidal quadrant of profile radius ρ, so that $r = R + \rho \sin\theta$, this becomes :

$$e_1 = \frac{d}{d\theta}\left(e_2 \frac{R + \rho\sin\theta}{\rho\cos\theta}\right)$$

and for a hemispherical head : $e_1 = \dfrac{d}{d\theta}(e_2 \tan\theta)$. (6)

For the correlation of stress with strain use can be made, firstly, of the Lévy-Lode relationship which can be written in the form

$$\frac{e_2}{e_1} = \frac{2 - x}{2x - 1} \tag{7}$$

and, secondly, of the strain-hardening (q, ψ) characteristic for the material. If the stress-ratio x remains effectively constant for any individual element during the development of the (finite) strain, then the radial stress $p_1 = \dfrac{q\sqrt{6}}{\sqrt{1 - x + x^2}}$, while the thickness change is given by

$$\ln\frac{t}{t_1} = -\psi \,.\, \frac{1 + x}{\sqrt{\frac{3}{2}(1 - x + x^2)}}\,. \tag{8}$$

These several conditions do not lend themselves to an explicit solution of the stress and strain distribution at any stage of the forming process, but conditions in any particular case could be investigated by an indirect trial-and-error method which can be described for the case of a hemispherical punch head.

In this case the stress equation (5) takes the form

$$\frac{d\,(p_1 t)}{p_1 t} = \frac{\frac{e_2}{e_1}(1 + 3\mu\tan\theta) - (1 - 3\mu\tan\theta)}{(2 + \frac{e_2}{e_1})\tan\theta}\, d\theta\,.$$

If some relationship is *assumed* between x and θ, then this equation can be integrated in some form :

$$\ln\frac{p_1}{p_0}\frac{t}{t_0} = \phi\,(\theta) - \phi\,(0)$$

where p_0, t_0 refer to the crown, at which $\theta = 0$. Substitution from equation (8) then gives

$$\phi - \phi_0 = \ln\frac{q}{\sqrt{1 - x + x^2}} - \ln q_0 - \psi\frac{\sqrt{\frac{2}{3}}(1 + x)}{\sqrt{1 - x + x^2}} + \psi_0\sqrt{\frac{8}{3}}$$

where q_0, ψ_0 refer to $\theta = 0$. Adopting the empirical strain-hardening relationship, this can be written in a form suitable for computation :

$$(a+\psi)\frac{\sqrt{\frac{2}{3}}(1+x)}{\sqrt{1-x+x^2}} - n\ln(a+\psi) + \frac{1}{2}\ln(1-x+x^2) - a\frac{\sqrt{\frac{2}{3}}(1+x)}{\sqrt{1-x+x^2}} + \phi$$

$$= (a+\psi_0)\sqrt{\frac{8}{3}} - n\ln(a+\psi_0) - a\sqrt{\frac{8}{3}} + \phi_0.$$

If x is expressed in terms of θ this equation can be solved graphically to give the distribution of ψ for any assumed value of the gross representative strain at the crown, $a + \psi_0$. The resultant thinning at any point can then easily be found from the strain ψ.

This result will of course only be correct if the assumed relationship between x, θ was itself correct, and this can be investigated by applying the same relationship to the solution of the strain equation (6), making use of the Lévy-Lode condition (7). Integration of the strain equation leads to an expression for the principal strain ratio $\frac{e_1}{e_0}$ in terms of θ, from which the thickness distribution $\frac{\epsilon_3}{\epsilon_0}$ immediately follows. If the assumed x, θ relationship was correct, this distribution will agree with that obtained from the stress analysis. Since the labour of computation involved in this procedure is considerable, it is convenient and does not seem improper to assume some x, θ relationship which conforms to experimental measurements, and to check its consistency through both stress and strain equations. An investigation along these lines is at present in hand.

Once the stress-strain distribution is known the inception of stability can be investigated without further difficulty. With a rigid convex punch the essential function of an elementary ring in the sheet metal is to transmit the force necessary to continue the strain of both the crown and the skirt of the pressing. If the ring fails to transmit this force, the crown of the pressing will cease to strain further, since the straining force on it will be relaxed, while the skirt will continue to strain under basically different conditions controlled by the degree and form of blank-holding and by the radial wedge action of the punch. The primary criterion of stability of the ring is therefore its ability to transmit the force which is represented by the stress p_1 but which has associated with it a hoop stress p_2 determined in relation to p_1 by the conditions of the stable strain. In fact the stability conditions at any given ring are similar to those in biaxial tension under a direct load with a second principal stress bearing an appropriate ratio x to the primary one.

In order to ascertain at what section instability is first reached, it is convenient to determine the state of strain which would be reached at the central point of the pressing at the juncture when each section reaches its own value of the subtangent z_1. That section which reaches its critical condition at the earliest stage of strain of the central point, as measured for example by its subtangent z_0, will in fact be the seat of instability. If no other section reaches its limit z_1 before the central pole, then instability will of course start there. Once the critical zone has been located the corresponding strain follows at once.

ACKNOWLEDGMENTS

The work embodied in this paper is part of a programme of research carried out in the University of Sheffield under the aegis of the *British Iron and Steel Research Association*. The author wishes to acknowledge help received from his colleagues, E. M. LOXLEY in computation and checking, and P. B. MELLOR in providing experimental data.

REFERENCES

BIJLAARD, P. P.	1940	*Pub. Int. Ass. Bridge and Structural Eng.*, **6**, 27.
BROWN, W. F. and SACHS, G.	1948	*Trans. A.S.M.E.*, **70**, 241.
BROWN, W. F. and THOMPSON, F. C.	1949	*Trans. A.S.M.E.*, **71**, 575.
HILL, R.	1950	*Phil. Mag.* (Ser. 7), **41**, 1133.
SACHS, G. and LUBAHN, J. D.	1946	*Trans. A.S.M.E.*, **68**, 271.

Vol.
1
1952/5

Journal of the Mechanics and Physics of Solids, 1952, Vol. 1, pp. 19 to 30. Pergamon Press Ltd., London.

ON DISCONTINUOUS PLASTIC STATES, WITH SPECIAL REFERENCE TO LOCALIZED NECKING IN THIN SHEETS

By R. Hill
Department of Theoretical Mechanics, University of Bristol

(*Received 27th. May*, 1952)

Summary

Permissible discontinuities of stress, velocity, and surface slope are investigated in a plastic-rigid sheet deformed in its plane. One such discontinuity of velocity is shown to be the mathematical idealization of localized necking ; the necessary restrictions on the stress-state and rate of work-hardening are obtained for any yield function and plastic potential. The results are illustrated by an examination of the modes of necking in notched tension strips. The constraint factors at the yield point are obtained for notches with wedge-shaped or circular roots.

ol.
1
2/53

1. Present State of Theory of Plane Plastic Stress

We consider the quasi-static distortion of a plane sheet by forces applied in its plane. The variation in thickness at any moment is supposed small enough to allow of the basic approximation of the theory of generalized plane stress; all components of stress and velocity are accordingly averaged through the thickness. The material is assumed to be plastic-rigid, with properties not dependent on the hydrostatic part of the stress.

When the velocity equations in a plastic state are hyperbolic the characteristics are the directions of zero rate of extension, whatever the plastic potential. When the yield function and plastic potential are identical these directions are also the characteristics for the stresses. The velocity relations along the characteristics have been derived for any potential and hardness distribution (Hill 1950, p. 306, eq. 52) and the stress relations for any yield function and thickness variation when the hardness is uniform (op. cit., p. 301, eq. 38). On the other hand, no general methods of integration are available for the part of the plastic zone where the equations are elliptic.

Complete solutions to non-trivial problems which involve a finite amount of distortion have been obtained only when the configurations are radially symmetric. These solutions relate to the expansion of a circular hole in an infinite sheet by internal pressure (op. cit., pp. 307-313), the contraction of an annular ring by internal tension (op. cit., pp. 284-287), and the bending of a sheet in its plane (Gaydon 1952 ; Lubahn and Sachs, 1950). The Tresca yield function and Mises potential were used in these solutions.

In more complicated problems it is to be expected, by analogy with the theory of plane strain, that the solutions may involve discontinuities in stress or velocity. The present paper examines these, and especially a discontinuity in velocity which is the mathematical idealization of localized necking.

2. THE CRITERION FOR A PERMISSIBLE DISCONTINUITY

In plastic-elastic theory no discontinuities in stress or velocity are admitted ; at least, none have so far been found necessary to ensure the existence of a solution. However, under certain circumstances, there may be found narrow transition zones through which some quantity varies rapidly. If the breadth of such a zone becomes vanishingly small, as YOUNG's modulus is indefinitely increased, there is obtained in the limit a plastic-rigid body containing a discontinuity in the quantity in question. If plastic-elastic theory is indeed self-contained, plastic-rigid solutions can require the admission of these discontinuities only. Others are merely *formally* possible (such as block-sliding across any plane) in the sense of not conflicting with the plastic-rigid equations as they stand ; a ' solution ' containing them could not be the correct analogue of the true solution for a plastic-elastic body.

A discontinuity in stress similar to that discussed by PRAGER (1948) is examined in Section 5. This discontinuity is permissible since it can be regarded as an evanescent strip of elastically-stressed material (HILL op. cit., p. 160 ; LEE 1951).

In Section 3 it is shown that under suitable stress conditions the velocity in a *non-hardening* material can be tangentially discontinuous across certain surfaces ; an element crossing one suffers a sudden finite shear. This again is permissible since such a surface is the limit of what would be an intense shear-zone in a plastic-elastic body, the breadth of the zone being small compared with the sheet thickness.

Since the theory of generalized plane stress treats the thickness as vanishingly small we must also admit a quite different kind of discontinuity. For if, in a sheet of any finite thickness h, the gradient of some quantity is of order $1/h$ in a zone of breadth comparable with h, this should appear in the generalized theory as a discontinuity. Now it is well-known that in a thin strip loaded in tension the final necking develops in such a zone (see, for example, NADAI 1951, pp. 319-320) ; simultaneously, the parts of the strip unload and move apart as rigid bodies, still in the same plane. It is observed that their relative velocity vector is inclined at a definite angle to the line of neck (BIJLAARD 1940). To take account of this and allied phenomena we have to admit a discontinuity in the normal, as well as the tangential, component of velocity across a line or curve, provided the rate of hardening does not exceed a certain critical value. It is not permissible to admit such discontinuities arbitrarily : they must bear a certain necessary relation to the local state of stress. According to the criterion just mentioned, this relation is to be obtained by regarding the discontinuity as the limit, when h is made vanishingly small, of a zone of intense strain accompanying the relative motion.

3. DISCONTINUITIES OF VELOCITY

It is supposed that the material is isotropic and that the yield function and plastic potential are identical (as required by the BISHOP-HILL theory of the plastic behaviour of a polycrystal, 1951). It is further supposed that they have six-fold symmetry, consequent on disregarding Bauschinger and related effects, when represented as a surface in principal stress-space (HILL 1950, pp. 18 and 36). Finally, the surface must not be concave outward at any point (a further requirement of the BISHOP-HILL analysis).

Vol.
1
1952/

Consider, first, the simple shear discontinuity in a non-hardening body. Isotropy necessitates the coincidence of the plane and direction of shear with the plane and direction of the maximum shear stress; moreover, the latter must be equal to the yield stress in pure shear. If the maximum shear stress lies in the sheet, the surface of shearing must be normal to the sheet and contain a maximum shear stress direction at each point. The principal stresses are $(k, -k, 0)$ for any potential whose surface in stress space has a finite radius of curvature at the point corresponding to pure shear. On the other hand, if the maximum shear stress is directed out of the plane, the principal stresses are $\pm (2k, k, 0)$. The plane and direction of shearing bisect the angle between the sheet normal and the axis of the greatest principal stress. Exceptionally, if the potential surface is plane in the neighbourhood of the point representing pure shear, the stress can take any value in this neighbourhood. In particular, for TRESCA's yield function and potential the stresses in the sheet satisfy $\sigma_1 - \sigma_2 = 2k$, $0 \leqslant \sigma_1 \leqslant 2k$, for shearing in the plane, and $\sigma_1 = 2k$, $0 \leqslant \sigma_2 \leqslant 2k$, for shearing out of the plane (also similar conditions with the signs reversed).

Consider, now, the necking type of discontinuity defined by a relative velocity $\mathbf{v}$, possibly varying from point to point. Let $\mathbf{v}$ have magnitude v and make an angle ψ with the neck (Fig. 1). The local breadth b of the neck and the sheet thickness h are comparable and are ultimately to be made infinitesimal in comparison with the length and radius of curvature of the trace of the neck. In the spirit of the theory of generalized plane stress we treat the strain-rate in the neck as if it were uniform. It is evident that the directions of zero rate of extension at each point are along the neck and perpendicular to the local direction of $\mathbf{v}$. As mentioned in Section 1 these directions are also the velocity characteristics in the material on either side (assuming for the moment that the stress varies continuously). Thus the incipient neck coincides with one characteristic and the discontinuity vector is perpendicular to the other; put otherwise, the velocity resolute along the other characteristic is continuous across the neck. When $\psi = 0$ there is no necking, only a relative sliding. Localized necking also cannot occur if the stress state is elliptic.

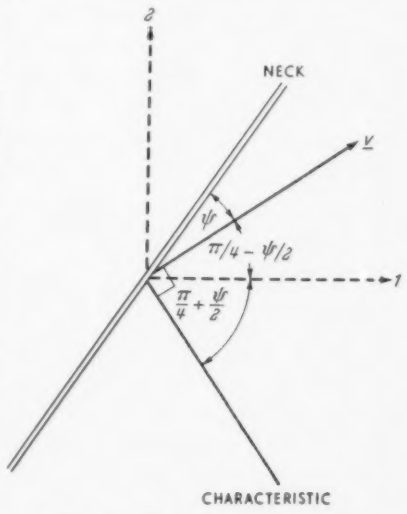

Fig. 1. Velocity discontinuity.

It is evident that in reality the relative displacement has only to become of order h for the neck to become so thin that fracture completes the separation. Correspondingly, if we adhere to a strict view of the theory, separation must be regarded as instantaneous once a neck is able to develop. Of course, the calculated stress at that moment is not necessarily that under which the ultimate fracture occurs.

It is easily shown that the strain-rate tensor in the neck has principal components

$$\dot{\epsilon}_1 = \frac{v}{2b}(1 + \sin\psi), \qquad \dot{\epsilon}_2 = -\frac{v}{2b}(1 - \sin\psi), \qquad \dot{\epsilon}_3 = -\frac{v}{b}\sin\psi,$$

where the third axis is along the sheet normal and the other two bisect the angles between the characteristics. The plastic work-rate per unit length of neck is thus

$$bh\,\dot{W} = bh\,(\sigma_1\,\dot{\epsilon}_1 + \sigma_2\,\dot{\epsilon}_2) = \tfrac{1}{2}\,hv\,[(\sigma_1 - \sigma_2) + (\sigma_1 + \sigma_2)\sin\psi]. \tag{1}$$

If f denotes the yield function and plastic potential,

$$f(\sigma_1, \sigma_2) = \text{const.}, \qquad \frac{\partial f}{\partial \sigma_1}\Big/\frac{\partial f}{\partial \sigma_2} = \dot{\epsilon}_1/\dot{\epsilon}_2, \tag{2}$$

where the constant depends on the degree of hardening. Hence

$$\left.\begin{aligned} \sin\psi &= \frac{\dot{\epsilon}_1 + \dot{\epsilon}_2}{\dot{\epsilon}_1 - \dot{\epsilon}_2} = \left(\frac{\partial f}{\partial \sigma_1} + \frac{\partial f}{\partial \sigma_2}\right)\Big/\left(\frac{\partial f}{\partial \sigma_1} - \frac{\partial f}{\partial \sigma_2}\right) \\ \text{where, for real } \psi, \qquad & -\frac{\partial f}{\partial \sigma_1} \leqslant \frac{\partial f}{\partial \sigma_2} \leqslant 0. \end{aligned}\right\} \tag{3}$$

In particular, $\dot{\epsilon}_1/\dot{\epsilon}_2 = -2$ for a thin strip pulled in tension, so that $\psi = \sin^{-1}\frac{1}{3} = 19^\circ\,28'$; thus the neck is inclined at $\frac{1}{4}\pi + \frac{1}{2}\psi = 54^\circ 44'$ to the tension axis while **v** is inclined at $\frac{1}{4}\pi - \frac{1}{2}\psi = 35^\circ 16'$.

In passing we may note that the work-rate (1), with stresses given by (2) and (3), is appropriate in the extremum principle for a plastic-rigid body at the yield point (HILL 1951; PRAGER and HODGE 1951; DRUCKER, PRAGER and GREENBERG 1952*) when the fictitious velocity field involves such a discontinuity. The adaptation of the principle to generalized plane stress is self-evident.

When the yield function is that of VON MISES,

$$\left.\begin{aligned} & f \equiv \sigma_1^2 - \sigma_1\,\sigma_2 + \sigma_2^2 = 3k^2 = Y^2, \\ & \frac{\sigma_1}{k} = \frac{1 + 3\sin\psi}{\sqrt{(1 + 3\sin^2\psi)}}, \qquad \frac{\sigma_2}{k} = \frac{-1 + 3\sin\psi}{\sqrt{(1 + 3\sin^2\psi)}}, \\ & \sin\psi = \frac{\sigma_1 + \sigma_2}{3\,(\sigma_1 - \sigma_2)}, \qquad bh\,\dot{W} = kvh\sqrt{(1 + 3\sin^2\psi)}. \end{aligned}\right\} \tag{4}$$

These equations are equivalent to those obtained by BIJLAARD (1940), who was concerned with the necking phenomenon itself and not with permissible discontinuities in a plastic-rigid solution. For the Tresca yield function, where k now denotes $\frac{1}{2}Y$ (Y = tensile yield stress),

$$f \equiv \sigma_1 - \sigma_2 = 2k, \qquad 0 < \sigma_1 < 2k, \qquad \psi = 0, \qquad \dot{\epsilon}_3 = 0, \tag{5a}$$

when σ_1 and σ_2 have opposite signs (the characteristics are orthogonal as in plane strain). When σ_1 and σ_2 have the same sign the characteristics are coincident and

$$f \equiv \sigma_1 = 2k, \qquad 0 < \sigma_2 \leqslant 2k, \qquad \psi = \tfrac{1}{2}\pi, \qquad \dot{\epsilon}_2 = 0. \tag{5b}$$

If, however, the stress is a uniaxial tension the only condition on the distortion

* The different points of view expressed by these various authors have recently been further discussed in a paper by LEE (1952), with comments by the present writer.

Vol 1 1952/

is that the greatest principal component of strain should coincide with this tension ; ψ can therefore have any value between 0 and $\frac{1}{2}\pi$. In all cases

$$bh\,\dot{W} = kvh\,(1 + \sin\psi). \tag{5c}$$

The so-called ' parabolic ' and ' generalized Tresca ' yield functions, recently proposed for plane stress by VON MISES (1949) and HODGE (1950) respectively, are not considered here since they make the yield stress in balanced biaxial tension different from that in uniaxial tension. They are therefore not appropriate for an isotropic material with properties independent of hydrostatic stress.

4. Influence of Work-Hardening

When the material work-hardens, a further condition is necessary for a localized neck to be able to develop : namely, that the hardening produced by the first increment of strain in the incipient neck should not be so great as to inhibit its immediate development and cause deformation to continue only elsewhere. If the parent stress-state is *uniform*, the neck is straight and the material on either side moves as a rigid body without strain-hardening. Hence, at the instant when continued necking *just* becomes possible, the stresses elsewhere are momentarily *unchanged* during the inception of the neck. The rate of hardening in the neck then exactly balances the rate of diminution in thickness, while the stress components there preserve constant ratios.

To evaluate the rate of hardening let us assume that the total amount of hardening is a function only of the plastic work W per unit volume, so that (2) may be written

$$f(\sigma_1, \sigma_2) = F(W).$$

Then
$$\dot{\sigma}_1 \frac{\partial f}{\partial \sigma_1} + \dot{\sigma}_2 \frac{\partial f}{\partial \sigma_2} = (\sigma_1\,\dot{\epsilon}_1 + \sigma_2\,\dot{\epsilon}_2)\,F'(W)$$

and so, since $\dot{\sigma}_1/\sigma_1 = \dot{\sigma}_2/\sigma_2$ in the neck when it is just able to develop,

$$\frac{\dot{\sigma}_1}{\sigma_1}\left(\sigma_1 \frac{\partial f}{\partial \sigma_1} + \sigma_2 \frac{\partial f}{\partial \sigma_2}\right) = (\sigma_1\,\dot{\epsilon}_1 + \sigma_2\,\dot{\epsilon}_2)\,F'(W).$$

Hence, by (2) and the properties of equal ratios,

$$\frac{\dot{\sigma}_1}{\sigma_1}\left(\frac{\partial f}{\partial \sigma_1} + \frac{\partial f}{\partial \sigma_2}\right) = (\dot{\epsilon}_1 + \dot{\epsilon}_2)\,F'(W).$$

But, as we have seen, progressive necking is just possible when

$$\frac{\dot{\sigma}_1}{\sigma_1} = -\,\dot{\epsilon}_3 = \dot{\epsilon}_1 + \dot{\epsilon}_2.$$

The rate of hardening must therefore satisfy

$$F'(W) \leqslant \frac{\partial f}{\partial \sigma_1} + \frac{\partial f}{\partial \sigma_2}$$

for localized necking to be possible. If $Y(\epsilon)$ is the uniaxial stress-strain relation (obtained by compression normal to the sheet or by balanced biaxial tension in its plane),

$$f(Y, 0) = F(W) \quad \text{where} \quad W = \int_0^\epsilon Y \, d\epsilon.$$

Hence $$F'(W) = r \frac{\partial f(Y, 0)}{\partial Y} \quad \text{where} \quad r = \frac{1}{Y} \frac{dY}{d\epsilon}.$$

Thus the stress and rate of hardening must satisfy

$$r \leqslant \left(\frac{\partial f}{\partial \sigma_1} + \frac{\partial f}{\partial \sigma_2} \right) \Big/ \frac{\partial f(Y, 0)}{\partial Y}, \tag{6}$$

and the conditions (3).

If the parent state of stress and hardness is not uniform we may nevertheless reasonably expect a good approximation to be obtained by satisfying (6) at every point of the neck. Since the neck will usually be curved and the direction of $\mathbf{v}$ will vary along it, the material on either side must also deform and harden; the amount is negligible, however.

If f is the Mises expression (4),

$$r \leqslant (\sigma_1 + \sigma_2)/2Y = \sqrt{3} \sin \psi / \sqrt{(1 + 3 \sin^2 \psi)}. \tag{7}$$

The angle ψ is therefore restricted to the range

$$\sqrt{3} \sin \psi \geqslant r / \sqrt{(1 - r^2)}. \tag{8}$$

In particular we note the otherwise obvious fact that a sliding discontinuity ($\psi = 0$) is possible only in a non-hardening material. Localized necking cannot be induced under any stress system whatever if $r > \sqrt{3}/2$.

In uniaxial tension of a thin strip it follows from (2) and (6), in view of $\dot{\epsilon}_1/\dot{\epsilon}_2 = -2$, that localized necking can occur when $r \leqslant \frac{1}{2}$. On the other hand, as is well-known, diffuse necking symmetrical about the tension axis can occur when $r \leqslant 1$*. Thus, in a strip of material whose stress-strain curve is rounded we should expect first a uniform extension, then diffuse necking, and finally localized necking when the requisite decrease in r has occurred. This is indeed observed (NADAI 1951, p. 326). As the analysis in Section 7 indicates, the shape and general direction of the final neck depend on the curvature of the diffuse neck, as well as on the hardness distribution there.

5. DISCONTINUITIES OF STRESS

For equilibrium the components of the stress acting over any surface are necessarily the same on both sides. We prove first that *all* components of stress are continuous across a velocity discontinuity (apart from exceptions to be mentioned). To show this for the shearing discontinuity in the plane, where the tangential stress is k, it is only necessary to observe that the normal components of stress in the plane must be equal; otherwise the maximum shear stress would exceed k, which is not possible when the yield function satisfies the conditions

* More generally, in a uniform biaxial state (σ_1, σ_2) diffuse necking symmetrical about the principal axes can first develop when $\dot{\sigma}_1/\sigma_1 = \dot{\epsilon}_1$, $\dot{\sigma}_2/\sigma_2 = \dot{\epsilon}_2$. This leads to the condition

$$r \leqslant \left[\sigma_1 \left(\frac{\partial f}{\partial \sigma_1} \right)^2 + \sigma_2 \left(\frac{\partial f}{\partial \sigma_2} \right)^2 \right] \Big/ \left(\sigma_1 \frac{\partial f}{\partial \sigma_1} + \sigma_2 \frac{\partial f}{\partial \sigma_2} \right) \frac{\partial f(Y, 0)}{\partial Y}.$$

The right-hand side here is always greater than that in (6), in view of the conditions (3).
In particular if f is the Mises expression we recover a result due to SWIFT (1950):

$$r \leqslant (\sigma_1 + \sigma_2)(4\sigma_1^2 - 7\sigma_1\sigma_2 + 4\sigma_2^2)/4Y^2.$$

Vol 1 1952/

previously laid down. Hence all components are continuous.* (Obviously, also, the velocity is continuous at a stress discontinuity for, if it were not, the stress would have to be continuous as just proved). A similar argument applies to shearing out of the plane, except for Tresca-type yield functions where there may indeed be a discontinuity.

To discuss necking it is convenient to introduce the envelope of circles for possible plastic states in MOHR's representation. Since the stress state in the neck is either hyperbolic or parabolic the associated circle has real contact with the envelope at the point whose coordinates are the shear stress along the neck and the normal stress across it (HILL 1950, p. 296). When the stress state is hyperbolic it is therefore impossible to find another stress circle through the same point that does not cut the envelope and so violate the yield condition. Hence the stress on either side of the neck is represented by the same circle and is therefore continuous. However, when the stress state is parabolic (both characteristics coinciding with the neck) infinitely many plastic stress circles can be drawn for a Tresca-type yield function; the stress may then be discontinuous. When the surface is not a characteristic a stress discontinuity is always possible since, through any point within the Mohr envelope, infinitely many stress circles can be drawn without violating the yield condition. In particular there are usually two such circles which represent possible plastic states, having real or imaginary contact with the envelope; the following analysis is concerned with these. Let σ_1 and σ_2 ($\leqslant \sigma_1$) be the principal components on one side of the discontinuity and σ_1', σ_2' ($\leqslant \sigma_1'$) those on the other; Fig. 2 shows the convention adopted in regard to the angles θ and θ' defining the orientation of the principal axes.

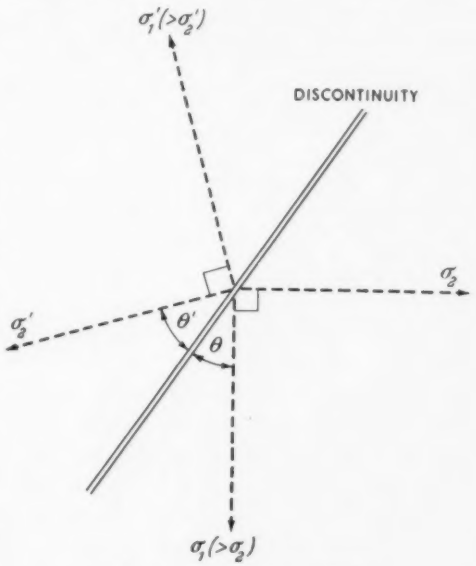

Fig. 2. Stress discontinuity.

For the Mises yield function it may be shown that

$$\left.\begin{aligned} \tan 2\theta' &= 2\sin 2\theta \Big/ \left(\cos\theta + \frac{\sigma_1+\sigma_2}{\sigma_1-\sigma_2}\right), \\ \sigma_1' + \sigma_2' &= \frac{1}{2}(\sigma_1 + \sigma_2) - \frac{3}{2}(\sigma_1 - \sigma_2)\cos 2\theta, \\ \sigma_1' - \sigma_2' &= [4k^2 - \tfrac{1}{3}(\sigma_1' + \sigma_2')^2]^{\frac{1}{2}}. \end{aligned}\right\} \qquad (9)$$

* Alternatively, this may be proved by showing that the velocity must be continuous across a stress discontinuity, as was done in the plane strain case by the writer (1950, p. 160). Such a method is a little less straightforward since it involves ruling out the possibility of a velocity discontinuity *alongside* the stress discontinuity; this was neglected in the later and otherwise similar discussion by LEE (1951).

For the Tresca yield function suppose that (σ_1, σ_2) is a hyperbolic state, so that $\sigma_1 - \sigma_2 = 2k$ and $|\sigma_1 + \sigma_2| \leqslant 2k$. We do not need to consider separately the case when (σ_1, σ_2) is a parabolic state since this is obtained by interchanging roles in the equations (10) below. It is found that

$$\left.\begin{aligned} \theta' &= \theta, \qquad \sigma_1' - \sigma_2' = 2k, \\ \tfrac{1}{2}(\sigma_1' + \sigma_2') &= \tfrac{1}{2}(\sigma_1 + \sigma_2) - 2k\cos 2\theta \end{aligned}\right\} \quad \text{when } \frac{\sigma_2}{2k} \leqslant \cos 2\theta \leqslant \frac{\sigma_1}{2k}. \tag{10a}$$

These are formally identical with the conditions at a discontinuity in plane strain. Further,

$$\left.\begin{aligned} \tan\theta' &= \left(1 + \cos 2\theta - \frac{\sigma_2}{k}\right) \Big/ \sin 2\theta, \qquad \sigma_1' = 2k, \\ \frac{\sigma_2'}{2k} &= -\frac{\sigma_2}{k}\left(\frac{\sigma_2}{2k} - \cos 2\theta\right) \Big/ \left(1 + \cos 2\theta - \frac{\sigma_2}{k}\right); \end{aligned}\right\} \quad \frac{\sigma_2}{2k} \geqslant \cos 2\theta. \tag{10b}$$

$$\left.\begin{aligned} \cot\theta' &= \left(1 - \cos 2\theta + \frac{\sigma_1}{k}\right) \Big/ \sin 2\theta, \qquad \sigma_2' = -2k, \\ \frac{\sigma_1'}{2k} &= -\frac{\sigma_1}{k}\left(-\frac{\sigma_1}{2k} + \cos 2\theta\right) \Big/ \left(1 - \cos 2\theta + \frac{\sigma_1}{k}\right). \end{aligned}\right\} \quad \frac{\sigma_1}{2k} \leqslant \cos 2\theta. \tag{10c}$$

Exceptionally, when the stress normal to the discontinuity is $\pm 2k$ the other principal components on either side can have any values between 0 and $\pm 2k$. The discontinuity is then not necessarily the limit of a narrow elastic zone since the jump can be bridged by a continuous sequence of plastic states.

We have seen that the velocity must be continuous across a stress discontinuity. If the velocity fields on either side satisfy this condition, and the condition that the plastic work-rate is everywhere positive, it follows that the rate of extension along the discontinuity is automatically zero. For in view of the convexity of f the values of $\partial f/\partial\sigma_x$ on either side are opposite in sign, where σ_x is the component parallel to the discontinuity. Since f is also the plastic potential the rates of extension in this direction have therefore different signs on either side (the work-rates being positive). Hence, if the velocity is made continuous, and therefore the rate of extension also, the latter must automatically be zero. The vanishing of the extension rate is thus not an *additional* condition to be imposed on the velocity fields; this is contrary to the view expressed by LEE (op. cit., p. 219, footnote).

6. DISCONTINUITIES IN SURFACE SLOPE

A discontinuity in the slope of the surface may be present in the undeformed sheet or may be created during the distortion. We note first that no part of the trace of such a discontinuity can currently coincide with a characteristic. This follows since the slope enters the differential relation governing the variation of the stress components along the characteristic; since the stresses are continuous, so is the slope. (Exceptions occur for a Tresca-type yield function but are not considered here). The trace can, however, coincide with an envelope of characteristics since the relation mentioned does not hold along the envelope. These

Vol. 1 1952/

remarks apply in particular to the boundary between the rigid and deforming parts of a hyperbolic plastic zone since this is a characteristic or envelope of characteristics (as when a hole is expanded in a sheet).

Consider, now, the possibility of a discontinuity in slope in a state of steady motion. We have seen that in general the trace cannot coincide with a characteristic; that is, the derivatives of the velocity components are continuous across the trace. Accordingly, if volume is to be preserved, the velocity component normal to the trace must vanish. Hence the trace, or thickness characteristic as we may regard it, must be a streamline. The equation of incompressibility furnishes the relation

$$\left(1 + \frac{\partial f/\partial \sigma_n}{\partial f/\partial \sigma_t}\right)\frac{dq}{q} + \frac{dh}{h} = 0 \tag{11}$$

for the variation of the speed q along a streamline, where (σ_n, σ_t) are the normal stress components perpendicular and tangential to the streamline. Taking (11) in conjunction with the yield condition and the four relations along the other two characteristics (referred to in Section 1) we have, in all, six canonical equations suitable for determining the three stress components, two velocity components, and the thickness as functions of position in a non-hardening material. Although the thickness gradient transverse to the stress characteristics enters the associated relations, the fact that it is continuous across them makes unnecessary, not to say disadvantageous, its elimination by means of the incompressibility equation in the manner detailed by HODGE (1951).

In a non-steady state, on the other hand, the thickness is known to begin with. When the initial stress and velocity fields have been computed, the incompressibility equation furnishes the rate of change of thickness Dh/Dt following an element:

$$\frac{1}{h}\frac{Dh}{Dt} = -\left(1 + \frac{\partial f/\partial \sigma_n}{\partial f/\partial \sigma_t}\right)\frac{\partial q}{\partial s}, \tag{12}$$

where s is arc-length measured along curves enveloping the momentary directions of flow. We may therefore calculate the approximate new thickness after some selected small interval. Thereafter, the procedure may be repeated for a succession of small intervals, at the beginning of each of which the thickness is a previously calculated and therefore known quantity.

7. Necking of Notched Strips

In illustration of the preceding results consider the extension of a long rectangular strip symmetrically notched in its plane. The material is supposed to be uniformly hardened and to obey the Mises yield criterion. When the notch is sufficiently deep and sharp, with a wedge-shaped root,* the relevant part of the characteristic field (Fig. 3a) is similar to that in the analogous plane strain problem. It may be proved (cf. HILL 1951, p. 872) that the plastically-stressed zone certainly extends at least as far as the field shown. There is, however, no need to determine the *actual* stress distribution elsewhere; to justify this partial field it is only necessary to prove the possibility of constructing elsewhere *some* distribution satisfying the

* In practice the radius of curvature of the notch root must be two or three times the sheet thickness if the theory of generalized plane stress is to be a satisfactory approximation.

boundary-conditions and not violating the yield criterion (PRAGER and HODGE 1951, p. 226). Such a construction, valid for sufficiently deep notches of any angle, has been given by BISHOP (to be published).

To describe the state of stress where one family of characteristics pass through the notch root it is convenient to introduce polar components σ_r, σ_ϕ, and $\tau_{r\phi}$. The yield condition and the equations of equilibrium are satisfied by

$$\sigma_r = k\cos\phi, \qquad \sigma_\phi = 2k\cos\phi, \qquad \tau_{r\phi} = k\sin\phi, \tag{13}$$

where the polar angle ϕ is measured from the base-line indicated in Fig. 3a. This is such that the angle between it and the farther surface of the notch is 2β where, as proved in Section 3, $\beta = \tan^{-1}\sqrt{2} = 54°44'$ is the inclination of the characteristics in the state of uniaxial tension adjacent to the side of the notch. From (4) we find that $\tan\psi = \frac{1}{2}\cot\phi$ and hence that the curved characteristics have equation $r^2\sin\phi = \text{constant}$. They are inflected where $\phi = \frac{1}{2}\pi - \beta$ and, if continued, approach the base-line asymptotically.

If 2α is the notch angle and ϕ is now restricted to refer to the *innermost* characteristic through the root, then

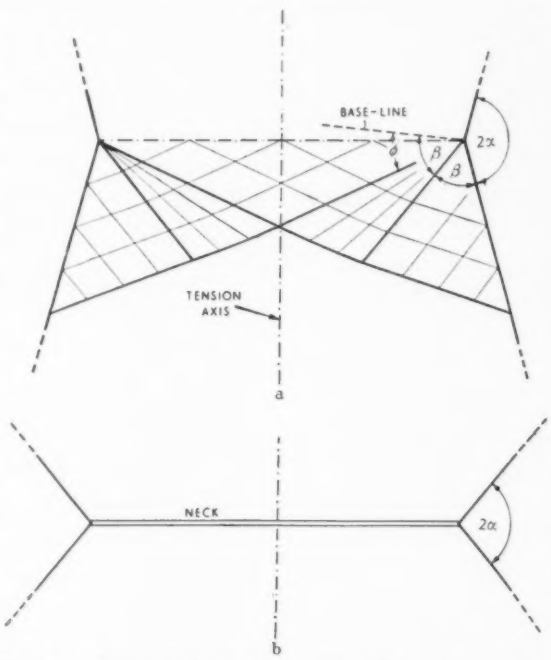

Fig. 3. Characteristic field in notched tension strip; root wedge-shaped. (a) $\alpha > 70°32'$ (b) $\alpha \leqslant 70°32'$.

$$2\tan\phi + \tan 2(\alpha + 2\beta - \phi) = 0 \tag{14}$$

in order that there should be no shear stress along the transverse axis of symmetry. The constraint factor, c, defined as the mean longitudinal stress in the minimum section divided by the uniaxial yield stress, is found to be

$$\left.\begin{aligned} c &= [\sqrt{(1 + 3\sin^2\phi)} + 3\cos\phi]/2\sqrt{3} \\ &\sim 1 + \left(\frac{2}{\sqrt{3}} - 1\right)\sin\left(\frac{\frac{1}{2}\pi - \alpha}{\frac{4\beta}{\pi} - 1}\right), \qquad \pi - 2\beta \leqslant \alpha \leqslant \tfrac{1}{2}\pi, \end{aligned}\right\} \tag{15}$$

empirically, with an overestimate of less than $\frac{1}{2}$ per cent. It will be observed that $\phi = 0$ and $c = 2/\sqrt{3}$ when $\alpha = \pi - 2\beta = 70°32'$; the field then shrinks to a coincident pair of characteristics along the transverse axis (Fig. 3b), where $\sigma_\phi = 2k$ and $\sigma_r = k$. This is also true for all sharper notches since, by the maximum

work principle, c cannot decrease when material is added in order to reduce the notch angle;* on the other hand, c certainly cannot exceed $2/\sqrt{3}$ since in view of (4) no stress component can exceed $2k$. It seems safe to expect that the solutions are valid when the fractional reduction of width at the notch is more than 25 per cent or so.

If the rate of hardening is sufficiently low two deformation modes are theoretically possible : (i) flow through an extended plastic zone ; (ii) localized necking along both characteristics through some point of the field. Only the diffuse mode (i) occurs when the hardening rate is sufficiently large ; when $r \leqslant \frac{1}{2}$ the mode (ii) can also occur, according to (7), and in practice presumably always will (in the case of Fig. 3b the condition $r \leqslant \frac{1}{2}$ must be approached as a limit by indefinitely increasing the curvature of the root). For definiteness, suppose that in mode (ii) both branches of the neck pass through the centroid. The velocity field between the branches is defined by the boundary condition that at any point of the neck the velocity resolute along the other characteristic is continuous (as mentioned in Section 3). If the ends of the strip are moved longitudinally with unit speed relative to the centroid the elements on the transverse axis travel inward with speed $\tan(\frac{1}{4}\pi - \frac{1}{2}\psi)$ where $\tan\psi = \frac{1}{2}\cot\phi$. The relative velocity vector at other points of the neck, together with the velocity field between the two branches, can be determined by integrating the relations along the characteristics. However, since fracture follows immediately according to a strict view of the present theory, there is no opportunity for distortion to occur elsewhere; in reality, displacements of order h would be expected.

Consider, next, deep notches with circular roots of radius ρ, distance $2a$ apart. It is believed that the relevant fields are as in Fig. 4, although no justifying stress distribution has yet been constructed in the remainder of the strip, nor is the extent of the diffuse mode known. For small values of a/ρ the field is radially symmetric (as in an annular ring under external tension) and is defined by the well-known parametric formulae

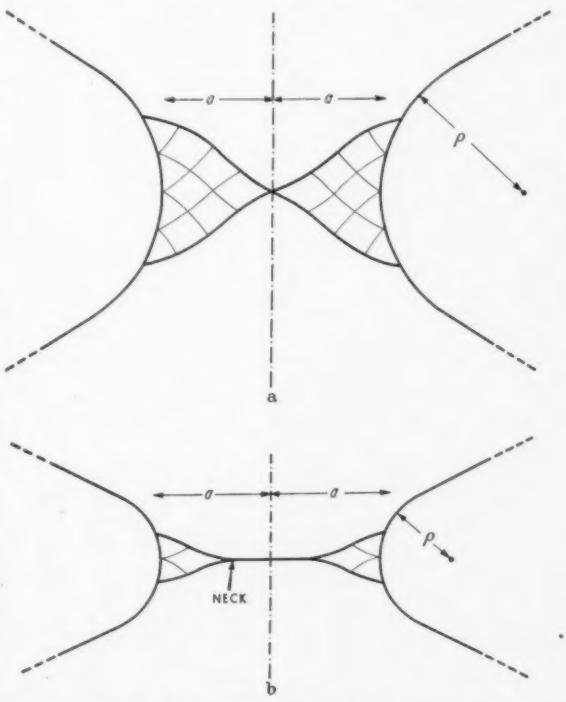

Fig. 4. Characteristic field in notched tension strip ; root circular. (a) $a/\rho \leqslant 1{\cdot}071$, (b) $a/\rho > 1{\cdot}071$.

* This incidentally disproves the surmise by HODGE (1950) that c for $\alpha = \pi - 2\beta$ exceeds its value for any neighbouring angle.

$$\left.\begin{aligned} &\sigma_r = 2k \sin(\theta - \tfrac{1}{6}\pi), \qquad \sigma_\phi = 2k \sin(\theta + \tfrac{1}{6}\pi), \\ &\text{where} \qquad \frac{r^2}{\rho^2} = \frac{\sqrt{3}}{2} \sec\theta \exp\{\sqrt{3}(\theta - \tfrac{1}{6}\pi)\}, \qquad \tfrac{1}{6}\pi \leqslant \theta \leqslant \tfrac{1}{3}\pi. \end{aligned}\right\} \tag{16}$$

When $\theta = \frac{1}{3}\pi$, $r/\rho = 2{\cdot}071$ and the characteristics coincide. Hence Fig. 4a and (16) apply only when $a/\rho \leqslant 1{\cdot}071$; furthermore, the angular span of the root must be greater than $4\beta - \pi = 38°56'$. The constraint factor is

$$\left.\begin{aligned} c = \int_\rho^{a+\rho} \sigma_\phi \, dr/\sqrt{3}\,ka &= (a+\rho)\,\sigma_r\,(a+\rho)/\sqrt{3}\,ka \\ &\sim 1 + 0{\cdot}226\,\frac{a}{a+\rho} \end{aligned}\right\} \quad 0 \leqslant \frac{a}{\rho} \leqslant 1{\cdot}071 \tag{17a}$$

empirically, with an underestimate of less than $\frac{1}{4}$ per cent. For sharper notches the characteristics coincide along the central part of the transverse axis (Fig. 4b), the stresses there being $2k$ and k. The constraint factor is

$$c = \frac{2}{\sqrt{3}} - 0{\cdot}040\,\frac{\rho}{a}, \qquad \frac{a}{\rho} \geqslant 1{\cdot}071. \tag{17b}$$

Localized necking at the yield point is to be expected when $r \leqslant \frac{1}{2}$.

Consider, finally, the solution for TRESCA's yield function and potential. The constraint factor c can certainly not exceed unity since no stress can exceed $2k$. That c is, on the other hand, not less than unity (whatever the shape of the notch) follows from the maximum work principle by comparison with a uniform tension $2k$ in a strip of width $2a$. Hence $c = 1$. The notched strip necks directly across the minimum section provided $r \leqslant 1$, according to (5b) and (6). The result that the Mises and Tresca constraint factors do not differ by more than a factor $2/\sqrt{3}$ is a particular example of a general comparison theorem (HILL 1952).

It is worth noting, as a general result, that the maximum constraint factor is equal to the ratio of the maximum shear stresses in pure shear and pure tension.

Vol 1 1952/

REFERENCES

BIJLAARD, P. P.	1940	*Pub. Int. Ass. Bridge and Structural Eng.*, **6**, 27.
BISHOP, J. F. W. and HILL, R.	1951	*Phil. Mag.*, **42**, 414 and 1298.
DRUCKER, D. C., PRAGER, W. and GREENBERG, H. J.	1952	*Quart. App. Math.*, **9**, 381.
GAYDON, F. A.	1952	*J. Mech. Phys. Solids*, in press.
HILL, R.	1950	*Mathematical Theory of Plasticity* (Clarendon Press).
	1951	*Phil. Mag.*, **42**, 868.
	1952	*Phil. Mag.*, **43**, 353.
HODGE, P. G.	1950	*J. Math. and Phys.*, **29**, 38.
	1951	*Quart. App. Math.*, **8**, 381.
LEE, E. H.	1950	*Proc. 3rd Symposium in App. Math., Am. Math. Soc.*, **3**, 214.
	1952	*Phil. Mag.*, **43**, 549.
LUBAHN, J. D. and SACHS, G.	1950	*Trans. Amer. Soc. Mech. Eng.*, **72**, 201.
MISES, R. VON	1949	*Reissner Anniversary Volume*, 415.
NADAI, A.	1950	*Theory of Flow and Fracture of Solids*, Vol. I (McGraw-Hill).
PRAGER, W.	1948	*Courant Anniversary Volume*, 289.
PRAGER, W. and HODGE, P. G.	1951	*Theory of Perfectly Plastic Solids* (Wiley).
SWIFT, H. W.	1950	Brit. Iron and Steel Res. Ass., Rep MW/E/52/50.

Journal of the Mechanics and Physics of Solids, 1952, Vol. 1, pp. 31 to 36. Pergamon Press Ltd., London.

CALCULATIONS ON THE INFLUENCE OF FRICTION AND DIE GEOMETRY IN SHEET DRAWING

By A. P. Green* and R. Hill†

* The British Iron & Steel Research Association, Sheffield.

† Department of Theoretical Mechanics, University of Bristol.

(*Received 28th. May*, 1952)

Summary

Calculations of the drawing stress on the basis of the Hill-Tupper theory of sheet-drawing are reported for an extended range of angles and reductions for both smooth and rough wedge-shaped dies. The results are summarized in convenient empirical formulae. It is shown that the fractional redundant work due to inhomogeneous distortion is virtually a function only of a single geometric parameter in frictionless drawing. The redundant work does not decrease steadily as the reduction is increased, but oscillates with a decreasing amplitude.

ol.
1
2/53

1. Introduction

In the particular forming process under consideration a uniform rectangular sheet is reduced in thickness by drawing it through a wedge-shaped die. When the width of the sheet is large compared with the length of the die channel, the deformation is essentially plane, since the rigid material on either side of the die prevents lateral expansion except very near the edges. The process may be regarded as the two-dimensional analogue of wire-drawing.

The only previous theory that adequately takes account of the inhomogeneous distortion is that of Hill and Tupper (1948). Their solution is an exact one for an ideal plastic-rigid material deforming under a constant maximum shearing stress k. In the present paper further calculations on this theory are presented and conveniently summarized in empirical formulae.

Hill and Tupper also suggested that the contribution of work-hardening to the drawing load could be estimated to a good approximation by assuming that the mean strain imparted by the die is independent of the hardening characteristics of the material‡ (see also Hill 1950, p. 172).

2. Drawing Stress for a Smooth Die

The calculations of Hill and Tupper for smooth dies cover the range of angles and reductions for which the zone of plastically-deforming material intersects the longitudinal axis in a single point in a typical plane of flow. This range of reductions is defined by the limits

‡ Green (1951a) has demonstrated by means of a scribed grid technique that the deformation in plasticine, a work-hardening material, is very like that calculated, even in detail. Wistreich (1951) has found, from observations of the total hardening during drawing, that the average strain is approximately the same for copper, stainless steel, and mild steel, all these metals being annealed before drawing.

$$\alpha\left(0{\cdot}230 + \frac{\alpha}{9}\right) \leqslant r \leqslant 2\sin\alpha/(1 + 2\sin\alpha) \qquad (1)$$

where α is the semi-angle of the die channel (radian measure) and r is the fractional reduction in thickness. The expression for the lower limit is empirical, with an error in r of less than 1 per cent. At reductions below the lower limit in (1) a bulge or standing wave of plastic material forms ahead of the die. At reductions beyond the upper limit in (1) the plastically-deforming zone extends over a finite portion of the axis. The calculations reported here relate to certain ranges of such reductions (namely those corresponding to Fig. 6a, HILL and TUPPER, op. cit., or to Fig. 35a, HILL 1950, and their analogues at higher reductions). These further ranges are defined by the limits

$$2\sin\alpha/(1 + 2\sin\alpha) \leqslant r \leqslant 2{\cdot}06\,\alpha - \alpha^2 \qquad (2)$$

and

$$3{\cdot}5\,\alpha - 4{\cdot}9\,\alpha^2 \leqslant r \leqslant 4\,\alpha - 5\,\alpha^2 \qquad (3)$$

to within 1 per cent. The solution for the intermediate range has been found qualitatively (GREEN 1951b) though no exact calculations have been made. However, the pressure distribution on the die has been calculated approximately in three instances (see Section 3), while close bounds from above and below to the drawing stress have been obtained by HILL (1951) and GREEN (1952).

The results are shown in Table 1 in terms of the ratio of the actual drawing stress t to the quantity $2k \ln\{1/(1-r)\}$ representing the drawing stress given by the SACHS theory, which assumes homogeneous deformation; this ratio is also equal to the quotient of the respective die loads or mean pressures. The extent by which the ratio exceeds unity is thus a measure of the relative amount of redundant work expended in inhomogeneous distortion during drawing. It is remarkable that the redundant work does not decrease steadily but varies in an oscillatory manner as the reduction is increased; it never quite reaches zero at the minima but the amplitude of the oscillations decreases steadily.

It is found that the ratio in Table 1 depends only on the single geometrical parameter c/d where d is the length of the contact with each die and c is the length of the circular arc which has its centre at the virtual apex of the channel and joins the midpoints of the two zones of contact (Fig. 1).

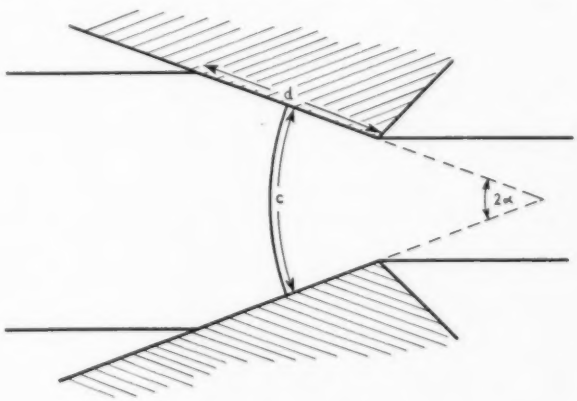

Fig. 1.

The variation from the mean of the calculated ratios is less than $\frac{1}{4}$ per cent over most of the ranges (1), (2) and (3), and about $\frac{1}{2}$ per cent near each end of (1) for semi-angles between 5° and 30° (the computational error in Table 1 is thought not to exceed $\frac{1}{4}$ per cent). It is easily shown that this parameter c/d is equal to $(2 - r)\,\alpha/r$.

Vol. 1 1952/5

Mech. Tool.
1
2/53

TABLE I

α	5°		10°		15°		20°		25°		30°	
	r	$t/2k.\ln\left(\frac{1}{1-r}\right)$	r	$t/2k.\ln\left(\frac{1}{1-r}\right)$	r	$t/2k.\ln\left(\frac{1}{1-r}\right)$	r	$t/2k.\ln\left(\frac{1}{1-r}\right)$	r	$t/2k.\ln\left(\frac{1}{1-r}\right)$	r	$t/2k.\ln\left(\frac{1}{1-r}\right)$
	0·022	2·43	0·043	2·48	0·068	2·40	0·094	2·35	0·123	2·28	0·152	2·22
	0·038	1·89	0·071	1·92	0·111	1·86	0·121	2·06	0·159	1·98	0·200	1·91
	0·057	1·48	0·104	1·55	0·162	1·49	0·155	1·79	0·203	1·72	0·254	1·66
	0·074	1·30	0·133	1·35	0·207	1·29	0·199	1·55	0·258	1·48	0·320	1·43
	0·097	1·13	0·173	1·17	0·265	1·13	0·252	1·34	0·325	1·28	0·359	1·33
	0·110	1·07	0·225	1·05	0·300	1·07	0·319	1·17	0·364	1·20	0·401	1·24
	0·127	1·04	0·258	1·02	0·341	1·03	0·360	1·10	0·409	1·13	0·448	1·16
	0·148	1·00	0·294	1·00	0·384	1·01	0·406	1·05	0·458	1·07	0·500	1·10
	0·172	1·00	0·330	1·01	0·427	1·01						
	0·276	1·00	0·456	1·01	0·467	1·02						
	0·312	1·00	0·501	1·00	0·582	1·02						
			0·544	1·01	0·627	1·01						

Suppose, now, that the die angle is indefinitely reduced. In the limit there is obtained a stress field in the plastically-deforming material which is identical with that in a strip of thickness c indented by an opposed pair of flat dies of width d. The solution of this problem when $c/d \geqslant 1$ has been given by HILL (1947 and 1950, p. 257) and when $c/d \leqslant 1$ by GREEN (1951b). Table 2 shows the calculated indentation pressures p at the yield point divided by $2k$, the yield stress in homogeneous plane compression.* If the previously-mentioned functional relation could legitimately be extrapolated to vanishingly small die-angles it

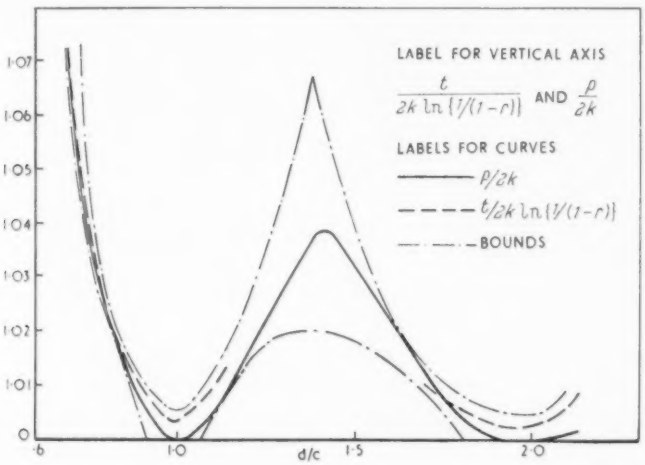

Fig. 2.

TABLE II

$p/2k$	c/d	$p/2k$	c/d	$p/2k$	c/d
2·57	8·72	1·43	2·75	1·03	0·77
2·48	8·04	1·32	2·35	1·04	0·72
2·31	6·88	1·22	2·01	1·04	0·71
2·14	5·90	1·13	1·71	1·04	0·69
1·98	5·06	1·06	1·45	1·03	0·65
1·83	4·34	1·02	1·21	1·01	0·58
1·69	3·73	1·00	1·00	1·00	0·50
1·55	3·20	1·01	0·86		

should be found to be identical with that in Table 2. This is indeed so, within the limits of variation stated. In the range where an exact theory is not available we appeal to the bounds referred to earlier; Fig. 2 illustrates this in the case of a 20° total angle.

We have thereby obtained a suggestive correlation between the respective redundant works in drawing and indenting. Moreover, to an accuracy sufficient

* FORD and WATTS (1952) have shown that the indentation pressures for work-hardened copper and brass are in excellent agreement with these theoretical values.

for practical purposes, interpolation of Table 2 with respect to the c/d ratio can be used in preference to the difficult interpolation of Table 1 with respect to the die angle and reduction simultaneously.

It should perhaps be emphasized that whereas the indentation pressure p is exactly $2k$ whenever d/c is integral, the redundant work in drawing appears never to be exactly zero ; it does, however, pass through successive minima near integral d/c values. The upper bounds to the unknown exact values show that the amplitudes of the oscillations when $d/c > 1$ decrease, probably steadily, both for drawing and indenting, and that the peaks probably occur near $d/c = \sqrt{\{n(n+1)\}}$, $n = 1, 2, \ldots$.

Equation (1) for the bulge limit may also be extrapolated to zero die angle. The " bulge limit " for indenting occurs when $c/d = 8{\cdot}72$, and hence $r/\alpha \to 2d/c = 0{\cdot}230$ when $\alpha \to 0$, which agrees with (1).

3. Pressure Distribution over the Die

Some typical distributions of pressure on the die, for a total angle 10°, are shown in Fig. 3, together with the Sachs distribution for comparison (broken curves).

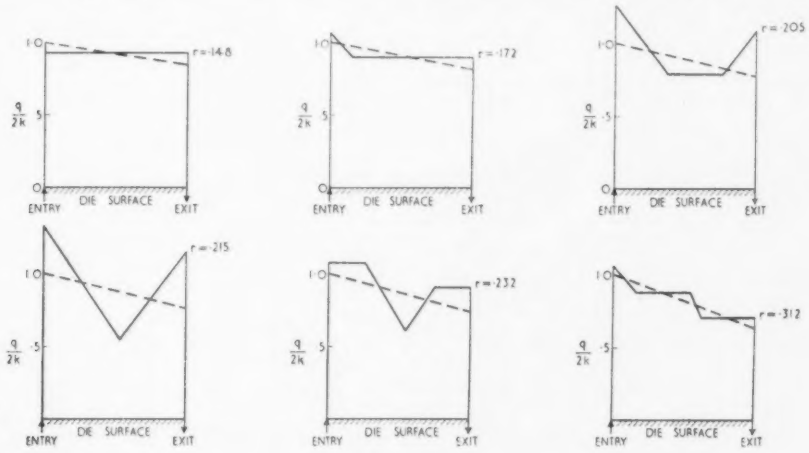

Fig. 3.

The latter is defined by $q/2k = 1 + \ln(1 - x)$ where x is the reduction up to the point under consideration. The local Sachs pressure is thus independent of the total reduction and the die angle α, in contrast to the exact value which depends on both these quantities.

In the range (1) the pressure on the die is distributed uniformly, its value being equal to $t(1 - r)/r$. In the range (2) the pressure falls steadily in a certain region near the entry but becomes uniform towards the exit. In range (3), which is in the neighbourhood of $d/c = 2$, there are two uniform regions and two steps down towards the exit ; in the neighbourhood of $d/c = 3$ there would be three uniform regions and three steps, and so on. Between (2) and (3) where no exact calculations are available, the pressure distributions shown are approximations ; the pressure falls near the entry, rises a smaller amount towards the exit and may be uniform either in the centre or at the entry and exit.

4. DRAWING STRESS FOR A ROUGH DIE

The exact theory for drawing through a rough die was also given by HILL and TUPPER in the ranges corresponding to (1), (2), and (3); numerical results were given for the highest reduction at which the plastically-deforming zone intersects the axis in a single point, for half-angles between 5° and 30°. The present calculations are for all lower reductions down to the bulge limit, for half-angles between 5° and 15°. Owing to the considerable difficulties of computation the numerical error is several times greater than it is when the die is smooth. We do not therefore consider it is worthwhile to quote the results individually; but instead we express them collectively in an empirical formula which is believed to be not more than 1 per cent in error. If t is the drawing stress for a smooth die (Table 1), and t' that for the same die when the coefficient of friction is μ, the formula is

$$\frac{t'}{t} = (1 + \mu \cot \alpha) - \mu\,(0{\cdot}2 + 0{\cdot}08\, r \cot^2 \alpha). \tag{4}$$

This has been fitted to calculations in a range approximately given by (1) when the half angle is between 5° and 15° and $\mu \leqslant 0{\cdot}15$; extrapolation is not advisable. If q and q' are the corresponding pressures on the die (uniformly distributed in this range),

$$\frac{q'}{q} = 1 - \frac{\mu\,(0{\cdot}2 + 0{\cdot}08\, r \cot^2 \alpha)}{1 + \mu \cot \alpha}. \tag{5}$$

The second terms on the right-hand sides of these equations are the corrections to HILL and TUPPER's suggested rough approximations $t'/t \sim 1 + \mu \cot \alpha$ and $q'/q \sim 1$.

ACKNOWLEDGMENT

We are grateful to the Director, *The British Iron & Steel Research Association*, for permission to quote material from restricted reports.

REFERENCES

COOK, P. M. and WISTREICH, J. G.	1952	*Brit. J. App. Phys.*, **3**, 159.
FORD, H. and WATTS, A. B.	1952	British Iron & Steel Research Association Report MW/B/8/52, to be published in *Proc. Inst. Mech. Eng.*
GREEN, A. P.	1951a	*Phil. Mag.*, **42**, 365;
	1951b	*Phil. Mag.*, **42**, 900;
	1952	British Iron & Steel Research Association Report MW/B/7/52.
HILL, R.	1947	*J. Iron & Steel Inst.*, **156**, 513;
	1950	*Mathematical Theory of Plasticity* (Clarendon Press, Oxford);
	1951	*Phil. Mag.*, **42**, 868.
HILL, R. and TUPPER, S. J.	1948	*J. Iron & Steel Inst.*, **159**, 353.
WISTREICH, J. G.	1951	British Iron and Steel Research Association Report MW/D/53/51 (to be published).

Journal of the Mechanics and Physics of Solids, 1952, Vol. 1, pp. 37 to 52. Pergamon Press Ltd., London.

RHEOLOGY OF METALS AT ELEVATED TEMPERATURES

By A. E. Johnson and N. E. Frost
Mechanical Engineering Research Laboratory, East Kilbride

(*Received 20th. June*, 1952)

Summary

An account is given of the outline and progress of an examination of the general stress, time, and temperature dependence of the creep, plastic strain, and relaxation properties of several metals and metallic alloys, which, while being typical practical engineering materials, are different in their basic structures. The temperature range examined for each of these materials has been in each case chosen as the practical temperature range of use at elevated temperatures in actual engineering practice.

The work involves simple tensile, torsion, and combined stress creep tests, and similar varieties of short period plastic strain tests and relaxation tests.

The results, so far obtained in the work, and the inferences drawn from them, are discussed in relation to such appropriate theory as has currently been advanced, and in several cases it has been possible to suggest relations modifying or replacing those implicit in such theory.

ol.
1
2/53

1. Introduction

In the past twenty or thirty years the rheology of time-independent plastic strain of engineering metals at room temperature has been the subject of considerable research. In contrast the investigation of the rheology of such metals at relatively elevated temperatures, where both time-independent strain, time-dependent or creep strain, and related relaxation and recovery phenomena occur has largely been restricted to pure tension or sometimes pure torsion creep tests, little data being available for the case of general stress systems. Also, while considerable speculation has been made concerning the physical principles underlying the mechanism of creep, it still appears to be a fact that even in the case of the pure tensile or torsion creep tests insufficient data of a type necessary to afford a really searching test of the validity of such theories is available.

A few years ago with much the above views in mind a programme of work was commenced at the National Physical Laboratory* in which it was the intention to make a thorough examination of the general stress, time and temperature dependences of several metals or metallic alloys which, while being typical practical engineering metals, were different in their basic structures and therefore presumably likely to allow the maximum divergence of behaviour. The temperature range examined for each of these materials was in each case chosen as the practical range of use of the materials at high temperatures in actual engineering practice.

In detail the programme has and will involve simple tensile, torsion, and combined tension and torsion creep tests, similar varieties of short period plastic

* Now continuing at the Mechanical Engineering Research Laboratory, East Kilbride.

strain tests (the degree of strain in general being limited to that occurring in the initial stages of normal creep tests), and finally similar varieties of relaxation tests.

The following paragraphs indicate briefly the various aspects of the work performed or contemplated, and also discuss the nature of and inferences from the results so far obtained.

2. MATERIALS CHOSEN FOR INVESTIGATION

The basic materials used in the research have been a 0·17 per cent C steel (of body-centred cubic lattice) an RR 59 type aluminium alloy (of face centred cubic lattice), and a magnesium alloy containing 2 per cent of aluminium (of close-packed hexagonal lattice); the respective temperature ranges of investigation being (apart from some individual tests) 350 to 550°C, 20 to 250°C and 20 to 150°C. Additionally limited series of tests have been made on selected materials (e.g. Nimonic 75 alloy, 0·5 per cent Mo steel or pure copper) for specific purposes.

In preparing the above mentioned materials for the work, great care has been taken to obtain the materials in an isotropic condition as regards creep and plastic strain properties by means of suitable mechanical and heat treatments. The test pieces used in the great majority of cases have been of a thin walled tubular type of 2 inches effective gauge length and a wall thickness of 0·02 to 0·03 inch, the grain size of the material being regulated to about six grains to the wall thickness. Recent work has involved tubular specimens of wall thickness 0·0625 inch, and of effective gauge length 8 inches, and also short compression specimens 0·25 inch diameter and 1 inch in length.

3. COMBINED-STRESS CREEP TESTS UNDER CONSTANT LOADING SYSTEMS

The initial work has largely been devoted to combined tension and torsion creep tests. Such tests have been taken as satisfactorily representing the general stress behaviour of metals at normal stresses and temperatures, on the assumption that an imposed hydrostatic stress of magnitude comparable to the stresses used in the creep tests would make no difference to the magnitude of creep occurring, and that tensile and compression creep at corresponding stresses and temperatures are similar in magnitude.

The former assumption has actually been tested experimentally by comparison of the creep of a tubular specimen of magnesium alloy at 20°C under several systems of combined tension and torsion, and the creep of a thin plate of similar material under biaxial tensile stress equivalent in principal stress system to the tension and torsion test apart from the addition or subtraction of a hydrostatic stress. Very close agreement between the two sets of principal creep rates was obtained indicating the validity of the principle in question. The second assumption has been based upon previous experience of the various materials used by the authors but it is intended to make an explicit check in the case of the materials used in the current research, and a compression creep machine (Fig. 1) has been designed and constructed for this purpose among others.

On the above mentioned bases, suggested rheological equations for combined stress creep have in the past been of the St. Venant-Mises type $C_i = F(J_2)(S_i)$ etc. ($i = 1, 2, 3$) where C_i is the creep rate at a given period and where J_2, S_i are

Vol. 1 1952/5

the second order invariant and stress deviator* of the system, and F denotes some function. More general expressions equally useful for both creep and plastic strain have been suggested by PRAGER and REINER and take the form for creep of

$$C_i = f(J_2, J_3)\left[p(J_2, J_3^2)\, J_3 (S_i^2 - 2/3\, J_2\, I) + q(J_2, J_3^2)\, S_i\right]$$

where C_i, etc. are principal values of the creep rate tensor, S_i etc. principal values of the stress deviator tensor, $J_2 = \frac{1}{2}(\Sigma S_i^2)$, $J_3 = \frac{1}{3}(\Sigma S_i^3)$, p and q are polynominals in J_2 and J_3, and I is the unit tensor.

BAILEY has maintained that certain tests of his making are not capable of representation by the St. Venant-Mises equation, and he has used the form

$$C_i = F(J_2)\left[(\sigma_i - \sigma_j)^n - (\sigma_k - \sigma_i)^n\right]$$

the creep being considered to be a function of slip on planes other than those of maximum shear stress (σ_i are the principal stresses).

In this connection it is to be noted that it may be shown on purely theoretical grounds that if the creep relations of a material obey the Mises criterion of plastic strain (indicated by the $F(J_2)$), and are also isotropic, then n in BAILEY's equation must be unity providing the relations involve power terms at all. Thus before accepting the validity of any results indicating a departure from the simple St. Venant-Mises relation it is necessary to make sure that this departure is not merely due to the occurrence of anisotropy. The degree of isotropy attained in all materials used in the author's tests made it virtually certain that this factor would not mask the true value of any results obtained.

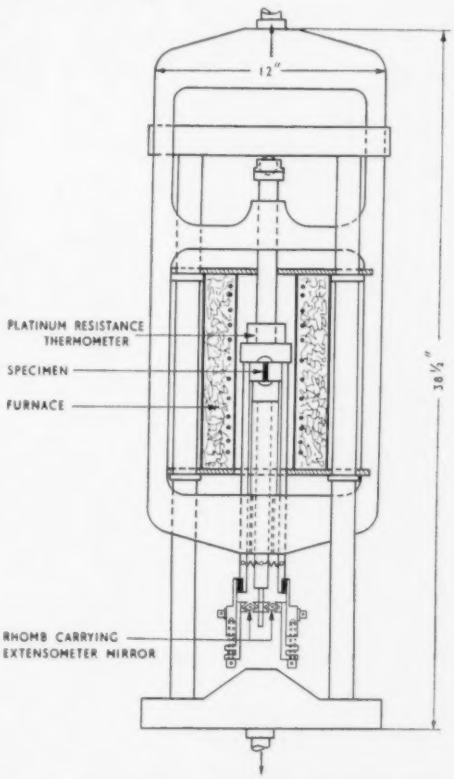

Fig. 1 Apparatus for compression creep tests on small specimens.

A series of results of tests on 0·17 per cent C steel at 350, 450 and 550°C on RR59 alloy at 150 and 200°C, magnesium alloy at 20 and 50°C, and Nimonic 75 at 550 and 600°C are summarised in Figs. 2 and 3. Here the octahedral stress is plotted against the octahedral creep rate, this constituting a direct check of the application of the Mises criterion. Obviously all points are closely disposed about a common curve indicating a close adherence to the Mises criterion. The other prominent feature of the figures is that in all cases the curve is comprised of two distinct portions; at lower and moderate stresses the curve is linear, such

* $S_i = (\sigma_i - \frac{1}{3}\Sigma\sigma_i)$.

portions of the curve for all materials being well represented by the St. Venant-Mises type of equation

$$C_i = [A\,(J_2)^p]\,S_i\,;$$

p lying between the values 0 and 1 for the quite wide range of materials and temperatures concerned. As regards time dependence it was found that for all materials and temperatures over a quite wide stress range the curves could be represented by simply affixing a function of time to the above equation ; in other words the curves were geometrically similar.

At higher stresses the curved portion of the characteristic curve required a more complex representation than is given by the above equation. In all materials anisotropy occurs at some stage in this stress range although, in one or two cases, isotropy is preserved to quite high stress levels. Further, the simple power function

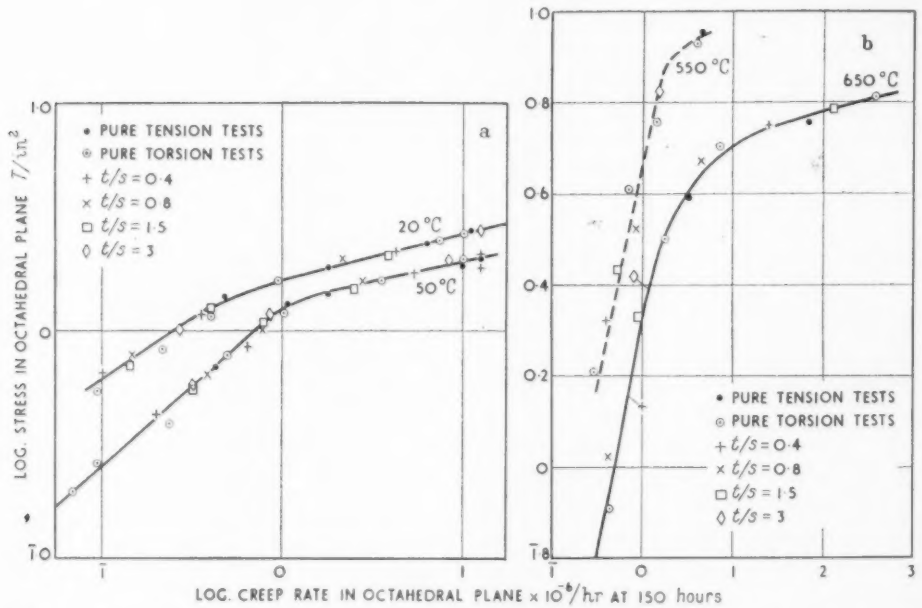

Fig. 2. Complex stress creep tests on various materials. (a) Magnesium alloy at 20°C and 50°C. (b) Nimonic 75 at 650°C and 550°C.

of J_2 becomes a multiple power function, the physical significance of which is yet to be fully understood.

Evidently, therefore, the representative equation appears to be a generalized St. Venant-Mises or a simplified Prager-Reiner equation.

With the exception of the carbon steel (where apparent metallurgical changes obscure the nature of the anisotropy) all anisotropy may be represented by general equations of type

$$C_i = F\,(J_2)\,[A_{ij}\,(\sigma_i - \sigma_j) - A_{ki}\,(\sigma_k - \sigma_i)] \quad \text{etc.}$$

where A_{ij} etc. are anisotropy coefficients. Actually, three differing anisotropy coefficients were only needed in the case of carbon steel at 450°C. In all other

cases except the magnesium alloy at 50°C, $A_{12} = A_{31}$, and the tubes apparently exhibit a considerable change of diameter, but not of wall thickness, the major principal creep being as in the case of complete isotropy. The value of A_{23} depends upon the stress system. The direction is that of major principal stress.

At 50°C for the magnesium alloy the reverse is true, A_{23} is unity and A_{12} and A_{31} have values depending on the stress system, but always such as to make

$$A_{12}(\sigma_1 - \sigma_2) - A_{31}(\sigma_3 - \sigma_1) \equiv (\sigma_1 - \sigma_2) - (\sigma_3 - \sigma_1)$$

The major principal stress creep is as in the case of isotropy, but a change of wall thickness and not of diameter is noted in the tubes. This disparity between the mechanisms of deformation of the magnesium alloy at the two temperatures of 20 and 50°C is in line with marked differences in mechanical working properties which have been noted for this material at these temperatures.

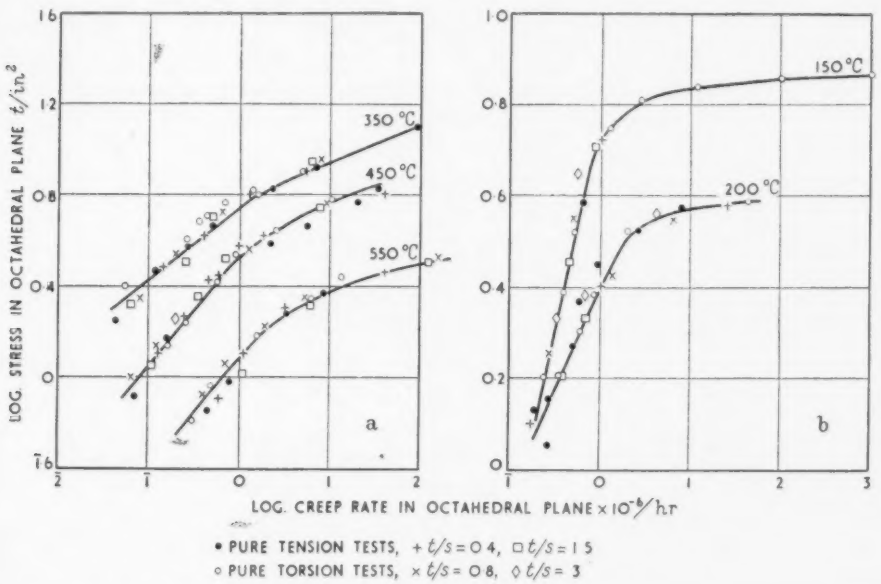

Fig. 3 Complex stress creep tests on various materials. Relations between log. stress and log. creep rate in the octahedral plane. (a) 0.17%C. steel at 350, 450 and 550°C. (b) Aluminium alloy at 150 and 200°C.

Evidently in general the anisotropy arising in these materials is of quite a complex nature, but is fortunately confined to stresses that are usually in excess of those which would be imposed by designers.

4. Combined-Stress Creep Tests under Variable Systems of Loading

Since engineering materials used at elevated temperatures may, preparatory to their use under a given system of complex stresses, be subjected to prestrain in preferential directions, or in the course of their use be subjected to a series of changed combined stress systems, it has been decided to investigate the

modification in the characteristic equations necessary to render them applicable to the case of prestrained material, or material subject to changing combined stress conditions.

Obviously a programme such as this will eventually involve a considerable volume of work, but in commencement a series of tests have been made upon magnesium alloy specimens at 20° C, these specimens having previously been the subject of creep tests in pure tension or pure torsion. Upon the results of this series of tests the framing of a major programme of work will depend. However, these preliminary tests have given several interesting indications.

Since the Mises criterion undoubtedly holds for simple loading, it might be thought that in a test in which the ratio of tension to torsion load was changed several times, the octahedral stress being maintained constant, the creep curve of octahedral strain would be continuous throughout the series of tests. Such however proved not to be the case, and evidently the $F(J_2)$ term of constant loading characteristics is subjected to modification by the degree of strain involved. However it has been found for this material and temperature that whatever the changes of loading system made (whether the same octahedral stress was maintained or not) the geometrical curve with respect to time was similar to that of the virgin material under constant loading conditions, and further that anisotropy (where produced) was similar to that occurring in the virgin material although the magnitude of the anisotropy coefficients was altered. An indication was also given that at lower stresses where isotropy was preserved modification of the $F(J_2)$ term for simple loading could be approximately represented for moderately small strains by the subtraction of a constant from the term, while at higher stresses and strains the modification might be proportional to $\sqrt{I_2}$, the second invariant of total strain. The above facts suggest a possible general equation of the type

$$C_i = [F(J_2) - (A + B\sqrt{I_2})]\,[A_{ij}(\sigma_i - \sigma_j) - A_{ki}(\sigma_k - \sigma_i)]\,f(t)$$

where A_{ij}, A_{ki}, A_{jk}, are modified anisotropy coefficients, A_{ij} and A_{ki} being unity for this material, and where $f(t)$ represents the time function appropriate to the material in the virgin condition. At low or moderate stresses this equation reduces to

$$C_i = [F(J_2) - A]\,[S_i]\,f(t).$$

However, the above indications are based upon only a few tests, and the major programme ahead may not confirm them.

5. Fracture after Creep under Combined Stress

It is hoped, for all materials, to investigate the criterion of fracture after creep under combined stress, although instability of specimens in the final stages of fracture may only make this possible for one or two materials.

However, an opportunity has occurred to examine the creep-fracture characteristics of a 0·5 per cent Mo steel which was particularly prone in certain temperature ranges to intercrystalline fracture, and the results obtained for this material, although unlikely to be typical of the materials used in the major programme, are worth noting.

The tests arose out of the consideration of a paper by W. Siegfried published

Vol. 1 1952/5

in 1943 which dealt with the creep failure of metals as influenced by general stress systems, over ranges of temperatures both above and below the so-called " equicohesive " temperature defined as that temperature below which fracture in creep is purely transcrystalline and above which it is intercrystalline depending in each case upon the supposed relative strength of crystal and boundary material. He suggested that below the equicohesive temperature the period to fracture depended upon the maximum stress deviator portion of the imposed stress system, while above the equicohesive temperature the period to fracture depended upon the hydrostatic component of that system, regarded as causing the fracture of boundaries. General experience suggested that SIEGFRIED's proposition should be modified in as much as that for any particular material and temperature the fracture occurring may not be wholly trans- or intercrystalline, but partly both. To check the theory tests were made at such a temperature and in such a stress range as gave virtually entirely intercrystalline failure in pure tensile creep.

The tests consisted of a pure tension test, a pure torsion test, and three tests in which the ratio of tension to torsion stress was respectively in the ratios 9:1, 9:5, and 1 to 2.

The SIEGFRIED theory would appear to suggest that the torsion-test fracture would be entirely transcrystalline. The two tests with stress ratios 9 to 1 and 9 to 5 had the same tension stress, and accordingly the same hydrostatic stress $= \frac{1}{3} \times$ tension stress. Thus, according to SIEGFRIED, in an intercrystalline range the two tests should have fractured in identical periods whatever the value of the torsion stress applied.

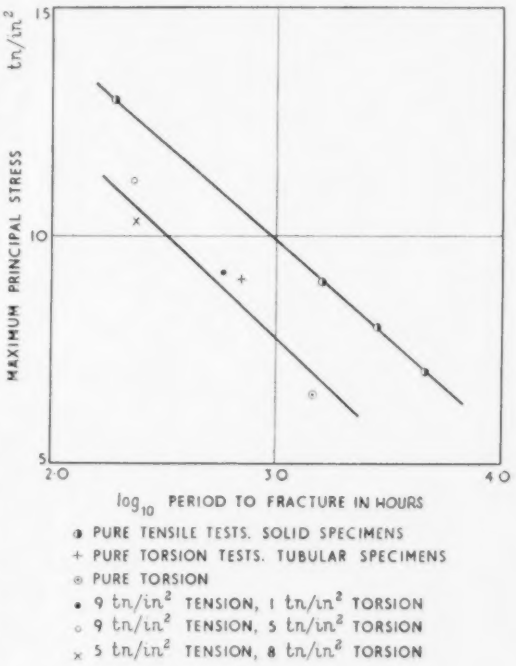

Fig. 4 Relation between maximum principal stress and log. period of fracture.

Actually the results of the tests indicated that, while fracture in the pure torsion creep test was transcrystalline, no other evidence in favour of the Siegfried hypothesis arose. The two tests of similar tensile stress fractured in quite dissimilar periods, and with quite differing fractures.

A criterion of failure was sought, and it became evident that for this material at this particular temperature the criterion was closely that of maximum principal stress. This is illustrated by Fig. 4. The actual relation was expressed by the equation $\log P = A - B\sigma_1$, where P is the period to fracture and σ_1 is the maximum principal stress.

6. TIME AND TEMPERATURE DEPENDENCE OF CREEP

For each of the basic materials concerned in this programme it is intended to examine the time and temperature dependence of the material; the former by a series of torsion creep tests carried either to fracture or the tertiary region, or into the secondary region for prolonged periods, at one or two chosen temperatures, and the latter by torsion creep tests of a moderate length at close intervals of temperature over the working range. It is thus hoped that sufficient data will be accumulated to provide reliable evidence to complete the general stress, time, and temperature relations for the materials in question.

At the moment, the temperature and time dependence tests of the aluminium alloy RR 59 have been completed, but whereas the former set of tests has been adequately analysed, the latter has not and will not be commented upon.

The temperature dependence tests were made at a common stress of 2 tons per sq. in. and 50°C intervals between 20 and 250°C. An additional test was also made at 300°C, but this lasted only a few hours, and analysis indicated immediately that the distortion was of a different character from that in the other tests. Creep recovery was measured at the completion of each forward creep test.

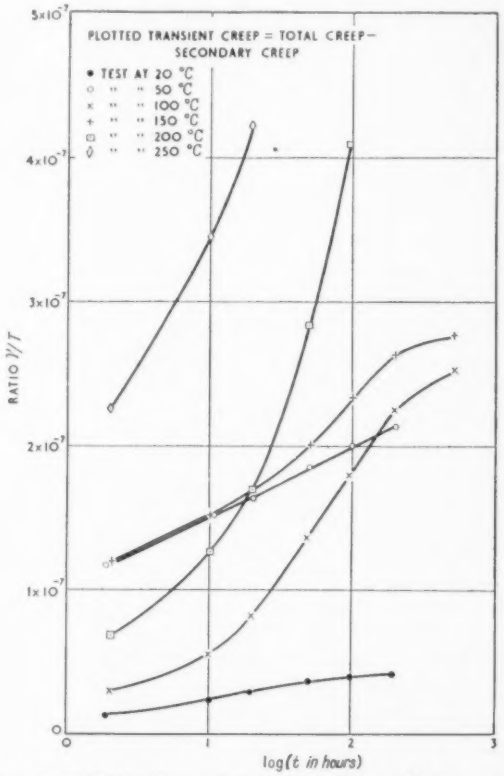

Fig. 5. R.R.59 Alloy. Application of SMITH's theory to transient creep in temperature range 20-250°C.

Comparison of the test data was made with the current physical theories for primary and steady stage creep, and with the semi-empirical theories such as that of Andrade; and of the recoverable creep with anelastic and superposition theory. Additionally, in view of the "phenomenological" equations put forward by LUBAHN, HOLLOMON, GRAHAM and others, an examination was made of the possibility of framing a phenomenological equation from the results. The comparison did not give very encouraging results from the point of view of current theories. The primary creep equations of MOTT and NABARRO, OROWAN, and SMITH (Fig. 5), although generalised where possible, did not adequately represent this stage of creep. The steady state equations of NOWICK, and MACHLIN, KAUZMAN, and FELTHAM (Fig. 6) based upon the Eyring rate process theory did appear to

agree with the asymptotic secondary creep rates measured up to a temperature of 200°C, above which temperature an abrupt discontinuity occurred, possibly due to complete change of creep mechanism. The ANDRADE equation represented the results only at the highest temperatures. The superposition theories of BOLTZMAN, BECKER, and BENNEWITZ did not adequately represent the recoverable creep.

In the face of the above negative evidence it was necessary to examine the data *ab initio*, to see whether any basis could be found for a general equation which might possibly form the basis for physical analysis. It was found that the creep curves at all temperatures corresponded with the relation

$$\epsilon = A\,t^{M_1} + B\,t^{M_2}$$

where t is time, and the first term represents recoverable creep and the second term irrecoverable creep, M_1 and M_2 both being fractional. M_1 is approximately constant with temperature. The detailed results are given in Table 1. Up to 150°C it was possible to form some sort of "phenomenological" equation, M_2 having the form $(DT - C)$ where T is absolute temperature and D and C are constants, but it appeared impossible to do so beyond this temperature.

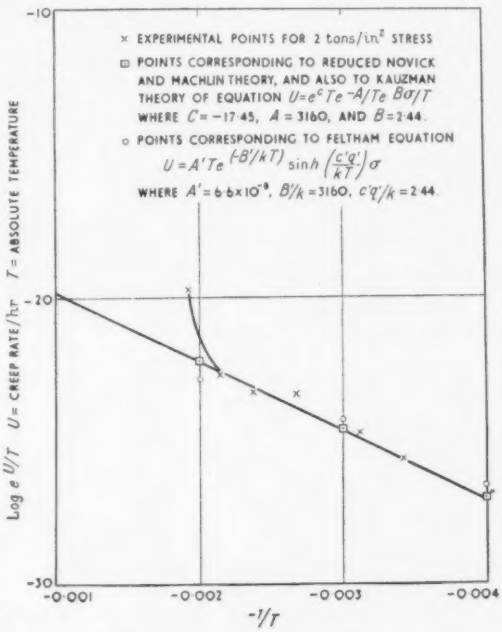
× EXPERIMENTAL POINTS FOR 2 tons/in.² STRESS
□ POINTS CORRESPONDING TO REDUCED NOVICK AND MACHLIN THEORY, AND ALSO TO KAUZMAN THEORY OF EQUATION $U=e^{C}Te^{-A/Te}B\sigma/T$ WHERE $C=-17{\cdot}45$, $A=3160$, AND $B=2{\cdot}44$.
○ POINTS CORRESPONDING TO FELTHAM EQUATION
$U=A'Te^{(-B'/kT)}\sinh\left(\frac{c'q'}{kT}\right)\sigma$
WHERE $A'=6{\cdot}6\times10^{-8}$, $B'/k=3160$, $c'q'/k=2{\cdot}44$.
Log e U/T U = CREEP RATE/hr T = ABSOLUTE TEMPERATURE
-10
-20
-30
-0·001
-0·002
-0·003
-0·004
-1/T

Fig. 6 R.R.59 Alloy. Application of various theories to secondary creep in the temperature range 20-250°C.

TABLE I

RR 59 Alloy

Equations for Creep and Recovery at 20–250°C

(*t* represents time in hours from the commencement of the creep and recovery tests)

Temperature	*Equation of curve of total forward creep less recoverable creep*	*Equation of creep recovery curve (excluding initial elastic strain*)*	*Equation of total forward creep curve*
20	All creep recoverable	*$0{\cdot}0000038\ t^{0{\cdot}28}$	$0{\cdot}0000038\ t^{0{\cdot}26}$
50	$0{\cdot}000038\ t^{0{\cdot}055}$	$0{\cdot}0000029\ t^{0{\cdot}36}$	$0{\cdot}000038\ t^{0{\cdot}055} + 0{\cdot}0000029\ t^{0{\cdot}36}$
100	$0{\cdot}000041\ t^{0{\cdot}10}$	$0{\cdot}0000029\ t^{0{\cdot}285}$	$0{\cdot}000041\ t^{0{\cdot}10} + 0{\cdot}0000029\ t^{0{\cdot}285}$
150	$0{\cdot}000031\ t^{0{\cdot}175}$	$0{\cdot}0000061\ t^{0{\cdot}34}$	$0{\cdot}000031\ t^{0{\cdot}175} + 0{\cdot}0000061\ t^{0{\cdot}34}$
200	$0{\cdot}00001\ t^{0{\cdot}44}$	$0{\cdot}000021\ t^{0{\cdot}27}$	$0{\cdot}00001\ t^{0{\cdot}44} + 0{\cdot}000021\ t^{0{\cdot}27}$
250	$0{\cdot}0000083\ t^{0{\cdot}75}$	$0{\cdot}000052\ t^{0{\cdot}22}$	$0{\cdot}0000083\ t^{0{\cdot}75} + 0{\cdot}000052\ t^{0{\cdot}22}$

* These terms acquire maximum values at the end of transient creep.

Now, considering the above equation, the inference seems to be that for this material primary and secondary stages of creep share a common mechanism. Such a suggestion has previously been made by ZENER. If the general idea that the diminishing creep rate is due to a gradual rise of the value of activation stress during strain hardening, and its converse (applied to tertiary creep) that a lowering of the value of activation stress occurs with time as thermal softening occurs, it seems possible that in view of the above results the whole creep curve might reasonably be represented by an equation $\epsilon = At^{M_1} + Bt^{M_2} + Ct^N$ where N is a number greater than unity, the value of C being chosen to make the third term negligible during primary creep. Actually in the case of 0·5 per cent molybdenum steel previously mentioned a third term of ϵ^{tN} appeared to be necessary. However it is hoped that since similarity in curve form has been indicated in the temperature-dependence tests the time-dependence tests at selected temperatures will indicate the nature of the time term corresponding to tertiary creep.

It is perhaps possible to suggest that for a simple stress system the whole creep field at a specific temperature may be represented by an equation of the general type

$$\epsilon = [ASt^{M_1}] + [A_1 S^{N_1} + A_2 S^{N_2} + -][Bt^{M_2} + B_3 t^{M_3} + B_4 t^{M_4} + -]$$

where the coefficients are chosen to simulate the various features of the creep field at high and low stresses and times. The first bracketed term represents purely anelastic strain.

Vol. 1 1952/5

7. RELAXATION AND ITS RELATION TO CREEP

The examination of relaxation under general stress conditions is of course one of the major objectives of the programme of research, but it is intended for reasons given below to leave this aspect of the work for the time being.

A considerable number of papers have been published in which relaxation equations have been derived from chosen creep equations using either the so-called "time-hardening" or "strain hardening" theories as a link between the two varieties of equation. The relaxation concerned of course relates to plastic creep strain as opposed to anelastic strain.

However, work some years ago by one of the authors on a carbon steel, and on a chromium molybdenum bolt steel, convinced him that neither of these theories constituted an adequate link between creep and relaxation data. This fact appeared to be bound up with the composite nature of the creep and relaxation concerned, and the part played by initial plastic strain in modifying the order of creep in the relaxation tests. It was decided therefore as a preliminary to undertaking the combined stress relaxation work to make some attempt under simple loading conditions to determine, for a chosen material (RR59 alloy), the relations between creep, recovery and relaxation, commencing at very low stresses where the relation was presumably entirely anelastic, and proceeding through the stress range where the creep occurring in both creep and relaxation tests was not associated with any appreciable degree of initial plastic strain, to a stress level at which the plastic strain became relatively heavy. In this way it is hoped that the effects of the factors concerned may be separated from each other, and a basis derived for framing the combined stress relaxation programme.

Accordingly a torsion creep machine was constructed* capable of measuring creep rates of the order of 10^{-9}/hour at correspondingly low stresses and of being used in creep recovery and relaxation tests. Using this machine a group of tests is being made on the RR59 alloy at 50°C following the lines indicated above. The initial results obtained have been most encouraging. At creep rates of the order 10^{-8} to 10^{-9}/hour the creep curve form has been found to be of the type $\epsilon_c = AS + BSt^{1/M_2}$ where A is a constant and the term AS representing time independent plastic strain, and the term BSt^{1/M_2} representing recoverable creep strain. The recovery curve was represented completely by the relation $\epsilon_r = Bst^{1/M_2}$, while the creep equivalent curve of the relaxation curve was given precisely by the relation $\epsilon = AS + BSt^{1/M_2}$ as in the case of the forward creep curve. Thus at rates of this order the three phenomena are simply related. Raising of the stress level will show the effects of the incidence of normal plastic creep strain, and also of initial plastic strain, it is hoped.

If and when the above tests clarify the relations between creep and relaxation sufficiently, the matter of combined stress relaxation will be taken up.

8. Time-Independent Plastic Strain at Elevated Temperatures, under Constant Loading Conditions

In the present context interest in plastic strain, stress, and temperature relations largely arises from the fact that appreciable time independent plastic strain is frequently associated with the early stages of the creep tests ; but from a practical point of view interest is limited to initial plastic strains of the order of 1 or 2 per cent only as a maximum. Accordingly a combined tension and torsion machine has been constructed, capable of making incremental short time tests in pure tension, pure torsion, and any reasonable combination of these†.

For each of the basic materials concerned in this work comparison is to be made with the theoretical equations normally suggested at room temperature for stress plastic strain relations, where possible both deformation and incremental theories, and the various theories associated with the build up of macroscopical strain from the consideration of microscopic slip being examined. When the whole of the data for the group of basic materials is available the possibility of building up a new version of the latter type of theory from the data will be considered if no existing theory is satisfactory.

At the time of writing a series of tests has been completed on the magnesium alloy at 20, 50, 100, and 150°C. These were in all cases tests at constant stress ratio. Difficulties associated with the marked tendency of this material to creep precluded any possibility of examining the relative application of deformation and incremental theories in this particular case.

The tests at 20°C and 150°C comprised pure tension, pure torsion, and combinations of tension and torsion approximately in the ratios $t/s = 0{\cdot}2$, $0{\cdot}5$, 1 and 3, while the tests at 50 and 100°C were limited to the one system $t/s = 1$ (s = shear stress).

It was found that at all temperatures the material obeyed the Mises rather that the maximum shear stress criterion of plastic strain. Up to 100°C the material

* See Johnson, A. E., 1950, *J. Sci. Instrum.*, **27**, 70.

† See Pollard, H. V. and Tapsell, H. J., 1951, *Engineering*, **171**, 58.

remained virtually isotropic up to strains of the order 2 per cent, and the results up to this temperature were well represented by an equation of the type

$$\epsilon_i = F(J_2)\, S_i,$$

where $F(J_2)$ was of the form $A\left[\Sigma(\sigma_1 - \sigma_2)^2\right]^n$, A and n varying with temperature.

At 150°C, however, the same type of anisotropy that was encountered in this material in creep at 50°C (i.e. the secondary deformation was mainly in reduction of wall thickness) made its appearance. The anisotropy constants involved, however, appeared to be linear functions of the stress invariant J_2. The general features of the stress-strain relations were again those of the St. Venant-Mises equation.

The actual equations concerned were of the type

$$\epsilon_1 \propto \left[A_{12}(\sigma_1 - \sigma_2) - A_{31}(\sigma_3 - \sigma_1)\right]$$
$$\epsilon_2 \propto \left[(\sigma_2 - \sigma_3) - A_{12}(\sigma_1 - \sigma_2)\right]$$
$$\epsilon_3 \propto \left[A_{31}(\sigma_3 - \sigma_1) - (\sigma_2 - \sigma_3)\right]$$

where A_{12} and A_{31} are of the form

$$A_{12} = B_0 - a_1\sqrt{J_2},\ A_{31} = C_0 + a_2\sqrt{J_2}$$

where J_2 is the stress invariant. a_1 and a_2 are virtually constant at all stress systems and B_0 and C_0 vary with the stress system.

In Figs. 7, 8 and 9 the plot of octahedral stress against octahedral strain is

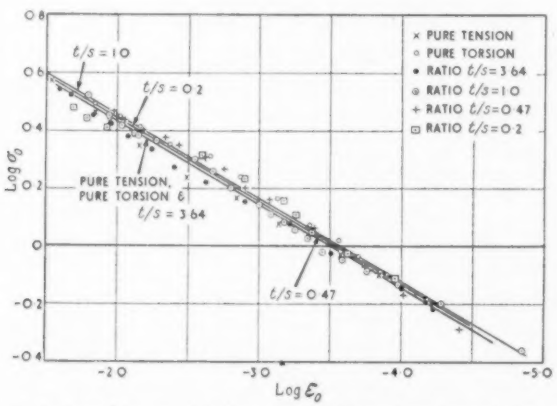

Fig. 7 Relations log. σ_0 with log. ϵ_0 at 20°C and various stress systems.

The lines shown in the diagram correspond with the equations.

$$\epsilon_1 = A\left[\Sigma(\sigma_1 - \sigma_2)^2\right]^n\left[(\sigma_1 - \sigma_2) - (\sigma_2 - \sigma_3)\right]$$
$$\epsilon_2 = A\left[\Sigma(\sigma_1 - \sigma_2)^2\right]^n\left[B(\sigma_2 - \sigma_3) - (\sigma_1 - \sigma_2)\right]$$
$$\epsilon_3 = A\left[\Sigma(\sigma_1 - \sigma_2)^2\right]^n\left[(\sigma_3 - \sigma_1) - B(\sigma_2 - \sigma_3)\right]$$

where $n = 1{\cdot}24$, $A = 3{\cdot}65 \times 10^{-6}$ and B has the following values :—
Pure tension $B = 1$, Pure torsion $B = 1$; $t/s = 0{\cdot}47$, $B = 0{\cdot}7$; $t/s = 1{\cdot}0$, $B = 2{\cdot}2$; $t/s = 3{\cdot}64$, $B = 0{\cdot}7$; and $t/s = 0{\cdot}2$, $B = 0{\cdot}8$.

σ_0 and ϵ_0 are octahedral stress and strain.

shown for the four temperatures, and the linearity of the curves gives quite convincing evidence of the adherence of the material to the simple St. Venant-Mises types of relation.

It will be recalled that the classical tests of TAYLOR and QUINNEY indicated a deviation from the equality between the Lode variables required by the Lévy-Mises equation. Their deviation has been expressed analytically by BAILEY, PRAGER, and others, the resulting expressions in several cases being exceedingly complex. With this in mind it is interesting to note that the first of the basic materials examined in the current research programme should have yielded relatively simple results in accord with the Mises equation as indeed did all these basic materials under conditions of creep. It appears not unreasonable to suggest that the TAYLOR and QUINNEY deviation might possibly be bound up with occurrence of anisotropy in specimens used.

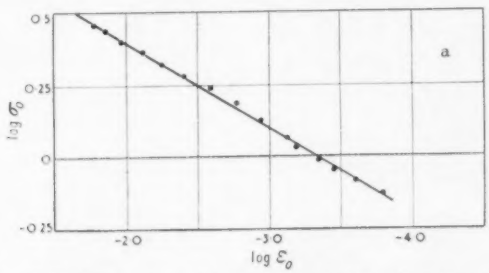

Fig. 8a Relation log. σ_0 with log. ϵ_0 at 50°C and ratio $t/s = 1{\cdot}13$.

The line shown in the diagram corresponds in principal stress relations of type.

$$\epsilon_1 = A\left[\Sigma(\sigma_1 - \sigma_2)^2\right]^n\left[(\sigma_1 - \sigma_3) - (\sigma_2 - \sigma_1)\right]$$
$$\epsilon_2 = A\left[\Sigma(\sigma_1 - \sigma_2)^2\right]^n\left[(\sigma_2 - \sigma_3) - (\sigma_1 - \sigma_2)\right]$$
$$\epsilon_3 = A\left[\Sigma(\sigma_1 - \sigma_2)^2\right]^n\left[(\sigma_3 - \sigma_1) - (\sigma_2 - \sigma_3)\right]$$

where $n = 1{\cdot}14$, $A = 6{\cdot}8 \times 10^{-6}$.

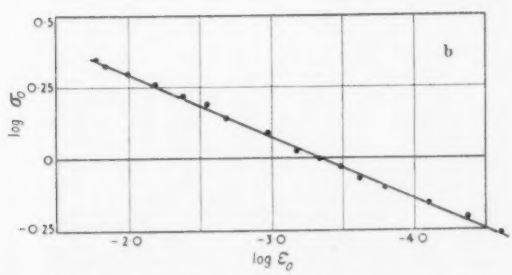

Fig. 8b Relation log. σ_0 with log. ϵ_0 at 100°C and ratio $t/s = 1{\cdot}14$.

The line shown in the diagram corresponds to principal stress relations of type.

$$\epsilon_1 = A\left[\Sigma(\sigma_1 - \sigma_2)^2\right]^n\left[(\sigma_1 - \sigma_2) - (\sigma_2 - \sigma_1)\right]$$
$$\epsilon_2 = A\left[\Sigma(\sigma_1 - \sigma_2)^2\right]^n\left[B(\sigma_2 - \sigma_3) - (\sigma_1 - \sigma_2)\right]$$
$$\epsilon_3 = A\left[\Sigma(\sigma_1 - \sigma_2)^2\right]^n\left[(\sigma_3 - \sigma_1) - B(\sigma_2 - \sigma_3)\right]$$

where $n = 1{\cdot}8$, $B = 2$, and $A = 1{\cdot}42 \times 10^{-6}$.
σ_0 and ϵ_0 are octahedral stress and strain.

In any case it will be interesting to see whether the further M.E.R.L. short time plastic strain results support the evidence in favour of adherence to the Mises criterion so far obtained.

9. Fracture at Elevated Temperatures in Short-time Plastic-strain Tests

As indicated in the previous section plastic strains beyond 2 per cent are not of interest in this programme of work. However, in carrying out a set of short time plastic strain tests on RR59 aluminium alloy (as yet incompletely analysed) at 20, 150 and 200°C, it has been found that strains of the order of 2 per cent coincided in several cases with actual fracture, this fracture being such that the section of the tubular test piece was virtually undistorted (that is from the point of view of unstable collapse) enabling evidence regarding the criterion of fracture to be put forward with some confidence. The results obtained for this material at the various temperatures are indicated in Table 2. It will be noted that the criterion appears to be between the octahedral stress, and the maximum shear stress, and is certainly not a direct function of the maximum principal stress.

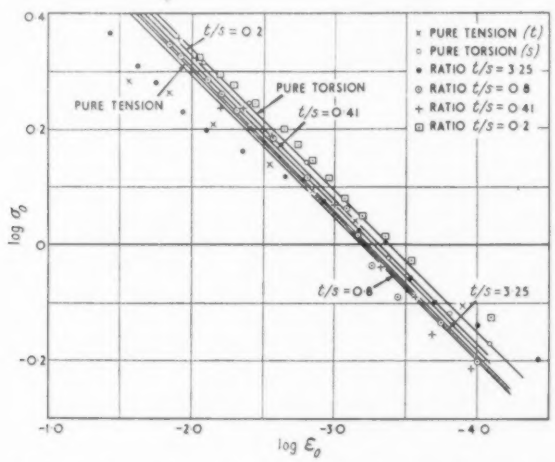

Fig. 9 Relations log. σ_0 with log. ϵ_0 at 150°C and various stress systems.

The lines shown in the diagram correspond with the equations.

$$\epsilon_1 = A\left[\Sigma(\sigma_1 - \sigma_3)^2\right]^n \left[B(\sigma_1 - \sigma_3) - C(\sigma_3 - \sigma_1)\right]$$

$$\epsilon_2 = A\left[\Sigma(\sigma_1 - \sigma_3)^2\right]^n \left[(\sigma_2 - \sigma_3) - B(\sigma_1 - \sigma_3)\right]$$

$$\epsilon_3 = A\left[\Sigma(\sigma_1 - \sigma_3)^2\right]^n \left[C(\sigma_3 - \sigma_1) - (\sigma_2 - \sigma_3)\right]$$

where $n = 1{\cdot}5$, $A = 3{\cdot}5 \times 10^{-8}$ and $B = B_0 - a_1\sqrt{J_2}$, $C = C_0 + a_2\sqrt{J_2}$.
B_0, C_0, a_1, a_2 are numerical constants.
J_2 is the second stress invariant.
σ_0 and ϵ_0 are octahedral stress and strain.

10. Generalized-loading Time-independent Plastic-strain Tests

For similar reasons to those given in Section 3, it is intended to investigate the modification in the criterion of time-independent plastic-strain necessitated by

generalized loading conditions. This knowledge will of course necessarily be complementary to the information gained in the corresponding creep tests since changes in loading system of various types may involve increased plastic strain as well as creep strain. As a preliminary to this part of the programme, the

TABLE II
RR 59 Alloy
Fracture tests at 20, 150 *and* 200°C

Test	*Temperature* °C	*Maximum principal stress*	*Maximum shear stress*	*Octahedral stress*
Pure tension	20	16·9	8·4	7·9
$t/s = 3{\cdot}1$		15·7	8·5	7·7
Varying tension Constant torsion $s = 5{\cdot}0$ tons per sq. in.		16·3	8·9	8·0
Pure tension	150	14·3	7·2	6·7
$t/s = 1{\cdot}25$		11·6	7·6	6·4
$t/s = 3{\cdot}8$		12·9	6·9	6·3
Varying tension Constant torsion $s = 5{\cdot}0$ tons per sq. in.		13·9	7·3	6·7
Pure tension	200	13·6	6·8	6·4
$t/s = 3{\cdot}72$		11·9	6·3	5·8
Varying tension onstant torsion $s = 2{\cdot}7$ tons per sq. in.		12·2	6·4	5·9

t = tension stress, s = shear stress.

effects of reversal of tensile stress to compression stress (e.g., Bauschinger effect), and reversals of torque will be investigated. A set of tests of the former type has already been completed for the three basic materials, and it would appear that in several instances the Bauschinger effect at high temperatures is small enough to be neglected in the framing of general loading equations.

ACKNOWLEDGMENT—This paper is published by permission of the Director of the *Mechanical Engineering Research Laboratory.*

REFERENCES

ANDRADE, E. N. da C.	1910	*Proc. Roy. Soc.* A. **84**, 1.
	1914	*Proc. Roy. Soc.* A. **90**, 329.
BECKER, R.	1925	*Zeits. fur Physik*, **33**, 185.
BENNEWITZ, L.	1924	*Phys. Zeits.*, **21**, 703.
	1928	*Ibid.*, **25**, 417.
BOLTZMAN, L.	1876	*Poggendorff Annalen der Physik und Chemie* **7**, 624.
EYRING, H.	1936	*J. Chem. Phys.* **4**, 283.
FELTHAM, P.	1950	*Iron & Coal Trades Rev.* **106**, 305.
GRAHAM, A.	1952	*Engineer* **193**, 198.
HOLLOMON, J. H. and LUBAHN, J. D.	1947	*General Electric Rev.* **50**, 28.

KAUZMAN, W.	1941	*Trans. Am. Inst. Min. & Met. Eng.* **143**, 57.
MOTT, N. F. and NABARRO, F. R. N.	1940	*Proc. Phys. Soc.* **52**, 86.
NOWICK, A. G. and MACHLIN, E. S.	1947	*J. App. Phys.* **18**, 79.
OROWAN, E.	1947	*West of Scotland Iron & Steel Inst.* **54**, 45.
SIEGFRIED, W.	1943	*J. App. Mech.* **10**, A202.
SMITH, C. L.	1948	*Proc. Phys. Soc.* **64**, 201.

Vol.
1
1952/

Journal of the Mechanics and Physics of Solids, 1952, Vol. 1, pp. 53 to 63. Pergamon Press Ltd., London.

THE TIME LAWS OF CREEP

By A. H. COTTRELL
Department of Metallurgy, University of Birmingham

(*Received* 16*th. July*, 1952)

SUMMARY

EXPERIMENTAL and theoretical studies of transient creep are briefly reviewed. Many creep curves begin with a rate of strain proportional to t^{-n} where t is time and n is usually 1 (logarithmic creep), 2/3 (ANDRADE creep) or 0 (steady state creep). Logarithmic creep can be explained by the exhaustion theory in which regions with low activation energies yield first and are then used up, leaving the less readily activated regions of higher energy to continue the process, so that the rate of creep diminishes. Experiments by WYATT confirm a deduction of his from the exhaustion theory that a mechanical equation of state is obeyed during logarithmic creep. It is proposed that the unit process in WYATT's creep is the cutting of one dislocation through another; this idea enables one to account quantitatively for the properties of the activation energy function obtained from WYATT's results. A brief discussion of the possibility of explaining ANDRADE creep by modifying the exhaustion theory is given. It appears unlikely that this problem can be solved until work hardening is introduced into the theory.

1. EXPERIMENTAL OBSERVATIONS

ONE method of studying the plastic properties of solids is to subject a specimen to a constant applied stress at a constant temperature and to observe the progress of its deformation as the time of application increases. This plastic flow under constant stress, or *creep*, usually begins very rapidly ("instantaneous" flow) as soon as the stress is applied, and then continues at a diminishing rate ("transient" creep). Fig. 1 illustrates characteristic forms of the creep curve. At low temperatures the rate diminishes so strongly that the instantaneous flow is practically all that can be seen, and the dimensions of the specimen soon become stable. At high temperatures, on the other hand, the rate diminishes more gradually, so that substantial amounts of flow continue to occur even when the stress has been acting for a long time; in many cases a stage may be reached where the rate of flow is constant ("steady-state" creep), and this is often followed by "accelerating"

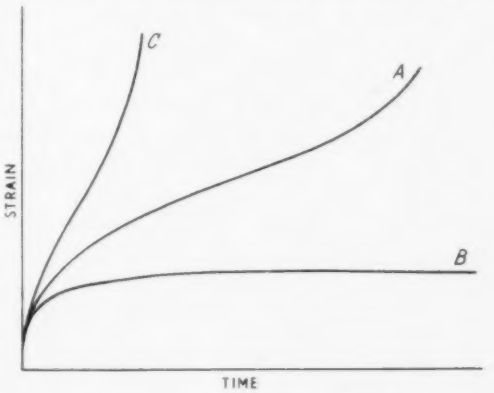

Fig. 1. Creep curves: (a) standard form; (b) at low stresses and low temperatures; (c) at high stresses and high temperatures.

creep and fracture. Practical interest has been focussed on high-temperature creep because of the engineering difficulties which arise when components are unable to support applied loads for long periods without continually changing their dimensions or breaking, and it is this that has led to the popular notion that creep only occurs at high temperatures.

During the accelerating stage the shape of the creep curve is determined by various structural changes, e.g., opening up of cracks, recrystallization, precipitation occurring in the material and differs from one specimen to another. There is no general time law of creep under these circumstances. On the other hand, the early parts of creep curves on different specimens and materials bear sufficient resemblances to each other for some general shapes to be recognised. Many investigators have shown that the beginning of creep can in most cases be represented accurately by functions for the creep rate $\dot{\gamma}$ of the type

$$\dot{\gamma} = A t^{-n}, \tag{1}$$

where γ is the strain, t the time, A and n are constants during the creep experiment, and $0 \leqslant n \leqslant 1$. One of the arguments for the use of such time laws as these is that $\dot{\gamma} = \infty$ at $t = 0$ when $n > 0$, which agrees with the experimental observation that the rate of strain at the beginning of creep is indefinitely large, even at the lowest temperatures. Thus MEISSNER, POLANYI and SCHMID (1930) obtained transient creep curves, which began with characteristic steepness, on crystals of zinc and cadmium at a temperature of only 1·2°K.

When the relation (1) is fitted to experimental creep curves certain values of n are preferred. The extreme case $n = 1$ is frequently observed and this leads to the *logarithmic* creep law,

$$\gamma = \alpha \log t, \qquad (t > 1) \tag{2}$$

where α is a constant, which PHILLIPS (1905) observed in experiments with rubber, glass, and various metals, and which has since been confirmed in other investigations (CHEVENARD 1934; LAURENT and EUDIER 1950; DAVIS and THOMPSON 1950).

At faster creep rates and large strains n is usually less than unity. Various values in the range 0 to 1 may then be observed, but very frequently the value 2/3 is especially preferred, and this leads to ANDRADE's transient creep law

$$\gamma = \beta t^{1/3}, \tag{3}$$

where β is a constant. ANDRADE (1910, 1914) showed that this was obeyed on some polycrystalline metals extended some 20 per cent in times of about 30 minutes. It has subsequently been confirmed on celluloid (FILON and JESSOP 1928), on single crystals of zinc (COTTRELL and AYTEKIN 1950), and on various other materials (LATIN 1948; HENDERSON 1951; WYATT 1951).

Whenever steady-state creep is observed it is necessary to add to the creep formula a term with $n = 0$ to represent it. This gives the *steady-state* or *quasi-viscous* creep strain

$$\gamma = \kappa t, \tag{4}$$

where κ is a constant.

Broadly, the effect of increasing the temperature of the creep experiment is to increase the proportion of creep strain which is contributed by the terms with

the smaller values of n. For example WYATT (1951) showed with polycrystalline copper that $\gamma = \alpha \log t$ gives the best fit at temperatures below about 200°K, that $\gamma = \beta t^{1/3}$ is best at temperatures around 400°K, and that a combination of these,

$$\gamma = \alpha \log t + \beta t^{1/3}, \tag{5}$$

is best at intermediate temperatures. The applied stress has a similar effect, and the temperature at which ANDRADE creep predominates over logarithmic creep can be lowered by increasing the level of stress at which the experiment is made. Working at temperatures and stresses where steady-state creep was appreciable, FILON and JESSOP (1928) using celluloid, and COTTRELL and AYTEKIN (1950) using single crystals of zinc, concluded that the relation

$$\gamma = \gamma_0 + \beta t^{1/3} + \kappa t \tag{6}$$

fitted their creep curves very well. Here γ_0 represents the 'instantaneous' strain which occurs on loading. FILON and JESSOP showed that this relation fitted their observed creep strains with an accuracy of about 1 part in 500, although in a few cases this extremely good fit was only obtained by permitting (small) negative values of β, the physical significance of which is not clear.

The magnitudes of the parameters A, α, β, and κ, in these creep formulae depend on the applied stress and the temperature. In transient creep the precise form of the dependence has still to be elucidated, but qualitatively the effect is that the creep curve bends away, with increasing strain, from its initial steep rise less sharply at high temperatures and stresses than low ones. Experiments on steady-state creep (KAUZMANN 1941; DUSHMAN, DUNBAR, and HUTHSTEINER 1944; COTTRELL and AYTEKIN 1950) show that κ increases exponentially with temperature and stress, suggesting a relation

$$\kappa = C \exp\{-U(\sigma)/kT\}, \tag{7}$$

where C is a constant, k is BOLTZMANN's constant and T is absolute temperature. This relation is typical of a thermally activated process, and the experimental observations can be accounted for if the activation energy $U(\sigma)$ is a decreasing function of the applied stress σ. Over a narrow range of σ this function can then be linearized into $U(\sigma) = U - b\sigma$, where U and b are constants for this stress level, and the coefficient of steady-state creep then becomes

$$\kappa = C \exp\{-(U - b\sigma)/kT\}, \tag{8}$$

which agrees well with its observed behaviour (COTTRELL and AYTEKIN 1950).

2. THERMAL ACTIVATION DURING CREEP

It is a remarkable fact that the time laws of creep described above apply to many radically different kinds of solids; examples of their observance have been obtained from metals, non-metals, single crystals, polycrystals, and amorphous materials. This must surely mean that the shapes of creep curves, in the initial stages at least, are largely independent of the precise atomic mechanism by which the movements are accomplished and depend instead only on the existence of general features common to all or most solids. Of course the magnitudes of the

coefficients A, α, β, and κ, in any particular example could only be explained by structural theories which considered particular processes involving, for example, dislocations, vacant lattice sites, and grain boundaries. On the other hand, it is reasonable to suppose that the general forms of the laws might be explained by formal theories which did not consider these structural details. Some of the theories that have been proposed involve very precise structural models; an example is the theory of MOTT and NABARRO (1948) which involves loops of dislocation lines jumping over regions of internal stress set up by precipitates in a crystal. However, one usually finds in such theories that the form of time law which they yield is largely independent of properties unique to the structural processes which they assume.

The basis on which all formal theories of creep have been built is the idea of BECKER (1925, 1926) that, during creep, the rate of flow is limited because thermal fluctuations are needed to bring it about. One may define a *yield stress* σ_Y as that value of the applied stress σ at which plastic flow can take place without the aid of thermal fluctuations. Roughly, this yield stress can be determined from a conventional rapid stress-strain experiment; more precisely, it is not quite determined by this since some thermally activated flow can take place at the rate of strain which is applied in such an experiment. BECKER's idea was that during creep σ_Y is greater than σ, i.e., that there is an activation stress $\sigma_a\,(=\sigma_Y-\sigma)$ which is finite and positive. An activation energy $U\,(\sigma_a)$ is associated with this activation stress and thermal stress fluctuations are needed in order to overcome, temporarily, the activation stress and allow some flow to take place.

The next important idea is that of OROWAN (1934, 1946-47). He supposed that at the beginning of creep the activation stress and, correspondingly, the activation energy are vanishingly small; as the creep strain increases the yield stress rises progressively, climbing further and further above the applied stress, so that the activation stress and activation energy rise. There are three points to notice about this idea:

(1) Since the rate of flow must depend on the activation energy through a relation of the type $\dot{\gamma} = C \exp\{-U\,(\sigma_a)/kT\}$, the vanishing of the activation stress at the beginning of creep implies (for a large value of C) an extremely high rate of flow even at a vanishingly small temperature.

(2) The increase of the yield stress and activation stress with the creep strain is in accordance with the property of work hardening that is possessed by many solids.

(3) The increase of the activation energy with creep strain implies that the flow slows down progressively, which is characteristic of transient creep. On this view steady-state creep is reached when the activation stress and activation energy no longer increase with increasing strain. A formal theory of steady-state creep can be developed along these lines (BAILEY 1926; OROWAN 1934; COTTRELL and AYTEKIN 1950) by supposing that a stage is reached where work hardening becomes exactly balanced by thermal softening ("recovery"), thereby maintaining constant values of σ_a and $U\,(\sigma_a)$.

3. EXHAUSTION THEORY OF TRANSIENT CREEP

Through the work of OROWAN (1946-47), MOTT and NABARRO (1948), and SMITH (1948), these ideas have culminated in the so-called exhaustion theory

of creep. An important feature here is that, because large thermal fluctuations of stress can only occur at an appreciable rate if they are localised to very small volumes of the material, the flowing specimen is to be regarded as an assembly of elementary ones. Each successful stress fluctuation affects in the first place only one element and produces an increment of plastic deformation in it. This does not rule out the possibility, of course, that an increment of deformation in one element may "trigger off" deformation in its neighbours. In structural theories of creep the elements can be identified with particular features, such as loops of dislocation lines, in the specimen, but this is not necessary for considering the time laws of creep.

The next assumption is that the material is inhomogeneous on a microscopic scale so that different elements have different activation stresses and energies. This allows a qualitative explanation of transient creep to be made. At the beginning of creep the rate of flow is high because of the presence of numerous "soft spots," i.e., elements with small activation stresses and energies. As these elements yield and make their contribution to the overall deformation they become used up or "exhausted," so that creep can continue only by the activation of elements with progressively larger energies, and the rate of flow becomes smaller.

To make a quantitative theory on this basis certain additional assumptions are necessary, and various possibilities then arise. The assumptions most usually made are as follows :—

(1) The activation energy $U(\sigma_a)$ is the same function of the activation stress σ_a for all elements. The precise form of this function depends upon the structural process involved. In the theory of BECKER (1925, 1926) the function is of the form $U \propto \sigma_a^2$, in that of MOTT and NABARRO (1948) it is $U \propto \sigma_a^{3/2}$, while in a recent theory to be described below, in which the elementary process is the cutting of one dislocation line by another, the function is $U \propto \sigma_a$. For mathematical simplicity in the following discussion we shall consider the case where

$$U(\sigma_a) = A\,\sigma_a, \tag{9}$$

A being a constant for constant applied stress ; the other functions are less tractable but do not lead to radically different results.

(2) When an element is thermally activated it contributes an increment v to the overall strain, this being the same for all elements.

(3) After it has been once activated the element makes no more contributions ; this is equivalent to assuming that its activation energy is raised to a prohibitively large value as a result of its plastic deformation.

(4) The elements are independent of each other in the sense that the activation stress of any one of them is unaffected by events occurring amongst its neighbours.

The chance per unit time that an element with an activation stress σ_a will be activated during an increment of time dt is

$$f(\sigma_a) = \nu \exp\{-U(\sigma_a)/kT\}, \tag{10}$$

where ν is the frequency of stress fluctuations in it. The rate of creep is then

$$\dot{\gamma} = v \int_0^\infty N(\sigma_a, t) f(\sigma_a)\, d\sigma_a, \tag{11}$$

where $N(\sigma_a, t)\, d\sigma_a$ is the number of elements in the range σ_a, $\sigma_a + d\sigma_a$. Since each element is activated not more than once the number of available ones is exhausted at a rate

$$\frac{\partial}{\partial t} N(\sigma_a, t) = -N(\sigma_a, t) f(\sigma_a), \tag{12}$$

which gives

$$N(\sigma_a, t) = N(\sigma_a, 0) \exp\{-f(\sigma_a)\, t\}, \tag{13}$$

where $N(\sigma_a, 0)$ is the initial distribution and t is the time of creep.

The creep rate is given by substituting equation (13) into equation (11). Using equations (9) and (10) to write $-(kT/A)\, df(\sigma_a)$ for $f(\sigma_a)\, d\sigma_a$ and assuming, for simplicity, that $N(\sigma_a, 0) = N$, a constant, over the range $0 \leqslant \sigma_a \leqslant \sigma_m$ and is zero outside it, the creep rate is then given by

$$\dot{\gamma} = -\frac{vNkT}{A} \int_0^{\sigma_m} e^{-f(\sigma_a)\, t}\, df(\sigma_a)$$

$$= \frac{vNkT}{At}\left[e^{-t/t_m} - e^{-t/t_0}\right] \qquad (t_0 < t < t_m), \tag{14}$$

where $t_0^{-1} = f(0) = \nu$ and $t_m^{-1} = f(\sigma_m) = \nu \exp(-A\sigma_m/kT)$. Over a wide range of time, $t_0 \ll t \ll t_m$, the factor in the bracket is almost unity, so that the time law of creep is essentially

$$\gamma = (vNkT/A) \log \nu t. \tag{15}$$

This logarithmic law is the prototype for exhaustion theories of creep. By varying the details of the model, laws of the kind $\gamma \propto (\log t)^x$ can be obtained (MOTT and NABARRO, 1948) and most models yield values of x in the range of 0·5 to 1. The assumption that $N(\sigma_a, 0)$ is a constant is not convincing and distributions such as that sketched in Fig. 2 seem more reasonable. However, unless $N(\sigma_a, 0)$ varies as nearly steeply with σ_a as does $\exp\{-f(\sigma_a)\, t\}$ its form cannot very much affect the shape of the creep curve; and with reasonable values for the physical parameters involved $\exp\{-f(\sigma_a)\, t\}$ is practically a step function of σ_a when $\nu t \gg 1$. Over most of the range of σ_a this function is either almost zero or almost unity, and it changes sharply from the one to the other at the value of σ_a for which $f(\sigma_a)\, t = 1$.

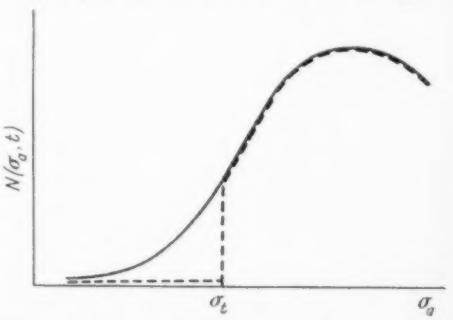

Fig. 2. The distribution of elements with activation energies in a given range: full curve – start of creep; broken curve – after creep for a time t.

This step-like form allows the time law to be deduced in a simple and instructive manner. After a time t practically all elements have been exhausted for which $\sigma_a < \sigma_t$, where

$$\sigma_t = (kT/A) \log \nu t. \tag{16}$$

and practically none of those for which $\sigma_a > \sigma_t$ have been used (Fig. 2). The creep strain is then

$$\gamma = v \int_0^{\sigma_t} N(\sigma_a, 0)\, d\sigma_a, \tag{17}$$

which, with $N(\sigma_a, 0) = N$ and substituting for σ_t, gives equation (15) again. The exhaustion process can thus be regarded as the advance of a vertical step along the axis of σ_a; as it sweeps through part of the distribution curve, all the elements in that part make their contribution to the creep strain and are then no longer available.

Because of this sharp step at σ_t a sudden increase in the applied stress at time t would not produce "instantaneous" flow unless it was at least equal to σ_t. From this point of view $\sigma + \sigma_t$ can be regarded as the yield stress of the material at this time. As MOTT (1951) has pointed out, this enables one to relate this form of exhaustion theory to an earlier and apparently different theory of transient creep proposed by OROWAN (1946-47). OROWAN starts with an expression of the type

$$\dot{\gamma} = C \exp\{-U(\sigma_t)/kT\} \tag{18}$$

for the creep rate, and then makes use of a work-hardening relation, e.g.

$$\sigma_t = h\gamma, \tag{19}$$

to replace σ_t by γ, where h is a coefficent of work hardening (or the slope of a tangential approximation to a non-linear stress-strain curve). Equation (18) is then a differential equation for γ as a function of t. If we substitute for U and σ_t from equations (9) and (19) OROWAN actually uses a Becker function instead of equation (9), equation (18) integrates to give a logarithmic time law

$$\gamma = (kT/Ah) \log\{(AhC/kT)\, t\} \tag{20}$$

4. Experiments on Logarithmic Creep

An experimental investigation of MOTT and NABARRO's form of the exhaustion theory has been made by DAVIS and THOMPSON (1950). They used a precipitation-hardened copper-silver alloy and showed that their creep strains increased proportionately with $(\log t)^{2/3}$, which agrees with the exhaustion theory when this is based on the MOTT and NABARRO activation energy function, $U \propto \sigma_a^{3/2}$, appropriate to a precipitation-hardened alloy. By making sudden small increments in the applied load during the course of a creep experiment DAVIS and THOMPSON were able to demonstrate the existence of a critical stress, σ_t, which could be reached by a suitable increment of load (e.g., 1·4 kg mm^{-2} after creep for 24 hours at room temperature at a stress of about 6 kg mm^{-2}); increments less than this merely increased the rate of flow, without producing "instantaneous" flow, whereas increments greater than this produced instantaneous flow. These experiments showed that the magnitude of the activation energy was of the right order to be accounted for by the MOTT and NABARRO theory of precipitation hardening but that the frequency ν was several orders of magnitude smaller than the expected value. This discrepancy, which concerns the structural part of the theory but not the formal one, has not yet been satisfactorily explained.

In his detailed study of the creep of polycrystalline copper WYATT (1951) showed that, in the range of temperature where the simple logarithmic law (equation 2) of creep was followed, his specimens obeyed a mechanical equation of state, i.e.,

$$\dot{\gamma} = F(\sigma, \gamma, T) \tag{21}$$

This means that at constant temperature, for example, the rate of strain at any instant depends only on the *current* values of stress and strain, and not on their previous values. This was proved by experiments in which sudden increments of load were made during the course of creep. The portions of the creep curve which followed such increments could always be fitted exactly on to earlier portions by sliding them backwards by a suitable amount.

WYATT points out that these results are to be expected from the exhaustion theory. If a specimen is allowed to creep for a time t_1 under constant stress, its activation stress is then given by $\sigma_1 = (kT/A) \log \nu t_1$. If the applied stress is then suddenly increased by an amount $\Delta\sigma\,(= \sigma_1 - \sigma_2)$, the activation stress is immediately reduced to σ_2. There was a point earlier in the deformation of the specimen when its activation stress was σ_2, so that the effect of making the increment $\Delta\sigma$ at time t_1 is to cause a new portion of the creep curve to start which is identical in form with that portion of the original curve that started from the time t_2 defined by $\sigma_2 = (kT/A) \log \nu t_2$. The mechanical equation of state is obeyed because, in the exhaustion theory, the rate of strain at any instant depends solely on the current value of the activation stress, and the activation stress itself depends entirely on the current values of the strain and the applied stress.

Vol
1
1952/

5. A STRUCTURAL THEORY OF WYATT'S LOGARITHMIC CREEP

From the distance along the time axis that it was necessary to slide his curves back, WYATT concluded that σ_t rises linearly with $\log t$. Since, in the exhaustion theory, the activation energy rises linearly with $\log t$, this implies a linear relation between activation stress and activation energy (equation 9), as WYATT has pointed out. We can use this result as a clue to the mechanism of creep in these specimens.

Plastic deformation in crystalline solids mostly occurs through the movement of dislocations in the crystals. Detailed accounts of the theory of dislocations are available (see, for example, COTTRELL 1948), and we shall merely summarize here a few relevant points. The atoms in a slip plane cannot all slip simultaneously over their neighbours in the next plane; slip must begin at one place and then spread from there throughout the rest of the plane. The line running through the slip plane which denotes the boundary of this slip front is called a *dislocation*. When the atoms in the slipped region have moved by only one atomic spacing the slip front is called a *unit* dislocation (or, more often, simply a " dislocation "). Slip fronts bounding regions of larger amounts of slip are regarded as composed of many unit dislocations. Because it is a source of internal stress, a dislocation line has energy. This energy varies with the configuration of the line, and with various other circumstances, but is always of order Ga^3 per atom spacing along the line, where G is the shear modulus and a is the atomic spacing.

The yield strength of a crystalline substance is the stress required to drive the dislocations in it through various obstacles, such as precipitates, solute atoms,

and other dislocations gliding in other directions, which they meet in their slip planes. A sufficiently large applied stress can accomplish this, but when the stress is smaller the dislocations can overcome their obstacles only with the aid of thermal fluctuations. For a given applied stress each obstacle is characterized by a certain activation stress and activation energy.

Many processes of interaction between dislocations and obstacles have now been considered but practically all of them do not give a linear relation between activation stress and activation energy. The one process at present known which gives the linear relation is that which happens when a dislocation line gliding in one slip plane cuts through an intersecting dislocation line lying in some other slip system. Since the passage of a dislocation through a slip plane implies the displacement of the crystal above that plane by one atomic spacing over the crystal below the plane, then, when one dislocation cuts through another, "jogs" will be formed in the dislocation lines, as shown in Fig. 3. The energies of the dislocations are increased through the presence of these jogs and so a force is needed to drive the dislocations through each other, as HEIDENREICH and SHOCKLEY (1948) first pointed out. The activation energy and stress for this process can be found as follows (COTTRELL, 1952). The energy of the jogs may be written as $\alpha\, Ga^3$, where α is a number of order unity. Suppose that a dislocation line is held up against a grid of intersecting dislocations spaced a distance l apart. One of these is cut through when a piece l of the dislocation moves forward a distance of about a. If the applied stress on the dislocation is σ the work done when the piece moves is, from the general theory of dislocations, $\sigma a^2 l$. Hence the activation energy is

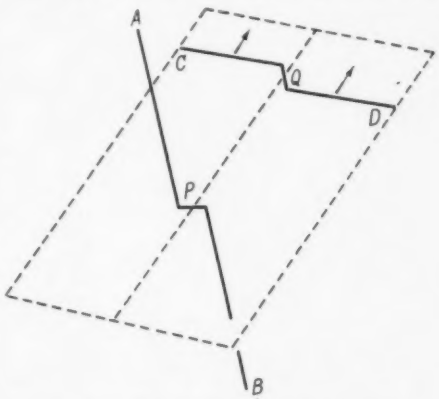

Fig. 3. Jogs P and Q formed in intersecting dislocation lines AB and CD.

$$U = \alpha\, Ga^3 - \sigma\, a^2\, l. \tag{22}$$

Let σ_Y be the applied stress at which $U = 0$. Then

$$U = a^2 l\,(\sigma_Y - \sigma) = a^2 l\,\sigma_a = (\alpha\, Ga^3)\,\sigma_a/\sigma_Y. \tag{23}$$

We shall suppose that the elements in WYATT's exhaustion creep are pieces of dislocation lines held up by intersecting dislocations. When a thermal fluctuation causes one of them to cut through its obstacle this piece then moves on towards the next obstacle, and, by moving, contributes to the creep strain. Several of WYATT's observations can be explained on this basis :

(1) As already mentioned, the activation energy is proportional to the applied stress.

(2) NABARRO (1952) has pointed out the following consequence of the theory. Suppose that, in experiments at the same temperature, two grossly different applied stresses, σ and σ', are used and that the material is allowed to deform freely until its creep rate is about the same in both cases. From equation (22)

this means that

$$l\,\sigma = l'\,\sigma', \tag{24}$$

where l and l' are characteristic values of l for these two conditions of the material. Differentiating equation (22) gives $d\,U/d\,\sigma = -\,a^2\,l$, so that in the two experiments the relation

$$\sigma\,\frac{dU}{d\sigma} = \sigma'\,\frac{dU'}{d\sigma'} \tag{25}$$

should be obeyed. The quantities $dU/d\sigma$ and $dU'/d\sigma'$ are determined in WYATT's incremental loading experiments, and NABARRO points out that the experimental values obtained satisfy the relation rather well.

(3) A numerical comparison is also possible. If we substitute $kT \log \nu t$ for U in equation (23) and then differentiate with respect to $\log t$, this equation becomes

$$\frac{1}{\sigma_Y}\,\frac{d\sigma_a}{d\,\log\,t} = \frac{kT}{\alpha G a^3}\,. \tag{26}$$

In typical experiments WYATT applied a stress of about 18 kg mm^{-2} and found that increments of 0·1 kg mm^{-2} changed the creep rate by amounts equivalent to those produced by changes in $\log t$ of about unity. Hence, in these experiments the left hand side of equation (26) is about 0·005, which means that $\alpha\,Ga^3 \simeq 200\,kT$, i.e. about 4 electron volts, which is reasonable since Ga^3 is 4 electron volts in copper.

6. THE PROBLEM OF ANDRADE CREEP

It is at first surprising that the exhaustion theory, which deals successfully with the creep behaviour when $n = 1$ in equation (1), should so far have had little success in explaining ANDRADE creep, for which $n = 2/3$. However, the model on which the exhaustion theory is based will have to be profoundly altered before it can also apply to ANDRADE creep, for WYATT has shown that the mechanical equation of state no longer holds for this kind of creep. It would be useless merely to apply the present exhaustion theory to an $N\,(\sigma_a, 0)$ curve deliberately shaped to yield a $t^{1/3}$ law.

The strain in ANDRADE creep is usually larger than that in logarithmic creep. Since in the exhaustion theory not all the elements are thermally activated, and those that are activated only jump once, the strains they produce are small unless each thermally activated jump "triggers off" many other jumps in nearby elements. But if this happens, and these stimulated elements are selected at random from the entire $N\,(\sigma_a)$ distribution, then to a first approximation all parts of the distribution are exhausted at the same rate. This rate of exhaustion is proportional to the creep rate and the resulting time law of creep is then similar to the law of radioactive decay.

Another way to obtain large strains from the model is to allow each element to jump more than once. This would certainly occur in, for example, the process discussed in Section 5, where a piece of dislocation line which had cut through the dislocation that was obstructing it would bulge out into the slip plane until it came to the next obstacle. The introduction of this idea changes the theory from one of *exhaustion* to one of *redistribution*. While creep is taking place there is a continual interchange of elements among the various parts of the $N\,(\sigma_a)$ distribution.

Vol 1 1952/

If the elements redistribute themselves within some fixed and finite range of activation stress, a *steady-state* distribution will eventually be set up in which the rates at which elements enter and leave any given part of the range are equal. When this happens the creep rate becomes constant. This steady state should be practically established by the time that every element has been able to jump at least once, so that not much creep may occur before the steady state sets in. It appears unlikely that such a redistribution theory could give a rate of transient creep substantially larger than the steady rate once the creep strain became large compared with the elastic strain.

At large creep strains some true work hardening is to be expected, i.e. hardening caused by an increase in the yield stresses of the obstacles and not merely by the exhaustion of elements facing the smaller obstacles. It appears that the best prospect for a theory of Andrade creep is to take account of this work hardening, perhaps by formulating a redistribution theory in which the range of allowed activation stresses is increased at a rate determined by the creep rate.

Acknowledgments—I am grateful to Dr. O. H. Wyatt for allowing me to refer to his experiments and to Mr. F. R. N. Nabarro for useful discussions.

ol.
1
2/53

References

Andrade, E. N. da C.	1910	*Proc. Roy. Soc.* A, **84**, 1 ; 1914, *ibid*, **90**, 329.
Bailey, R. W.	1926	*J. Inst. Metals*, **35**, 27.
Becker, R.	1925	*Phys. Zeit.*, **26**, 919 ;
	1926	*Zeit. Tech. Phys.*, **7**, 547.
Chevenard, P.	1934	*Rev. Mét.*, **31**, 473.
Cottrell, A. H.	1948	Chapter II, *Progress in Metal Physics I* (Ed : B. Chalmers) (Butterworth's, London), p. 77 ;
	1952	*Report of 9th Solvay Conference*, p. 421.
Cottrell, A. H. and Aytekin, V.	1950	*J. Inst. Metals*, **77**, 389.
Davis, M., and Thompson, N.	1950	*Proc. Phys. Soc.* B, **63**, 847.
Dushman, S., Dunbar, L. W., and Huthsteiner, H.	1944	*J. Appl. Physics*, **15**, 108.
Phillips, F.	1905	*Phil. Mag.*, **9**, 513.
Filon, L. N. G., and Jessop, H. T.	1928	*Phil. Trans. Roy. Soc.* A, **223**, 89.
Henderson, C.	1951	*Proc. Roy. Soc.* A, **206**, 72.
Kauzmann, W.	1941	*Trans. Amer. Inst. Min. Met. Eng.*, **143**, 57.
Latin, A.	1948	*J. Inst. Metals*, **74**, 259.
Laurent, P., and Eudier, M.	1950	*Rev. Mét.*, **47**, 39.
Meissner, W., Polanyi, M., and Schmid, E.	1930	*Zeit. Phys.*, **66**, 477.
Mott, N. F.	1951	*Proc. Phys. Soc.* B., **64**, 729.
Mott, N. F., and Nabarro, F. R. N.	1948	*Report on the Strength of Solids* (London : Physical Society), p. 1.
Nabarro, F. R. N.	1952	*Advances in Physics*, Supplement to *Phil. Mag.*, **1**, 269.
Orowan, E.	1934	*Zeit. Phys.*, **89**, 614, 635 ;
	1946-47	*J. West Scotland Iron and Steel Inst.*, **54**, 45.
Smith, C. L.	1948	*Proc. Phys. Soc.*, **61**, 201.
Wyatt, O. H.	1951a	*Nature*, **167**, 866 ;
	1951b	Thesis, Cambridge.

Journal of the Mechanics and Physics of Solids, 1952, Vol. 1, pp. 64 to 73. Pergamon Press Ltd., London.

THE YIELD PHENOMENON IN POLYCRYSTALLINE MILD STEEL

By W. M. Lomer*
Cavendish Laboratory, Cambridge

(*Received 23rd July*, 1952)

Summary

While Cottrell's theory of the yield point in single crystals is now widely accepted, it has to be combined with some form of grain boundary theory to explain the strength of polycrystalline iron. This paper tries to summarise and interrelate the most important macroscopic features of the yield in polycrystalline iron, and to single out the fundamental properties which must be explained. It appears that the drop in stress after the first yield is responsible for the localisation of plastic flow, and that this localisation may in turn be responsible for the macroscopic shear associated with the Lüders deformation. The existence of this shear influences the pattern of the bands in the specimen and, therefore, the regularity or otherwise of the progress of the yield. It is suggested that the two essential quantities to be derived from any theory are the magnitude of the Lüders strain and the sharpness of its localisation.

1. Introduction

The stress-strain curve of low-carbon iron or mild steel is very different from the approximately parabolic curves typical of metals like aluminium and copper. Fig. 1 shows a somewhat idealised curve for a low-carbon iron, and the important quantities which will help to specify the yield behaviour of the specimen are marked. There is a long *elastic range*, which is sharply terminated when the *upper yield stress* is reached. After this point plastic deformation begins locally. The strain in these small regions is another important characteristic of the material, and is called the *Lüders strain*, and the regions which have been deformed *Lüders bands*, after their discoverer (Lüders 1860). As the extension of the specimen increases, the *Lüders bands* spread and cover a steadily larger area of the specimen until at A the extension corresponds to a

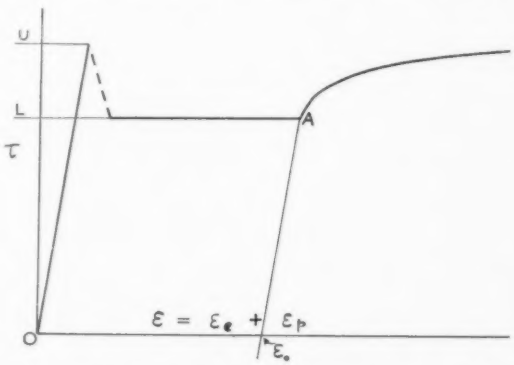

Fig. 1. Stress versus total (elastic and plastic) strain for annealed mild steel. U – Upper yield stress. L – Lower yield stress. ϵ_0 – Lüders strain. A – End of lower yield.

*Now at A.E.R.E., Harwell

mean strain equal to the Lüders strain and the bands cover the whole specimen. The constant stress under which the bands spread is the *lower yield stress*. After the point A the deformation is homogeneous throughout the specimen and the stress rises as the material work-hardens. There appears to be no way of investigating the mechanical properties of steel at plastic strains less than the Lüders strain. The horizontal part of the curve does not mean that mild steel can be used as an ideally plastic material to confirm experimentally the results of plasticity theory as developed for instance by HILL (1950). A mean strain less than the Lüders strain will be inhomogeneous and probably has a rather complicated stress pattern associated with it.

A theory proposed by COTTRELL (1948) and developed with his co-workers (COTTRELL and BILBY, 1949; COTTRELL and CHURCHMAN, 1949) attributes the long elastic range of iron single crystals, and the drop in stress when yielding starts, to the attraction between not very mobile atoms of carbon or nitrogen in solution and the dislocations which are responsible for plastic flow. The yield occurs when the stresses are large enough to pull the dislocations away from their "atmospheres" of impurity atoms. The treatment of polycrystalline material on the basis of this theory (COTTRELL 1951) is rather less satisfactory, in that the grain boundaries have to act as additional barriers to dislocations, and although a plausible account of the upper yield point can be given in terms of this modified theory, the dependence of the lower yield point and the Lüders strain on grain size cannot be dealt with.

The purpose of this paper is to try to interrelate the macroscopic features of yielding in polycrystalline material as far as possible in order to show more clearly which properties may be considered as fundamental.

2. Testing Machine and Variables

The type of testing machine used can materially affect the appearance of the stress-strain curve. The curve of Fig. 1 is drawn for a test on a long thin wire specimen tested at constant crosshead velocity on a hard machine, in which a small extension of the specimen can produce a large decrease in the stress. There is little inertia in the stress-measuring device, and the abrupt fall from the upper yield point can be recorded. In many conventional machines the load is the variable under direct control, and the extension is measured; in these machines there is obviously no way of recording the suddenness of the fall in stress, and if the machine has considerable inertia, complex effects of "overshooting" may apply larger loads than intended for short times. The curves obtained in this way are considerably more difficult to interpret and we shall always refer to curves of the type of Fig. 1. The strain measurement in normal testing practice is often not very accurate in the region of less than 5 per cent which interests us here. HALL and SYLWESTROWICZ (1951), HALL (1951 a and b), and ELAM (1938) have described tests on suitable machines, but in some of the earlier work it is quite difficult to assign values to the stresses and strains we are interested in, owing to the lack of control of testing velocity (see the curves of EDWARDS and PFEIL, 1925). It will appear later in this paper that it is valuable to observe not only the quantities indicated in Fig. 1, but also the appearance of the surface during deformation, both microscopically and on a larger scale. Reproducible measurements of the

upper yield stress are very difficult to carry out, for they are determined largely by stress concentrations which vary from specimen to specimen, but, when some reliable technique is found, it appears that the upper yield point always follows the same trends with external variables as does the lower yield point. Attention is, therefore, focussed on the dependence of lower yield stress and Lüders strain on the various variables, and on the qualitative appearance of the specimen. The most important variables whose effect is to be investigated are :—

(1) Grain size.
(2) Alloying composition.
(3) Testing temperature.
(4) Heating and strain history.
(5) Specimen size and shape.
(6) Testing velocity.

In order to limit the scope of this paper we shall consider only fully recrystallized material, tested at or below room temperature, thus eliminating the complex effects of strain aging and blue brittleness (see KENYON and BURNS 1940, HALL 1952).

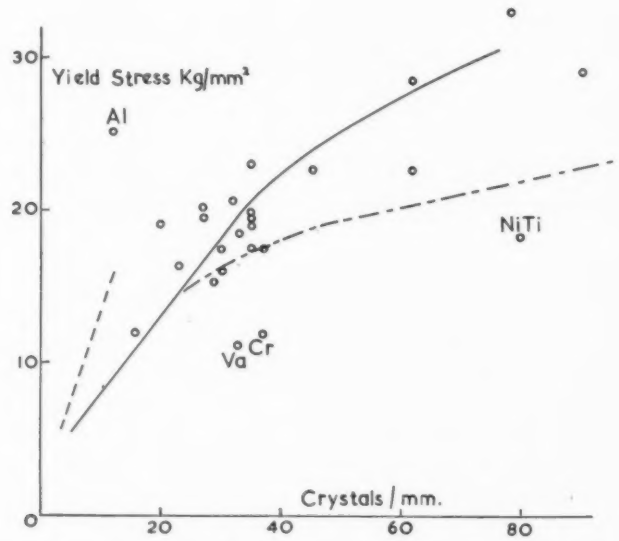

Fig. 2. Lower yield stress versus grain size for many alloys. Dashed line – Imperfectly decarburised iron (EDWARDS and PFEIL 1925). Full line – Mean of many plain carbon steels (EDWARDS, JONES and WALTERS 1939). Circles – Various alloy steels (EDWARDS, PHILLIPS and JONES 1940). Chain line – Simple bands in low carbon irons (HALL 1951b).

It is found that the grain size of the specimen is one of the most important variables determining the lower yield stress (HALL 1951b). A re-analysis of the results of EDWARDS and his co-workers (1925, 1940, 1943) in terms of grain size alone (Fig. 2) shows that the main effect of many alloying elements is to control the grain size, and thus, indirectly, the yield point. The carbide-forming elements Ti, Va, and Cr are exceptions to this, and their presence materially lowers the yield point, presumably by removing almost all the carbon from solution in the lattice.

(The lowering of the yield point does not, of course, imply a decrease in the ultimate strength or toughness of the material, but only that plastic deformation begins more easily in these alloys than in plain carbon steels of the same grain size). Another exception appears to be large-grained aluminium-bearing alloys, which have abnormally high yield points. No explanation of this result has been given.

The work by HALL on thin wires shows a similar dependence on grain size, but all his figures lie consistently below those of EDWARDS (Fig. 2). It is not thought that this is a true size effect, for tests on an intermediate size ($\frac{1}{4}'' \times \frac{1}{8}''$ cross-section) have shown that points may be obtained near either curve, but not between. The higher one is associated with the propagation of complex bands (see Fig. 3a) and the lower with simple bands (Fig. 3b). Not only do the complex bands raise the mean value of the lower yield, but they also make the curve much less smooth. There is a drop of stress associated with the formation of each new tongue of deformation.

The grain size and specimen size both affect the type of band pattern. HALL (1950) has described how the bands become less sharply defined and much more difficult to see as the grain size increases beyond about 1/30 mm diameter. He has distinguished between these diffuse bands, and the sharp ones observed in fine grained material. The specimen size determines the pattern of the bands ; broadly speaking, heavy stiff specimens yield in complex patterns, while lighter flexible ones give single bands.

The temperature of test has a marked effect on the observed yield strength as is shown by experiments carried out by GEIL and CARWILE (1950) and by ELDIN and COLLINS (1951). The results are rather similar to those got by COTTRELL and CHURCHMAN (1949) for single crystals, and follow a law of the type $\text{Y.S.} = a + bT^{\frac{1}{2}}$ fairly well up to room temperature. Above this temperature aging effects become important, and the whole behaviour of the material is different. This form of curve is what would be deduced from a BECKER-OROWAN stress assisted thermal activation process, as pointed out by COTTRELL and BILBY (1949).

The yield stress rises fairly rapidly with the velocity of testing (ELAM 1938, HALL and SYLWESTROWICZ 1951), which emphasises the desirability of keeping this variable under direct control.

3. GEOMETRY OF DEFORMATION

The actual strains in, and the dispositions of, the Lüders bands have been studied by NADAI (1931), FELL (1935, 1937), and HALL and SYLWESTROWICZ (1951), but the earlier work was done on complex bands, which do not in general give truly homogeneous strains within the bands, and some of the observations were limited to one face of the specimen. Most of the results are consistent with the picture given below.

A Lüders band is normally bounded by a plane which is near a plane of maximum shearing stress. In a series of ten tensile tests the plane normal made an angle of $48° \pm 1{\cdot}5°$ with the tensile axis, in excellent agreement with the figure quoted by NADAI. This seems to be a true deviation from 45°. The angle made on the broad face of strip specimen by the trace of the band edge may take any value consistent with the plane being at 48°, but is often at about 65° to the axis. No explanation of the frequency with which this angle occurred was found.

In torsion tests on tube specimens the band front was a plane normal to the tube axis, which is the plane of maximum shear.

Measurements by FELL showed that the material undergoes a sharp and well defined shear at the band front. This shear has been confirmed by HALL and SYLWESTROWICZ, who also point out, however, that the shear strain alone cannot account for the observed decrease in all diameters of an initially circular wire after the passage of a band front. HALL (1951a) has, therefore, suggested that the deformation should be regarded as due to two separate contributions ; first, a pure shear at the band front which takes the material locally through the yield, followed by the second contribution of decelerating flow under constant stress. The assumption is made that this " flow " is not necessarily pure shear, and will give equal contractions to all diameters.

The sharpness of the band front has been investigated using the opaque-stop microscope (LOMER and PRATT 1952). Fig. 4 shows the appearance of the edge of a band, at a magnification of about $\times$ 200. It will be seen that the shear of the surface, which produces the contrast between the dark and light parts of the image, develops in about one crystal diameter. The deformed area is very much roughened by the deformation.

It was hoped that more detailed information about the actual strains in the Lüders bands would be informative, and specimens of pentagonal cross-section as shown in Fig. 5 were prepared by milling from $\frac{1}{4}'' \times \frac{1}{8}''$ bar. This shape was chosen to allow the strain tensor to be completely determined. The strains on the now rather narrow faces were measured by photographing the lightly etched surface before and after deformation at a very carefully fixed magnification on a projection microscope. It was necessary to replace the specimen accurately on the stage so that the same field was photographed the second time, which avoided errors from the distortion of the objectives, and to avoid using the fine-focus adjustment which altered the tube length of the microscope. It was found that strains of 5 per cent could be measured to within about 0·1 per cent on a gauge length of about 1 mm. The axial strain, which should have been the same on all faces, did not always agree well, and it was soon found that in fact the strain on these small gauge lengths was far from homogeneous, although they were some thirty crystals long. For instance, on two lengths, 1 mm long and 1 mm apart, the strains were respectively 2·8 per cent and 3·2 per cent. Presumably these fluctuations average out over longer lengths, but as it is not possible to use wider specimens without getting complex bands, it seems that the inaccuracy of the method must be put at something more like $\pm$ 0·3 per cent. A typical result

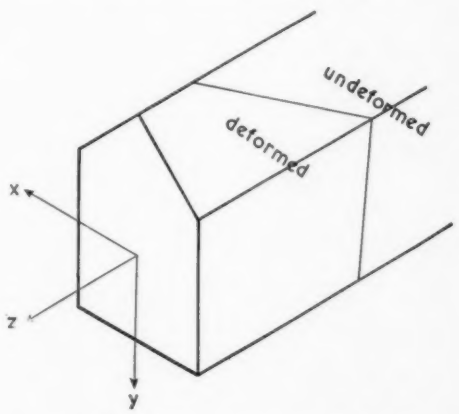

Fig. 5. Pentagonal specimens used for complete strain measurement.

Vol.
1
2/53

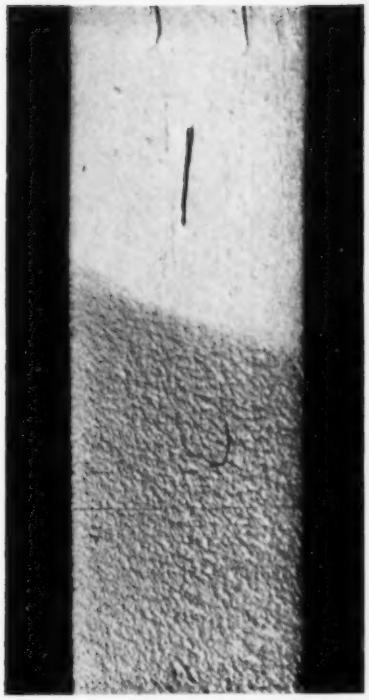

Fig. 3a. Simple Lüders band in strip specimen.

Fig. 3b. Complex Lüders band in $\frac{1}{8}'' \times \frac{1}{4}''$ bar specimen.

Fig. 4. Edge of Lüders band under opaque stop microscope ($\times$ 200, reduced by $\frac{1}{4}$). The contrast arises from the tilt of the deformed left-hand side. Note the sharpness of the edge and the crumpled appearance of the deformed part.

Vol.
1
1952/

was that the strain tensor referred to the axes shown in the figure was :—

$$\begin{pmatrix} -2{\cdot}06 & -0{\cdot}93 & -0{\cdot}10 \\ -0{\cdot}93 & -1{\cdot}66 & 0{\cdot}30 \\ -0{\cdot}10 & 0{\cdot}30 & 3{\cdot}14 \end{pmatrix}$$

or, when rounded to make the dilatation zero :—

$$\begin{pmatrix} -1{\cdot}85 & -0{\cdot}9 & -0{\cdot}1 \\ -0{\cdot}9 & -1{\cdot}45 & 0{\cdot}3 \\ -0{\cdot}1 & 0{\cdot}3 & 3{\cdot}30 \end{pmatrix}$$

or resolved into the two components suggested by HALL, using independent direct measurements of the plane of the band front to determine the direction of the line of greatest slope, which decides the new axes to which to refer the shear :—

$$\begin{pmatrix} -1{\cdot}9 & 0 & 0 \\ 0 & 0 & 0 \\ 0 & 0 & 1{\cdot}9 \end{pmatrix} + \begin{pmatrix} -0{\cdot}7 & 0{\cdot}4 & -0{\cdot}3 \\ 0{\cdot}4 & -0{\cdot}7 & 0{\cdot}3 \\ -0{\cdot}3 & 0{\cdot}3 & 1{\cdot}4 \end{pmatrix}$$

The non-diagonal terms in the second tensor are not much outside the experimental error, and can be ignored.

The conclusion of HALL and SYLWESTROWICZ that there is a considerable contribution to the extension apart from the pure shear is supported fully, but it may be questioned whether the resolution of the strain in this way justifies the introduction of two distinct mechanisms of deformation.

4. EFFECT OF MACROSCOPIC CONSTRAINTS

The picture of the Lüders phenomena which emerges is this. The bands in small-grained material are sharply bounded by a surface which approximately a plane of maximum shearing stress. A distinct shear occurs at this boundary, and in the case of material containing 40 grains/mm. accounts for about half the total extension. In large-grained material, diffuse bands are observed (HALL 1951b) and there is no appreciable surface kink or associated shear. The type of band, sharp or diffuse, is determined by the grain size. On the other hand, the type of band pattern observed depends primarily on specimen size and shape, though complex diffuse bands have not been recognised, if they exist. Thus in all grain sizes, a slender specimen gives a smooth single band, while in stiff specimens fine-grained material gives complex bands.

It seems reasonable to suggest that the complex bands are a consequence of the attempts of the specimen to remain aligned in the grips of the machine, and to have the characteristic shear across each band front. Clearly, large fibre stresses would be necessary to bend the specimen back into line if all the shear occurred at a single plane right across the specimen. The magnitude of these stresses near the kink is about

$$\sigma = \frac{Er\alpha}{\lambda} \coth \frac{l}{2\lambda}$$

for the case of an elastic bar with an angle 2α at the mid-point ; where E = effective elastic modulus (plastic tangent modulus) ; r, l = radius, length of specimen,

respectively ; $\lambda^2 = EI/YA$, I = moment of inertia of cross-section ; Y = applied tensile stress ; A = cross-sectional area. It is not quite clear what value to use for E, but the slope of the join OA in Fig. 1 is perhaps a reasonable average value, and $E/Y = 1/\epsilon_0 \sim 30$. For a circular bar then $\lambda \simeq 3r$.

If $l/6r > 2$, $\coth l/6r \simeq 1$, and the fibre stress for $\alpha = 2°$ is about $E/100$, or $1/3$ yield stress. As $l/6r$ decreases below unity, the fibre stresses rise rapidly, and at $l/r = 3$, are almost equal to the yield stress. This suggests that to minimise the disturbance introduced by the shear kink the length to diameter ratio should be twelve to one or more ; this seems reasonable, for specimens much over $\frac{1}{4}''$ diameter give complex bands on a gauge length of $4''$ or $5''$.

That complex bands are not a result of overall size is demonstrated by the fact that torsion tests on tube of wall thickness $\frac{1}{16}''$ and internal diameter $\frac{1}{2}''$ always gave smooth propagation of clean bands. In this case the sharp shear does not produce any substantial disturbance in the macroscopic shape of the specimen and does not disturb the stress distribution. A tensile test on a similar tube specimen gave a complex pattern.

5. Mechanism of Deformation

The inhomogeneity of the deformation of iron is a direct result of the fact that there is a falling part of the stress-strain curve, so that once some plastic strain has occurred, this is the part of the specimen which deforms further. Some modification or elaboration of COTTRELL's theory of the yield point of single crystals of iron will probably explain this. There remains the question of why the deformation should consist largely of a shear across the boundary of the deformed region. To this there may be two possible solutions ; either there is some characteristic mechanism of deformation associated only with the initial yield and involving a small shear naturally, such as " kinking " first described by OROWAN (1942), or, alternatively, it may be a consequence of the localisation of the strain, and only secondarily due to the properties of the material.

In order to examine the first possible explanation, it is clearly advantageous to examine specimens which have had the least possible plastic strain, so that any features characteristic of the yield phenomenon are not swamped by the subsequent deformation. The most noticeable feature of specimens extended by the Lüders strain of some 5 per cent is the very great " crumpling " of the surface, on the scale about a crystal diameter (see Fig. 4). The surface is as rough as that of copper or aluminium after about 20 per cent extension. This effect was not found in the torsion experiments which showed quite well marked Lüders bands, and so cannot be regarded as being truly an essential feature of the yield. The appearance and number of slip lines seen varies greatly with the method of preparation of the surface. Electro-polishing in the acetic acid – chromic anhydride bath recommended by MORRIS (1949) led to the slip lines being very difficult to see ; they were apparently neither so sharp nor so high as when mechanical polishing was used. These observations are in accord with those of BROWN and HONEYCOMBE (1951) on aluminium, and of PAXTON, ADAMS and MASSALSKI (1952) on single crystals of iron. The main difference is the short electropolishing treatment of the polycrystalline iron which serves to remove the effects of mechanical polishing.

Vol. 1 1952/5

The worked layer on the surface is presumably much thinner on the hard polycrystals than on the soft single crystals.

NADAI (op. cit. Fig. 62) has pointed out that occasional large areas of roughly oriented slip, over regions of some tens of crystals, are often observed. There seems to be no obvious connection between the orientation of these groups and the direction of the Lüders band trace as it passed through the region. The fact that these areas occur is probably a consequence of the fact that the " pencil slip " of iron, which does not occur on a single family of crystallographic planes, can comparatively easily pass continuously through a grain boundary if the crystals on either side have their slip directions not too far from parallel.

We may conclude from these observations that there is no direct evidence for a new deformation mechanism associated with the primary yield phenomena in iron.

The possibility that the characteristic shear deformation is a consequence of the constraints at the elastic-plastic boundary which is the edge of the Lüders band seems more attractive. In order to retain continuity of displacements across the boundary the compressive strains in directions parallel to the boundary must be equal on either side of the boundary, and so are both small, of the order of the elastic deformations. If we assume there is no volume change on plastic deformation there can only be small changes in the compressive strains normal to the plane. It is easy to see that there cannot be a discontinuity in the shear strain in the plane of the boundary. There remain only the two shear strains involving displacements parallel to the boundary, representing the sliding of layers parallel to the boundary. These are not hindered by the plastic-elastic boundary, and are therefore the only strains permitted to the first few layers which are close to the elastic region. As we move away from the boundary the constraint must become less effective, and more general deformation is possible. No progress towards a full solution of the plastic problem involved has proved possible yet. If the relative importance of the two components of the strain is to be assessed, it is clearly necessary to treat the full three-dimensional case, and also, to limit the strain in the plastic region, to include work hardening.

There is, however, one experimental fact which seems to support this explanation. In large-grained specimens the band edge is diffuse, and so only a small amount of the deformation is severely constrained by the elastic material, and the theory sketched above would predict a very small pure shear contribution. This is in excellent accord with experience, for diffuse bands are always difficult to see, and can only be found by close examination of the surface, and not by looking for a tilt of the surface shown by the reflection of a light.

There is one further complicating factor in the tensile test. The initial pure shear deformation produces a kinked bar, which is pulled straight by the applied load. This involves plastic bending under a net tension, which always produces a greater extension than would be expected from the tension alone (see for instance SWIFT 1948). It seems that this effect could make a considerable contribution to the extension; for small linear strain hardening the extension at the end of bending and straightening is nearly the mean of the strain at the centre plane at the outside edge of the bent specimen. Since the curvature of the specimen in the plastic region may be such as to give a change of angle of about 2° in a specimen

diameter, the extreme fibre strain may be about 3 per cent, and the effect discussed could lead to a net extension of $1\frac{1}{2}$ per cent. This figure is to be regarded as an upper limit, since in fact the strain hardening is neither small nor linear. This kind of factor does not enter into the torsion test, but it is not easy to use this comparison to test its importance since the stress and strain systems are not the same in the two cases. Rough measurements indicate that the shear stress across the plane of the band front is the same in the two cases (TRESCA's criterion of yielding; see also MORRISON 1939) and that the plastic work done in the torsion test is some 20-30 per cent smaller than in the tensile test, as would be expected if the plastic extension is increased above its 'natural' value by the bending effect just discussed. The interpretation of the results is, however, too difficult to allow any definite statement to be made.

6. SUMMARY AND CONCLUSION

This paper has briefly summarized some of the better-established facts about yielding in low-carbon iron. The properties of polycrystalline iron are controlled very markedly by the grain size, and COTTRELL's theory of the yield point must again use the idea of the boundaries being a barrier to plastic deformation. The initial deformation is localized in Lüders bands, within which the strain is made up of roughly equal components of shear and normal extension. The shear component causes the bar to become sharply kinked, and this in turn introduces large bending moments which influence the band pattern. There is further evidence that the appearance of the slip lines on deformed metal depends on the mode of preparation of the surface, but no evidence for a special mechanism of deformation associated with the primary yield. It is, however, possible to explain qualitatively the shear strain as a consequence of constraints imposed by the elastic-plastic boundary of the Lüders band. The value of the Lüders strain must be determined by the strain-hardening properties of the material, and if this could be explained and the sharpness of the band front predicted, it seems that most of the macroscopic peculiarities of the yield strains could be explained on the lines indicated here.

Vol. 1 1952/

ACKNOWLEDGMENTS

It is a pleasure to thank Dr. E. OROWAN for suggesting this field of study, Dr. E. O. HALL for many fruitful discussions, and Prof. Sir W. L. BRAGG for ensuring the availability of facilities in the Cavendish Laboratory. The work was started while the author was in recept of a maintenance grant from D.S.I.R., to whom grateful acknowledgment is made.

REFERENCES

BROWN, A. F. and HONEYCOMBE, R. W. K. 1951 *Phil. Mag.*, **42**, 1146.

COTTRELL, A. H. 1948 *The Strength of Solids* (London : Physical Soc.), 30.

1951 *Rep. 9th Solvay Conference on Physics* (Brussels ; Stoops), 487.

COTTRELL, A. H. and BILBY, B. A. 1949 *Proc. Phys. Soc.* A, **62**, 49.

COTTRELL, A. H. and CHURCHMAN, A. T. 1949 *J. Metals* (*Metals Trans.*), **185**, 877.

Edwards, C. A., Jones, H. N. and Walters, B.	1939	*J. Iron Steel Inst.*, **139**, 375.
Edwards, C. A. and Pfeil, L. B.	1925	*J. Iron Steel Inst.*, **112**, 79.
Edwards, C. A., Phillips, D. L. and Jones, H. N.	1940	*J. Iron Steel Inst.*, **142**, 199.
Edwards, C. A., Phillips, D. L. and Liu, Y. H.	1943	*J. Iron Steel Inst.*, **147**, 153.
Elam, C. F.	1938	*Proc. Roy. Soc. A*, **165**, 568.
Eldin, A. S. and Collins, S. C.	1951	*J. Appl. Phys.*, **22**, 1296.
Fell, E. W.	1935	*J. Iron Steel Inst.*, **132**, 75.
	1937	*Carnegie Inst. Memoirs*, **32**, 124.
Geil, G. W. and Carwile, N. L.	1950	*J. Bur. Stand.*, **45**, 129.
Hall, E. O.	1950	*Proc. Phys. Soc.* B, **63**, 724.
	1951 a	*Proc. Phys. Soc.* B, **64**, 742.
	1951 b	*Proc. Phys. Soc.* B, **64**, 747.
	1952	*J. Iron Steel Inst.*, **170**, 331.
Hall, E. O. and Sylwestrowicz, W.	1951	*Proc. Phys. Soc.* B, **64**, 495.
Hill, R.	1950	*Mathematical Theory of Plasticity* (Clarendon Press).
Kenyon, R. L. and Burns, R. S.	1940	*Symposium on Age Hardening of Metals*, (Amer. Soc. Metals, Cleveland, Ohio).
Lomer, W. M. and Pratt, P. L.	1952	*J. Inst. Met.*, **80**, 409.
Lüders, W.	1860	*Dinglers polytech. J.*, **155**, 18.
Morrison, J. L. M.	1939	*Proc. Inst. Mech. Eng.*, **142**, 193.
Morris, C. E.	1949	*Metals Progress*, **56**, 696.
Nadai, A.	1931	*Plasticity* (New York, McGraw Hill).
Orowan, E.	1942	*Nature*, **149**, 643.
Paxton, H. W., Adams, M. A. and Massalski, T. B.	1952	*Phil. Mag.*, **43**, 257.
Swift, H. W.	1948	*Engineering*, **166**, 334.

ol.
1
2/53

BOOK REVIEWS

H. M. HANSEN and P. F. CHENEA: **Mechanics of Vibration.** John Wiley & Sons, Inc., New York: Chapman & Hall, London. 1952, 417 pp., $8 or 64s.

THE aim of the authors has been to provide a thorough and elementary treatment of the basic principles of vibration theory which would serve as a text in an engineering course. The book succeeds admirably in this purpose, an especially attractive feature being the collection of some 350 graded problems and solutions. Forced vibrations of systems of one and two degrees of freedom are treated for the most part. LAGRANGE's equations are introduced, somewhat briefly, but not the classical theory of normal modes. The book closes with chapters on transient vibrations, both linear and non-linear.

The method described for finding the frequencies and modes of an n-degree of freedom system is the well-known and popular one of HOLZER; this, however, is applicable only when the masses and springs are distributed as in a torsional system. Curiously enough, considerable space is given to GRAEFFE's root-squaring method for solving the frequency equation; this method seems to have little to commend it in this context, since the frequency determinant has first to be expanded and the modes have afterwards still to be found. One wonders why the STODOLA iterative method was not given for preference, even though the proof of convergence would probably have to be omitted in a book at this level. Continuous systems are mentioned only briefly, mainly to illustrate the approximate estimate of the fundamental frequency by RAYLEIGH's principle (the proof of which is not given).

The distinctive part of the book, in the reviewer's opinion, is the very thorough exposition of the so-called mobility method. Essentially, this is a systematic way of treating a complex system as a combination of a few standard units whose responses to forced vibrations are known. A direct setting-up and solution of the equations of motion is thereby avoided, while at the same time more insight is gained into the interaction and relative importance of the component parts. These advantages should commend the method to engineers.

The book is attractively produced and the illustrations are numerous and lucid.

R. HILL

Vol. 1 1952/5

W. PRAGER and P. G. HODGE, Jr.: **The Theory of Perfectly Plastic Solids.** John Wiley and Sons, Inc., New York; Chapman and Hall Ltd., London. 1951, 264 pp. + x, $5.50 or £2.2s.

THE subject of plasticity is neither flesh, fowl nor good red herring in that it does not belong wholly to metal physics, to conventional engineering nor to applied mathematics. It is therefore difficult to write a book on plasticity which will be readily understandable by all those interested, and yet which is still rigorous and comprehensive. Indeed, the widely different training of engineers, physicists, and mathematicians makes it virtually impossible to satisfy their several needs simultaneously. The literature can consequently be classified fairly sharply into three groups, reflecting the approach of the author, and the kind of audience for which he is catering.

The present book is based on a Brown University Survey Report designed for theoretical research workers, which has been modified to appeal to pre- and post-graduate students of engineering. The authors state that the book gives an introductory treatment on an intermediate level, but a brief survey will convince the informed reader that such a claim is too modest. The authors confine themselves to the theory of "perfectly plastic," i.e., non-hardening and isotropic, solids, which they feel to have reached a sufficiently definitive form to be included in a course for first year and graduate engineers. Even this branch of the subject has now developed to a sufficient magnitude to require several volumes for an exhaustive treatment of both theoretical and experimental aspects. A compromise has been reached by dealing exclusively with the mathematical theory. The mode of approach and the mathematics used have been selected to be acceptable to engineering students, although the authors have not allowed a desire for simplicity to preclude the use of more advanced mathematical techniques where necessary, e.g. in the discussion of extremum principles. The book commences with an introduction to the con-

cepts of stress and strain and tensor invariants, leading to a mathematical discussion of the Tresca and von Mises yield criteria and the Reuss stress-strain relations. A short chapter on the plastic-elastic behaviour of beams is followed by a discussion of the twisting of prismatic bars, and the combined torsion and tension of a circular cylinder. The three following chapters deal with plane strain, giving specific solutions to several initial yield and steady motion problems. The book concludes with chapters on limit analysis and extremum principles. Some particular applications of plastic limit analysis were first published in the book.

It is inevitable that in a book of this size and scope the research worker will find the treatment too curtailed, but the authors have given references to enable most of the original papers to be consulted. Those entering the field for the first time will be able to feel that the problems handled are of current, and often research, interest.

J. F. W. BISHOP.

Progress in Metal Physics : Vol. 3 Edited by BRUCE CHALMERS. Pergamon Press Ltd., London 1952. 9¾ x 6. pp. viii x 334 with numerous illustrations. 48s.

ol.
1
2/53

IN this series reviewing progress in metal physics at approximately yearly intervals the editor and publishers have undertaken a task which some regard as primarily the responsibility of the scientific societies rather than of "private enterprise." They did so, of course, because the societies most concerned have not catered adequately for the demand that undoubtedly exists. With the appearance of the third volume in the series it may be opportune to consider how far the objects set forth in the foreword to the first volume have been achieved and whether the pattern now emerging will, on a long term basis, satisfy the need for authoritative reviews of the present state of knowledge in specialised fields of metal physics.

The standard of the articles in Volume I was almost uniformly high but although several of the later articles can also be regarded as authoritative reviews of the kind aimed at, some are of considerably lower standard and do not justify inclusion in this series. It would, perhaps, be remarkable if the high quality of the best articles in each volume were reached by every contributor but one feels that a little more discrimination by the editor would enable this goal to be more closely approached. After all, if an article does not reach the required standard it need not be printed.

In the volume under review the chapter on "Crystallography of Transformations" by J. S. BOWLES and C. S. BARRETT is first-rate and could be taken as a model by future contributors ; it could with advantage be studied by classical metallographers as well as by metal physicists. After reading the title, most metallurgists will expect something quite different from D. K. C. MACDONALD'S article on "The Properties of Metals at Low Temperatures." Contrary to the author's opening sentence, practical metallurgists are greatly interested in the effect of low temperatures on mechanical properties of metals and they will be disappointed to find that this chapter only summarises recent work on fundamental electrical and thermal properties of metals and makes no reference to mechanical properties as such. The subject discussed by Dr. MACDONALD is a very specialised one and the wisdom of including it in the series at this stage may be questioned. "Recent Advances in the Electron Theory of Metals" with particular reference to the problems posed by the modern theory of dislocations and of other lattice defects are reviewed in a characteristic manner by N. F. MOTT and his article will be widely appreciated.

The subject of twinning is ripe for review even though much remains to be learnt about it. It is therefore unfortunate that the article on "Twinning" by R. CLARK and G. B. CRAIG does not reach the high standard required ; something more than a summary of literature is needed to give a clear impression of the present state of knowledge. The chapters by URSULA MARTIUS on "Ferromagnetism" and by G. B. GREENOUGH on "Quantitative X-ray Diffraction Observations on Strained Metal Aggregates" are both competent reviews by workers in the respective fields. In many respects the treatment of "Recrystallisation and Grain Growth" by J. E. BURK and D. TURNBULL will be better appreciated by experts than by those who claim

no special knowledge of the subject. Nevertheless, the section on annealing twins is much more readily understood than the corresponding section of the article on "Twinning."

In the final chapter BRUCE CHALMERS describes the advances that have been made regarding the "Structure of Crystal Boundaries" since the subject was reviewed in the first volume. More progress reports of this type and quality will be welcomed in future volumes.

To sum up, the best of the articles so far published in this series serve a most useful purpose; if the remainder approached their high standard "Progress in Metal Physics" would be assured of a permanent place in the literature of metallurgy.

A. G. QUARRELL

ANNOUNCEMENTS

ACTA METALLURGICA

The Interim Board of Governors of Acta Metallurgica announce that this International Journal, which will be devoted to the fundamental Physics and Chemistry of metals, will commence publication in January, 1953. Acta Metallurgica will contain papers that describe original research, either theoretical or experimental, which leads to a fuller understanding of the properties and behaviour of metals in terms of fundamental particles, forces and energies. It will also contain letters to the editor, critical book reviews and occasional review articles. The Editor is BRUCE CHALMERS of the University of Toronto, and he will be assisted by a distinguished panel of associate editors. The business management is in the hands of Mr. WALLACE WATERFALL, of the American Institute of Physics.

Vol.
1
1952/5

Journal of the Mechanics and Physics of Solids, 1953, Vol. 1, pp. 77 to 89. Pergamon Press Ltd., London.

LIMIT ANALYSIS OF ARCHES

By E. T. Onat and W. Prager
Division of Applied Mathematics, Brown University, Providence, R.I.

(*Received* 31*st July*, 1952)

Summary

In the limit analysis of frames it is usually assumed that the limiting bending moment of a cross section is not significantly reduced by the presence of axial forces. In the limit analysis of flat arches this assumption is not permissible as a rule. In the present paper the basic concepts of limit analysis are extended to members in which axial forces as well as bending moments must be taken into account. Methods of determining the critical load intensity of arches are developed and illustrated by numerical examples.

ol.
1
2/53

1. Introduction

The basic concepts of limit analysis† were developed in connection with the design of statically indeterminate beams.†† If the influence of the shear force is neglected, as is customary, the mechanical behaviour of a beam made of an elastic-plastic material can be described in terms of the bending moment, M, and the angle of flexure per unit length, ψ. The typical M versus ψ diagram obtained in a flexure experiment exhibits a more or less sharply defined "turn" when the absolute value of the bending moment reaches a critical value M_0 : a small increase of the absolute value of the bending moment beyond M_0 causes a very significant increase in the absolute value of the angle of flexure. Practically, this means a "yield hinge" forms at any cross section where the bending moment reaches M_0 in absolute value.

As the loads acting on a statically indeterminate beam are increased, each new yield hinge reduces the degree of indeterminacy of the beam. Eventually, yield hinges will form in a number sufficient to cause excessive plastic deformation and hence render the beam unserviceable. Limit analysis is concerned with the determination of the load intensity at which this stage is reached.

The same ideas have been applied to frames‡ in spite of the fact that in this case the plastic behaviour of the members should be described in terms of bending moment and axial force on one hand, and angle of flexure and axial extension (or

† The term "limit analysis" seems preferable to the customary term "limit design" when the problem under consideration concerns the determination of the carrying capacity of a given structure. Use of the term "limit design" should be reserved for cases where the basic concepts of limit analysis are employed to design a structure so as to combine a prescribed carrying capacity with other desirable characteristics such as low weight. For a discussion of certain aspects of limit design for minimum weight see J. Heyman, 1951, *Quart. App. Math.*, **8**, 373.

†† For a comprehensive bibliography of early work in this field see H. Maier-Leibnitz, Preliminary Publication of the Second Congress of the International Association for Bridge and Structural Engineering, Berlin, 1936, 103.

‡ See, for instance, J. F. Baker, 1949, *J. Inst. Civ. Eng.*, **32**, 188; P. S. Symonds, Graduate Division of Applied Mathematics, Brown University, Report All-S6 to ONR, May 1950; P. S. Symonds and B. G. Neal, 1951, *J. Franklin Inst.*, **252**, 383 and 469.

compression) on the other hand. The excuse usually offered for the neglect of axial forces and extensions is the fact that, for solid sections at least, a moderate axial force does not lower the critical bending moment M_0 appreciably. While the neglect of axial forces and extensions may be justified in the case of frames of conventional design, it is not likely to be permissible in the case of arches. In this paper the basic concepts of limit analysis are therefore extended to members in which axial forces as well as bending moments must be taken into account.

2. Plastic Behaviour of Typical Sections

Consider the solid rectangular section shown in Fig. 1 (a). To find a critical combination of axial force N and bending moment M assume a "fully plastic" stress distribution such as shown in Fig. 1 (b): from the top fibre down to a depth y the section is under the yield stress in, say, compression, while the rest of the section is under the yield stress in tension. In the following, these yield stresses will be assumed to have the same absolute value σ_0. With the notations of Fig. 1 (a), the resultant of these stresses is then found to be

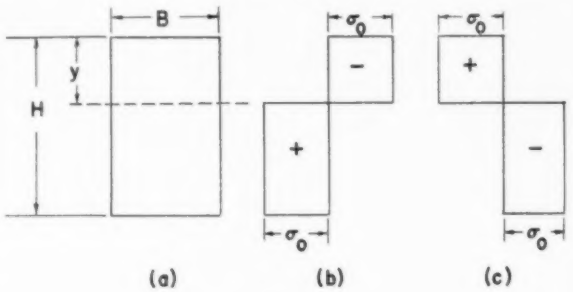

Fig. 1

$$N = B\,(H - 2y)\sigma_0, \tag{1}$$

and the resulting moment with respect to the horizontal through the centroid of the section is found as

$$M = B\,(H - y)\,y\sigma_0. \tag{2}$$

For $y = 0$, the section is stressed in simple tension:

$$M = 0, N = BH\sigma_0 = N_0, \tag{3}$$

where N_0 denotes the limiting value of the axial force in the absence of bending. For $y = H$, the section is stressed in simple compression:

$$M = 0, N = -BH\sigma_0 = -N_0, \tag{4}$$

and for $y = H/2$, the section is stressed in pure bending:

$$M = BH^2\sigma_0/4 = M_0, N = 0, \tag{5}$$

where M_0 denotes the limiting value of the bending moment in the absence of axial force. For values of y between 0 and H, limiting combinations of axial force and bending moment can be obtained by eliminating y from (1) and (2). With the use of N_0 and M_0 as given by (3) and (4), the relation resulting from this elimination of y can be written in the form

$$\left(\frac{N}{N_0}\right)^2 + \frac{M}{M_0} = 1. \tag{6}$$

Vol 1 1952/

In Fig. 2, where N/N_0 and M/M_0 are used as rectangular coordinates, equation (6) is represented by the parabolic arc ABC. If the fully plastic stress distribution of Fig. 1 (c) had been used instead of that shown in Fig. 1 (b), the parabolic arc ADC would have been obtained instead of the arc ABC.

Points within the area bounded by these parabolic arcs in Fig. 2 represent "safe" combinations of axial force and bending moment, while points on these arcs represent critical combinations.

Under any such critical combination of axial force and bending moment a certain type of plastic deformation becomes possible which is characterized by the value of the ratio between the unit axial extension, ϵ, and the angle of flexure per unit length, ψ. Note that the values of N and M do not determine the values of ψ and ϵ but only the ratio ϵ/ψ, since the material can flow plastically under constant stress. For $N = 0$, $M = M_0$, for instance, the plastic deformation must be pure bending with $\epsilon = 0$, but the angle of flexure ψ remains undetermined.

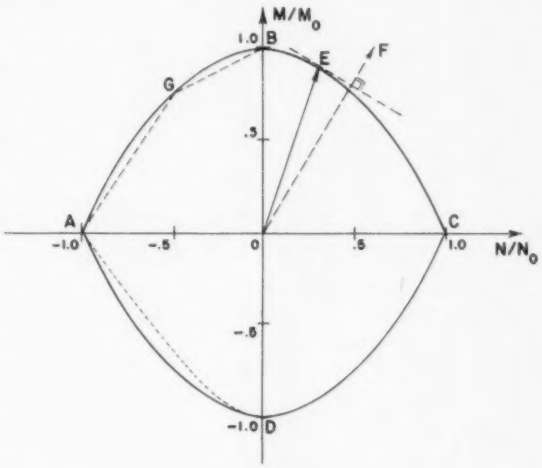

Fig. 2

For the stress distribution of Fig. 1 (b) (for which $M > 0$) the neutral fibre which does not experience any axial extension is at the depth y below the top fibre. If it is assumed that the cross section remains plane, the following relation between the unit extension ϵ of the centroidal fibre and the angle of flexure ψ is obtained :

$$\epsilon = \left(\frac{H}{2} - y\right)\psi. \tag{7}$$

From (10,) (2), (4) and (7), it follows that

$$\frac{N_0\epsilon}{M_0\psi} = 2\,\frac{N}{N_0}. \tag{8}$$

If the left-hand side of (6) considered as a function of N/N_0 and M/M_0 is denoted by F, (8) can be written as

$$\frac{N_0\epsilon}{M_0\psi} = \frac{\partial F}{\partial\,(N/N_0)}\Big/\frac{\partial F}{\partial\,(M/M_0)}. \tag{9}$$

Equation (9) establishes the following important fact : if a critical combination N, M is represented in Fig. 2 by the point E on the boundary of the safe domain, and a corresponding plastic deformation by the vector OF with the components $N_0\epsilon$ and $M_0\psi$, this vector has the direction of the exterior normal to the boundary of the safe domain at the point E. The following consideration leads to a physical

interpretation of this fact. Since the plastic deformation ϵ, ψ develops under constant values N, M, the mechanical energy dissipated in this deformation is given by

$$D = N\epsilon + M\psi = \left(\frac{N}{N_0}\right)(N_0\epsilon) + \left(\frac{M}{M_0}\right)(M_0\psi). \tag{10}$$

The last expression proves D to be the scalar product of the vectors OE and OF in Fig. 2, that is, the product of OF and the projection of OE on OF. Inspection of Fig. 2 shows then that the energy dissipation computed from a given plastic deformation ϵ, ψ and the critical combination N, M causing this deformation is larger than the energy dissipation computed from the given deformation and any safe combination of axial force and bending moment. This is the special form which HILL's (1948) principle of maximum plastic work assumes for the case of combined tension and bending.

Other cross sections can be treated along similar lines. When the results for symmetrical sections are plotted in the manner of Fig. 2 with the appropriate values of N_0 and M_0, the safe domain is found to differ less from that obtained for the solid rectangular section than might be expected. For instance, for the I section shown in Fig. 3, the safe domain in the third quadrant of Fig. 2 would

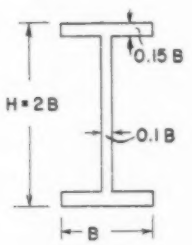

Fig. 3

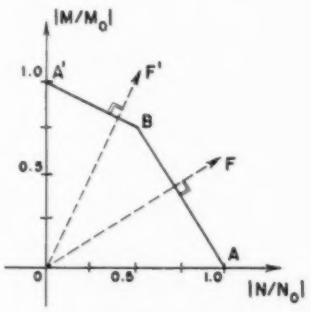

Fig. 4

be bounded by the dotted line AD instead of the full line which corresponds to the rectangular section. For unsymmetrical sections, however, the safe domain is no longer symmetrical with respect to the N/N_0 axis. In all cases the safe domain is found to be convex. When the safe domain has been established, the relation between the plastic deformation ϵ, ψ and the critical combination N, M which causes this deformation is established by the principle of maximum plastic work.

In the following, it will be found convenient to approximate the curved boundary of the safe domain by a polygon. As the dotted line AGB in Fig. 2 indicates, a reasonably good approximation in the case of a solid rectangular section is given by the octagon with the vertices $(\pm 1, 0)$, $(\pm \frac{1}{2}, \pm \frac{3}{4})$, $(0, \pm 1)$. Since this approximating polygon does nowhere protrude beyond the curved boundary furnished by the theory, the carrying capacity computed on the basis of the polygonal approximation cannot exceed the true carrying capacity.

When the boundary of the safe domain is thus modified with the view to simplifying the mathematical work, the relation between ϵ, ψ and N, M must

also be modified so as to preserve the validity of the principle of maximum work. This necessity was first pointed out by HEYMAN (1951) in a paper on the limit analysis of frames with members subjected to bending and torsion.

On account of the symmetry of the safe domain in Fig. 2 with respect to the coordinate axes, it is possible to restrict the following discussion to one quadrant or, what amounts to the same, to consider only the absolute values of N/N_0 and M/M_0 disregarding the signs of these quantities. The aforementioned approximation to the boundary of the safe domain for a solid rectangular section is shown in this manner in Fig. 4. If the principle of maximum plastic work is to remain valid, the vector with the components $N_0|\epsilon|$, $M_0|\psi|$ must have the direction OF for all critical combinations of axial force and bending moment represented by interior points of the segment AB, and the direction OF' for all critical combinations represented by interior points of the segment $A'B$. In the first case,

$$\frac{N_0|\epsilon|}{M_0|\psi|} = \frac{3}{2}, \tag{11}$$

and in the second case

$$\frac{N_0|\epsilon|}{M_0|\psi|} = \frac{1}{2}. \tag{12}$$

For a plastic deformation satisfying (11), the mechanical energy dissipated can be evaluated, by means of (10), from the critical combination represented by any point on AB, for instance from that represented by A. Thus,

$$D = N_0|\epsilon| \text{ if } N_0|\epsilon|/M_0|\psi| = 3/2 \text{ and } \left|\frac{N}{N_0}\right| + \frac{2}{3}\left|\frac{M}{M_0}\right| = 1, \left|\frac{N}{N_0}\right| > \frac{1}{2}. \tag{13}$$

Similarly,

$$D = M_0|\psi| \text{ if } N_0|\epsilon|/M_0|\psi| = 1/2 \text{ and } \frac{1}{2}\left|\frac{N}{N_0}\right| + \left|\frac{M}{M_0}\right| = 1, \left|\frac{N}{N_0}\right| < \frac{1}{2}. \tag{14}$$

For critical combinations of axial force and bending moment represented by the vertices A, B, or A', the type of plastic deformation is not so narrowly restricted. For the vertex B, for instance, any value of $N_0|\epsilon|/M_0|\psi|$ between the limits set by (11) and (12) is possible. Thus,

$$D = \frac{1}{2}N_0|\epsilon| + \frac{3}{4}M_0|\psi| \text{ if } \frac{1}{2} \leqslant \frac{N_0|\epsilon|}{M_0|\psi|} \leqslant \frac{3}{2}, \text{ and } \left|\frac{N}{N_0}\right| = \frac{1}{2}, \left|\frac{M}{M_0}\right| = \frac{3}{4}. \tag{15}$$

Similarly

$$D = N_0|\epsilon| \text{ if } \frac{N_0|\epsilon|}{M_0|\psi|} \geqslant \frac{3}{2} \text{ and } \left|\frac{N}{N_0}\right| = 1, \frac{M}{M_0} = 0, \tag{16}$$

and

$$D = M_0|\psi| \text{ if } 0 \leqslant \frac{N_0|\epsilon|}{M_0|\psi|} \leqslant \frac{1}{2} \text{ and } \frac{N}{N_0} = 0, \left|\frac{M}{M_0}\right| = 1. \tag{17}$$

As is indicated by (17), the manner in which the boundary of the safe domain has been modified in the neighbourhood of the point $N/N_0 = 0$, $M/M_0 = 1$, implies that the response to the loads $N = 0$, $M = M_0$ is no longer necessarily pure bending with $\epsilon = 0$.

3. Plastic Behaviour of Arches

Limit analysis of beams made of highly ductile materials such as structural steel is based on the following empirical fact : when large plastic deformations first develop, they are highly localized so that the deformation of the beam can be adequately described in terms of rigid lengths of beam joined by yield hinges. In fact, for a beam made of a perfectly plastic material large plastic deformations can be shown to occur only in the vicinity of certain critical sections. The same is true for arches made of a perfectly plastic material so that the term " yield hinge " is equally appropriate in this case. There is this difference, however, that a yield hinge in a beam permits only the relative rotation of adjoining sections, whereas a yield hinge in an arch must permit approach or separation of adjoining sections as well as relative rotation.

The mechanical behaviour of a yield hinge in a beam is completely defined by the statement that the bending moment must have the absolute value M_0 while the sense of the relative rotation must correspond to the sign of the bending moment. The mechanical behaviour of a yield hinge in an arch is more complex. If the approximation discussed in connection with Fig. 4 is accepted for the solid rectangular section, equations (13) to (17) define the mechanical behaviour of such a yield hinge provided that ϵ is now interpreted as the separation (or approach) of the sections joined by the hinge and ψ as their relative rotation.

The method of limit analysis of arches presented in the following is based on theorems which were first established by Greenberg and Prager (1951) in the case of beams and frames, then extended by Drucker, Greenberg, and Prager (1951) to problems of plane strain in a continuous medium obeying the stress-strain law of Prandtl and Reuss, and finally extended by the same authors (1952) to more general types of elastic-plastic materials. An alternative proof of these theorems containing a different approach to the problem based on an extended form of an earlier theorem (Hill 1950) has been given by Hill (1951), and the advantages and disadvantages of the two types of approach have been discussed in detail by Lee (1952).

A two-hinged arch is simply indeterminate and a built-in arch is triply indeterminate. In the first case the horizontal thrust is best chosen as the redundant quantity, and in the second case the thrust and the clamping moments at the two ends. In each case, the statically determinate base structure is an arch with a fixed hinge at, say, the left-hand end and a movable hinge at the other end. All distributions of axial force and bending moment which are produced in this base structure by the given loads together with assumed intensities of the redundant quantities will be referred to as " statically admissible states of stress." If such a statically admissible state of stress provides, at each cross section, values of the axial force and bending moment which are represented by a point inside the safe domain of Fig. 4, this state of stress is called a " safe statically admissible state of stress." With this terminology, the first fundamental theorem of limit analysis can be stated as follows :

Theorem I. The given loads cannot be critical if a safe statically admissible state of stress can be found for these loads.

To illustrate the application of this theorem to the limit analysis of arches, consider a two-hinged circular arch of uniform rectangular cross section carrying

Vol. 1 1952/

a single vertical load at the centre of span (Fig. 5). The vertical component of the reaction R at each support equals P, while the horizontal component is the redundant thrust T. For any assumed value of T, the axial force N and the bending moment M are readily computed for any section of the arch. The dangerous sections are the central section 1 and the sections 2 where the tangents to the centre line of the arch are parallel to the reactions R. Indeed, the axial force as well as the bending moment assume higher values at 2 than at the sections immediately to the left or right of 2. The location of the sections 2 depends, of course, on the assumed value of T. According to Theorem I the given load $2P$ cannot be critical if a value of T can be found such that the corresponding values of N and M at the dangerous sections are represented by points inside the safe domain of Fig. 4.

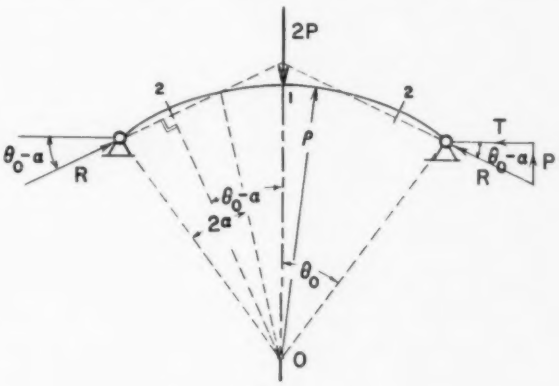

Fig. 5

With the notations of Fig. 5, the values of N and M at the dangerous sections are

$$N_1 = -R\cos(\theta_0 - \alpha),\quad M_1 = \rho R\left[\cos\alpha - \cos(\theta_0 - \alpha)\right], \tag{18}$$

$$N_2 = -R, \qquad M_2 = -\rho R(1 - \cos\alpha), \tag{19}$$

where

$$R = \mathrm{P}\,\mathrm{cosec}\,(\theta_0 - \alpha). \tag{20}$$

Since $T = P\cot(\theta_0 - \alpha)$, the angle α is determined by the value of T: this angle therefore plays the role of a statically indeterminate quantity in equations (18) to (20). A way of determining α is indicated by the following reasoning. Whereas complete neglect of axial forces would not be justified, this influence is secondary compared to that of the bending moments in the case of single loads such as considered here. For the purpose of a rough estimate of the carrying capacity of the arch, the influence of the axial forces may therefore be neglected. To produce yield hinges at the dangerous sections, the moment arms of the reactions R must therefore be the same with respect to these sections. With the notations of Fig. 5, this condition may be written as follows:

$$1 - \cos\alpha = \cos\alpha - \cos(\theta_0 - \alpha). \tag{21}$$

After α has been determined from this equation by trial and error, the absolute value of the bending moment at, say, the section 2 is set equal to M_0, and the resulting equation is solved for P. Thus

$$P = \frac{M_0}{\rho}\,\frac{\sin(\theta_0 - \alpha)}{1 - \cos\alpha}. \tag{22}$$

For $\theta_0 = 45°$, $\rho = 30'$, for instance, one finds $\alpha = 18° 35{\cdot}5'$ from (21) and then $P\rho/M_0 = 8{\cdot}50$ from (22).

In view of the preponderant influence of the bending moments, it may be assumed that $|N/N_0| < \frac{1}{2}$ throughout the arch. Accordingly, (14) must be used in assessing the influence of the axial forces. With the expressions (18) and (19), the condition that sections 1 and 2 be equally dangerous then takes the form

$$\frac{1}{2} + \frac{4\rho}{H}(1 - \cos\alpha) = \frac{1}{2}\cos(\theta_0 - \alpha) + \frac{4\rho}{H}[\cos\alpha - \cos(\theta_0 - \alpha)], \tag{23}$$

where N_0/M_0 has been replaced by $4/H$ in accordance with (4) and (5). After α has been determined from (23) by trial and error, $\frac{1}{2}|N/N_0| + |M/M_0|$ at, say, the section 2 is set equal to unity in accordance with (14), and the resulting equation is solved for P. Thus,

$$P = \frac{M_0}{\rho}\frac{\sin(\theta_0 - \alpha)}{1 - \cos\alpha + (H/8\rho)}. \tag{24}$$

For $\theta_0 = 45°$, $\rho = 30'$, $H = 2'$, for instance, one finds $\alpha = 18° 32{\cdot}6'$ from (23) and then $P\rho/M_0 = 7{\cdot}40$ from (24). With this value of P, the value of $|N/N_0|$ at section 2 is found to be

$$\left|\frac{N}{N_0}\right| = \frac{P}{N_0}\operatorname{cosec}(\theta_0 - \alpha) = \frac{P\rho}{M_0}\frac{H}{4\rho}\operatorname{cosec}(\theta_0 - \alpha) = 0{\cdot}278. \tag{25}$$

Since this value is below 1/2, the use of (14) in establishing (23) was justified.

In the case of the present example, taking account of axial forces thus does not shift the dangerous sections appreciably but lowers the critical load by 13 per cent.

Whereas the first fundamental theorem of limit analysis takes a statical approach to the problem, the second theorem takes a kinematical approach. Yield hinges are assumed at a sufficient number of sections to allow infinitesimal displacements in the structure even though the lengths between successive yield hinges are treated as rigid. Any state of infinitesimal displacement obtained in this manner will be called "kinematically admissible." The work done by the given loads on a kinematically admissible state of displacement is then compared to the mechanical energy dissipated in the yield hinges. If this energy, evaluated from equations (13) to (17), should turn out to be smaller than the work done by the given loads the considered kinematically admissible state of displacement will be called "unsafe." With this terminology, the second fundamental theorem of limit analysis can be stated as follows :

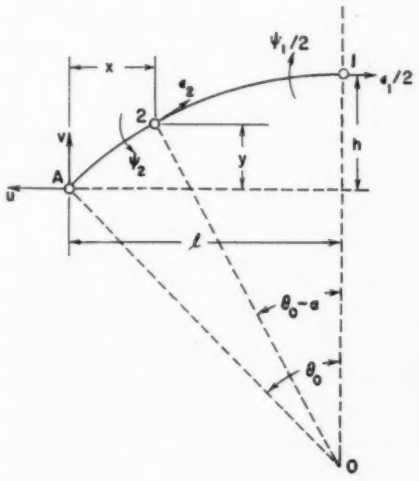

Fig. 6

Theorem II. The given loads exceed the critical loads if an unsafe kinematically admissible state of displacement can be found for the given loads.

To illustrate the application of this theorem to the limit analysis of arches, consider again the problem indicated in Fig. 5. As has been shown above, the statical analysis which neglects the influence of the axial forces furnishes a good approximation to the actual location of the yield hinges even though it gives a too high value for the critical load intensity. The location of the hinges 2 in Fig. 5 will therefore be assumed to correspond to the value $\alpha = 18° 35{\cdot}5'$ which was obtained from (21).

Fig. 6 shows the notations used in evaluating the displacements from the deformations in the yield hinges. It is convenient to determine the displacements relative to the centre of the yield hinge 1. The section immediately to the left of this hinge then moves horizontally to the right by $\epsilon_1/2$ and rotates in the sense indicated in Fig. 6 by $\psi_1/2$. Here, ϵ_1 and ψ_1 denote the approach and the relative rotation, respectively, between the sections which are joined by this yield hinge. Similarly, ϵ_2 and ψ_2 in Fig. 6 indicate the approach and relative rotation between the sections which are joined by the yield hinge 2. Since (14) has been found to apply at all hinges,

$$\epsilon_1 = \beta\psi_1, \; \epsilon_2 = \beta\psi_2, \tag{26}$$

where

$$\beta = \frac{M_0}{2N_0} = \frac{N}{8}. \tag{27}$$

The ratio ψ_2/ψ_1 can now be found from the condition that the left-hand end A of the arch must not have any horizontal displacement u with respect to the centre of the hinge 1. With the notations of Fig. 6, the condition $u = 0$ furnishes

$$\frac{\psi_1}{\psi_2} = \frac{2\left[y + \beta\cos(\theta_0 - \alpha)\right]}{h - \beta} = \frac{2\left[\left(1 + \dfrac{H}{8\rho}\right)\cos(\theta_0 - \alpha) - \cos\theta_0\right]}{1 - \dfrac{H}{8\rho} - \cos\theta_0}. \tag{28}$$

The vertical displacement of the end A relative to the centre of the yield hinge 1 is found to be

$$\begin{aligned} v &= \frac{\psi_1}{2}\,l - \psi_2\left[x - \beta\sin(\theta_0 - \alpha)\right] \\ &= \frac{\psi_2\rho}{2}\left[2\left(1 + \frac{H}{8\rho}\right)\sin(\theta_0 - \alpha) - \left(2 - \frac{\psi_1}{\psi_2}\right)\sin\theta_0\right]. \end{aligned} \tag{29}$$

The central load $2P$ does the work $W = 2Pv$ and, according to (14), the total mechanical energy dissipated at all yield hinges of the arch is $D = M_0(\psi_1 + 2\psi_2)$. Thus, the considered kinematically admissible state of displacement is unsafe if P exceeds the value

$$P^* = \frac{M_0\left(2 + \dfrac{\psi_1}{\psi_2}\right)}{\rho\left[2\left(1 + \dfrac{H}{8\rho}\right)\sin(\theta_0 - \alpha) - \left(2 - \dfrac{\psi_1}{\psi_2}\right)\sin\theta_0\right]}. \tag{30}$$

Here, ψ_1/ψ_2 must be evaluated from (28). With $\theta_0 = 45°$, $\rho = 30'$, $H = 2'$, and $\alpha = 18° 35{\cdot}5'$, one finds $P^* = 7{\cdot}45\, M_0/\rho$. Since an approximate location rather than the exact location of the yield hinges has been used, P^* must exceed the

actual critical load P in accordance with Theorem 2. In fact, the critical load found above from statical considerations was $P = 7{\cdot}40\, M_0/\rho$.

4. Examples

In the case of distributed loads the dangerous sections are less readily determined than in the case of concentrated loads. Moreover, if the load is uniformly distributed over the entire span, it is no longer possible to determine the approximate locations of the dangerous sections by neglecting the axial forces. Indeed, for such a load an arc can be so designed that $N = N_0$, $M = 0$ at all cross sections.

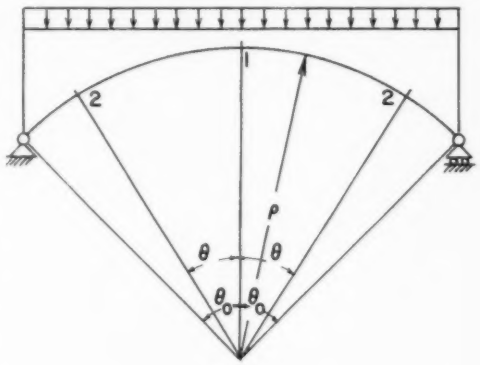

Fig. 7

Consider a two-hinged circular arch of uniform rectangular cross section carrying the distributed load p per unit length of the span. If three yield hinges are assumed as in Fig. 7, some of the previous kinematical formulas remain valid. Only, in view of the preponderance of the axial forces, (13) must now be used instead of (14). This means that in equations (28) and (29) the ratio $H/8\rho$ must be replaced by $3H/8\rho$; also, the angle $\theta_0 - \alpha$ must be replaced by the angle θ indicated in Fig. 7. Thus,

$$\frac{\psi_1}{\psi_2} = \frac{2\left[\left(1 + \frac{3H}{8\rho}\right)\cos\theta - \cos\theta_0\right]}{1 - \frac{3H}{8\rho} - \cos\theta_0}, \tag{31}$$

and

$$v = \frac{\psi_2 \rho}{2}\left[2\left(1 + \frac{3H}{8\rho}\right)\sin\theta - \left(2 - \frac{\psi_1}{\psi_2}\right)\sin\theta_0\right], \tag{32}$$

where ψ_1 and ψ_2 are assumed to have the directions shown in Fig. 6.

The work of the given load is now found to be

$$W = 2\left\{p\rho v \sin\theta_0 - \frac{\psi_1}{2}\frac{p\rho^2}{2}\sin^2\theta_0 - \epsilon_2 p\rho\,(\sin\theta_0 - \sin\theta)\sin\theta + \psi_2\frac{p\rho^2}{2}(\sin\theta_0 - \sin\theta)^2\right\}. \tag{33}$$

According to (13),

$$\epsilon_2 = 3\psi_2\, M_0/2N_0 = \frac{3H}{8}\psi_2. \tag{34}$$

Substitution of this and (32) into (33) furnishes

$$W = \psi_2\, p\rho^2\left[\left(\frac{1}{2}\frac{\psi_1}{\psi_2} - 1\right)\sin^2\theta_0 + \left(1 + \frac{3H}{4\rho}\right)\sin^2\theta\right]. \tag{35}$$

The mechanical energy dissipated in the yield hinges is now

$$D = N_0(\epsilon_1 + 2\epsilon_2) = \frac{3H}{8} N_0(\psi_1 + 2\psi_2) = \frac{3}{2} M_0(\psi_1 + 2\psi_2). \tag{36}$$

By setting D equal to W and solving the resulting equation for p, one finds

$$p = \frac{3M_0\left(2 + \dfrac{\psi_1}{\psi_2}\right)}{\rho^2\left[\left(\dfrac{\psi_1}{\psi_2} - 2\right)\sin^2\theta_0 + \left(2 + \dfrac{3H}{2\rho}\right)\sin^2\theta\right]}, \tag{37}$$

where ψ_1/ψ_2 must be computed from (31). Since this value of p is found from an arbitrarily assumed location θ of the yield hinges 2, it cannot be smaller than the critical value of p. This critical value can therefore be found by determining θ so that the right-hand side of (37) is minimized. This is most readily done by computing p from (37) for a few values of θ and determining the minimum from a graph of p versus θ.

For $\theta_0 = 45°$, $\rho = 30'$, $H = 2'$ the critical value of $2p\rho \sin\theta_0$, i.e. the total load on the arch, is found to be $68{\cdot}1\, M_0/\rho$. This result should be compared with the critical load $2P = 14{\cdot}8\, M_0/\rho$ which this arch can carry as a concentrated load applied at the central cross section.

As a final example, consider the same arch when only the left-hand half of the span carries the uniformly distributed load p. Under such unsymmetric loading the bending moments are preponderant, and the axial forces may be neglected in a preliminary analysis. Consider separately the bending moment diagrams

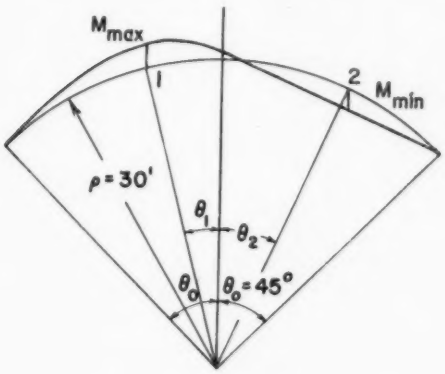

Fig. 8

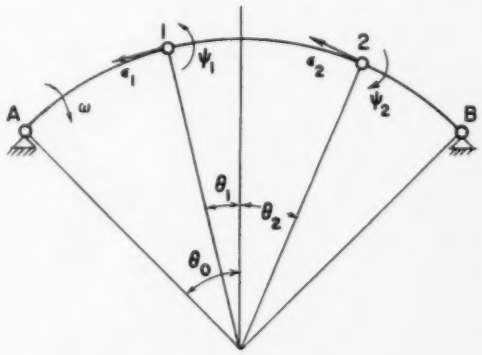

Fig. 9

corresponding to (1) the load and the vertical reactions, and (2) the horizontal thrust. To a suitable scale, the second diagram is given by the centre line of the arch. By trial and error, the first diagram must now be drawn to such a scale that after superposition of the two diagrams the extreme bending moments for the two sides of the arch have equal absolute values (Fig. 8). These extreme bending moments are found to occur at the sections defined by $\theta_1 = 14°$, $\theta_2 = 24°$. The scale of the bending moment diagram of Fig. 8 is determined by the fact that the absolute value of these extreme bending moments must be M_0. From this, the load is found to be $p = 32{\cdot}1\, M_0/\rho^2$ and the thrust $T = 0{\cdot}217\, N_0$. The

axial forces at the sections 1 and 2 of Fig. 8 can now be computed; one finds $N_1/N_0 = 0{\cdot}22$ and $N_2/N_0 = 0{\cdot}23$. Since these values are both smaller than $\frac{1}{2}$, (14) will be used in the following kinematic analysis.

Fig. 9 shows the displacements in the hinges as well as the angular displacement ω of the left-most portion of the arch. The conditions that the horizontal and vertical displacement components of the right-hand end B vanish are

$$\psi_1\rho\,(\cos\theta_1 - \cos\theta_0) - \epsilon_1\cos\theta_1 - \psi_2\rho\,(\cos\theta_2 - \cos\theta_0) - \epsilon_2\cos\theta_2 = 0, \tag{38}$$

$$2\omega\rho\sin\theta_0 - \psi_1\rho\,(\sin\theta_0 + \sin\theta_1) + \epsilon_1\sin\theta_1 + \psi_2\rho\,(\sin\theta_0 - \sin\theta_2) - \epsilon_2\sin\theta_2 = 0. \tag{39}$$

According to (14),

$$\frac{\epsilon_1}{\psi_1} = \frac{\epsilon_1}{\psi_2} = \frac{H}{8}. \tag{40}$$

When this is substituted into (38) and (39), one finds

$$\psi_2/\psi_1 = 1{\cdot}20, \qquad \omega/\psi_1 = 0{\cdot}416. \tag{41}$$

The work of the applied load is

$$W = \omega\frac{p\rho^2}{2}\sin^2\theta_0 + \epsilon_1 p\rho\sin^2\theta_1 - \psi_1\frac{p\rho^2}{2}\sin^2\theta_1$$

$$= \psi_1\frac{p\rho^2}{2}\left[\frac{\omega}{\psi_1}\sin^2\theta_0 - \left(1 - \frac{H}{4\rho}\right)\sin^2\theta_1\right]. \tag{42}$$

Finally, according to (14) the mechanical energy dissipated in the hinges is

$$D = M_0\,(\psi_1 + \psi_2). \tag{43}$$

From $W = D$ it follows that

$$p = \frac{2M_0\left(1 + \dfrac{\psi_2}{\psi_1}\right)}{\rho^2\left[\dfrac{\omega}{\psi_1}\sin^2\theta_0 - \left(1 - \dfrac{H}{4\rho}\right)\sin^2\theta_1\right]} = 29{\cdot}1\,\frac{M_0}{\rho^2}. \tag{44}$$

Since the hinge locations used in this kinematic analysis are only approximate, this value of p cannot be smaller than the actual critical value. If this seems desirable, the influence of small variations of θ_1 and θ_2 in the neighbourhood of the values used above may be studied with the purpose of minimizing p and thus obtaining the actual critical load. According to the authors' experience with this and other problems, however, this is an unnecessary refinement by which a small correction of one or two per cent is obtained at a disproportionate expense in labour.

In conclusion, a word of caution seems to be in order. Limit analysis is based on a more realistic representation of the actual mechanical behaviour of many structural materials than the customary elastic analysis. Limit analysis therefore may eventually replace elastic analysis. As elastic analysis, however, limit analysis must be supplemented by a study of structural stability whenever com-

Vol
1
1952/

pressive axial forces of significant intensity exist in the structure. The preceding discussion thus represents only the first step in a complete analysis of the structure.*

Acknowledgment

The results presented in this paper were obtained in the course of research conducted under Contract N7onr-35801 between the Office of Naval Research and Brown University.

References

Drucker, D. C., Greenberg, H. J. and Prager, W.	1951	*J. Appl. Mech.*, **18**, 371.
Drucker, D. C., Prager, W. and Greenberg, H. J.	1952	*Qu. App. Math.*, **9**, 381.
Greenberg, H. J. and Prager, W.	1951	*Proc. Am. Soc. Civ. Eng.*, **77**, Separate No. 59.
Heyman, J.	1951	*J. Appl. Mech.*, **18**, 157.
Hill, R.	1948	*Qu. J. Mech. App. Math.*, **1**, 18.
	1950	*J. Appl. Mech.*, **17**, 64.
	1951	*Phil. Mag.*, **42**, 868.
Lee, E. H.	1952	*Phil. Mag.*, **43**, 549.

* After the present study had been completed, the authors' attention was drawn to a series of papers by W. Swida, *Der Stahlbau*, 1950, 19, 17 and 29; 1951, 20, 25, in which the same problem is discussed. The method proposed in these papers is exclusively based on considerations of statics (corresponding to Theorem I of the present paper). While the fundamental equations are written in a quite general form special simplifying assumptions are introduced in the examples in order to reduce the amount of algebraic and numerical work. The combination of statical and kinematical considerations discussed in the present paper eliminates the need for such special assumptions, the appropriateness of which is not always easy to judge.

Journal of the Mechanics and Physics of Solids, 1953, Vol. 1, pp. 90 to 102. Pergamon Press Ltd., London.

THE STABILITY AND STRENGTH OF STOCKY BEAMS

By A. R. Flint
Department of Civil Engineering, University of Bristol

(*Received 20th August* 1952)

Summary

A brief analysis has been made of the ultimate strengths of short span I-beams bent in their planes of maximum stiffness by pure terminal couples. In the cases treated, primary failure would occur by lateral buckling in all but the most stocky members. The critical applied moments were less in magnitude than the fully plastic moment, the practical collapse load coinciding with that causing full plasticity of the flanges.

The principle discussed by Shanley (1947) has been assumed applicable to problems of beam stability and the theory has been extended to beams the materials of which exhibit both discontinuous and continuous stress-strain relationships. Estimates of the buckling moments of typical stocky beams have been compared with the results of a series of tests, the theory predicting a lower limit to the range of possible collapse loads.

Vol.
1
1952/5

1. Introduction

The trend towards limit design of complex engineering constructions has led to detailed investigations into the ultimate load-carrying capacity of entire structures, in the course of which the lateral stability of beams stressed beyond the elastic limit has been found to be an important factor. It is known that even stocky beams, the spans of which are not large in relation to their cross-sectional dimensions, will never attain their full strength under pure bending without prior collapse by buckling out of the plane of loading. Thus a complete knowledge of the inelastic behaviour of beams is desirable before design may be safely based upon ultimate strength.

A recent theoretical analysis of the behaviour of yielded mild steel beams of rectangular cross-section has been made by Neal (1949), who compared his solution with the results of tests on small beams under uniform bending moment. These results showed that, although the failing loads predicted by his theory could with great care be attained, collapse might occur at lower loads, even under laboratory conditions. Thus, while providing an estimate of the critical loads for ideal beams, Neal's method gives no indication of the lowest loads at which practical members may fail if subject to small disturbing forces. The load at which bifurcation of the equilibrium position may first occur differs from the conventional critical load, as indicated by Shanley (1947). Columns stressed into the plastic range have usually collapsed at loads slightly greater than those based on a tangent modulus theory, but considerably below the critical loads given by the reduced modulus approach developed by von Karman (1910). It might, therefore, be expected that the Shanley principle could be advisedly

extended to beam problems as providing a theoretical lower limit to the range of applied loads within which lateral buckling may occur. Furthermore, the adoption of this principle considerably simplifies the analysis, especially when treating materials exhibiting a continuous stress-strain relationship.

The present analysis of the inelastic behaviour of symmetrical I-beams is based upon the SHANLEY concept, and is confined to members loaded under uniform bending moment. Materials having both discontinuous and continuous stress-strain relationships are considered.

2. LATERAL BUCKLING UNDER UNIFORM BENDING MOMENT

The critical condition for lateral buckling of a perfect beam loaded in its plane of maximum flexural stiffness is defined by the moment required to maintain the system in a state of neutral equilibrium. A solution to the critical loading under any conditions of support may be derived from the equations of flexural and torsional equilibrium of a member slightly displaced from its stable position. Employing the methods of REISSNER (1904) and CHWALLA (1939) these equations may be written as

$$Bu'' = M\left(1 - \frac{B}{A}\right)\theta, \tag{1}$$

$$C\theta + C_1\theta''' = T_z, \tag{2}$$

where u is the lateral displacement of the shear centre,

θ is the angle of twist,

A and B are the primary and secondary flexural rigidities,

C and C_1 are the torsional and warping rigidities,

M and T_z are the bending moment and torque at any section, and primes denote derivatives with respect to z, the co-ordinate along the longitudinal beam axis, with origin at a support.

It is assumed that the ratio C/A is small compared with unity in deriving equation (1).

For a beam bent by pure terminal couples, M, and supported with rigid torsional supports but with no end restraint to bending actions, M is constant and $T_z = -Mu'$. Hence the general solution for θ may be obtained from (1) and (2) in the form

$$\theta = a \sin mz + b \cos mz + ce^{nz} + de^{-nz} \tag{3}$$

in which

$$m = \left[-\frac{1}{2p^2} + \sqrt{\left(\frac{1}{4p^4} + \frac{1}{q^4}\right)}\right]^{1/2},$$

$$n = \left[\frac{1}{2p^2} + \sqrt{\left(\frac{1}{4p^4} + \frac{1}{q^4}\right)}\right]^{1/2},$$

and

$$p^2 = C_1/C, \qquad q^2 = \frac{C}{M^2}\frac{B}{\left(1 - \frac{B}{A}\right)}.$$

The critical value of the bending moment is then derived by satisfying the end conditions and eliminating the arbitrary constants from (3). The stipulation of no rotation at the supports furnishes the conditions

$\theta = o$ at $z = 0$ and $z = L$, where L is the span.

The remaining conditions are governed by the degree of restraint to sectional warping afforded by the supports. When warping is unrestrained, $\theta'' = 0$ at $z = 0$ and $z = L$, and the critical moment becomes

$$M_{crit} = \frac{\pi}{L}\sqrt{\frac{BC}{\left(1 - \frac{B}{A}\right)}}\left[1 + \frac{\pi^2 C_1}{CL^2}\right]^{1/2}. \tag{4}$$

This expression is similar to that obtained by TIMOSHENKO (1936), with the addition of the term in the denominator.

When warping is rigidly restrained at the supports, as it must be in any experimental attempt to simulate terminal loading, the governing end conditions are $\theta' = 0$ at $z = 0$ and $z = L$. The expression controlling the value of the critical moment becomes

$$(n^2 - m^2) \sin mL \sinh nL + 2mn\,(1 - \cos mL \cosh nL) = 0. \tag{5}$$

The corresponding critical moment is given by

$$M_{crit} = \frac{m}{L}\sqrt{\frac{BC}{\left(1 - \frac{B}{A}\right)}}\left[1 + \frac{m^2 C_1}{C}\right]^{1/2}. \tag{6}$$

Putting $n^2 = m^2 + C/C_1$, the value of the critical moment may be determined from (5) and (6) for any assumed value of CL^2/C_1 by a process of trial and error.

By application of the strain energy method developed by TIMOSHENKO (1910), an approximate solution has been found to the critical moment for a beam having end warping restraint, given by

$$M_{crit} = \frac{\pi}{L}\sqrt{\frac{BC}{\left(1 - \frac{B}{A}\right)}}\left[1 + \frac{4\pi^2 C_1}{CL^2}\right]^{1/2}. \tag{7}$$

This expression shows reasonable agreement with the above analytical solution over a large range of values of CL^2/C_1, and proving simple in application, has been adopted in the present analysis.

It is seen that the magnitude of the buckling moment depends not only upon the initial secondary flexural and torsional stiffnesses of the beam, but also upon its primary flexural and warping rigidities. When a part of the cross-section has been stressed into the plastic range under applied bending actions, these properties are modified, the flexural rigidities decreasing with increased applied moment. Thus, the stability of a partially plastic beam is determined by the relationships between these rigidities and the bending moment, and in the following discussion the problems of the stability of I-beams having two different material properties are treated.

3. SYMMETRICAL MILD STEEL I-BEAMS

(a) *Stress-strain relation*

The material to be considered in the first instance is assumed to have identical properties in tension and compression and to exhibit the stress-strain relation

Vol. 1 1952/5

shown in Fig. 1. The material is wholly elastic until the upper yield stress, rY, is attained, at which a drop in stress occurs at constant strain. On further straining, the stress remains at the lower yield value, Y, until the range of work-hardening is reached. Such properties may be found in annealed mild steel. In contrast, rolled structural steel may show no marked upper yield, and may have differing properties in tension and compression, as discussed by KLINGLER and SACHS (1948).

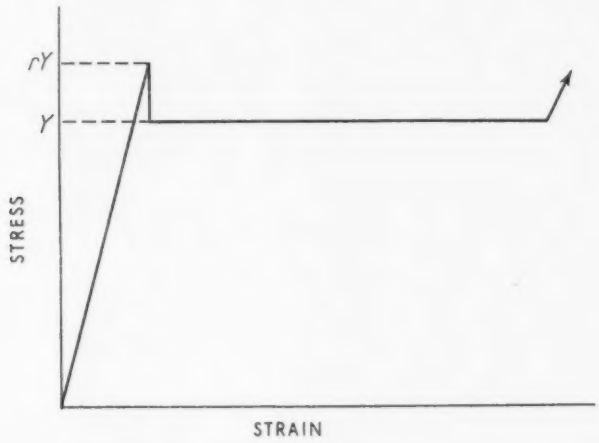

Fig. 1

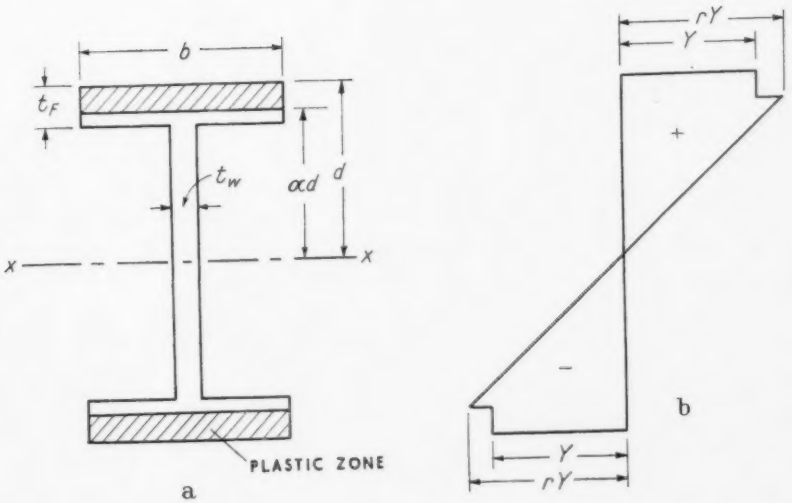

Fig. 2

(b) *Moment of resistance*

In a beam subjected to pure end couples applied about a principal axis, it is evident from symmetry that cross-sectional planes remain plane during bending. Longitudinal strains vary directly with distance from the neutral axis and the

distribution of bending stress in an I-beam bent in its plane of greatest stiffness is consequently similar to that shown in Fig. 2b. The upper yield stress is reached at a distance αd from the neutral axis, $x - x$, beyond which the material is stressed at the lower yield stress as in Fig. 2a.

The equilibrium condition that the moment of resistance afforded by the internal forces must equal the applied moment leads to a relationship between the applied moment, the yield stress and the geometry of the cross-section. Where the flange is only partly plastic this relation may be written as

$$\frac{M}{Yd^2} = b(1 - \alpha^2) + 2r\left[\frac{\alpha^2 b}{3} - \frac{\beta^3}{3\alpha}(b - t_w)\right] \tag{8}$$

where $\beta = 1 - t_F/d$.

Similarly, when the flanges are wholly stressed to the yield stress and the web is partly plastic,

$$\frac{M}{Yd^2} = b(1 - \beta^2) - t_w\left[(1 - \alpha^2) - (1 - \beta^2) + \frac{2r\alpha^2}{3}\right]. \tag{9}$$

The fully plastic moment at which the entire section is stressed at the lower yield stress is attained when $\alpha = 0$, and is given by

$$\frac{M_p}{Yd^2} = b(1 - \beta^2) - t_w\beta^2. \tag{10}$$

This represents the maximum moment that the beam will sustain before collapse in the plane of loading, and is used as a basis for comparison in further discussion.

(c) *Primary flexural rigidity*

The stiffness of the beam in the plane of loading has an influence upon the critical load at which lateral buckling occurs, as shown in Section 2, and is determined by the primary flexural rigidity, A, defined by

$$A = M/\rho \tag{11}$$

where ρ is the primary curvature.

In a partially plastic member $\rho = \rho_y/\alpha$, where ρ_y is the curvature at which yield commences in the extreme fibres; hence, putting $\rho_y = rY/Ed$, the primary rigidity becomes

$$A = E\frac{\alpha d}{rY}M, \tag{12}$$

where E is Young's modulus. The ratio between the plastic and elastic primary rigidities may be written as

$$\tau_1 = \frac{A}{EI_1} = \frac{\alpha M}{M_y}$$

where M_y is the moment causing onset of yield in the extreme fibres. For a given value of α, M is known from (8) and (9), and hence τ_1 may be estimated.

(d) *Secondary flexural rigidity*

In accordance with the SHANLEY principle it is assumed that the beam becomes unstable by a gradual process of combined primary and secondary flexure. In this

Vol 1 1952/

way the bending actions may be so co-ordinated that no reversal of stress occurs anywhere in the section, despite differential straining in the flanges. This basic assumption is more likely to be satisfied under practical conditions than the supposition that a beam remains undisplaced laterally and free from disturbing forces until the critical load is reached.

In the case of partially plastic mild steel I-beams the estimation of the secondary flexural rigidity is greatly simplified by the adoption of this principle. The material stressed beyond yield under primary bending may be regarded as totally ineffective when considering secondary bending actions, and the remainder of the section is treated as fully elastic (*cf.* Fig. 2). Thus the ratio of the secondary flexural rigidity, B, to the elastic value, B_e, may be expressed as

$$\tau_2 = \frac{B}{B_e} = \frac{(\alpha - \beta)\, b^3 + \beta t_w{}^3}{(1 - \beta)\, b^3 + \beta t_w{}^3}, \qquad 1 > \alpha > \beta. \tag{14}$$

Similarly
$$\tau_2 = \frac{\alpha t_w{}^3}{(1 - \beta)\, b^3 + \beta t_w{}^3}, \qquad \beta > \alpha > 0. \tag{15}$$

(e) *Torsional rigidity*

The phenomenon of lateral buckling involves failure by instability in a combined flexural and torsional mode. In consequence the stability of a beam depends in part upon its torsional rigidity under pure torsion, defined by the initial relation between applied torque about its longitudinal axis and the ensuing angle of twist, while under constant bending loads. It has been shown experimentally by Morrison and Shepherd (1950) that the initial torsional rigidity of a thin-walled tube overstrained in tension remains at its elastic value, and Neal (1949) has verified, both in theory and experimentally, that the same observation is true for a partially plastic narrow beam. Thus it may be reasonably assumed that no modification need be made to the term representing the elastic torsional rigidity of an I-beam when partly stressed beyond yield in bending.

In addition to the resistance to applied torque provided by the system of shear stresses arising in pure torsion, a beam of open cross-section supported at its ends will exhibit resistance due to shear stresses induced by the restraint of sectional warping.

In the case of an I-beam this resistance is due to differential bending of the flanges alone, and in the range of stocky beams may prove an important factor governing stability. Furthermore, the magnitude of the warping term in the stability equation varies considerably with the conditions of support, as shown in Section 2.

Once the yield stress is attained in the flanges, however, their flexural rigidity in their own plane decreases rapidly with increased bending moment, and the warping rigidity is reduced in proportion. On the assumption that warping displacements occur conjointly with primary and secondary bending displacements, the ratio of the warping rigidity of a partially plastic beam to its elastic value may be seen to be

$$\tau_3 = \frac{\alpha - \beta}{1 - \beta}, \qquad 1 > \alpha > \beta, \tag{16}$$

and
$$\tau_3 = 0, \qquad \beta > \alpha > 0. \tag{17}$$

(f) *Method of solution*

On introducing the modified values of the beam properties into (4) and (7), the critical bending moments for a partially plastic beam may be derived from the equation

$$M_{crit} = \frac{\pi}{L}\sqrt{\frac{BC\tau_2}{\left(1 - \frac{\tau_2 B}{\tau_1 A}\right)}}\left[1 + k\frac{\pi^2 C_1 \tau_3}{CL^2}\right]^{1/2} \tag{18}$$

where $k = 1$ for free warping at the supports,

$k = 4$ for restrained warping at the supports,

and $C_1 = \frac{EI_F h^2}{2}$ for I-beams, in which I_F is the maximum second moment area of one flange and h is the distance between flange centroids.

Moreover, the critical moment must equal the moment of resistance given by (8) and (9).

The method of solution involves the determination of the critical span for an assumed value of the parameter α. Thus the moment of resistance and the reduced rigidities may be simply estimated from the foregoing results, and hence the corresponding value of L is obtained by solution of the quadratic equation obtained by re-forming (18).

Owing to the complexity of the solution it is not possible to present the relationship between slenderness and the ratio of buckling moment to fully plastic moment in a general form for a given material. Thus each section must be treated independently.

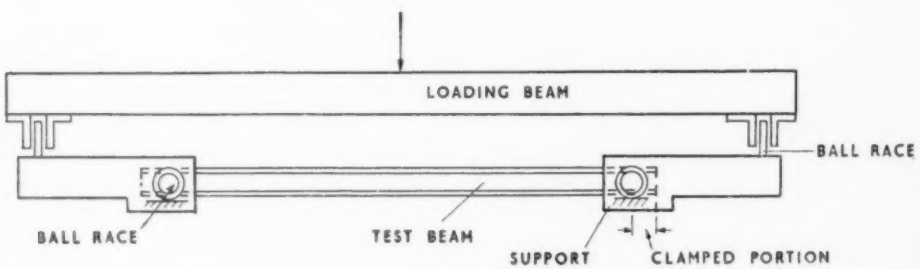

Fig. 3

(g) *Experimental results*

As an example of the behaviour of stocky beams under uniform bending, the buckling moments of 1″ x ¾″ x ⅛″ mild steel I-beams have been estimated by means of the foregoing solution. This theory has been compared with the results of several tests carried out in the Engineering Laboratories of the University of Bristol. A number of I-beams were fabricated from ¾″ x ½″ x ⅛″ Tee section welded web to web. The material was in the condition as rolled and its properties were determined from control tests on specimens cut from the section. In tension the steel had an upper yield stress of 22·00 tons/in.^{2} and a lower yield of 20·94

tons/in.^{2}. The compressive yield stress corresponded to the lower yield in tension but no upper yield was observed in compression, owing to eccentricities of loading inherent in the testing system.

A diagram of the bending rig in which the beams were tested is shown in Fig. 3. The apparatus was designed by T. E. CARMICHAEL (1952) to provide conditions of loading and support closely simulating those assumed in theory, with rigid restraint to warping at the supports. The ends of the test beams were held by clamping blocks, housed in the lever arms through which the terminal couples were applied. The arms were supported on ball races in line with the ends of the test beams and were loaded at their ends through transversely mounted races attached to a loading beam.

Six beams, of spans varying from 9 in. to 39 in., were tested, and their collapse loads were observed, the test results being compared with the theory in Fig. 4. No

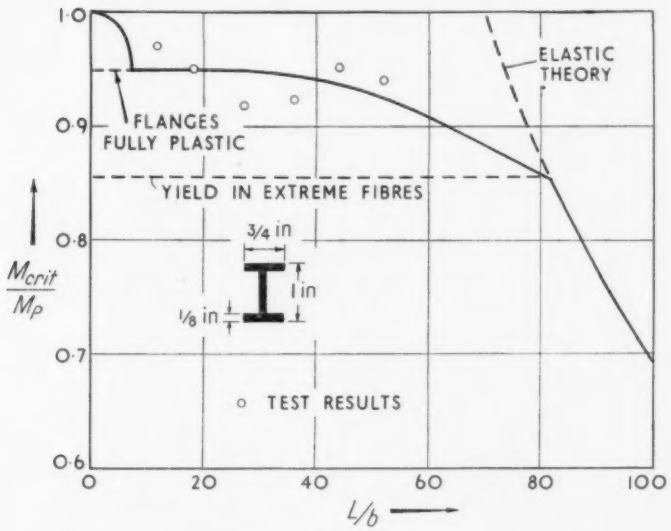

Fig. 4

intentional disturbing force was applied to the beams during testing, although appreciable lateral and torsional displacements developed at loads approaching the buckling load in most instances. The theoretical solution is seen to provide a reasonable estimate of the load carrying capacity of these members, although two failed at rather lower loads than predicted.

It is of interest to note that, over a large range of stocky beams, the buckling moment is nearly equal to that causing full plasticity in the flanges. Thus the fully plastic moment can never be attained, except for very short spans, and it must be expected that primary failure will occur by buckling at the lower moment. For more slender beams the buckling moment decreases gradually with increased span until the span at which the critical moment is equal to that causing onset of yield in the extreme fibres. For further increases in span the buckling moment falls rapidly, the critical value being given by the elastic theory.

4. Symmetrical Aluminium Alloy I-Beams

(a) *Stress-strain relation*

In contrast to the mild steel beams previously discussed, it is of interest to analyse the behaviour of typical beams whose material has a continuous stress-strain relation of the form shown in Fig. 5. The material is assumed to be entirely elastic until the elastic limit, σ_e, is reached. On further straining the stress-strain relation becomes non-linear until a stress, Y, is reached at which the strain continues to increase at constant stress. The properties are typical of many aluminium alloys in structural use, as well as of cold-rolled steel.

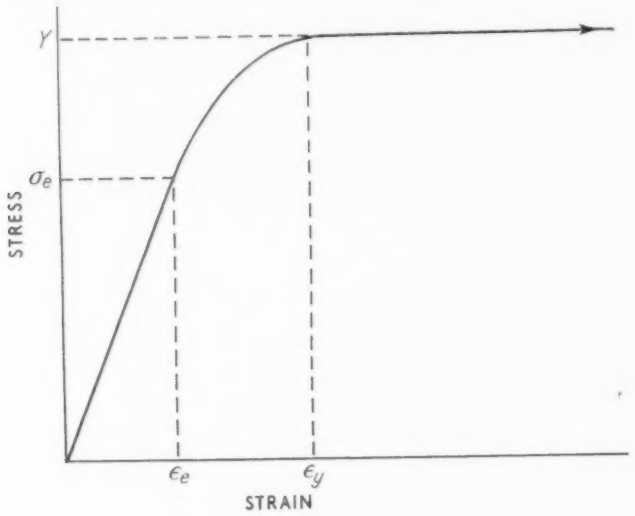

Fig. 5

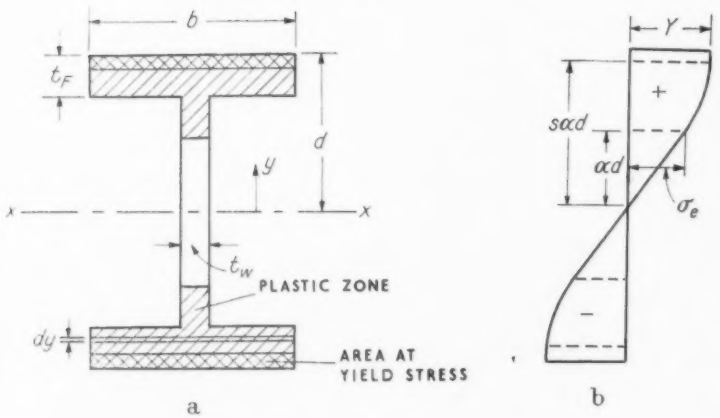

Fig. 6

(b) *Moment of resistance*

The zones of plasticity and the distribution of stress within the section of an I-beam of the assumed material, bent by pure terminal couples into the inelastic

range, are shown in Figs. 6a. and 6b. respectively. The elastic limit is reached at a distance αd from the neutral axis and the strain at any point is $\epsilon_e y/\alpha d$. Thus the stress distribution may be represented as a function of y, say $\sigma = F(y)$. If the ratio of the strain at yield to the strain at the elastic limit is s, the yield stress is reached at a height $\alpha s d$ above the neutral axis.

The moment of resistance is again expressed as a function of α. When $1 > \alpha > \beta$, assuming $\beta > 1/s$,

$$M = \frac{\sigma_e I_e}{\alpha d} + 2b \int_{\alpha d}^{d} F(y)\, y\, dy \tag{19}$$

where I_e is the second moment of area of the elastic portion of the section about $x - x$. Similarly, when $\beta > \alpha > 1/s$,

$$M = \frac{\sigma_e I_e}{\alpha d} + 2t_w \int_{\alpha d}^{\beta d} F(y)\, y\, dy + 2b \int_{\beta d}^{d} F(y)\, y\, dy. \tag{20}$$

When the yield stress is attained in the flanges the moment of resistance becomes

$$M = \frac{\sigma_e I_e}{\alpha d} + 2t_w \int_{\alpha d}^{\beta d} F(y)\, y\, dy + 2b \left\{ \int_{\beta d}^{\alpha s d} F(y)\, y\, dy + \int_{\alpha s d}^{d} Y\, y\, dy \right\}. \tag{21}$$

A similar expression may be used when the yield stress is reached in the web and the fully plastic moment is given by (10).

(c) *Reduced rigidities*

The primary flexural rigidity may again be estimated from (13) in which M_y is replaced by M_e, the applied moment required to stress the extreme fibres to the elastic limit. Thus, in the critical moment equation,

$$\tau_1 = \alpha \frac{M}{M_e}. \tag{22}$$

Calculation of the secondary flexural rigidity is made possible by the adoption of the SHANLEY concept, whereas any attempt to apply a "reduced modulus" approach for a material having a continuous stress-strain relation would prove extremely laborious. The reduced value of this lateral rigidity may be estimated by replacing the elastic modulus by a tangent modulus, μE, in the inelastic parts of the section. Considering an elementary rectangular strip of flange of thickness dy and width b, as in Fig. 6a, it will be seen that its flexural rigidity is given by $\mu E b^3 dy/12$. Thus when the flanges are only partly plastic the total secondary rigidity is given by

$$B = \frac{E}{6} \left[b^3 \left\{ \int_{\alpha d}^{d} \mu\, dy + d\,(\alpha - \beta) \right\} + t_w{}^3\, d\, \beta \right]. \tag{23}$$

When the web is partly plastic this expression becomes

$$B = \frac{E}{6} \left[b^3 \int_{\beta d}^{d} \mu\, dy + t_w{}^3 \left\{ \alpha d + \int_{\alpha d}^{\beta d} \mu\, dy \right\} \right]. \tag{24}$$

As in the case of mild steel beams, the portion of the section stressed to the yield stress is assumed to be ineffective in providing lateral stiffness, and the upper limit to the integrals must be reduced when $\alpha < 1/s$.

Where the web is very thin compared with the flange breadth, its contribution to overall lateral stiffness may be ignored and the ratio of the secondary flexural rigidity to its elastic value becomes

$$\tau_2 = \frac{1}{1-\beta}\left[\frac{1}{d}\int_{\alpha d}^{d} \mu\, dy + \alpha - \beta\right], \qquad 1 > \alpha > \beta, \tag{25}$$

and

$$\tau_2 = \frac{1}{1-\beta}\int_{\beta d}^{d} \mu\, dy, \qquad \beta > \alpha > 1/s, \tag{26}$$

the upper limit to the integral being reduced to $s\alpha d$ when $\alpha < 1/s$.

It may reasonably be assumed that the initial torsional rigidity of the beam again remains unaffected by plastic bending. The warping rigidity, governed by the lateral flexural stiffness of the flanges, decreases as the section is stressed farther into the plastic range; the ratio of its plastic to elastic values, τ_3, will be identical to the expressions given for τ_2 in (25) and (26). Thus $\tau_3 = 0$ when $\beta > s\alpha$.

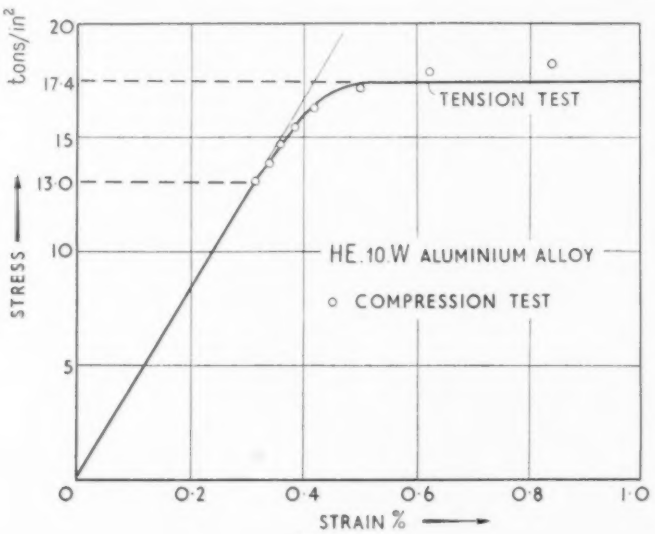

Fig. 7

(d) *Method of solution*

The values of the critical spans for beams having the assumed material properties may again be deduced from (18). For assumed values of α, the reduced rigidities may be estimated from the above expressions by introducing the tangent modulus function, μ, in terms of the variable. Thus, as $\sigma = F(y)$ and $\epsilon = \frac{\epsilon_e y}{\alpha d}$, the tangent modulus is given by

$$\mu E = \frac{d\sigma}{d\epsilon} = \frac{\alpha d}{\epsilon_e}\frac{dF(y)}{dy}. \tag{27}$$

The corresponding end moments may then be obtained from the expressions for moment of resistance and the relationship between critical loading and slenderness may be plotted for any given beam.

(e) *Experimental results*

A further series of tests, carried out with 1″ x 1″ x $\frac{1}{16}$″ extruded I-beams of HE.10.W aluminium alloy material, has afforded an experimental comparison with the tangent modulus theory. The tensile and compressive stress-strain curves for the material are shown in Fig. 7, being identical in the early stages of plasticity but exhibiting slightly differing yield stresses. A function was chosen in the analysis to fit the tensile curve as providing a lower limit to the probable range of mean properties.

The critical moments were estimated as outlined in Section 3 (d), the critical lengths being determined for assumed values of α, and the relation between the ratio of critical to fully plastic moments and slenderness is shown in Fig. 8. The elastic limit is reached at a moment $M = 0{\cdot}666\, M_p$, a much lower fraction than usual in similar mild steel beams. Beyond this value the critical moment drops below the elastic value and tends towards the moment causing full plasticity in the flanges, only $2\frac{1}{2}$ per cent below the fully plastic moment. The fully plastic moment is only attainable for unpractically short spans.

ol.
1
2/53

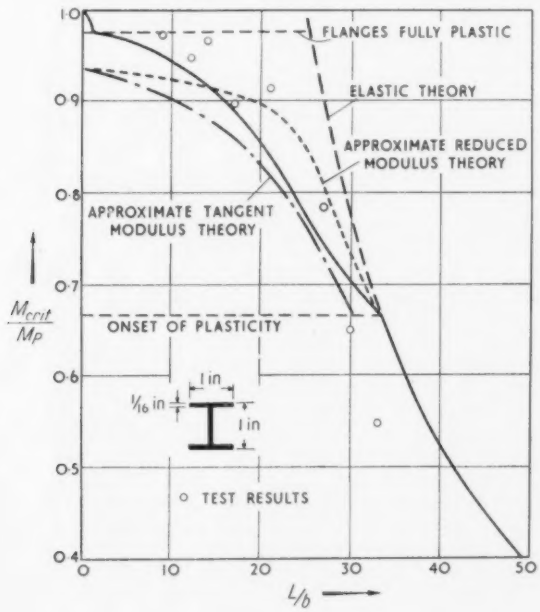

Fig. 8

It has been suggested by Bleich (1952) that a satisfactory approximate solution might be obtained by simply replacing the value of E throughout the section by its tangential value corresponding to the stress in the extreme fibres, when estimating the lateral flexural rigidity. Timoshenko (1936) proposed a similar use of the corresponding reduced modulus. The curves based on both of these assumptions are plotted in Fig. 8, from which it is apparent that the tangent modulus approxi-

mation provides a safe design basis, whereas the reduced modulus curve may prove unsatisfactory in the more slender range of spans.

A number of beams were tested under uniform bending moment in the rig described above, and the observed collapse loads are indicated in Fig. 8. It was found that the more slender beams failed at lower moments than predicted, owing to initial imperfections. The critical loads predicted from measured displacements, by the method due to SOUTHWELL (1932), agreed with the elastic theory however. In the plastic range the degree of scatter was considerable, again possibly owing to the different imperfections encountered. It was evident, however, that the theoretical curve did provide a lower limit for failure within the plastic range and that the moment causing fully plastic flanges was not exceeded.

REFERENCES

BLEICH, F. 1952 *Buckling Strength of Metal Structures*, p. 165 (McGraw Hill).

CARMICHAEL, T. E. 1952 *Thesis*, University of Bristol.

CHWALLA, E. 1939 *Forschungshefte auf dem Gebeite des Stahlbaues*, No. 2 (Berlin).

KARMAN, TH. VON 1910 *Forschungsarbeiten*, No. 81 (Berlin).

KLINGLER, L. J. and SACHS, G. 1948 *J. Aero. Sci.* **15**, 151.

MORRISON, J. L. and SHEPHERD, W. M. 1950 *J. Inst. Mech. Engrs.*, **163**, 1.

NEAL, B. G. 1949 *Phil. Trans. Roy. Soc.* A, **242**, 197.

REISSNER, H. 1904 *S. B. berl. Math. Ges.*, **3**, 53.

SHANLEY, F. R. 1947 *J. Aero. Sci.*, **14**, 261.

SOUTHWELL, R. V. 1932 *Proc. Roy. Soc.* A, **135**.

TIMOSHENKO, S. 1936 *Theory of Elastic Stability*, p. 273 (McGraw Hill).

Vol. 1 1952/

Journal of the Mechanics and Physics of Solids, 1953, Vol. 1, pp. 103 to 112. Pergamon Press Ltd., London.

AN ANALYSIS OF THE PLASTIC BENDING OF A THIN STRIP IN ITS PLANE

By F. A. Gaydon
Department of Theoretical Mechanics, University of Bristol

(*Received 23rd September*, 1952)

Summary

The problem is treated as one of generalized plane stress, and a solution by successive approximation is carried sufficiently far to cover strains realisable in practice. Full account is taken of the variation in thickness and the movement of the neutral surface. The extreme fibre-strain, predicted on the basis of the Mises yield criterion and stress-strain relations, agrees well with experimental data of Sangdahl, Aul, and Sachs (1948).

ol.
1
2/53

1. Introduction

The problem considered is that of a thin rectangular strip bent in its plane by end couples sufficiently large to cause the whole volume to become plastic. It is assumed that there are no through-thickness components of stress, the problem being treated as one of generalized plane stress. The solution given in this paper is one of successive approximation ; it appears to be impossible to obtain an exact analytic solution. Lubahn and Sachs (1950) have obtained numerical solutions for various cases, but their results differ in some respects from those presented here.*

To simplify the analysis a linear yield criterion involving two parameters is used. By special choice of the parameters either the Tresca yield criterion or a sufficient approximation to the Mises yield criterion can, for example, be obtained. Further assumptions are (i) that strain-hardening is negligible, (ii) that the strip is sufficiently long for the stress and strain to be considered uniform along each longitudinal fibre except near the ends, and (iii) that the bending is caused by end-couples only.

It follows from (ii) and (iii) that the radial stress σ_r and circumferential stress σ_θ are the principal stresses. Let a, b (Fig. 1) be the internal and external radii of curvature when the angle of bending is α per unit *original* length, and let (r, θ) be the polar coordinates of any point P of the centre longitudinal section, (it will be verified *a posteriori* that the surfaces are concentric cylinders). Let h be the local thickness at any instant; h varies with r.

* Lubahn and Sachs' numerical work shows that the height $(b - a)$ has decreased by 10 per cent when the ratio height/(external radius of curvature) has reached 5/6. However, according to the analysis given here the height is constant to a high degree of approximation. Again, in their treatment of *plane strain* bending it is tacitly assumed that the fibre whose *resultant* change in length is zero at each stage is the one coinciding with the neutral surface. An exact analysis by Hill (1950) shows, however, that this fibre is actually the one lying midway between the inner and outer surfaces, for bending under conditions of plane strain.

Initially the strip is straight, of height t and thickness h_0, a and b being infinite. At any subsequent time there will exist a surface concentric with the inner and outer ones, such that longitudinal fibres which are being momentarily compressed and those which are being extended lie on opposite sides of it. Let c be the radius of curvature of this surface.

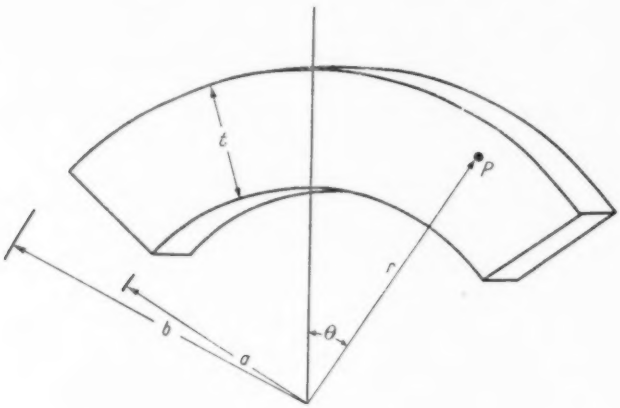

Fig. 1.

In a further small strain, in which the angle of bending increases by an amount $d\alpha$, it is supposed that a particle has displacements $ud\alpha$ radially outwards and $vd\alpha$ circumferentially in the direction of increasing θ. A solution is found for which u is a function of r only and $v = r\theta/\alpha$, and is shown to be consistent with all equations. In this solution plane radial cross-sections remain plane, while the inner and outer surfaces remain concentric and cylindrical throughout the deformation. The equations which have to be satisfied are the yield criterion (discussed in Section 2); the equation of equilibrium

$$\frac{d}{dr}(h\sigma_r) = \frac{h(\sigma_\theta - \sigma_r)}{r}; \tag{1}$$

the LÉVY-MISES relation

$$\frac{\dot{\epsilon}_r}{\dot{\epsilon}_\theta} = \frac{2\sigma_r - \sigma_\theta}{2\sigma_\theta - \sigma_r} \tag{2}$$

where a ' dot ' denotes rate of change with respect to α, following a particle; and the equation of incompressibility,

$$\dot{\epsilon}_r + \dot{\epsilon}_\theta + \frac{\dot{h}}{h} = 0. \tag{3}$$

2. THE YIELD CRITERION

This is taken in the form

$$\left.\begin{aligned} \sigma_\theta - \lambda\sigma_r &= Y, \qquad r \geqslant c \\ \sigma_\theta - \mu\sigma_r &= -Y, \qquad r \leqslant c \end{aligned}\right\} \tag{4}$$

where Y is the uniaxial yield stress. The TRESCA, or maximum shear stress, criterion is obtained from (4) by putting $\lambda = 1, \mu = 0$, since σ_r is everywhere compressive. The relevant portions of the yield locus are in the immediate neighbourhood of the points representing pure tension and compression. The tangents at these points to the MISES ellipse

$$\sigma_\theta^2 - \sigma_r\sigma_\theta + \sigma_r^2 = Y^2$$

are therefore a good approximation to the ellipse itself, and correspond to $\lambda = \frac{1}{2}$ and $\mu = \frac{1}{2}$ in (4).* Other values of λ and μ in the ranges $\frac{1}{2} \leqslant \lambda \leqslant 1$, $0 \leqslant \mu \leqslant \frac{1}{2}$, provide an intermediate locus.

3. FIRST APPROXIMATION

For the first approximation the thickness h is regarded as uniform in equation (1). Then, on substituting in (1) for σ_θ from the first of equations (4), it is found that for $r \geqslant c$

$$\frac{\sigma_r}{Y} = \begin{cases} \dfrac{1}{\lambda - 1}\left[\left(\dfrac{r}{b}\right)^{\lambda-1} - 1\right], & \lambda \neq 1; \\ \ln\left(\dfrac{r}{b}\right), & \lambda = 1. \end{cases}$$

Put $r = b - x$ and expand the right hand side, discarding terms of higher degree than $(x/b)^2$; this still allows consideration of large strains. Then

$$\frac{\sigma_r}{Y} = -\frac{x}{b} + \frac{(\lambda - 2)x^2}{2b^2} \quad \text{for all } \lambda. \tag{5}$$

For $r \leqslant c$ substitute in (1) for σ_θ from the second of equation (4); then

$$\frac{\sigma_r}{Y} = \begin{cases} \dfrac{1}{\mu - 1}\left[1 - \left(\dfrac{r}{a}\right)^{\mu-1}\right], & \mu \neq 1; \\ -\ln(r/a), & \mu = 1. \end{cases}$$

Put $b - a = t$ and $r = b - x$ and expand the right hand side as before; then

$$\frac{\sigma_r}{Y} = \frac{x}{b} - \frac{t}{b} - \frac{(\mu - 2)x^2}{2b^2} + \frac{(\mu - 1)xt}{b^2} - \frac{\mu t^2}{2b^2} \quad \text{for all } \mu. \tag{6}$$

For equilibrium σ_r is continuous at $r = c$, that is at $x = b - c$. Hence, from (5) and (6), a first approximation to c is given by

$$\frac{c}{b} = 1 - \frac{t}{2b} - \frac{(\lambda + \mu)t^2}{16b^2}. \tag{7}$$

From equation (2), since

$$\dot{\epsilon}_r = \frac{\partial u}{\partial r} \quad \text{and} \quad \dot{\epsilon}_\theta = \frac{1}{r}\frac{\partial v}{\partial \theta} + \frac{u}{r}$$

it follows that

* This approximation is of the same order as that used later in other equations.

$$\frac{\partial U}{\partial r}\Big/\left(1+\frac{U}{r}\right)=\frac{2\sigma_r-\sigma_\theta}{2\sigma_\theta-\sigma_r}$$

where $U=u\alpha$. Substitute in the above equation for σ_θ from the first of (4) and for σ_r from (5). Expand the right-hand side retaining terms up to the first degree in x/b; these are all that are required to obtain U to the second degree. Then

$$\frac{\partial U}{\partial x}-\frac{U}{2b}\left(1+\frac{5x}{2b}\right)=\frac{1}{2}\left(1+\frac{3x}{2b}\right).$$

The solution of this equation is

$$\frac{U}{b}=\frac{x}{b}+\frac{x^2}{2b^2}+A\left(1+\frac{x}{2b}+\frac{3x^2}{4b^2}\right),\qquad 0\leqslant x\leqslant b-c. \tag{8}$$

At the neutral surface $\dot{\epsilon}_\theta$ must be continuous; since it changes sign it is therefore zero. Hence

$$U=-c \quad \text{when} \quad \frac{x}{b}=\frac{t}{2b}+\frac{(\lambda+\mu)\,t^2}{16b^2},$$

and therefore $$A=-1+\frac{t}{2b}+\frac{(\lambda+\mu-1)t^2}{16b^2}.$$

Equation (8) thus becomes

$$\frac{U}{b}=-1+\frac{t}{2b}-\frac{x^2}{4b^2}+\frac{xt}{4b^2}+\frac{(\lambda+\mu-1)\,t^2}{16b^2},\qquad 0\leqslant x\leqslant b-c. \tag{9}$$

Similarly, from (6) and the second of (4) it is found that

$$\frac{U}{b}=\frac{x}{2b}+\frac{x^2}{2b^2}-\frac{3xt}{4b^2}+B\left(1+\frac{x}{2b}+\frac{3x^2}{4b^2}-\frac{3xt}{4b^2}\right),\qquad b-c\leqslant x\leqslant t. \tag{10}$$

The condition at the neutral surface determines

$$B=-1+\frac{t}{2b}+\frac{(\lambda+\mu-1)\,t^2}{16b^2}$$

and therefore

$$\frac{U}{b}=-1+\frac{t}{2b}-\frac{x^2}{4b^2}+\frac{xt}{4b^2}+\frac{(\lambda+\mu-1)\,t^2}{16b^2},\qquad b-c\leqslant x\leqslant t. \tag{11}$$

Put $x=0$ in (9) and $x=t$ in (11); then

$$\alpha\frac{da}{b}=\alpha\frac{db}{b}=\left[-1+\frac{t}{2b}+\frac{(\lambda+\mu-1)\,t^2}{16b^2}\right]d\alpha. \tag{12}$$

Therefore, to this order of approximation, $db-da=0$ and $b-a=t$ is constant throughout the deformation. Integration of (12) leads to

$$\alpha=\frac{1}{b}\left[1+\frac{t}{2b}+\frac{(\lambda+\mu+7)\,t^2}{32b^2}\right]. \tag{13}$$

4. Variations in Thickness

Before the equation for h can be found it is necessary to obtain the relation between the original coordinate x_0 of a particular particle and its current coordinate x.

Vol. 1 1952/5

When α increases by $d\alpha$ the incremental radial displacement is $ud\alpha$; b increases algebraically by db and x by dx. Therefore $ud\alpha = db - dx$; that is

$$\frac{Dx}{Db} = 1 - u\frac{d\alpha}{db},$$

where D/Db denotes differentiation following the particle. Substitute in this equation from (9) and (12); then

$$\frac{Dx}{Db} = \frac{xt}{4b^2} - \frac{x^2}{4b^2}.$$

The solution to the present degree of approximation is

$$\frac{x}{b} = \frac{x_0}{b} - \frac{x_0 t}{4b^2} + \frac{x_0^2}{4b^2}. \tag{14}$$

The inverse relation, which is also required, is

$$\frac{x_0}{b} = \frac{x}{b} + \frac{xt}{4b^2} - \frac{x^2}{4b^2}. \tag{15}$$

To obtain h to the second degree, the through-thickness strain rate is required to the second degree and therefore also $\dot{\epsilon}_r$. Hence it is not sufficient to differentiate U as given by (9). Instead the LÉVY-MISES equation (2) must be used.

Now, since $v = r\theta/\alpha$,

$$\alpha\dot{\epsilon}_\theta = 1 + \frac{u\alpha}{r} = -\frac{x}{b} + \frac{t}{2b} - \frac{5x^2}{4b^2} + \frac{3xt}{4b^2} + \frac{(\lambda+\mu-1)\,t^2}{16b^2}, \qquad 0 \leqslant x \leqslant t, \tag{16}$$

and so, from (2),

$$\alpha\dot{\epsilon}_r = \begin{cases} \dfrac{x}{2b} - \dfrac{t}{4b} + \dfrac{11x^2}{8b^2} - \dfrac{3xt}{4b^2} - \dfrac{(\lambda+\mu-1)\,t^2}{32b^2}, & 0 \leqslant x \leqslant b-c; \\ \dfrac{x}{2b} - \dfrac{t}{4b} + \dfrac{11x^2}{8b^2} - \dfrac{3xt}{2b^2} - \dfrac{(\lambda+\mu-13)\,t^2}{32b^2}, & b-c \leqslant x \leqslant t. \end{cases}$$

From these, together with (16) and (3), it follows that

$$\frac{\alpha}{h}\frac{Dh}{D\alpha} = \begin{cases} \dfrac{x}{2b} - \dfrac{t}{4b} - \dfrac{x^2}{8b^2} - \dfrac{(\lambda+\mu-1)\,t^2}{32b^2}, & 0 \leqslant x \leqslant b-c; \qquad (17) \\ \dfrac{x}{2b} - \dfrac{t}{4b} - \dfrac{x^2}{8b^2} + \dfrac{3xt}{4b^2} - \dfrac{(\lambda+\mu+11)\,t^2}{32b^2}, & b-c \leqslant x \leqslant t. \qquad (18) \end{cases}$$

Substitution from (12) and (14) in (17) gives

$$\frac{b}{h}\frac{Dh}{Db} = \frac{t}{4b} - \frac{x_0}{2b} - \frac{x_0 t}{8b^2} + \frac{(\lambda+\mu+3)\,t^2}{32b^2}.$$

On integrating and afterwards substituting for x_0 from (15),

$$\frac{h}{h_0} = 1 + \frac{x}{2b} - \frac{t}{4b} + \frac{xt}{16b^2} - \frac{(\lambda+\mu+1)\,t^2}{64b^2}, \qquad 0 \leqslant x \leqslant b-c \tag{19}$$

Similarly,

$$\frac{h}{h_0} = 1 + \frac{x}{2b} - \frac{t}{4b} + \frac{7xt}{16b^2} - \frac{(\lambda + \mu + 13)\, t^2}{64b^2}, \qquad b - c \leqslant x \leqslant t \tag{20}$$

5. Second Approximation

Return now to (1) and substitute

$$\frac{h}{h_0} = 1 + \frac{x}{2b} - \frac{t}{4b}.$$

For $0 \leqslant x \leqslant b - c$ the equation becomes

$$\frac{\partial}{\partial x}\left\{\left(1 + \frac{x}{2b} - \frac{t}{4b}\right)\frac{\sigma_r}{Y}\right\} = -\frac{1}{b}\left(1 + \frac{x}{b}\right)\left(1 + \frac{x}{2b} - \frac{t}{4b}\right)\left[1 + (\lambda - 1)\frac{\sigma_r}{Y}\right].$$

Only first degree terms need be retained on the right-hand side. The solution of this equation is then

$$\frac{\sigma_r}{Y} = -\frac{x}{b} + \frac{(2\lambda - 3)\, x^2}{4b^2}, \qquad 0 \leqslant x \leqslant b - c. \tag{21}$$

Similarly,

$$\frac{\sigma_r}{Y} = \frac{x}{b} - \frac{t}{b} - \frac{(2\mu - 3)\, x^2}{4b^2} + \frac{(2\mu - 1)\, xt}{2b^2} - \frac{(2\mu + 1)t^2}{4b^2}, \qquad b - c \leqslant x \leqslant t. \tag{22}$$

On equating the right-hand sides of equations (21) and (22) for $x = b - c$, a second approximation for c is found to be

$$\frac{c}{b} = 1 - \frac{t}{2b} - \frac{(\lambda + \mu + 1)\, t^2}{16b^2}. \tag{23}$$

The first order terms in equations (21) and (22) are the same as those in the first approximation for the stresses given by (5) and (6). It follows that these stresses will not alter U to second degree as given by (8) and (10). However, the constants A and B are altered in consequence of the use of (23) in the boundary condition instead of (7). The alterations amount to replacing $\lambda + \mu$ by $\lambda + \mu + 1$, so that the second approximation to U is

$$\frac{U}{b} = -1 + \frac{t}{2b} - \frac{x^2}{4b^2} + \frac{xt}{4b^2} + \frac{(\lambda + \mu)\, t^2}{16b^2}, \qquad 0 \leqslant x \leqslant t. \tag{24}$$

Note that this second approximation still gives $dt = db - da = 0$. In like manner (13) becomes

$$\alpha = \frac{1}{b}\left[1 + \frac{t}{2b} + \frac{(\lambda + \mu + 8)\, t^2}{32b^2}\right], \tag{25}$$

and the equations for h/h_0 become

$$\frac{h}{h_0} = 1 + \frac{x}{2b} - \frac{t}{4b} + \frac{xt}{16b^2} - \frac{(\lambda + \mu + 2)\, t^2}{64b^2}, \qquad 0 \leqslant x \leqslant b - c\,; \tag{26}$$

$$\frac{h}{h_0} = 1 + \frac{x}{2b} - \frac{t}{4b} + \frac{7xt}{16b^2} - \frac{(\lambda + \mu + 14)\, t^2}{64b^2}, \qquad b - c \leqslant x \leqslant t. \tag{27}$$

From (4), (21) and (22) the circumferential stress is given by

$$\frac{\sigma_\theta}{Y} = 1 - \frac{\lambda x}{b} + \frac{\lambda(2\lambda - 3)x^2}{4b^2}, \quad 0 \leqslant x \leqslant b - c; \tag{28}$$

$$\frac{\sigma_\theta}{Y} = -1 + \frac{\mu(x-t)}{b} - \frac{\mu^2(x-t)^2}{2b^2} + \frac{\mu(x-t)(3x+t)}{4b^2}, \quad b - c \leqslant x \leqslant t. \tag{29}$$

Equations (23) to (27) involve λ and μ in the combination $\lambda + \mu$ only. These equations are thus identical for the TRESCA and the linearised MISES criteria, since $\lambda + \mu = 1$ for both. The stresses, however, are different.

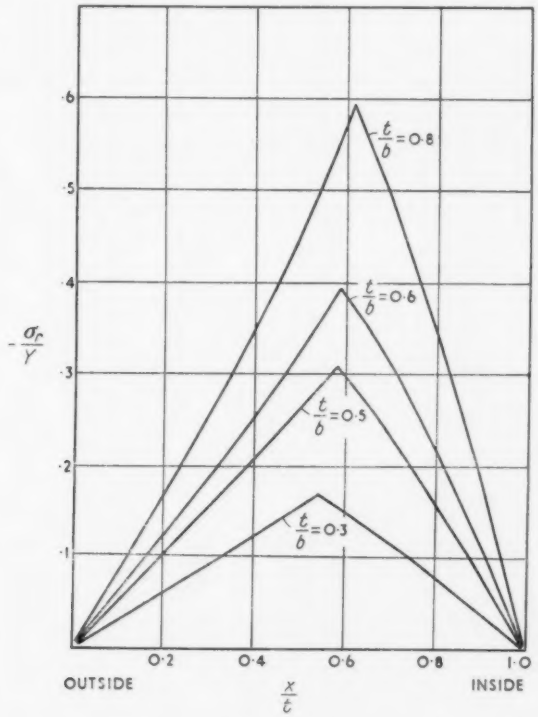

Fig. 2. Variations of radial stress as bending progresses (TRESCA yield criterion).

6. THIRD APPROXIMATION TO THE STRESSES

σ_r can now be found correct to the third power of x/b by substituting in (1) the second degree expressions for h/h_0, namely equations (26) and (27). Then

$$\frac{\sigma_r}{Y} = -\frac{x}{b} + \frac{(2\lambda - 3)x^2}{4b^2} - \frac{(4\lambda^2 - 16\lambda + 21)x^3}{24b^3} + \frac{3x^2 t}{32b^3}, \quad 0 \leqslant x \leqslant b - c; \tag{30}$$

and

$$\frac{\sigma_r}{Y} = \frac{x}{b} - \frac{t}{b} - \frac{(2\mu - 3)x^2}{4b^2} + \frac{(2\mu - 1)xt}{2b^2} - \frac{(2\mu + 1)t^2}{4b^2} + \frac{(4\mu^2 - 16\mu + 21)x^3}{24b^3}$$
$$- \frac{(16\mu^2 - 32\mu + 33)x^2 t}{32b^3} + \frac{(8\mu^2 + 7)xt^2}{16b^3} - \frac{(16\mu^2 + 32\mu + 27)t^3}{96b^3}, \quad b - c \leqslant x \leqslant t, \tag{31}$$

from which the third degree expression for c/b is found to be

$$\frac{c}{b} = 1 - \frac{t}{2b} - \frac{(\lambda + \mu + 1)\, t^2}{16b^2} - \frac{(\lambda^2 - \mu^2 + 5\lambda + 7\mu + 6)\, t^3}{192b^3}. \tag{32}$$

σ_r/Y is plotted against x/t for different values of t/b in Fig. 2 for the TRESCA criterion $\lambda = 1$, $\mu = 0$, and in Fig. 3 for the linearised MISES criterion $\lambda = \frac{1}{2}$, $\mu = \frac{1}{2}$. For both criteria equation (32) reduces to

$$\frac{c}{b} = 1 - \frac{t}{2b} - \frac{t^2}{8b^2} - \frac{t^3}{16b^3}. \tag{33}$$

It is interesting to observe that this value of c is the same as that given by the first four terms of the expansion of $c = \sqrt{(ab)}$ in powers of t/b. It is remarkable that $\sqrt{(ab)}$ is also the radius of the neutral surface in the plane strain problem whatever criterion is used (HILL 1950); moreover t remains strictly constant there.

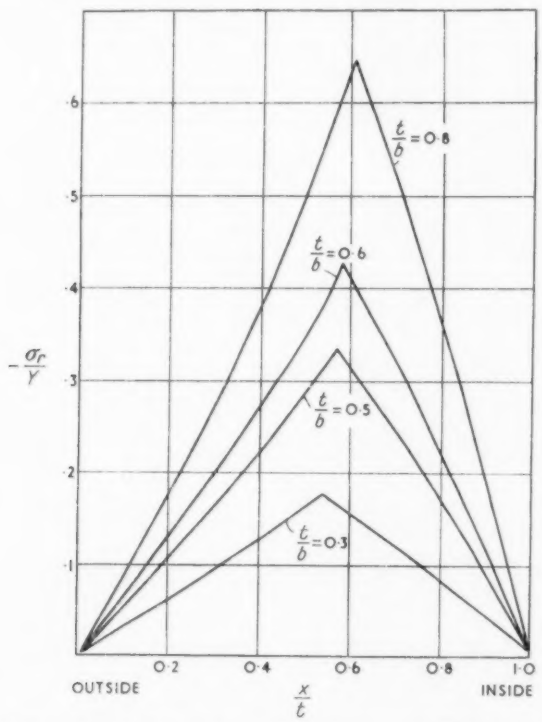

Fig. 3. Variation of radial stress as bending progresses (MISES yield criterion).

7. THE BENDING COUPLE

The couple is given by

$$G = -\int_0^{b-c} \sigma_\theta\, h x dx - \int_{b-c}^{t} \sigma_\theta\, h x dx$$

where, for convenience, moments are taken about $x = 0$. After integration, this gives

$$G = \frac{1}{4} Y h_0 t^2 \left[1 - \frac{(\lambda - \mu) t}{12b}\right]. \tag{34}$$

It is to be remarked that the couple remains constant, to this approximation, for the MISES yield criterion ($\lambda = \mu = \frac{1}{2}$).

8. COMPARISON WITH EXPERIMENT

The total logarithmic strain ϵ_θ at the outer surface is

$$\epsilon_\theta = \ln b\alpha = \frac{t}{2b} + \frac{(\lambda + \mu + 4) t^2}{32b^2}, \text{ from (25).}$$

This reduces to

$$\epsilon_\theta = \frac{t}{2b} + \frac{5t^2}{32b^2},$$

for $\lambda + \mu = 1$ (Fig. 4). The exact solution for the same quantity in the corresponding plane strain problem is

$$\epsilon_\theta = \ln\left(\frac{2b}{a+b}\right) \sim \frac{t}{2b} + \frac{t^2}{8b^2},$$

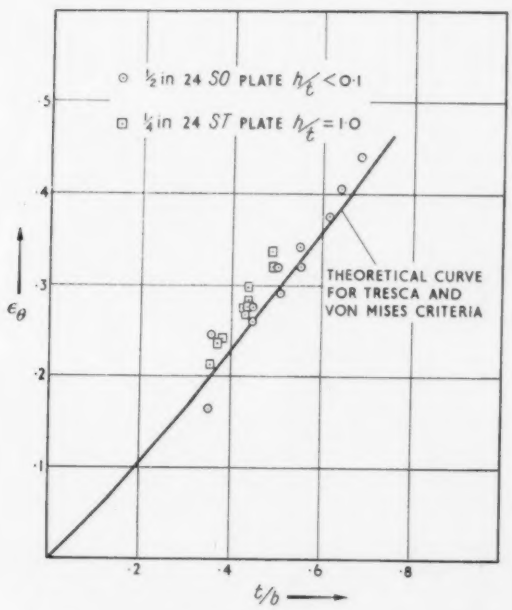

Fig. 4. Variation of external circumferential strain.

which, on the scale used, is indistinguishable from that shown. Also plotted on Fig. 4 are the results of experiments by SANGDAHL, AUL, and SACHS (1948) on an aluminium alloy. It can be seen that these agree as well as can be expected in view of the assumptions of isotropy and no strain-hardening. A small decrease

in height t was observed in these experiments (5 per cent when $t/b = 0{\cdot}6$); this can probably be attributed to anisotropy or strain-hardening, or both together.

ACKNOWLEDGMENTS

I wish to thank Dr. R. HILL for many helpful suggestions and criticisms, and Mr. S. T. NEWING for checking part of the calculations.

REFERENCES

HILL, R. 1950 *Mathematical Theory of Plasticity* (Clarendon Press, Oxford), pp. 287-292.

LUBAHN, J. D. and SACHS, G. 1950 *Trans. Am. Soc. Mech. Eng.*, **72**, 201.

SANGDAHL, G. S., AUL, E. L. and SACHS, G. 1948 *Proc. Soc. Exp. Stress Analysis*, **6**, 1.

Vol. 1 1952/

Journal of the Mechanics and Physics of Solids, 1953, Vol. 1, pp. 113 to 128. Pergamon Press Ltd., London.

AN INVESTIGATION OF THE PLASTIC BEHAVIOUR OF METAL RODS SUBJECTED TO LONGITUDINAL IMPACT

By J. D. Campbell
Department of Engineering Science, University of Oxford

(*Received 30th September*, 1952)

Summary

The difficulties inherent in attempts to obtain dynamic stress-strain relations by conventional experimental methods are discussed. A new method of test is described, in which these difficulties are avoided ; in this test a cylindrical specimen is subjected to compressive impact and the strain developed in it is measured electrically. Results of tests on aluminium alloy specimens are given, and a dynamic stress-strain relation is derived.

ol.
1
2/53

1. Introduction

Many investigations have been made in order to obtain data concerning the behaviour of metals subjected to rapid loading. One of the earliest was that of Hopkinson (1905) who carried out experiments in which a wire was subjected to tensile impact by means of a falling weight. The results of these experiments indicated that iron wire was able to withstand stresses considerably greater than the static yield stress for a time of the order of 10^{-4} sec., without appreciable permanent set occurring. Later, various investigators (Ginns 1937; Clark and Datwyler 1938; Brown and Vincent 1941) devised apparatus designed to give direct measurement of the stress and strain occurring during an impact test, and thus to give a dynamic stress-strain relation. However, the accuracy of results obtained in this way is seriously limited, owing to a number of difficulties which are discussed in Section 2 below. It appears that no accurate measurement has been made of the part of the dynamic stress-strain curve in which the plastic and elastic strains are of the same order.

The present paper describes some experiments carried out in order to obtain information regarding the onset of plastic deformation in a metal under impact loading, using a new method of test in which, it is believed, some of the main difficulties of impact testing are avoided.

2. Method of Test

(i) *General Considerations*

There appear to be three main difficulties inherent in any attempt to derive a dynamic stress-strain curve directly by measurement during tensile impact tests on short specimens.

(a) *Inertia of the specimen.* If the velocity of impact is great enough to cause even moderately rapid straining, wave propagation effects will cause large variations of strain along the length of the specimen at any given instant. The theory of plastic wave propagation, developed independently by TAYLOR (1946) and VON KARMAN (1946), has been applied to the tensile impact test by CLARK and DUWEZ (1948). They have shown that, owing to wave propagation effects, an impact test in which the stress is measured at one end of a tension specimen and the strain is derived from the total extension of the specimen will give a diagram different from the stress-strain relation of the material.

(b) *Inertia of the weighbar.* A number of investigators have used apparatus in which the stress is determined by measurement of the strain in an elastic weighbar in series with the specimen. With this arrangement, stress waves are propagated along the weighbar and give rise to oscillations in the weighbar signal, thus rendering accurate interpretation of the results very difficult. An analysis of this effect has also been made by CLARK and DUWEZ.

(c) *Eccentricity of loading.* In a tensile test, it is necessary to attach to the specimen an anvil which is struck by a hammer. Owing to the very small time intervals involved, it is almost impossible to ensure axiality of loading with this arrangement. For example, if the strain at yield is 10^{-3}, and the rate of strain is assumed to be 10 sec.$^{-1}$, yield will occur in 10^{-4} sec. Thus, assuming that impact between the anvil and hammer occurs at two diametrically opposite points, the time between the two blows must be small compared with 10^{-4} sec. Moreover, at all times the difference between the forces exerted at the two points must be exceedingly small if serious bending effects are to be avoided. These conditions appear to be impossible to fulfil in practice.

Vol. 1 1952/5

(ii) *Repeated impact tests*

In view of the difficulties discussed in Section 2 (i) an entirely different method of test was devised. This method is one of repeated compressive impact on each specimen, and uses the inertia of the specimen itself to generate the stress. It depends on the fact that if a free cylindrical specimen is subjected to axial compressive impact each element of the specimen will be subjected to stress for a short interval of time. At the instant of impact a compressive stress wave is propagated into the specimen, and this is reflected from the free end as a wave of unloading. The impact is terminated soon after this reflected wave reaches the impact end, and the specimen then moves on at a speed greater than the impact velocity, both its ends being free of stress. The magnitude of the stress to which a given element of the specimen is subjected depends on the impact velocity, and the duration of the stress depends mainly on the distance of the element from the free end of the specimen. From measurements of the strain occurring at any given point in the specimen some of the dynamic properties of the material may be derived.

The advantages of this method of test are that since no anvil or weighbar is attached to the specimen effects due to the measuring apparatus itself are eliminated, and that by using a compressive impact the eccentricity of loading can be reduced to an acceptable amount.

The strain-time variation at any position may be recorded by means of resistance

strain gauges of small gauge length, in conjunction with a cathode ray tube and camera. The record thus obtained will indicate for the gauge position

(a) the maximum strain occurring during the impact (ϵ'),

(b) the permanent strain after unloading (ϵ''),

and (c) the rate of loading and unloading.

It would in principle be possible to determine the dynamic elastic limit by carrying out a series of tests on a specimen, increasing the impact velocity until permanent set first occurred. If the value of ϵ' were then ϵ_0, the stress at the elastic limit would be given by

$$\sigma_0 = E\,\epsilon_0 \tag{1}$$

where E is the dynamic modulus of elasticity.

The value of this modulus may be obtained from a vibration test; however, since it must lie between the values for isothermal and adiabatic conditions, and it can be shown that for most metals these values differ by less than 0·5 per cent, a static test may be used.

The value of σ_0 can be obtained accurately by the above method only for a metal with a sharp yield point. If there is no definite yield point, the permanent set may be small after unloading from stresses considerably greater than σ_0. However, the dynamic proof stress corresponding to a given permanent set ϵ'' may be calculated if it is assumed that the metal unloads elastically, as in a static test. This stress is given by

$$\sigma' = E\,(\epsilon' - \epsilon'') \tag{2}$$

From a number of tests on different specimens at various impact velocities a dynamic stress-strain diagram may be obtained by plotting corresponding values of σ' and ϵ'. If it is assumed that on reloading a specimen the metal follows the original stress-strain diagram as soon as the stress exceeds the previous maximum, the diagram may be obtained by repeated tests on the same specimen. Thus, if the suffix n refers to the values obtained in the nth test on a particular specimen, a point on its dynamic stress-strain curve is given by

$$\left.\begin{aligned} \sigma &= \sigma_n' = E\,(\epsilon_n' - \epsilon_n''), \\ \epsilon &= \epsilon_n' + (\epsilon_1'' + \epsilon_2'' + \ldots + \epsilon_{n-1}'') \end{aligned}\right\} \tag{3}$$

This eliminates the necessity of testing a large number of different specimens, with the consequent probable scatter due to variation between specimens.

3. Details of Apparatus

(i) *Mechanical*

The specimens used were cylindrical, $\frac{1}{2}$ inch in diameter and 11 inches in length, the strain gauges being placed 1 inch from the impact end. During the test the specimen was mounted in guides with its axis vertical; a rubber disc was used to apply sufficient friction to prevent the specimen falling under its own weight, but apart from this the specimen was free to move vertically.

The impact was applied by a steel disc $1\frac{1}{2}$ inches in thickness, which formed part of a falling weight. This weight could be raised to any height up to 18 feet and was guided by steel wires. The arrangement of specimen and weight as used originally is shown in Fig. 1 (a). It was found that with this arrangement

large eccentricity of loading occurred when plane ended specimens were used; this was due to the impossibility of ensuring simultaneous contact over the whole end plane of the specimen. A great improvement was effected by machining the end of the specimen to a spherical shape, of radius 1 inch. Considerable eccentricity of loading was, however, still evident (see Section 5 (ii)); this was due to the fact that, owing to tilting oscillations during its descent, the impacting surface of the falling weight was not exactly horizontal at the moment of impact. A modified arrangement was therefore used in which the impact was transmitted through a hardened steel rod coaxial with the specimen. This rod was supported in guides with its plane end in contact with the rounded end of the specimen, as shown in Fig. 1 (b). This arrangement ensured that initially the surface transmitting the impact stress to the specimen was normal to the axis of the specimen. Moreover, flexural displacements in an elastic rod are transmitted more slowly than axial displacements, the velocity of propagation of the former decreasing with increasing wavelength. Thus it was expected that during the time of loading of the specimen the motion of the end of the steel rod would be little affected by disturbances due to non-axial impact by the falling weight. Evidence that with this arrangement the effect of eccentricity of loading was small was given by tests in which the difference between the outputs of diametrically opposite strain gauges was measured (see Section 5 (ii)). It was found that with this method of loading the experimental results were consistent and repeatable.

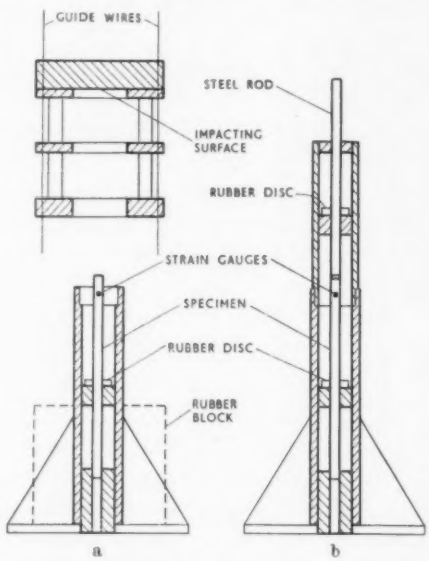

Fig. 1. Impact apparatus.
(a) Arrangement for direct impact, showing falling weight. (b) Arrangement for impact transmitted through steel rod.

Shortly after the impact the falling weight was arrested by a rubber block. The specimen and steel rod were free to move axially, apart from the small friction forces exerted by the rubber discs used to bring them to rest (see Fig. 1.).

(ii) *Electrical*

The resistance strain gauges used were of Type 6H manufactured by *H. Tinsley & Co. Ltd.* This type of gauge has a resistance of about 50 ohms and a gauge length of 8 mm; its mass is small (about 0·04 gm), thus minimizing inertia effects.

On each specimen two gauges were cemented diametrically opposite to each other and connected in series. The gauges were connected in a simple potentiometer circuit, the output being fed to an amplifier. For some tests the potentiometer formed part of a Wheatstone Bridge circuit, so that the permanent strain could be measured after impact (see Section 5 (iii)).

Vol 1 1952/

The amplified signal was applied to the Y-plates of a high-speed cathode ray tube (type VCR 87). To the X-plates was applied the output of a single stroke generator, triggered by the signal. The duration of the sweep could be varied, and was usually set at about 400 microseconds. The "writing speed" of the spot was of the order of 10^5 cm/sec. and it was found that in order to obtain a satisfactory photographic record of the trace it was necessary to switch the beam to full brightness during the movement of the spot. This was done by means of a brightening pulse generator, also triggered by the signal, whose output was applied to the grid of the cathod ray tube.

In order to provide a timing mark on the record, the beam was interrupted every 10 microseconds by means of a crystal-controlled resistance-capacity oscillator.

(iii) *Photographic*

The camera used was a Cossor Model 427 oscillograph camera with an $f/3{\cdot}5$ lens. The film used was Ilford Recording Film Type 5G91. The negatives obtained were inserted in an enlarger, and the image projected on to squared paper and traced.

ol.
1
2/53

4. Calibration

The voltage output of the potentiometer circuit is given by

$$\Delta e = \frac{R_1}{R_1 + R} . I \Delta R \tag{4}$$

where R is the total gauge resistance, ΔR is the change in R, R_1 is the resistance in series with the gauges, and I is the gauge current.

If the change of resistance ΔR is due to a mechanical strain ϵ,

$$\Delta R = RS\epsilon \tag{5}$$

where S is the gauge factor. This factor is a constant for any particular gauge. It is determined by the manufacturers for each batch of gauges and the accuracy claimed is $\pm$ 2 per cent. In order to check the response of the gauges under dynamic conditions, however, a series of tests under elastic conditions was carried out (see Section 5 (ii)).

From equations (4) and (5) the output due to a strain ϵ is

$$\Delta e = \frac{RR_1}{R_1 + R} . IS\epsilon \tag{6}$$

For any given type of gauge, R and S are fixed, and there is a maximum allowable current. For maximum sensitivity, therefore, the gauge should be run at this maximum current, and the series resistance R_1 should be large. Little advantage is gained, however, by making R_1 greater than two or three times the gauge resistance R.

The calibration signal was produced by closing a switch inserting a high resistance R_c in parallel with the gauges. The alternative method of short-circuiting a small series resistance was found to be unsatisfactory, owing to the very rapid switching required and the extremely small allowable contact resistance.

The closing of the parallel circuit causes a sudden decrease of resistance $\Delta R = R^2/(R + R_c)$, and is thus equivalent to a mechanical strain $\epsilon = R/\{S(R + R_c)\}$. Since in most cases $R_c > 200\,R$, a sufficiently accurate value was usually given by $\epsilon = R/(SR_c)$.

Immediately before each test, a series of calibration signals was recorded photographically using different values of R_c. These signals gave the deflections corresponding to known values of strain and thus a calibration curve for the test could be drawn.

Since the time between calibration and test was only a few seconds, it is considered that this method of calibration eliminates possible inaccuracies due to change of amplifier gain or alteration of gauge current.

5. Experimental Results

(i) *Static tests*

The material used was an aluminium alloy containing 2 per cent magnesium, $\frac{1}{4}$ per cent manganese, supplied by the *Northern Aluminium Company Ltd.* Specimens for static tension and compression tests were machined from the same bar as was used for the impact specimens. All specimens were annealed for 1 hour in air at 350°C after machining.

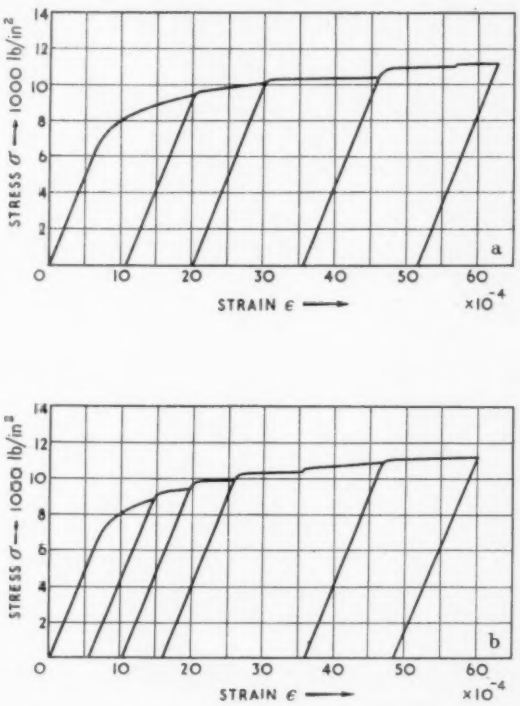

Fig. 2. Static stress-strain curves showing unloading lines. (a) Tension test using Cambridge extensometer. (b) Compression test using 3 resistance strain gauges.

Fig. 2 (a) shows the result of a tensile test using a Cambridge extensometer, and Fig. 2 (b) that of a compression test using three type 6H resistance strain gauges. It will be seen that there is little difference between the stress-strain curves for tension and compression. During these tests, the specimen was periodically unloaded before continuing the test, and the unloading lines are shown in Figs. 2 (a) and 2 (b). It was found that these unloading lines were straight, and that their slopes were equal to that of the initial elastic loading line, within the limits of experimental error.

(ii) *Elastic range dynamic tests*

In order to check the method of calibration, two series of tests were carried out at low impact velocities such that with axial loading no plastic strain would occur in the specimen (except locally at the spherical end).

(a) *Direct impact.* The relation between the impact velocity V and the strain ϵ' propagated into the specimen is

$$\epsilon' = \frac{V}{\sqrt{(E/\rho)}} \tag{7}$$

where ρ is the density of the specimen. This relation is plotted in Fig. 3, using the value of E obtained from static tests.

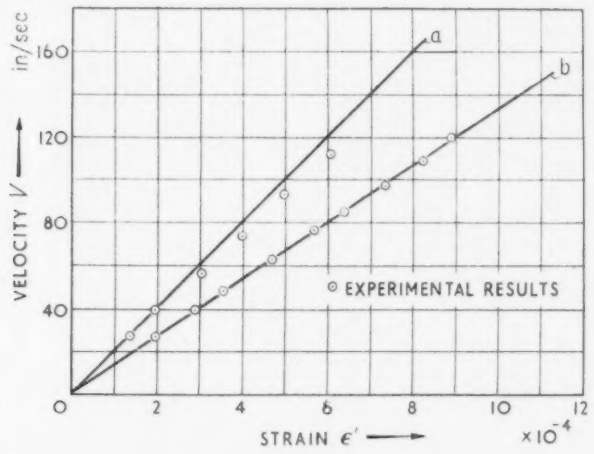

Fig. 3. Relation between velocity of impact (V) and strain in specimen (ϵ') – elastic conditions. (a) Theoretical relation for direct impact (Eq. 7). (b) Theoretical relation for impact through steel rod (Eq. 8).

Results of repeated impact tests at increasing velocities are also shown in Fig. 3. It can be seen that for impact speeds greater than 40 in./sec. the measured strains are appreciably larger than those given by equation (7). It was thought that this was due to bending effects, and this was confirmed by a test in which the difference between the strains in the two gauges was measured and found to be considerable. It was then decided to apply the impact through a steel rod as described in Section 3 (i).

(b) *Impact through steel rod.* The relation between V and ϵ' for this case is

$$\epsilon' = \frac{V}{\sqrt{(E/\rho)}} \cdot \frac{2}{1 + \sqrt{(E\rho/E_s\,\rho_s)}} \tag{8}$$

where E_s and ρ_s are respectively the modulus of elasticity and density of the steel. This relation is also plotted in Fig. 3, using the value of E_s obtained from a vibration test on the steel rod used.

The results of a number of tests on different specimens are plotted in this figure, and it is seen that they lie very close to the line given by equation (8). The fact that the eccentricity of loading was small was confirmed by tests in which the difference between the two gauge outputs was recorded. It was found that the variation between the gauges was less than $\pm$ 10 per cent from the mean. This corresponds to an eccentricity of $2\frac{1}{2}$ per cent of the radius, or less than 0·007 in.

Fig. 4 (a) shows a typical record for an elastic impact, and Fig. 4 (b) the record for a repeat impact at the same velocity. It may be noted that after unloading there is a small elastic wave travelling up and down the rod, i.e. the rod is vibrating slightly. This is a consequence of the finite acceleration of the impact end at the moment of impact.

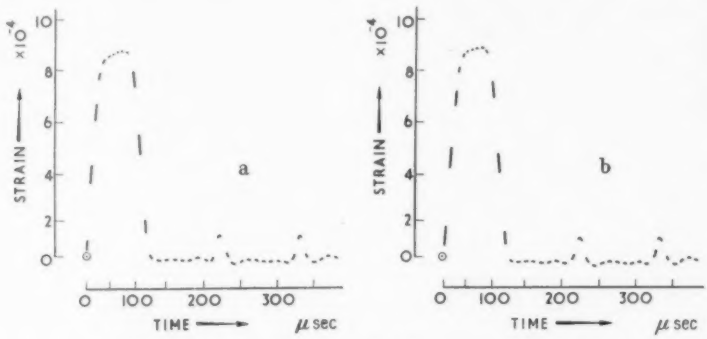

Fig. 4. Strain-time records (elastic conditions).
(a) Impact at 120 in./sec; peak strain = $8{\cdot}8 \times 10^{-4}$. (b) Repeat impact at 120 in./sec; peak strain = $8{\cdot}9 \times 10^{-4}$.

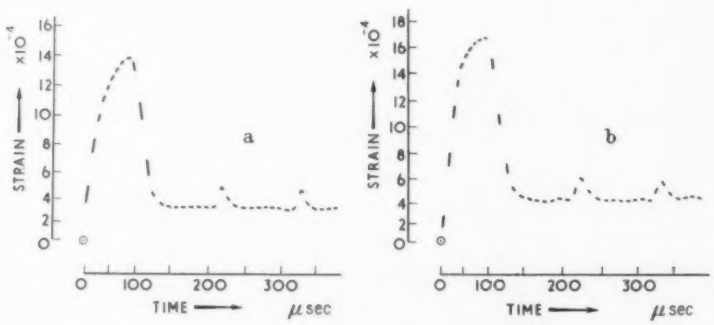

Fig. 5. Strain-time records (plastic conditions).
(a) Impact at 153 in./sec; previous permanent strain = $4{\cdot}6 \times 10^{-4}$; peak strain = $13{\cdot}9 \times 10^{-4}$; additional permanent strain = $3{\cdot}7 \times 10^{-4}$. (b) Impact at 192 in./sec; previous permanent strain = $42{\cdot}5 \times 10^{-4}$; peak strain = $16{\cdot}7 \times 10^{-4}$; additional permanent strain = $4{\cdot}5 \times 10^{-4}$.

(iii) *Plastic range dynamic tests*

These tests were carried out using the steel rod to transmit the stress.

Fig. 5 shows typical records obtained when plastic deformation occurred. It will be seen that the increase of strain is more gradual than that obtaining under elastic conditions (see Fig. 4). This is due to local plastic deformation at the impact end, and to the smaller velocity of propagation of the larger plastic strains. The records also show that after unloading the specimen continues to vibrate elastically.

In order to check the assumptions made in interpreting the strain-time records a theoretical analysis was made of the wave propagation effects occurring in the

specimen. From this analysis strain-time curves for the gauge position were calculated, using the static stress-strain relation. The exact shape of these curves depends not only on the stress-strain relation but on the local deformation occurring at the impact end of the specimen; in order to allow for the latter effect an exponentially increasing end velocity was assumed.

The general shape of the calculated curves was similar to that of the strain-time records obtained experimentally and it was confirmed that the first peak of the curve gives the maximum strain reached at the gauge position, while the mean height of the latter part of the curve gives the permanent strain there. The permanent strain was therefore measured by taking this mean height and using the calibration curve obtained as described in Section 4. As a further check the value of the permanent strain was also obtained by measuring the permanent change in the gauge resistance by means of a sensitive Wheatstone Bridge circuit; the values obtained agreed well with those obtained from the strain-time records.

ol.
1
2/53

Each specimen was subjected to repeated impacts at increasing velocities, and values of σ and ϵ were calculated by equations (3). Fig. 6 shows the results obtained in this way for two different specimens, together with the mean static stress-strain curve. It will be seen that the points obtained from the impact tests lie appreciably above the static stress-strain curve, except at stresses below the static elastic limit. Thus, under the conditions of these tests, the stress necessary to cause a given plastic strain is greater than that which would cause the same strain in a static test. The two curves of Fig. 6 indicate that the 0·1 per cent proof stress is raised above the " static " value by 15 per cent and 18 per cent respectively.

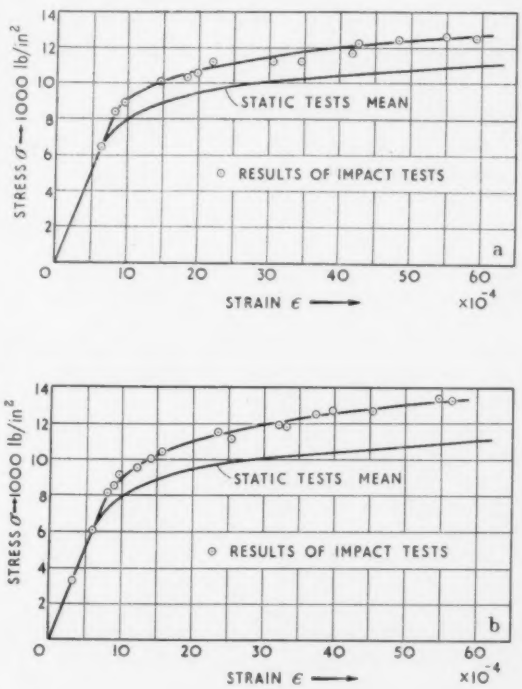

Fig. 6. Static and dynamic stress-strain curves. (a) Specimen 1. (b) Specimen 2.

This increase is of the same order as that found by NADAI and MANJOINE (1941) for the ultimate stress of pure aluminium; their tests indicate that the ultimate stress of pure aluminium when tested in tension at a strain rate of 10 sec.$^{-1}$ is about 25 per cent higher than when tested at a strain rate of 10^{-4} sec.$^{-1}$.

It is not possible to specify an exact figure for the rate of strain in the present

tests, as it appears from the strain-time records (Fig. 5) that the rate decreases as the strain increases. The time taken to reach the maximum strain was, however, very nearly constant in all tests, being rather less than 10^{-4} sec. Thus the average rate of strain during loading was of the order of 15 sec.$^{-1}$, though the initial rate in any test was several times this value.

6. Conclusions

It has been established that the resistance strain gauge is capable of responding accurately to the rapidly varying strains occurring during the longitudinal impact of metal rods. For impacts at low velocities the measured strains agree well with those calculated from the theory of elastic wave propagation.

The plastic strains caused by longitudinal impacts at higher velocities have been measured, and dynamic stress-strain curves have been derived from repeated impact tests. For the aluminium alloy tested, the results indicate that under the conditions of these tests the plastic strain caused by a given stress is considerably less than would be caused by that stress applied statically. In the plastic range investigated, the stress-strain curve is found to be raised by 15 – 20 per cent.

Vol.
1
1952/5

Appendix

Derivation of equation (8)

It may be shown from considerations of continuity and momentum that under elastic conditions the speed of propagation of a longitudinal wave in a thin rod is

$$c = \sqrt{(E/\rho)} \tag{9}$$

and that across a wave front the increases in compressive stress ($\Delta\sigma$) and particle velocity (Δv) are related by

$$\Delta\sigma = \pm \rho c \Delta v. \tag{10}$$

The sign here depends on the direction of propagation of the wave; it is positive when this direction is the same as that in which the particle velocity is measured. A direct impact on the specimen at velocity V therefore causes the propagation of a stress $\rho cV = \sqrt{(E\rho)}V$, and hence the strain propagated into the specimen is $V/\sqrt{(E/\rho)}$ (Eq. (7)).

When an impact at velocity V is transmitted through the steel rod, the stress propagated into this rod is, according to (10),

$$\sigma_1 = \rho_s c_s V \tag{11}$$

where $c_s = \sqrt{(E_s/\rho_s)}$, the elastic wave velocity for steel. On arrival at the interface between the two rods this wave causes the propagation of a stress σ' into the specimen. From (10), therefore, the particle velocity in the specimen becomes

$$v' = \sigma'/\rho c. \tag{12}$$

Since the two rods are equal in diameter, the stress at the end of the steel rod must become σ' also; further, if the rods are to remain in contact, the particle

velocity there must become v'. Thus a reflected wave is propagated back into the steel rod, with velocity $-c_s$. Across this wave : $\Delta\sigma = \sigma' - \sigma_1$ and $\Delta v = v' - V$. Substituting these values into (10) and using (12) to eliminate v' we obtain

$$\sigma' (1 + \rho_s c_s/\rho c) = \sigma_1 + \rho_s c_s V$$
$$= 2 \rho_s c_s V \qquad \text{from (11).}$$

From (9) this may be written

$$\sigma' \left(\frac{1}{\sqrt{(E\rho)}} + \frac{1}{\sqrt{(E_s \rho_s)}} \right) = 2V.$$

Hence the strain propagated into the specimen is given by

$$\epsilon' = \sigma'/E = \frac{V}{\sqrt{(E/\rho)}} \cdot \frac{2}{1 + \sqrt{(E\rho/E_s \rho_s)}} \qquad (8) \text{ bis.}$$

For the steel and alloy used, $\sqrt{(E\rho/E_s \rho_s)} = 1/3$ very nearly, so this becomes

$$\epsilon' = \frac{3}{2} \cdot \frac{V}{\sqrt{(E/\rho)}}, \qquad \text{approximately.}$$

Thus, under elastic conditions, the effect of the steel rod is to increase by a factor of 3/2 the strain propagated into the specimen due to an impact of given velocity.

References

Brown, A. F. C. and Vincent, N. D. G.	1941	*Proc. Inst. Mech. Eng.*, **145**, 126.
Clark, D. S. and Dätwyler, G.	1938	*Proc. Am. Soc. Test. Mat.*, **38**, 98.
Clark, D. S. and Duwez, P. E.	1948	*J. Appl. Mech.*, **15**, 243.
Ginns, D. W.	1937	*J. Inst. Met.*, **61**, 61.
Hopkinson, B.	1905	*Proc. Roy. Soc.* A, **74**, 498.
Karman, Th. v. and Duwez, P. E.	1946	*6th Int. Cong. App. Mech.* (Paris).
Nadai, A. and Manjoine, M. J.	1941	*J. Appl. Mech.*, **8**, 77.
Taylor, G. I.	1946	*6th Int. Cong. App. Mech.* (Paris).

Journal of the Mechanics and Physics of Solids, 1953, Vol. 1, pp. 124 to 133. Pergamon Press Ltd., London.

THE AUTOFRETTAGE OF THICK TUBES WITH FREE ENDS

By D. G. B. Thomas
British Iron & Steel Research Association, Sheffield

(*Received 30th October*, 1952)

Summary

A numerical analysis is made of the expansion by internal pressure of a partially plastic open-ended tube of wall-ratio 2 : 1. This is based on the Prandtl-Reuss incremental stress-strain relations, together with the Tresca yield criterion. The calculated surface strains are described by simple formulae. Comparison is made with previous solutions based on total stress-strain relations.

Vol
1
1952/

1. Introduction

The expansion of a thick-walled tube by internal pressure has been treated by many authors, mainly because of the importance of the problem in connection with the autofrettaging (or pre-stressing) of gun barrels and pressure vessels. There are three main forms of the problem, namely, one in which the tube is considered to be in a state of plane strain, one in which the tube is closed by plugs firmly attached to it (a " closed-end " tube) and one in which the tube is closed by floating pistons (an " open-end " tube). The first two have been adequately dealt with in the past (see Hill 1950), but the third has only been treated using the total strain theory of Hencky (Steele 1952; Allen and Sopwith 1951; MacGregor, Coffin, and Fisher 1948).

In this paper the stress and strain distributions in a moderately thick partially plastic tube (wall ratio 2 : 1) are found by means of a numerical integration of the Prandtl-Reuss equations of incremental plastic strain in conjunction with Tresca's yield condition. The results of this integration are compared graphically with the results of previous workers. It is found, further, that the calculated surface strain can be described quite closely by extremely simple formulae.

2. Analysis of the " Open-End " Problem

This section contains as much of the analysis set out by Hill (1950) as is necessary for an understanding of the difference equations in the next section.

Consider the expansion of a thick-walled tube by a uniform internal pressure, the external pressure being zero. At any instant after the bore has yielded, the annulus contained by the bore ($r = a$) and some internal surface ($r = c$) is plastic, while the outer annulus, contained by $r = c$ and the outer surface ($r = b$) is in an elastic state of stress. It is assumed that

(i) The tube is sufficiently long to make the stresses and strains independent of the axial co-ordinate.

(ii) The ends of the tube are not loaded, and the tube is free to expand axially (open-end condition).

(iii) The axial stress is the intermediate principal stress in the plastic region.

(iv) The maximum shear stress in the plastic region is constant (TRESCA's yield criterion).

The first assumption implies that plane sections of the tube remain plane throughout the expansion, and hence that the axial strain ϵ_z is constant throughout the tube at any instant.

When the tube is wholly elastic, $\sigma_\theta \leqslant \sigma_z \leqslant \sigma_r$, which suggests assumption (iii). As will be seen later, this does not hold near the outer surface of the tube when the elastic annulus has almost disappeared. An adequate solution after this stage would require a complete reanalysis of the problem, which is not undertaken.

The fourth assumption implies that strain-hardening is neglected.

In the elastic region, $c \leqslant r \leqslant b$, the elastic equations can be solved under the boundary conditions

$$\sigma_r = 0 \text{ on } r = b \text{ and } \sigma_\theta - \sigma_r = Y \text{ on } r = c, \tag{1}$$

where σ_r, σ_θ and Y are respectively the radial and tangential stresses and the yield stress of the material in tension. The result is

$$\left.\begin{aligned} \sigma_r &= -\frac{Yc^2}{2b^2}\left(\frac{b^2}{r^2} - 1\right), \\ \sigma_\theta &= +\frac{Yc^2}{2b^2}\left(\frac{b^2}{r^2} + 1\right), \\ \sigma_z &= E\,\epsilon_z + \nu\,Y\,\frac{c^2}{b^2}, \end{aligned}\right\} \qquad c \leqslant r \leqslant b \tag{2}$$

where ϵ_z is the axial strain, E is Young's modulus, and ν is Poisson's ratio (taken as 0·3 throughout this paper). The radial displacement of a point in the elastic region is therefore

$$u = \frac{r}{E}\{\sigma_\theta - \nu\sigma_z - \nu\sigma_r\} = -\nu r\epsilon_z + (1+\nu)\frac{Yc^2}{2Eb^2}\left\{(1-2\nu)\,r + \frac{b^2}{r}\right\}. \tag{3}$$

In the plastic region, $a \leqslant r \leqslant c$, the equation of equilibrium combined with the yield criterion gives

$$\frac{\partial\sigma_r}{\partial r} = \frac{\sigma_\theta - \sigma_r}{r} = \frac{Y}{r}. \tag{4}$$

Integrating, and using the condition that σ_r must be continuous across $r = c$,

$$\left.\begin{aligned} \frac{\sigma_r}{Y} &= -\ln\left(\frac{c}{r}\right) - \tfrac{1}{2}\left(1 - \frac{c^2}{b^2}\right), \\ \frac{\sigma_\theta}{Y} &= -\ln\left(\frac{c}{r}\right) + \tfrac{1}{2}\left(1 + \frac{c^2}{b^2}\right); \end{aligned}\right\} \qquad a \leqslant r \leqslant c \tag{5}$$

so that the internal pressure is

$$p = Y\ln(c/a) + \tfrac{1}{2}\,Y\,(1 - c^2/b^2). \tag{6}$$

The inner surface of the tube yields initially when $c = a$ or

$$p_0 = \tfrac{1}{2} Y (1 - a^2/b^2) \tag{7}$$

and the tube is first completely plastic when $c = b$ or

$$p_1 = Y \ln (c/b). \tag{8}$$

According to TURNER (1909), if $p_1 < 2 p_0$ all elements recover elastically on unloading and, provided there is no Bauschinger effect, a subsequent application of p_1 does not cause the tube to yield. This condition is satisfied here, as can be seen by putting $b/a = 2$ in equations (7) and (8). However, there seems to be some doubt (WARREN 1947) as to whether the recovery would actually be entirely elastic.

The stresses σ_r and σ_θ throughout the tube are, from equations (2), (5) and (6), statically determined in terms of the pressure p (via the parameter c) independently of the end conditions or of the strains, provided variations of the internal and external radii can be neglected. On the other hand, the axial stress can only be found by following the strain history. None of the stresses can be statically determined if the VON MISES yield criterion is used, as this criterion involves the axial stress in its enunciation (see equation 21 below).

Since the plastic flow is restrained by the external elastic annulus while the tube is only partly plastic, and since only a moderately thick tube ($b/a = 2$) is considered, variations of the internal and external radii can be neglected to a first approximation.

The REUSS incremental stress-strain relations for a plastic material are

$$E d\epsilon_r = d\sigma_r - \nu d\sigma_\theta - \nu d\sigma_z + \sigma_r' \, d\lambda \tag{9}$$

with two other similar equations for $E d\epsilon_\theta$ and $E d\epsilon_z$. $d\lambda$ is a proportionality factor which varies over the field, $\sigma_r' = \sigma_r - \tfrac{1}{3}(\sigma_r + \sigma_\theta + \sigma_z)$, and the increments refer to an element of material, not to an element of space.

The elimination of $d\lambda$ from the three equations (9) leads to

$$\partial u/\partial r + u/r + \epsilon_z = (1 - 2\nu) \{q - 3 \ln (c/r) + 3c^2/2b^2\} \, Y/E, \tag{10}$$

and

$$\{1 - \tfrac{2}{3} q (1 - 2\nu)\} \, \partial q/\partial c + (1 - 2\nu)(2q - 1)(1 - c^2/b^2)/c + (4q/3r)(\partial/\partial c)(Eu/Y) + (\tfrac{2}{3} q - 1)(\partial/\partial c)(E\epsilon_z/Y) = 0 \tag{11}$$

where

$$q = 3\sigma_z'/2Y = \sigma_z/Y + \ln (c/r) - c^2/2b^2. \tag{12}$$

The third equation for the three unknowns, u, q and ϵ_z, is supplied by the condition that the total axial load across any cross-section is zero, so that

$$\int_a^b 2\pi r (\sigma_z/Y) \, dr = \int_a^c 2\pi r q \, dr + \pi a^2 p/Y + \pi (b^2 - c^2) \{E\epsilon_z/Y - (1 - 2\nu) c^2/b^2\} = 0. \tag{13}$$

Finally, since u and σ_z are continuous across $r = c$, the elastic equations (2) and (3) give the relations

$$Eu/Y = -\nu c E\epsilon_z/Y + (1+\nu)(1-2\nu+b^2/c^2)\,c^3/2b^2 \tag{14}$$

and

$$q = E\epsilon_z/Y - (1-2\nu)\,c^2/2b^2 \tag{15}$$

on the plastic-elastic boundary.

It may be shown by the usual methods that the equations (10), (11) and (13) are hyperbolic with, to our degree of approximation, characteristics r = constant and c = constant in the (r, c) plane. They must be integrated numerically along these characteristics. For this purpose suitable finite difference approximations are outlined in the next section.

3. Numerical Integration

The (r, c) plane was divided into a rectangular mesh, with mesh-lengths $\Delta c = \delta r = a/10$ for $b/a = 2$. The internal radius a was put arbitrarily equal to unity. Referring to Fig. 1, suppose that all the required quantities have been found for all mesh points within and on the sides of the triangle OAP. Let the operator d represent a difference along a line parallel to the diagonal $r = c$, and the operator Δ a difference along a line parallel to the ordinates r = constant.

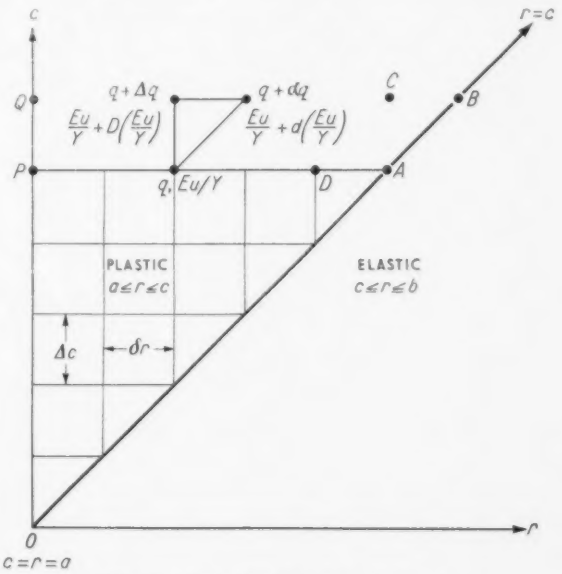

Fig. 1. Notation in the (r, c) plane.

On the plastic-elastic boundary $r = c$, the values of Eu/Y and q at B are given in terms of c, $E\epsilon_z/Y$ and the constants of the system by equations (14) and (15) respectively. Thus, if AP is the characteristic c,

$$d(Eu/Y)_A = -\nu(c+\Delta c)\,d(E\epsilon_z/Y) - \nu\Delta c E\epsilon_z/Y +$$

$$3(1+\nu)(1-2\nu)(c+\Delta c)\,c\Delta c/2b^2 + \tfrac{1}{2}\Delta c(1+\nu) = 0, \tag{16}$$

$$dq_A = d(E\epsilon_z/Y) - (1-2\nu)(c+\tfrac{1}{2}\Delta c)\,\Delta c/b^2. \tag{17}$$

The difference $d(E\epsilon_z/Y)$ between the values of $E\epsilon_z/Y$ on AP and on BQ must, initially, be estimated by extrapolation from previous values. Using this estimate, Eu/Y and q can be found at B from equations (16) and (17) (using $\nu = 0{\cdot}3$). Their values at C can now be computed in terms of $(Eu/Y)_B$ and q_B from finite difference approximations to equations (10) and (11). In equation (12), which provides the differential relation along BQ, the differentials $d(Eu/Y)$ and dq are replaced by the differences $(d-\Delta)(Eu/Y)$ and $(d-\Delta)q$. Simiarly in equation (13), which

holds along the lines r = constant (parallel to AC), the differentials are replaced by $\Delta(Eu/Y)$ and Δq respectively. Also, the value of a function in an interval is taken to be the mean of its values at the ends of that interval. Making these substitutions, equations (10) and (11) become

$$\Delta(Eu/Y)\, r/(r + \tfrac{1}{2}\delta r) + \tfrac{1}{2}(1 - 2\nu)\,\delta r\,\Delta q$$
$$= \delta r\, d(E\epsilon_z/Y) + d(Eu/Y) + E(u + \tfrac{1}{2}du)\,\delta r/Y(r + \tfrac{1}{2}\delta r) + (E\epsilon_z/Y)\,\delta r$$
$$+ (1 - 2\nu)\,\delta r\left\{3\ln\left[(c + \Delta c)/(r + \tfrac{1}{2}\delta r)\right] - 3(c + \Delta c)^2/2b^2 - (q + \tfrac{1}{2}dq)\right\} \qquad (18)$$

and

$$-\tfrac{1}{3}(1 - 2\nu)(\Delta q)^2 + (2/3r)\,\Delta q\Delta(Eu/Y)$$
$$+ \Delta q\left\{1 - \tfrac{2}{3}q(1 - 2\nu) + (1 - 2\nu)\,\Delta c/(c + \tfrac{1}{2}\Delta c) + (1 - 2\nu)(c + \tfrac{1}{2}\Delta c)\,\Delta c/b^2\right.$$
$$\left. + \tfrac{1}{3}d(E\epsilon_z/Y)\right\} + (\tfrac{2}{3}q - 1)\,d(E\epsilon_z/Y) + (4q/3r)\,\Delta(Eu/Y) +$$
$$(1 - 2\nu)(2q - 1)\,\Delta c/(c + \tfrac{1}{2}\Delta c) + (1 - 2\nu)(2q - 1)(c + \tfrac{1}{2}\Delta c)\,\Delta c/b^2 = 0. \qquad (19)$$

A simultaneous solution of equations (18) and (19) for $\Delta(Eu/Y)$ and Δq then leads to q_C and $(Eu/Y)_C$. We therefore know, by subtraction, the $d(Eu/Y)$ and dq corresponding to the interval CD, and, continuing in a similar manner, we can find in turn values of the unknowns at all the mesh-points on the characteristic BQ. The resulting q-values are substituted in equation (6) in the form

$$d\left(\frac{E\epsilon_z}{Y}\right) = \frac{-1}{b^2 - (c + \Delta c)^2}\int_a^{c+\Delta c} 2rq\,dr + \frac{a^2}{2b^2} + \frac{(1 - 2\nu)}{2b^2}(c + \Delta c)^2$$
$$+ \frac{a^2}{b^2 - (c + \Delta c)^2}\ln\frac{(c + \Delta c)}{a} - \frac{E\epsilon_z}{Y} \qquad (20)$$

to give a second estimate of $d(E\epsilon_z/Y)$, which is used in a repeat of the entire process from equations (16) and (17) onwards. The iteration is, of course, continued until two successive values of $d(E\epsilon_z/Y)$ are identical to within the computational error. Finally, the last set of q-values is substituted in equation (12), together with the appropriate parameters, to give σ_z/Y over the whole field.

When c was greater than about 1·3 this straightforward process was, however, not feasible, as the values of $d(E\epsilon_z/Y)$ either did not converge or converged very slowly. It was then necessary to use the empirical property that any small increment in $d(E\epsilon_z/Y)$ causes an approximately equal increment in both Δq and dq at each mesh point along BQ. This permits the calculation of a series of values of the right hand side of equation (23), from which the value of $d(E\epsilon_z/Y)$ which satisfies the equation most closely can be selected. This value was usually found to be practically unaltered by a further iteration.

4. Approximations to the Yield Criterion

After the completion of the solution, it was found that at one point (2, 2) in the (r, c) net, the axial stress was no longer the intermediate principal stress. The discrepancy was fortunately comparatively small (see Fig. 2), for at (2, 2) $\sigma_r - \sigma_z = 0{\cdot}0784\,Y$. However, this fact prevents the continuation of the solution beyond

Vol. 1 1952/5

the point at which all the tube becomes plastic, without a complete reformulation of the theory. This was not considered practicable.

Since VON MISES' yield criterion

$$(\sigma_\theta - \sigma_r)^2 + (\sigma_r - \sigma_z)^2 + (\sigma_z - \sigma_\theta)^2 = 2Y^2 \tag{21}$$

is generally held to give a more accurate description of the behaviour of most metals than the TRESCA criterion, it is interesting to see whether the present TRESCA solution can be used to give a fair approximation to a solution using the MISES criterion. If the yield criterion is considered as a surface in stress space with σ_r, σ_θ and σ_z as cartesian axes, the curve of section of the MISES surface by the plane $\sigma_r + \sigma_\theta + \sigma_z = 0$ is a circle. A small arc of this circle in the range of deviatoric stress with which we are concerned can be approximated by the chord

$$\sigma_\theta - \sigma_r = mY \tag{22}$$

which is equivalent to the TRESCA criterion with a modified yield stress. Equation (21) can, in view of (12), be rearranged as

$$\sigma_\theta - \sigma_r = 2Y\sqrt{(1 - q^2)/3}. \tag{23}$$

Therefore, the best value of m will be the mean of the local values of $2\sqrt{(1-q^2)/3}$ over the mesh points in the plastic part of the (r, c) field. This mean value is 1·132 in the present case. The local relative error in replacing (21) by (22) then has a maximum value of 17 per cent at the outer surface of the tube when $c/a = 2{\cdot}0$, decreasing rapidly to 1 per cent at (1·7, 2·0). The error also decreases with decreasing c to 5 per cent at (1·7, 1·7).

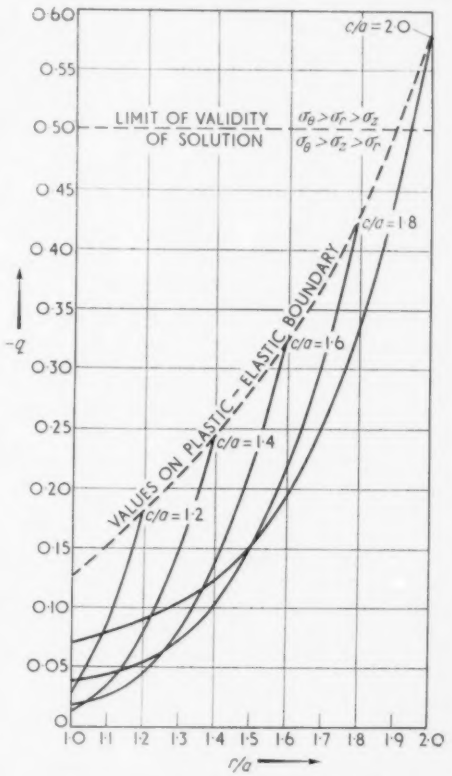

Fig. 2. Distributions of $q = 3\sigma_z'/2Y$.

These errors compare with a maximum local error of 2 per cent in the plane-strain solution and of 0·3 per cent in the closed-end solution. The comparatively large error corresponds to a rotation of the radius vector in the deviatoric stress plane through $33\frac{1}{2}°$, compared with 14° in the plane-strain solution, and 10° in the closed-end solution.

The only available VON MISES solution of the open-end tube problem is that of MACGREGOR, COFFIN and FISHER, who, however, used the HENCKY total strain theory. It is interesting to note that the ratio of their values of the radial stress to the values given by equations (2) and (3) is about 1·21. For the other stresses and strains, however, the corresponding ratios are greater than this.

5. SUMMARY OF ALTERNATIVE SOLUTIONS

All the other solutions of the problem under consideration involve, either directly or indirectly, the equation

$$E\epsilon_r = \sigma_r - \nu\sigma_\theta - \nu\sigma_z + \lambda\sigma_r' \tag{24}$$

with two other similar equations for $E\epsilon_\theta$ and $E\epsilon_z$. λ here is a factor which is zero in the elastic region and which varies in the plastic region. A comparison with the REUSS equations (9) shows that the difference lies in the fact that in equations (9) the components of the *increments* of plastic strain are proportional to the corresponding deviatoric stress components, while in equations (24) (the HENCKY equations), the *total* plastic strain components are proportional to the deviatoric stress components. It is well known (see, e.g. HILL 1950) that the REUSS equations reduce to the HENCKY equations when the reduced stresses maintain constant ratios to one another, i.e. when the reduced stress vector in the geometric representation does not rotate.

The maximum rotation of the stress vector for a single element occurs at $r/a = 1{\cdot}4$, and is about 9°. The maximum rotation for a tube in plane strain is about 6° at $r/a = 1$. Since these two angles are similar, we might expect the discrepancy between the HENCKY and REUSS solutions to be similar and fairly small for plane-strain and open-ended tubes. When the TRESCA yield condition is used, the radial and tangential stresses are, of course, still given by equations (2) and (5).

We consider, for comparison purposes, the solutions of STEELE (1952) and of ALLEN and SOPWITH (1951), which assume the TRESCA yield criterion, are in closed form, and permit a correction for strain hardening. We put $b/a = 2$, $\nu = 0{\cdot}3$ and neglect strain hardening, as in sections (2) and (3) of this paper.

TABLE I. *Summary of Computed Qualities*

c/a	p/Y	$(E\epsilon_\theta/Y)_a$	$(E\epsilon_\theta/Y)_b$	$-E\epsilon_z/Y$	$(\sigma_z/Y)_e$
1·0	0·3750	0·738	0·250	0·0750	0·0000
1·1	0·4441	0·896	0·303	0·0909	− 0·0002
1·2	0·5023	1·077	0·360	0·1016	+ 0·0004
1·3	0·5551	1·280	0·422	0·1256	+ 0·0012
1·4	0·5915	1·503	0·489	0·1450	+ 0·0020
1·5	0·6242	1·748	0·562	0·1670	+ 0·0018
1·6	0·6500	2·012	0·640	0·1925	− 0·0005
1·7	0·6694	2·295	0·724	0·2235	− 0·0068
1·8	0·6828	2·597	0·816	0·2622	− 0·0192
1·9	0·6906	2·915	0·915	0·3122	− 0·0414
2·0	0·6932	3·250	1·024	0·3784	− 0·0784

6. RESULTS AND COMPARISONS

Numerical values of the surface strains $(E\epsilon_\theta/Y)_a$, $(E\epsilon_\theta/Y)_b$ and $E\epsilon_z/Y$, the axial stress in the elastic region $(\sigma_z/Y)_e$ and the expanding pressure p/Y, as obtained in Sections (2) and (3), are given in the Table.

Since the tangential and radial stresses, as expressed by equations (2) and (3), have been published previously (HILL 1950), they will not be shown here. Axial stress distributions are shown in Fig. 3 for various positions of the plastic elastic boundary.

A comparison is made in Figs. 4 and 5 between the various values of the axial stress and strain. Although the different shapes of the curves of σ_z/Y in Fig. 4 prevent any useful numerical evaluation of the discrepancies, these are considerably more than the 5 per cent found previously for the plane-strain and closed-end

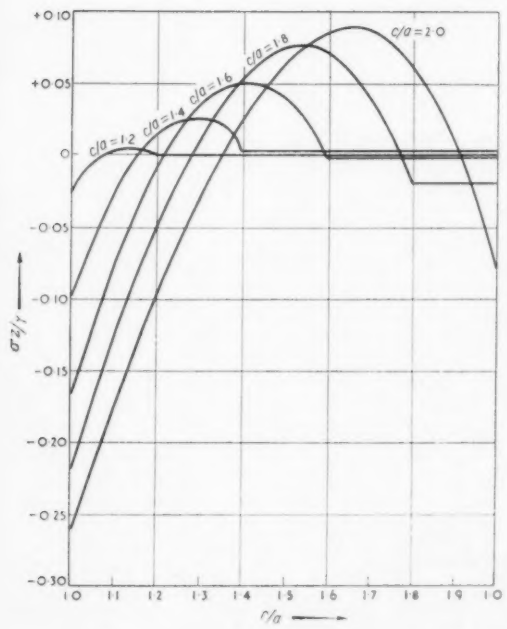

Fig. 3. Axial stress distributions.

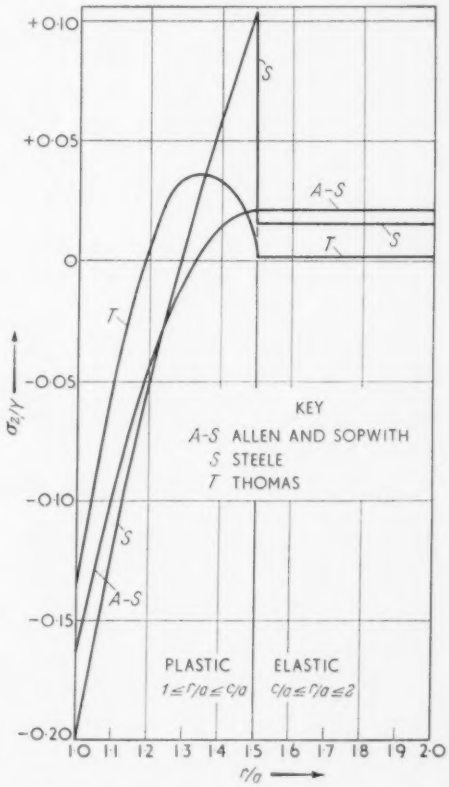

Fig. 4. Comparison of axial stresses at $c/a = 1{\cdot}5$.

tubes. In Fig. 5, again, there is a considerable difference between the axial strain curves, the maximum variation from the REUSS solution being 25 per cent and 16 per cent respectively for the solutions of ALLEN and SOPWITH and of STEELE.

The various internal and external expansions are plotted in Fig. 6, where it can be seen that the maximum difference between the REUSS solution and the HENCKY solution of ALLEN and SOPWITH is only 2 per cent on both surfaces. The abscissa scale of this Figure and of Fig. 5 was chosen to be c/a, instead of the physically more appropriate p/Y, to emphasize the differences between the three solutions. It is to be noticed that the ordinate scale in Fig. 6 is very much compressed compared with that in the other Figures.

It can also be seen qualitatively that the axial stress and strain are likely to be more sensitive to the type of solution than are the other strains for, since the variations in σ_z' in the incremental solution are proportionately much greater than the variations in σ_θ' or σ_r', and the HENCKY theory implies equal proportional changes in the reduced stresses, ϵ_z is likely to be affected more by the type of theory than either ϵ_θ or ϵ_r.

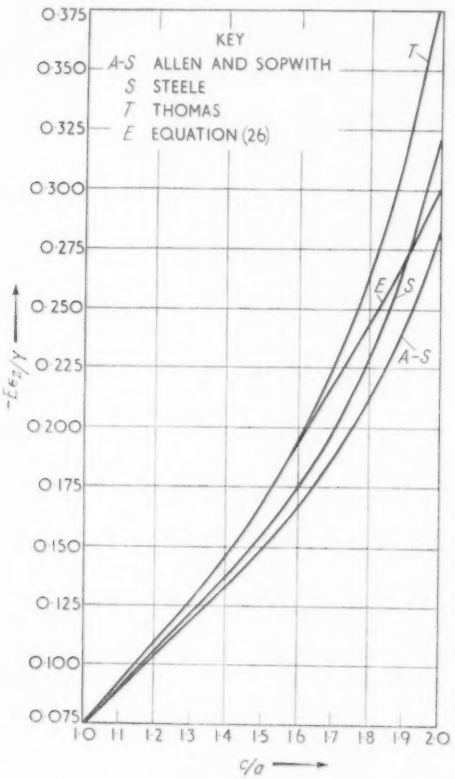

Fig. 5. Comparison of axial strains.

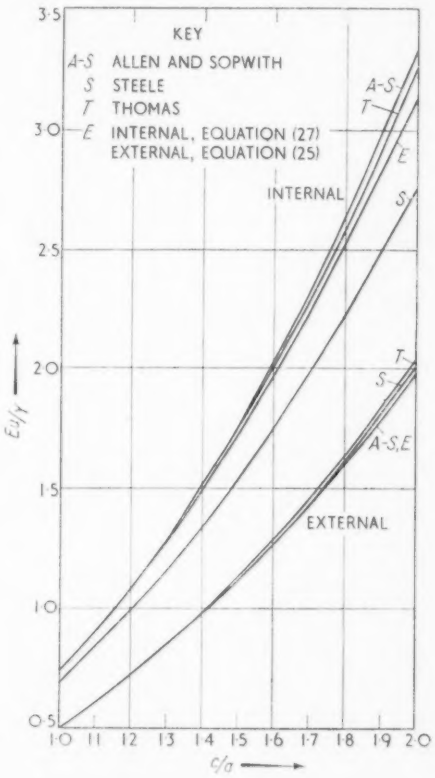

Fig. 6. Comparison of radial expansions.

The agreement in the external expansions is also partly due to the fact that the plastic component of strain at the outer surface is much smaller than the elastic component, which is the same in all theories.

On putting $\sigma_z = 0$ in equations (2) and (3), we find the approximations

$$\left(\frac{E\epsilon_\theta}{Y}\right)_b = \frac{1}{b}\left(\frac{Eu}{Y}\right)_b = \frac{c^2}{b^2}, \tag{25}$$

$$\frac{E\epsilon_z}{Y} = -\frac{\nu c^2}{b^2}, \tag{26}$$

for the external and axial strains. The substitution of (26) in STEELE's expression for the internal expansion gives, using a correction term derived by inspection, the third equation

$$\left(\frac{E\epsilon_\theta}{Y}\right)_a = \frac{1}{a}\left(\frac{Eu}{Y}\right)_a = \frac{c^2}{b^2}(4 + 5\nu)\left(1 + 0{\cdot}075\,\frac{c}{a}\right). \tag{27}$$

The formulae (25) and (27) underestimate the external and internal expansions by $2\frac{1}{2}$ per cent at the most. On the other hand, the error in equation (26) for $E\epsilon_z/Y$ is, from equation (2), equal to σ_z/Y in the elastic annulus, so that, from the last two columns of the Table, it has a maximum of 21 per cent but decreases very rapidly with decreasing c/a.

7. Conclusions

It has been shown that the use of a total strain theory instead of the more accurate incremental strain theory introduces an error of only 2 per cent in the radial expansions. The difference between the two theories is, however, quite marked as regards the axial stress and strain.

The assumption of incompressibility in the plastic region, which is made by Steele, leads to a maximum error of 18 per cent in the external expansion, as compared with the other two solutions. This assumption also leads to unrealistic discontinuities at the plastic-elastic boundary. Since Steele's aim was to produce a set of simple formulae which would sufficiently accurate be for ordinary use, it does not appear that this aim has been fully achieved, for his equations are more complex and, usually, farther from the solution of this paper than the equations (25), (26) and (27).

ol.
1
2/53

Acknowledgments

I wish to thank Mr. A. P. Green for his interest and advice throughout the work, and Dr. R. Hill for his valuable comments.

This paper is Report MW/B/74/52 of the Solid Mechanics Group of the British Iron & Steel Research Association.

References

Allen, D. N. de G. and Sopwith, D. G. 1951 *Proc. Roy. Soc.* A, **205**, 69.

Hill, R. 1950 *Mathematical Theory of Plasticity* (Clarendon Press, Oxford).

MacGregor, C. W., Coffin, L. F. Jr. and Fisher, J. C. 1948 *J. Franklin Inst.*, **245**, 135.

Steele, M. C. 1952 *J. Appl. Mech.*, **19**, 133.

Turner, L. B. 1909 *Trans. Camb. Phil. Soc.*, **21**, 377.

Warren, A. G. 1947 *Symposium on Internal Stresses in Metals and Alloys* (Inst. Metals), p. 209.

Journal of the Mechanics and Physics of Solids, 1953, Vol. 1, pp. 134 to 141. Pergamon Press Ltd., London.

THE MECHANISM OF FATIGUE OF METALS

By A. K. Head*
Aeronautical Research Laboratories, Melbourne

(*Received 8th November*, 1952)

Summary

Experiments have shown, mainly by microscopic observation, that there are three stages in the fatigue of metals. The initial stage is one of bulk deformation of the metal which work hardens to the level of the applied stress. The details of this deformation, particularly for high frequency stresses, differ from work hardening under static stresses. During the intermediate stage, which is the major part of the life, isolated regions of the metal become increasingly deformed, and it is in these regions that a crack forms and extends in the final stage. An element of randomness is present during the intermediate stage. No current theory of fatigue is entirely satisfactory, and an explanation at an atomic level depends on an indentification of this random element.

Vol.
1
1952/5

1. Introduction

The failure of metals by fatigue has been an important problem for more than a century. Some of the early discussions have been brought to light by Peterson (1950) and the question which was asked then still remains to be answered completely to-day. It can be stated simply : why does a metal fail, with little or no warning, under repeated applications of a load which it could support indefinitely if applied statically ? Much work has been done to try and prevent failure by fatigue and a biblography (Division of Aeronautics, 1945) lists over 900 contributions. Many of these are to provide data and design methods which will minimize fatigue failure in service. This aspect has been summarized by the staff of the Battelle Memorial Institute (1941) and will not be considered here. Another important field has been to find tests, preferably non-destructive, by which incipient fatigue failures may be detected. There have been many attempts to correlate the progress of fatigue with changes in other properties of the metal, and, although there is as yet no practical method of detecting the fatigue of an arbitrary shaped part in service, this work has provided information on the subject of this review, the basic mechanism of fatigue.

2. Experimental Methods

The techniques and precautions of fatigue testing, and the types of machines used, have been described by Gough (1926) and the Battelle Memorial Institute (1941). The experimental work to be referred to has been done with nominal uniaxial stress alternating symmetrically about zero. This may be produced by

*At present at : H. H. Wills Physical Laboratory, University of Bristol.

alternate flexure, by rotating bending or by direct push-pull of a specimen. Fatigue under biaxial stresses, or with a superimposed direct stress, although of engineering importance, will not be considered as the nature of fatigue appears to be the same under all stress systems.

The typical variation of N, the number of stress cycles endured before failure, with S, the amplitude of the applied alternating stress, for 24ST aluminium alloy is shown in Fig. 1 (MANN 1950). The scatter of experimental points appears to be an inherent feature of fatigue, and the presentation of fatigue data by curves of equal probability of failure is more realistic than drawing a mean $S - N$ curve and ignoring the scatter. In Fig. 1 the 5%, 50% and 95% probability contours have been calculated from the statistical properties of the test results (HEAD 1950) and it will be seen that even carefully controlled laboratory fatigue tests contain a considerable element of statistical variability. As a result of this scatter, and of the time involved in testing specimens which may last for tens of millions of cycles, the fatigue properties of metals are usually not known with any great precision.

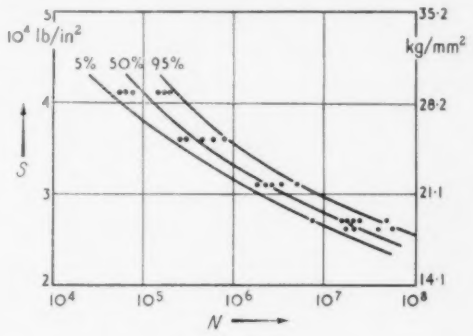

Fig. 1.

The mean fracture curve of Fig. 2 (BENNETT 1946) for X4130 steel illustrates the alternative form of $S - N$ curve found for many steels. Instead of a smooth variation of N with S there appears a sharp discontinuity at the *fatigue limit*, and a stress below this limit apparently never produces failure. There is a curious lack of information as to whether the possession of a fatigue limit is essentially limited to some ferrous materials. It would appear that the position of the discontinuity, which is at the order of one million cycles for these ferrous materials, is at much greater N for non-ferrous materials if it exists at all. However, for stresses above the fatigue limit, the fatigue of ferrous and non-ferrous metals appear to be by the same basic mechanism.

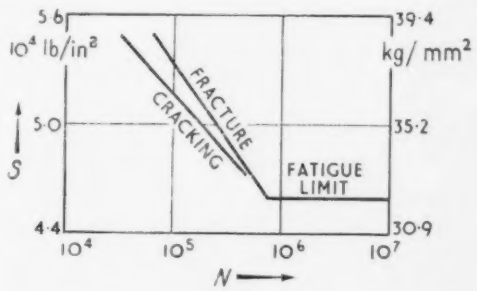

Fig. 2.

One experimental technique which is usually not mentioned explicitly is that at the start of the fatigue test the peak stress is generally not applied immediately but brought on gradually over a number of cycles. This feature is inherent in many types of testing machines and is important when testing a metal with an initial yield point below the test stress. Otherwise a large unidirectional deformation may be caused which may produce dynamic unbalance especially in rotating

bending machines, and also may mask the smaller deformations of fatigue which follow.

3. Experimental Observations

The work of Gough (1933) and his collaborators has shown that fatigue has much in common with plastic flow and fracture of metals under static stresses. They demonstrated that under repeated stresses the metal deforms by slip on the same planes and in the same directions as static slip, and that the operative slip system is, in general, given by the same resolved shear stress law as for static loading. The shape of the specimen, on a macroscopic scale, remains unchanged because alternate half cycles reversed the deformation. However, microscopic observations showed that the reverse deformation was never exactly on the same plane but on a neighbouring one. Cracks formed in regions of heavy slip and tended to propagate initially along the active slip planes. Experiments with single crystals, polycrystalline specimens, and specimens containing two or three large crystals, all showed essentially the same features. This and later work has shown that there are three stages during fatigue and these form convenient divisions for further discussion.

Vol.
1
1952/5

4. Primary Stage

This initial period is most noticeable in the softer metals where the peak applied stress is above the initial yield point and it may be absent when the stress is below this limit. During this period there is bulk plastic deformation until the metals have hardened sufficiently to withstand the applied stress. Damping and the hysteresis loop are initially large and quickly decrease to a constant value (Duce 1950). If slip is visible, it is widespread and a number of slip systems may operate (Duce 1950 ; Wood, Bullen and Head 1952). If the applied stress is above the initial yield point the metal quickly hardens and tensile tests show that the yield point has been raised to approximately the peak of the applied alternating stress. However, particularly if the frequency of the applied stress is high enough, the structural changes producing this hardening differ from those occuring under static stresses (Wood and Thorpe 1940 ; Wood and Head 1951 ; Wood, Bullen and Head 1952). In this work the frequency had to be greater than 400 cycles per minute. For static stresses, slip, hardening, and disorientation and fragmentation of the crystals (as revealed by X-ray diffraction) increase together. Under alternating stresses the hardening is practically completed in the first hundred cycles whilst slip may only become visible after one thousand cycles. What disorientation occurs, appears in the first hundred cycles, but it is smaller than for static stress, and for high frequency stresses it is very small. High frequency stresses also produce an essentially different form of slip line which may both start and end in the interior of the grain, unlike static or low frequency slip which extends from grain boundary to grain boundary. In either case the bulk of the metal is hardened to withstand the applied stress. As a consequence of this widespread deformation there are changes in many other bulk properties of the metal.

5. Intermediate Stage

This long middle-period, which forms the major part of the life of the specimen, is usually taken as extending from the end of the initial widespread settling down (which is absent for many high strength materials) until a crack becomes visible. Microscopic observation (Gough 1933 ; Duce 1950 ; Forsyth 1951 ; Craig 1952 ; Brown 1952 ; Wood, Bullen and Head 1952), aided by the electron microscope, have shown during this period the gradual thickening of a small number of slip bands that formed in the initial stage. These slip bands are usually in the directions of greatest shear stress. These thick bands can be resolved by the electron microscope (and sometimes by the optical microscope) into a finer structure of ragged slip lines. Finally a crack becomes visible in these heavily deformed regions and the propagation of the crack forms the final stage of fatigue.

In view of the extremely localized nature of these distortions and the very small volume of material involved, it is not surprising that the many attempts to correlate progressive damage during fatigue with changes in physical properties of the bulk metal have been generally unsuccessful. Changes have been observed in damping and elastic modulus (Hanstock and Murray 1946 ; Duce 1950), electromagetic properties (Cavanagh 1947), X-ray diffraction patterns (Gough and Wood 1936 and 1938 ; Wood, Bullen and Head 1952), X-ray strain measurements (Wood and Thorpe 1940 ; Schaal 1949 ; Bennett 1951) and coefficient of thermal expansion (Rosenholtz and Smith 1952), but such changes are usually small or difficult to interpret.

6. Final Stage

Fig. 2 illustrates the typical point at which a fatigue crack is first observed, being then of the order of 0·005 cm in length. Measurements of the rate of extension of the crack (De Forest 1936 ; Bennett 1946 ; Bennett and Baker 1950) show that the length increases approximately exponentially until the cross-sectional area has been reduced to such an extent that the remainder fails abruptly with a tensile fracture. In single crystals the direction of the crack is along the slip planes that carry the largest shear stress, i.e. those which were active in the middle period (Gough 1933 ; McClintock 1951). In polycrystalline specimens the general direction of the crack is perpenicular to the direction of maximum tensile stress (Cox and Field 1952) but microscopic observation (Gough and Hanson 1923 ; Lucas 1927) shows that the crack zig-zags from one grain to the next. McClintock (1952) has shown that, if it is assumed that within each grain the direction of the crack is along the slip plane with the highest shear stress and the grains in the polycrystal are randomly oriented, then the average direction of the crack is perpendicular to the tensile stress, as observed, and with deviations from the mean direction which agree with experiment. At high stresses the number of cracks observed (Bennett 1946) may be as many as one hundred and fracture will be very rapid due to the high rate of growth of individual cracks and also to the coalescence of several cracks to form larger ones. At lower stresses there is usually one crack visible and its rate of growth is slower.

In all these observations the size of the crack when first observed is already large by atomic dimensions. It is pertinent to ask how long it had taken to grow

to this size, i.e. when did the crack really start, rather than when it was first observed. Unfortunately, it is not possible to extrapolate the crack growth curves backwards because of the scatter of the experimental points and the present direct methods of crack detection (Hanson 1951) are not sensitive to smaller cracks. However, there are a few observations which indicate that the fatigue crack can be formed quite early in the life of the specimen. Ferguson (1944) has found that cracks could be made visible by a 5% static extension after only 10% of the number of cycles required to fractive a similar specimen. On the assumption that the initiation of a fatigue crack is preceded by a period of local work hardening, Sinclair and Dolan (1951) periodically interrupted the fatigue test and recrystallized the specimen to see if its life could be extended by removing work hardening. Ten such recrystallizations equally spaced during the test did not extend the life beyond that of an unrecrystallized specimen. They concluded that submicroscopic cracks were the only form of damage which would not have been removed by this treatment, and that these are formed in the first 10% of the life of the specimen.

Direct evidence of the early formation of cracks was found by Fenner, Owen Phillips (1951) who observed that, for a very sharply notched specimen, a crack could be detected at the root of the notch after one or two thousand cycles under an alternating stress which did not produce failure for ten or twenty million cycles. This indicates that in certain cases a fatigue crack may be formed very quickly and then spread extremely slowly, and also that a fatigue crack may not be as severe a stress concentration as a machined notch.

Vol
1
1952/

7. Theories of Fatigue

A number of theories have been proposed to explain fatigue in terms of the familiar concepts of the deformation and fracture of the bulk metal under static stresses. Although the inhomogeneity of deformation in fatigue is recognized, the regions of deformation are usually ascribed properties of the same kind as the bulk.

Dehlinger (1940, 1941) proposes that the cause of fatigue lies in the essential inhomogeneity of a polycrystalline metal. Due to the differing orientation of the grains there is a variation in the effective elastic and plastic properties of the metal from point to point. Also, the surface grains (which are the ones usually observed) are in a special position with less constraint than those in the interior. Again, many of the applied stress systems are inhomogeneous. Dehlinger considers that under repeated loadings lock-up internal stresses develop due to the inhomogeneous deformation and, when large enough, cause a crack to form.

Orowan (1939) considers a more localized inhomogeneity and takes as a model a small plastic region embedded in an elastic matrix. He argues that under an applied stress the plastic region can yield and transfer part of the local stress to the elastic surrounding. In doing so it work hardens and under repeated loadings he shows that the work hardening per cycle decreases and that the total work hardening tends to a finite limit which depends on the applied stress. If this limit is below the local "fracture strength," the metal can withstand an infinite number of cycles. If the stress is higher, then the work hardening will reach the fracture strength in a finite number of cycles. A crack then forms and is assumed

to propagate by a similar mechanism applying to a small plastic region at its tip. By making a rather arbitrary assumption about the variation of rate of strain hardening with magnitude of applied stress, the predicted $S - N$ curve can be given the right shape. However, quantitative agreement is secured only by assuming extreme values for the physical properties of the plastic region, e.g. a coefficient of strain hardening two to four orders of magnitude less than the static coefficient of the bulk metal. A more detailed analysis is given by AFANASIEV (1940, 1941) using similar ideas to DEHLINGER; the $S - N$ relation obtained is identical with that of OROWAN.

FREUDENTHAL (1946) considers hypothetical " bonds " in the material which have a certain probability of breaking at each load application, and from a " weakest link " argument the probability of complete failure after N load applications can be calculated. Although this gives a $S - N$ curve of the right form the basis of the analysis has been criticized by EPSTEIN (1948) and it appears (FREUDENTHAL 1949) that the theory can be applied to brittle materials only.

MACHLIN (1948 a, b; 1949) has considered fatigue of a material which initially contains cracks. The cracks are presumed to extend by the generation of dislocations in the stress field at the tip of the crack with the aid of thermal fluctuations. Although this is the only published theory which considers a basic atomic process of fatigue, it does not appear to apply to any real situation. It does not seem possible (FRANK 1950) that suitable cracks with sufficiently large stress concentration are invariably present in all metals. Moreover, the large temperature dependence of fatigue predicted by this theory does not agree with the small variation observed (TEED 1950).

As each of these theories can predict a $S - N$ curve which can be fitted to some experimental results, it appears that this is not a very sensitive test of the correctness of a theory of fatigue, particularly as the experimental curves are not precisely determined due to the scatter of test points.

8. DISCUSSION

Due perhaps to the more easily observed changes, the initial and final stages are better understood than the intermediate stage. The initial stage (if present) appears to be essentially the bulk deformation of the metal until it has work hardened sufficiently to withstand the applied stress. The actual mechanism of this hardening is intrinsically of interest as it differs from static hardening in important respects and also differs at high and low frequencies of application. These differences may affect the generation and propagation of the ultimate fatigue crack. Two opposing consquences are apparent, one that the smaller disorientation of the bulk may make the propagation of a crack along the slip planes easier than it would be in a statically deformed metal, the other that the same small internal distortion would not aid the formation of a crack as would the larger disorder in the static case. These two opposing effects may also be the explanation of the many observations that a small amount of prior static cold work can improve the fatigue resistance of a metal whereas a large amount is detrimental.

However, the crux of the problem of fatigue appears to lie in the long middle period. During this, deformation is occurring in very limited regions and it is there that a crack is ultimately seen. It is usually assumed that the crack is formed

finally as a result of the intense distortion of these regions. But recent observations that a crack can sometimes be detected very early in the life of a specimen suggest that the converse interpretation should not be overlooked, namely that the deformation in localized regions is the result of the stress concentration round a submicroscopic crack.

In either case the difficulty is to explain a process which progresses so slowly. For instance, the average rate of extension of the cracks observed by FENNER, OWEN and PHILLIPS (1951) is of the order of one atom per stress cycle, and during part of the growth would be even less. Although very little is known of the atomic mechanism of formation and propagation of a crack it does not appear probable that it could extend in a continuous manner at such low rates of extension. Similarly microscopic observations of the thickening of slip bands during the middle stage of fatigue suggest that the individual slip lines of the cluster are formed, complete, at irregular time intervals. In this respect their formation is similar to slip lines under static stress and the same explanation can be given, namely, that the group of dislocations producing the slip line are generated by a FRANK-READ source (1950).

If deformation in fatigue is an intermittent process then it is necessary that there be an element of randomness present. For, if not, then if one stress cycle produces no irreversible effect, neither should any of the indentical cycles which follow. That there is an element of randomness in fatigue is also suggested by the large scatter of experimental $S - N$ points. Due to the small temperature dependence of fatigue, it does not seem sufficient to propose a simple explanation in terms of random thermal stresses occasionally aiding the applied stress to start a FRANK-READ source generating dislocations on a nearby slip plane. If thermal fluctuations are the cause of the randomness, it must be by a more involved or indirect process. Progress in formulating a theory of fatigue at an atomic level appears to depend on an indentification of this random element. The only current theory which attempts to do this is that due to MACHLIN, but the process he uses does not appear to correspond with reality.

Vol
1
1952/

ACKNOWLEDGMENTS

I would like to acknowledge many discussions with Professor N. F. MOTT, University of Bristol, and Dr. W. A. WOOD, University of Melbourne, although opinions expressed here do not necessarily coincide with theirs. This review is published by permission of The Commonwealth of Australia, Department of Supply, of which the author is an Officer.

REFERENCES

AFANASIEV, N. N. 1940 *J. Tech. Phys. U.S.S.R.*, **10**, 1553.
1941 *J. Tech. Phys. U.S.S.R.*, **11**, 349.

BATELLE MEMORIAL INSTITUTE 1941 *Prevention of the Failure of Metals under Repeated Stress*, (John Wiley and Sons, New York).

BENNETT, J. A. 1946 *Proc. Am. Soc. Test. Mat.*, **46**, 693.
1951 *J. Res. Nat. Bur. Standards*, **46**, 457.

BENNETT, J. A. and BAKER, J. L. 1950 *J. Res. Nat. Bur. Standards*, **45**, 449

BROWN, A. F. 1952 *Advances in Physics*, **1**, 427.

Cavanagh, P. E.	1947	*Proc. Am. Soc. Test. Mat.*, **47**, 639.
Cox, H. L. and Field, J. E.	1952	*Aero. Quart.*, **4**, 1.
Craig, W. J.	1952	*Eng. Exp. Station, Univ. of Illinois, Tech. Rep. No.* 27.
De Forest, A. V.	1936	*J. Appl. Mech.* **58**, A. 23.
Dehlinger, U.	1940	*Zeits. Physik.*, **115**, 625.
	1941	*Zeits. Metallkunde*, **32**, 199.
Division of Aeronautics	1945	*Bibliography on the Fatigue of Metals*, C.S.I.R. (Melbourne).
Duce, A. G.	1950	*A Study of some Fatigue Phenomena in Pure Metals and Alloys*, Ph.D. Thesis, University of Cambridge.
Epstein, B.	1948	*J. Appl. Phys.*, **19**, 140.
Fenner, A. J., Owen, N. B. and Phillips, C. E.	1951	*Engineering*, **171**, 637.
Ferguson, L.	1944	*Metal Progress*, **45**, 512.
Forsyth, P. J. E.	1951	*J. Inst. Metals*, **80**, 187.
Frank, F. C.	1950	*Carnegie Inst. of Technology Symposium on the Plastic Deformation of Crystalline Solids*, p. 92.
Frank, F. C. and Read, W. T.	1950	*Phys. Rev.*, **79**, 722.
Freudenthal, A. M.	1946	*Proc. Roy. Soc. A*, **187**, 416.
	1949	*Cold Working of Metals*, (Am. Soc. Metals, Cleveland) p. 248.
Gough, H. J.	1926	*The Fatigue of Metals*, (Ernest Benn Ltd., London)
	1933	*Proc. Am. Soc. Test. Mat.*, **33**, 3.
Gough, H. J. and Hanson, D.	1923	*Proc. Roy. Soc. A*, **104**, 538.
Gough, H. J. and Wood, W. A.	1936	*Proc. Roy. Soc. A*, **154**, 510.
	1938	*Proc. Roy. Soc. A*, **165**, 358.
Hanstock, R. F.	1951	*The Nondestructive Testing of Metals*, (Inst. of Metals, London).
Hanstock, R. F. and Murray, A.	1946	*J. Inst. Metals*, **72**, 97.
Head, A. K.	1950	*Am. Soc. Test. Mat. Bull.*, 51.
Lucas, F. F.	1927	*Trans. Am. Soc. Steel Test.*, **11**, 531.
McClintock, F. A.	1951	*Proc. First Nat. Congress Appl. Mech.* (to be published).
	1952	*J. Appl. Mech.*, **19**, 54.
Machlin, E. S.	1948	*N.A.C.A. Tech. Note No.* 1489.
	1948	*Fracturing of Metals.* (Am. Soc. Metals, Cleveland) p. 282.
	1949	*N.A.C.A. Tech. Report No.* 929.
Mann, J. Y.	1950	*Aeronautical Research Laboratories, Melbourne, Report SM.* 147.
Orowan, E.	1939	*Proc. Roy. Soc. A.*, **171**, 79.
Peterson, R. E.	1950	*Am. Soc. Test. Mat. Bull.*, 50.
Rosenholtz, J. L. and Smith, D. T.	1952	*Metal Progress*, **61**, 85.
Schall, A.	1949	*Zeits. Metallkunde*, **40**, 417.
Sinclair, G. M. and Dolan, T. J.	1951	*Proc. First Nat. Congress Appl. Mech.* (to be published).
Teed, P. L.	1950	*The Properties of Metallic Materials at Low Temperatures*, (Chapman and Hall, London).
Wood, W. A., Bullen, F. P. and Head, A. K.	1952	*Proc. Roy. Soc.* (in press).
Wood, W. A. and Head, A. K.	1951	*J. Inst. Metals*, **72**, 97.
Wood, W. A. and Thorpe, P. L.	1940	*Proc. Roy. Soc. A.*, **174**, 310.

ol.
1
2/53

Journal of the Mechanics and Physics of Solids, 1953, Vol. 1, pp. 142 to 145. Pergamon Press Ltd., London.

A NOTE ON THE BACK-PULL FACTOR IN STRIP-DRAWING

By R. Hill
Department of Theoretical Mechanics, University of Bristol

(*Received 7th November*, 1952)

Summary

An expression is derived for the back-pull factor in strip-drawing, based on the slip-line field theory of Hill and Tupper. It is shown that the currently accepted formula of MacLellan, based on the approximate theory of Sachs, is appreciably in error when the reduction or the coefficient of friction is large.

Vol.
1
1952/

1. Introduction

In a recent paper, Green and Hill (1952) have obtained a formula for the load needed to draw a wide strip of non-hardening plastic-rigid material through a rough wedge-shaped die. The formula applies to a range of reductions and die-angles where the pressure on the die is distributed uniformly. In the present note it is shown how the load for drawing with back-pull may be derived from the load calculated by Green and Hill for drawing without back-pull.

2. Theory for Back-pull Drawing

Consider the slip-line field in the deformation zone in drawing, without back-pull, through a die of angle 2α, fractional reduction r, and coefficient of friction μ^*. Let t^* be the drawing stress and q^* the die pressure, in the range of reductions and angles where this is distributed uniformly:

$$\alpha\left(0{\cdot}230 + \frac{\alpha}{9}\right) \leqslant r \leqslant 2\sin\alpha/(1 + 2\sin\alpha), \text{ approximately.} \tag{1}$$

This is the range where the redundant work is appreciable.

A uniform hydrostatic tension σ may be superimposed on the stress system in the deformation zone without affecting the equilibrium equations, the yield condition, or the plastic stress-strain relations. The die pressure becomes $q^* - \sigma$, but the frictional stress is unaltered; the new coefficient of friction is therefore

$$\mu = \mu^* q^*/(q^* - \sigma). \tag{2}$$

The drawing stress becomes $t^* + \sigma$. The rigid part of the plastic region bordering the deformation zone is, of course, changed but this need not be considered here. It is only necessary to be sure that the non-plastic material can support the proposed stresses in the deformation zone, and this appears certain so long as

$q^* + \sigma$ does not exceed the tensile yield stress in plane strain.†

We have thus derived, from a solution for no back-pull and friction coefficient μ^*, a solution for back-pull σ and friction coefficient μ given by (2). It is evident that this method fails when the die pressure is not distributed uniformly, which is so for all reductions greater than (1).

According to the computations by GREEN and HILL, q^* is given, for r in the range (1) and $5° \leqslant \alpha \leqslant 15°$, $\mu^* \leqslant 0{\cdot}15$, by

$$\frac{q^*}{q_0} = 1 - \frac{\lambda^* \epsilon}{1 + \lambda^*}, \qquad \lambda^* = \mu^* \cot \alpha, \tag{3}$$

where q_0 is the die pressure for zero friction, and ϵ is a parameter dependent only on die geometry and given by

$$\epsilon = 0{\cdot}2 \tan \alpha + 0{\cdot}08\, r \cot \alpha. \tag{4}$$

Since ϵ is less than 0·2 where (3) holds, the term involving ϵ in (3) is always less than 0·1.

The solution of (2) and (3) for q^* and μ^* is

$$\frac{q^*}{q_0} = 1 - \frac{(1 - \sigma/q_0)\,\lambda\epsilon}{1 + (1 - \sigma/q_0)\,\lambda}, \qquad \lambda = \mu \cot \alpha, \tag{5}$$

$$\frac{\mu^*}{\mu} = (1 - \sigma/q_0)\left[1 - \frac{\lambda\epsilon\sigma/q_0}{1 + (1 - \sigma/q_0)\,\lambda}\right], \tag{6}$$

with neglect of terms of order ϵ^2. The error so committed is less than the computational error involved in (3).

3. THE BACK-PULL FACTOR

Let q be the die pressure and $Q\,(o)$ the axial component of die load in drawing without back-pull through a rough die with friction coefficient μ, and $Q\,(\sigma)$ that when the back-pull stress is σ. Then, if H is the initial strip-thickness,

$$Q\,(o) = (1 + \lambda)\, rHq, \qquad Q\,(\sigma) = (1 + \lambda)\, rH\,(q^* - \sigma).$$

Also, as in (3),

$$\frac{q}{q_0} = 1 - \frac{\lambda\epsilon}{1 + \lambda} \tag{7}$$

provided $\mu \leqslant 0{\cdot}15$. Then

$$\begin{aligned} Q\,(o) - Q\,(\sigma) &= rH\sigma\,(1 + \lambda)\left(1 - \frac{q^* - q}{\sigma}\right) \\ &= rH\sigma\left[1 + \lambda - \frac{\lambda\epsilon}{1 + (1 - \sigma/q_0)\,\lambda}\right] \end{aligned} \tag{8}$$

from (3), (6) and (7), neglecting, as before, terms of order ϵ^2.

The reduction in die load is thus not strictly proportional to the back-pull, in contrast to previous theories. The curvature of the $Q\,(\sigma)$ relation is, however, small : in the range of validity of (3) the slope decreases by not more than a few

† MACLELLAN (1952) has criticized the HILL-TUPPER theory on the ground that the sum of the die pressure and the drawing stress exceeds the yield stress. The die pressure is, however, not the mean transverse stress in the exit plane, and is in fact much greater.

per cent as σ increases up to an amount sufficient to reduce Q to zero ($\sigma/q_0 \sim 1/(1+\lambda)$). This may be contrasted with BARON and THOMPSON's observations (1950) that, in drawing brass *wires* pre-strained to a yield stress of about 18 tons/in.^{2}, the slope decreases by 20-30 per cent.; the reductions were, however, such that the redundant work was slight.† MACLELLAN (1952), on the other hand, found a hardly perceptible change in slope for copper wire pre-strained to a yield stress of about 18 tons/in.^{2}; his dies had, however, parallel extensions which appreciably changed the influence of back-pull.

For practical purposes we may put $Q(\sigma) = Q(o) - b\,\sigma\,H$ where b, the back-pull factor, is here taken as the *initial* slope of the $Q(\sigma)$ relation:

$$b = r\left(1 + \lambda - \frac{\lambda\epsilon}{1+\lambda}\right). \tag{9}$$

3. COMPARISON WITH PREVIOUS THEORIES

According to the writer's previous approximate theory (1949), in which the influence of friction on die pressure was neglected,

$$b = r(1+\lambda). \tag{10}$$

According to MACLELLAN's extension (1948) of SACHS' theory, which disregards the inhomogeneity of the deformation,

$$b = 1 - (1-r)^{1+\lambda}. \tag{11}$$

Formula (11) underestimates, and formula (10) overestimates, the true value of b given by (9). The proportionate error in (11) increases (i) with increasing r and (ii) with increasing μ (at any rate, where (3) is valid). (ii) is to be expected since in SACHS' theory no account is taken of the influence of friction on the assumed trajectories of principal stress. (i) is perhaps unexpected since the SACHS formula for the *frictionless* drawing load is known to become, on the whole, more accurate the larger the reduction. However, the actual distribution of pressure on the die, and the mode of deformation, are considerably different from those in SACHS' theory (cf. GREEN and HILL, op. cit.). One may suspect, therefore, that the good approximation of the SACHS die load in frictionless drawing is fortuitous; the present results confirm this. The analogous SACHS and MACLELLAN formulae for wire-drawing may also be expected to involve greater errors than has hitherto been supposed.

Table 1 compares equations (9), (10) and (11) at the largest reductions for which (9) has been established.

For large r and μ the formula (10) is better than MACLELLAN's, and indeed better than the original method of derivation might suggest. In fact, however, (10) may alternatively (and preferably) be derived from the less drastic assumption that the application of a back-pull stress diminishes the die pressure by exactly the same amount; there is then no need to assume anything about the effect of friction on die pressure.

† BARON and THOMPSON inferred that the observed curvature is due to a decrease in the friction coefficient as the die pressure is reduced; the present theory shows that this inference is not well-founded. They also argued the same conclusion from the increase in slope with increasing pre-strain, coupled with another dubious prediction of earlier theories, viz., that the $Q(\sigma)$ relation is independent of the stress-strain curve.

4. Derivation of μ from Back-pull Data

If b is obtained from the experimental Q (σ) relation, μ can be deduced by solving (9). It may be shown that

$$\lambda = \mu \cot \alpha = (b/r - 1) + (1 - r/b)\,\epsilon, \tag{12}$$

with neglect of ϵ^2 terms (the resulting error in μ is entirely negligible).

It may be remarked that the error in MacLellan's formula for b is greatly magnified in the derived value of μ. For example, if $b = 0{\cdot}387$ happens to be the

Table I

Comparative back-pull factors

μ	0·05	0·10	0·15	
Equation (9)	0·224	0·305	0·387	$\alpha = 5°$
,, (10	0.232	0.317	0.403	
,, (11)	0.222	0·290	0·352	$r = 0{\cdot}148$
,, (9)	0·397	0·455	0·513	$\alpha = 15°$
,, (10)	0·404	0·468	0·532	
,, (11)	0·391	0·435	0·478	$r = 0{\cdot}341$

observed value for $\alpha = 5°$, $r = 0{\cdot}148$, then, according to Table 1 or (12), 0·150 is the true value of μ. MacLellan's formula would, however, give $\mu = 0{\cdot}180$, an overestimate of 20 per cent. Again, if $b = 0{\cdot}513$ is observed for $\alpha = 15°$, $r = 0{\cdot}341$, the true μ is 0·150 while MacLellan's μ is 0·195 with an error of 30 per cent. (10) gives 0·141 and 0·135 respectively.

5. Further Work

At sufficiently large reductions, where the redundant work is small, only the approximate formulae (10) and (11) are available (the extrapolation of (9) could possibly be risked). It appears that (10) is preferable, though the errors are still appreciable. It is evidently highly desirable to obtain a more accurate formula in this range. An exact determination based on the slip-line field would involve an enormous amount of labour. There are, however, prospects that a sufficiently good approximation may be obtained by the method of upper and lower bounds (Hill 1951).

References

Baron, H. G. and Thompson, F. C. 1950 *J. Inst. Metals*, **78**, 415.

Green, A. P. and Hill, R. 1952 *J. Mech. Phys. Solids*, **1**, 31.

Hill, R. 1949 *J. Iron and Steel Inst.*, **161**, 41.

1951 *Phil. Mag.*, **42**, 868.

Hill, R. and Tupper, S. J. 1948 *J. Iron and Steel Inst.*, **159**, 353.

MacLellan, G. D. S. 1948 *J. Iron and Steel Inst.*, **158**, 347.

1952 *J. Inst. Metals*, **81**, 1.

BOOK REVIEWS

P. W. BRIDGMAN: **Studies in Large Plastic Flow and Fracture.** McGraw-Hill Book Company, Inc., New York. 1952. 362 pp. $8.

IN this book Prof. BRIDGMAN has assembled a valuable store of experimental data from his numerous published papers and wartime reports. The investigations reflect his lifelong interest in the construction of 'pressurized laboratories.' His virtuosity in this field is well-known; his enthusiasm leads him to such ventures as hardness testing, extrusion, and wire-drawing – all under hydrostatic pressure. Prof. BRIDGMAN writes conversationally, even colloquially at times. Unexpectedly, his reflections on fundamental problems of flow and fracture are often naive, but the experimental observations are reported with admirable clarity for all to interpret.

The most thorough-going group of experiments are tension tests on high-strength steels under pressures up to 30,000 atmospheres. The main conclusions would appear to be as follows. (i) To a very rough approximation, fracture occurs when the greatest principal stress attains a critical (positive) value. A universal criterion, reasonably accurate for all the steels tested, could, however, not be found in terms of macroscopic stress and strain. (ii) The strain to fracture is notably enhanced by an ambient fluid pressure. (iii) Strain-hardening continues at a roughly constant rate. (iv) The stress-strain curve is, to a first approximation, independent of the superposed pressure. (v) There is a suggestion (hardly more, in view of the uncertain influence of creep or the unknown accuracy of the author's correction for necking) that a superposed pressure causes a slight raising of the stress-strain curve in tension. A further complication is the marked development of crystallographic anisotropy during the enormous deformation obtained under these conditions.

Comparative data for non-ferrous metals is unfortunately only fragmentary; so also is that for uniaxial compression combined with hydrostatic pressure. It is to be hoped that Prof. BRIDGMAN will eventually be able to extend his investigations in these directions.

A large hydrostatic component of stress can, of course, be obtained otherwise than in a pressurized laboratory. In the several methods described here, however, the results are difficult to interpret owing to the complex distribution of stress in the plastic zone. With the exception of a stress analysis of compressed tubes, Prof. BRIDGMAN has by no means made what use he could of the mathematical theory of plasticity to estimate correction factors. Similarly, his observations of directional effects in two-dimensional compression could have been systematized with the help of the theory of plasticity for anisotropic metals. Such omissions render a large part of the book merely interesting in a general way, and many of the results should probably not be taken at face-value.

R. HILL

Imperfections in Nearly Perfect Crystals. Edited by W. SHOCKLEY, J. H. HOLLOMON, R. MAURER and F. SEITZ. John Wiley and Sons Inc., New York; Chapman and Hall., London. 1952, 490 pp. + xii. $7.50 or £3.

Recently the National Research Council of the U.S.A., with financial support from the Office of Naval Research, has organized Conferences of which the printed Report is likely to be of even greater value than the meeting itself. The symposium on Imperfections in Nearly Perfect Crystals, held in October, 1950, gathered the leading American experts in the field, together with MOTT and BRAGG from England, CHALMERS from Canada, and GUINIER from France. The Report consists of 17 papers, together with selected contributions to the discussion. Most of the papers summarize particular aspects of the subject. The student beginning research will be well advised to read a selected group of these papers. The expert reading the papers on his own speciality

Vol. 1 1952/5

will find much which is familiar and, almost certainly, a good deal which is new to him. To the expert, however, the main value of the book is likely to lie in its surveys of fields related to his own, particularly now that the interdependence of the various properties studied is proving such a profitable subject of research.

This idea of interdependence is emphasized in the introductory paper, by F. SEITZ, who ambitiously attempts to prepare a synthesis comparable to YUKAWA's proposal of a meson theory of nuclear forces. No one is better qualified than SEITZ to attempt such a programme, and his survey of the whole field of imperfections in crystals is a remarkable feat of virtuosity, most stimulating to the reader. It states explicitly an approach which SEITZ himself and many others have for some time been using without a definite formulation. "Assume that we know a great deal about one type of imperfection, such as a free electron. From effects induced by interaction with another imperfection we may deduce properties of the second imperfection. From the knowledge gained about the second imperfection and additional information about its interaction with a third imperfection, we may obtain information about the third. This may then be cross-checked by studying the interaction of the third imperfection and an electron. It is noteworthy that the theory of imperfections and the experimental techniques for studying them have finally reached a state in which it is conceivable to undertake interlocking investigations of this type in a systematic way." Despite these virtues, the reviewer feels that the article fails in its primary aim of presenting a synthesis already largely achieved. Indeed, the aim seems to him impossible: the field of imperfections in crystals is, like the London Underground map, irreducibly complicated, not, like the Washington street plan, subject to grand synthetic principles.

The second introductory paper, on the geometry of dislocations, is by W. T. READ and W. SHOCKLEY, and forms an excellent introduction to the rather complicated properties of dislocations which these authors and F. C. FRANK have recently found to be of outstanding importance in the theory of crystal plasticity.

There follows a group of papers on the role of imperfections in deformation. C. S. BARRETT contributes an excellent survey of stacking faults which are induced by plastic deformation and phase changes. W. T. READ gives a review of experimental information on slip lines, eschewing the temptation to devise theoretical explanations. B. E. WARREN and A. L. AVERBACH outline their technique for the X-ray analysis of stresses in cold-worked metals. They find support for the assumption that the stress distribution is essentially isotropic. In discussion, READ and SHOCKLEY say "these investigations are probably the most direct evidence ever presented that the cold-worked state consists of a substantially uniform distribution of dislocations." N. F. MOTT contributes the next paper, on the dislocation theory of mechanical strength and creep in metals. E. OROWAN, in discussion, shows that the usual rather naive presentation of the theory of exhaustion creep is not self-consistent. The section closes with a paper by J. S. KOEHLER on the influence of dislocations on the damping of metal single crystals, which, though beginning with a survey, is essentially an important original paper. Its importance is not reduced by the rather negative conclusion that the observed damping is far too great to be explained by KOEHLER's very reasonable mechanism, taken in conjunction with available estimates of the resistance to the motion of a dislocation.

The third group of papers, on diffusion and related phenomena, begins with an account by R. G. BRECKENRIDGE of relaxation effects in ionic crystals, including recent studies on mechanical damping. This is followed by a survey, by L. APKER and E. TAFT, of studies of alkali halides by photoelectric methods, a subject on which much quantitative information has been accumulated. The concluding papers in this section, on diffusion in metals and alloys, form a curiously well-matched pair. J. BARDEEN and C. HERRING treat diffusion and the Kirkendall effect by considering vacant lattice sites as an independent component of the system. They clear up many obscurities in the theory, and show why dislocations are effective sources of vacant sites in diffusion, but not in sintering. They give no discussion of the temperature dependence of the rate of diffusion. This is given in the following paper by C. ZENER, who, in the course of a general treatment, resolves the ambiguities which appear when the heat of activation is not a constant, but is a linear function of temperature.

The last six papers deal with the properties of grain boundaries in metals, and of the sub-boundaries which sometimes appear within a single grain. The first of the group, by J. C. FISHER and C. G. DUNN, collects the available data on surface and interfacial tensions of metals, adding some new results, and reinterpreting some of the old experiments. Observations on the variation

of grain boundary angle with orientation are also reported. In the next paper, W. T. READ, and W. SHOCKLEY give the latest development of their theory of this variation. CYRIL S. SMITH extends the analysis of FISHER and DUNN to a comparison of the surface energy between two grains of the same phase with the surface energy of an interphase boundary in a two-phase alloy. Remarkably, the latter is nearly always lower. SMITH makes an ingenious attempt to relate this to the fact that two plane lattices with the same co-ordination number can only be joined by introducing atoms with the wrong co-ordination number, while lattices with co-ordination numbers $n+1$ and $n-1$ can always be joined systematically by a row of atoms with co-ordination number n. There follows an excellent account of sub-structures in crystals, by A. GUINIER. B. CHALMERS contributes a brief essay on the properties and effects of grain boundaries, and R. SMOLUCHOWSKI closes the volume with a paper on movement and diffusion in grain boundaries, emphasizing the importance of the grain boundary as a channel of easy diffusion.

There are full name and subject indices, though only moderate care seems to have been used in compiling the former. Thus, BAEDEKER, whose name appears on p. 5, is mentioned neither in the references nor, surprisingly, in the index, which atones with separate entries for FRENKEL, I. and FRENKEL, J. An adequate distinction is made between SMITH, CHARLES S., and SMITH, CYRIL S., but one paper is impartially attributed to both. This, and a frequency of mis-spelt proper names remarkable in a book otherwise so carefully prepared, are practically the only imperfections in this nearly perfect book.

F. R. N. NABARRO.

Vol.
1
1952/

Journal of the Mechanics and Physics of Solids, 1953, Vol. 1, pp. 149 to 163. Pergamon Press Ltd., London.

FLANGE BUCKLING IN A BENT I-SECTION BEAM

By J. F. Davidson
Engineering Laboratory, Cambridge

(*Received 20th November*, 1952)

Summary

Buckling loads are given for a flat and infinitely long elastic plate compressed in its own plane by thrusts which act parallel to two opposite edges, and which vary linearly between them. One of these edges is free, and the other fixed in position but elastically clamped. The Rayleigh-Ritz method is used in most of the calculations, a method originated by Schwarz being used as an accurate check. The results may be applied to calculate the flange buckling load of a thin walled section subjected to end load and bending. This has been done in the case of an I-section under pure bending, and the results have been verified by experiment.

ol.
1
2/53

1. Introduction

When a thin walled structural member is subjected to end load and bending, failure may be caused by buckling of the most severely compressed walls. The calculation of the critical load in such cases is necessary for the design of the most efficient structural sections. The present paper deals with one aspect of this problem, namely, flange buckling in an I-section beam bent by pure couples inclined at angles between 0 and 90 degrees to the web. The information given has been verified by experiment and will, together with previous work, facilitate the calculation of flange buckling in an I-section under any combination of axial thrust and bending.

In the theoretical analysis, the buckled flange has been treated as a flat and infinitely long elastic plate, compressed by thrusts in its own plane and parallel to two opposite edges. One of these edges is free, the other being fixed in position but elastically clamped. Under these conditions the deformations follow equations of the type originated by Bryan (1891). When the thrusts in the plane of the plate vary linearly across its width, solution of these equations in terms of known functions is not possible. Two approximate methods were therefore used to calculate the critical load, which is given over a wide range of values of the three independent variables. These are

(i) The wavelength of the buckled plate.
(ii) The amount of elastic clamping.
(iii) The amount of variation of thrust across the plate width.

The Rayleigh-Ritz method was used for the bulk of the calculations, while a method originated by Schwarz (1890) has been used as an accurate check at selected points. Some theoretical interest is attached to the application of the first method, in that the assumed deformation of the plate satisfied only the geometrical edge conditions, but did not satisfy statical edge conditions. This

possibility was noted by RAYLEIGH (1894) and by RITZ (1909), but has been neglected by many subsequent writers who have used functions which satisfy all the boundary conditions.

In any particular case, such as an I-section beam, it is necessary to calculate the amount of elastic clamping at the inner edge of the flange in order to use the curves given by the above analysis. This clamping is provided by the remainder of the I-section, which resists rotation of the buckled flange about the line in which it joins the web. The amount of clamping may be estimated from tables given by KROLL (1943), so that the I-section is treated as a series of plates, any of which may be compressed by loads parallel to the junction lines.

2. THEORY OF BUCKLING

The state of stress in an I-section beam, bent by pure couples acting in a plane at angle θ to the web, is shown in Fig. 1. The couple required to cause local buckling of the compressed flange may be calculated on the basis of four assumptions

(i) The beam is treated as five thin plates rigidly joined along the lines DC and EF, and simply supported at the ends of the beam.

(ii) The curvature due to the applied moment is neglected.

(iii) The junction lines DC and EF are assumed to remain straight during buckling.

(iv) The variation of stress across the thickness of each constituent plate is neglected.

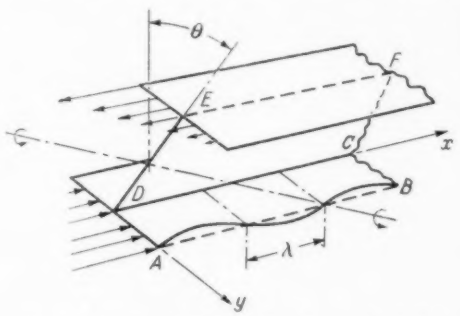

Fig. 1. Stresses in I-section beam bent by couples at angle θ to web.

On this basis, we may apply the well-known equation of deformation,

$$\frac{\partial^4 w}{\partial x^4} + \frac{2\partial^4 w}{\partial x^2 \partial y^2} + \frac{\partial^4 w}{\partial y^4} = -\frac{N}{D}\frac{\partial^2 w}{\partial x^2}, \tag{2·1}$$

to the buckling of the most severely compressed flange $ABCD$. Dx and Dy are coordinate axes shown in Fig. 1, w is the deflection of the buckled flange out of its own plane, $D = Et^3/12(1-\sigma^2)$ is the flexural rigidity, t being the plate thickness, E Young's modulus and σ Poisson's ratio. N is the compressive load per unit length which acts in the direction Dx and may be a function of y.

Edge conditions of the buckled flange

(1) At the ends of the beam, we have simple support so that

$$w = \frac{\partial^2 w}{\partial x^2} = 0. \tag{2·2}$$

(ii) Along AB where $y = b$ the plate width,

$$\left.\begin{aligned} &\frac{\partial^2 w}{\partial y^2} + \sigma \frac{\partial^2 w}{\partial x^2} = 0 \\ &\frac{\partial^3 w}{\partial y^3} + (2 - \sigma) \frac{\partial^3 w}{\partial x^2 \partial y} = 0, \end{aligned}\right\} \tag{2·3}$$

giving zero moment and shear.

(iii) Along DC where $y = 0$,

$$w = 0. \tag{2·4}$$

Also, rotation $\partial w/\partial y$ of the plate about DC (Fig. 1) is resisted by couples due to the deformation of the remainder of the I-section. These couples are proportional to $\partial w/\partial y$ so that

$$D \frac{\partial^2 w}{\partial y^2} = K \frac{\partial w}{\partial y}, \tag{2·5}$$

K being a constant, the couple per unit length per unit rotation.

Non-dimensional forms

The above equations may be simplified and reduced to non-dimensional terms by using

$$\frac{w}{b} = F(\xi) \sin \frac{\pi x}{\lambda} \tag{2·6}$$

where $\xi = y/b$, and λ is the half wavelength in the x direction. (2·6) satisfies the edge condition (2·2) and when substituted in (2·1) gives

$$\frac{d^4 F}{d\xi^4} - 2\beta^2 \frac{d^2 F}{d\xi^2} + \beta^4 F = kF\Omega \tag{2·7}$$

$\beta = \pi/\mu$, $\mu = \lambda/b$, $k = N_1 b^2/\pi^2 D$, and N_1 is the value of N at $\xi = 1$, so that k is referred to the stress at the outer edge of the plate. Also, $N = N_1 [\alpha + (1\text{-}\alpha)\xi] = N_1 \Omega/\beta^2\pi^2$, so that α gives the ratio of the stress at the fixed edge to the stress at the free edge.

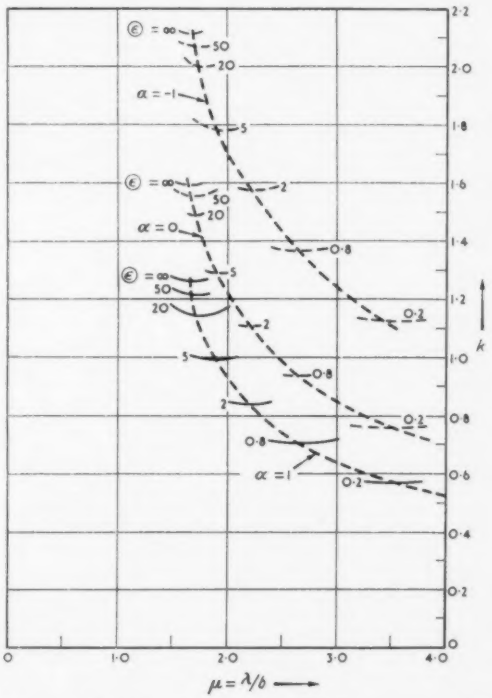

Fig. 2. Buckling load (RAYLEIGH-RITZ 3 terms) against μ for various fixity and bending.

The edge condition (2·3) becomes, after substitution of (2·6), at $\xi = 1$,

$$\left.\begin{aligned} &F'' - \sigma\beta^2 F = 0, && \text{(i)} \\ &F''' - (2 - \sigma)\beta^2 F' = 0, && \text{(ii)} \end{aligned}\right\} \tag{2·8}$$

dashes denoting differentiation with respect to ξ. Similarly, at $\xi = 0$, from (2·4) and (2·5),

$$\left.\begin{aligned} &F = 0 && \text{(i)} \\ &F'' = \epsilon F', && \text{(ii)} \end{aligned}\right\} \tag{2·9}$$

where $\epsilon = Kb/D$.

When $\alpha = 1$, so that the stress is uniform across the width of the plate, a solution of (2·7) in terms of known functions has been given by LUNDQUIST and STOWELL (1942) and by BAKER and RODERICK (1948), who give k plotted against μ at various values of ϵ as shown in Fig. 2.

TABLE I.

Ratio :— (Maximum critical load)/(Minimum critical load) at constant ϵ, $\alpha = 1$.

ϵ	∞	20	10	1·0	0·4
m					
3	1·042	1·065	1·058	1·038	1·018
4	1·021	1·038	1·032	1·020	1·008
5	1·012	1·025	1·019	1·012	1·006
6	1·010	1·018	1·012	1·010	1·004

For a plate in which ϵ *is constant*, if we vary the length $m\lambda$, m being the number of half waves, the buckling load k will be a minimum at the value of λ given by the minimum in Fig. 2. When the buckling load is the same for m or $m - 1$ half waves, its value will be a maximum, whose ratio to the previous minimum is given in Table I.

Now in practical cases $\epsilon > 0{\cdot}4$, so that $\lambda/b < 3$, from Fig. 2, and since the ratio (section length)/(flange width b) will usually be more than 12, $m > 4$. Thus from Table I the error will be less than 4% if only minimum values of k are used at *constant* ϵ. The minimum values of k, together with the corresponding values of μ have, therefore, been plotted against ϵ in Fig. 3.

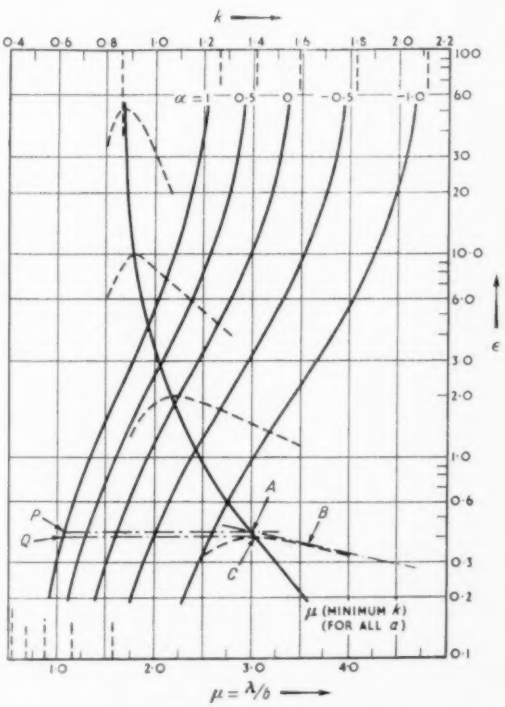

Fig. 3. Minimum buckling load k against fixity ϵ with varying bending. Dotted curves give ϵ against μ at constant k ($\alpha = 1$).

When the fixity ϵ is a function, obtainable from the tables of KROLL (1943), of μ, the dotted curves in Fig. 3 which give ϵ against μ at constant k, are required. Thus if the line AB is the known relation between ϵ and μ, whose slope is always negative, the minimum k will be at point B where AB is a tangent to one of the family of dotted curves. BC being a line of constant k, we find the minimum value of k from the point Q. A slightly larger

value of k is obtained from P corresponding with the intersection A on the minimum line AC. Now it will be seen from Fig. 3 that each of the dotted curves reaches a maximum negative slope $-(\partial\epsilon/\partial\mu)$ max, and that if this is numerically less than the slope of the line AB, the minimum k will be much smaller than the value at point P.

Table II gives $-(\partial\epsilon/\partial\mu)$ max at various ϵ, and the error in k when the line AB takes this maximum slope and the intersection A is used in place of B. Note that each maximum slope $-(\partial\epsilon/\partial\mu)$ max refers to a point on the line AC. In using Table II to test a particular $\epsilon - \mu$ relationship, AB, for the validity of the "intersection A" method, the position of point A, as well as the slope of the relationship, must be known.

TABLE II

Percentage increase in k due to use of minimum curve AC Fig. 3. $\alpha = 1$.

ϵ_c	k_P	% error in k_P	μ_B	μ_A	$(-\partial\epsilon/\partial\mu)$ max.
0·4	0·635	1·1	3·5	3·05	0·11
0·8	0·710	1·6	3·0	2·65	0·24
2	0·865	3·0	2·8	2·14	1·01
5	1·02	2·5	2·25	1·86	3·2
20	1·15	0·8	1·95	1·70	27·8

Thus, while the change in μ is large, the error in k is small enough to justify the use of the minimum curve, *provided* the slope AB is not greater than the value given, $-(\partial\epsilon/\partial\mu)$ max, at the point A in question.

The requirements for critical load calculations for $\alpha \neq 1$ are thus :

(i) Curves of k against μ to give minimum k at constant ϵ (Fig. 2).

(ii) These minimum k's and the corresponding values of μ to be plotted against ϵ (Fig. 3).

(iii) Examination of the maximum slope of the families of dotted curves in Fig. 3 for $\alpha \neq 1$.

(iv) Examination of the percentage error in k due to the use of this maximum slope with the intersection A in place of the true minimum point B (Fig. 3).

3. The Rayleigh-Ritz Method

When $\alpha \neq 1$, so that Ω varies with ξ, it is not possible to solve (2·7) in terms of known functions. The critical value of k may be then be obtained by equating the potential energy of bending to the work done by the buckling loads in the manner originated by Rayleigh (1894) and the expression for the critical load is

$$k = \frac{2\beta^2(1-\sigma)(FF')_{\xi=1} + \epsilon(F')^2_{\xi=0} + \int_0^1 (F'' - \beta^2 F)^2 \, d\xi}{\int_0^1 F^2 \Omega d\xi} = \frac{V}{T} \text{ say.} \qquad (3{\cdot}1)$$

Then applying Ritz's extension (1909) of Rayleigh's principle, we substitute for F in (3·1) an assumed shape

$$F = \psi_0 + \sum_{r=1}^{n} a_r \psi_r, \qquad (3{\cdot}2)$$

and put $\partial k/\partial a_1 = 0$, $\partial k/\partial a_2 = 0 \ldots \partial k/\partial a_n = 0$. Then by RAYLEIGH's principle k thus determined will always be greater than the true value, and will, from RITZ's extension, approach the true value as n is increased.

The question then arises as to whether ψ_r must satisfy the boundary conditions (2·8) and (2·9). RAYLEIGH (1894), using the method to find the fundamental frequency of a clamped-free bar, uses a shape for which $y''' \neq 0$ at the free end. RITZ (1909) states that the ψ_r must satisfy the boundary conditions " in so far as these do not themselves come from the variation problem." Many subsequent writers merely state that the boundary conditions must be satisfied. Thus TEMPLE and BICKLEY (1933) solve numerous problems in which all the boundary conditions are satisfied. Applying RITZ's argument to (3·1), we have in the present case, if $\delta(V - kT) = \delta V - k\delta T - T\delta k = \delta V - k\delta T = 0$,

$$[(F''' - \sigma\beta^2 F)\,\delta F' - (F'''' - (2-\sigma)\,\beta^2 F')\,\delta F]_{\xi=1} + [(\epsilon F' - F'' + \beta^2 F)\,\delta F' + (F''' - \beta^2 F')\,\delta F]_{\xi=0} + \int_0^1 (F^{iv} - 2\beta^2 F'' + \beta^4 F - k\Omega F)\,\delta F\, d\xi = 0. \qquad (3\cdot3)$$

Then since the exact solution for F satisfies (2·7) (2·8) and (2·9), small variations will not violate (3·3) unless they involve $\delta F \neq 0$ at $\xi = 0$. Hence ψ_r must satisfy (2·9) (i) only.

The physical basis of this result is illustrated by considering a strut, whose deflection u is prevented at the ends, while its slope γ there is resisted by a couple $G\gamma$, G being constant. If the ends of the strut are brought towards each other, so that buckling occurs, and then rigidly fixed in position, it will be found *experimentally* that the strut is in stable equilibrium. If now the strut is distorted by external forces, the potential energy $\frac{1}{2}\int_0^l B\,(u'')^2\,dz + G\gamma^2$ will thus be increased. z is measured along the strut whose length is l and flexural rigidity B. Hence the ratio (potential energy)/(strut shortening) will be increased in the distorted position, since the position of the ends, and therefore $\frac{1}{2}\int_0^l (u')^2\,dx$, the shortening, are fixed. This justifies RAYLEIGH's principle, and, as one distortion is obtained by applying end moments (still keeping the ends fixed in position), the end condition $G\gamma = Bu_0''$ need not be satisfied. Hence, in general, it is not necessary to satisfy conditions of *statics* at the ends.

If now $G \to \infty$ so that the ends are clamped, and RAYLEIGH's method is applied to an assumed shape for which $\gamma \neq 0$ at the ends, the term $G\gamma^2$ in the potential energy expression, and also the critical load, becomes infinite. Thus while the method is still valid it is useless, and only those deformations which give $\gamma = 0$ at the ends give a finite critical load. Hence in general it is necessary to satisfy *geometrical* end conditions in any assumed shape.

Analysis in normal modes

These results may also be justified by an analysis in normal modes. Following the method given, for example, by DEN HARTOG (1940) and by SOUTHWELL (1936), we expand the assumed shape in the form

$$F = \sum_{n=1}^{\infty} b_n F_n \qquad (3\cdot4)$$

where F_n is the nth mode associated with the critical load k_n. The modes obey the following orthogonality relations (see Appendix I), if $n \neq m$,

$$\left.\begin{aligned} &(1-c)\,\beta^2\,[(F_m F_n' + F_m' F_n)]_{\xi=1} + \epsilon\,[(F_n' F_m')]_{\xi=0} \\ &+ \int_0^1 (F_n'' - \beta^2 F_n)(F_m'' - \beta^2 F_m)\,d\xi = 0, \qquad \text{(i)} \\ &\int_0^1 \Omega F_n F_m\,d\xi = 0. \qquad \text{(ii)} \end{aligned}\right\} \qquad (3\cdot5)$$

If now we assume that (3·4) may be differentiated twice, direct substitution of (3·4) in (3·1), and use of the nth equation of type (3·1), yields the result

$$\frac{k}{k_1} = \frac{\int_0^1 \sum_{n=1}^{\infty} (k_n/k_1)\,b_n^2 F_n^2\,\Omega d\xi}{\int_0^1 \sum_{n=1}^{\infty} b_n^2 F_n^2\,\Omega d\xi}, \qquad (3\cdot6)$$

Vol 1 1952/

giving $k/k_1 > 1$ which justifies RAYLEIGH's principle.

The conditions under which (3·4) may be twice differentiated can be obtained by following the procedure for Fourier series given, for example, by JEFFREYS (1946). To find the coefficients b_n in (3·4), multiply each side by $\Omega\ F_n$ and integrate, giving

$$b_n \int_0^1 F_n^2\ \Omega d\xi = \int_0^1 F\ F_n\ \Omega d\xi \tag{3·7}$$

in view of (3·5ii). Then substituting for $F_n\ \Omega$ from (2·7),

$$b_n \int_0^1 F_n\,(F_n^{\mathrm{iv}} - 2\beta^2\ F_n'' + \beta^4\ F_n)\,d\xi = \int_0^1 F\,(F_n^{\mathrm{iv}} - 2\beta^2\ F_n + \beta^4\ F_n)\,d\xi.$$

Then integrating by parts we obtain

$$\begin{aligned} & b_n\left[2\beta^2\,(1-\sigma)\,(F_n'\ F_n)_{\xi=1} + \epsilon\,(F_n')^2{}_{\xi=0} + \int_0^1 (F_n'' - \beta^2\ F_n)^2\,d\xi\right] \\ &= \beta^2\,(1-\sigma)\,(F_n' F + F_n F')_{\xi=1} + \epsilon\,(F_n' F')_{\xi=0} + \int_0^1 (F_n'' - \beta^2\ F_n)\,(F'' - \beta^2\ F)\,d\xi \\ &\quad - \left[F\,(F_n''' - \beta^2\ F_n')\right]_{\xi=0}. \end{aligned} \tag{3.8}$$

If it is possible to differentiate (3·4) twice, we may also find the coefficients b_n by using the first orthogonality relation (3·5i), so that substituting for F in

$$(1-\sigma)\,\beta^2\left[(F\ F_n' + F'\ F_n)\right]_{\xi=1} + \epsilon\left[(F\ F_n')\right]_{\xi=0} + \int (F_n'' - \beta^2\ F_n)\,(F'' - \beta^2\ F)\,d\xi$$

we get

$$\begin{aligned} & b_n\left[2\beta^2(1-\sigma)\,(F_n'\ F_n)_{\xi=1} + \epsilon\,(F_n')^2{}_{\xi=0} + \int_0^1 (F_n'' - \beta^2\ F_n)^2\,d\xi\right] \\ &= \beta^2\,(1-\sigma)\,(F_n'\ F + F_n\ F')_{\xi=1} + \epsilon\,(F_n'\ F')_{\xi=0} + \int_0^1 (F_n'' - \beta^2\ F_n)\,(F'' - \beta^2\ F)\,d\xi. \end{aligned} \tag{3·9}$$

Subtracting (3·8) from (3·9) we get $(F)_{\xi=0} = 0$, from the last term in (3·8), as the condition for differentiation of (3·4), and hence for fulfilling RAYLEIGH's principle.

This method is illustrated in Fig. 4 which shows the state of affairs at $\xi = 0$ when the assumed function F is not zero there. An analysis in normal modes leads to the graph shown, having infinite first and second derivatives at $\xi = 0$. A similar result would obtain at a boundary where F' was fixed, but if F'' has a fixed value at a boundary the assumed F'' need not take this value. Thus while an analysis of the form $F'' = \Sigma b_n\ F''_n$ leads to an infinite F''', this last does not occur in (3·1) so the critical load will not be affected. Since the geometric boundary conditions fix F and F', while the static ones fix F'' and F''', we are led to the same conclusion as before.

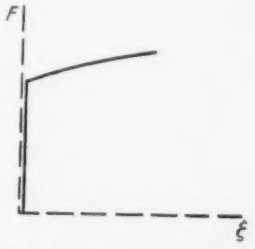

Fig. 4. Assumed function at $\xi = 0$.

The shape used in the present case was

$$F = \phi_0 + \sum_{r=1,2,3,}^{n} a_r\ \phi_r = a_0\ \xi + \sum_{R=1,3,5,}^{N} a_R\left(1 - \cos\frac{R\pi\xi}{2}\right), \tag{3·10}$$

which satisfies the condition $F = 0$ at $\xi = 0$. The first term was included since exact analysis gives a linear relation between F and ξ when $\epsilon = \beta = 0$. Thus the linear relation satisfies the conditions (2·8), (2·9) and also (2·7) which becomes $d^4F/d\xi^4 = 0$. Substitution of $F = a_0\ \xi$ in (3·1) gives the critical load

$$k = \frac{1-\sigma}{\pi^2\,(1/8 + \alpha/24)}. \tag{3·11}$$

Also, the work of PLAAS (1949) who considered the case when $\alpha = -1$ (pure bending), shows an almost linear relation when ϵ and β are small. The first term $a_0\ \xi$ has to be deleted when $\epsilon \to \infty$, since then $F' = 0$ at $\xi = 0$ giving a second geometrical boundary condition to be satisfied.

Then writing (3·1) in the form $k = V/T$, we apply RITZ's method, as given for example by TEMPLE and BICKLEY (1933), and get $n+1$ equations of the type $\partial V/\partial a_r - k\partial T/\partial a_r = 0$. To eliminate the a_r's between these equations requires a determinant of order $n+1$, giving an equation in k of the same order.

A slightly less convergent, but easier, process is to fix the a_n's step by step. Thus we substitute (3·10) in (3·1), and get

$$(V - kT) = \sum_{r=0}^{n} (A_{rr}\, a_r^2 + \sum_{t=0}^{r-1} 2a_r\, a_t\, A_{rt}) = 0 \tag{3·12}$$

where

$$A_{rt} = A_{tr} = \beta^2 (1-\sigma)(\psi_r\, \psi_t' + \psi_r'\, \psi_t)\xi=1 + \epsilon(\psi_r'\, \psi_t')\xi=0$$

$$+ \int_0^1 (\psi_r'' - \beta^2\, \psi_r)(\psi_t'' - \beta^2\, \psi_t)\, d\xi - k\int_0^1 \psi_r\, \psi_t\, \Omega\, d\xi.$$

Also by putting $$\partial V/\partial a_n - k\,\partial T/\partial a_n = 0,$$

we have $$A_{nn}\, a_n^2 + a_n \sum_{t=0}^{n-1} a_t\, A_{nt} = 0. \tag{3·13}$$

Subtracting twice (3·13) from (3·12), and then substituting for a_n from (3·13), gives

$$\sum_{r=0}^{n-1} (A_{rr}\, a_r^2 + \sum_{t=0}^{r-1} 2a_r\, a_t\, A_{rt}) = \Big(\sum_{t=0}^{n-1} a_t\, A_{nt}\Big)^2 \Big/ A_{nn}. \tag{3·14}$$

Then if a_1 to a_{n-1} are known, (3·14) gives a quadratic in k, and a_n may be found from (3·13) so that a more accurate value of k may be found from the $n+1$ th equation (3·14). Hence starting from a_1, a_0 being indeterminate, we get a series of values of k, converging towards, but not necessarily to, the true value.

The dotted lines in Fig. 2 are values obtained by this method with $\sigma = 0{\cdot}32$, using 3 terms ($N = 3$) in (3·10). It will be seen that at any given value of ϵ the μ to give minimum k is independent of α, so that in Fig. 3, the single $\epsilon - \mu$ curve suffices for all α. The minimum values of k, recalculated with 4 terms ($N = 5$), are plotted in Fig. 3 and shown in Table III together with the values of BAKER and RODERICK (1948) for $\alpha = 1$.

TABLE III

Minimum values of k at given ε. σ = 0·32

	$\alpha =$	1	0·5	0	− 0·5	− 1
ϵ	μ for minimum k					
	1·66	1·26	1·41	1·59	1·82	2·11
50	1·67	1·21	1·36	1·54	1·77	2·06
20	1·71	1·14	1·29	1·48	1·70	1·99
5	1·89	0·990	1·12	1·28	1·49	1·78
2	2·20	0·840	0·955	1·10	1·30	1·57
0·8	2·66	0·700	0·808	0·936	1·11	1·36
0·2	3·54	0·568	0·649	0·756	0·904	1·12
0	∞	0·413	0·473	0·550	0·659	0·827

The differences between the values of k with 3 and 4 terms are not greater than 1%, suggesting satisfactory convergence.

We have thus fulfilled requirements (i) and (ii), Section 2, and now consider (iii) and (iv).

Calculations show that for $1 > \alpha \geqslant -1$ the curvature and maximum slopes of the $\epsilon - \mu$ curves (constant k) are greater than for $\alpha = 1$. Use of the maximum slope ($-\partial\epsilon/\partial\mu$) max given in Table II shows that the percentage errors in k when using the minimum curve AC (Fig. 3) are less than those in Table II. Table II therefore gives the maximum errors in k due to use

of the intersection A for $1 \geqslant \alpha \geqslant -1$ *provided* the slope of AB does not exceed the values given at the point A in question.

4. The Schwarz Method

A method originated by Schwarz (1890) has been used as an independent check on the results of Section 3. We start with an assumed shape for the buckled plate $\phi_1(\xi)$, which can be analysed in normal modes so that $\phi_1 = \sum_{n=1}^{\infty} b_n F_n$, and substitute ϕ_1 in those terms of the governing differential equation which are multiplied by the critical load. (2·7) then becomes

$$F^{\mathrm{iv}} - 2\beta^2 F'' + \beta^4 F = k\Omega\phi_1 = k\Omega \sum_{n=1}^{\infty} b_n F_n. \tag{4·1}$$

The solution of (4·1), $\phi_2(\xi)$, will be in the form of a particular integral, linear in k, and a complementary function whose four arbitrary constants are also linear in k, since ϕ_2 satisfies the boundary conditions (2·8), (2·9). Hence $\phi_2 = k\,\omega(\xi)$, where ω is now known. Now considering the equation for the nth mode, $F_n^{\mathrm{iv}} - 2\beta^2 F_n'' + \beta^2 F_n = k_n \Omega F_n$, we obtain $F_n = k_n \omega_n$ whence from (4·1),

$$\omega = \sum_{1}^{\infty} b_n \omega_n = \sum_{1}^{\infty} b_n F_n / k_n \tag{4·2}$$

so that

$$\phi_2 = k \sum_{1}^{\infty} b_n F_n / k_n. \tag{4·3}$$

Thus ϕ_2 is a better approximation to the first mode than ϕ_1. This method of improving a guessed shape was used for strut problems by Engesser (1893) and Vianello (1898), for whirling shafts by Stodola (1905), and more recently by Southwell and others (1941), when (4·1) was solved by relaxation.

Following Vianello, we put $\phi_2 = \phi_1$ to find the critical load, giving k as a function of ξ,

$$k(\xi) = \frac{\sum_{1}^{\infty} b_n F_n}{\sum_{1}^{\infty} b_n F_n / k_n}. \tag{4·4}$$

Then Schleussner (1938) has shown (see also Appendix II) that $k(\xi)$ must take values above and below the first critical load provided F_1, ω and Ω are positive throughout the range of ξ.

A more accurate method is to write

$$\int_0^1 \phi_1 \phi_2 \, \Omega d\xi = \int_0^1 \phi_2^2 \, \Omega d\xi \tag{4·5}$$

which becomes, on substituting the expanded forms for ϕ_1 and ϕ_2,

$$\frac{k}{k_1} = \frac{\int_0^1 \Omega \sum_{1}^{\infty} b_n^2 F_n^2 k_1 / k_n \, d\xi}{\int_0^1 \Omega \sum_{1}^{\infty} b_n^2 F_n^2 k_1^2 / k_n^2 \, d\xi}. \tag{4·6}$$

A comparison with (3·6) shows that this is the same as applying Rayleigh's method to the improved mode ϕ_2, without the trouble of calculating ϕ_2' and ϕ_2''. The equivalent of (4·5) was given by Schleussner (1938) who attributed it to Schwarz (1890). A less accurate method is to put

$$\int_0^1 \phi_1^2 \, \Omega d\xi = \int_0^1 \phi_1 \phi_2 \, \Omega d\xi \tag{4·7}$$

which gives

$$\frac{k}{k_1} = \frac{\int_0^1 \Omega \sum_{1}^{\infty} b_n^2 F_n^2 \, d\xi}{\int_0^1 \Omega \sum_{1}^{\infty} b_n^2 F_n^2 k_1 / k_n \, d\xi}. \tag{4·8}$$

In applying this method we have to solve (4·1) with assumed values for ϕ_1. The most convenient solution is to have the particular integral in integral form so that the complete solution is

$$\phi_2 = c\cosh\beta\xi + d\sinh\beta\xi + \xi(e\cosh\beta\xi + f\sinh\beta\xi)$$
$$+ k\int_{\tau=0}^{\xi} \Omega(\xi-\tau)\,\phi_1(\xi-\tau)\left[\frac{\beta\tau\cosh\beta\tau - \sinh\beta\tau}{2\beta^3}\right]d\tau. \qquad (4\cdot9)$$

The four arbitrary constants c, d, e, f are found from the condition that ϕ_2 must satisfy (2·8) and (2·9). It is not necessary for ϕ_1 to satisfy these conditions, but merely that ϕ_1 can be expanded in terms of normal modes as in (4·1). More accurate approximations, ϕ_3, ϕ_4 etc. to the first mode can be obtained by substituting ϕ_2, ϕ_3 etc. successively in (4·9).

Results obtained by this method are shown in Table IV, in comparison with exact results for $\alpha = 1$ (pure compression) from the calculations of BAKER and RODERICK (1948).

TABLE IV

Schwarz method compared with exact values $\sigma = 0{\cdot}32$, $\alpha = 1$ (*pure compression*) $\mu = 1{\cdot}67$, $\epsilon = 50$, $k = 1{\cdot}213$

			First integration		Second integration	
			Equation (4·4)		Equation (4·4)	
ξ	True shape $F(\xi)$	First shape (Rayleigh) $\phi_1(\xi)$	$\phi_2(\xi)/\phi_2(1)$	$k(\xi)$	$\phi_3(\xi)/\phi_3(1)$	$k(\xi)$
0	0	0	0		0	
0·2	0·0921	0·0642	0·0893	0·935	0·0912	1·192
0·4	0·278	0·212	0·275	1·003	0·278	1·202
0·6	0·508	0·431	0·503	1·114	0·508	1·206
0·8	0·749	0·702	0·744	1·227	0·747	1·215
1·0	1·000	1·000	1·000	1·302	1·000	1·218
k from equation	(4·5)			1·213		1·212
	(4·7)			1·219		1·212

The first shape ϕ_1 was obtained from the RAYLEIGH-RITZ process using 2 terms in (3·10). ϕ_3, the result of two integrations, is correct to 1%. Nevertheless, k obtained from VIANELLO's method (4·4) has a maximum error of 3%. At the same time the results from (4·5) and (4·7) are accurate to the number of decimals used after the *first* integration. This latter method has, therefore, been used in comparisons with the RAYLEIGH-RITZ process when $\alpha \neq 1$.

Such a comparison is given in Table V where values of k from the RAYLEIGH-RITZ process, with 4 terms in (3·10), and exact values are given. The exact values at $\alpha = 1$ are those of BAKER and RODERICK (1948), the remainder coming from (4.5). The values of ϵ, ∞, 50 and 0·2, are the extremes required, and μ is taken from Table III.

TABLE V

Rayleigh-Ritz (values bracketed) compared with exact values of k ($\sigma = 0{\cdot}32$).

ϵ	μ	$\alpha = 1{\cdot}0$		$\alpha = 0{\cdot}0$		$\alpha = -1{\cdot}0$	
∞	1·66	1·260	(1·270)	1·582	(1·593)	2·098	(2.112)
50	1·67	1·213	(1·224)	1·532	(1·542)	2·048	(2·059)
0·2	3·54	0·568	(0·569)	0·754	(0·756)	1·118	(1·121)

It will be seen that the bracketed values, and hence those of Table III, have an error nowhere greater than 1%.

The way in which (3·10) fails to satisfy the boundary conditions, whilst giving an upper limit for k in accordance with the argument of Section 3, is shown in Fig. 5. This gives, in a typical case, values of F and F'' from the two methods. Thus F'' from the RAYLEIGH-RITZ process approaches the true values slowly, owing to (3·10) having a zero in F'' at $\xi = 1$. This zero makes it impossible for (3·10) to satisfy the boundary condition (2·8(i)) *at* $\xi = 1$, although F'' from (3·10) is approaching the true values *near* $\xi = 1$ as the number of terms is increased.

5. EXPERIMENTS

A preliminary experiment was carried out on an aluminium alloy I beam approximately 13in. long. The section was $2\frac{1}{2}$in. deep, the flange width was 3in. and the web and flanges were nominally 0·11in. thick. The material had a 0·1% proof stress of about 28 tons/in². and Young's modulus was 4,660 tons/in². Pure bending was applied in the plane of the web by a four point loading system described in a previous paper (1952), using bearings described by NEAL (1950). At the ends of the specimen, the web and flanges were each clamped, although the fact that the compression flange buckled in four half waves made this effect unimportant.

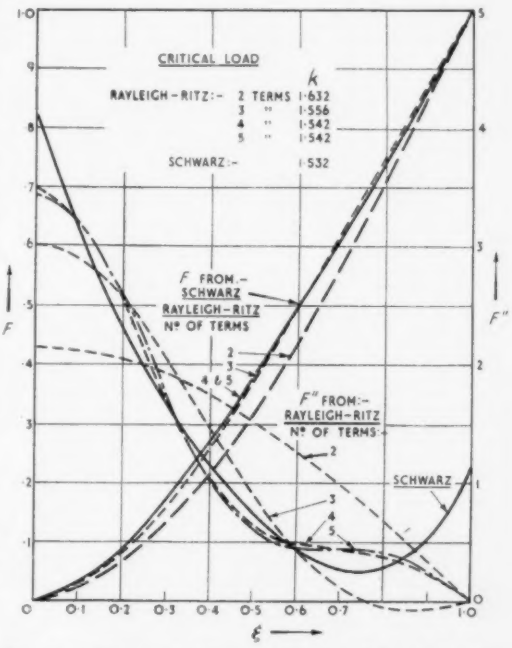

Fig. 5. Shape of deformation F and its derivative F'' from RAYLEIGH-RITZ and SCHWARZ methods. $\alpha = 0$, $\epsilon = 50$, $\mu = 1{\cdot}67$, $\sigma = 0{\cdot}32$.

Buckling was detected by means of six electric strain gauges fixed to the compression flange as shown in Fig. 6. The figure also shows Δ/q plotted against Δ in the manner originated by SOUTHWELL (1932). Δ is the maximum strain in any gauge minus the nominal maximum strain due to bending, and is thus the strain due to buckling. q is the nominal maximum stress. The linearity of the experimental relation between Δ/q and Δ, and the close agreement between the experimental buckling stress of 22·6 tons/in.² (the inverse slope of the line) and the theoretical buckling stress of 22·0 tons/in.², was felt to justify the use of the Southwell plot method in subsequent experiments.

The theoretical buckling stress was obtained by using the data of KROLL (1943) with Fig. 3. The applied bending moment being in the plane of the web, it was first assumed that the web was encastered by the tension flange. The ratio (moment per unit length)/(rotation of lower edge of web) can then be obtained from the quantity S given by KROLL at various λ/h, h being the web depth. The web moment is then taken to be divided equally between the buckling flanges, so that by assuming various λ, we can get the curve AB in Fig. 3 of ϵ against

$\lambda/b = \mu$. The use of intersection A, which was justified by Table II, gave the critical load.

In a second calculation, also based on the data of KROLL, the top flange was assumed to be free from tension, thereby providing a smaller restraint to the web than in actual fact. This showed the error of the previous assumption, that the web was encastré, to have been negligible.

Three series of tests were then carried out on an I beam of similar material to the first, having Young's modulus of 4,740 tons/in.^{2} The section depth and flange width were both 2½in., and for the first series of tests the flanges were machined to about 0·060in. thickness, the web thickness being about 0·110in. For the second series, the web thickness was reduced to about 0·030in., the flanges remaining unaltered. A fillet between web and flanges, of about 0·050in. radius, which remained after reduction of the web, necessitated a third series with a sharp corner between the 0·030in. web and 0·060in. flanges. In all cases the buckling was elastic.

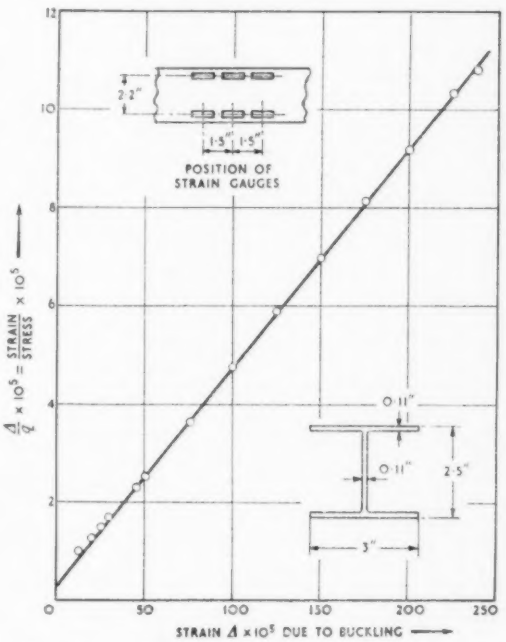

Fig. 6. "Southwell" plot of strain due to buckling. Theoretical buckling stress 22·0 ton/in.^{2}. Experimental buckling stress 22·6 ton/in.^{2}.

The end bearings used are shown in Fig. 7, the design being based on the bearings used in the preliminary test, so as to allow freedom of rotation of each end of the beam. Loading, as before, was by two equal lever arms, each forming an extension of the specimen, and each carrying an equal weight. In setting up, it was possible to twist the specimen about its own axis so that the bending moments, which must always act in a vertical plane, make any desired angle with the web. In Fig. 7, θ is 60°, and the distance between the bearings (i.e. the effective length of the specimen) is 17ins.

Four mirrors, visible in Fig. 7, were fixed in pairs to the two most highly compressed flanges. The members of each pair were an inch apart, and held by plasticine to the edges of the flanges at the centre section. Four horizontal telescopes sighting perpendicularly to the specimen then gave the rotations of the flanges, about the axis of the specimen, by deflections on a scale. The scale deflections were then used to give the buckling load by means of the Southwell plot.

The results are shown in Fig. 8, the theoretical curves being obtained from the curves in Fig. 3 using the "intersection A" method. The $\epsilon - \mu$ curve was obtained from the tables of KROLL (1943), treating the web and unbuckled flanges

ol.
1
2/53

Fig. 7. End bearings. Specimen bent by pure couples at 60 degrees to web.

Vol
1
1952/

as a series of plates. When $\theta \neq 0$, the mean compressive stress in the unbuckled half of the bottom flange was used when calculating the contribution to the fixity ϵ. The tensile stress in the top flanges was neglected.

The only plausible reason for the rather large differences between theory and experiment is the inaccuracy of the "Southwell plot" method. This has been considered by Hu, Lundquist and Batdorf (1946) and by Cox (1951) who

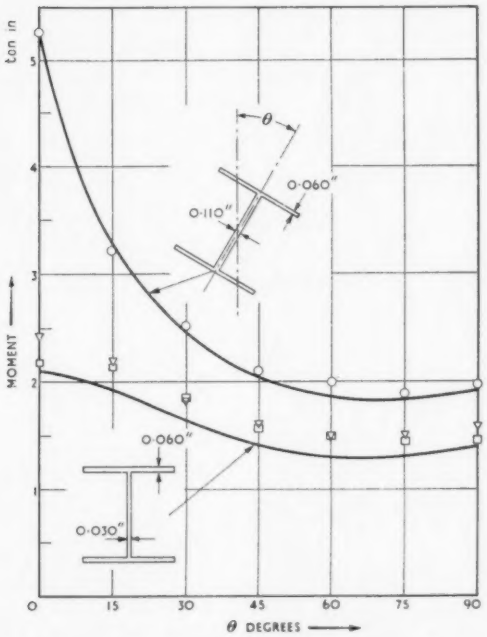

Fig. 8. Buckling moments from mirror readings. 0·110 in web ○; 0·030 in. web with 0·050 in. fillet ▽; sharp corners □. Theoretical curves—.

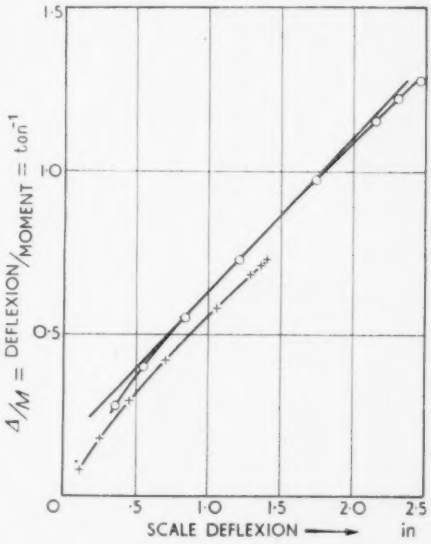

Fig. 9. "Southwell" plots of mirror readings. 0·030 in. web, $\theta = 15$.

showed, from the theory of large deflections of plates, that the Southwell plot method is likely to give a curved relationship between Δ/q and Δ, even when the initial curvature of the plate is quite modest. Such was the case with the present tests, the worst example being shown in Fig. 9, from which it is difficult to determine the critical moment within 10 per cent, in sharp contrast with the results of Fig. 6. However, the results confirm the predictions of Hu, Lundquist and Batdorf and Cox, in giving an experimental critical load *above* the theoretical, and to that extent are satisfactory.

Acknowlegments

The author would like to express his thanks to Dr. E. N. Fox for much helpful discussion of Section 3, and to the Aluminium Development Association who sponsored the work.

APPENDIX I

To obtain the orthogonal relations (3·5) we write

$$\int_0^1 F_n^{\text{iv}} F_m \, d\xi = [F_m F_n''' - F_m' F_n'' + F_m'' F_n' - F_m''' F_n]_0^1 + \int_0^1 F_m^{\text{iv}} F_n \, d\xi$$
$$= 2\beta^2 (F_m F_n' - F_m' F_n)_{\xi=1} + \int_0^1 F_m^{\text{iv}} F_n \, d\xi, \tag{I·1}$$

integrating by parts and using (2·8) and (2·9). Similarly,

$$\int_0^1 F_n'' F_m \, d\xi = (F_m F_n' - F_m' F_n)_{\xi=1} + \int_0^1 F_m'' F_n \, d\xi. \tag{I·2}$$

Then from (I·1) and (I·2),

$$\int_0^1 [F_n^{\text{iv}} F_m - F_m^{\text{iv}} F_n - 2\beta^2 (F_n'' F_m - F_m'' F_n)] \, d\xi = 0,$$

so that substituting from (2·7),

$$(k_n - k_m) \int_0^1 \Omega F_n F_m \, d\xi = 0. \tag{I·3}$$

giving (3·5 ii) if $n \neq m$.

Also, substituting for ΩF_n from (2·7) in (I·3), and integrating by parts, and using (2·8) and (2·9),

$$0 = \int_0^1 (F_n^{\text{iv}} - 2\beta^2 F_n'' + \beta^4 F_n) F_m \, d\xi$$
$$= [F_m F_n''' - F_m' F_n'' - \beta^2 (F_n' F_m - F_n F_m')]_0^1 + \int_0^1 (F_n'' - \beta^2 F_n)(F_m'' - \beta^2 F_m) \, d\xi$$
$$= (1 - \sigma) \beta^2 [F_m F_n' + F_m' F_n]_{\xi=1} + \epsilon [F_n' F_m']_{\xi=0} + \int_0^1 (F_n'' - \beta^2 F_n)(F_m'' - \beta^2 F_m) \, d\xi$$

i.e. (3·5 i).

APPENDIX II

To find the conditions under which (4·4) shall give upper and lower limits to k_1, we multiply numerator and denominator by $\Omega F_1(\xi)$ and integrate, giving,

$$\int_0^1 k(\xi) \, \Omega\omega F_1 \, d\xi = b_1 \int_0^1 \Omega F_1^2 \, d\xi \tag{II·1}$$

in view of (3·5 ii) and (4·2).

Then using (4·2) and putting $k(\xi)/k_1 = 1 + \delta(\xi)$, (II·1) becomes

$$\int_0^1 \delta(\xi) \, \Omega\omega F_1 \, d\xi = 0. \tag{II·2}$$

Then $\delta(\xi)$ must change sign if Ω, F_1 and ω are positive throughout the range.

REFERENCES

BAKER, J. F. and RODERICK, J. W.	1948	*The Strength of Light Alloy Struts.* Aluminium Development Assn. Res. Rep. No. 3.
BRYAN, G. H.	1891	*Proc. Lond. Math. Soc.* **22**, 54.
COX, H. L.	1951	*R. and M.* 2696.
DAVIDSON, J. F.	1952	*Proc. Roy. Soc.* A, **212**, 80.
DEN HARTOG, J. P.	1940	*Mechanical Vibrations* 2nd. ed., p. 192 (New York : McGraw Hill).
ENGESSER, F.	1893	*Z. d. Oest. Ing. u. Ark. V.* **45**, 506.
HU, P. C. LUNDQUIST, E. E. BATDORF, S. B.	1946	*N.A.C.A. Technical Note No.* 1124.

Jeffreys, H. and B. S.	1946	*Mathematical Physics*, p. 412 (Cambridge University Press).
Kroll, W. D.	1943	*N.A.C.A. Rep. No. ARR* 3 *K* 27.
Lundquist, E. E. and Stowell, E. Z.	1942	*N.A.C.A. Rep. No.* 734.
Neal, B. G.	1950	*Phil. Trans. A*, **242**, 197.
Plaas, H. J.	1949	*Rep. Dep. Mech. Eng.* Stanford Univ. Calif.
Rayleigh, Lord	1894	*Theory of Sound*, Vol. 1, p. 287 (London : Macmillan).
Ritz, W.	1909	*J. f. reine u. ang. Math.* **135**, 1 (Also *Gesammelte Werke* p. 192. Paris : Gauthier Villars, 1911).
Schleussner, A.	1938	*Zur Konvergenz des Engesser – Vianello – Verfahrens* (Berlin : Teubner).
Schwarz, H. A.	1890	*Gesammelte Mathematische Abhandlungen*, p. 241 (Berlin : Springer).
Southwell, R. V.	1932	*Proc. Roy. Soc.* A, **135**, 601.
Southwell, R. V.	1936	*Theory of Elasticity*, p. 445 (Oxford, Clarendon Press).
Southwell, R. V., Allen D. N. de G., Fox L., and Motz, H.	1941	*Phil. Trans*, A, **239**, 488.
Stodola, A.	1905	*Steam Turbines* 2nd ed., p. 185 (London : Constable).
Temple G. and Bickley W. G.	1933	*Rayleigh's Principle* (Oxford University Press).
Vianello, L.	1898	*Z. V. D. I.* **42**, 1436.

ol.
1
2/53

Journal of the Mechanics and Physics of Solids, 1953, Vol. 1, pp. 164 to 171. Pergamon Press Ltd., London.

DIE PRESSURE IN PLANE STRAIN DRAWING: COMPARISON OF EXPERIMENT WITH THEORY†

By J. G. WISTREICH
British Iron and Steel Research Association, Sheffield.

(*Received 25th November*, 1952)

SUMMARY

THE problem of drawing the ideal solid of the mathematical theory of plasticity through a wedge-shaped die in plane strain has been solved by HILL and TUPPER, and by GREEN. Different solutions have been proposed earlier, by SACHS and others, based on a more elemeatary theory of plastic deformation. COOK and WISTREICH have measured the pressure on the die face during the plane-strain drawing of solder.

In this paper, COOK and WISTREICH's measurements and those obtained in two further experiments are interpreted in terms of the SACHS and HILL theories. The SACHS theory is rejected. Significant similarities are found between the experimental and theoretical patterns of pressure according to the other authors mentioned above. It seems likely that patterns of deformation characteristic of the ideal solid are substantially preserved in a work-hardening metal. The quantitative comparison of mean die pressures is inconclusive on account of short-comings of the experimental data. In particular, the question of the validity or otherwise of HILL and TUPPER's correction for work-hardening remains open.

Vol.
1
1952/5

1. INTRODUCTION

PLANE-STRAIN drawing*, though uncommon compared with other wire-drawing processes, is nevertheless of particular interest because an exact solution for it exists in the mathematical theory of plasticity. This solution, of course, is true only of a solid with idealized mechanical properties. The prospects of an analogous solution for a real metal are, at present, remote, so that one would like to know to what extent the ideal solution is applicable in practice.

Drawing experiments are, in general, difficult to analyse because of the presence of friction which is not amenable to close control and cannot readily be measured. The die pressure, however, turns out to be fairly insensitive to light friction, so that it is a particularly attractive criterion of comparison between theory and experiment.** If the die is made of an optically stress-sensitive material, the pressure between stock and tool may be found by photo-elastic methods. Experiments of this kind have been performed by COOK and WISTREICH (1952), who give full particulars of the experimental and analytical techniques, and of their limitations.

† Paper MW/D/67/52 of the Drawing Committee of the British Iron and Steel Research Association.

* Electric Conductor strip is sometimes produced by drawing through a wedge-shaped die without lateral constraint. The spread is negligible, even when the ingoing strip is only three times as wide as it is thick. Thus the process is practically one of plane deformation.

** The investigation was planned before GREEN and HILL's (1952) more exact study of the friction effect. It now appears that the effect is negligible for relatively large die angles and small reductions, but otherwise it *may* be appreciable.

The purpose of the present paper is to compare results of such experiments with theory.

2. Theory

The theoretical solution referred to above is the one by Hill and Tupper (1948), amplified by Green (1951). In this theory the die pressure at a particular distance from the die entry depends not only on the distance, but also on the die angle and on the *total* reduction achieved in the die. If the length of the die face is not more than the thickness of the outgoing strip, then the pressure is constant along the die, its value varying with die angle and reduction. For other proportions of the reduction zone the pressure remains constant over parts of the die face and varies elsewhere ; in some instances the variation has a minimum in the central region of the face (see also Green and Hill 1952). Finally, the pressure may exceed the yield stress by as much as a factor of two. These features of the theory are in marked contrast with those of earlier and more elementary theories (e.g. Sachs 1927) according to which, for the same ideal solid and in the absence of friction, the pressure decreases continuously from entry to exit, depends only on the distance from entry, and nowhere exceeds the yield stress.

Hill and Tupper also suggest how to calculate the *mean* die pressure for work-hardening metals. The method rests on the assumption that the mean strain imparted to the metal does not depend on its hardening properties, but only on the die configuration. In the Sachs theory the die pressure rises or falls, depending on whether the rate of work-hardening is greater or less than the value obtaining at the necking point in the tensile test (Wistreich 1948) ; since hardening rates invariably decrease monotonically with increasing strain, a drop in die pressure can never be followed by a rise, so that no minimum is possible.

Friction reduces the pressure, but provided it is small and the die is short compared with the thickness of the stock, its effect is negligible (Green and Hill, op. cit.) because the frictional shear stress at the interface is small compared with the other stresses present.

3. Experiments

Some mention must be made of the practical limitations of the photo-elastic method used by Cook and Wistreich. Owing to the low strength of the die material only soft solders were suitable for drawing stock. Even with these, die configurations which are associated with high pressure could not be employed. As for the condition of plane strain, it was not practicable to draw wide strip without lateral constraint ; instead, strip narrower than it was thick was constrained by glass plates. Unfortunately the elasticity of the glass plates and supporting frame made some lateral spread inevitable, so that the condition of plane strain was only imperfectly realized (the spread amounted to about 0·002″ in 0·148″). Moreover, lateral pressure on the glass plates caused appreciable friction, so that the drawing force was larger than would otherwise be necessary ; this in turn, placed an upper limit on reduction. In short, the choice of metals and of die configurations was limited. Finally, when it came to the stress analysis, the pressures at the points of entry and exit could not be computed with any

certainty, and in one experiment, A, the calculations of the pressure some distance in front of the die exit were subject to appreciable error. Elsewhere, the accuracy of measurement was estimated to be better than $\pm 5\%$.

It is evident from the brief outline of the theory that two kinds of experiment are of particular interest. In the first, the metal should preferably have a low work-hardening rate, and die configurations should be chosen for which the two theories give widely different results. In the second, metals with widely differing work-harding rates should be drawn through the same die. Four experiments have been performed, as specified in Table I. Experiments A and B belong to the first of the above categories, C and D to the second ; that is to say, A and B are meant to distinguish between HILL's and earlier theories and, of course, to provide a test of their practical use ; C and D are meant to be a sensitive test of the assumption underlying HILL and TUPPER's correction for work-hardening.

TABLE I

Particulars of Experiments

Experiment	A	B	C	D
Metal	I (5/95 Sn/Pb Hard)	I (5/95 Sn/Pb Hard)	II (3/97 Sn/Pb Annealed)	III (3/97 Sn/Pb Hard)
Die Semi-Angle	10°	10°	4·5°	4·5°
Reduction	16%	25%	21%	21%

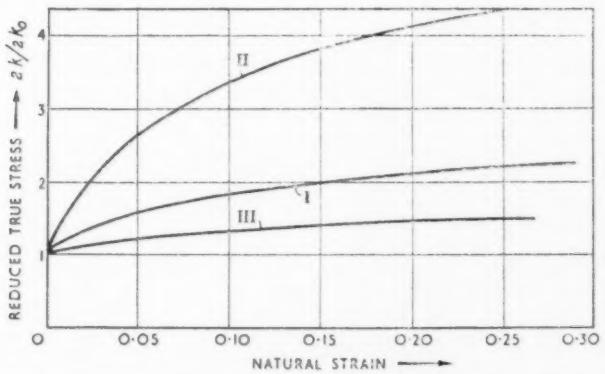

Fig. 1. Reduced plane-strain stress-strain curves of undrawn strips (current plane-strain yield stress $2k$ divided by initial plane-strain yield stress $2k_0$).

The stress-strain curves of the metals were determined before the experiments by compressing small cylinders cut from the undrawn strip, with their axes normal to the plane of deformation during drawing. The compression specimens remained circular in cross section during the test, indicating isotropy in the plane of deformation ; anisotropy in the direction normal to the plane of deformation is however not excluded. In order to be applicable to plane deformation the data had to

be corrected ; the correction was made with the assumption that the metals obeyed v. MISES' criterion of yield. The corrected data, reduced to a common denominator for ease of comparison, are plotted in Fig. 1.

The coefficient of friction in these experiments varied from point to point, but, judging by the inclination of the principal stresses at the interface, nowhere did it exceed 0·05.

4. COMPARISON OF EXPERIMENT WITH THEORY.

(i) *Test of Sachs Theory.* Experiments A and B, which have metal and die angle in common, afford a crucial test of the SACHS theory. If this theory is correct, the local pressures along the face of the ' A ' die should be indentical with those for ' B ' up to a point 64% of the length of the ' B ' die away from the entry (except for second order differences due to differences in friction). The experimental results are plotted in Fig. 2 ; they clearly contradict the theory. It is also evident from the figure that with A the pressure is locally greater than the yield stress ; this, too, is in contradiction to theory. Turning now to experiments C and D, it is seen in Fig. 4 that in both cases the pressure curves contain a minimum. The presence of a minimum is predicted by GREEN and HILL (see below), but is generally inadmissible according to the SACHS theory.

The SACHS theory has been criticized before on purely theoretical grounds, but this is the first instance of a crucial experimental test of its salient features. The test is decisive because it is practically independent of friction and work-hardening. It is also relevant to recent variants of the SACHS theory, which seek to remedy its defects by making an allowance for the effect of die angle (e.g. KÖRBER and EICHINGER 1940). Since the die angle is the same in both experiments, the correction does not enter into the comparison, and these variants of the SACHS solution also fail.

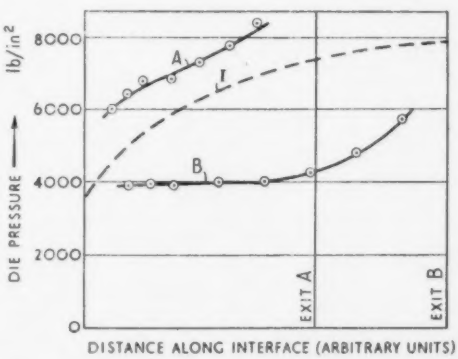

Fig. 2. Die pressures in experiments A and B (- - - stress-strain curve of metal I plotted on the assumption of uniform straining).

(ii) *Qualitative comparison with Hill and Tupper's, and Green and Hill's solutions.* HILL and TUPPER, and GREEN and HILL, express the die pressures as fractions of the yield stress ; this is constant for the ideal solid, but in a work-hardening metal varies with strain. It will be appreciated, therefore, that for a quantitative comparison of theoretical and experimental curves the yield stress of the metal must be known at each point along the die face. The local yield stresses can, in principle, be deduced from the equivalent stress-strain curve and from strain measurements on partly drawn strip. This was tried ; the attempt was successful in demonstrating that straining does not proceed uniformly along the die face, but

the measurements were not sufficiently accurate for the purpose envisaged. In the circumstances, only a qualitative discussion of the variation of pressure along the die face is possible.

The theoretical pressure curves are plotted in Fig. 3. Of these, the curve marked 'C and D' is, clearly, of greatest interest from the point of view of comparison with experiment, because of its unusual shape. Of the two experiments for which the pattern is appropriate, D is to be preferred for the purpose of comparison because of the relatively low rate of work-hardening of metal III (see Fig. 1).

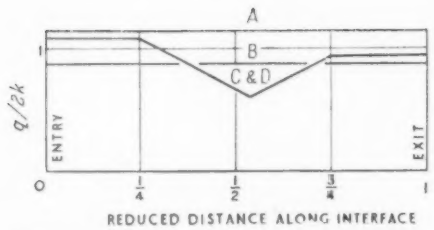

Fig. 3. Reduced theoretical die pressures in frictionless drawing (theoretical die pressure q divided by plane-strain yield stress $2k$).

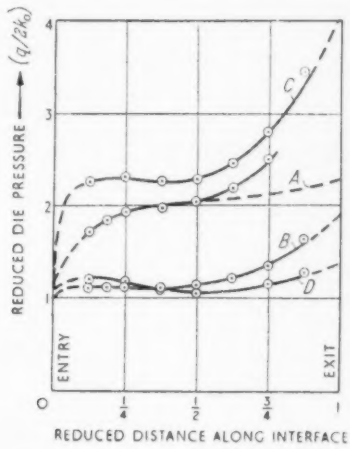

Fig. 4. Reduced experimental die pressures (experimental die pressure q divided by initial plane-strain yield stress $2k_0$).

Now, referring to Fig. 4 in which the experimental pressures are plotted, the pressure curve of D does indeed significantly resemble the theoretical pattern: it, too, comprises a minimum, and this occurs roughly where it is predicted by theory. As for experiment C, the resemblance is tenuous, but if anything, it is better than the great difference in work-hardening between metal II (cf. Fig. 1) and the theoretical solid would lead one to expect.

The theoretical and experimental curves for A and B seem, at first sight, quite unlike. However, an argument will be presented as to the reason for this and it will be shown that the differences are plausibly accounted for as work-hardening effects which, moreover, in their details follow logically from the theory.

In this connection something must first be said about the theoretical pattern of deformation. In the mathematical theory of plasticity the plane deformation patterns are often built up of regions in which the ideal solid moves as a rigid whole, and of regions in which it strains more or less gradually; moreover, in entering and leaving the zone of deformation, and sometimes in moving from one region to another, the ideal solid strains instantaneously by a finite amount, the amount varying from case to case. The corresponding picture for a work-hardening metal is likely to be one of varying rates of strain. For instance, where the ideal solid

strains *instantaneously* the real metal can only strain *rapidly* ; where the ideal solid moves rigidly, the real metal may actually strain, though probably only slowly.

The theoretical deformation patterns of A and B in the vicinity of the die face are shown schematically in Fig. 5. They are similar in that they consist of an extended central region of motion without straining, flanked by smaller regions of gradual straining, and bounded by " jumps " in strain at die entry and exit. At the same time the two patterns differ, for in A " jumps " are smaller than in B, and in the " transition " regions of A straining proceeds more gradually than in those of B. Moreover, the first " transition " region in B is vanishingly small, i.e. the strain " jump " at die entry is almost contiguous with the region of no change in strain.

Let us now modify this picture so as to allow, in a plausible manner, for the work-hardening of metal I. In experiment ' B,' one may expect the yield stress to increase very quickly close to the die entry, to remain substantially constant over the larger part of the die face, and to increase fairly rapidly in the vicinity of the die exit. In ' A,' on the other hand, the yield stress probably increases more gradually and over larger portions of the die face near both entry and exit. Since the theoretical pressure is, in both instances, a constant fraction of the yield stress, it will faithfully reproduce these variations. Examining the experimental curves of Fig. 4 in the light of this argument, but ignoring for the time being the " dashed " extrapolations, one concludes that curve B does, in fact, conform to the anticipated shape, and that curve A, though devoid of any constant pressure interval, nevertheless is not inconsistent with what has been said. One may indeed go a stage further by extending the experimental curves to die entry and exit (cf. dashed intervals in Fig. 4). However, instead of extrapolating in the usual manner and checking the end points against theory, it seems preferable to calculate the end points from theory, and to check whether they can be joined with the experimental data by means of smooth curves. That this is, indeed, the case in all instances save that of the die exit of ' A,' may be gauged from Fig. 4. The dashed curves are also consistent with the preceding argument.

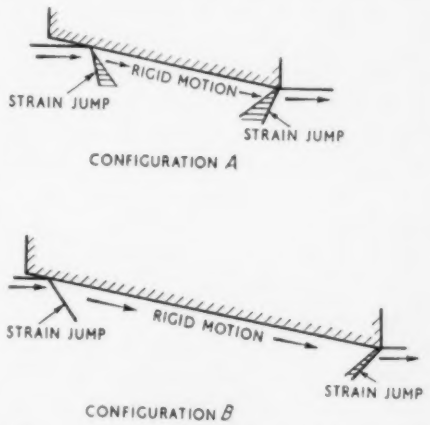

Fig. 5. Ideal flow patterns of frictionless drawing (note – horizontally shaded areas are regions of gradual straining).

Summarizing, the experimental pressure curves resemble the theoretical ones of Hill and Tupper and of Green in some vital particulars, and the dissimilarities are consistent with the idea that *the characteristic theoretical pattern of deformation, which is determined by the die geometry, is substantially preserved — even in a metal which work-hardens.*

(iii) *Quantitative Comparison of Mean Die Pressures.* Encouraged by the above evidence one is tempted to make a quantitative comparison, notwithstanding the uncertainties arising from the extrapolation of curves, and from previously mentioned experimental shortcomings. The results are tabulated below.

TABLE II

Experimental and Theoretical Mean Die Pressures

Equipment	A	B	C	D
Mean pressure, psi, computed*	6900/6700	5600/5400	4400/4000	6200/5600
Mean pressure, psi, measured	6800	4500	3500	6100

It will also be recalled that experiments C and D, with indentical die angle and reduction but with metals of different work-hardening rates, were meant, among other things, as a test of the aforementioned argument concerning the mean total strain. If the argument is justified, then the ratio of mean die pressure to mean yield stress is invariant with respect to the shape of the stress-strain curve. The ratio is 0·91 for the ideal solid, 0·73-0·80 for the annealed metal II, and 0·90-0·98 for the cold-worked metal III.

One gathers from Table II that both theoretical and experimental pressures increase in the order C, B, D, A; but the agreement is poor (save for A; but this is the experiment with the least reliable measurements). The ratios of die pressure to yield stress are, of course, functionally related to the data of Table II.

It appears then, that the HILL-TUPPER theory adequately accounts for the complicated and rather unusual patterns of the observed variations of pressure, and yet it seems to miss the mark when put to the less discriminatory test of *mean* values. This is an unexpected situation, and it is suggested that its explanation is to be found in shortcomings of the experiments rather than of the theory. For instance, although the lateral spread was small and apparently did not cause the pattern of pressure variation to change significantly, it might nevertheless have caused an appreciable drop in the hydrostatic component of the pressure. The yield stress of the metal in the plane of deformation may well have been different in magnitude from the measured yield stress which was used in its stead in the computations. Added to this, there is the computational error of the photoelastic stress analysis, estimated at up to $\pm 5\%$ by COOK and WISTREICH, and the error of extrapolation. Finally, in the computations from theory the uncertainty of how much to allow for the effect of friction on pressure is small only in the case of experiments A and B.

5. DISCUSSION

Although the experimental investigation fell short in several respects of what was required, one can nevertheless draw useful conclusions about the relative merits of the SACHS and HILL theories, and also about the effect of work-hardening in the latter theory.

* The method of computation is based on the procedures outlined by HILL (1950 pp. 172-3) and GREEN and HILL (1952). The effect of friction is neglected in the first figures; the second figures are calculated on the assumption of a constant coefficient of friction of 0·05. The configurations 'C' and 'D' are outside the range for which the errors inherent in GREEN and HILL's method are known to be small, so that the second figures for 'C' and 'D' are uncertain.

Vol. 1 1952/5

SACHS' theory, including its recent variants, fails to account for the observed pronounced effect of *total* reduction on the pressure in the vicinity of the die entry ; it cannot explain the rise of pressure near the die exit ; it does not admit of the observed presence of minima in the pressure curves and of the excess of local pressure over yield stress ; and it predicates a uniform increase of strain along the die face, contrary to observation. All these contradictions remain, even when due allowance is made for the shortcomings of the experiments.

The argument in favour of the HILL-TUPPER-GREEN theory derives its strength from the resemblance of patterns of pressure variation, particularly in experiment D, the metal of which work-hardens least ; from the fact that the differences between the theoretical and experimental patterns for the other metals, which work-harden more, are precisely what one would expect them to be ; and also from the fact that, in seven out of eight instances, the calculated end points of the curves fit in with a plausible extrapolation of measured pressures. One may, in fact, venture the suggestion that, *in spite of work-hardening, a real metal deforms substantially in accordance with the patterns predicated for the ideal solid.* In contrast with these strong indications of the applicability of the HILL-TUPPER theory, the data of Table II inform us otherwise. These discrepancies, however, may well be due to to experimental shortcomings, and cannot be safely taken as evidence against the theory.

In the circumstances the question, as to how accurately one may predict the die pressure from the theory of the ideal solid and the stress-strain curve of the metal, remains open. It is doubtful whether COOK and WISTREICH's experimental approach is capable of yielding results of sufficiently high accuracy for an unequivocal answer. Nevertheless, it is felt that the investigation, and the analysis presented here, have served a useful purpose in clearly distinguishing between the SACHS and HILL theories by recourse to experiment. The analysis should also prove helpful in the planning and execution of investigations of the validity of HILL and TUPPER's method of allowing for work-hardening.

ol.
1
2/53

ACKNOWLEDGMENTS

Experiments A and B were performed by MR. T. K. LOCKETT, to whom my colleague MR. P. M. COOK gave indispensable advice on experimental procedure and on the method of stress analysis. The data of experiments C and D are taken from the paper by COOK and WISTREICH.

The views expressed in this paper are the author's and are not necessarily endorsed by the Drawing Committee of B.I.S.R.A. as a body.

REFERENCES

COOK, P. M. and WISTREICH, J. G.	1952	*Brit. J. Appl. Phys.*, **3**, 59.
GREEN, A. P.	1951	*Phil. Mag.*, **42**, 900.
GREEN, A. P. and HILL, R.	1952	*J. Mech. Phys. Solids.*, **1**, 31.
HILL, R.	1950	*Mathematical Theory of Plasticity* (Clarendon Press, Oxford).
HILL, R. and TUPPER, S. J.	1948	*J. Iron and Steel Inst.*, **159**, 353.
KÖRBER, F. and EICHINGER, A.	1940	*Mitt. K. W. I. Eisenf.*, **22**, 57.
SACHS, G.	1927	*Z.A.M.M.*, **7**, 235.
WISTREICH, J. G.	1948	Unpublished report

Journal of the Mechanics and Physics of Solids, 1953, Vol. 1, pp. 172 to 181. Pergamon Press Ltd., London.

ON THE GENERALITY OF THE CUBIC CREEP FUNCTION

By A. J. Kennedy
The Davy Faraday Laboratory of the Royal Institution, London

(*Received* 1st *January*, 1953)

Summary

The fit of a cubic creep function to a wide variety of materials is examined and the results compared with the fit to a general power law. The behaviour of a simple mechanical model, composed essentially of bi-stable units, is shown to approximate to the observed type of transient creep in real materials. A statistical approach to the problem is outlined.

1. Introduction

The fact that a wide variety of materials exhibit transient creep curves of a very similar parabolic nature has been commented upon in the past; in particular, it has been noted that a cubic creep function of the form first proposed by Andrade (1910, 1914), is of remarkably general application. This point has been recently discussed by Cottrell (1952).

It is the purpose of this paper to bring together the evidence for this creep function, and to examine in detail the fit of various materials to a creep formula of the Andrade form. The question as to whether a general power law (i.e., one not restricted to $\frac{1}{3}$) is in better agreement will be considered, and, finally, an approach to the mechanics of the problem outlined.

2. The Andrade Equation

The Andrade equation expresses the length, l, of a specimen flowing under constant stress as

$$l = l_0 (1 + \beta t^{\frac{1}{3}}) \exp (\kappa t)$$

where t is time, and l_0, β and κ are constants. The close fit of this equation to the creep curves of metals was demonstrated by Andrade and since then a number of experimenters working with lead, cadmium and other non-ferrous metals have found that their results can be very accurately fitted by an equation of this form (see Orowan 1946-7). A variety of experiments has established that the division of the creep process into a transient flow with a function of the form (time)$^{\frac{1}{3}}$, and a permanent flow represented by the exponential term, leads to a rational interpretation of the results of experiments on the change of resistivity during creep (Andrade and Chalmers 1932), the effect of pre-strain prior to creep (Kennedy 1949), the influence of the surface and composition (Andrade and Kennedy 1951), and creep under pure shear (Andrade and Jolliffe 1952). A successful treatment of the problem of the creep of lead under interrupted stress

has been developed on the basis that this function is part-recovered during the recovery period (KENNEDY 1952) and the method has been applied also to the behaviour of copper under similar testing (KENNEDY 1953).

A number of creep curves for non-ferrous metals, selected from the literature as examples of both cubic and hexagonal structures, are plotted in Fig. 1, the continuous lines being the experimental curves and the points those calculated from the values of the constants given in Table 1. Examples of such curves are

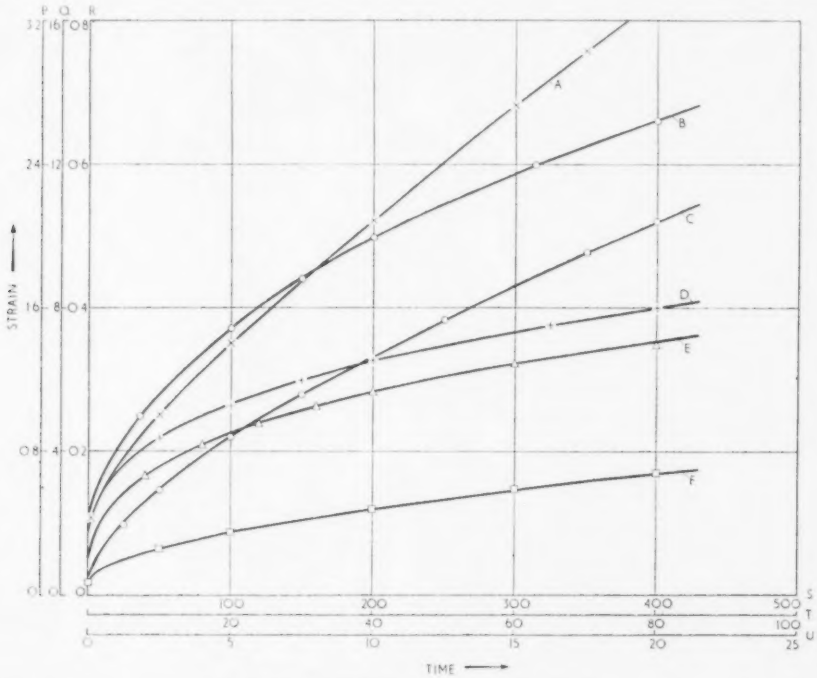

Fig. 1. Creep curves for various metals.

abundant, as reference to the literature will reveal, but even where the ANDRADE equation has been tested, the best values for the constants have not always been taken, as in the case of HASIGUTI and OWADANO (1951) working with aluminium : the best fit to their results has been indicated by ANDRADE (1951), and it has been shown that the equation provides quite as good a fit as the HASIGUTI 4-constant formula. Other workers (for instance, LATIN 1948) have also not deduced the best values. It is essential that accurate 3-point fitting be used, or else a method such as that used by KENNEDY (1948) which is advantageous when a large number of curves have to be fitted.

GRAHAM (1953) has made an exhaustive investigation of the fit of experiment with various formulae, and has been led to the conclusion that the most successful general fit is obtained by using a series of terms with those involving the powers $\frac{1}{3}$ and 1 being the dominant ones.

A number of investigators, working with non-metallic materials, have also found that a function (time)$^{\frac{1}{3}}$ fits the results of their creep tests very closely

TABLE I

Curve	Material	Author(s)	Graph Scales		Andrade constants		
			% Length	Time	l_0	β (min$^{-\frac{1}{3}}$)	κ (min^{-1})
A	Al alloy	STURM, R. G. DUMONT, C. and HOWELL, F. M. (1936)	$Q/10$	S (hrs.)	1·0007	$8{\cdot}28 \times 10^{-4}$	$2{\cdot}47 \times 10^{-5}$
B	Lead (1% Sn)	HOPKIN, L. M. T. (1950)	Q	S (hrs.)	1·0097	$1{\cdot}29 \times 10^{-2}$	$7{\cdot}4 \times 10^{-5}$
C	Cadmium	ANDRADE, E. N. da C. and CHALMERS, B. (1932)	$P \times 10$	$S/10$ (min.)	1·0053	$2{\cdot}88 \times 10^{-2}$	$1{\cdot}89 \times 10^{-3}$
D	Lead (0·05% Te)	KENNEDY, A. J. (1950)	Q	T (min.)	1·010	$1{\cdot}33 \times 10^{-2}$	0
E	Copper	ANDRADE, E. N. da C. (1910)	$Q/4$	$T/4$ (min.)	1·000	$6{\cdot}55 \times 10^{-3}$	0
F	Lead (1% Sn)	KENNEDY, A. J. (1950)	Q	T (min.)	1·017	$7{\cdot}24 \times 10^{-3}$	$2{\cdot}4 \times 10^{-5}$

Note: B and F show results for the same material, B for long-time and F for short-time testing.

Vol
1
1952/

under certain conditions. Fig. 2 shows the creep curves for various materials : the continuous lines representing the experimental results taken from the publications under reference, and the marked points those calculated according to the formulae given in Table II. In the case of non-tensile tests the formula has been suitably modified, but retains the essential cubic function. Some examples of the early stages of creep curves of steel in tension and in torsion are included as the behaviour of steels is often quoted as evidence against the cubic law.

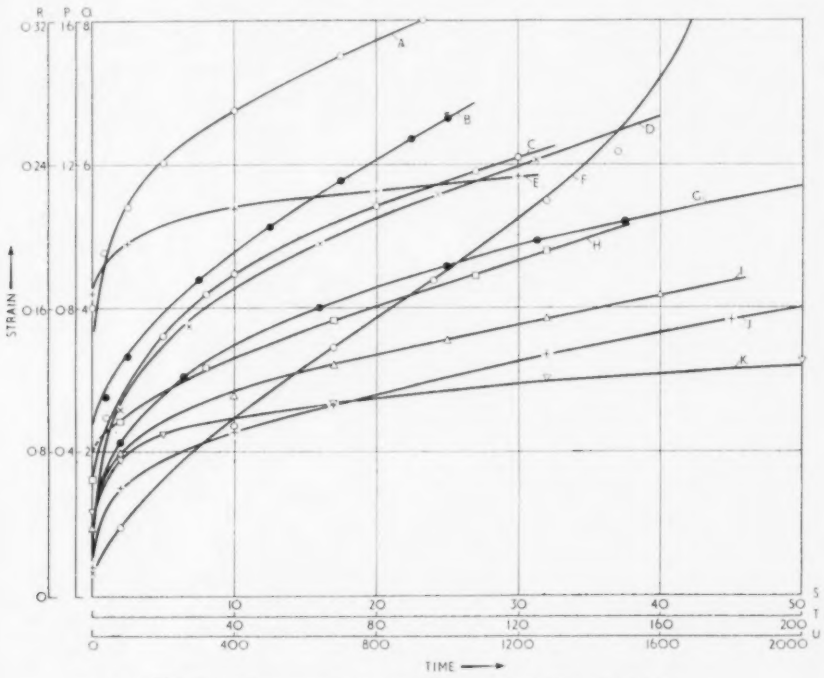

Fig. 2. Creep curves for various non-metallic materials.

The agreement demonstrated by Fig. 2 is certainly very good. Further evidence is provided by various workers (their results are not shown) who have discussed the fit of experimental results to a function (time)$^{\frac{1}{3}}$: for instance, Filon and Jessop (1923) working with celluloid over a small strain range, Saal and Labout (1940) working with plastic asphalt (they quote 0·38 as the power of the time), and Henderson (1951) working in the region of reversible creep strain on cadmium and lead. Henderson has also shown that the function applies to the results of Schofield and Scott Blair (1933) on the creep of dough.

It is not claimed, of course, that all materials, under all test conditions, exhibit creep curves which can be fitted as closely as these, but it *is* suggested that the (time)$^{\frac{1}{3}}$ law has a far wider application, and provides much closer agreement, than is generally realized. Indeed, some materials exhibit curves which are remarkably good cubic parabolae, with $\kappa = 0$ in the Andrade equation, over a large strain range. The creep curves of concrete and of concrete mixes, obtained by Glanville (1933) are examples of this, and the very accurate fit of this simple

TABLE II

Curve	Material	Author(s)	Graph Scales		Andrade Constants		
			% Length	Time	l_0	β (min$^{-\frac{1}{3}}$)	κ (min$^{-\frac{1}{3}}$)
A	0·17%C Steel	JOHNSON, A. E. (1941)	$P/10$	$T \times 10$ (hrs.)	1·0008	$5{\cdot}17 \times 10^{-5}$	$3{\cdot}33 \times 10^{-7}$
B	Macerated fabric-filled phenoplast	GAILUS, W. J. and TELFAIR, D. (1945)	$Q/10$	$T \times 10$ (hrs.)	1·0018	$2{\cdot}76 \times 10^{-4}$	$2{\cdot}59 \times 10^{-6}$
C	Plasticized polyvinyl chloride	LEADERMAN, H. (1943)	P	S (mins.)	1·0016	$3{\cdot}49 \times 10^{-3}$	0
D	Mortar *	BINGHAM, E. C. and REINER, M. (1933)	Q (mm)	T (days)	0·30	1·15	0
E	Cuprammonium filaments	STEINBERGER, R. L. (1936)	Q	$T/10$ (mins.)	1·042	$7{\cdot}10 \times 10^{-3}$	0
F	Graphite	MALSTROM, KEEN and GREEN (1951)	Q	T (mins.)	0·9972	$4{\cdot}62 \times 10^{-3}$	$2{\cdot}5 \times 10^{-4}$
G	Concrete	GLANVILLE, W. H. (1931)	$Q/100$	T (days)	1·000028	$9{\cdot}3 \times 10^{-5}$	0
H	Celluloid (15% camphor)	McNALLY, J. G. and SHEPPARD, S. E. (1931)	Q	S (mins.)	1·016	$5{\cdot}57 \times 10^{-3}$	$4{\cdot}0 \times 10^{-4}$
I	0·34%C Steel†	EVERETT, F. L. (1933)	Q (shear strain)	T (hrs.)	0·9474	0·507	$2{\cdot}7 \times 10^{-3}$
J	Nylon	DILLON, J. H. and PRETTYMAN, I. B. (1945)	Q	S (hrs.)	1·004	$6{\cdot}98 \times 10^{-3}$	$1{\cdot}73 \times 10^{-4}$
K	Rubber	BRAUN, M. L. (1936)	$Q/24$	T (mins.)	1·048	$1{\cdot}49 \times 10^{-2}$	0

* Beam under load at mid. pt.
† Torsional creep under constant shear stress

Constants are for the equation $l = l_0 + \beta t^{\frac{1}{3}} + \kappa t$

Vol. 1 1952/53

equation may be compared with that proposed by THOMAS (1933) for concrete :

$$l = A\left[1 - \exp\left[-B\left\{(t + C)^x - C^x\right\}\right]\right]$$

where A, B, C and x are constants, and in which the power x is found empirically, for different cases, as 0·3 and 0·4. MCHENRY (1943) has proposed another complicated formula for concrete :

$$l = \alpha\left[1 - \exp(-rt)\right] + \beta \exp(p\kappa)\left[1 - \exp(-mt)\right]$$

where α, β, r, p, m and κ are constants. Equations for the creep of particular substances are, in fact, numerous : they are usually built up of exponential functions, with several constants, and are difficult to intepret in terms of physical processes. They have been surveyed by POPOV (1947).

An examination of the published work reveals that where deviations from the cubic law occur, they can be most generally classified as (1) deviations from the initial infinite rate of creep which the formula gives – that is, the curves are of

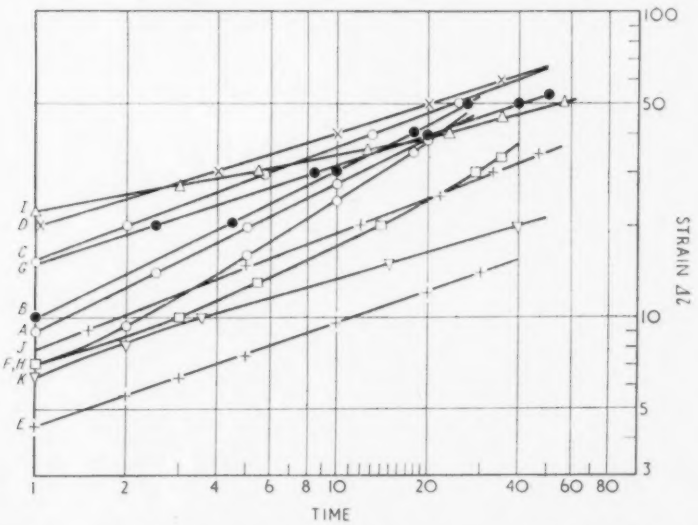

Fig. 3. The curves of Fig. 2 plotted on a log-log scale (arbitrary units) ; the symbols and letters correspond to those on Fig. 2. The initial and average slopes of the lines are, respectively, as follows :–

A :	0·47, 0·47.	B :	0·50, 0·50.	C :	0·38, 0·38.
D :	0·33, 0·31.	E :	0·35, 0·35.	F :	0·34, 0·60.
G :	0·33, 0·33.	H :	0·29, 0·45.	I :	0·18, 0·20.
J :	0·38, 0·38.	K :	0·33, 0·33.		

the pre-strained character previously observed in lead (KENNEDY 1949), or (2) deviations from the law at longer creep times, where the strain observed is less than that given by the formula. It is true that fundamental changes may occur during extension : in the case of rayon fibres, for instance, the water content changes as extension proceeds. In the case of metals, the radical geometrical rearrangement of crystals in a polycrystalline wire, after a large creep extension,

changes the basic nature of the material, so that some deviation from a simple initial deformation law is not unexpected.

3. The General Power Law

The question of the representation of creep data as a simple power relationship, of the general form $\epsilon = \beta t^p$, has received widespread attention. The approach has often been in conflict with that followed by those who apply the ANDRADE equation, and it is true that frequently the same experimental results may be very closely fitted to either equation. The curves plotted in Fig. 2, when re-plotted on a log-log scale, appear as in Fig. 3. The average and the initial slopes of these lines are given beneath the Figure : whilst the values are near to 0·33, there is a distinct scatter about this value. Examination reveals that the addition of an ANDRADE permanent (linear) component enables the curves to be closely fitted using the power value obtained from the initial slope. It is not possible to say, on this basis, which is the more valid approach. If it can be shown that the results of experiments (such as those on interrupted creep) can be treated successfully only when a cubic function is used then this would constitute strong support for the view that the power $\frac{1}{3}$ expresses a fundamental process. This line of enquiry is being pursued.

4. Statistical Model

The thesis which is here proposed is that the (time)$^{\frac{1}{3}}$ law (or a law very near to this) is the basic transient creep law of an aggregate which may be said to possess units of structure (these may be called dislocations, cross-linkages, miscelles, cells – all the terms exist in the literature) which are essentially defined by patterns of "weakness" or "strength" centres, distributed throughout the aggregate. The deviations from the law arise from deviations in the pattern of the linkages, in their randomness of distribution, and not in the basic mechanism by which deformation proceeds. The mechanism may be pictured, in general terms, as one by which the units of the structure each contribute a finite strain to the aggregate by changing over from one (stable) state to another.

Let us consider a simple mechanical model. In Fig. 4(a) a random network is shown made up of studs inter-connected by taut threads. These threads form an array of smallest triangles, the studs to which they are fixed being placed on a smooth surface coated with a heavily viscous medium. A second set of (loose) interconnections is then made, superposed on the first, the length of each link bearing a fixed ratio to the link it duplicates (say twice as long). Before loading this array, an experiment is carried out on a "perfect" or regular array of the same general shape. That is, if the random array is p units long and q units wide, and is made up of n nodes, then a perfect lattice must have a columns and b rows, where $ab = n$, $a/b = p/q$. Thus, working with this perfect lattice, failure will occur when the load equals aL, L being the breaking load of one thread. Returning to our random network, we now load this with a load $< aL$, (say 0·75 aL) and observe its behaviour. On loading, those links will break in which the breaking stress is exceeded, and the studs will move until the second link eventually takes the stress, the rearrangement occuring in a time dictated by the viscous material.

Vol. 1 1952/5

Stresses are thus redistributed as orientations alter and the breaking stress is exceeded in some of the other links. The stress is thus gradually transferred from the first set of weak links to the second set of strong links chosen to be of such strength that breakage of these does not occur. The process thus involves the breakdown of units which are bi-stable (being either " short " or " long ") the whole controlled by viscous forces. The matrix was photographed as the extension occurred, measurements being made directly from the photographs. The results are plotted in Fig. 4 (b), and demonstrate how a quite simple aggregate can provide a curve of the required form.

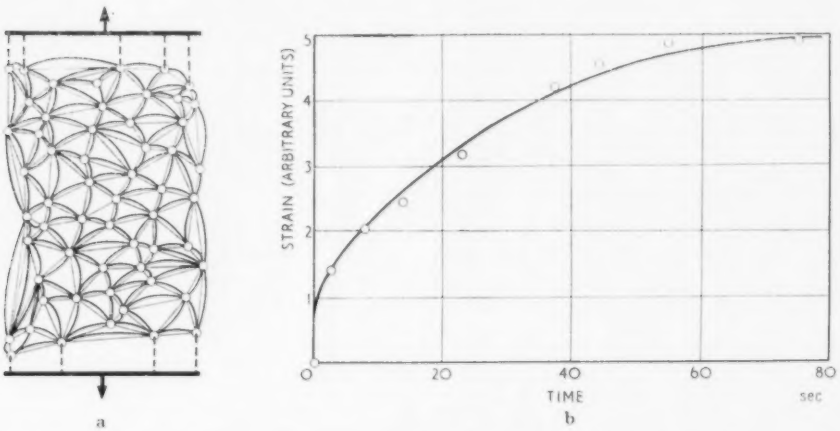

Fig. 4. (a) The model represented diagramatically before the application of the load. (b) The creep curve exhibited by the model.

5. Discussion and Conclusions

We are, then, confronted with the possibility that an aggregate possessed of very simple properties may provide, statistically, a cubic creep law. It is interesting that the problem has an analogy to the behaviour of a two-party electoral system. Kendall and Stuart (1950) have discussed and examined the relation between the ratio (r) of the number of votes cast for each party and the ratio (R) of the number of seats each gains. In this country, at the present time, the relationship is very close to $R = r^3$. In a sense, it is unfortunate that the particular electoral distribution should lead to the very power which we have noted as of common occurrence in solids. The significant fact is that any power law at all should appear, and that this power should depend upon the way in which voters of like party are aggregated in certain areas. These considerations enable us to propose the following general system.

The system is defined by two types of primary element : (a) cells, and (b) stress centres distributed at random throughout the cells of the matrix. We assume that the division of the matrix into cells is made in some arbitrary manner. If a stress is applied to the system, then, under thermal activation, breakdown occurs at the stress centres in such a way that the average rate at which such centres " fire " is a constant. We say that each such breakdown is followed by a multiplication of weakness centres *throughout* the matrix (it is convenient to call these

dislocations). Each avalanche of dislocations (softening) is terminated by the "operation" of a cell (hardening), the operation being said to take place when the number of dislocations in that cell exceeds the number of stress centres it contains. Thus each primary softening event ends in a single hardening event, and this constitutes the time scale. The total strain achieved by the matrix at any time is defined as being proportional to the total number of dislocations generated in that time. Under such conditions, the matrix exhibits a power creep law which, with a particular type of distribution of stress centres, could be of the one-third power form. COTTRELL (1952) has already indicated how little is achieved by simply shaping a distribution curve to provide the required function. Shaping in this case, however, is a direct consequence of a physical arrangement of centres in the matrix and it might thus be very profitable to consider whether fairly elementary aggregation laws may not lead to the required pattern.

The model has, of course, deliberately been given just those properties which will lead to the results observed with real materials, and these properties are, indeed, somewhat strange. It is difficult to see why, physically, the process of dislocation multiplication throughout the matrix should be halted by the operation of one particular fragment of it. It is reasonable to assume that operation may create a *barrier* of some form, and by some such compromise, a model may be developed on firmer physical lines, with properties approximating to the other.

It is clear that before such an approach as this can be developed in detail this crucial property, which we may describe as the mechanical feedback between the twin processes of softening and hardening, must be given sensible crystallographic form (at least so far as a metal is concerned) and experiments framed to test it. Upon its validity rests the whole of this particular statistical model. The statistics are more easily examined, and this is now going forward with the aid of a specially-built apparatus.

Vol. 1 1952/5

REFERENCES

ANDRADE, E. N. da C.	1910	*Proc. Roy. Soc. A*. **84**, 1.
	1914	*Proc. Roy. Soc. A*, **90**, 329.
	1951	*Nature*, **168**, 1007.
ANDRADE, E. N. da C. and CHALMERS, B.	1932	*Proc. Roy. Soc. A*, **138**, 348.
ANDRADE, E. N. da C. and JOLLIFFE, K. H.	1952	*Proc. Roy. Soc. A*, **213**, 3.
ANDRADE, E. N. da C. and KENNEDY, A. J.	1951	*Proc. Phys. Soc. B*, **64**, 363.
BINGHAM, E. C. and REINER, M.	1933	*Physics*, **4**, 92.
BRAUN, M. L.	1936	*Physics*, **7**, 421.
COTTRELL, A. H. and AYTEKIN, V.	1950	*J. Inst. Metals*, **17**, 389.
COTTRELL, A. H.	1952	*J. Mech. Phys. Solids*, **1**, 53.
DILLON, J. H. and PRETTYMAN, I. B.	1945	*J. Appl. Phys.*, **16**, 159.
EVERETT, F. L.	1933	*Physics*, **4**, 120.
FILON, L. N. G. and JESSOP, H. T.	1923	*Phil. Trans. Roy. Soc. A*, **223**, 89.
GAILUS, W. J. and TELFAIR, D.	1945	*Mod. Plastics*, **22**, 149.
GLANVILLE, W. H.	1933	*Struct. Eng.*, 11, 54 and 143.
		D.S.I.R. Bldg. Res. Tech. Paper No. 12.
		D.S.I.R. Bldg. Res. Tech. Paper No. 21.

Graham, A.	1953	*Research* (in press).
Hasiguti, R. R. and Owadano, T.	1951	*Nature*, **168**, 706.
Henderson, C.	1951	*Proc. Roy. Soc. A*, **206**, 72.
Hopkin, L. M. T.	1950	*Proc. Phys. Soc., B*, **63**, 346.
Jenkins, C. H. M., Tapsell, H. J., Mellor, G. A. and Johnson, A. E.	1936	*Trans. Chem. Eng. Congr.* World Power Conf. London, **1**, 122.
Johnson, A. E.	1941	*Proc. Inst. Mech. Eng.*, **145**, 210.
Kendall, M. G. and Stuart, A.	1950	*Brit. J. Sociology*, **1**, No. 3.
Kennedy, A. J.	1948	*Proc. Phys. Soc.*, **61**, 510.
	1949	*Proc. Phys. Soc., B*, **62**, 501.
	1950	*Ph.D. Thesis*, London.
	1952	*Proc. Roy. Soc., A*, **213**, 492.
	1953	*Nature*, (in press).
Latin, A.	1948	*J. Inst. Metals*, **15**, 259.
Leaderman, H.	1943	*Ind. Eng. Chem.*, **35**, 274.
Malstrom, C., Keen, R. and Green, L., Jr.	1951	*J. Appl. Phys.*, **22**, 593.
McHenry, D.	1943	*Proc. Amer. Soc. Test. Materials.* Prep. No. 64.
McNally, J. G. and Sheppard, S. E.	1931	*J. Phys. Chem.*, **35**, 2398.
Orowan, E.	1947	*J. West Scotland Iron and Steel Institute* Session 1946-7.
Popov, E. R.	1947	*Trans. Am. Soc. Mech. Eng.*, 14.
Saal, R. N. J. and Labout, J. W. A.	1940	*J. Phys. Chem.*, **44**, 149.
Schofield, R. K. and Scott Blair, G. W.	1933	*Proc. Roy. Soc. A*, **141**, 72.
Steinberger, R. L.	1936	*Tex. Res. J.*, **6**, 325.
Sturm, R. G., Dumont, C. and Howell, F. M.	1936	*J. Appl. Mech.*, **58**, 62.
Thomas, F. G.	1933	*Struct. Eng.*, **11**, 69.

ol.
1
2/53

Journal of the Mechanics and Physics of Solids, 1953, Vol. 1, pp. 182 to 188. Pergamon Press Ltd., London.

THE "ELASTIC HYSTERESIS" OF URANIUM

By E. R. W. Jones and W. Munro
A.E.R.E., Harwell

(*Received 26th January*, 1953)

Summary

It is shown that the "elastic" properties of polycrystalline uranium at room temperature are very sensitive to the mechanical history of the sample. The metal exhibits "elastic hysteresis" losses that are a factor 10 greater than those found in steel and brass. The energy dissipated per stress cycle has been measured for samples of various grain size and orientation; the results show that the micro-structure of the metal affects the degree of energy loss. It is concluded that the energy loss in stress cycling is due to mechanical twinning.

Vol
1
1952/

1. Introduction

The values quoted in the literature for the mechanical properties of uranium vary widely and this may be attributed to differences of the purity of the metal tested.

In particular most workers agree that the load-extension line is curved from the origin, which makes the value of Young's modulus deduced from static measurements unreliable. In the course of our work this experience has been confirmed.

An attempt was made to raise the elastic limit, without seriously affecting the modulus, by prestraining. However, even after 300 cycles of stress, the stress-strain graph was still curved from zero stress, and the loading and unloading line for a complete cycle formed a loop. This loop was similar to "elastic hysteresis" loops found in other metals when stressed beyond the primitive elastic limit.

2. Experimental Details

(*a*) *Tests on wrought uranium*

The specimen used was wrought rolled bar of 99·95 per cent purity. It was first stressed in compression to a maximum stress of 76,000 lb./in.^{2}. The stress was applied in a standard testing machine and the longitudinal strain was measured with an extensometer having a strain sensitivity of 3×10^{-6}; lateral strain was measured to a sensitivity of 4×10^{-6}.

The specimen was then subjected to 300 cycles of compression stress. In some of the cycles the stress was both applied and removed by increments, and the strain measured. For the other cycles the stress was both applied and removed continuously at a rate of approximately 3,700 lb./in^2. per sec. The maximum stress in most of the cycles was 70,000 lb./in^2. but five cycles were measured with a maximum stress of 56,000 lb./in.^{2}.

Fig. 1 shows stress × longitudinal-strain graphs for cycles 1, 4, 30 and 100. The stress-strain graphs are all looped and the unloading line cuts the strain axis at a point farther from the origin than the loading line. This means that each cycle puts some permanent strain into the specimen. The permanent strain from cycle No. 1 is $2{\cdot}5 \times 10^{-4}$; from cycle No. 4, 8×10^{-5}; and from cycles Nos. 30 and 100, of order 2×10^{-5}. After cycle No. 100 the specimen was left in position in the testing machine with no external stress; it was found that the apparent permanent strain disappeared after 30 minutes. Although the strain lags behind the stress, by an amount of order 2×10^{-5}, this will not account for the loop since its width is equivalent to strain of order 4×10^{-4} at the widest point. It will also be noted from Fig. 1 that the area of a loop, which is proportional to the energy dissipated, varies with the number of previous cycles of stress. Table I gives the loop areas for cycles having maximum stress of 70,000 lb./in^2. or 56,000 lb./in.^{2}. The Table shows that the energy dissipated decreases up to about the 50th cycle; thereafter a more or less constant amount of energy is dissipated per cycle, the energy loss depending on the range of stress.

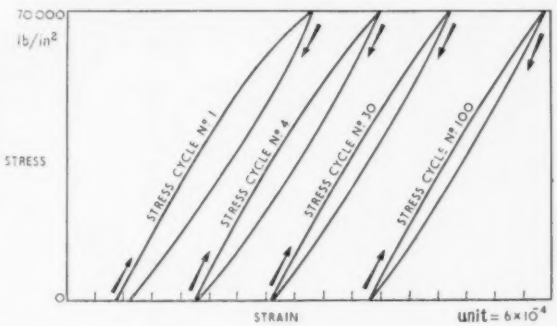

Fig. 1. Hysteresis loops for wrought uranium.
Note: Horizontal scales are displaced to separate the loops.

TABLE I. *Energy dissipated per cycle of compression stress applied to wrought uranium*

Stress cycle No.	*Maximum stress of cycle* lb./in^2.	kg/cm^2	*Energy dissipated* ergs/cc × 10^{-5}
10	70,000	5,000	17·6
30	70,000	5,000	13·3
50	70,000	5,000	12·4
75	70,000	5,000	11·9
100	70,000	5,000	11·9
9	56,000	4,000	7·5
51	56,000	4,000	6·0
101	56,000	4,000	6·2
300	56,000	4,000	6·0

It was impossible to measure strain in both directions for any one cycle because the two extensometers available could not be used simultaneously. Therefore Fig. 2 shows stress × lateral-strain graphs for cycles No. 7 and 8 and stress × longitudinal-strain graphs for cycles Nos. 9 and 10. The stress × lateral-strain graphs are loops similar in shape to the stress longitudinal-strain loops. There is a small amount of permanent strain in the lateral as well as in the longitudinal

direction. For cycle No. 7 the permanent lateral strain is of order of 1×10^{-5} and for cycle No. 10 the permanent longitudinal strain is of order 5×10^{-5}; the ratio of the two (0·2) is of order of Poisson's ratio. On the lower part of Fig. 2, Poisson's ratio/stress curves are plotted for two cases. These curves were derived by comparing the incremental strains on the loading and unloading lines of the

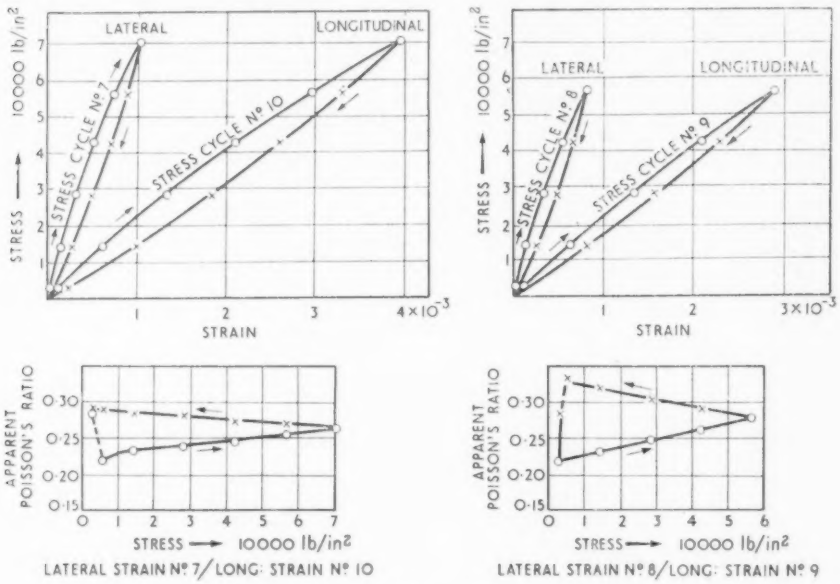

Fig. 2. Relations between lateral and longitudinal strains for wrought uranium.

lateral strain loop with the corresponding increments of strain on the longitudinal strain loop of the same maximum stress. It will be noted that the apparent Poisson's ratio varies throughout the cycle. It has a minimum value shortly after stress is first applied and then increases as the stress increases. After the maximum stress it continues to increase as the stress decreases, and reaches a maximum value shortly before the applied stress is completely removed. How the ratio varies at low stresses, i.e. between the maximum and minimum, is not clear from the observed strain readings. This is possibly due to the inaccuracy of measuring lateral strains at low stresses. For the stress cycle of maximum stress 70,000 lb./in². Poisson's ratio varies between 0·22 and 0·29 and at the maximum stress point it is 0·26. For the 56,000 lb./in.² cycles it varies between 0·22 and 0·33 and is 0·28 at the maximum stress. Thus Poisson's ratio is not an invariant quantity for uranium. Values of Poisson's ratio quoted in the literature (Katz and Rabinowitch 1951) vary from 0·20 to 0·49 depending on the condition of the metal.

After the specimen had been subjected to the 300 cycles of stress, a further 6 cycles of stress with different upper limits were applied by increments and the strain measured. The energy dissipated per cycle (ergs/cc) is plotted against maximum stress of cycle (kg/cm²) in Fig. 3. The results show the energy loss increases rapidly with the upper stress of the cycle.

(*b*) *Tests on cast uranium*

This specimen was machined from vacuum cast bar of 99·92 per cent purity. It was stressed in tension by a standard testing machine and the longitudinal strain was measured with an extensometer having strain sensitivity of 2×10^{-6}.

The specimen was subjected to 200 cycles of stress. As before, for some of the cycles the stress was both applied and removed by increments and the longitudinal strain measured : for the others it was applied and removed continuously at a rate of approximately 2,600 lb./in^2. per sec. The maximum stress used was 48,000 lb./in.^{2}.

These tests gave stress × longitudinal-strain loops similar to those for wrought uranium. Table II gives values for energy dissipated in stress cycles 50, 70, 100 and 200, and shows that the energy loss is greater than for the wrought uranium and continues to decrease throughout the 200 cycles ; for wrought uranium it reached a steady value after 50 cycles.

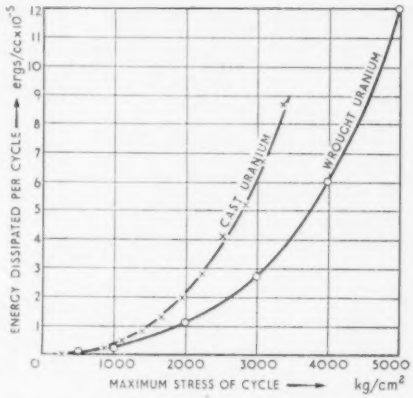

Fig. 3. Relation between energy dissipated and maximum stress for consecutive cycles of stress.

After the 200 cycles of stress, a further 12 cycles with different upper limits were applied. Fig. 3 shows that, as with the wrought uranium, the energy loss increases rapidly with stress.

TABLE II. *Energy dissipated per cycle of tensile stress applied to cast uranium*

Stress cycle No.	*Maximum stress of cycle* lb./in^2.	kg/cm^2	*Energy dissipated* ergs/cc × 10^{-5}
50	48,000	3,375	10·6
70	48,000	3,375	10·3
100	48,000	3,375	9·9
200	48,000	3,375	8·7

(*c*) *Tests on steel and brass*

It was obvious that uranium was showing more marked elastic hysteresis than common metals and a few tests were made on steel and brass to provide numerical comparisons. These tests should strictly be compared with the early cycles on uranium since it was found that the steel and brass loops tended to disappear as cycling continued. A few tests on steel below the elastic limit confirmed that the hysteresis was not due to the extensometers.

The testing technique was essentially similar to that adopted for uranium. The results are given in Fig. 4 and Table III, with comparable data on wrought uranium. Figures for cast uranium are not included because loops were recorded only after

50 cycles of stress. The energy loss in the uranium is approximately 12 times that for the steel and 8 times that for the brass.

3. Discussion of Results

It is clear from these experiments that uranium is very different from the other two metals discussed since the " elastic " properties derived from the stress-strain curves are very sensitive to the mechanical history of the sample. In view of this, precise elastic calculations on uranium would appear to be pointless.

" Elastic hysteresis " can be explained by non-uniform yielding in polycrystalline samples as follows. At a very early stage in the loading the deformation is elastic and all grains deform uniformly. Then one of the grains yields and the stress in the surrounding grains is increased, so that they in turn yield as the applied load is further increased. By this mechanism the total strain is partly elastic and partly plastic, and so the stress × total-strain line is curved. If the applied load is tensile and is now reduced, the grains which have yielded go into compression and deform elastically. At an early stage in the unloading the grain that first yielded on loading should again yield first. The compressive stress on the surrounding grains will now be increased and they in turn will yield as the applied load is further decreased. Thus, as for loading, the strain on unloading is partly elastic and partly plastic and the stress × total-strain line is a curve. The unloading line of the elastic hysteresis loop should be the same as the loading line, except that it is inverted. That this is approximately so can be noted from the elastic hysteresis loops shown on Fig. 1. The energy dissipated is used in plastically deforming some of the metal.

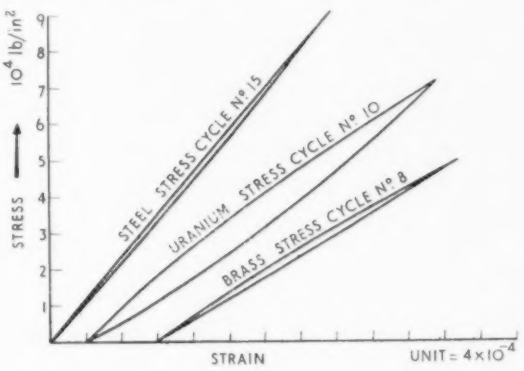

Fig. 4. Hysteresis loops for uranium steel and brass.
Note: Horizontal scales are displaced to separate the loops

Table III.

Material	*Steel*	*Uranium*	*Brass*
Ultimate tensile strength lb./in.^{2} × 10^{-4}	10·7	13·0	7·5
Maximum stress of cycle lb./in^2. × 10^{-4}	9·1	7·1	5·0
Energy dissipated per cycle ergs/cc × 10^{-5}	1·4	17·6	2·1
Number of stress cycle	15	10	8

It has been found that the energy dissipated in uranium is a factor 10 greater than in steel or brass. This relatively large dissipation of energy is probably due to some difference in the mode of plastic deformation in uranium. Cahn (1953)

Vol. 1 1952/5

has shown that at low temperatures uranium deforms mainly by twinning whereas it is known that steel and brass deform mostly by slip. The above description of elastic hysteresis is still applicable, twinning occurring when the grains yield as the load is applied and untwinning as the grains yield as the load is removed. Evidence of untwinning on reversal of stress can be seen in JILLSON's photographs of zinc (1950). With regard to the energies involved, CHALMERS (1935) has shown by a ballistic technique that the twinning energy for tin is 8×10^5 ergs/cc, so that our value of 6-17 $\times$ 10^5 ergs/cc for partial twinning of uranium (a harder metal) is of reasonable magnitude. The difference between cast and wrought uranium may lie in the different grain size, as it has been shown by CAHN and others that twinning is facilitated by a large grain size. This suggestion was verified by a comparative experiment on a uranium specimen whose grain size had been enlarged by strain annealing. The grain size of the strain annealed specimen (0·032 mm) was approximately 50 per cent larger than that of the cast specimen (0·023 mm). For stress cycles of maximum stress 2,000 kg/cm^2 the hysteresis losses were 5×10^5 ergs/cc for strain annealed and $2{\cdot}2 \times 10^5$ ergs/cc for cast material. Thus the specimen having the larger grain size dissipates the greater energy.

TABLE IV.

*Specimen**	*Energy dissipated per cycle ergs/cc* $\times 10^{-5}$	*Grain size mm.*	*Orientation*
HR 2	11·4	0·01 to 0·18	Random
CS 2	13·0	0·01 to 0·15	
HR 3	30·0	0·23	Random
CS 3	27·0	0·20	
HR 4	5·8	not measurable	In CS 4 (010) predominates normal to stress axis
CS 4	5·6	not measurable	
HR 5	31·0	0·045	Both samples show very strong orientation of (131) normal to stress axis
CS 5	26·0	0·035	

* The numeral in the specimen number denotes the heat treatment given. The letters give the mode of fabrication. HR = hot rolled. CS = cold swaged.

4. FURTHER EXPERIMENTAL WORK AND DISCUSSION

Eight more uranium specimens have been examined in an attempt to obtain confirmation of the suggestion made above. Four of the specimens had been made by hot rolling and the other four by swaging at a lower temperature.

Four different heat treatments were given and the grain sizes and preferred orientations in these materials together with the energy losses on cycling are given in Table IV.

The results on the specimens with random orientation (treatments 2 and 3) show that the energy loss does increase with grain size. That grain size is not

the only important variable can be seen by comparing specimens given heat treatment 5 with those given heat treatment 2, since the former have a larger energy loss and a smaller grain size. This is consistent with the concept that the loss is due to twinning since the specimens given heat treatment 5, having (131) normal to the stress axis, can twin more readily than the average. This follows from Fig. 5, which is due to Cahn, and shows that if a stress is applied in certain directions to uranium the crystal cannot deform by twinning. Similarly the fact that HR 4 has a higher energy loss than CS 4 is consistent with the fact that CS 4 has a larger proportion of (010) normal to the stress axis and this is an orientation which does not twin in tension.

It follows that the large energy loss in polycrystalline uranium is due to mechanically induced twinning and untwinning. The variation apparent in Poisson's ratio is not surprising on this hypothesis if uranium is elastically anisotropic, as would be expected from its other properties. As far as we are aware there has been no determination of the single crystal elastic constants of uranium, but we may cite as an example beryllium for which the dependence of Poisson's ratio on stress orientation can be calculated from the data given by Gold (1949). If the transverse strain is measured in the basal plane Poisson's ratio changes from 0·35 to −0·28 as the stress axis moves from being perpendicular to being parallel to the basal plane.

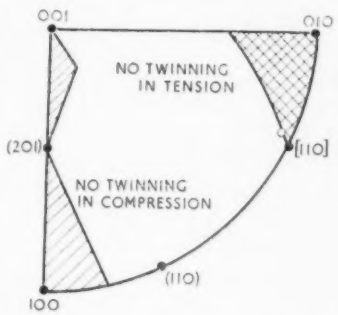

Fig. 5. Restrictions on twinning in uranium. (After Cahn).

Haig (1935) has previously suggested that twinning and untwinning may be the direct cause of elastic hysteresis in metals, and this work confirms his suggestion. However, there must be some other mechanism operating, which dissipates less energy, to explain the behaviour of steel and brass in which deformation twinning has not been demonstrated at these rates of strain. It is interesting to speculate whether annealing twins could grow under stress as do deformation twins, and thus dissipate energy. Further work would be required to demonstrate this possibility.

Acknowledgments

Thanks are due to Dr. J. Adam and Mr. E. C. Sykes, who determined the preferred orientation and grain size respectively, and to the Director of the Atomic Energy Research Establishment for permission to publish this paper.

References

Cahn, R. W. 1953 *Acta Metallurgica*, **1**.

Chalmers, B. 1935 *Proc. Phys. Soc.*, **47**, 733, also discussion by Haig, B. P.

Gold, L. 1949 *U.S.A.E.C ref. A.E.C.D. 2644. An Evaluation of stiffness coefficients for Beryllium from ultrasonic measurements in polycrystals and single crystals.*

Jillson, D. C. 1950 *Trans. Am. Inst. Min. Met. Eng.*, **188**, 1009.

Katz and Rabinowitch 1951 *The Chemistry of Uranium*, Vol. VIII-5 (McGraw Hill, New York).

Journal of the Mechanics and Physics of Solids, 1953, Vol. 1, pp. 189 to 206. Pergamon Press Ltd., London.

THE COMBINED BENDING AND TWISTING OF THIN CYLINDERS IN THE PLASTIC RANGE

By M. P. L. Siebel
Department of Mechanical Engineering, University of Bristol

(*Received 10th November*, 1952)

Summary

Many applications of the theory of plasticity are based on the Reuss stress-strain relations. The present investigation was undertaken to test their validity under conditions where the plastic and elastic components of the strain increments are comparable and where the stresses and the strains are not uniformly distributed. The problem chosen was the overstraining of thin tubes by the simultaneous action of bending and twisting couples. The material was a steel with a stress-strain curve closely approximating the idealized one assumed in the theory.

The test results were found to be predicted very accurately by the theory. Certain small discrepancies are attributable to the effects of stress gradient and small imperfections. The Maxwell-Mises yield criterion and the Lévy-Mises relation were found to be good approximations for this material.

ol.
1
2/53

1. Introduction*

Most applications of the mathematical theory of plasticity are based on the Reuss stress-strain relations (Hill 1950, p. 39). These assume that any infinitesimal increment of strain in an overstrained material can be treated as composed of two distinct and additive parts: one, the elastic part, given by the ordinary elastic equations; the other, the plastic part, given by the Lévy-Mises relations. Evidence as to the validity of the Reuss relations when the plastic and the elastic parts of the strain increment are comparable appears, however, only to have been obtained under conditions where the stress and strain distributions are uniform (Morrison and Shepherd 1950). The present investigation was undertaken to examine the validity of the Reuss relations when conditions are non-uniform. The experiment selected is the overstraining of thin tubes by the simultaneous action of bending and twisting couples. This was chosen for the following reasons:

(i) Direct information is obtained about the yield criterion (The Reuss relations can, in principle, be used with any criterion).

(ii) The relation between Lode's variables μ_L and ν_L can be deduced. (The Lévy-Mises relation postulates $\mu_L = \nu_L$).

(iii) Apart from the autofrettage of pressure vessels, the combined bending and twisting of thin tubes is the only problem that has been solved theoretically where the plastic and the elastic components of the strain increment are comparable (Hill and Siebel 1951), except for trivial cases where the distribution is uniform or for simple cases of non-uniform distribution such as the torsion of a solid circular cylinder.

* This paper is an abridged version of a Dissertation (University of Bristol).

The experiments were not designed to discriminate between the predictions of the so-called "incremental" and the "total" strain theories. The physical inadequacy of the latter is well known (e.g. HILL 1950, p. 47). The present intention is purely to test predictions based on the REUSS relations and also, in this case, on the MAXWELL-MISES yield criterion.

In a tube subjected to simultaneous bending and twisting, a plastic region is eventually initiated in the extreme fibres and gradually spreads under monotonic loading towards the neutral plane. The distortion of the plastic zone is constrained by the remaining elastic zone to be of an elastic order of magnitude until about one half of the tube has become plastic. It is in this range of strain that the REUSS relations are examined. As the loads are increased, the elastic zone shrinks and finally becomes negligibly small. The stresses are then effectively uniformly distributed in a non-hardening material and can easily be calculated from the measured couples. At this stage, therefore, the yield criterion of a non-hardening material can be directly checked. The material used was a steel which in fact did not work-harden in the relevant range of strain. In this "fully" plastic state the stresses remain constant, so that the validity of the LÉVY-MISES relation can also be independently investigated.

2. MATERIAL

Ten 2 in. diameter bars, 13½ in. long, of a special steel (E steel) were available. The cast from which the bars had been rolled had the following pit sample analysis: C, 0·22 per cent; Si, 0·21 per cent; Mn, 1·48 per cent; S, 0·031 per cent; P, 0·029 per cent; Ni, 0·63 per cent; Cr, 0·19 per cent; Mb, 0·36 per cent. The heat treatment originally given to the bars was:

Water hardened	850°C	(1½ hrs. soak),
Tempered	630°C	(1½ hrs. soak),
Re-tempered	650°C	(2 hrs. soak).

The bars then had a Brinell hardness equivalent to a tensile strength of 55 tons/in.². This was considered too high, and after a complete re-heat treatment the hardness was reduced to one corresponding to 50 tons/in.² tensile strength.

Microscopic examination showed the steel to have a small number of slag threads enclosed in the sorbitic structure normal of the heat treatment given.

In order to eliminate machining stresses as far as possible, all the specimens were subjected to a stress relief anneal after machining. This consisted of a one hour soak at 550°C ± 5° and was carried out in the vacuum furnace described by MORRISON (1939).

3. CONVENTIONAL TESTS

The material of tubes subjected to combined torsion and bending is stressed in tension, in compression and in shear. The stress-strain curves of the steel under these three loading conditions were determined separately; for this purpose nine specimens were made from one of the bars (No. 6). It was considered essential to have three specimens available for each type of test. The specimens were so distributed that it should clearly appear from the tests whether there was a variation of properties along or round the bar at a radius where the walls of the tubes would normally lie.

Check specimens for direct testing were obtained from each of the bars from which tubular specimens were made. After the material necessary for one tubular specimen had been cut

from each end, only a " slice " 1·75 in. long from the middle of each bar was left. From this, transverse and longitudinal compression specimens were made (Fig. 1). From further bars, not used for tubes, oblique specimens were obtained. All the compression check specimens were similar and therefore provide, not only the stress-strain curve of the material of each bar, but also a check of the isotropy and homogeneity.

Fig. 1. Position and numbering of compression check specimens. The reference mark of each specimen consists of the letters as shown, preceded by the number of the bar from which it was taken.

As a further check, Brinell hardness tests were made along and through the cross-sections of the bars.

The torsion specimens from bar No. 6 had a parallel test section 1·5 in. long and 0·4 in. in diameter, joined to enlarged keyed ends by a 3 in. radius transition curve. The profile of the test section was ground. The tests were carried out in a torsion testing machine designed by Mr. B. Crossland (University of Bristol). The torque is applied through shackles which cause neither bending nor axial stressing of the specimen ; it is measured by the twist in a long steel bar. The strain was measured by a torsionmeter consisting of two clips carrying mirrors and fixed an accurately set distance apart.

All the tension and compression tests were carried out in a 10-ton Robertson machine (Robertson and Newport 1927), in which a very close approach to axial loading is possible. The weighbar (Siebel and Smallman 1949) was recalibrated.

The tension and compression specimens from bar No. 6 had a 1·125 in. parallel section, 0·357 in. in diameter, joined by a 3 in. radius fillet to heavy ground ends which were a push fit in the sockets of the load bars.

The compression check specimens had a total length of only about 1·7 in. A central parallel section 1 in. long and 0·357 in. diameter is joined by a 1 in. radius fillet to a very short parallel end section, $\frac{7}{16}$ in. in diameter. To ensure axiality of loading the flat ends of these specimens were located on half steel balls, also of $\frac{7}{16}$ in. diameter, by means of short sleeves. A pair of adapters made it possible to test these specimens in the 10-ton Robertson machine (Fig. 2).

In all the tension and compression tests the strains were measured by means of the triple Martens extensometer described elsewhere (Morrison 1939). From the readings the maximum as well as the average strain in the specimen may be determined and hence the true upper yield stress.

The technique used for the axial loading tests and for the torsion tests was the same. In the elastic range the load was raised by decreasing amounts as the proportional limit was approached. In the plastic range readings were taken twenty minutes after the application of each load increment. This wait was necessary to allow the load-bar-specimen system to reach an approximate equilibrium.

The compression check specimens were strained to a permanent set of about 0·7 per cent, and their " roundness " then measured.

4. Design of the Tubular Specimens and Testing Machine

Absence of buckling was essential to the success of the investigation. Preliminary pure bending tests under four point loading were therefore carried out on two tubes made from the ' E ' steel. Both had a 1 in. diameter bore ; the first had a wall thickness, $t = 0{\cdot}050$ in., and did not buckle at a strain three times that at yield ; the second with $t = 0{\cdot}020$ in., buckled at yield.

A bore diameter of 1 in. and a wall thickness of 0·060 in. were therefore considered suitable, allowing for the possibility that, after delivery, certain machining processes might still be necessary to correct any eccentricity or taper. That this wall thickness does not lead to appreciable errors when its *mean* radius, a, is used in the theoretical " thin-tube " formulae is shown in Appendix 1.

The specimens were given a parallel section of 3·5 in. to ensure that at least 2 in. of it was free from end effects, since three different types of extensometer had to be fitted for each test. The test section was joined to the enlarged ends of the specimens by a fillet of 3 in. radius, equal to about six times that of the specimens or to about fifty times its wall thickness. Thereby it was hoped not only to avoid premature yielding at the fillets, but also to obtain a longitudinally

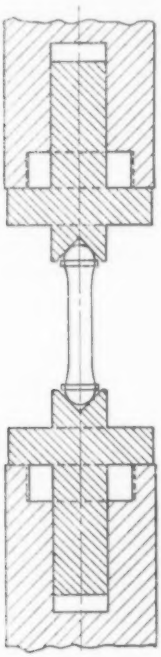

Fig. 2. Section through compression testing rig.

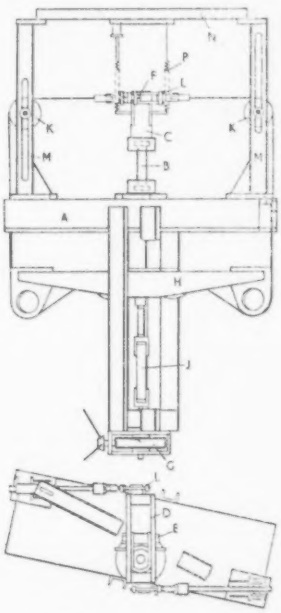

Fig. 3. General arrangement of testing machine set for pure torsion test.

uniform stress distribution about 0·5 in. away from the root of the fillet. The enlarged end sections of the specimen were keyed flanges. The total length 5·75 in., was such that a length of about 1·8 in. was left from the middle of each bar after two specimens had been cut off. This remainder was used to make the compression check specimens.

In the testing machine one couple only is applied. Its axis can be made to lie at any angle to that of the specimen. The ratio B/T of the bending to the twisting component of the couple is held constant during a test.

The main features of the machine are shown in Figs. 3 and 4a. The lower end of the specimen, B, is firmly held on the rigid base, A ; to its upper end is fitted the loading head, C. This consists of a heavy member to which a frame, D, is attached by one bolt, E. The frame can be pivoted about this bolt to set its angular position, and is locked in position by tightening the bolt.

Equal and opposite forces act on each end of the loading frame. Their lines of action are parallel to the axis of the pivot bolt, so that any desired ratio of bending to twisting moment can be applied to the specimen by adjustment of the frame angle. The forces are applied through thin steel tapes leading from each end of a loading beam, H, over pulleys, K, to the frame. At the ends of the tapes the shackles, L, are fitted with a hard steel surface which bears on the

ol.
1
2/53

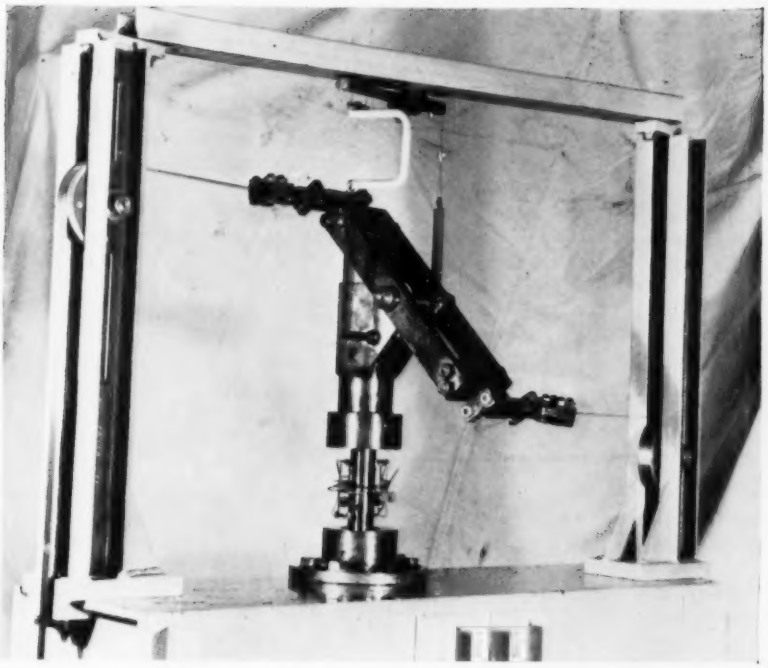

Fig. 4a. The combined bending and torsion testing machine.

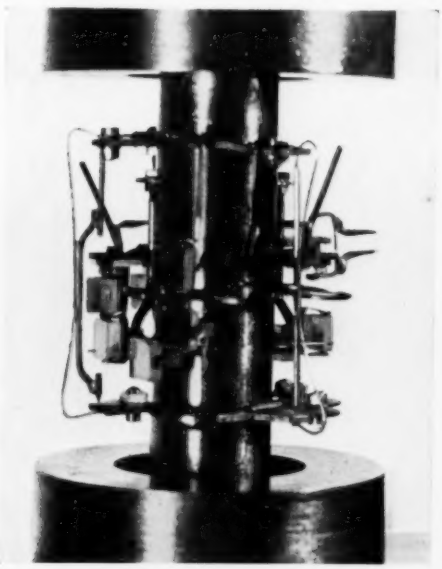

Fig. 4b. Extensometers.

Vol.
1
1952/5

hard steel balls, F, set in the frame. The positions of the pulleys and their supports, M, can be so adjusted that the tape is parallel to the pivot bolt.

Since the torsional and bending stiffnesses of the tube are different the rotation of the frame due to the straining of the specimen, has two components with axes respectively perpendicular to the plane of the forces and in the plane of the forces, parallel to their common perpendicular. To minimize the " cosine " effect due to the first component, the balls are offset from the centre-line of the frame in a direction opposite to that of the applied forces. The apparent initial increase in the effective moment arm, when the frame rotates under load, is almost balanced by the decrease due to the rolling of the steel balls on the load applying surfaces. The calculated correction never exceeded 0·15 per cent even at the ends of the tests when the frame had turned through 5 or 6°. The effect of the second component on the B/T ratio can be disregarded, since the rotation is less than 2° and also because the points of application of the forces are very near its axis.

The load is applied to the beam by means of worm, gear and nut arrangement, G, and through a proving ring, J. In the design of this ring particular care was taken to eliminate errors due to frictional effects and small additional bending moments. The ring and its dial gauge were calibrated by dead weights and a 5 : 1 yard arm. A reading on the dial gauge for a given load can be relied upon to within 0·2 to 0·3 of a division in the range 0–450 divisions. (One division = 2·68 lb.). It was checked that the tensions in the two tapes were the same. The frictional resistance in the pulleys was found to be negligible.

The tops of the pulley supports are connected by a rigid member, N. This greatly increases the effective stiffness of the supports, and thus reduces their necessary width. This member also supports the heavy loading head which is suspended from it by means of two springs, P, of low stiffness.

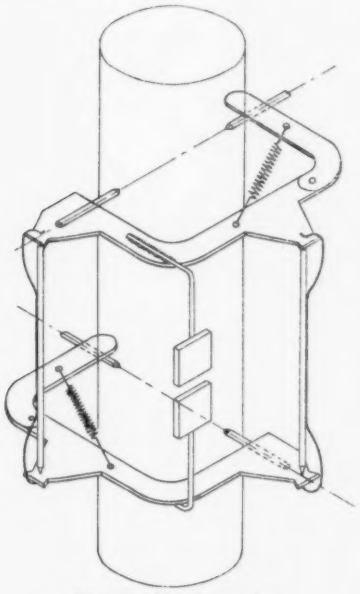

Fig. 5. Torsionmeter.

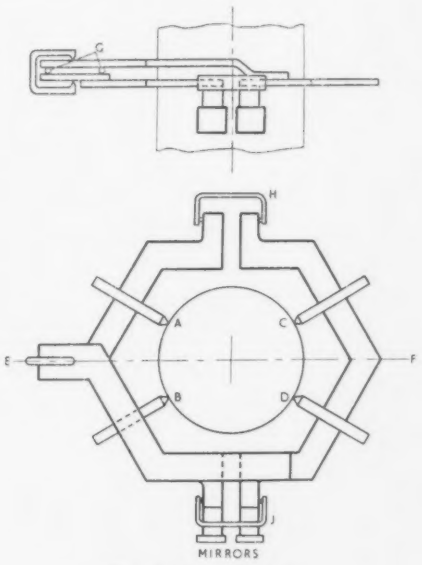

Fig. 6. Warpmeter.

5. Extensometers

The deformations that had to be independently measured were the angles of twist and of bend and the axial warping of the cross section. Three types of mechanical-optical extensometers were used (Fig. 4b).

The angle of bend was measured by two Martens extensometers held in position at the extreme fibres by a spring loaded clip.

The torsionmeter* (Fig. 5) consists essentially of two clips carrying mirrors and fixed to the specimen a known distance apart. Each clip touches the tube at two diametrically opposed points. To prevent pivoting about this diameter, the clips are disposed on two perpendicular diameters, and are so connected that they remain parallel to each other. This ensures that the measurement of twist will not be affected by bending of the specimen.

In designing the warpmeter advantage was taken of the anti-symmetry of the warp. It has been shown (HILL and SIEBEL 1951) that the warping takes the same value at points lying at opposite ends of a diameter, while the values at points on a pair of diameters symmetrically disposed about the plane of bending are equal and opposite.

The extensometer consists of two members carrying mirrors and each fixed to the specimens at two points, A, B and C, D, respectively (Fig. 6). When warping occurs, both members rotate in opposite senses about EF. The relative rotation, which is proportional to the amount of warping, is measured by means of the mirrors, a scale and a telescope.

Two hard steel points fitted to each member are the only contacts between the warping extensometer and the specimen ; two spring clips, H and J, provide the force necessary to position the extensometer.

To prevent the members rotating about the lines through AB and CD, a rigid extension of one member is hinged to the other on the line EF. The hinge is found by two small steel balls, G, lying on EF and held between flat plates. The use of balls permits the extensometer to adjust itself to small changes in the shape of the specimen cross-section. This extensometer, in effect, only measures the warp at four points lying at angles of 60° from the axis of bending.

6. TECHNIQUE OF TUBE TESTS

The tubes were manufactured with great care to ensure that the test section was parallel and that its outer profile was concentric with the bore. Both profile and bore were ground.

None of the specimens was perfect on delivery. To correct the imperfections the bores were first made parallel by using a Precision Honing Machine. The taper of the bore in the test section was less than 0·0001 in., while the outer profiles were parallel to a similar accuracy. Then, to correct the eccentricity, excess metal was removed from the bores by rubbing with emery paper held on a round steel rod. Finally the roundness of the bores was restored by again honing. The relative eccentricity of bore and outer profile was reduced to 0·00015 in. or less. After the stress-relief anneal, the dimensions were re-checked, and the positions on the specimens where the extensometers would be located were accurately marked out. The thickest and the thinnest parts of the walls were arranged to be as near as possible to the neutral axis.

The tests were carried out in two series. In the first B/T ratios of 0, ∞, $\frac{1}{2}$, 1 and 2 were used in that order. The pure torsion and bending tests were performed first, with all extensometers in position, to check that one kind of deformation did not affect extensometers measuring any other.

The load was raised by decreasing amounts until the proportional limit was reached. Thereafter definite strain increments were applied and readings taken ten minutes after straining. The "creep rate" was then roughly the same in the tubes as it had been after twenty minutes in the conventional test specimens.

The tests were stopped at a strain of order two or three times that at the proportional limit. The elastic constants obtained from these tests differed by up to 2·5 per cent from those obtained from the conventional tests. It was found that, after stressing the specimens several times to a stress about 0·8 of that at

* I am indebted to Professor J. L. M. MORRISON for suggesting the design.

Vol 1 1952/

the proportional limit, the elastic constants were very nearly in accord with those in the conventional tests. This cyclic pre-strain had no other observable effect on the behaviour of the tubes.

All tubes used in the second series of tests were subjected to about eight such preliminary loading cycles. Otherwise the testing procedure remained unchanged, the B/T values being, 2, 1, $\frac{1}{2}$, and 1/10. To facilitate the comparison of results, specimens taken from the same bar of 'E' steel were used when repeating tests under the same B/T ratio.

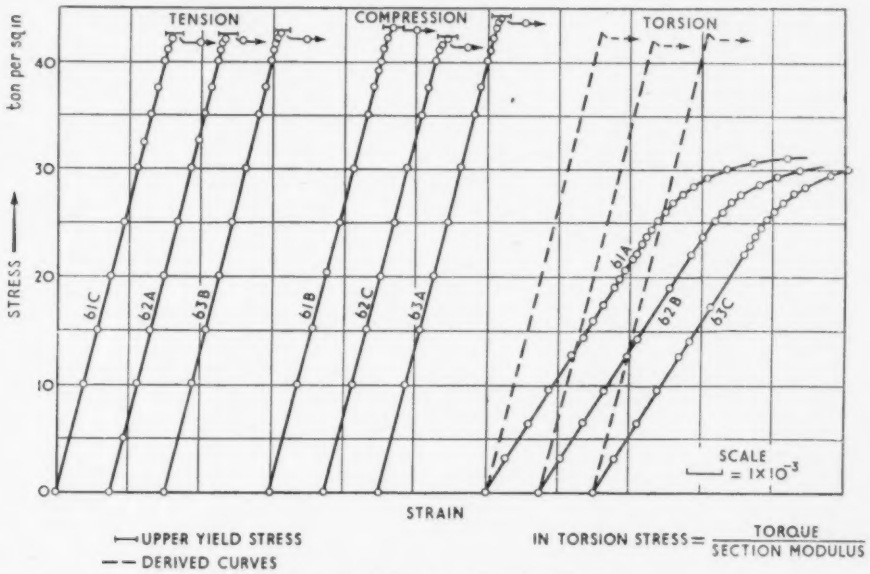

Fig. 7. Bar No. 6 stress-strain curves.

TABLE 1

Specimen	*Test*	*E* *tons/in.²*	*G* *tons/in.²*	*Upper Yield Stress* *tons/in.²*	*Lower Yield Stress* *tons/in.²*
61A*	Torsion	—	5300	—	42·2†
61B	Compression	13430	—	43·1	42·8
61C	Tension	13440	—	42·5	41·7
62A	Tension	13500	—	42·5	41·7
62B	Torsion	—	5250	—	41·4†
62C	Compression	13330	—	42·3	41·2
63A	Compression	13450	—	44·0	43·5
63B	Tension	13460	—	42·8	42·0
63C	Torsion	—	5230	—	42·0†

7. Results of the Conventional Tests

The stress-strain curves for Bar No. 6 are shown in Fig. 7 and the numerical results in Table 1. In tension and in compression the relation is linear until, at

* Numbers 1, 2 and 3 indicate position along the bar, while letters A, B and C indicate position round the bar.
† Derived quantities: $\sqrt{3} \times$ shear yield stress.

a stress 1 to 2 tons/in.^{2} below the upper yield, a small curvature appears even when the axiality of loading is almost perfect. A small drop of stress of between 1 and 4 per cent occurs after yield. The material then deforms under a constant stress up to strains of 1·3 per cent when the tests were stopped. No Lüders markings were observed.

TABLE 2. COMPRESSION CHECK SPECIMENS–TEST RESULTS

Specimen	*E* tons/in.^{2}	*Upper Yield Stress* tons/in.^{2}	*Lower Yield Stress* tons/in.^{2}
2LA	13600	42·0	41·1
2LB	13550	42·3	41·1
2TA	13600	42·6	41·9
2TB	13650	42·7	42·2
3LA	13650	42·2	41·5
3LB	13600	42·8	41·3
3TA	13600	43·0	41·9
3TB	13600	43·0	42·1
4LA	13600	42·7	41·6
4LB	13700	42·8	42·0
4LC	13650	41·5	40·7
5LA	13600	42·0	40·7
5LB	13600	42·0	40·7
5LC	13750	42·7	41·7
7LA	13550	43·8	42·5
7LB	13700	43·6	42·3
7TA	13700	43·8	43·4
7TB	13600	43·8	43·4
8LA	13700	43·7	43·0
8LB	13600	43·6	43·0
8OA	13850	45·5	45·2
8OB	13850	45·5	45·1
9LA	13650	43·0	42·2
9LB	13650	43·0	42·1
9OA	13900	44·8	44·5
9OB	13800	44·5	44·2
10LA	13800	43·0	41·7
10LB	13800	42·5	41·3
10OA	13850	44·0	42·9
10OB	13850	44·2	42·9

L denotes longitudinal specimens ; T denotes transverse specimens ; O denotes oblique specimens

The torque-twist curves were converted to shear stress-strain curves by the well-known NADAI construction. The tensile stress-strain curves were then derived, assuming the ratio between tensile and shear yield stresses to be $\sqrt{3}$;

Vol. 1 1952/5

this is shown to be justified later. From the values of E and G, Poisson's ratio, ν, was calculated to be $0{\cdot}275 \pm {\cdot}01$.

There appears to be no significant variation of properties either along or round the bar. The scatter of the lower yield stress values is about 4 per cent; the mean values are 42·5 tons/in.² in compression and 41·8 tons/in.² in tension. In these tests the eccentricity of loading was kept small; the maximum stress exceeded the mean by between 0·4 per cent (61C) and 2·5 per cent (62C). In torsion the mean derived value of the lower yield stress is 41·9 tons/in.².

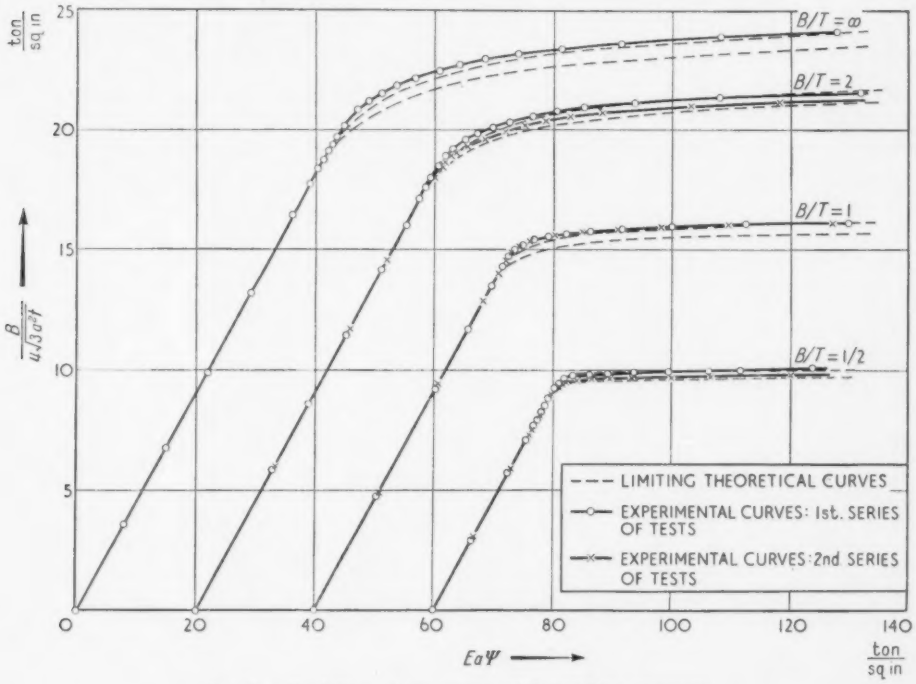

Fig. 8. Variation of curvature with bending moment.

The results of the tests on the compression check specimens are given in Table 2; the stress-strain curves are similar to those for Bar No. 6 (Fig. 7). It may be seen that the material is not absolutely homogeneous; all transverse and oblique specimens have higher compressive yield stresses than the corresponding longitudinal ones; the longitudinal specimen 5LC from the core of Bar 5 (Fig. 1) has also a higher yield stress than specimens 5LA and 5LB. Generally it may be said that specimens with gauge lengths near the cores of the bars have higher yield stresses than those with gauge lengths from the outer layers. The yield stress of specimens taken from similar positions in any bar agree to within 1 per cent (except in Bar No. 4); the yield stresses of specimens from dissimilar positions may vary by 5 per cent.

No ovality of section was found in any specimen after testing. The axiality of loading in these tests was good; in the elastic range the maximum stress exceeded the mean by an average of 1·85 per cent only, the limits being 0 and 5·3 per cent.

Brinell hardness tests revealed no significant variation of properties along the bars. The cores are, however, somewhat harder than the outer layers. In an extreme case (Bar No. 3) the hardness numbers were 269 at the core and 217 at a radius of $\frac{3}{4}$ in.

8. Results of Tests on Tubes

(*a*) *The bending moment-curvature relations*

In Fig. 8 the experimental results have been plotted together with those predicted by the theory. $Ga\psi/k$ was first converted to $Ea\psi/k$ using a Poisson's ratio of 0·3 as in the theoretical calculations; a is the mean radius of the wall of thickness t while ψ is the angle of bend per unit length. The predicted curves were then obtained by multiplying the dimensionless quantities $B/4\sqrt{3}\,a^2\,t\,k$ and $Ea\psi/k$ by the measured shear yield stress k. From the compression check specimens a small range of values was found for the lower yield stress in each

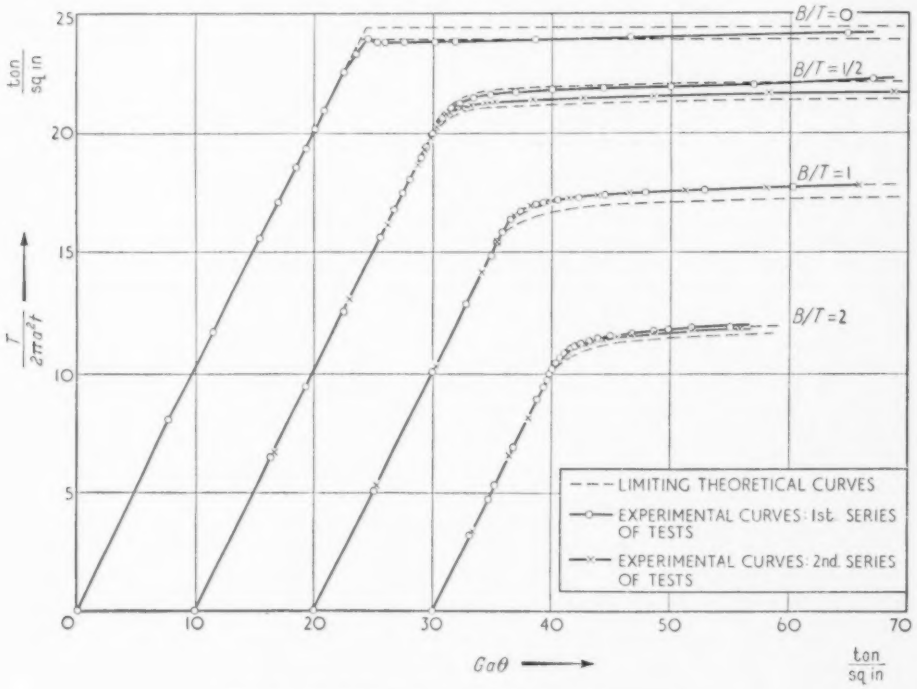

Fig. 9. Variation of twist with twisting moment.

bar. The extreme values of this range were used to plot two calculated curves for each B/T ratio. The effect of plotting $B/4\sqrt{3}\,a^2\,t$ against $Ea\psi$ is that the calculated and the experimental curves have the same slope, $\pi/4\sqrt{3}$ in the elastic range. It should be noted that the relation between $B/4\sqrt{3}\,a^2\,t$ and $Ea\psi$ is completely independent of ν (cf. equation 13, Hill and Siebel, *op cit.*).

In the early part of the plastic range some curves have a raised "knee" and

the applied bending moment is greater than predicted, but, as the plastic zone spreads, all the curves return to the predicted range. At the ends of the tests they are almost horizontal.

The experimental curve for $B/T = 1/10$ is not shown. Almost immediately after yield $B/4\sqrt{3}\,a^2t$ attains the constant value of 2·14 tons/in². This test is interesting only from the point of view of warping.

(*b*) *The Twisting-Moment-Twist Relations*

The experimental twisting moment twist curves are shown in Fig. 9 together with the two limiting curves calculated for each B/T ratio from the corresponding extreme values of k.

The calculated $T/2\pi a^2t$ is independent of ν. θ, the angle of twist per unit length is proportional to $(1 + \nu)$ in the elastic range and becomes steadily less dependent on ν as the elastic zone shrinks. When $T/2\pi a^2t$ is plotted against $Ga\theta$ the slope of the line in the elastic line is, of course, unity regardless of the value of ν.

The curve for pure torsion ($B/T = 0$) departs from linearity about 8 or 10 per cent below the upper yield point, where a very small drop of twisting moment occurs. The curve lies in the predicted zone except for a short range immediately after yield.

The curves for $B/T = 2$, 1 and $\frac{1}{2}$ are exact replicas of the bending curves. Their position relative to the predicted curves is the same and the "knees" are of the same relative magnitude. The curve for $B/T = 1/10$ is not shown; it is very close to the pure torsion curve, but the ultimate twisting moment is 1·5 per cent lower.

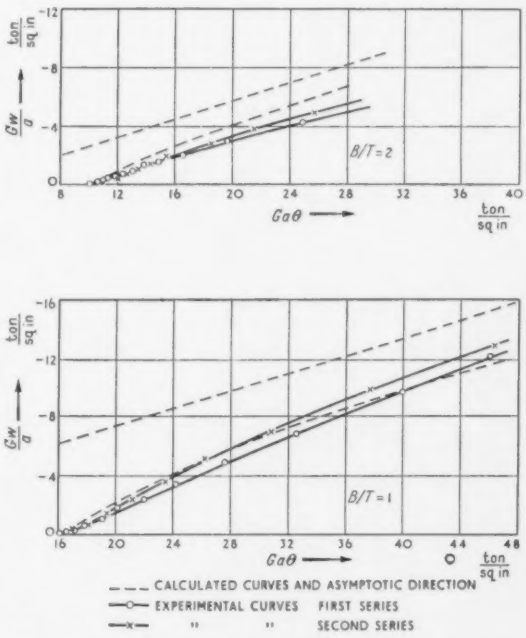

Fig. 10. The relationship between warp at $\theta = 60°$ and twist.

(*c*) *Warping*

The experimental curves of the warp, w, at $\phi = 60°$ in relation to the twist, θ, are shown in Figs. 10 and 11, together with the theoretical curves and asymptotic direction (Appendix 2). The vertical scale is such that one unit is equivalent to a warp of approximately 0·001 in.

The predicted curves have been obtained by multiplying the calculated dimensionless quantities Gw/ka and $Ga\theta/k$ by the highest value of the yield stress, k, obtained from the appropriate bar of steel.

The experimental curves for $B/T = 2$ lie below the calculated curve. Their shape is similar to that predicted and they possess the characteristic inflexion; their final slope is about 0·25. The curves for $B/T = 1$ lie astride the calculated one, the inflexion being again present. The final slope is about 0·36. The two curves for $B/T = \frac{1}{2}$ are similar in the early part of the test. In the first test the warp-meter slipped after the last reading shown, and the readings were then erratic and meaningless. The inflexion is again present. The final slope of the second curve is about 0·31. When $B/T = 1/10$, the experimental curve has no point of inflexion and the amount of warp remains small. The final slope of the curve is about 0·03. The sense of the warp was, in every case, as predicted.

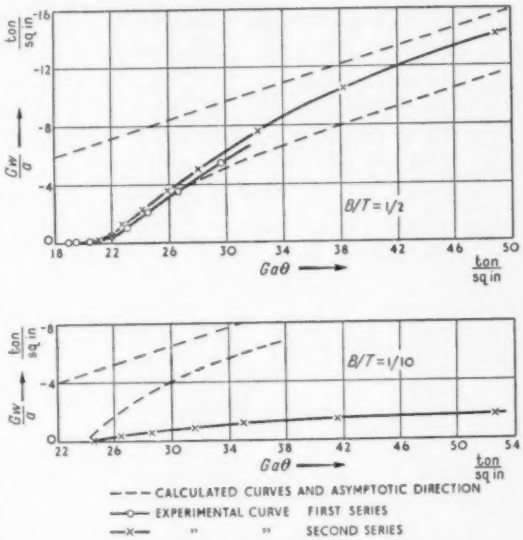

Fig. 11. The relationship between warp at $\theta = 60°$ and twist.

(*d*) *The Yield Criterion*

The last load reading in each experiment was used to calculate the shear and axial stresses (τ_∞ and σ_∞) in the tube which by then should be uniformly distributed (Fig. 12). Three MAXWELL-MISES ellipses ($\sigma^2 + 3\tau^2 = 3k^2$) are also shown representing the highest, the lowest and the mean values obtained from the compression check specimens from all the bars from which tubular specimens were made.

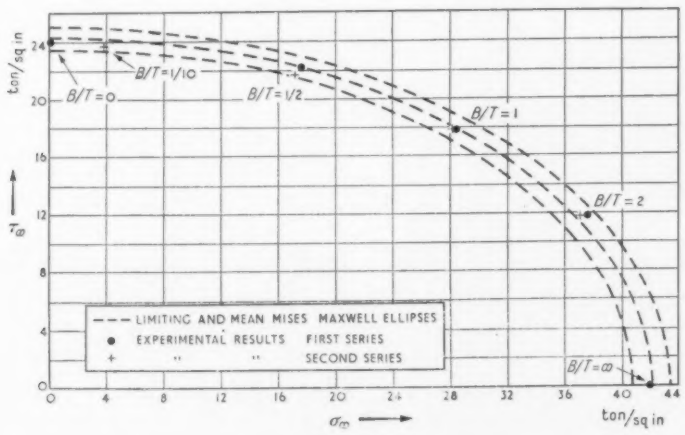

Fig. 12.

(e) Lode's Variables

The experimental relations between $Ga\theta$ and $Ea\psi$ are shown in Fig. 13. The theoretical curves were calculated using the upper value of k in the range for the appropriate bar.

LODE's variable ν_L is calculated from

$$\nu_L = -\left[1 + \left(\frac{\pi}{3}\cdot\frac{d\theta}{d\psi}\right)^2_{\infty}\right]^{-\frac{1}{2}}$$

using the asymptotic slope $(d\theta/d\psi)_{\infty}$. The derivation of this relation is given in Appendix 3. μ_L is given by

$$\mu_L = -\left[1 + \left(\frac{2\tau_{\infty}}{\sigma_{\infty}}\right)^2\right]^{-\frac{1}{2}}.$$

The (μ_L, ν_L) relation is shown in Fig. 14.

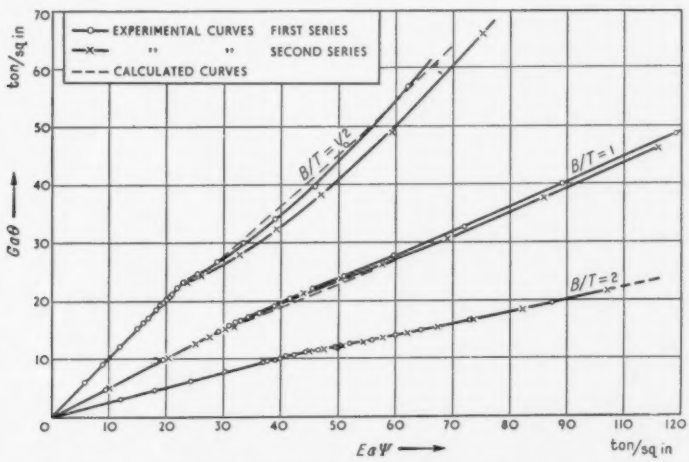

Fig. 13. The relationship between curvature and twist.

9. DISCUSSION OF RESULTS

(a) Tension, Compression, Torsion and Hardness Tests

The tests on the nine specimens made from Bar No. 6 show that the stress-strain curve of the steel in tension is effectively identical with that in compression. From the torsion tests the ratio of tensile to shear yield stress is shown to be $\sqrt{3}$ within the accuracy possible for this material. All the wanted properties of the steel may therefore determined from the compression tests on the check specimens alone. The small drop of stress at yield (less than 4 per cent) should not unduly influence the torsion or the bending test results. The properties of the steel do not vary excessively along or round the bar. In other words, it would appear from these nine tests that this steel fulfils all the theoretical requirements as well as an engineering material can be expected to do.

However, the hardness tests and the compression tests on the longitudinal,

transverse and oblique compression check specimens reveal that this material is not uniform radially. Also, higher yield stress is frequently allied to a higher value of Young's modulus, E. These effects are particularly marked in the compression check specimens taken from Bars No. 5, 8, 9, and 10. The variation appears greatest in the bars where the gauge lengths of the specimens lie particularly close to the axis (Bars 5, 8, 9 and 10). Some tests on thin tubes designed to reveal anisotropy in the steel were negative.

The conclusion is that the steel is isotropic but not homogeneous in its elastic and in its plastic properties. E decreases by up to 1·5 per cent from the axis to the outside of a bar while the lower yield stress decreases by 2 to 5 per cent in the same distance.

The properties of all elements of the material at the same radius from the axis of the bar may be expected to have identical properties; this is confirmed by the fact that specimens from opposite sides of the same bar always have almost the same value of E and k. The lack of radial homogeneity is therefore not significant in the tests on the tubes, since these are centred on the axis of the bar. The walls are too thin for any effect of the radial variation of properties to be felt.

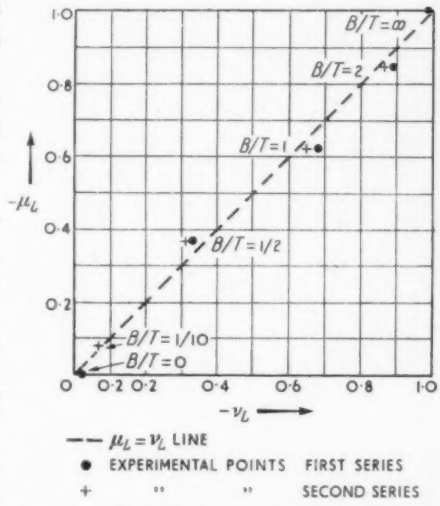

Fig. 14. The relationship between LODE's variables μ_L and ν_L.

(*b*) *The Yield Criterion*

The ordinate of the last experimental point of each moment-angle curve was taken to represent the limiting value of the applied couple, and the axial and shear stresses in the tubes were calculated on this assumption. This is equivalent to saying that, at the ends of the tests, the stress distribution round the tubes is uniform. This assumption is strictly true only for torsion. In pure bending only about 85 per cent of the tube is plastic at the end of the test when the curvature is three times that at first yield. For the intermediate B/T ratios the extent of the plastic zone at the ends of the tests probably lies between these two values.

The theoretical curves indicate that when the angles of twist and of bend are two to three times those at yield, the applied couples have reached values less than 1 per cent below their limiting values. It is, therefore, permissible to take the final load reading in each test as the limiting load. Greater strains would not necessarily give more accurate values, since work-hardening would occur at the extreme fibres. The experimental points all lie within the range predicted and, moreover, they all lie within 1·5 per cent of the mean MAXWELL-MISES ellipse.

This, taken in conjunction with the results of the tests for the correlation of the properties of the steel (Bar No. 6), appears to be sufficient proof that the MAXWELL-MISES criterion is a close approximation for this steel.

(c) Lode's Variables

These tests were not expressly designed to investigate the (μ_L, ν_L) relation, but it may be found approximately from the results at the final stages of the tests when the stresses in the tubes are effectively uniform. Errors in the calculation of μ_L and ν_L arise from this assumption of uniformity and from the uncertainty in the derived final slopes of the θ-ψ curves. This slope is independent of k but is inversely proportional to $(1 + \nu)$. It is therefore somewhat fortuitous that the agreement between the theoretical ($\nu = 0{\cdot}3$) and the experimental curves should be so close when $B/T = 1$ and 2. A steeper slope might have been expected. For $B/T = 1/2$ the experimental slope is steeper than that calculated.

The experimental points are scattered in a random fashion about the $\mu_L = \nu_L$ line. The scatter is small, and it is concluded that undue errors will not be made if the LÉVY-MISES relations are used for the prediction of the plastic part of the strain increment.

(d) Moment-Angle Relations

It is sufficiently accurate to compare torque-twist curves calculated with $(1 + \nu) = 1{\cdot}3$ with experimental curves for material where $(1 + \nu)$ is not far different. Consider two such curves, both for $B/T = 1$, the one calculated with a value $\nu_1 = 0{\cdot}3$, the other with $\nu_2 = 0{\cdot}26$, i.e. $(1 + \nu_1)/(1 + \nu_2) = 1{\cdot}03$. The two curves are coincident when the tube is wholly elastic and also when it is wholly plastic. A small discrepancy between the two curves will, however, be observed in the transition between these extreme states. At a given value of $Ga\theta$ such that about one third of the tube is plastic, the difference in the applied moment is estimated, from a scrutiny of the calculations, to be about 0·05 per cent. As the plastic zone spreads the discrepancy diminishes.

When the tubes are partly plastic, several of the moment-angle curves show that, for a given value of the angle, the applied moment is slightly greater than predicted. This is the case for $B/T = \infty$, 2 (1st series) and 1; the curve for $B/T = 2$ (2nd series) also shows this tendency to a raised knee in this portion, although the whole curve lies within the predicted range. The curves for $B/T = \frac{1}{2}$ are entirely as predicted and lie well within the range defined by the two limiting calculated curves. The curve for $B/T = 0$ is, as was to be expected, a replica of the shear stress-strain curve. The portion round the yield point is somewhat less sharply defined owing to the finite thickness of the tube. A small amount of work-hardening occurs; but is less than 1 per cent at a strain three times that at yield.

The small difference between the predicted and experimental moment-angle curves cannot be attributed to a lack of reliability of the REUSS relations. These were not used in the calculation of the *bending* curves. They were, however, used for the calculation of the *torsion* curves, and the torsion curves are the exact replicas of the bending curves.

The explanation of the knee was, at first, thought to be connected with the drop of stress at yield. It is known that the drop of stress is one of less than 4 per cent. Calculations show that the moment-angle curve for pure bending derived on this basis is almost indistinguishable from the one calculated using the idealized stress-strain curve with no drop of stress.

It was noticed that the maximum discrepancy between the predicted and the experimental curves decreases from 1·5 per cent to 0 as the B/T ratio decreases from ∞ to $\frac{1}{2}$. The existence of the "knee" may therefore be linked in some way with the amount of bending, that is, with the "steepness" of the stress gradient in the tubes. The influence of the local stress gradient has been observed also by COOK (1932 and 1937) and by MORRISON (1939 and 1948). The alloy steel used here has a much smaller drop of stress at yield than annealed mild steel, so that the "size-effect" theory suggested by MORRISON cannot explain the observations.

Apart from the initial "knee," the moment angle curves then all lie in the predicted range. Most experimental curves coincide with the upper one of the two calculated curves. This is not surprising since the upper curve was calculated generally on the basis of the yield stress obtained from the transverse or centrally disposed compression specimens. The gauge lengths of these specimens lie in the same region of the original bar as do the walls of the tubes.

The curves for $B/T = \frac{1}{2}$, from tubes made out of Bar No. 4, lie between the two limiting curves. The latter were calculated from the extreme yield stresses of three longitudinal specimens all lying at about the same distance from the centre of the bar as the walls of the tubes.

The curves for pure torsion and for $B/T = 2$ (2nd series) are rather lower than would be expected. The difference is one of less than 1·5 per cent and may well be due to a small axial variation in the properties of the bar concerned.

Generally speaking, then, the moment-angle curves can be predicted very accurately by the theory put forward by HILL and SIEBEL (1951).

Vol.
1
1952/

(*e*) *Warping*

The experimental curves rise from zero as soon as yield is initiated at the extreme fibres. In fact, the measurement of warp was found to be a very sensitive method of detecting the initiation of yield, and the warp-meter was usually the first instrument to give a warning of this. The curves for $B/T = 2$, 1 and $\frac{1}{2}$ have the predicted form, that is concave first upwards and then downwards. The quantitative agreement with theory is, however, less good. The predicted warping is only little affected by small variations in k and $(1 + \nu)$; the relatively small scatter of the warp curves about the predicted values may be attributed tentatively to 'imperfections' in the material. The theory predicts the same rate of warping whatever the value of B/T providing B and $T = 0$ (Appendix 2). In actuality, however, some transition must presumably exist between warping at intermediate B/T's and no warping at $B/T = 0$ or ∞. Indeed, the warping for $B/T = 1/10$ was found to be far less than predicted. Since the B/T and the t/a ratios are here comparable, the failure of the theoretical solution may possibly be attributed to the breakdown of the thin-wall approximation.

APPENDIX 1

If, in a thin walled tube, the mean radius is used in the present theoretical formulae, only small errors will accrue. Thus, when the tube is wholly plastic with uniform shear stress, τ, the true applied torque is

$$2\pi\tau \int_{a-t/2}^{a+t/2} r^2\, dr = 2\pi\tau a^2 t \left[1 + \frac{t^2}{12a^2}\right].$$

If the mean radius, a, is used, the torque is approximately equal to $2\pi\tau a^2 t$. When t/a is about 0·11, as in these tests, the error in torque is about 0·1 per cent; this is not measurable. A similar argument applies to the error in the bending moment.

Appendix 2

Asymptotic Direction of the Warp-Twist Curves

The warping increases without limit, but the w-θ curve has an asymptotic direction. Hill and Siebel have shown that, when the tube is fully plastic,

$$\frac{\partial}{\partial s}\left(\frac{dw}{d\theta}\right)_\infty = \frac{3\tau}{|\sigma|}\,|y|\,\frac{d\psi}{d\theta} - 2\,\frac{\partial A_s}{\partial s}$$

where s is the distance measured round the perimeter, A the cross-sectional area, A_s the sectional area, and the suffix ∞ denotes the limiting value of any quantity for indefinitely great strain.

Hence

$$\frac{\partial}{\partial s}\left(\frac{dw}{d\theta}\right)_\infty = 2\left[\frac{A\,|y|}{\oint y\,ds} - \frac{\partial As}{\partial s}\right],$$

since, for continuity of $\partial w/\partial\theta$ round the tube,

$$\oint \frac{\partial}{\partial s}\left(\frac{\partial w}{d\theta}\right) ds = 0.$$

Therefore

$$\left(\frac{dw}{d\theta}\right)_\infty = 2\left[\frac{A\int^s |y|\,ds}{\oint y\,ds} - A_s\right].$$

This in independent of B/T (B and $T \neq 0$). Since this relation does not depend on $3\tau/|\sigma|$ it is actually valid whatever the yield criterion and the (μ_L, ν_L) relation.

For a circular tube

$$\frac{G}{ka}\left(\frac{dw}{d\theta}\right)_\infty = \frac{Ga}{k}\left(\frac{\pi}{2}\sin\phi - \phi\right)$$

where ϕ is the angle subtending s at the axis.

Appendix 3

Derivation of Equation for ν_L

From equations (1) and (2) given by Hill and Siebel,

$$\frac{\partial}{\partial s}\left(\frac{dw}{d\theta}\right) = \frac{\dot\gamma}{\dot\epsilon}\,|y|\,\frac{d\psi}{d\theta} - 2\,\frac{\partial As}{\partial s}.$$

When the tube is fully plastic $\dot{\gamma}/\dot{\epsilon}$ is a function only of τ/σ depending on the (μ_L, ν_L) relation, and this ratio is constant round the tube. Hence

$$O = \oint \frac{\partial}{\partial s}\left(\frac{dw}{d\theta}\right) ds = \frac{\dot{\gamma}}{\dot{\epsilon}} \frac{d\psi}{d\theta} \oint |y|\, ds - 2A,$$

and so

$$\frac{\dot{\gamma}}{\dot{\epsilon}} = \frac{2A}{\oint |y|\, ds} \cdot \frac{d\theta}{d\psi},$$

from which follows the equation for ν_L.

ACKNOWLEDGMENTS

I am much indebted to Professor J. L. M. MORRISON for his supervision, guidance and helpful advice in all matters relating to the work described in this paper. I am also very grateful to Dr. R. HILL for his many valuable suggestions regarding the mathematical and the practical aspects of the experiments. I wish to express my thanks to the *English Steel Corporation Ltd.*, for giving the material used. Thanks are due also to the University of Bristol, Faculty of Engineering Workshop staff who constructed the testing machine and the extensometers, and prepared the specimens.

REFERENCES

COOK, G.	1932	*Proc. Roy. Soc.* A, **137**, 559.
COOK, G.	1937	*Trans. Eng. and Shipbuilders in Scotland*, **81**, 371.
DONNELL, L. H.	1933	*Nat. Adv. Comm. Aero.*, Tech. Rep. No. 479.
HILL, R.	1950	*The Mathematical Theory of Plasticity* (Oxford, Clarendon Press).
HILL, R. and SIEBEL, M. P. L.	1951	*Phil. Mag.*, **42**, 722.
MORRISON, J. L. M.	1939	*Proc. Inst. Mech. Eng.*, **142**, 194.
MORRISON, J. L. M.	1948	*Proc. Inst. Mech. Eng.*, **159**, 81.
MORRISON, J. L. M. and SHEPHERD, W. M.	1950	*Proc. Inst. Mech. Eng.* (W.E.P. No. 55), **163**.
NADAI, A.	1931	*Plasticity* (McGraw Hill Book Co.).
ROBERTSON, A.	1929	*Aero. Res. Council*, Rep. and Mem. No. 1185.
ROBERTSON, A. and NEWPORT, A. J.	1927	*Aero. Res. Council*, Rep. and Mem. No. 1161.
SIEBEL, M. P. L. and SMALLMAN, E. W.	1949	*Unpublished Report for the Degree of B.Sc. in Engineering in the University of Bristol.*
TAYLOR, G. I. and QUINNEY, H.	1931	*Phil. Trans. Roy. Soc.* A, **230**, 323.
TIMOSHENKO, S.	1936	*Theory of Elastic Stability* (McGraw Hill Book Co.).

Vol. 1 1952/5

Journal of the Mechanics and Physics of Solids, 1953, Vol. 1, pp. 207 to 214. Pergamon Press Ltd., London.

ON THE PLASTIC DISTORTION OF SOLID BARS BY COMBINED BENDING AND TWISTING

By R. Hill* and M. P. L. Siebel†
*Department of Theoretical Mechanics, University of Bristol
†Department of Mechanical Engineering, University of Bristol

(*Received 11th December*, 1952)

Summary

Experimental moment-angle relations are reported for steel bars of circular section plastically strained by combined bending and twisting couples in constant ratio. The bending and twisting moments approach, and practically attain within an overstrain of elastic magnitude, the theoretical values calculated for the fully-plastic state of a plastic-rigid material. Very good estimates of the latter values are obtained by bracketing between upper and lower approximate values. A general relation is proposed between the fully-plastic values of bending moment, torque and axial force when all three are applied together. This relation applies for a wide variety of sections and is suitable for plastic limit design.

ol.
1
2/53

1. Introduction

The overstraining of a thin-walled tube of arbitrary section by combined bending and twisting couples has been treated analytically by Hill and Siebel (1951). Their calculations of the moment-angle relations and amount of warping, for monotonic loading of a circular tube under constant ratio of bending to twisting couples, have received excellent experimental confirmation by Siebel (1953). The material was an alloy steel with basic properties closely simulating those assumed. These are that yielding is governed by the Maxwell-Mises criterion ; that there is no subsequent hardening in the strain range concerned ; and that the plastic part of any strain-increment is related to the stress according to the Lévy-Mises hypothesis. The overall agreement between experiment and theory indicates that no practically significant errors arise from the additional assumptions : namely, that each increment of strain can be resolved into additive elastic and plastic parts (the one governed by the generalized Hooke's law and the other by the Lévy-Mises relations); that stress gradient does not affect the behaviour of material elements, and that stresses and strains may be averaged through the wall-thickness if this does not exceed about one tenth of the tube diameter.

It has not been found possible to treat by exact analysis, or even by tolerable approximation, the partial overstraining of a solid bar by combined bending and twisting couples. It is, however, possible to calculate for a Maxwell-Lévy-Mises material the loading that first causes local yielding (the elastic limit) and, to sufficient accuracy, also the loading that produces a fully plastic state. Strictly, the latter is calculated as the yield point of a fictitious plastic-rigid material ; one,

that is, in which the rigidity modulus is assigned an indefinitely great value, and in which distortion cannot begin, in the present instance, until the plastic zone has spread through the whole body. For an actual material with a finite rigidity, HILL and SIEBEL showed theoretically that the moment-angle relations for a thin-walled tube approach asymptotically with increasing strain to the plastic-rigid yield point values. The approach is not steady, nor even complete in any finite strain, but the discrepancy is less than a per cent or two after an overall distortion of three times that at the elastic limit. Such an asymptotic approach is a purely mathematical phenomenon : the consequence of neglecting dimensional changes, as in the linear theory of elasticity. If these changes were to be incorporated in the analysis, the moment-angle relation in a non-hardening material would still be expected to come most near the level representing the plastic-rigid yield point within a strain of elastic magnitude, but afterwards diverge. SIEBEL's experiments confirm these expectations, within the range of strain for which the steel did not work-harden.

In such circumstances the plastic-rigid yield point load has the practical significance that the actual load may be raised to within a few per cent of it, and yet cause a permanent distortion of elastic magnitude only. Furthermore, the yield point may be shown not to depend on the history of loading up to the final combination of loads, nor on the locked-up stresses initially present in the body. These ideas are, of course, fundamental in the well-known method of plastic limit design of structures.

For comparison with the calculated yield point of a solid bar of circular section under combined bending and torsion, we report here experimental data for the alloy steel previously used by SIEBEL. The theoretical values are found to have a significance comparable with that already demonstrated for thin-walled tubes. A similar significance has been previously demonstrated for bars of various sections under pure bending (RODERICK and PHILLIPPS 1949 ; SHACKELL and WELSH 1952). No general theorem has yet been found for predicting in any particular circumstances how rapidly and closely the load-distortion relation approaches the corresponding plastic-rigid yield point. In addition to the cases mentioned, present knowledge rests on a few special theoretical solutions such as the over-straining of moderately thick-walled tubes by internal pressure (HILL 1950a, p. 121 ; THOMAS 1953) ; combined torsion and tension of a bar of circular section (GAYDON 1952) ; stretching by external tension of a circular sheet with a central cut-out (HODGE 1953).

2. METHOD FOR APPROXIMATE ESTIMATE OF YIELD POINT

Suppose, for simplicity, that the section has two orthogonal axes of symmetry. Let T_0 be the yield point under pure torque, F_0 the yield point under pure axial load, and B_0 the yield point for pure bending about an axis of symmetry. The stress state for pure axial load is a uniform normal stress of amount $\sqrt{3}k$, while that for pure bending consists of stresses $\pm\sqrt{3}k$ on opposite sides of the neutral surface (which coincides with a plane of symmetry). If an axial load F and bending moment B are applied together, the stress state at the yield point still consists simply of stresses $\pm\sqrt{3}k$ on opposite sides of the neutral surface (no longer a plane of symmetry). At the yield point F and B satisfy some relation

$$\phi\left(\frac{B}{B_0}, \quad \frac{F}{F_0}\right) = 0 \tag{1}$$

where ϕ is a purely numerical function depending on the shape of the section.

Consider now, the combined action of axial load, bending moment, and torque. A solution in general terms for the fully plastic state has been described by HILL (1950, pp. 313-6) for a MAXWELL-LÉVY-MISES body. The resulting non-linear differential equation has, however, not been solved; instead we obtain close approximations from above and below to the relation between the yield point loads by means of the continued inequality due to HILL (1950a, p. 67 ; 1950b). This particular method of applying the inequality is due to DRUCKER, GREENBERG and PRAGER (1951); further illustrations have been given by HILL (1951) and PELL and PRAGER (1951).

(i) *Approximation from below*

For this we take a fictitious distribution of shearing stress similar to that in pure torsion, but of amount $\tau < k$. The corresponding torque T^* satisfies

$$\frac{T^*}{T_0} = \frac{\tau}{k}. \tag{2}$$

We combine with this a uniform distribution of normal stress of amount $\sigma < \sqrt{3}k$, but having opposite signs on either side of a quasi-neutral plane. From (1) the corresponding bending-moment B^* and axial force F^* satisfy

$$\phi\left(\frac{\sqrt{3}kB^*}{\sigma B_0}, \qquad \frac{\sqrt{3}kF^*}{\sigma F_0}\right) = 0. \tag{3}$$

Since the artificial state must not violate the yield criterion, the best approximation is obtained by taking

$$\sigma^2 + 3\tau^2 = 3k^2. \tag{4}$$

The elimination of $\sigma/\sqrt{3}k$ and τ/k between (2), (3), and (4) leads to a relation between B^*/B_0, F^*/F_0 and T^*/T_0, which, considered as a surface, lies inside that corresponding to the actual yield point state.

(ii) *Approximation from above*

For this we take a fictitious distribution of velocity

$$u = \tfrac{1}{4}(x^2 - y^2 + 2z^2)\dot{\psi} - \tfrac{1}{2}x\dot{\epsilon} - yz\dot{\theta},$$
$$v = \tfrac{1}{2}xy\dot{\psi} - \tfrac{1}{2}x\dot{\epsilon} + xz\dot{\theta},$$
$$w = -xz\dot{\psi} + z\dot{\epsilon},$$

where z is the axis of the bar, and x and y are the axes of symmetry, y being the axis of B. This distribution represents a combination of uniform bending, twisting, and extension, at rates $\dot{\psi}$, $\dot{\theta}$, and $\dot{\epsilon}$ per unit length, without warping or volume change. Substitution in HILL's inequality leads to

$$B\dot{\psi} + F\dot{\epsilon} + T\dot{\theta} \leqslant k\iint[3(\dot{\epsilon} - x\dot{\psi})^2 + (x^2 + y^2)\dot{\theta}^2]^{1/2}\,dxdy = W, \text{ say,}$$

where the integral is taken over a cross-section. For given ratios of B, F, T, the best approximations to their magnitudes are given by

$$B \leqslant B^* = \frac{\partial W}{\partial \dot{\psi}}, \qquad F \leqslant F^* = \frac{\partial W}{\partial \dot{\epsilon}}, \qquad T \leqslant T^* = \frac{\partial W}{\partial \dot{\theta}}, \tag{5}$$

where the associated ratios of the fictitious strain-rates are such that

$$B/B^* = F/F^* = T/T^*. \tag{6}$$

Now the stresses that would correspond to the fictitious strain-rates according to the MAXWELL-LÉVY-MISES relations are given by

$$\sigma/(\dot{\epsilon} - x\dot{\psi}) = -3\tau_x/y\dot{\theta} = 3\tau_y/x\dot{\theta}, \qquad \sigma^2 + 3(\tau_x^2 + \tau_y^2) = 3k^2. \tag{7}$$

If the derivatives in (5) are evaluated, it will be found that B^*, F^*, T^* are precisely the loads that would be obtained as the resultants of the stresses (7). This is remarkable, seeing that the distribution (7) is not in equilibrium and also entails a resultant transverse shearing force and tangential surface stresses.

In short, then, the surface representing the actual relation between the yield point loads lies inside the one that is calculated if warping is disregarded (together with attendant inconsistencies).

Vol. 1 1952/5

3. YIELD POINT OF CIRCULAR SECTION

When the section is a circle of radius a, equation (1) is the result of eliminating β between

$$B/B_0 = \cos^3\beta, \qquad F/F_0 = (2\beta + \sin 2\beta)/\pi,$$

where $B_0 = 4ka^3/\sqrt{3}$, $F_0 = \sqrt{3}\pi ka^2$, and $a\sin\beta$ is the distance of the neutral plane from the longitudinal axis. It is found that

$$\frac{B}{B_0} + \frac{F^2}{F_0^2} = 1 \tag{8}$$

approximately, with an underestimate of less than $1\frac{1}{2}$ per cent in the magnitudes of B and T for a given ratio B/T. For a thin-walled circular tube, where $B/B_0 = \cos\beta$, $F/F_0 = 2\beta/\pi$, (8) overestimates the true magnitudes by less than 4 per cent; for a solid rectangular section, (8) is in fact the exact relation (with the appropriate values of B_0 and F_0). The comparative independence of geometry exhibited by the (B, F) relation has also been remarked for other sections by ONAT and PRAGER (1953). From (2), (3), (4), and (8) there results

$$\left(\frac{F^*}{F_0}\right)^2 + \left(\frac{T^*}{T_0}\right)^2 + \frac{B^*}{B_0}\left(1 - \frac{T^{*2}}{T_0^2}\right)^{1/2} = 1 \tag{9}$$

as the approximation from below.

For combined torsion and tension the exact yield point solution is known (HILL 1950, p. 76). It is

$$\left.\begin{aligned} T/T_0 &= (1+\mu^2)^{3/2} - 3\mu^2(1+\mu^2)^{1/2} + 2\mu^3 \\ F/F_c &= 2\mu(1+\mu^2)^{1/2} - 2\mu^2 \end{aligned}\right\} \quad \begin{aligned} &\text{where } \mu = \sqrt{3}\,\dot{\epsilon}/a\dot{\theta} \\ &\text{and } T_0 = \tfrac{2}{3}\pi k a^3. \end{aligned}$$

Since this solution for a MAXWELL-LÉVY-MISES body involves no warping it coincides with (5), the approximation from above. Moreover, it differs from the approximation from below,

$$\left(\frac{F^*}{F_0}\right)^2 + \left(\frac{T^*}{T_0}\right)^2 = 1,$$

by less than $1\frac{1}{2}$ per cent (comparing radius vectors to the two curves).

The exact solution for combined torsion and bending is not known. From (5) and (6), however, we obtain the upper approximation

$$\frac{B^*}{B_0} = \int_0^{\frac{1}{2}\pi} \frac{\sqrt{3}\lambda \sin^2\phi\, d\phi}{\sqrt{(1+3\lambda^2\sin^2\phi)}}, \quad \frac{T^*}{T_0} = \frac{2}{\pi}\int_0^{\frac{1}{2}\pi} \frac{d\phi}{\sqrt{(1+3\lambda^2\sin^2\phi)}}, \qquad \lambda = \dot{\psi}/\dot{\theta}. \quad (10)$$

These are elliptic integrals; they are not, however, convenient to evaluate from available tables. Instead we have computed the integrals directly (Table 1).

TABLE 1

$\lambda = \dot{\psi}/\dot{\theta}$	B^*/B_0	T^*/T_0	$\{(B^*/B_0)^2 + (T^*/T_0)^2\}^{\frac{1}{2}}$	B^*/T^*
0	0	1·000	1·000	0
0·408	0·476	0·904	1·022	0·580
0·577	0·602	0·835	1·029	0·800
1·000	0·776	0·688	1·037	1·250
1·826	0·900	0·502	1·031	1·980
5·774	0·982	0·235	1·009	4·620
∞	1·000	0·000	1·000	∞

The penultimate column indicates that (10) exceeds the lower approximation

$$\left(\frac{B^*}{B_0}\right)^2 + \left(\frac{T^*}{T_0}\right)^2 = 1 \quad (11)$$

by less than 4 per cent.

These results suggest that (9) may be relied upon to provide an approximation involving an error of not more than a few per cent in the general case when B, F and T act simultaneously in given ratios. It is a *safe* formula for a circular section since the true yield point relation is under-estimated. It may also be used with reasonable accuracy for all sections for which (8) is a sufficient approximation.

4. EXPERIMENTS

To investigate the rapidity of approach to the plastic-rigid yield point values, steel bars of circular section were strained in combined torsion and bending. In each test the ratio of bending and twisting moments was held constant. The material and the machine have been described by SIEBEL (op. cit.). The specimens

had a diameter of 0·800 in., a parallel length of 3·625 ins. (the gauge length being 2·35 ins.), and end fillets of radius 3 ins. After manufacture the specimens were given a stress-relief annealing in vacuo.

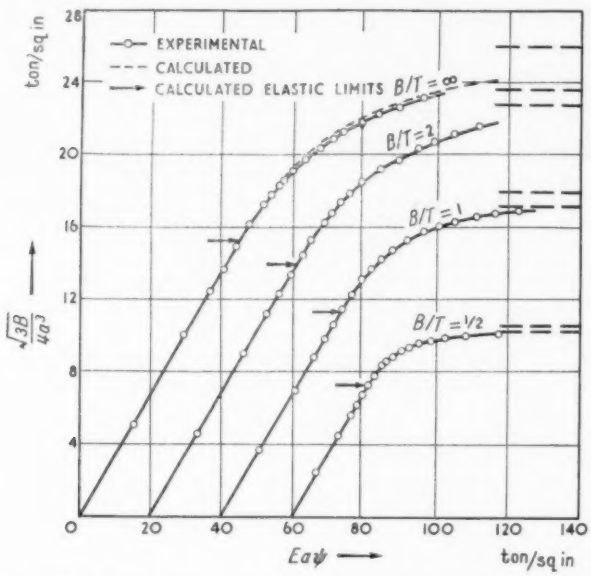

Fig. 1. Relation between bending moment, B, and angle of bend, ψ.

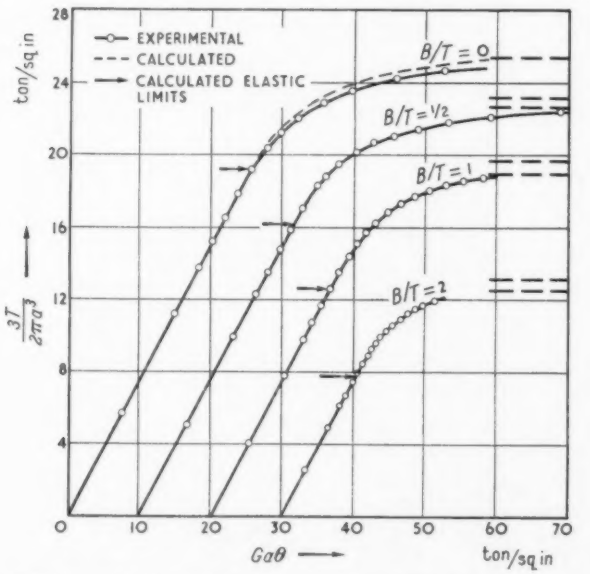

Fig. 2. Relation between torque, T, and angle of twist, θ.

The (B, ψ) and (T, θ) relations are shown in Figs. 1 and 2 for $B/T = 0, \frac{1}{2}, 1, 2, \infty$. Also shown are the theoretical curves for pure torsion and pure bending :

$$T/T_0 = 1 - c^3/a^3, \qquad B = 0,$$

where c is the radius of the plastic-elastic boundary, and

$$B/B_0 = \sin^3\alpha + \tfrac{3}{8}(\tfrac{1}{2}\pi - \alpha + \tfrac{1}{4}\sin 4\alpha), \qquad T = 0,$$

where $a\cos\alpha$ is the distance of the plastic-elastic boundary from the neutral plane. The latter formula is based on the customary engineering approximation which, in effect, disregards elastic compressibility (cf. HILL 1950, p. 82); dimensional changes are also ignored. For $B/T = \frac{1}{2}$, 1, 2 it is only possible to show the theoretical elastic limits, the lower approximation (11) to the yield point, and the upper approximation (10) interpolated from Table 1. The values of k (Table 2) were obtained from compression specimens taken from the same part of the original bar as the gauge lengths of the torsion and bending specimens; the elastic constants are those measured in the actual tests.

TABLE 2

B/T	E (tons/in.^{2})	G (tons/in.^{2})	$E/2G - 1$	k (tons/in.^{2})
0	–	5350	–	25·6
$\frac{1}{2}$	13500	5360	0·26	24·8
1	13400	5330	0·26	25·6
2	13650	5330	0·28	26·0
∞	13500	–	–	26·0

The results show that the plastic-rigid yield points may be used in design calculations. The total distortion is less than about twice that at the elastic limit so long as the actual loads do not approach within, say, 5 per cent of the theoretical yield point values.

Fig. 3 shows the (θ, ψ) relations. From these may be derived the strain ratios $\dot{\psi}/\dot{\theta}$ in the elastic range and also when the bar is virtually completely plastic (Fig. 4). The limiting strain-ratio at large strains should be comparable with that at the yield point of a plastic-rigid body. According to the maximum work principle,

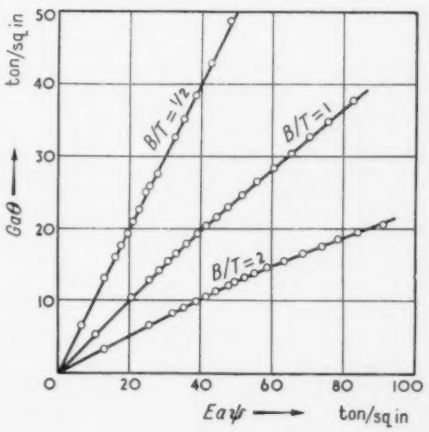

Fig. 3. Relation between angle of twist, θ, and angle of bend, ψ.

$$\dot{\psi}/\dot{\theta} = \frac{\partial f}{\partial B}\Big/\frac{\partial f}{\partial T}$$

where $f(B, T) = 0$ is the relation between the bending and twisting moments at the yield point. If (10) is taken as an approximation to f, the corresponding

strain-ratio turns out to be just λ itself, as given in Table 1. If (11) is taken as an approximation to f, the corresponding strain-ratio is

$$\frac{\dot{\psi}}{\dot{\theta}} = \frac{B}{T} \Big/ \left(\frac{B_0}{T_0}\right)^2 = \frac{\pi^2 B}{12T}. \tag{12}$$

This, incidentally, is the exact value for a thin-walled circular tube (HILL and SIEBEL, op. cit.).

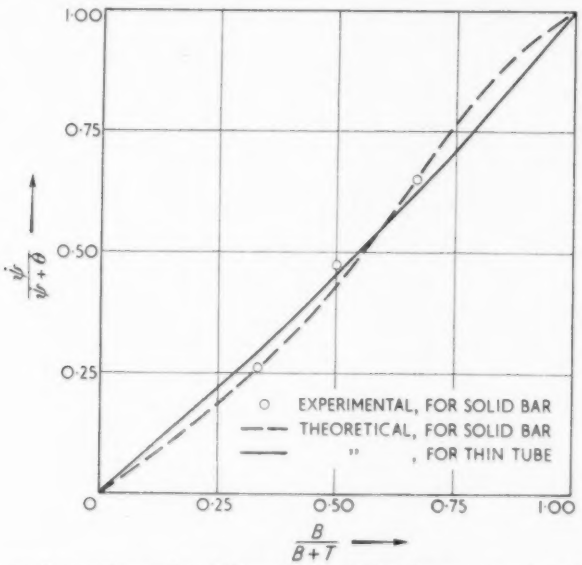

Fig. 4. Comparison of experimental and theoretical relations between strain-ratio and couple-ratio in fully plastic state.

The experimental data in Fig. 4 is too meagre to indicate which approximation is the better. Independent support for (10) is perhaps furnished by the observation that the warping of the solid bars (measured on the surface at a fixed station 60° from the axis of bend) was very small, being less than one tenth of that observed in tubes.

REFERENCES

DRUCKER, D. C., GREENBERG, H. J. and PRAGER, W.	1951	*J. Appl. Mech.*, **18**, 371.
GAYDON, F. A.	1952	*Quart. J. Math. Appl. Mech.*, **5**, 29.
HILL, R.	1950a	*Mathematical Theory of Plasticity* (Clarendon Press)
	1950b	*J. Appl. Mech.*, **17**, 64.
	1951	*Phil. Mag.*, **42**, 868.
HILL, R. and SIEBEL, M. P. L.	1951	*Phil. Mag.*, **42**, 722.
HODGE, P. G., Jr.	1953	*J. Appl. Mech.* (to be published).
ONAT, E. T. and PRAGER, W.	1953	*J. Mech. Phys. Solids*, **2**, 77.
PELL, W. H. and PRAGER, W.	1951	*Proc. 1st U.S. Nat. Congress of Appl. Mech.*
RODERICK, J. W. and PHILLIPPS, I. J.	1949	*Research, Supplement on Engineering Structures*, 9. (Butterworth's Scientific Publications).
SIEBEL, M. P. L.	1953	*J. Mech. Phys. Solids*, **3**, 149.
SHACKELL, K. K. and WELSH, J. H.	1952	*Proc. Inst. Mech. Eng.*, **166**, 112.
THOMAS, D. G. B.	1952	*J. Mech. Phys. Solids*, **2**, 124.

Vol. 1 1952/5

BOOK REVIEWS

H. W. GILLETT: **The Behavior of Engineering Materials.** New York. John Wiley & Sons. (London: Chapman and Hall). 1951. xvi + 395 pp. with 58 illustrations and diagrams. $6.50 or 52s.

THERE is little doubt that this book will be very useful to a great number of people who want to know something about the properties of metals and alloys. It was written by the late H. W. GILLETT of the Battelle Memorial Institute, a metallurgist whose outlook on design seems to be exclusively that of the empiricist, and who has little respect for those who try to relate measurable properties of materials to the predicted behaviour of a machine element which is to be subjected to given loading.

The author's view point, and his object in writing the book, is, however, clearly stated in the Preface and he has been faithful to his object throughout. This is "to present the viewpoint of the metallurgist for those who have not specialised in this field. Since it is intended to help in choosing suitable engineering materials, the behaviour of these materials is discussed rather than the sometimes abstruse theories that seek to explain their behaviour." The references, as far as possible, have been purposely chosen from the more "popular" kind of technical journals.

The first chapter defines and explains briefly some of the metallurgical terms and concepts and deals cursorily with the mechanical test properties. While some sound pointers are given here, the essentially elementary nature of the book should be remembered as otherwise it may lead to misconceptions.

In subsequent chapters, considerations of the requirements to meet manufacturing and service conditions, the use and limitations of acceptance tests and specifications, the effect of notches and surface finish, and the economics of using the statistical approach both in the control of manufacture and modification in service, are all dealt with in a practical and easily readable fashion.

After a chapter on chemical and physical properties including those properties concerned with Atomic Energy, the author gives five chapters on steels, including one on cold-working. This latter chapter is disappointing in view of the many and far-reaching consequences of cold-working, and while it is true that there are many incidental references throughout the book, it is felt that a more systematic treatment would have been an advantage. The more "metallurgical" chapters on heat treated steels and castings are much more detailed and show the writer's wide knowledge and experience.

There are some very useful practical chapters on non-ferrous materials, and the remainder of the book is devoted to special characteristics which may effect the selection of metals and alloys, including such topics as: the effect of hydrogen, machinability, coating and cladding, powder metallurgy, bearing metals, wear and corrosion, and some effects of high and low temperature. Considerations of cost and availability of materials form the subject of the final chapter.

The book contains an enormous amount of interesting miscellaneous information. It is not the sort of book which can be consulted for systematic treatment of any of the particular subjects to be found in its index: but the broad object behind it is so well achieved that it will certainly be found useful in helping the engineer to make a sound choice of materials. The book is written particularly for the American reader, and the references are almost entirely to American publications.

HUGH FORD.

E. E. SECHLER: **Elasticity in Engineering.** John Wiley & Sons, Inc. New York, 1952. + ix. 419 pp. $8.50.

THIS book is designed as an undergraduate text of structural analysis for engineers. The author makes no claim to originality and freely acknowledges his debt to LOVE, TIMOSHENKO, SOUTHWELL *et al.* The text, like Gaul, is divided into three parts: the first part is a presentation of the fundamentals of the theory of elasticity, the second discusses problems in elasticity in stable structures, the third deals with problems in unstable elastic structures.

In the first section, the author's debt to TIMOSHENKO is particularly apparent. The order of presentation is slightly different, the detail is greater at some points, the number of illustrative problems is more complete, but it is reminiscent of TIMOSHENKO's style and method of presenting the fundamentals of his *Theory of Elasticity*.

The second section comprises a chapter on solution of such two-dimensional problems as the

displacement of simply-supported beams, stress states in hollow cylinders, curved beams subjected to pure bending, stress concentrations due to a hole, stress distributions in a semi-infinite body due to a distributed load or a concentrated load, all solved primarily by the aid of AIRY's stress function ; a chapter on simple beam theory, including a liberally instanced presentation of graphical solutions of beam equations, a discussion of the RAYLEIGH-RITZ approximation method and its comparison in various cases with exact solutions, harmonic analysis methods for beams with their flanges ; a chapter on energy methods of solving statically indeterminate truss systems; a chapter giving energy methods of solving torsion problems and lastly a chapter on the stable bending of plates and shells. The choice of these particular problems was determined, the author tells us, by the needs of aeronautical structural engineers, although it must be admitted that the problems are of interest to almost everyone who needs to undertake an undergraduate course in elasticity.

The third section, consisting of three chapters, explains the standard methods of solution by differential equations energy methods, and successive approximation, of the buckling of columns with different end constraints, lateral buckling of thin beams, channels and I-beams, the instability of rods under torsion, and the instability of plates and shells both unstiffened and stiffened under various loads (including shearing).

Although the problems treated are for the most part elementary, the author takes pains to illustrate the methods used in solving general non-linear large-deflection problems involving second-and higher-order terms, and warns the reader against the pitfalls arising from the assumptions involved in elasticity formulae encountered in such problems.

In keeping with the undergraduate character of the book, all references (with one or two exceptions) are directed to secondary sources rather than to original papers. The text is clearly written, well illustrated, supplemented with numerous test problems, and certainly passes muster as a worthwhile undergraduate text.

W. M. BALDWIN.

Vol.
1
1952/5

H. M. WESTERGAARD : **Theory of Elasticity and Plasticity.** Harvard University Press, Cambridge, Massachusetts : John Wiley and Sons, Inc. : New York, 1952. xiii + 176pp. $5.00. AN untimely death overtook Professor WESTGAARD before he could complete this book as he had originally envisaged it. What his overall plan was we can only guess (although his preface hints at the completed plan). In the precious time that he could allow himself he could not create a broad and balanced text but he could and did produce a small, but sturdy book for graduate students: concise, lucid and logical in its development.

Professor WESTERGAARD in his preface writes, " When a colleague asked me at what level the book was to be, the best answer that I could give was that the trail begins at the foot of the mountain." This is a particularly apt description of the book, for although the book attains an advanced level - and rather quickly too - the reader is brought there by a smooth, steady route from a lowly starting point.

The emphasis of the book, as Professor WESTERGAARD tells us, is on elasticity. Indeed it is not too untrue to say that plasticity is treated only in those respects in which it is an extension of the theory of elasticity. There are nearly forty pages devoted to the history of the subject from Galileo to present day trends. The treatment is scholarly, and carried out in considerable detail, although the author's treatment of the more recent history reveals his own bias. Two chapters are devoted to the elements of the theory : stress tensor, strain tensor, compatibility equations, Hooke's Law. The conciseness of the book is epitomized in the author's treatment of the compatibility equations. They are directly introduced and their derivation is thereafter explained in three perspicuous sentences. The strain potential is described and several of Lamé's solutions are presented and interpreted : formulas for stresses in hollow cylinders, examples of stress concentration, stresses in rotating discs. Some fifty pages are devoted to the use of biharmonic functions and Galerkin's vector in the solution of problems. Detailed applications of the method to Kelvin's, Cerruti's, Boussinesq's and Mindlin's problems are given for various values of Poisson's ratio.

The book, because it is unfinished, may never be read as widely as the great classics of elasticity, but it is classic : it is simple, elegant, and masterful.

W. M. BALDWIN.

Journal of the Mechanics and Physics of Solids, 1953, Vol. 1, pp. 217 to 226. Pergamon Press Ltd., London.

LIMIT ANALYSIS OF TWO AND THREE DIMENSIONAL SOIL MECHANICS PROBLEMS*

By D. C. Drucker
Division of Engineering, Brown University

(*Received 27th September*, 1952)

Summary

Previous work on the implications of assuming soil to be a perfectly plastic body is extended. A brief discussion is given of suitable general forms of the yield or sliding criterion for soils. Coulomb's equation is interpreted in terms of a modified Tresca as well as a modified Mises rule. Particular attention is given to a soil unable to take tension but which exhibits both cohesion and internal friction in sliding action. Indication is given of an interesting development of complete solutions.

The stability of unbraced vertical-walled cuts is then treated. A brief description of the application of the general limit theorems to inhomogeneous soil is also included to demonstrate their power.

1. The Yield Criterion

Coulomb's rule relating the normal and the shearing stress in two-dimensional (plane strain) problems is represented in Fig. 1. The radius R of Mohr's circle at the instant of slip is assumed to depend linearly upon the mean normal stress in the plane :

$$R = c \cos \phi - \frac{\sigma_x + \sigma_y}{2} \sin \phi \tag{1}$$

where c is the cohesion and ϕ is the angle between the tangent to the Mohr's circles at slip and the negative σ axis.

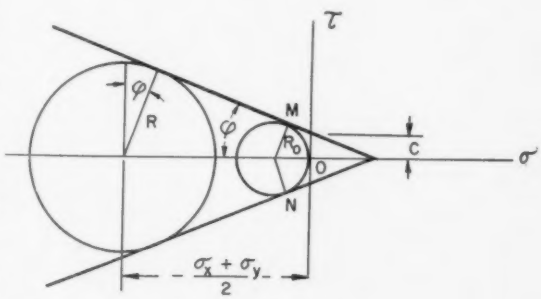

Fig. 1. Coulomb rule.

As shown previously (Drucker and Prager 1952), the modified Mises yield function

$$f \equiv \alpha J_1 + J_2^{1/2} = k \tag{2}$$

is a proper generalization of the Coulomb rule to three dimensions if

$$3\alpha^2 = \frac{\sin^2 \phi}{3 + \sin^2 \phi} \qquad \text{and} \qquad k^2 = \frac{3c^2 \cos^2 \phi}{3 + \sin^2 \phi}. \tag{3}$$

* The results presented in this paper were obtained in the course of research sponsored by the Office of Naval Research under Contract N7onr-35801 with Brown University.

J_1 is the sum of the principal stresses and J_2 is the second invariant of the stress deviation,

$$\frac{1}{6}\left[(\sigma_x - \sigma_y)^2 + (\sigma_y - \sigma_z)^2 + (\sigma_z - \sigma_x)^2\right] + \tau_{xy}^2 + \tau_{yz}^2 + \tau_{xz}^2.$$

The yield surface in principal stress space is a right circular cone equally inclined to the principal axes as shown in Fig. 2. Also shown are parts of the intersections with the three coordinate planes. The assumption that the soil cannot take tension cuts off all parts of the cone for which any principal stress is positive and leaves the convex body *OELA*. These tension cut-offs appear in the plane strain case of Fig. 1 as the circular arc *MON* of radius $R_0 = c \tan(\frac{1}{4}\pi + \frac{1}{2}\phi)$. Fig. 3a shows a section through the σ_3 axis and the axis of the cone; Fig. 3b is the elliptical plane stress intersection on which the tension cut-offs are indicated by heavy lines.

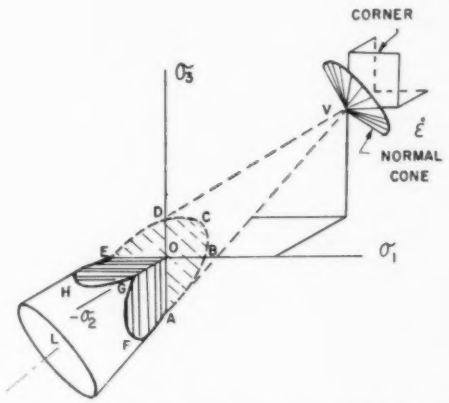

Fig. 2. Modified MISES criterion. *ABCDE* is the plane stress intersection. *OGFA* and *OEHG* are tension cut-off planes. Plastic strain-increment (rate) vectors lie on or inside normal cone.

A modified TRESCA criterion is probably more in the spirit of the Coulomb postulate for soils than is the modified MISES. The yield surface in principal stress space is a right regular hexagonal pyramid instead of a cone (Fig. 4). Plane

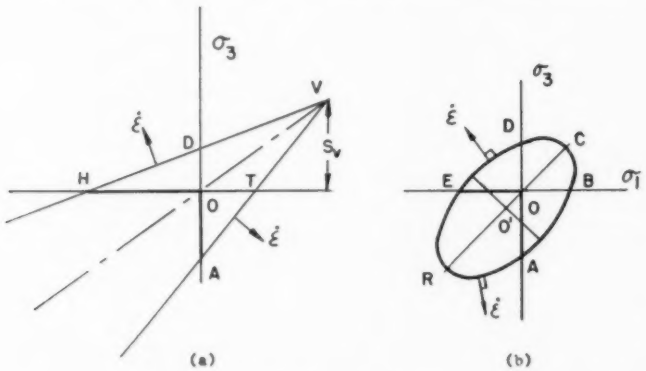

Fig. 3. Sections of the cone.

$$OA = OE = c\cos\phi\left[(3 + \sin^2\phi)^{\frac{1}{2}} + \sin\phi\right]$$
$$OB = OD = c\cos\phi\left[(3 + \sin^2\phi)^{\frac{1}{2}} - \sin\phi\right]$$
$$OC = OT = \sqrt{2}\,c\left[(3 + \sin^2\phi)^{\frac{1}{2}} - 2\sin\phi\right]/\cos\phi$$
$$OR = OH = \sqrt{2}\,c\left[(3 + \sin^2\phi)^{\frac{1}{2}} + 2\sin\phi\right]/\cos\phi$$
$$OO' = 2\sqrt{2}\,c\tan\phi$$

Vol. 1 1952/

strain conditions (Fig. 1) will be met if the dimensions are as given for the section through the axis of the pyramid and the σ_3 axis (Fig. 5a) and for the plane stress intersection (Fig. 5b). Tension cut-offs are indicated in these Figures also.

There is, of course, no limit to the number of yield surfaces or functions which may be devised. In particular, many convex surfaces of revolution, $f(J_1, J_2) =$ constant or modifications of them, may be found useful to correlate actual test data more closely. So few problems of soil mechanics have been solved completely, however, that it does not seem worthwhile at this time to consider more elaborate yield functions for exact or approximate solutions. It is likely that simple anisotropic forms will be found desirable after a few solutions have been obtained with isotropic yield functions.

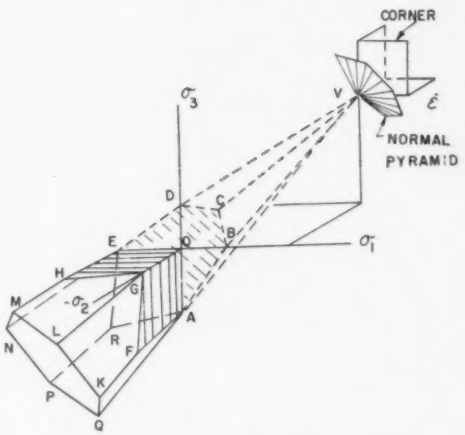

Fig. 4. Modified TRESCA criterion.

2. PLASTIC STRAIN-INCREMENT VECTORS

As is customary in many branches of soil mechanics (TERZAGHI 1943), the concept of ideal or perfect plasticity is here arbitrarily assumed valid. The plastic

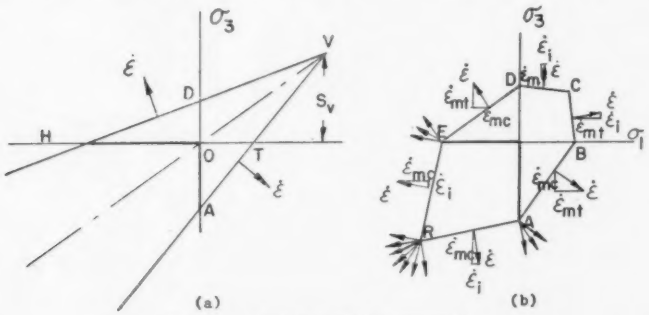

Fig. 5. Sections of the pyramid.

$$OA = OE = \frac{6c\cos\phi}{3-\sin\phi} \qquad OB = OD = \frac{2c\cos\phi}{1+\sin\phi}$$

$$OC = OT = \frac{6\sqrt{2}\,c\cos\phi}{3+5\sin\phi} \qquad OR = OH = \frac{2\sqrt{2}\,c\cos\phi}{1-\sin\phi}$$

The three principal strain rates for the faces of the pyramid are $\dot{\epsilon}_{mt} : \dot{\epsilon}_i : \dot{\epsilon}_{mc} = 3(1+\sin\phi) : 2\sin\phi : -(3\sin\phi)$.

strain increment is therefore represented by a vector normal to the yield surface at a smooth point on the surface or by a vector which lies within the directions of the normals to adjacent points at a corner or pointed vertex (see, for example,

DRUCKER 1950). Some of the plastic strain increment, or strain rate, vectors $\dot{\epsilon}$ are shown in Figs. 2-5. The projections of $\dot{\epsilon}$ appearing in Figs. 3b and 5b are likewise normal to the plane stress intersections at a smooth point or lie in a fan bounded by normals to adjacent points at a vertex. In all cases plastic shearing action must be accompanied by an increase in volume if the soil obeys the laws of plasticity.

The plastic strain increment vectors along any generator are necessarily parallel except at corners or vertices of the surfaces. Any one section such as Fig. 3b for the cone and Fig. 5b for the pyramid therefore gives complete information when the third component of plastic strain is known. The three components are always in the ratios

$$3(1 + \sin\phi) \quad : \quad 2\sin\phi \quad : \quad -(3 - \sin\phi) \tag{4}$$

for the faces of the pyramid. A linear combination of the possible components for the intersecting faces gives the possible components for the edges of the pyramid. If the state of stress, or stress point, lies on a tension cut-off plane, the strain increment vector is normal to the plane. Strain-increment vectors for the stress points on the boundaries of the tension cut-off planes are linear combinations of the normal vectors to the cut-off plane and to the lateral surface of the pyramid or the cone. This means that the direction of the projection of the strain-increment vector on the cut-off plane must remain constant as the perpendicular tensile strain increment is increased relative to the two components in the plane. The cut-off arc MO of Fig. 1 corresponds to one point on the boundary of a cut-off plane.

There is thus no difficulty in determining which stress points correspond to a given plastic strain increment vector or conversely which increments are permissible at a given stress point.

3. LIMIT THEOREMS

The two main limit theorems for any body or assemblage of bodies of elastic – perfectly plastic material are (DRUCKER GREENBERG and PRAGER 1952) :

(i) Collapse will not occur if any state of stress can be found which satisfies equilibrium and the boundary conditions on stress and for which all stress points lie inside the yield surface (or are points on the surface at which the rate of dissipation of energy is zero).

(ii) Collapse must occur if for any flow pattern, considered as plastic only, the rate at which the external forces do work on the bodies equals or exceeds the rate of internal dissipation.

Discontinuous states of stress satisfying the required conditions, and discontinuous velocity patterns, are permissible and are especially useful in soil mechanics problems.

4. THE DISSIPATION FUNCTION

As stated in the limit theorems, it is necessary to compare external work and internal dissipation. The dissipation function D, or the rate of dissipation of energy per unit volume, is therefore of primary importance.

Vol.
1
1952/5

The expression for D is especially simple in the case of the complete cone or pyramid :

$$D = c \cot \phi \,.\, (\dot{\epsilon}_1 + \dot{\epsilon}_2 + \dot{\epsilon}_3) \tag{5}$$

since $c \cot \phi$ is the 1, 2, and 3 coordinate of the vertex.

In the case of the cone,

$$\dot{\epsilon}_1 + \dot{\epsilon}_2 + \dot{\epsilon}_3 \geq \frac{\sqrt{2} \sin \phi}{(1 + \sin^2 \phi)^{1/2}} (\dot{\epsilon}_1^{\,2} + \dot{\epsilon}_2^{\,2} + \dot{\epsilon}_3^{\,2})^{1/2} \tag{6}$$

where the inequality applies at the vertex only. No such simple relation exists between the length of all strain-rate vectors and their projections on the axis for the edge rays of the pyramid.

However, the modified TRESCA criterion is as easy or easier to use than the cone. The basic difficulty with the cone is illustrated by the plane stress ellipse (Fig. 3b). Unlike the usual MISES ellipse which is centred about the origin of coordinates and which may be expressed in the form of a homogeneous function of stress set equal to a constant, the ellipse of Fig. 3b does not lead to a simple expression for D in terms of components of strain rate in the plane. Referring to the hexagon of Fig. 5b and designating a neighbouring point to A on the line AB as A^+ and a neighbouring point to C on the line BC as C^-, etc., a convenient form of the dissipation function for the portion

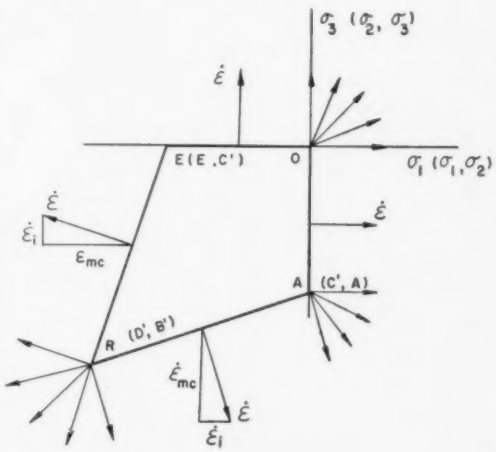

Fig. 6. Tension cut-off.

$$A^+BC^- \text{ is } \frac{2c \cos \phi}{1 + \sin \phi} \dot{\epsilon}_1, \quad \text{for } C^+DE^- \text{ is } \frac{2c \cos \phi}{1 + \sin \phi} \epsilon_3,$$

$$\text{for } D^+ER^- \text{ is } \frac{6c \cos \phi}{3 - \sin \phi} |\dot{\epsilon}_1|, \quad \text{for } R^+AB^- \text{ is } \frac{6c \cos \phi}{3 - \sin \phi} |\dot{\epsilon}_3|,$$

and for point

$$C \text{ is } \frac{6c \cos \phi}{3 + 5 \sin \phi} (\dot{\epsilon}_1 + \dot{\epsilon}_3), \text{ and for } R \text{ is } \frac{2c \cos \phi}{1 - \sin \phi} (-\dot{\epsilon}_1 - \dot{\epsilon}_3). \tag{7}$$

It is of interest to note that the dissipation function may be written as

$$D = \frac{2c \cos \phi}{1 + \sin \phi} \cdot \dot{\epsilon}_{mt} \quad = \frac{6c \cos \phi}{3 - \sin \phi} \cdot \dot{\epsilon}_{mc} \quad = c\dot{\gamma}_m \cos \phi \tag{8}$$

for the faces of the complete pyramid, where $\dot{\epsilon}_{mt}$ is the maximum tensile plastic strain-rate, $\dot{\epsilon}_{mc}$ is the magnitude of the maximum compressive plastic strain-rate,

and $\dot{\gamma}_m = \dot{\epsilon}_{mt} + \dot{\epsilon}_{mc}$ is the maximum plastic shear-rate. Edges VB, VD, and VR of the pyramid follow the first form of (8) while edges VA, VC, VE follow the second. All reduce to $2c|\dot{\epsilon}_m|$ when $\phi = 0$.

For a material unable to take tension, the portion $OERAO$ (Fig. 6) gives complete information when considered in turn as being in the σ_1, σ_3 plane, in the σ_1, σ_2 plane, and in the σ_2, σ_3 plane. As an explanation of the notation of Fig. 6, point E in the σ_1, σ_3 plane remains E in the σ_1, σ_2 plane and becomes C' in the σ_2, σ_3 plane. C' is the intersection of VC with the σ_2, σ_3 plane. Actually there is no need to consider anything but the σ_1, σ_3 plane unless some extraneous ordering system is employed for the principal stresses.

In all cases, with or without the tension cut-off planes, the yield surface is convex with respect to every interior point (the meaning of interior is clear despite the open-ended shape). Therefore the dissipation function D is uniquely determined by the components of $\dot{\epsilon}$. Equation (5) is simplest if the strain rate vector is normal to the lateral surface, or if the stress point is at the vertex of the cone or pyramid.

It is important to keep in mind that the choice of a flow pattern for application of the theorem (ii) is arbitrary except that for the cone inequality (6) must be satisfied, and for the pyramid there are equivalent conditions, as given pictorially at V in Figs. 2 and 4. Permissible strain rate directions clearly must lie on or inside the normal cone or pyramid. If the material can not take tension, $D = 0$ on or inside the corner which is shown inside the normal cone and the normal pyramid. Vectors lying on this corner correspond to stress points on the cut-off planes; vectors inside correspond to a stress point at the origin; while vectors between the normal cone or pyramid and the corner correspond to stress points on the boundary of the cut-off planes. Although the three-dimensional picture is helpful in visualizing the strain rate vectors, the two-dimensional Fig. 6 is much more convenient when there are cut-off planes. As there is then no upper limit to the tensile strain rate $\dot{\epsilon}_2$ for points on the boundary $OERAO$ in the (σ_1, σ_3) plane, and as σ_2 does no work, the in-the-plane expressions (7) should be used for the pyramid.

The determination of which stress point or points correspond to a given strain rate vector is straightforward for the pyramid. If the largest compressive strain rate, assuming there is one, is taken as $\dot{\epsilon}_3$ and the maximum tensile strain rate is denoted by $\dot{\epsilon}_1$, the strain rate vector is a permissible one for the faces of the pyramid if

$$\left|\frac{\dot{\epsilon}_1}{\dot{\epsilon}_3}\right| \geqslant \frac{3\,(1 + \sin\phi)}{3 - \sin\phi}. \tag{9}$$

The greater than sign requires the stress point to be on RA.

The stress point is then on R^+A^- if $\dot{\epsilon}_2/\dot{\epsilon}_3$, which by definition cannot exceed unity, equals $-2\sin\phi/(3\text{-}\sin\phi)$. The stress point is at R if the ratio is algebraically greater, and at A if the ratio is algebraically less, than this fraction. D is given by the expressions (7) for R^+AB^- and R.

If there is no compressive strain-rate the stress point is on the tension cut-off planes, or their boundaries, and $D = 0$.

Vol. 1 1952/5

5. Plane Strain

The various possible plastic strain rate vectors for plane strain are shown in projection in Fig. 7a for the lateral surface of the complete pyramid and 7b for the case of no tension. Again, if no extraneous 1, 2, 3 ordering is employed, there is really just one independent vector in Fig. 7a, but there is some advantage in looking at all the projections.

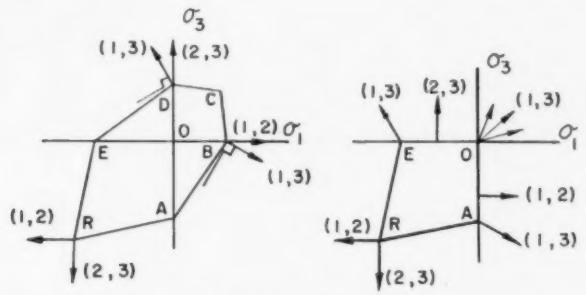

Fig 7. Plane strain vectors. (1, 2) indicates that the strain increment vector lies in the 1, 2 plane, etc.

By considering the vector at B which lies in the 1, 3 plane and which must be a linear combination of the vectors for points on each side of B, it follows that

$$\dot{\epsilon}_2 = 0 = a\,[2 \sin \phi] + b\,[-(3 - \sin \phi)]$$

where a and b are constants. Linear combination also gives

$$\dot{\epsilon}_1 = a\,[3\,(1 + \sin \phi)] + b\,[3\,(1 + \sin \phi)] \text{ and } \dot{\epsilon}_3 = a\,[-3\,(1 - \sin \phi)] + b\,[2 \sin \phi].$$

Therefore, for plane strain, the ratio of the maximum tensile strain rate to the maximum compressive rate is given by

$$-\frac{\dot{\epsilon}_1}{\dot{\epsilon}_3} = \frac{1 + \sin \phi}{1 - \sin \phi} = \tan^2 (\tfrac{1}{4}\pi + \tfrac{1}{2}\phi). \tag{10}$$

The corresponding expression holds at point R for the complete pyramid. If *OEARO* is a cut-off plane, however, the equality sign is replaced by a greater than or equal sign.

The dissipation function is given by (7) or (8) for continuous velocity fields and may be applied to a discontinuous velocity field by considering each discontinuity as the limit of a continuous variation through a small transition layer when the thickness of the layer goes to zero (Drucker and Prager 1952).

6. Stability of Vertical Cuts under their own Weight

The assumption of the inability of soil to take tension suggests the introduction of tension cracks in the flow pattern. If the velocity of the soil on one side of the crack relative to the other is perpendicular to the crack, no energy is dissipated on the surface of discontinuity, $D = 0$. In general, calling the tangential change in velocity $\delta \dot{u}$, if the relative velocity is at an angle θ to the crack, $\theta \geqq \phi$,

$$D_A = c\,\delta\dot{u}.\,\frac{\tan(\frac{1}{4}\pi + \frac{1}{2}\phi)}{\tan(\frac{1}{4}\pi + \frac{1}{2}\theta)} \tag{11}$$

where D_A is the rate of dissipation per unit area of the surface of discontinuity (DRUCKER and PRAGER, *op. cit.*).

Fig. 8 depicts a two-dimensional flow pattern containing a simple tension crack and a constant state flow field. A region Δ in width and almost H in height is shown rotating about P with an angular velocity ω. Boundary conditions for the region PTL of constant state are that PL is at rest and the velocity along PT is normal to PT and varies linearly with the distance from P. The velocity vector at each point in the region is at an angle ϕ to PL and its magnitude is linear with the distance of the point from PL. This action may be thought of physically as shearing parallel to PL plus an expansion perpendicular to it. The shear rate $\dot{\gamma}$ for axes parallel and perpendicular to PL is constant and equal to ω, so that $D = c\omega$. An alternative method of arriving at this result is to observe that, for these axes, the normal strain rate is zero along PL and is $\omega \tan\phi$ perpendicular to PL. Equation (5) then gives $D = c \cot\phi \times \omega \tan\phi = c\omega$. The total rate of dissipation of internal energy for unit dimension perpendicular to the plan of flow is just D times the area of the triangle PTL or $D\Delta^2 \tan(\frac{1}{4}\pi + \frac{1}{2}\phi)$. The rate at which work is done by the gravitational force when Δ is very small is closely $\frac{1}{2}\omega\, w H \Delta^2$, where w is the unit weight of the soil. Letting Δ approach zero and equating internal and external work leads to an upper bound for the critical height of a vertical bank :

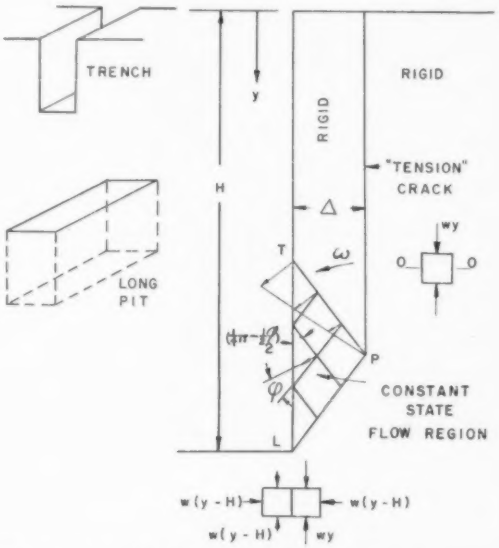

Fig. 8. Critical height for soil unable to take tension.

$$H_c \leq \frac{2c}{w} \tan(\tfrac{1}{4}\pi + \tfrac{1}{2}\phi). \tag{12}$$

The coefficient 2 is an improvement over the admittedly crude value of 2·5 given previously by DRUCKER and PRAGER, and in fact when coupled with the lower bound result shows that the right hand side of (12) is H_c. The lower bound is obtained simply by observing that the elementary discontinuous stress distribution shown in Fig. 8, which is not the true state of stress, is in equilibrium and satisfies the boundary conditions on stress. Referring to Fig. 1, if wH is less than $2R_0$ the stress points are all inside the yield surface or at the origin. Therefore from theorem (i)

$$H_c \geqq \frac{2R_0}{w} = \frac{2c}{w} \tan\left(\tfrac{1}{4}\pi + \tfrac{1}{2}\phi\right). \tag{13}$$

It is of interest to note also that many "complete solutions" (HILL 1950; LEE 1952), taking into account both velocity and stress fields, can be devised which include tension cracks. This topic certainly seems worthwhile pursuing along with application of the limit theorems in order to obtain a better understanding of the implications of plasticity for soil mechanics.

7. INHOMOGENEOUS MEDIA

Inhomogeneous media are very often encountered in practical applications. The limit theorems are apt in fact to be of greatest use in such cases because of the enormous difficulty in obtaining exact solutions. A simple plane strain example, with specially chosen angles to eliminate all calculation, is shown in Fig. 9. To avoid obscuring the basic points, the friction angle ϕ is taken as zero, and the weight of the soil is considered negligible.

The problem is to find the maximum uniform surcharge p_m which can be carried for various ratios of the cohesion c_2 of the weak soil to the cohesion c_1 of the stronger soil which lies under the load.

Using theorem (ii), the unsophisticated flow pattern* in the weak soil (Fig. 9c) gives

$$p_m \leqq 2c_1 + (2 + \tfrac{1}{2}\pi)\, c_2. \tag{14}$$

If the weak soil has no strength, $c_2 = 0$, Fig. 9a and (14) give the obvious answer $p_m = 2c_1$. Suppose next that $c_2 = c_1/2$. The discontinuous stress pattern of Fig. 9b coupled with the flow pattern for half a homogeneous wedge, Fig. 9d, give

$$3c_1 \leqq p_m \leqq (2 + \tfrac{1}{3}\pi)\, c_1.$$

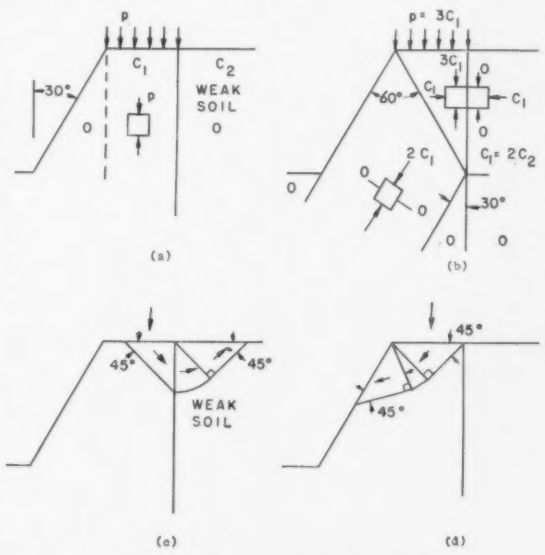

Fig. 9. Inhomogeneous soil $\phi = 0$.
(a) is always an equilibrium solution; (b) is valid for $c_1 = 2c_2$; (c) and (d) are velocity fields composed of a fan and two regions of constant state. *O* indicates zero stress.

Equation (14) leads to a still higher value for the upper bound. Any further increase in the value of c_2 will be of no real help as the bounds are already very close. All bounds apply equally well to materials which cannot take tension.

* More elaborate types of flow and stress patterns are discussed in R. T. SHIELD and D. C. DRUCKER, "The Application of Limit Analysis to Punch Indentation Problems," Brown University Report A11-75 to the Office of Naval Research.

8. CONCLUSION

The application of the limit theorems to soil mechanics, and the consequences of assuming soil unable to take tension, should prove both interesting and useful. It should not be forgotten, however, that answers obtained are correct for the material postulated but may have no relevance to any actual material. Of greatest significance in this connection is that the theory of perfect plasticity requires a volume increase under shearing action if hydrostatic pressure increases the shearing strength.

REFERENCES

DRUCKER, D. C.	1950	*Qu. Appl. Math.*, **7**, 411.
DRUCKER, D. C. and PRAGER, W.	1952	*Qu. Appl. Math.*, **10**, 157.
DRUCKER, D. C., GREENBERG, H. J. and PRAGER, W.	1952	*Qu. Appl. Math.*, **9**, 381.
HILL, R.	1950	*Mathematical Theory of Plasticity* (Clarendon Press, Oxford).
LEE, E. H.	1952	*J. Appl. Mech.*, **19**, A97.
TERZAGHI, K.	1943	*Theoretical Soil Mechanics* (Wiley & Sons).

Vol.
1
1952/

Journal of the Mechanics and Physics of Solids, 1953, Vol. 1, pp. 227 to 233. Pergamon Press Ltd., London.

THE BRITTLE FRACTURE OF METALS

By E. O. Hall
Engineering Laboratory, University of Cambridge*

(*Received 10th March*, 1953)

Summary

A study has been made of the theory of the brittle fracture of metals, where plastic deformation arises during the cleavage process. By the use of X-rays, the magnitude of this plastic work has been investigated on single crystal and polycrystal cleavage surfaces. A theoretical study has also been made of the depth of the plastic zone in single crystals with varying crack velocity.

ol.
1
2/53

1. Introduction

The usual definition of a brittle fracture is one in which little or no plastic deformation precedes fracture. This concept has caused some confusion, and in certain theoretical investigations has led to too close an identification of fracture in ceramics and glasses with fracture in metals. In glasses and ceramics no deformation accompanies fracture; the pieces may be re-joined and fit perfectly. With metals this can never be done, even when material outside the zone of fracture is clearly undeformed. This indicates that plastic deformation in metals is an integral part of fracture, and seriously modifies the theory of fracture derived from ceramics and glasses.

2. The Initiation of Fracture

In Griffith's (1920) theory of brittle fracture, the material is considered to contain numerous internal cracks or flaws which approximate to plane ellipses. For a surface crack of length c, or an internal crack of length $2c$, the strain energy of the plate is decreased by an amount $\pi \sigma^2 c^2/E$ where σ is the applied stress and E is Young's modulus. Griffith supposed that the crack length would increase catastrophically when this energy was numerically greater than that required to create new surface. The surface energy for the crack is $4cT$, where T is the surface tension of the metal; thus, the crack can increase when

$$\frac{\partial}{\partial c}\left(-\frac{\pi\sigma^2 c^2}{E} + 4cT\right) \leqslant 0;$$

i.e., when

$$\sigma \geqslant \sqrt{\frac{2ET}{\pi c}}. \qquad (1)$$

*Present address: Physics Department, University of Sheffield.

This result has been examined in detail by SACK (1946) and ELLIOTT (1947), who both showed that, for slightly different shapes of crack, the only alteration to the formula (1) is in the numerical factor $2/\pi$. The GRIFFITH formula is thus true to an order of magnitude.

This formula does not take into account any plastic work during the growth of the crack. OROWAN (1947) and KLIER (1950) showed by the use of X-rays that the surface of a brittle fracture suffers a high degree of plastic deformation. This seriously alters the GRIFFITH formula, for it adds a term to the surface energy T. If plastic deformation occurs with the spreading of the crack, then the work needed to increase the crack length by dc is no longer $4T\,dc$, but

$$4\,(T + w)\,dc$$

where w is the plastic work done in the process. Thus, the fracture stress is

$$\sigma = \sqrt{\frac{2E\,(T + w)}{\pi c}}. \qquad (2)$$

OROWAN (1950) has made an estimate of w. From an examination of a polycrystalline fracture surface, he estimated that a layer, strained to an average of 2 per cent, existed to a depth of $\frac{1}{2}$ mm below the fracture surface. Assuming that this arose under a stress of about 2×10^9 dynes/cm^2, $w = 2 \times 10^{-2} \times 5 \times 10^{-2} \times 2 \times 10^9$ ergs/cm^2. $= 2 \times 10^6$ ergs/cm^2. This is about 2,000 times larger than the surface energy T, which may therefore be neglected in comparison with w. The value of w however, can vary greatly : a discussion of this follows later. OROWAN's analysis raises the critical crack length for a free internal crack by a factor of 2,000 from a few microns to several millimetres. Usually there are other stress-raisers present, such as precipitates and grain boundaries, which act to reduce the critical length. This estimate of several millimetres is therefore probably too large.

Vol. 1 1952/5

3. THE PROPAGATION OF A BRITTLE CRACK

There have been a few attempts to estimate the velocity at which a GRIFFITH crack spreads once the critical length has been exceeded. Some (PONCELET 1946, HOLLOMON 1948, SAIBEL 1948), based on rate-process theories, are almost certainly incorrect, because fracture takes place at sonic velocities. This means that the vibrational energy of the atoms is not equally divided amongst their degrees of freedom : the system is not in equilibrium, and thus it is improbable that thermodynamic reasoning will give a satisfactory answer.

The only reasonable estimate of the crack velocities is by MOTT (1948). MOTT added a term to the GRIFFITH ' potential energy ' term to allow for the kinetic energy of the moving plate material, where the stress has been relaxed by the passage of the crack. In this way he calculated the velocity of a GRIFFITH crack as

$$V = \left[\frac{E}{\rho}\cdot\frac{4\pi}{k} - \frac{8E^2\,T}{ck\sigma^2\,\rho}\right]^{\frac{1}{2}}$$

where ρ is the density of the plate, and k is a dimensionless constant.

The plastic work factor w may be introduced rigorously into MOTT's argument, and leads to the following expression for the crack velocity :

$$V = \left[\frac{E}{\rho}\frac{4\pi}{k} - \frac{8E^2(T+w)}{ck\sigma^2\rho}\right]^{\frac{1}{2}}. \tag{3}$$

It follows from this that a crack, once longer than the critical length, can only come to a stop by a sudden increase in w; that is, by the expenditure of a considerable amount of energy in plastic deformation. TIPPER and SULLIVAN (1950) have shown examples of this.

A more striking example of this phenomenon in polycrystalline material has been given by TIPPER (1951). Here a composite plate in three parts was welded together and tested at about $-3°C$. The centre plate was internally notched, and was notch-brittle at this temperature. The two parts on either side were notch-ductile. Under stress, the centre plate failed in a brittle manner from the notch with no obvious plastic deformation, but as soon as the crack ran into the notch-ductile plates on either side it became a ductile crack and stopped, with a considerable amount of plastic deformation. The heat generated from the distortion was sufficient to melt the frost on the surface in a wide ring around the end of the crack.

When V approaches the velocity of sound, MOTT's analysis based on static elasticity theory breaks down and a full analysis must be made in terms of elastic waves. YOFFE (1951) has shown that in an isotropic solid at high crack velocities ($V \simeq \frac{1}{2} \times$ velocity of elastic shear waves), a type of shock wave builds up around the tip of the crack, and it is found that very nearly equal stresses exist over a wide arc in front of the advancing crack. The result is that the crack branches. This type of phenomenon has been demonstrated experimentally by OROWAN (1950) in cellophane, and is seen in the studies by PONCELET (1948a) on glass. By examining cellophane under polarized light, OROWAN was able to show that while the plastic work factor w was high, the crack is very like a ductile crack in its behaviour and spreads only slowly. As soon as catastrophic failure occurs, V rapidly increases, the crack branches, and under polarized light the edges of the crack are seen to be almost free of plastic deformation. *This result does not, however, explain why w falls rapidly as soon as the crack accelerates*: a discussion of this follows in the next section.

4. The Magnitude of the Plastic Work Factor

In the two previous sections the magnitude of the plastic work factor w has been assumed constant. Actually, it may vary considerably, and an analysis of the factors that influence it will now be made.

The occurrence of plastic deformation on the cleavage surface of a specimen can be estimated by standard back reflection X-ray techniques, but care must then be taken to exclude the plastic deformation which precedes fracture. In this instance, it is difficult to know how much weight should be attached to the X-ray photographs by KLIER (1950), who, by using notched specimens, had concentrated any deformation before fracture into the very zone he wished to study.

OROWAN's estimate of w (Section 2) was for a polycrystalline specimen. Microscopic studies of such fracture surfaces by TIPPER (1948) revealed that many grains have failed in a ductile manner in a predominantly brittle fracture, and

it was thought that OROWAN's published pictures might give an unduly high value for w for this reason. As a preliminary, a comparison was made between X-ray pictures of fractures surface from polycrystal and single crystal specimens.

A marked difference was immediately found. Fig. 1 (a) is a back-reflection Laue pattern from a polycrystalline specimen of carbonyl iron, with a grain size of about 1 mm diameter, broken in liquid air. Severe distortion is evident. A microsection taken across this surface shows that several of the grains have indeed been severely distorted (Fig. 1 (b)), and it must be these that contribute to the distortion in the X-ray picture. Fig. 1 (c) on the other hand is taken from a large crystal of silicon iron, broken in tension at room temperature. No deformation occurred before fracture. In this case, the distortion is much less. Consequently, while OROWAN's estimate is true for the material he used, it is several times too large for single crystals.

It is to be expected that the magnitude of w will depend on the velocity of the crack front. For, even with no delayed yield in the specimen, the faster the motion of the stress field around the tip of the crack, the less time there is for plastic deformation to spread (as plastic waves) into the bulk of the material on either side of the crack before the stress concentration has passed. If a delayed yield is present, this results holds *a fortiori*.

Such a result is needed to explain the observations of OROWAN on the fracture of cellophane. The spread of a crack should accelerate as soon as the instability condition is reached, i.e. as soon as the length of the crack given by equation (2) is exceeded, whether or not w diminishes on passing this point. Thus, an additional relation is needed between w and V which, when incorporated into an equation such as (3), will give a complete solution to the propagation of a brittle crack.

Analogous results appear to hold for silicon iron. Fig. 1 (c) is typical of X-ray patterns from single crystals broken by static loading, and by further examination, again by X-rays, the plastically deformed zone was shown to extend about $\frac{1}{2}$ mm into the specimen on each side of the crack. On the other hand, a specimen of the same material, which was broken under dynamic conditions by making a punch mark in the surface, showed no deformation at all by X-ray examination (Fig. 1 (e)). Since it can be shown that the X-ray beam can only penetrate some 8μ into the metal, an exceedingly thin deformed layer, say 100 Å or less, could be present on the surface and escape detection. An electron diffraction investigation was therefore kindly carried out by Dr. J. W. MENTER, which showed that a deformed layer was in fact present, but was only some 20 Å thick.

There were interesting differences in microstructure between these two cases. In the first case, a dense collection of Neumann lamellae had formed across the path of the crack. In the second case, there were none. In the first case, then, it seems reasonable to suppose that the differing orientations of the lamellae hold up the propagation of the crack : its velocity is therefore kept low. In the second case, there is nothing except occasional precipitate particles to hold up the crack, and so its velocity may approach the speed of sound. In this case, the chevron pattern is regular (Fig. 1 (f)) while in the former, it is exceedingly complex (Fig. 1 (d)).

It is possible, by a simple model, to estimate the magnitude of w and study its variation with the crack velocity V. Consider a point P in an infinite solid at a distance r from the path of the crack (Fig. 2 (a)), which is moving with a velocity

Vol. 1 1952/5

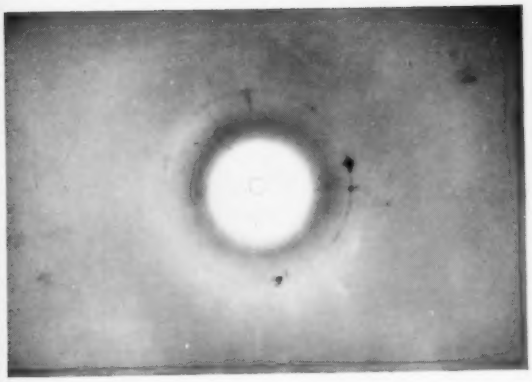

Fig. 1 (a)

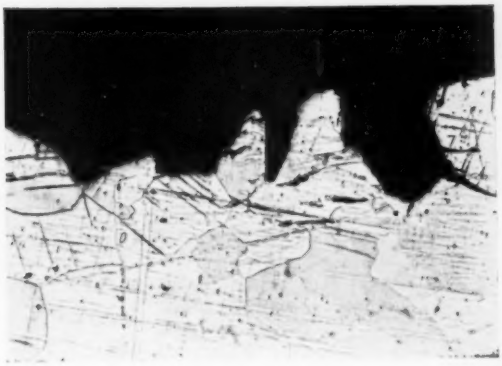

Fig. 1 (b)

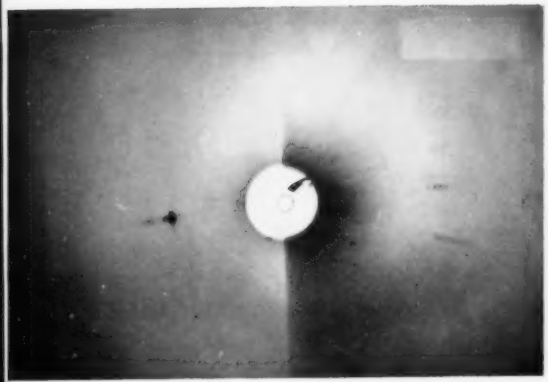

Fig. 1 (c)

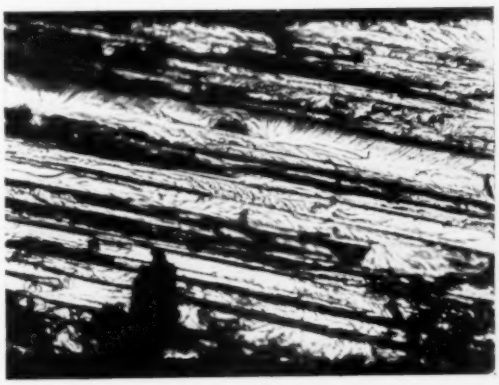

Fig. 1 (d)

Fig. 1 (e)

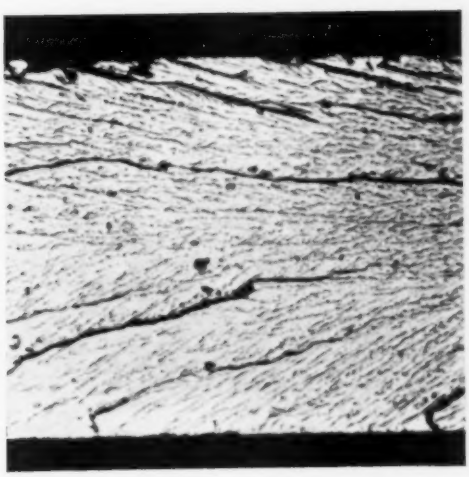

Fig. 1 (f)

Fig. 1. X-ray pictures and corresponding microphotographs of fracture surfaces.

Vol.
1
1952/

V. Around the tip of the crack there exists a zone of stress concentration, which, in the dynamic case considered here, consists of a complicated series of dilatational and shear stress *waves*. As the crack progresses, points lying immediately adjacent to the path of the crack find themselves in a stress field that increases up to a

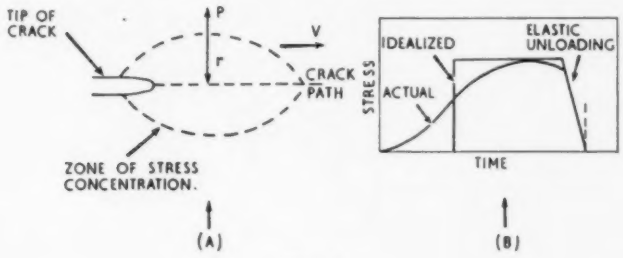

Fig. 2

maximum and then is unloaded as the crack passes. The shape of this wave can be calculated from the work of YOFFE; it would, presumably, be of the form illustrated in Fig. 2 (b). As a simplifying assumption, it is assumed instead that the pulse is square-fronted, and is unloaded elastically as the crack tip passes. Following YOFFE's work, we also assume that the limiting velocity of the crack is the shear wave velocity.

Under the influence of this stress pulse, plastic and elastic stress waves spread into the two half-spaces on each side of the crack, until their progress is stopped a time t' later by the elastic unloading wave. VON KARMAN and DUWEZ (1950) have shown that the velocity of plastic waves is given by

$$v_1 = \sqrt{\frac{1}{\rho} \cdot \frac{\partial \sigma}{\partial \epsilon}}$$

where $\partial\sigma/\partial\epsilon$ is the slope of the shear-stress strain curve at strain ϵ; the velocity of the elastic unloading shear waves is

$$v_2 = \sqrt{\frac{G}{\rho}}$$

where G is the shear modulus. Thus, plastic waves of strain amplitude ϵ and velocity v_1 reach out a distance r given by

$$r = v_1 t = v_2 (t - t').$$

Hence

$$t = \frac{v_2 t'}{v_2 - v_1}, \qquad r = \frac{v_1 v_2 t'}{v_2 - v_1}.$$

The velocity of plastic waves for varying strain was calculated from the tensile stress-strain curve of another single crystal, which extended some 3 per cent before fracture. This was converted into a true shear-stress strain curve, and the slope of the curve determined at various strains. The resulting graph of strain amplitude against plastic wave velocity is given in Fig. 3.

Before w can be calculated, the variation of the time of application of the stress pulse (t') with crack velocity must be determined. This varies because the length of the stress pulse suffers a type of relativistic contraction. t' is equal to the time between the arrival of the first (elastic) wave and the arrival of the crack, or

$$t' = \frac{l}{V} - \frac{l}{v_2}$$

where l is a parameter with the dimensions of length. Thus, finally,

$$\frac{r}{l} = \frac{v_1}{v_2 - v_1}\left(\frac{v_2}{V} - 1\right).$$

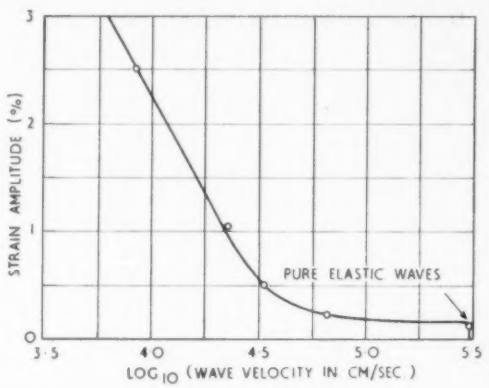

Fig. 3

From this formula, it is seen that plastic deformation extends to an infinite distance when $V = 0$, in accord with experience, and tends to zero as $V \to v_2$. This is in accord with the theory and results of VON KARMAN and DUWEZ, who state $\epsilon = 0$ for all $V > v_2$.

Values of r/l have been determined for three different values of ϵ, and plotted against V/v_2. These are in Fig. 4. As a final step, the plastic work factor w can be calculated by numerical integration from this graph, for

$$w = \sigma \int_0^\infty \epsilon_r \, dr.$$

Inspection of the graph indicates that w should fall by a factor of 100 as V increases from $v_2/10$ to $9v_2/10$. A variation of this magnitude is needed to explain the X-ray results previously mentioned in this section.

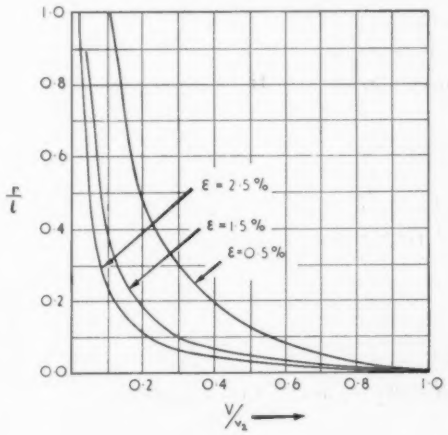

Fig. 4

This analysis has omitted the variation of the yield stress of the material with rate of deformation, which has not yet been measured at such high rates of strain; the effect would be to lower w still further. This would reinforce the present argument.

5. Discussion

It has been shown that the fracture stress of a metal is given by

$$\sigma = \sqrt{\frac{2E\,(T + w)}{\pi c}}$$

where w is the plastic work necessary to produce a crack of length c. In polycrystalline material w is high but in single crystals is much lower. Thus, a grain-size effect in the fracture strength of metals is to be expected, apart from any effect such as MOTT has analysed. A separate experimental determination is needed to analyse the effect of grain size on the plastic work factor.

It has also been shown that the plastic work factor and the microstructure on the cleavage surface are related. An X-ray microbeam is therefore needed for the point-to-point determination of the plastic work factor, and its correlation with the microstructure. A more accurate theoretical analysis, dealing in particular with the variation of crack velocity V with crack length c at high crack velocities, is also required to replace MOTT's formula, accurate at only very low crack velocities.

ACKNOWLEDGMENTS

This work was undertaken on behalf of the Admiralty Ship-Welding Subcommittee under the direction of Professor J. F. BAKER, O.B.E., Sc.D., in the Engineering Department, Cambridge University. The writer would like to thank Professor BAKER for his interest; Professor Sir LAWRENCE BRAGG for the use of an X-ray set in the Cavendish Laboratory; and Dr. J. W. MENTER for undertaking the electron-diffraction work mentioned in the text. Helpful discussions were held with Dr. C. F. TIPPER and Dr. W. M. LOMER. Acknowledgment is made to the Admiralty for permission to publish this paper.

ol.
1
2/53

REFERENCES

ELLIOTT, H. A.	1947	*Proc. Phys. Soc.*, **59**, 208.
GRIFFITH, A. A.	1920	*Phil. Trans. Roy. Soc.*, A **221**, 180.
HOLLOMON, J. H.	1948	*Fracture of Metals*, p. 262 (A.S.M.).
KLIER, E. P.	1950	*Trans. Am. Soc. Metals*, **43**, 935.
MOTT, N. F.	1948	*Engineering*, **165**, 16.
PONCELET, E. F.	1948a	*Verres et Réfractaires*, **2**, 203.
	1948b	*Fracture of Metals*, p. 201 (A.S.M.).
OROWAN, E.	1947	*J. West of Scotland Iron & Steel Inst.*, p. 45.
	1950	*Conference on Fatigue and Fracture of Metals*, M.I.T., June.
SACK, R. A.	1946	*Proc. Phys. Soc.*, **58**, 729.
SAIBEL, E.	1948	*Fracture of Metals*, p. 275 (A.S.M.).
TIPPER, C. F.	1948	Admiralty Ship-Welding Committee Report R 3, H.M.S.O.
	1951	Unpublished Admiralty Ship-Welding Committee Report.
TIPPER, C. F. and SULLIVAN, A. M.	1950	*Trans. Am. Soc. Metals*, **43**, 906.
VON KARMAN, T. and DUWEZ, P.	1950	*J. Appl. Phys.*, **21**, 987.
YOFFE, E. H.	1951	*Phil. Mag.*, **42**, 739.

Journal of the Mechanics and Physics of Solids, 1953, Vol. 1, pp. 234 to 243. Pergamon Press Ltd., London.

THE YIELD STRESS OF PURE LEAD IN COMPRESSION

By N. Loizou* and R. B. Sims†
British Iron and Steel Research Association, Sheffield

(*Received* 16*th March*, 1953)

Summary

The variation of the yield stress of pure lead in uniaxial compression with temperature, strain and strain-rate is described together with experiments designed to test the accuracy of the results. The average coefficient of friction between the platens and specimen has been measured for lubricated and unlubricated compression, and its dependence on strain rate demonstrated. The effect of previous strain-rate history on the yield stress is also discussed.

Vol.
1
1952/5

1. Introduction

The measurement of the yield stress of pure lead at relatively high rates of strain, and over a wide range of deformation, has been carried out as a part of a programme of research into hot rolling to examine the accuracy of the various rolling theories.

The yield stress of lead is known to depend on the temperature, strain rate and magnitude of the current strain, but in the past no measurements have been made at strain rates above the creep level or at large plastic deformations. The compression test has been used in the present work since, in tension, necking occurs at relatively small strains compared with those found in rolling.

A plastometer built to give a constant speed of compression by Mr. J. Los at Sheffield University was loaned for these experiments by Professor H. W. Swift. A second plastometer, designed by Orowan and Los (1950) to deform specimens at a constant strain-rate, was used to investigate the effect of variations of strain rate on the yield stress.

2. Apparatus and Materials

The experiments were carried out in a plastometer consisting essentially of a rigid framework supporting two horizontal compression platens of hardened, ground and lapped steel. The upper platen was attached to a load measuring device, and the lower platen could be driven towards the upper platen by means of a rotating cam. Before each experiment the platens and the cam were adjusted so that the specimen was held between them and the movement of the lower platen gave the required strain displacement. The cam speed was selected on a gearbox on the drive, and when the motor was running at constant speed a trigger connected the shaft to the cam which rotated once and compressed the specimen.

*Now with Shell Petroleum, Ltd., Cyprus.
†Now with Davy-United Engineering Co. Ltd., Sheffield.

ol.
1
2/53

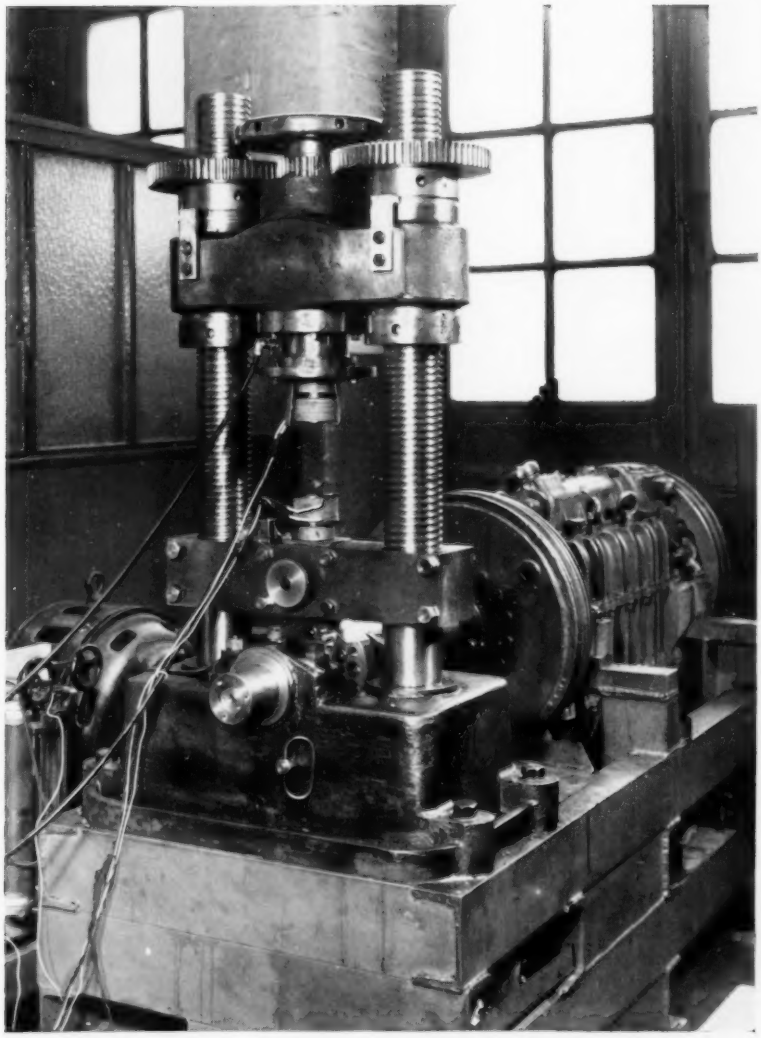

Fig. 1. The plastometer giving constant speed of compression.

Vol.
1
1952/5

In the plastometer shown in Fig. 1 the cam moved the lower platen at constant speed. A second plastometer of similar general arrangement was used in which the cam was designed to provide a constant strain-rate in the specimen.

The loadmeter of the constant speed apparatus was of the capacity type. An insulated brass disc formed one plate of the condenser, the second plate being a threaded plug which could be adjusted to change the total capacitance of the instrument. This condenser was in the circuit of a 2 megacycles-per-second oscillator. The change in capacity proportional to the applied load varied the frequency of the oscillator which was followed by a frequency modulation circuit and amplifier connected to the Y plates of a cathode ray oscilloscope.

The anvil travel was also measured by a capacity gauge. A plate fastened to the anvil moved between two insulated plates attached to a fixed crosshead, thus forming a condenser of variable capacity. The displacement was measured by a second frequency modulation circuit and oscilloscope. The load and displacement signals were recorded simultaneously by a high speed, drum type, camera. The loadmeter was calibrated directly by a proving ring and the displacement meter by a dial gauge. Calibrations made at various times were linear, and agreed to within $\pm$ 2%.

The constant strain-rate plastometer was equipped with a glass block dynamometer similar to that described by Orowan, Scott and Smith (1950). Electrolytically refined lead of very high purity was used in the experiments. It was cast in cylindrical moulds $1\frac{1}{8}$ in. in diameter and 4 in. long, care being taken to exclude impurities, particularly sulphur. The cast bars were then hammered down to $\frac{3}{4}$ in. in diameter approximately, and cold formed in a container of 1·000 in. internal diameter. The specimens were then faced in a lathe to final dimensions of 1·500 in. $\pm$ 0·001 in. long and 1·000 in. in diameter and left to anneal at room temperature. Some specimens 0·750 in. long and 1·000 in. in diameter were used to investigate the effect of end friction.

Table 1

Reduction in height %	*Compression rate* (*in./sec.*)	*Temperature increase* °C	*Work of deformation* *ins.-tons*	*Calculated temperature increase* °C
57·3	0·83	17·0	2·016	17·5
57·3	3·4	18·0	2·142	18·6
57·3	7·77	18·5	2·154	18·7
57·3	10·0	18·3	2·154	18·7
57·3	11·75	18·6	2·154	18·7
57·3	13·5	18·8	2·154	18·7
57·3	15·25	19·0	2·189	19·0

3. Results

Experiments at 0°C, 20°C, 40°C, 70°C and 110°C were made, ranging in strain rate from 0·8/sec. to 20/sec. For the 0°C experiments the specimens were kept at temperatures slightly below the freezing point of pure water and compressed

between polished insulating pads to reduce heat transfer to the specimens from the main body of the plastometer.

For the 40°C, 70°C and 110°C experiments the specimens were heated by conduction from the two compression pads in which heater wires were embedded, the temperature being checked by a thermocouple. The maximum temperature reached during compression was measured by a copper-constantan thermocouple peened into each specimen. Table 1 shows a comparison between the measured temperature rise and the values calculated from the work done on the specimens.

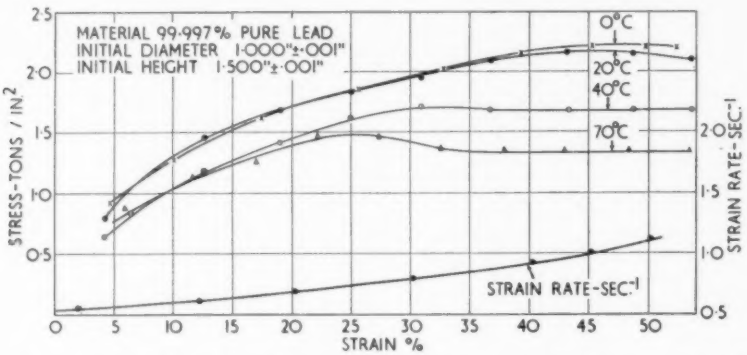

Fig. 2. Results obtained from constant speed plastometer (speed of compression 0·83″/sec.).

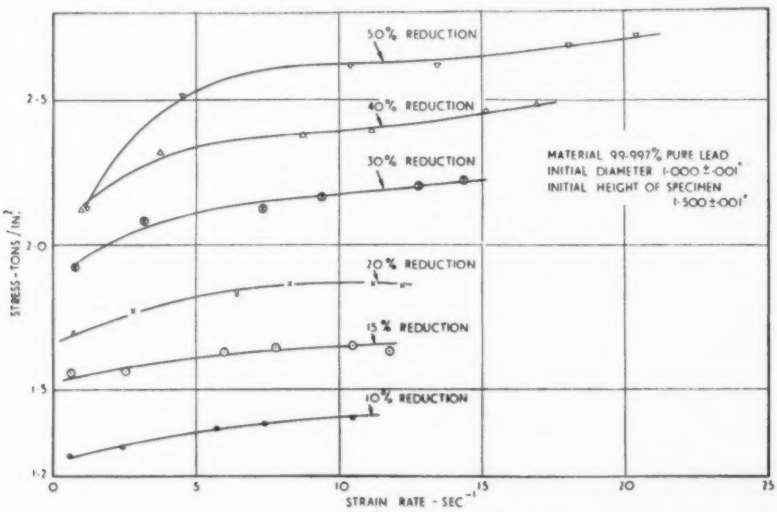

Fig. 3. Yield stress v. strain-rate of pure lead at 0°C (values of reduction marked on curves).

In Fig. 2 a typical set of results is given for a constant rate of compression of 0·83 ins./sec. at various temperatures. These results have been replotted, in Figs. 3 to 7, as yield stress against strain rate ($= dh/hdt$, where h is the instantaneous height of the specimen and t is time), and for various fractional reductions ($= (H - h)/H$, where H = the initial height of the specimen).

4. Accuracy of Experiments

The object of the present experimental work was to measure the yield stress of pure lead accurately at various strain rates, strains and temperatures. Since there is little information available on similar experiments using relatively soft metals, additional experiments were made to investigate the magnitude of the possible errors in the measurements.

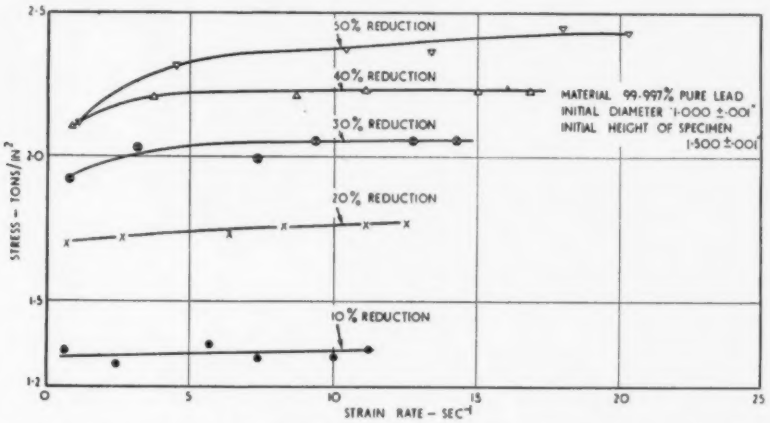

Fig. 4. Yield stress *v.* strain-rate of pure lead at 20°C (values of reduction marked on curves).

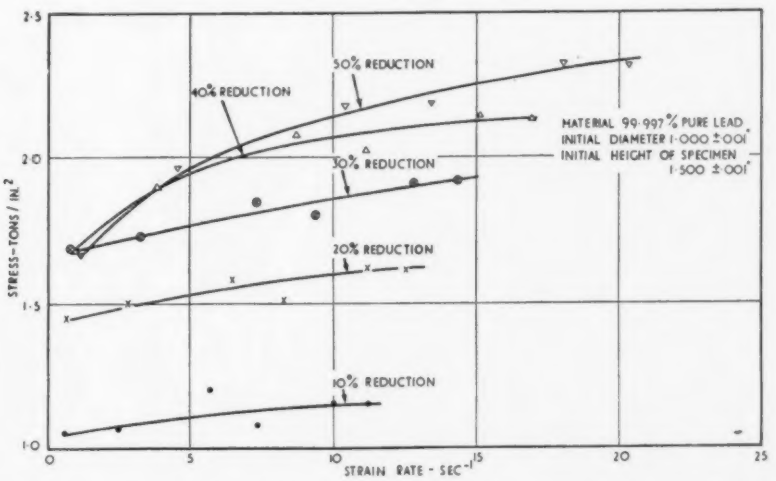

Fig. 5. Yield stress *v.* strain-rate of pure lead at 40°C (values of reduction marked on curves).

The reason for using the compression test has been explained above. Probably the largest single error in this method arises from the frictional forces between the compression platens and the material which alter the stress distribution near the ends of the specimen from a uniaxial to a triaxial system, thus inhibiting the radial flow of the material and causing barrelling. In this work efficient lubrication

was provided by an oil with a free fatty acid additive which was entrapped in concentric grooves 0·002 in. deep machined on each end of the specimen. The depth and number of these grooves were found by experiment : too few grooves resulted in barrelling and too many entrapped so much oil that the ends of the specimen were splayed outwards. With a spacing of 32 grooves per inch radius barrelling was eliminated, and, as the ends of the specimen were plane and parallel

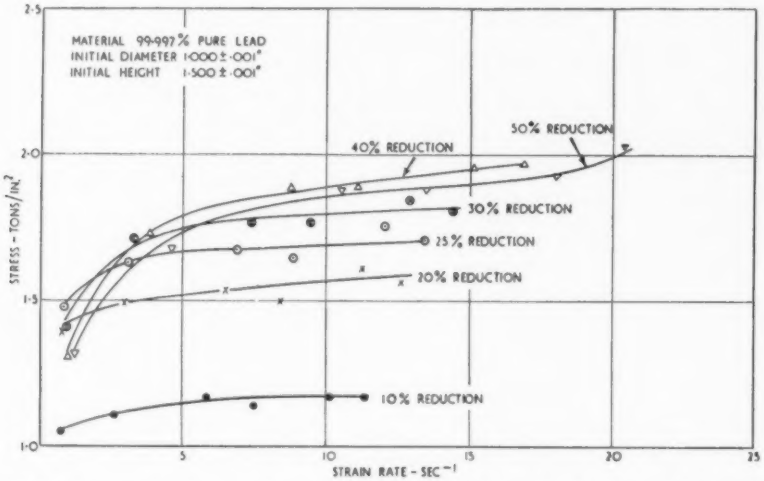

Fig. 6. Yield stress *v.* strain-rate of pure lead at 70°C (values of reduction marked on curves).

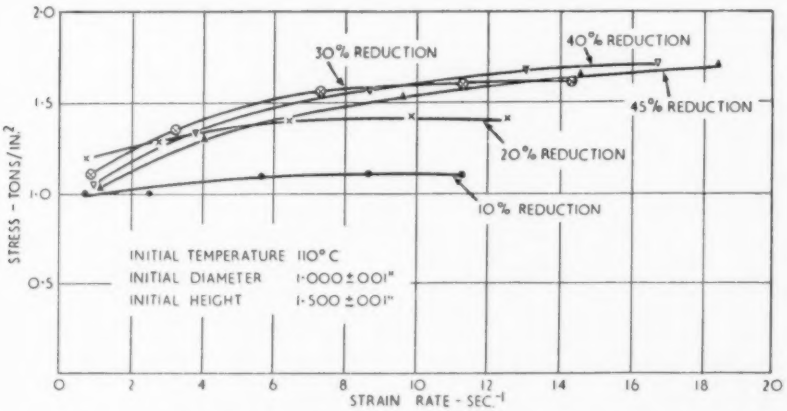

Fig. 7. Yield stress *v.* strain-rate of pure lead at 110°C (values of reduction marked on curves).

after compression, it is concluded that the deformation was very nearly uniaxial throughout. A photograph of specimens before and after compression is shown in Figs. 8a and 8b. The grooving can be clearly seen. This method of overcoming end friction, is, therefore, distinct from the method of Siebel and Pomp (1928) who used coned tools to remove the effects of barrelling, but deformed their specimens in a non-uniform manner.

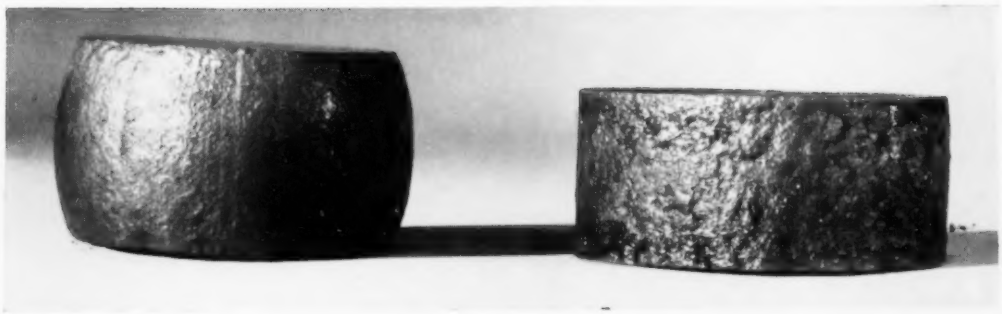

Fig. 8a. Barrelling on lubricated specimens with and without grooving.

ol.
1
2/53

Fig. 8b. Grooving of specimens before and after compression.

Vol.
1
1952/5

Experiments were carried out on specimens with height/diameter ratios of 1·5 and 0·75 : (i) with grooves cut in the ends and lubricated with oil ; (ii) with lapped and polished ends and lubricated with oil ; (iii) with lapped and flat ends, but both platens and specimens degreased with magnesium oxide. Fig. 9 shows results from experiments (i) and (iii). Within the experimental accuracy the measured yield stress is unaffected by the height/diameter ratio of the specimens when the ends are grooved, but large differences occur when there is no lubricant. Additional support is provided by these results for the view that a close approximation to the true yield stress is obtained with specimens grooved at the ends.

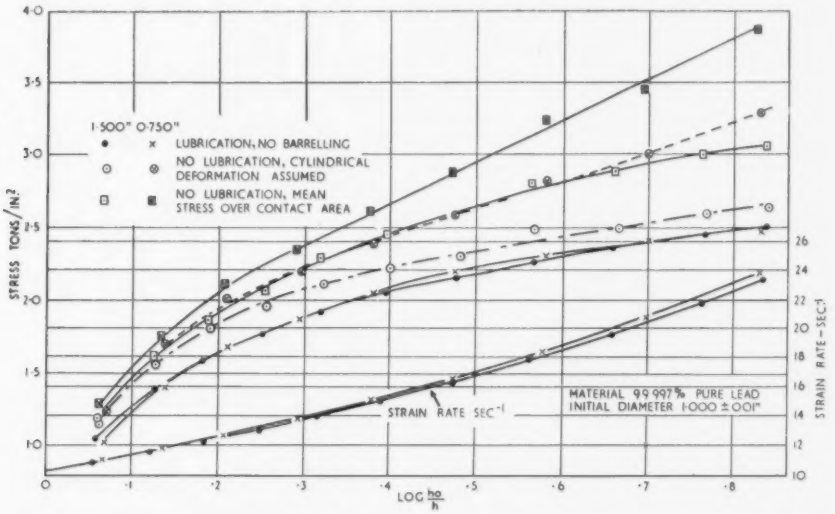

Fig. 9. Effect of friction on the measured yield stress (initial temperature ≏ 20°C).

Siebel (1923) has shown that the average pressure on a cylindrical specimen compressed with end friction is

$$p = Y\left(1 + \frac{2\mu a}{3h}\right)$$

where p = average pressure, a = maximum radius, μ = coefficient of friction, h = instantaneous height, and Y = yield stress in uniaxial compression. If the yield stress is known accurately the average coefficient of friction may be calculated and the results are shown for experiments (ii) in Fig. 10 and (iii) in Fig. 11. There is close agreement between the value of the coefficient of friction and the strain rate, and in the case of the 31 unlubricated specimens the correlation is 0·851. The best line through the experimental values has the equation $\log\mu = \log 0{\cdot}38 - 0{\cdot}0101\lambda$, where λ = the strain rate (sec.$^{-1}$).

The decrease in yield stress observed by Polakowski (1949) in specimens showing barrelling was not found in the present experiments.

Another possible error in the experiments was the variation of yield stress with crystal size in the specimen. The results in Fig. 12 show the effect to be large between a specimen in the as-cast condition (12 crystals per sq. cm.) and a

specimen in which the crystal size had been reduced by plastic forming to 3440 crystals per sq. cm. It is thought that in the present work this effect is negligible since the crystal size in the finished specimens was very much smaller than in the as-cast state and it is known that the yield stress is sensitive to crystal size only in coarse-structured materials.

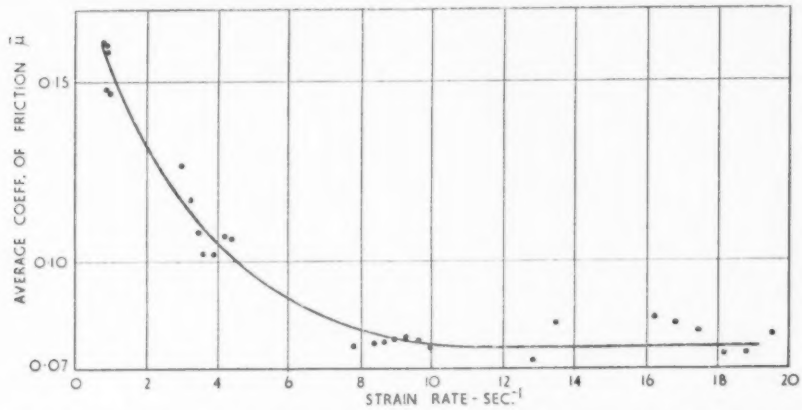

Fig. 10. Mean coefficient of friction for lubricated specimens of pure lead with lapped ends.

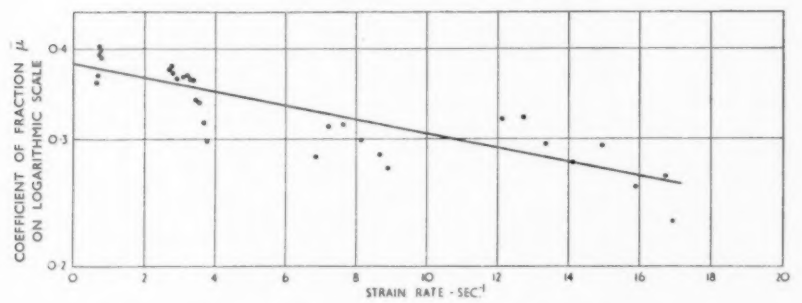

Fig. 11. Mean coefficient of friction for non-lubricated specimens.

The results given in Table 1 show that little or no exchange of heat occurs between the metal and its surroundings during compression. It is clear, therefore, that the results in Figs. 2 and 7 for the temperature of the specimen before compression do not give the true yield stress v. temperature relationship. All the results in Figs. 3 to 7 have not been corrected for the effect, since in use, particularly in rolling, it is the initial temperature of the material which is known, and not the temperature at various stages of the deformation. The correction has been made in Fig. 13, however, on a section of the results, and the variation of yield stress is shown against specimen temperature at various strain rates and reductions. The magnitude of the correction may be found from Fig. 13 by comparing the yield stress at the experimental points on the curves with the corresponding values at the initial temperature of the experiment.

The experiments described above were carried out on the plastometer in which the lower platen moved at constant velocity. Some experiments were made with the second apparatus in which the specimen was compressed at a constant strain rate. It was possible, therefore, to compare the yield stress at various tempera-

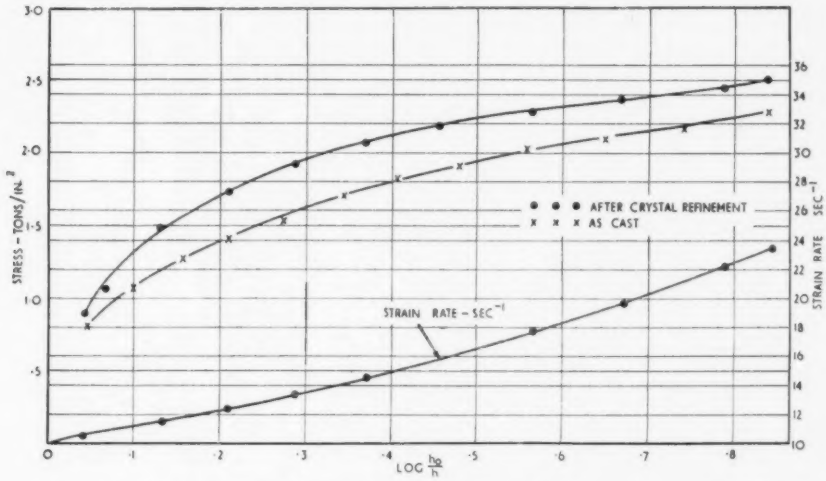

Fig. 12. Effect of crystal size on the yield stress (initial temperature ≏ 20°C).

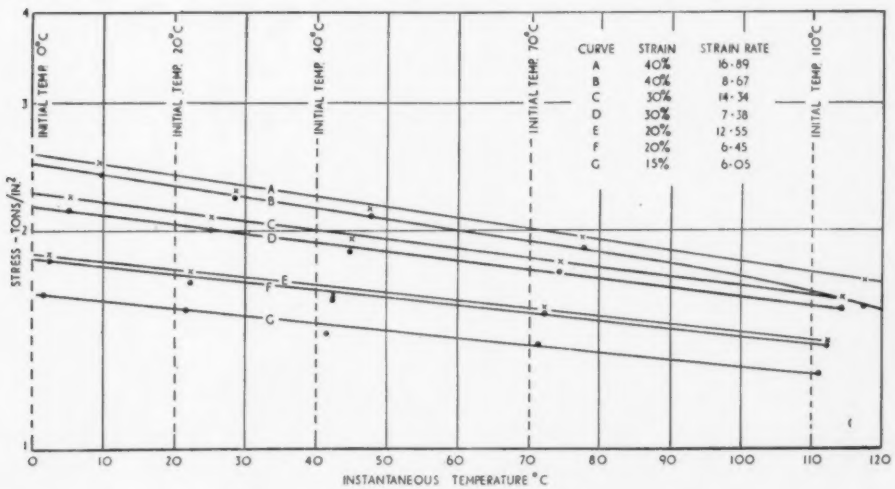

Fig. 13. True variation of yield stress with temperature.

tures, reductions and strain rates for specimens with differing strain-rate history. Since the yield stress at any temperature depends on the recovery within the material and the rate of re-crystallization, both of which are functions of time and the amount of plastic deformation, it is to be expected that the measured yield stress will depend not only on the instantaneous values of strain and strain-rate, but also on the mode of deformation from the annealed condition.

The experiments were carried out at an initial temperature of 100°C on specimens case from a single melt of lead. All specimens were grooved and lubricated. Typical results are shown in Figs. 14a and 14b, and Table 2 shows the ratio of the yield stresses at the same strain and strain-rate.

Table 2

$\frac{Y_2}{Y_1}$	*Strain-rate* $sec.^{-1}$	*Reduction at equal strain-rates* %	*Speed of compression for* Y_1 *inches/sec.*	*Initial strain-rate for* Y_1 sec^{-1}
1·068	1·063	43·8	0·83	0·593
1·053	3·045	26·2	3·40	2·266
1·085	7·75	34·0	7·77	5·180
1·034	11·53	31·8	11·75	7·830
1·047	17·50	42·0	15·25	10·166

Y_2 = yield stress measured in constant strain-rate plastometer.
Y_1 = yield stress measured at constant speed of compression.

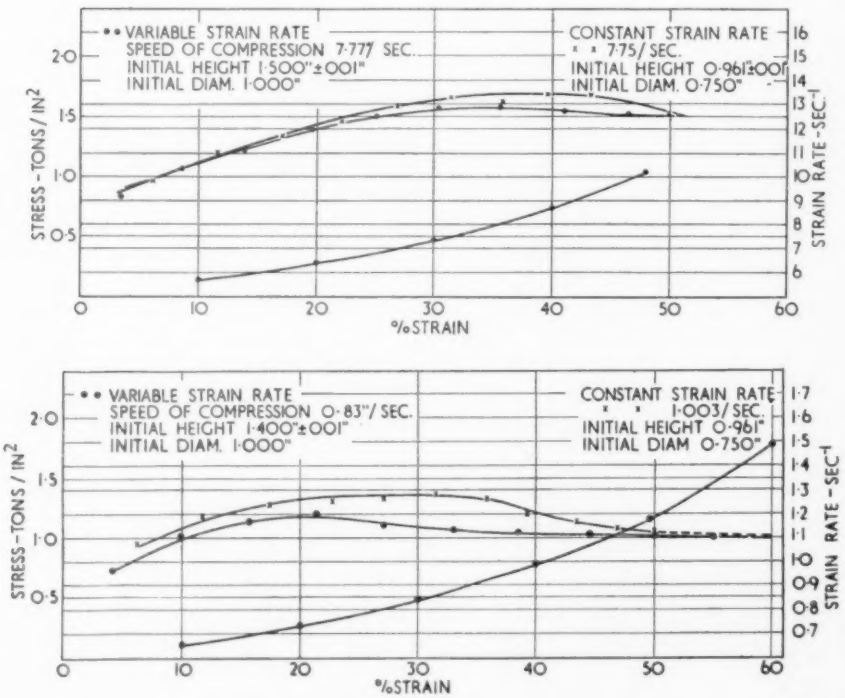

Figs. 14a and b. Yield stress at variable strain-rates and constant strain-rates of 7·75 and 1·063 $sec.^{-1}$ (temperature 110°C).

It will be seen in Figs. 14a and 14b that the two yield stress-strain curves intersect, a characteristic of all the results with the exception of the measurements

made at the strain rate of 17·50 sec.$^{-1}$. The data at these points of intersection, including the time taken for the total deformation, are shown in Table 3.

TABLE 3

Stress	*Reduction*	*Strain rate*		*Time*	
		Const. strain rate m/c. sec.$^{-1}$	*Const. speed m/c. sec.$^{-1}$*	*Const. speed m/c. secs.*	*Const. strain rate m/c. secs.*
tons./in.$^{-2}$	%				
1·05	63	1·063	1·602	1·062	0·930
1·26	51·8	3·045	4·77	0·225	0·240
1·48	51·8	7·75	10·75	0·100	0·942
1·62	48·2	11·75	15·122	0·061	0·061

Although there are too few results in Table 3 on which to base firm conclusions it would seem that the yield stress of a metal is dependent not only on the instantaneous temperature, strain and strain rate, but also in a complex manner on the total time taken to deform the specimen from the annealed condition, on the rate of deformation and on the time required for recovery and recrystallization.

The values of the yield stress given in Figs. 3 to 7 are, therefore, not the true values for deformation at a constant strain rate, and, as mentioned above, they are not corrected for the rise in temperature which occurs during the deformation. The results may be corrected for these two effects, but in view of the fact that only approximate equations are available at present for the mechanical working process, it is considered that the uncorrected data is of sufficient accuracy to be used in a quantitative manner with results of experiments using lead as a model for metals which hot work only at elevated temperatures.

ACKNOWLEDGMENTS

The authors are grateful to the Director of the British Iron and Steel Research Association and to the Chairman of its Rolling Committee for permission to publish this paper No. MW/A/50/52.

REFERENCES

OROWAN, E. 1950 *B.I.S.R.A. Restricted Report* MW/F/22/50.

OROWAN, E., SCOTT, F. H. and SMITH, C. L. 1950 *J. Sci. Instrum.*, **27**, 118.

POLAKOWSKI, N. H. 1949 *J. Iron and Steel Inst.*, **163**, 250.

SIEBEL, E. 1923 *Stahl und Eisen*, **43**, 1295.

SIEBEL, E. and POMP, A. 1928 *Mitt. K.W.I. Eisenf.*, **10**, 55.

Journal of the Mechanics and Physics of Solids, 1953, Vol. 1, pp. 244 to 257. Pergamon Press Ltd., London.

EINE THEORIE DES KRIECHENS VON EINKRISTALLEN*

By O. G. FOLBERTH** und A. KOCHENDÖRFER†
Institut für theoretische und angewandte Physik der Technischen Hochschule und
Max-Planck-Institut für Metallforschung, Stuttgart

(*Received 26th April* 1953)

SUMMARY

IN order to describe the phenomena of creep in single crystals, the assumptions of KOCHENDÖRFER's theory of plastic deformation are extended by taking the rate of dissipation of dislocations to be proportional to the number of bound dislocations, instead of independent of this number. This extension finds support in electron-microscopic studies of the formation of slip-lines. In comparison with the previous investigations this alters the form of the hardening curve, but not its dependence on temperature and rate of deformation. The previous assumptions also remain applicable to flow under high stresses, at which substantial amounts of shear occur, and many glide planes are activated, before stationary flow is reached. They lead to the result, in agreement with KORNFELD's observations, that the rate of flow is practically independent of stress.

With this extension, the laws of creep are well reproduced, both with respect to the form of the creep curve and also its dependence on temperature and stress. The theory thus covers the entire range of plastic behaviour, from creep to impact deformation.

Integration of the fundamental equations could only be performed by graphical-numerical methods. By a suitable simplification, however, a good approximation can be obtained in closed form. For intermediate time ranges, this gives a linear relationship between log (creep rate) and log (time), with slopes changing from -1 at low temperatures (logarithmic creep) to $-2/3$ at high temperatures ($t^{1/3}$ creep). It also correctly reproduces the empirically found regularities of transient creep, and the temperature and stress dependence of steady state creep in experiments of long duration. The initial creep velocity and the total amount of transient creep have finite values.

1. EINLEITUNG

UNTER Kriechen wird die plastische Verformung unter konstanter Spannung mit kleinen Gleitgeschwindigkeiten (Grössenordnung 10^{-6} sec^{-1}) verstanden. Qualitativ haben die Kriechkurven (Abgleitung a als Funktion der Zeit t) von Einkristallen dieselbe Form wie die von polykristallinen Materialien (SULLY 1949). Die Kriechgeschwindigkeit fällt nach anfänglich grossen Werten mit zunehmender Verformung ab, um nach einiger Zeit einen konstanten Wert anzunehmen‡. Formal kann somit der Kriechvorgang in zwei additive Teile zerlegt werden :

(a) Das Übergangskriechen (transient or primary creep), dessen Gleitgeschwindigkeit $v = v_{tr}$ sich mit wachsender Zeit asymptotisch dem Wert Null nähert.

*Auszug aus der Dissertation von O. G. FOLBERTH an der Technischen Hochschule Stuttgart (1952)

** Nunmehr Siemens-Schuckert-Werke, Erlangen.

† Nunmehr Max-Planck-Institut für Eisenforschung, Düsseldorf.

‡ Von dem sich an das stationäre Kriechen anschliessenden, dem Bruch vorausgehenden beschleunigten dritten Kriechen (tertiary creep) sehen wir hier ab.

(b) Das stationäre Kriechen (steady state or secondary creep) mit konstanter Gleitgeschwindigkeit $v = v_{st}$.

Für die mathematische Erfassung der Kriechkurven wurden verschiedene Ausdrücke vorgeschlagen (ANDRADE 1914; SMITH 1948; COTTRELL und AYTEKIN 1950; SLIFKIN und KAUZMANN 1950; TYNDALL 1950; NEURATH und KOEHLER 1951). Eine einheitliche Schreibweise dieser Vorschläge ist möglich, wenn man an Stelle der Abgleitung die Gleitgeschwindigkeit als Funktion der Zeit anschreibt (Kriechgeschwindigkeitskurven):

$$v = da/dt = \beta \,.\, t^{-n} + v_{st}. \tag{1}$$

β, n, v_{st} sind Materialkonstanten. n kann Werte zwischen 2/3 und 1 annehmen; ihm entspricht eine Zeitabhängigkeit der Abgleitung zwischen $t^{1/3}$ und $\log t$. Der Streubereich der Konstanten von Versuch zu Versuch ist sehr gross. Eine systematische Temperatur- und Spannungsabhängigkeit konnte bisher lediglich für v_{st} gemessen werden. Es ergab sich, dass v_{st} exponentiell mit der Gleitschubspannung τ wächst und ebenfalls exponentiell mit der reziproken absoluten Temperatur $1/T$ fällt (siehe Gleichung (8)).

Die exponentielle Zunahme von v_{st} mit τ tritt jedoch nur bei " echten " Kriechversuchen mit kleinen Gleitgeschwindigkeiten auf. Oberhalb einer bestimmten Schubspannung steigt v_{st} allmählich weniger als exponentiell an. Wenn τ etwa das zehnfache der normalen kritischen Schubspannung τ_0 beträgt, wird v_{st} (im Rahmen der Genauigkeit der Experimente) unabhängig von τ (KORNFELD 1936). Die Gleitgeschwindigkeiten sind dabei von der Grössenordnung 1/10 sec^{-1}. Es handelt sich bei diesen Versuchen also nicht mehr um eigentliche Kriechversuche, sondern um Fliessversuche bei mittleren (10^{-2} sec^{-1}) bis grossen (10^{2} sec^{-1}) Gleitgeschwindigkeiten.

Das Kriechen von Vielkristallen erfolgt durch gleichzeitige plastische und quasiviskose Vorgänge, im Gegensatz dazu tritt bei Einkristallen rein plastisches Gleiten auf. Die Plastizität, einschliesslich Verfestigung und Erholung, wird heute auf die Existenz von Versetzungen zurückgeführt. Mit Hilfe der Versetzungstheorien konnten eine grosse Anzahl plastischer Probleme gelöst oder der Lösung nähergebracht werden (CHALMERS 1949). Von meheren Autoren wurde auch das Kriechen versetzungstheoretisch behandelt. Diese Theorien ergeben jedoch entweder nur ein Übergangskriechen (OROWAN 1947; SMITH 1948; MOTT und NABARRO 1948; COTTRELL 1952) oder Kriechkurven, die nicht der experimentellen Beziehung (1) entsprechen (LAURENT 1945; LYONS 1948). Über die Temperatur und Spannungsabhängigkeit des Kriechens können diese Theorien nur unvollständige Angaben machen.

Für die plastischen Erscheinungen ist von KOCHENDÖRFER (1941) eine Versetzungstheorie entwickelt und mit Erfolg auf eine Anzahl von Versuchsgruppen angewendet worden. Insbesondere ergibt sich unter konstanter Schubspannung τ sowohl ein Übergangsfliessen wie auch ein stationäres Fliessen, letzteres aber unabhängig von τ (KOCHENDÖRFER 1952) wie bei den Versuchen von KORNFELD bei hohen Fliessspannungen.

Im folgenden wird gezeigt, dass diese Ansätze zwanglos so erweitert werden können, dass damit auch die echten Kriechversuche bei kleinen Gleitgeschwindigkeiten quantitativ erfasst werden.

2. Erweiterung der bisherigen Ansätze

Die von Kochendörfer (1941) und Vorgängern entwickelte Versetzungstheorie auf halbempirischer Basis geht von einem zweidimensionalen Modell aus. Die Aussagen der Theorie entstehen mit Hilfe einer Statistik über die Versetzungen; die dreidimensionale Erweiterung der Theorie wird dadurch vollzogen, dass die statistischen Mittelwerte entsprechend abgeändert werden. Die Zahlenwerte der auftretenden Konstanten sind nämlich aus der Theorie nicht abzuleiten, sondern erst durch einen Vergleich von Theorie und Experiment bestimmbar. Diese halbempirische Methode vermeidet die mathematischen Schwierigkeiten einer vollständigen atomistischen Durchrechnung des Problems, geht aber wesentlich über die rein phänomenologische Beschreibung der Messergebnisse hinaus.

Die Grundgedanken der Theorie sind folgende :

Die Wahrscheinlichkeit für die Bildung von Versetzungen ist nach dem Boltzmann'schen Prinzip gegeben durch :

$$W_1 = \alpha_1 \cdot \exp(-\Delta A/kT). \tag{2a}$$

Dabei ist die Aktivierungsenergie ΔA von der Gleitschubspannung τ und der Verfestigung $\tau_v = \tau - \tau_0$ gemäss

$$\Delta A = A_1 \cdot \left(1 - \frac{\tau - \tau_v}{\tau_{01}}\right)^2 \tag{2b}$$

(A_1, τ_{01} Konstanten) abhängig.

Plastisch wirksam sind im wesentlichen nur Versetzungen, die Abgleitungen in Richtung der Gleitschubspannung hervorrufen. Die gegensinnigen (indirekten) Versetzungen können auch bei kleinen Gleitgeschwindigkeiten meist vernachlässigt werden. Die Abgleitung des Kristalls ist proportional zur Anzahl der jeweils gewanderten Versetzungen pro Volumeinheit.

An gewissen Fehlstellen des Gitters (Mosaikblockgrenzen, mittlerer Abstand L) werden die Versetzungen aufgehalten (gebunden) und rufen eine Verfestigung des Gitters hervor. Diese ist bei hexagonalen Kristallen und bei kubischen Kristallen bei Einfachgleitung (Lücke und Lange 1952 ; Röhm und Diehl 1952) proportional zur Dichte der gebundenen Versetzungen (N) :

$$\tau_v = c \cdot N \quad (c = \text{Verfestigungsparameter}). \tag{3}$$

Für die Auflösung der gebundenen Versetzungen wird ebenfalls das Boltzmann-'sche Prinzip angewendet. Sie hat eine Erholung des Kristalls zur Folge, die von der Gleitgeschwindigkeit abhängt (dynamische Erholung) und von der Erholung im unbelasteten Kristall (statische Erholung) quantitativ verschieden ist.

Die erste Grundgleichung der Theorie ist demnach ein Ausdruck für die Änderungsgeschwindigkeit der Zahl der gebundenen Versetzungen pro (zweidimensionaler) Volumeinheit :

$$\frac{dN}{dt} = \frac{1}{L} \cdot \left\{ \alpha_1 \cdot \exp\left[\frac{-A_1}{kT} \cdot \left(1 - \frac{\tau - cN}{\tau_{01}}\right)^2\right] - \alpha_2 \cdot \exp\left[\frac{-A_2}{kT} \cdot \left(1 - \frac{\tau - cN}{\tau_{02}}\right)^2\right] \right\}. \tag{4}$$

Der erste Summand in Gleichung (4) gibt die Änderungsgeschwindigkeit der gebildeten Versetzungen an, der zweite die der aufgelösten Versetzungen.

Vol. 1 1952/5

Die zweite Grundgleichung ergibt die Gleitgeschwindigkeit

$$v = da/dt = \alpha_1 \lambda \,.\, \exp\left[(-A_1/kT)\left(1 - \frac{\tau - cN}{\tau_{01}}\right)^2\right]. \tag{5}$$

Bei der Ableitung der Gleichungen ist von der Annahme ausgegangen worden, dass die Auflösungsgeschwindigkeit unabhängig ist von der Zahl der gebundenen Versetzungen (α_2 unabhängig von N). Sie ist gleichbedeutend damit, dass die Zahl der betätigten Gleitebenen sich im Laufe der Verformung nicht ändert, da dann die neu entstehenden Versetzungen in den schon betätigten Ebenen hinter den vorher entstandenen Versetzungen auflaufen und erst aufgelöst werden können, wenn die vorhergehenden schon aufgelöst sind. Praktisch ist diese Annahme nur nach grösseren Abgleitungen erfüllt, wenn schon viele Gleitebenen betätigt worden sind. Aus diesem Grunde führt sie auch zu der erwähnten richtigen Beschreibung der Befunde von Kornfeld, da bei hohen Fliessspannungen vor dem stationären Fliessen Abgleitungen bis über 50 per cent auftreten. Bei kleineren Abgleitungen nimmt die Zahl der betätigten Gleitebenen nach den elektronenmikroskopischen Befunden von Heidenreich und Shockley (1948) von Brown (1949) sowie von Wilsdorf und Kuhlmann-Wilsdorf (1952) stetig und näherungsweise linear mit der Abgleitung zu. Im Rahmen der beschriebenen Vorstellungen besagt dies, dass die Zahl der auflösungsfähigen Versetzungen proportional zur Zahl der gebundenen Versetzungen zunimmt, also

$$\alpha_2 = \beta_2 N \tag{4a}$$

zu setzen ist. Wir legen für das folgende die Gleichungen (4) und (5) mit dieser Erweiterung zugrunde.

Die Gleichungen (4) und (5) haben sich zur Berechnung der Geschwindigkeits – und Temperaturabhängigkeit der Verfestigungskurven bewährt, ohne dass die Erweiterung (4a) benutzt wurde. Das hat folgenden Grund : Mit der Versuchsbedingung $v = \text{const.}$, $T = \text{const.}$ ergibt die Integration dieser Gleichungen $N = a.\,\phi\,(v, T)$, also eine linear mit der Abgleitung ansteigende Zahl der gebundenen Versetzungen, wobei der Anstieg von den Versuchsparametern v und T abhängt. Bei Berücksichtigung von (4a) führt die Integration auf einen nichtlinearen Zusammenhang zwischen N und a, wobei aber der Einfluss von Geschwindigkeit und Temperatur auf die gegenseitige Lage der Kurven $N = N\,(a)$ praktisch derselbe ist, wie im ersten Fall. Auf diesen Einfluss kommt es, wie bereits früher erwähnt (Kochendörfer 1941 ; Seite 90/91), bei dieser Problemstellung auch in erster Linie an und nicht auf den Verlauf der Verfestigungskurve $\tau = \tau(a)$ im einzelnen. Dieser hängt überdies noch ab von der Beziehung zwischen τ_v und N, die heute noch keineswegs bekannt ist und meist in der einfachen Form $\tau_v \sim N$ oder $\tau_v \sim \sqrt{N}$ angesetzt wird. Mit diesen Ansätzen erhält man ohne Berücksichtigung von (4a) geradlinige bzw. parabelförmige Verfestigungskurven, welche ausreichende Näherungen für die gemessenen Kurven darstellen und durch die Parameter τ_v/a bzw. $\tau_v{}^2/a$ gekennzeichnet werden können. Bei Berücksichtigung von (4a) würde diese einfache Darstellung verloren gehen, ohne dass über den wesentlichen Punkt, die Geschwindigkeits – und Temperaturabhängigkeit der Verfestigungskurven, tiefere Aussagen gewonnen werden könnten. Bei den Kriechkurven dagegen besitzt gerade der Einfluss der Schubspannung auf die

Kriechgeschwindigkeit eine entscheidende Bedeutung, so dass (4a) hierbei grundsätzlich berücksichtigt werden muss. Es kommt also ganz auf die Fragestellung an, ob (4a) berücksichtigt werden muss oder nicht.

Wenn auf diese Weise eine wirkliche Vervollständigung der Theorie erzielt worden sein soll, so müssen die gemessenen Kriechkurven mit den bisherigen Zahlenwerten der Konstanten ohne weitere Annahmen (mit Ausnahme der durch (4a) neu eingeführten Konstanten β_2) richtig wiedergegeben werden. Wir stellen daher zunächst die Werte dieser Konstanten zusammen. Sie besitzen zum Teil für alle Metalle ungefähr übereinstimmende, zum Teil für die verschiedenen Metalle spezifische Werte. Die ersteren sind*

$$\begin{aligned} A_1/k &= 2{\cdot}5 \times 10^4 \text{ Grad}, & \alpha_1 \lambda &= 1{\cdot}5 \times 10^{10} \text{ sec}^{-1}, \\ A_2/A_1 &= 0{\cdot}95, & \tau_{01}/\tau_{02} &= 0{\cdot}996, & L &= 10^{-4} \text{ cm}. \end{aligned} \tag{6a}$$

Die spezifischen Materialkonstanten sind für Zinkkristalle, von denen die Ergebnisse der Kriechmessungen benutzt werden†

$$\begin{aligned} \tau_{01} &= 160 \text{ g/mm}^2, & \lambda &= 2{\cdot}7 \times 10^{-8} \text{ cm}, \\ c/(\lambda L) &= \tau_v/a\,(T=0) = 2300 \text{ g/mm}^2. \end{aligned} \tag{6b}$$

Aus (6a) und (6b) ergibt sich

$$\alpha_1 = 5{\cdot}6 \times 10^{17} \text{ sec}^{-1} \text{ cm}^{-1}, \quad c = 0{\cdot}6 \times 10^{-10} \text{ (g/mm}^2\text{) cm}^2. \tag{6c}$$

Diese Grössen sind störungsempfindlich, ihre Werte hängen stark von der Herstellung, dem Reinheitsgrad, und der Vorbehandlung der Proben ab und können daher (mit Ausnahme der Werte der Konstantenverhältnisse) im Einzelfall bis zu 50 per cent von den angegebenen Mittelwerten abweichen (bei α_1 bezieht sich dies auf den Logarithmus). Die Forderung kann dasher nur lauten, dass die zur Wiedergabe der Kriechkurven erforderlichen Zahlenwerte innerhalb dieses Streubereichs mit den angegebenen Mittelwerten übereinstimmen.

3. Berechnung der Kriechkurven und Vergleich mit den experimentellen Ergebnissen

Die Berechnung dieser Kurven erfordert die Integration von Gleichung (4) mit α_2 nach (4a) mit der Anfangsbedingung $N = 0$ für $t = 0$. Das Integrationsergebnis $N = N(t\,;\ T, \tau)$ liefert, in Gleichung (5) eingesetzt, den gesuchten funktionellen Zusammenhang zwischen v und t. Diese Berechnung kann nicht in geschlossener analytischer Form durchgeführt werden, die folgenden Ergebnisse sind daher auf graphisch numerischem Wege gewonnen worden. Zum Vergleich dienen die experimentellen Ergebnisse von Cottrell und Aytekin (1950) an spektroskopisch reinem Zink. Da die experimentellen Kurven stark streuen, so kann mit festen Zahlenwerten der Konstanten nur eine bestimmte experimentelle Kurve möglichst gut wiedergegeben werden. Die Zahlenwerte sind so gewählt worden, dass dies für die Kurve Nr. 3 in der Veröffentlichung von Cottrell und Aytekin zutrifft.

* Nach Kochendörfer (1941) S. 76 f. u. 89. Es ist zu beachten, dass dort als Einheit der Gleitgeschwindigkeit Abgleitung $10/h$ benutzt worden ist.

† Nach Kochendörfer (1941) S. 28, 88 u. 124. Der Verfestigungskoeffizient τ_v/a für $T = 0$ ist auf S. 88 für Kadmium mit 469 g/mm² angegeben, für Zink beträgt er nach den bei E. Schmid u. W. Boas (1935) wiedergegebenen Verfestigungskurven rund das 5 fache.

Fig. 1 zeigt, dass eine sehr gute Übereinstimmung zwischen der theoretischen Kurve und den experimentellen Ergebnissen erzielt werden kann. Die hierfür erforderlichen Zahlenwerte sind folgende:

$$A_1/k = 2 \times 10^4 \text{ Grad}, \quad \alpha_1 = 8{\cdot}3 \times 10^{21} \text{ sec}^{-1} \text{ cm}^{-1},$$
$$\tau_{01} = 250 \text{ g/mm}^2, \qquad c = 3 \times 10^{-10} \text{ (g/mm}^2\text{) cm}^2, \quad \beta_2 = 3 \times 10^{10} \text{ sec}^{-1} \text{ cm}. \tag{7}$$

Für A_2/A_1 und τ_{01}/τ_{c2} sind die Zahlenwerte (6a) übernommen worden, da diese durch die früheren Messungen schon genau festgelegt sind (vgl. KOCHENDÖRFER 1941; Seite 89). Wie man sieht, liegen die Werte der anderen Konstanten innerhalb des oben angegebenen Streubereichs um die Mittelwerte (6a-c). Neu hinzugetreten ist lediglich der Wert von β_2. Eine ausgiebige Untersuchung hat ergeben, dass die Werte der Konstanten gegenüber denen in (7) nicht merklich abgeändert werden dürfen, wenn die Übereinstimmung zwischen der berechneten und gemessenen Kriechkurve bestehen bleiben soll. Ferner hat sich gezeigt, dass durch geeignete, etwas, davon verschiedene Werte jede der von COTTRELL und AYTEKIN gemessenen Kurven mit gleicher Genauigkeit wiedergegeben werden kann wie die Kurve in Fig. 1.

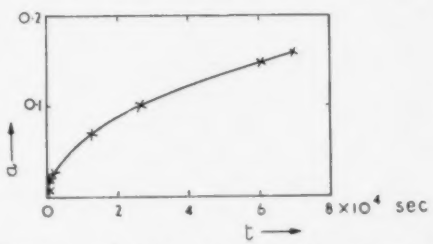

Fig. 1. Vergleich der mit den Zahlenwerten (7) berechneten Kriechkurve mit der von COTTRELL und AYTEKIN (1950) gemessenen Kurve Nr. 3 (Messpunkte x). Die "spontane Abgleitung" wurde nicht berücksichtigt.

Die mit den Zahlenwerten (7) berechneten Kriechgeschwindigkeitskurven für verschiedene Schubspannungen und Temperaturen sind in den Figs. 2 und 3 und die daraus durch graphische Integration gewonnenen Kriechkurven in den Figs.

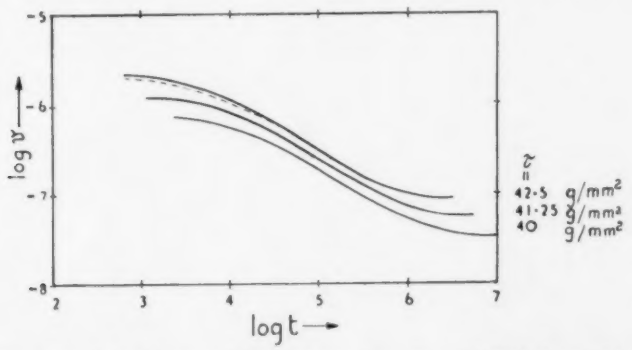

Fig. 2. Kriechgeschwindigkeitskurven für die Temperatur $T = 300°$K bei verschiedenen Schubspannungen τ, graphisch-numerisch berechnet. v in sec^{-1}, t in sec

4 und 5 dargestellt. Auch diese Ergebnisse stimmen gut mit den experimentellen Befunden überein. Wie bereits einleitend erwähnt worden ist, konnte eine definierte Temperatur – und Spannungsabhängigkeit der gesamten Kriechkurven bisher noch nicht aufgestellt werden, so dass die Übereinstimmung nur allgemeiner Natur sein kann. Wir werden darauf in der Diskussion zurückkommen.

Günstiger liegen die Verhältnisse bezüglich des stationären Kriechens. Cottrell und Aytekin fanden, dass die stationäre Fliessgeschwindigkeit v_{st} in Abhängigkeit von der Temperatur T und der Schubspannung τ gut durch eine Beziehung der Form

$$v_{st} = C_1 \exp(-C_2/T) \cdot \exp(C_3 \tau/T) \tag{8}$$

dargestellt werden kann. Die Werte der Konstanten C_i streuen stark von Versuch zu Versuch und liegen für den Spannungsbereich von 20 bis 50 g/mm² und den Temperaturbereich von 273 bis 400°K innerhalb folgender Grenzen:

$C_1 = 10^{10}$ bis 10^{13} sec^{-1}, $C_2 = 16000$ bis 21000 Grad, $C_3 = 75$ bis 150 (mm²/g) Grad. (8a)

Wie man sieht, sind die Streuungen von log C_1, C_2 und C_3 von derselben Grösse, wie sie oben für log (α_1 λ) und für die übrigen Konstanten in (6a-c) angegeben wurde, obwohl es sich im vorliegenden Falle um sehr reines Versuchsmaterial handelt.

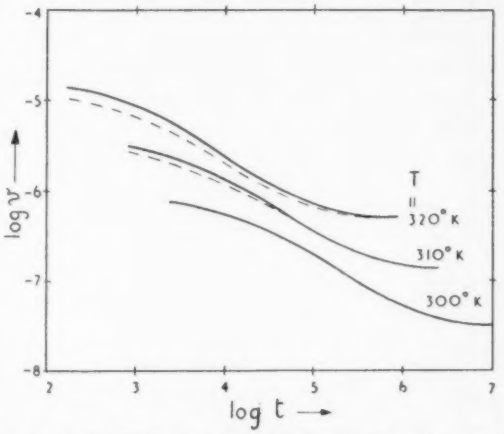

Fig. 3. Wie in Fig. 2 für Schubspannung $\tau = 40$ g/mm² bei verschiedenen Temperaturen T.

Theoretisch ergibt sich die Abhängigkeit $v_{st} = v_{st}(T, \tau)$ aus den Gleichungen (4), (4a), und (5) mit $dN/dt = 0$ durch Elimination von N. Da die Gleichungen transzendent sind, so ist ihre Auflösung nach N nicht in geschlossener Form, sondern nur auf graphischnumerischem Wege möglich. Die mit den bisherigen Werten (7) der Konstanten erhaltenen Ergebnisse für verschiedene

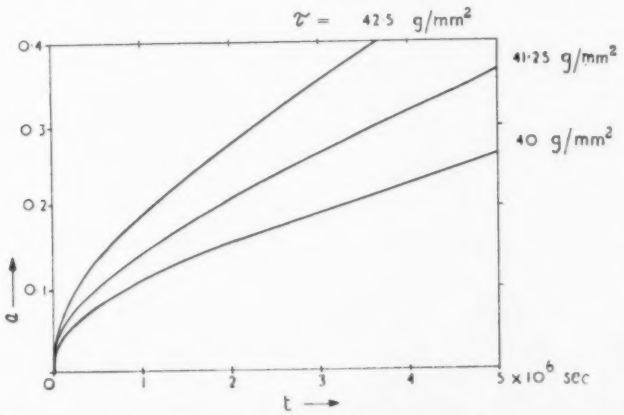

Fig. 4. Aus den Kurven von Fig. 2 sich ergebende Kriechkurven.

Temperaturen und Schubspannungen zeigen die Figs. 6 und 7. Wie man sieht, sind die Kurven log v_{st} als Funktion von τ für festes T und von $1/T$ für festes

τ in sehr guter Näherung Geraden, genügen also der experimentell ermittelten Beziehung (8). Für die darin auftretenden Konstanten C_1 ergeben sich folgende Werte :

$$C_1 = 2{\cdot}74 \times 10^{11}\ \text{sec}^{-1}, \quad C_2 = 17910\ \text{Grad}, \quad C_3 = 121\ (\text{mm}^2/\text{g})\ \text{Grad}. \qquad (8b)$$

Diese Werte liegen genau im Streubereich der experimentellen Werte (8a). Das gesamte über Kriechen vorliegende Tatsachenmaterial wird also durch die bisherigen Ansätze mit der Erweiterung (4a) und mit den bisherigen Zahlenwerten der Konstanten bestens widergegeben.

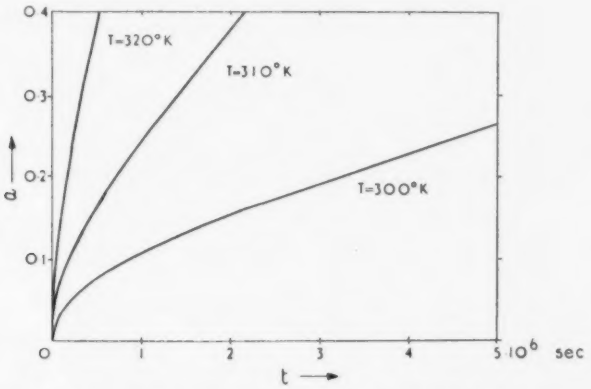

Fig. 5. Aus den Kurven von Fig. 3 sich ergebende Kriechkurven.

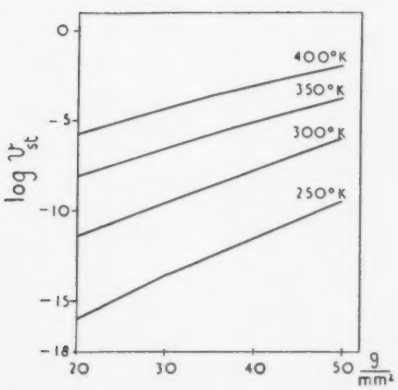

Fig. 6. Abhängigkeit der stationären Kriechgeschwindigkeit v_{st} (sec^{-1}) von der Schubspannung τ bei verschiedenen Temperaturen T, graphisch-numerisch berechnet. Abscissa τ.

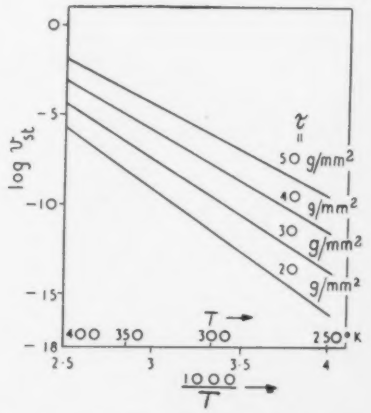

Fig. 7. Abhängigkeit der stationären Kriechgeschwindigkeit v_{st} (sec^{-1}) von der reziproken Temperatur $1/T$ bei verschiedenen Schubspannungen τ, graphisch-numerisch berechnet.

Wenn auch, wie erwähnt, der Einfluss von T und τ auf das Übergangskriechen sich nicht in gleicher Weise einfach formelmässig beschreiben lässt, so ergibt sich doch eine in etwa quantitative Übersicht, wenn man die Anfangskriechgeschwin-

digkeit v_0 in Beziehung setzt zur stationären Geschwindigkeit v_{st}. Bezeichnen wir das Verhältnis v_0/v_{st} mit Ω, so bedeutet $\Omega \gg 1$ ausgeprägtes, $\Omega \sim 1$ geringes Übergangskriechen. Die beschriebene numerische Auswertung der Gleichungen ergibt in guter Näherung

$$\Omega = c_1 \exp(c_2/T) \,.\, \exp(c_3\,\tau/T). \tag{9}$$

Diese Beziehung ist in Übereinstimmung mit den experimentellen Beobachtungen. Wir werden weiter unten von ihr Gebrauch machen.

Für die Versuchswerte

$$T^1 = 300^\circ\,\mathrm{K}, \quad \tau^1 = 40\ \mathrm{g/mm^2}, \tag{9a}$$

ergibt die Auswertung (vgl. Fig. 2)

$$\ln \Omega^1 = 3{\cdot}19. \tag{9b}$$

4. Vereinfachter Ansatz und Näherungslösung

Der Verlauf der Kriechgeschwindigkeitskurven und ihre Temperatur- und Spannungsabhängigkeit lässt sich mit folgenden Vereinfachungen unmittelbar analytisch angeben:

Da nach (6a) A_2/A_1 und τ_{01}/τ_{02} nahezu gleich 1 sind, so setzen wir beide Grössen gleich 1 und beschränken uns ferner in der Entwicklung der Exponentialfunktionen auf die linearen Glieder. Da die Konstanten dann eine andere Bedeutung und andere Werte annehmen als bisher mit den vollständigen Gleichungen, so unterscheiden wir sie von den bisherigen mit einem Strich. Dann lautet die erste Grundgleichung statt (4):

$$dN/dt = [(\alpha_1' - \beta_2' N)/L'] \,.\, \exp\left[\left(-A_1'/kT\right)\left(1 - 2\,\frac{\tau - c' N}{\tau_{01}'}\right)\right], \tag{10}$$

und die zweite Grundgleichung statt (5):

$$v = da/dt = \alpha_1' \lambda' \exp\left[\left(-A_1'/kT\right)\left(1 - 2\,\frac{\tau - c' N}{\tau_{01}'}\right)\right]. \tag{11}$$

Wir betrachten zunächst das stationäre Kriechen, für das N-const., d.h. $dN/dt = 0$ ist. Damit ergibt (10)

$$N_{st} = \alpha_1'/\beta_2'. \tag{12}$$

Nach (11) wird

$$v_{st} = \alpha_1' \lambda' \exp\left[(-A_1'/kT)\left(1 + 2\,(\alpha_1'/\beta_2')\,(c'/\tau_{01}')\right)\right] \exp\left[(2A_1'/kT)(\tau/\tau_{01}')\right]. \tag{13}$$

Diese Beziehung besitzt deselbe Form wie die schon diskutierte Beziehung (8). Durch Vergleich ergibt sich

$$C_1 = \alpha_1' \lambda', \quad C_2 = (A_1'/k)\left(1 + 2\,(\alpha_1'/\beta_2')\,(c'/\tau_{01}')\right), \quad C_3 = 2\,(A_1'/k)/\tau_{01}'. \tag{14}$$

Man sieht nun deutlich, dass durch die vorgenommene Vereinfachung der Charakter der funktionalen Zusammenhänge gegenüber bisher erhalten bleibt, aber Bedeutung und Zahlenwerte der auftretenden Konstanten geändert werden (vgl. (7) und (8b)).

Vol. 1 1952/5

Wir berechnen nun die Kriechgeschwindigkeitskurven selbst und führen hierzu an Stelle von N die Variable Z ein durch

$$\ln(1/Z) = (N_{st} - N)\,(2A_1'/kT)\,(c'/\tau_{01}'). \tag{15}$$

Zu Beginn des Kriechens ($t = 0$, $N = 0$) hat Z unter Berücksichtigung von (12) den Wert

$$Z_0 = p = p(T) = \exp\left[(-2A_1'/kT)\,(\alpha_1'/\beta_2')\,(c'/\tau_{01}')\right] < 1, \tag{15a}$$

und am Ende des Kriechens ($t = \infty$, $N = N_{st}$) den Wert

$$Z_\infty = 1. \tag{15b}$$

Setzen wir ferner

$$F = F(T, \tau) = (\beta_2'/L')\exp\left[(-A_1'/kT)\left(1 - 2\,\tau/\tau_{01}' + 2\,(\alpha_1'/\beta_2')\,(c'/\tau'_{(1)})\right)\right] \tag{16}$$

so lässt sich (10) in der Form

$$\frac{dZ}{\ln Z} = -F\,dt \tag{17}$$

schreiben. Die Integration ergibt, mit $N = 0$ für $t = 0$,

$$F \,.\, t = li\,(p) - li\,(Z), \tag{18}$$

wo li den Integrallogarithmus bezeichnet, der z.B. bei JAHNKE-EMDE (1948) tabelliert ist. In dem nach (15a, b) interessierenden Bereich von $Z = 0$ bis $Z = 1$ nimmt $li\,(Z)$ von 0 nach $-\infty$ ab, dementsprechend t von 0 für $Z = p = Z_0$ bis ∞ für $Z = 1$ zu, wie es wie es auch sein muss.

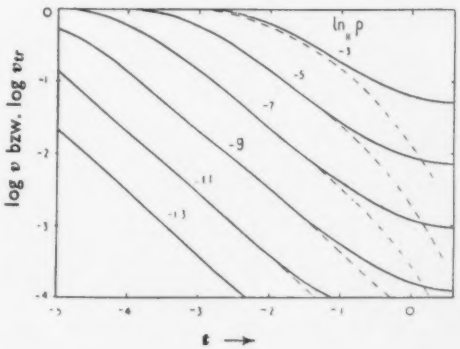

Fig. 8. Nach (21) berechnete normierte Kriechgeschwindigkeitskurven für das gesamte (ausgezogene Kurven) und für das Übergangskriechen (gestrichelte Kurven).

Elimination von N aus (11) und (15) ergibt Z als Funktion von v und dies in (18) eingesetzt den gesuchten Zusammenhang zwischen v und t. Führt man die normierte Zeit $\boldsymbol{t}$ und die normierte Geschwindigkeit $\boldsymbol{v}$ ein durch

$$\boldsymbol{t} = F(T, \tau)\,.\,t \quad \text{und} \quad \boldsymbol{v} = G(T, \tau)\,.\,v \tag{19a, b}$$

mit F nach (16) und

$$G = G(T, \tau) = (1/\alpha_1'\,\lambda')\exp\left[(A_1'/kt)\,(1 - 2\tau/\tau_{01}')\right], \tag{20}$$

so ergibt sich als Gleichung für die normierten Kriechgeschwindigkeitskurven

$$\boldsymbol{t} = \mathrm{li}\,(p) - li\,(p/\boldsymbol{v}). \tag{21}$$

Für $\boldsymbol{t} = t = 0$ wird $\boldsymbol{v} = 1$, also nach (19b) und (20),

$$v = v_0 = \alpha_1'\,\lambda'\exp\left[(-A_1'/kT)\,(1 - 2\tau/\tau_{01}')\right] \tag{22a}$$

und für $\boldsymbol{t} = t = \infty$ wird $\boldsymbol{v} = p$, also nach (19b), (20) und (15a),

$$v = v_\infty = p/G = v_{st}, \tag{22b}$$

wie es auch sein muss. Der Verlauf der Kriechgeschwindigkeitskurven nach (21) ist in Fig. 8 in einem doppeltlogarithmischen Koordinatensystem gezeichnet. Die eigentlichen doppellogarithmischen Kriechgeschwindigkeitskurven erhält man daraus bei vorgegebenen Werten von T und τ und bekannten Funktionswerten p, F und G, indem man jeweils die Kurve mit dem Parameterwert p um $\log F$ bzw. um $\log G$ in Abszissen- bzw. Ordinatenrichtung verschiebt.

Nach (11) ergibt sich für das Verhältnis $\Omega = v_0/v_{st}$ von Anfangsgeschwindigkeit $v_0\,(N = 0)$ und stationärer Geschwindigkeit $v_{st}\,(N = N_{st} = \alpha_1'/\beta_2')$

$$\Omega = \exp\,(2A_1'/kT)\,(\alpha_1'/\beta_2')\,(c'/\tau_{01}') \tag{23}$$

$$= \exp\,(c_2'/T). \tag{23a}$$

Dieser Ausdruck ist als Folge der Vereinfachung unabhängig von τ im Gegensatz zum vollständigen Ausdruck (9).

Zur Berechnung der Zahlenwerte der gestrichenen Konstanten kann man von den mit der vollständigen Theorie erhaltenen Ergebnissen verschiedene Kombinationen benutzen. Zweckmässig ist zu fordern, dass die Konstanten C_i in (14) und für die Versuchswerte (9a) der Parameter Ω in (23) die Werte (8b) und (9b) annehmen. Man erhält auf diese Weise unmittelbar

$$\begin{aligned} &A_1'/k = 16960\ \text{Grad}, && \tau_{01}' = 280\ \text{g/mm}^2, \\ &\alpha_1'\,\lambda' = 2{\cdot}74 \times 10^{-11}\ \text{sec}^{-1}, && \gamma = 1/\left[(\alpha_1'/\beta_2')\,(c'/\tau_{01}')\right] = 35{\cdot}5. \end{aligned} \tag{24a}$$

Damit wird nach (15a), (20) und (16) für die Versuchswerte (9a),

$$\ln p^1 = -\ln \Omega^1 = -3{\cdot}19, \qquad \log G^1 = 6{\cdot}1, \tag{25a}$$

$$\log F^1 = \log\,(\beta_2'/L') - 18{\cdot}95.$$

Zur Bestimmung von $\log\,(\beta_2'/L')$ ist die nach (21) erhaltene Kriechgeschwindigkeitskurve in Richtung der Abszissenachse so zu verschieben, dass sie mit der nach der vollständigen Theorie berechneten Kurve möglichst gut zur Deckung gelangt. Auf diese Weise ergibt sich

$$\log F^1 = -6{\cdot}3 \tag{25b}$$

und somit

$$\log\,(\beta_2'/L') = 12{\cdot}65. \tag{24b}$$

Damit sind die Werte der Konstanten und der Parameter, um welche die Kurve $(T^1,\ \tau^1)$ in Fig. 8 in Richtung der Koordinatenachsen verschoben werden muss, bekannt. Nach (15a), (16) und (20) lassen sich damit diese Parameter für alle Versuchswerte berechnen. Die so gewonnenen Kriechgeschwindigkeitskurven sind in den Figs. 2 und 3 gestrichelt eingezeichnet worden. Wie man sieht, stimmen sie mit den nach der vollständigen Theorie berechneten Kurven gut überein. Nur wenn die $(T,\ \tau)$-Werte stark von den für die Anpassung benutzten Werten $(T^1,\ \tau^1)$ verschieden sind, treten merkliche, aber immer noch verhältnismässig geringe Abweichungen auf. Sie sind dadurch bedingt, dass Ω nach der Näherungsgleichung (23a) im Gegensatz zur vollständigen Gleichung (9) nur von T, nicht aber von τ abhängt.

Vol. 1 1952/5

5. Diskussion der Ergebnisse

Eine formelmässige Erfassung der experimentellen Kriechgeschwindigkeitsmessungen nach Art der Beziehung (1) weist, was das Übergangskriechen betrifft, erhebliche Mängel auf. Es wird durch eine solche Formel weder der Tatsache Rechnung getragen, dass für $t = 0$ die Kriechgeschwindigkeit endlich ist, noch dass die gesamte durch das Übergangskriechen hervorgerufene Ableitung endlich bleibt. Eine solche Formel kann daher nur den mittleren, auch fast ausschliesslich messbaren Teil einer Kurve sachgemäss wiedergeben. Im Gegensatz hierzu liefert die vorliegende Theorie Kriechgeschwindigkeitskurven, die diese Mängel nicht aufweisen. Sie besitzen für $t \to 0$ horizontale Asymptoten, also endliche, wenn auch verhältnismässig grosse Anfangsgeschwindigkeiten und für $t \to \infty$ Geschwindigkeiten des Übergangskriechens, die rascher gegen Null gehen als nach dem $t^{-1/n}$ – Gesetz, also endliche Gesamtabgleitungen für das Übergangskriechen ergeben. Dies ist aus den Abweichungen der gestrichelten Kurven in Fig. 8, die das Übergangskriechen angeben, von den t^{-n} – Geraden zur ersehen. Dabei sind diese Kurven in den mittleren Teilen, wie auch in den Figs. 2 und 3, in sehr guter Näherung Geraden mit Neigungen zwischen $-2/3$ bis -1 und geben somit die experimentellen Befunde genau wieder. Insbesondere wird dem Umstand Rechnung getragen (Wyatt 1951), dass bei tiefen Temperaturen (kleine Werte von p) die Neigung bei -1 liegt und sich mit wachsenden Temperaturen dem Wert $-2/3$ annähert, also ein Übergang vom logarithmischen zum $t^{1/3}$ – Kriechen stattfindet. Der gleichwertige Einfluss wachsender Spannung ist in Fig. 8 wegen der Vereinfachungen nicht enthalten, aber in den vollständigen Gleichungen, wenn er auch in Fig. 2 nicht klar hervortritt, da der Spannungsbereich von 40 bis 42·5 g/mm² zu klein ist.

Eine Schwierigkeit beim Vergleich von Experiment und Theorie bereiten auch die verschiedenen Anfangsbedingungen. Während die Theorie mit definierten Anfangsbedingungen rechnen muss (volle Spannung ab $t = 0$, vorher Spannung gleich Null), sind diese im Experiment mehr oder weniger unbestimmt. Ehe eine bestimmte konstante Schubspannung sich eingestellt hat, erfolgt meist schon eine gewisse mit einer Verfestigung verbundene "spontane Abgleitung." Es ist auch aus diesem Grunde verständlich, wenn genaue Vergleiche von Theorie und Experiment erst für spätere Kriechstadien möglich sind. Deshalb haben wir auch unsere Näherungslösungen vorzugsweise in diesen Stadien den vollständigen Lösungen angepasst.

Bei sehr kleinen Gleitgeschwindigkeiten (Grossenordnung 10^{-10} sec^{-1}) treten diffusionsartige Vorgänge einzelner Atome als plastisch wirksam in Erscheinung (Cottrell 1948)*. Da solche Vorgänge in unsere Ansätze nicht mit einbezogen worden sind, so sind die Erscheinungen des "Mikrokriechens" (Chalmers 1936) in der vorliegenden Theorie nicht enthalten.

Berücksichtigt man die genannten Umstände, so erkennt man, dass durch die vorliegende Theorie das Gebiet der Kriech – und Fliesserscheinungen in seinen gesamten Umfang quantitativ richtig wiedergegeben wird. Entscheidend ist dabei, dass die Zahlenwerte der benutzten Konstanten (bis auf einen einzigen) aus Messungen in ganz anderen Bereichen des plastischen Gleitens gewonnen worden

* Von Kochendörfer (1941) wurden Verschiebungen der Mosaikblöcke als Ganzes angenommen, da das Kriechen bald praktisch zum Stillstand kommt.

sind. Insgesamt beschreibt also die Theorie das ganze Erscheinungsgebiet der Kristallplastizität. Wir sind uns bewusst, dass die zur Ableitung der Grundgleichungen benutzten modellmässigen Vorstellungen im Rahmen der Theorie der Versetzungen gewisse Schwierigkeiten bereiten. Es ist aber zu beachten, dass die Grundgleichungen sehr viel weniger spezielle Annahmen enthalten also das zugrundegelegte Modell, im wesentlichen die Grundgesetze der Statistik, die sich in verschiedener Weise atomistisch interpretieren lassen. Wir sehen es als eine Aufgabe an, diese Interpretation an Hand der Theorie der Versetzungen durchzuführen.

Auf Grund der vorliegenden Untersuchungen scheint uns eine Unterteilung des Kriechvorgangs in ein Übergangskriechen und ein stationäres Kriechen zwar formal zweckmässig, aber nicht physikalisch sinngemäss zu sein, denn es spielen sich in beiden Bereichen keine grundsätzlich verschiedenen Vorgänge ab, sondern nur das Verhältnis der beiden einander gegenläufig wirkenden Vorgänge – Bildung und Auflösung der Versetzungen – ändert sich stetig.* Es ist daher auch verständlich, dass die Zerlegung in verschiedener Weise, zum Teil additiv, zum Teil multiplikativ vorgenommen worden ist (vgl. Sully 1949).

Auf vielkristalline Metalle kann die Theorie bei Temperaturen unterhalb etwa $0{\cdot}4\ T_s$ (T_s absolute Schmelztemperatur), bei denen die Verformung vornehmlich durch Gleiten der einzelnen Körner erfolgt (abgesehen von der unter besonderen Bedingungen stattfindenden Zwillingsbildung) im wesentlichen unverändert übertragen werden (Kochendörfer 1952), genauere Untersuchungen sind in Angriff genommen worden. Bei höheren Temperaturen erfolgt die Verformung zusätzlich durch "quasi-viskoses" Fliessen der Korngrenzen, dem natürlich durch eine entsprechende Erweiterung der bisherigen Ansätze Rechnung getragen werden muss.

Abschliessend sei noch bemerkt, dass der Verlauf der Erholungs-isothermen, der sich mit den früheren Vorstellungen schon recht gut beschrieben lässt (Kuhlmann, Masing und Raffelsieper 1949), mit der Erweiterung (4a) in Einzelheiten verbessert werden kann. Wir werden darauf in einer besonderen Mitteilung eingehen. Dabei werden wir auch auf die Bedenken, die gegen den Ansatz (2b) erhoben worden sind (Laurent 1945; Vitovec und Nowotny 1951, 1952), zu sprechen kommen.

Literaturverzeichnis

Andrade, E. N. da C.	1914	*Proc. Roy. Soc.* A **90**, 329.
Bailey, R. W.	1926	*J. Inst. Metals*, **35**, 27.
Brown, A. F.	1949	*J. Inst. Metals*, **76**, 103.
Chalmers, B.	1936	*Proc. Roy. Soc.* A, **156**, 427.
	1949	*Progress in Metal Physics* (Pergamon Press, London).
Cottrell, A. H. u. Aytekin, V.	1950	*J. Inst. Metals*, **77**, 389.
Cottrell, A. H.	1948	*Rep. Conf. Strength of Solids*, S. 30 (Phys. Soc., London).
	1952	*J. Mech. Phys. Solids*, **1**, 53.
Heidenreich, R. D. u. Shockley, W.	1948	*Rep. Conf. Strength of Solids*, S. 57 (Phys. Soc., London).
Jahnke, E. u. Emde, F.	1948	*Tafeln höherer Funktionen* (B. G. Teubner, Leipzig).

* Dieses Bild entspricht dem bon Bailey (1926), nach dem das Kriechen durch ein Wechselspiel von Verfestigung und Erholung bestimmt ist.

Vol 1 1952/

Kochendörfer, A.	1941	*Plastische Eigenschaften von Kristallen und metallischen Werkstoffen* (J. Springer, Berlin).
	1952	*Archiv. Eisenhüttenwesen*, **23**, 183.
Kornfeld, M. O.	1936	*Phys. Z. Sowjetunion*, **10**, 605.
Kuhlmann, O., Masing, G. und Raffelsieper, J.	1949	*Z. Metallkunde*, **40**, 241.
Laurent, M. P.	1945	*Rev. Métallurgie*, **42**, 79, 125, 156, 194, 230.
Lyons, J.	1948	*Phys. Rev.*, **73**, 413.
Mott, N. F. und Nabarro, F. R. N.	1948	*Rep. Conf. Strength of Solids*, S. 1 (Phys. Soc., London).
Neurath, P. W. und Koehler, J. S.	1951	*J. Appl. Phys.*, **22**, 621.
Orowan, E.	1947	*J. West of Scotland Iron and Steel Inst.*, **54**, 45.
Slifkin, L. und Kauzmann, W.	1950	*Phys. Rev.*, **78**, 631.
Smith, C. S.	1948	*Proc. Phys. Soc.*, **61**, 201.
Sully, A. H.	1949	*Metallic Creep* (Butterworths, London).
Tyndall, E. P. T.	1950	*Pittsburgh Symposium on the Plastic Deformation of Crystalline Solids*, S. 49.
Vitovec, F. u. Nowotny, H.	1951	*Z. Phys.*, **131**, 41.
Vitovec, F.	1952	*Z. Metallkunde*, **43**, 128.
Wilsdorf, H. und Kuhlmann-Wilsdorf, D.	1952	*Z. angew. Phys.*, **4**, 361, 409.
Wyatt, O. H.	1951	*Nature*, **160**, 866.

Vol. 1 52/53

Journal of the Mechanics and Physics of Solids, 1953, Vol. 1, pp. 258 to 264. Pergamon Press Ltd., London.

EXPERIMENTAL INVESTIGATION OF THE BEHAVIOUR OF SOIL UNDER A PUNCH OR FOOTING*

By W. Sylwestrowicz
Graduate Division of Applied Mathematics, Brown University

(*Received 27th February*, 1953)

Summary

The displacement field and volume changes in sand, soil and clay, when indented by a punch, are investigated experimentally under conditions of plane strain. The pressure-penetration relations are also determined. Comparison is made with recent theories of the plastic behaviour of materials whose properties are influenced by hydrostatic pressure.

Vol.
1
1952/

1. Introduction

In three recent papers (Drucker and Prager 1952; Shield 1953; Drucker 1953), dealing with theoretical problems of soil mechanics, the implications were investigated of the assumption that soil can be treated as a perfectly plastic material for which hydrostatic pressure increases the yield stress. For plane strain the criterion for slip in soil is presented in Fig. 1 in the form of Mohr's circles and their enevlope, where the dotted line represents a criterion proposed by Drucker and Prager for the case of soils unable to take tension. One of the especially significant implication of the proposed theory is the necessity of increase in volume accompanying shearing action.

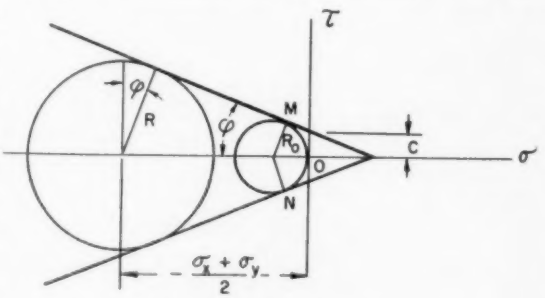

Fig. 1. Coulomb rule.

It was considered advisable to check the validity of this assumption experimentally and to obtain more data for the deformation of the soil. The experiments described in this report were designed mainly to observe the two-dimensional displacement field in the soil during the indentation of a punch or footing, and also to construct the pressure-penetration curve. These experiments deal mainly with sand although a few were performed using a garden soil and a commercial oil modelling clay called Plasteline.

* The results presented in this paper were obtained in the course of research sponsored by the Office of Naval Research under Contract N7onr-35801 with Brown University.

ol.
1
2/53

Fig. 2.

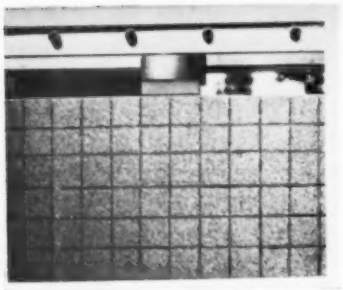

(a)

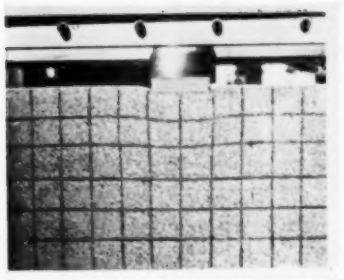

(b)

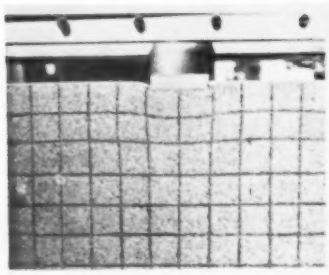

(c)

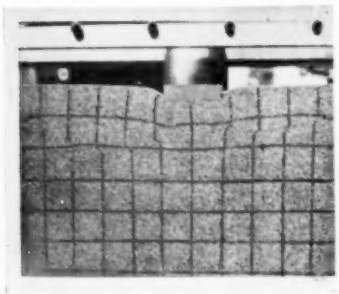

(d)

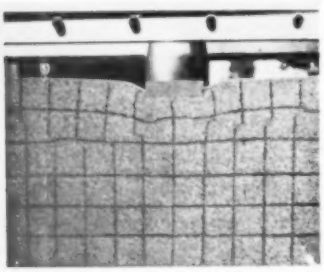

(e)

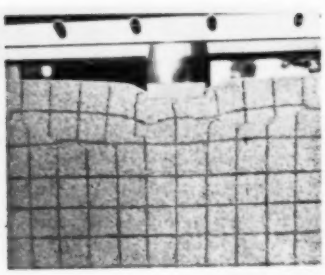

(f)

Fig. 3. Successive stages in deformation of sand.

Vol.
1
1952/5

2. Experimental Technique

For the experiments described in this report a special container was constructed with removable side panels made of $\frac{1}{2}$ in. thick glass (Fig. 2). The inside dimensions of this container are 10 in. high, 15 in. wide and 6 in. deep. A grid system was produced on the side surface of the material and the deformation of the grid system was observed in the glass container (Fig. 3 a-f). By taking photographs of different stages of the punch penetration, and tracing from them the grid systems corresponding to each position of the punch, a displacement field could

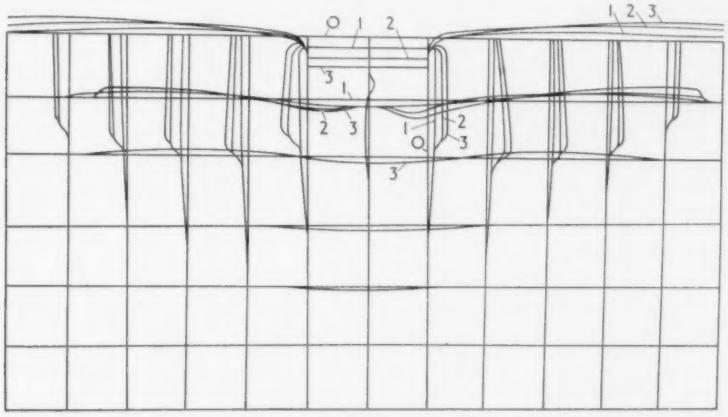

Fig. 4. Experimental displacement field for sand.

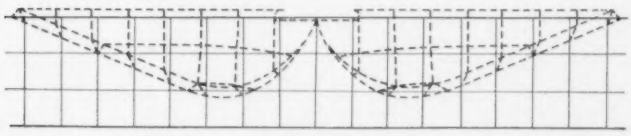

Fig. 5. Theoretical displacement field.

be constructed (Fig. 4) and compared with that predicted theoretically by Shield (Fig. 5). Horizontal lines in the centre of Fig. 4 represent the respective positions of the punch for each stage.

It was found possible to demonstrate the movement of the individual grains of sand by the superposition of photographs of two consecutive states of deformation. Fig. 6 is a composite of two such photographs of the sand taken for two positions of the punch, differing by 0·08 inch of penetration and superimposed in such a way as to match the reference marks (A on Fig. 6) made on the glass of the container. The streaks give the streamlines of the flow.

A conventional beam-type universal testing machine was used, and a much greater load than was expected in the experiments was applied to the beam of the machine. A thin-walled tube with strain gauges was placed between the head of the machine and the punch (2 in. wide and 6 in. deep) and was rigidly attached to the head of the machine. It was found in the initial experiments that the punch, when not rigidly attached, had a strong tendency to slide to one side.

The loads were measured by four resistance strain gauges connected in a Wheatstone bridge arrangement on the thin-walled tube. The out-of-balance current was measured by a sensitive galvanometer. The penetrations of the punch into the soil were measured by a dial gauge indicator.

3. EXPERIMENTS

(a) *Sand.* A white sandblast sand was used, with specific density 90 lbs./ft.^{3} and angle of repose 37° (ϕ in Fig. 1). The angle of repose was measured from a photograph of the cone of the sand produced on a glass plate from a funnel fixed above the plate. This sand was packed in the container by tamping with a steel rod, resulting in the increase of specific density to 103 lbs./ft.^{3} This increase of density was consistent for all the experiments with the sand. After the packing the top surface of the sand was supported by a wooden block, and the container then laid on its side and the front glass panel removed to make the grid system on the sand. Horizontal and vertical grooves were made in the sand, one inch apart and approximately 0·005 in. deep. The grooves were filled with aniline dyed sand. Finally the front panel was replaced and the container was ready for the test.

The important point in the analysis of the pressure-penetration curve is that the penetration was essentially fixed by the movement of the head of the machine and the resulting load was measured but not controlled. A form of creep appears

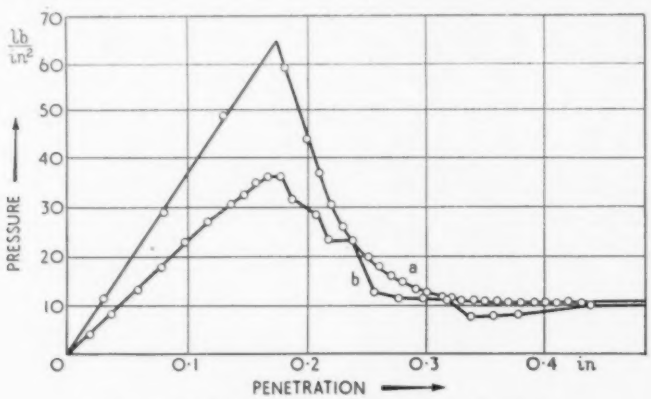

Fig. 7. Pressure-penetration relations for sand.

in the drop of load while the displacement is held constant. Two characteristic types of pressure-penetration curves are shown in Fig. 7. They differ in the numerical values but have the same general character. Up to the greatest pressure the relation between pressure and punch penetration is linear. It should be noticed, at this point, that there is no analogy to the linear part of the stress-strain curves for metals as sand does not exhibit appreciable elastic recovery properties on this scale.

Up to the greatest pressure the displacement field is somewhat like the flow of a fluid (Fig. 8), starting from the punch and ending on the top free surface of the sand. A part of the motion is also directed downward into the container. There

ol.
1
2/53

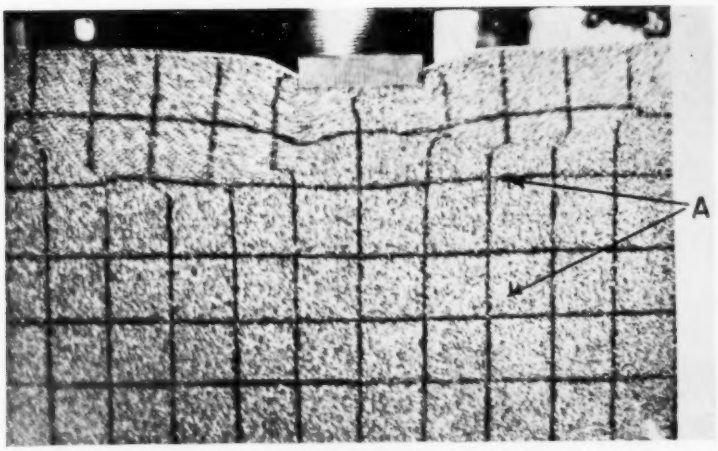

Fig. 6. Composite photograph from penetrations 0·08 in. apart in sand (after maximum pressure).

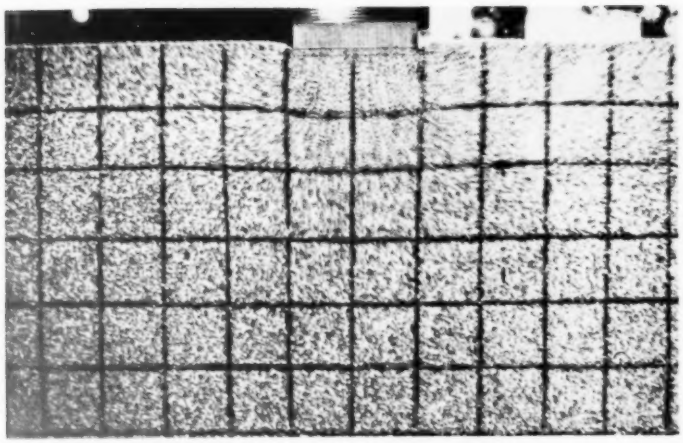

Fig. 8. Displacement field before maximum pressure.

Vol.
1
1952/

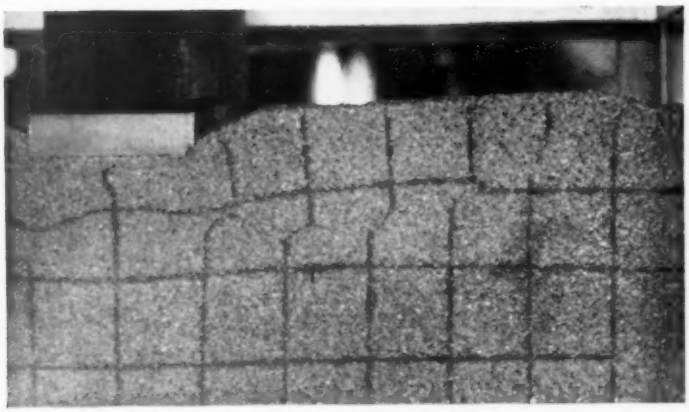

Fig. 9. Step on surface of sand.

is no discontinuity layer between the sand that moves and the sand at rest. When the maximum pressure is reached a new field of displacements starts to form. A surface of discontinuity of movement of grains appears. Below this surface no displacements of sand are apparent (Fig. 6). During the formation of this new displacement field the pressure decreases with the increasing indentation of the punch, but not in a smooth manner, until a definite layer of discontinuity is formed and further displacement of the sand takes place under almost constant pressure. An example of the displacement field is presented in Fig. 4. The discontinuity layers end on the free surface to form distinct steps (Fig. 9).

The change of volume was measured after the experiments, and an increase was observed in all experiments with the sand. The ratio of the increase of the volume to the sand displaced by the punch was approximately 2 (for an indentation of about 0·4 in.). No exact measurements were made of the areas where the change of volume took place. Only the changes of grid areas were measured. However, from these measurements and the character of the deformation of the grid, it is clear that the main change of the volume takes place in the discontinuity layer.

(b) *Garden Soil.* The garden soil used for these experiments was of rather fine structure, specific density 62 lbs./ft.^{3} (after sifting), moisture content 6·5 per cent (measured by the change of weight after heating for 5 hrs. at 75°C), with an apparent angle of repose of 44° (measured in the same way as for the sand). The same technique was used as for the sand. With the same method of packing, the resulting specific density varied from 80 to 120 lbs./ft^3.

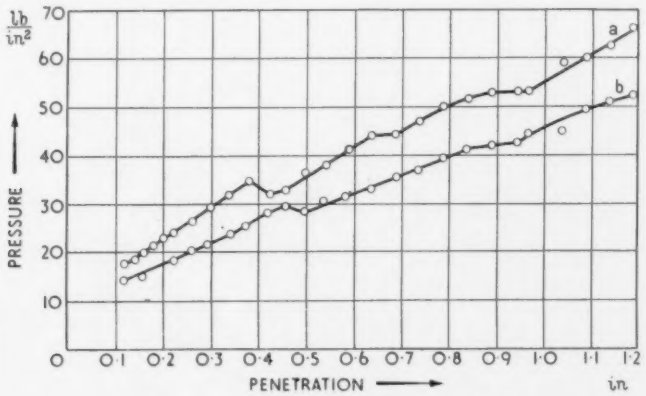

Fig. 10. Pressure-penetration relation for soil.

The pressure-penetration curve (Fig. 10) gradually increased up to the moment when the experiments were stopped, at which stage there was interference from the sides of the container.

After some indentation by the punch a separation of the soil in the form of cracks appears at a distance from the bottom corners of the punch. They are inclined at approximately 45° downwards. After some further indentation, a second set of cracks appears below the first ones. At that phase of deformation, the main displacement takes place in the column of soil under the punch forming

two distinct vertical layers of discontinuity. Between these layers and cracks there is small movement of the soil. In the area above the cracks there is practically no displacement of the soil. In the experiments with the garden soil, there is no appreciable change of the upper free surface, and the penetration is accommodated by an increase in density in the region below the cracks. Fig. 11 gives the displacement field for the experiment with the soil.

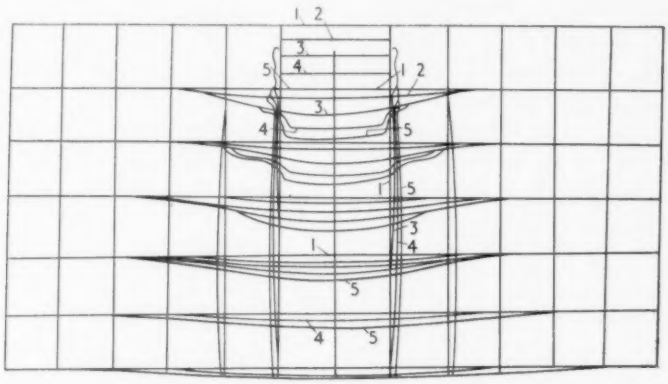

Fig. 11. Experimental displacement field for soil.

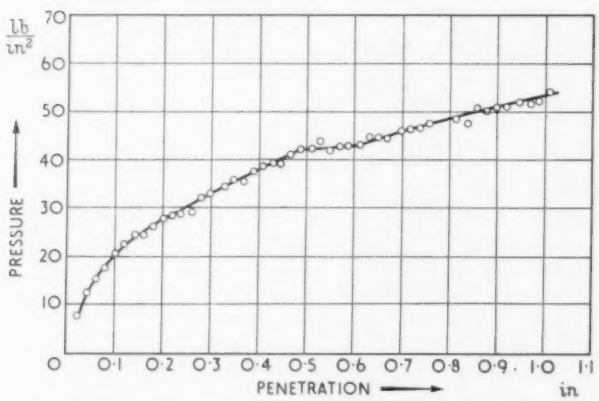

Fig. 12. Pressure-penetration relation for modelling clay.

The pressure-penetration curve shows a few changes of the slope corresponding approximately to the point of formation of cracks. Quite appreciable creep appears nearly from the beginning of the experiment (curve (b), Fig. 10), and other noticeable visco-elastic properties are exhibited by the soil.

(c) *Modelling Clay.* Commercial oil-modified modelling clay, Plasteline, of specific density 90 lbs./ft.^{3}, was used for the experiment. During packing into the container special care was taken to prevent the formation of horizontal layers. The glass panels were covered by a thin layer of viscous mineral oil to prevent sticking of the Plasteline to the glass.

Vol. 1 1952/5

The pressure-penetration curve is presented in Fig. 12. It was not continued because of interference by the sides of the container. Quite appreciable elastic deformation was exhibited by the Plasteline. There is no sign of formation of discontinuity layers. Displacement patterns are presented in Fig. 13.

4. Discussion

It appears from the deformation of the grid system (Fig. 4) that some packing still takes place in the sand up to the maximum value of the pressure (see changes of the lower grid's levels) although there is already present the movement of the sand in the directions which produce the discontinuity layers in the next stage of deformation. At that point, two symmetrical slip surfaces start to develop and portions of the sand above them move as a rigid body. With the formation of the slip surfaces, the force required for the further movement decreases, and a discontinuity layer is formed, which starts to move under approximately constant load.

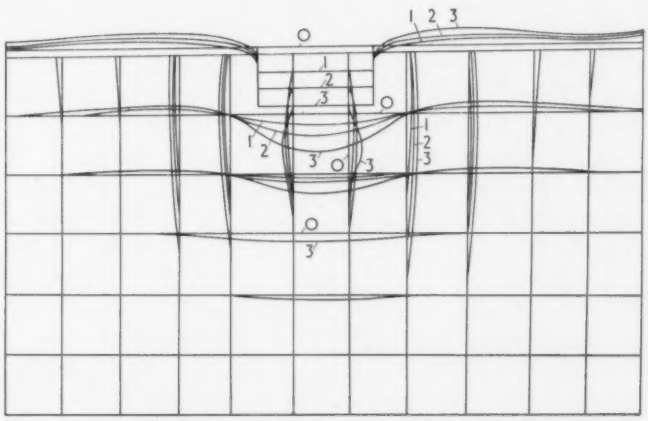

Fig. 13. Experimental displacement field for modelling clay.

The displacement field in the sand (Fig. 4) is then in good agreement with the deformation field given by Shield (Fig. 5) and obtained as an alternative to Prandtl's solution. The displacement of the grid system in Fig. 7 was computed for the angle of friction, $\phi = 37°$, obtained experimentally for the sand. Comparison of two pictures in Figs. 4 and 5 shows the same order of magnitude and character in the change of thickness of the discontinuity layer, and in the ratio of the distance from the punch to the step on the upper free surface to the width of the punch (according to Shield this ratio is 3·2; experimental value approximately 2·7). This agreement is still more surprising in view of the fact that the theoretical computations have been made with the assumption of very small displacements while in the experiments we were dealing with quite appreciable deformations. Although the increase of volume in the experiments (Fig. 4) corresponds in a sense to the theoretical prediction (Fig. 5). one should remember that the latter was computed for a very small movement of the punch while in

the experiments the penetration is quite large. Also the rapid decrease in load on the punch after the maximum load is reached seems to imply that the sand behaves in an unstable manner.

It is obvious from the results that sand under the compression of a punch behaves in a completely different way from garden soil or Plasteline. Much more must be learned about the validity of applying the mathematical theory of plasticity to soil, but these preliminary results on sand are encouraging.

ACKNOWLEDGMENTS

The author is greatly indebted to Dr. D. C. DRUCKER for his helpful advice and criticism and to Dr. F. D. STOCKTON for his suggestions and assistance in the experiments.

REFERENCES

DRUCKER, D. C. and PRAGER, W. 1952 *Qu. Appl. Math.*, **10**, 157.
DRUCKER, D. C. 1953 *J. Mech. Phys. Solids*, **1**, 217.
SHIELD, R. T. 1953 *Qu. Appl. Math.*, **11**, 61.

Vol.
1
1952/5

Journal of the Mechanics and Physics of Solids, 1953, Vol. 1, pp. 265 to 270. Pergamon Press Ltd., London.

ON THE MECHANICS OF CUTTING METAL STRIPS WITH KNIFE-EDGED TOOLS

By R. Hill
Department of Theoretical Mechanics, University of Bristol

(*Received 8th May*, 1953)

Summary

A theoretical investigation is made of a particular cutting operation in which a strip is split in two across its thickness by a tool whose cutting edge is wedge-shaped. The analysis is particularly concerned with the details of the deformation, the load variation, and the expenditure of work. The influences of friction and strain hardening are also treated.

ol.
1
2/53

1. Statement of the Problem

The process to be considered is one in which a flat strip or sheet of metal is cut in two by means of a tool whose cutting edge is wedge-shaped. The tool spans the width of the strip, which lies on a rigid horizontal base and is not otherwise constrained. It is supposed that the width/thickness ratio of the strip is great enough for edge effects to be neglected and the deformation treated as plane strain.

Two periods in this operation can be distinguished. In the first, the strip is merely indented (as in a hardness test) and the plastic zone does not extend to the base. Eventually, the sideways force exerted by the wedge rises to a value such that the opposing tension in the remaining thickness is sufficient to render it completely plastic. The ensuing separation of the halves constitutes the second period. During this, the plastic junction is reduced on one side by the continued cleaving action of the wedge and on the other by a contraction under the tension load, producing a small depression in the lower surface of the strip.

The present investigation is concerned with a calculation of the cutting load and expenditure of work, and with the deformation in the cut halves. The material is assumed to remain rigid up to a sharp yield point and to harden at a negligible rate.

2. First Stage : Indenting

The orthogonal indentation of a semi-infinite block by a smooth wedge has been treated by Hill, Lee and Tupper (1947). The deformation is restricted to zones $PQRST$ which extend from the tip T of the wedge to the free surface at Q (Fig. 1 (a), upper part). The raised lip PQ is straight, with inclination ϕ and of length equal to that of the contact face $PT = h$ say. The contact pressure is distributed uniformly and is of amount

$$p = 2k\,(1 + \theta - \phi), \tag{1}$$

where k is the yield stress in pure shear and 2θ is the apex angle of the wedge. In Table 1 p, ϕ, and c/h, where c is the penetration, are given for various wedge angles.

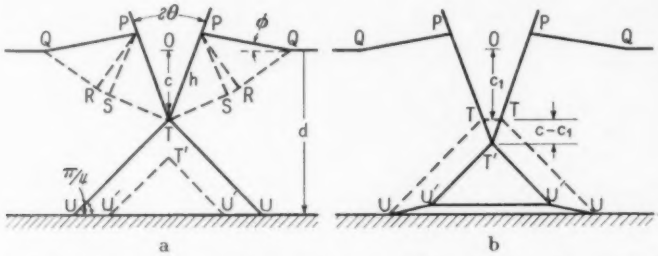

Fig. 1. Deformation zones when wedge angle is less than 44°20′: (a) at the instant when separation begins, and (b) at some later time.

TABLE 1

Wedge angle 2θ	0°	10°	20°	30°	40°	60°	120°	180°
Slope of lip ϕ	0°	4° 14′	7° 20′	9° 34′	11° 4′	12° 40′	9° 10′	0°
c/h	1	0·922	0·857	0·800	0·748	0·647	0·341	0
$p/2k$	1	1·013	1·047	1·095	1·156	1·302	1·887	2·571
γ_1	0	0·162	0·306	0·433	0·549	0·732	0·771	0
c_1/d	$\frac{1}{2}$	0·477	0·453	0·430	0·407	0·310	0·079	0
d/h_1	2	1·932	1·888	1·858	1·834	2·088	4·338	8·766

Note: as $\theta \to 90°$, $c \tan \theta/h \to 2/3$.

A mean shear strain, γ_1, can be defined for the deformed material, such that the work done by the applied load, $2 \times p \times$ triangle $OPT = pch \sin\theta$ (per unit width of strip), is equal to the energy of distortion, $2 \times k\gamma_1 \times$ area $PQRST$. From (1) and the geometry of Fig. 1 (a) it follows that

$$\gamma_1 = \frac{2c \sin\theta}{h} \cdot \frac{1 + \theta - \phi}{1 + \frac{1}{2}(\theta - \phi)} \simeq \frac{\sqrt{3}}{2} \sin 2\theta \qquad (2)$$

with an absolute error of less than 0·01.* The equivalent logarithmic strain in a uniaxial compression test is equal to $\gamma_1/\sqrt{3}$ or $\frac{1}{2}\sin 2\theta$.

If the wedge is rough, the pressure is still uniformly distributed provided the friction is. The lip remains straight but is diminished both in height and slope, so that PQ exceeds PT. Inspection of the calculations of LONGMAN (1952) for moderate coefficients of friction, μ, shows that the length of the contact face is decreased by a fraction $\frac{1}{4}\mu \sin 2\theta$ (very nearly) and that the normal load on a

* A formula given by HILL, LEE and TUPPER (op. cit.) relates only to the uniformly strained material originally occupying triangle OST, and not, as was stated, also to the material finally occupying triangle PQR.

face is increased by a fraction μ, with an error generally less than 1 per cent if μ is less than 0·1. Correspondingly, the pressure is increased by a fraction $\mu\,(1 + \frac{1}{4}\sin 2\theta)$, also with an error less than 1 per cent.

3. End of the First Period

During the first period the boundaries of the *deformation* zones remain geometrically similar. Eventually, in the rigidly constrained material below the wedge tip, the plastic zone spreads so far that the halves begin to separate. With small-angled wedges and a smooth base this happens when the sideways thrust on each contact face, $ph\cos\theta$, reaches the value $2k\,(d - c)$, where d is the strip thickness. If c_1 is the penetration then,

$$\frac{d}{c_1} = 1 + \frac{ph\cos\theta}{2kc}. \tag{3}$$

The incipient deformation zone, UTU in Fig. 1 (a), is a right-angled triangle in which the state of stress is just a uniaxial tension $2k$ parallel to the base. This solution is valid provided the rigid material in the angles UTS is not overstressed, which requires that

$$2\theta \leqslant \tfrac{1}{2}\pi - 1 + \phi, \text{ or } 2\theta \leqslant 44°\,20', \tag{4}$$

when the wedge is smooth.

If the wedge is more obtuse than this, the incipient deformation zone extends continuously downwards from the already-strained material (Fig. 2). Immediately below the tip, in the square $TEFE$, the stress is uniform, the transverse component being less than $2k$ (and becoming compressive for angles greater than about 100°). In $FCBC$ the transverse stress increases from F to B, while in the right-angled triangle ABA it is a uniform tension $2k$. When the wedge angle is 60° B is virtually on the base; when the angle is 120° B is at a height $0{\cdot}12\,h_1$; and when the angle is 180° (flat die) the height is $0{\cdot}91\,h_1$.*

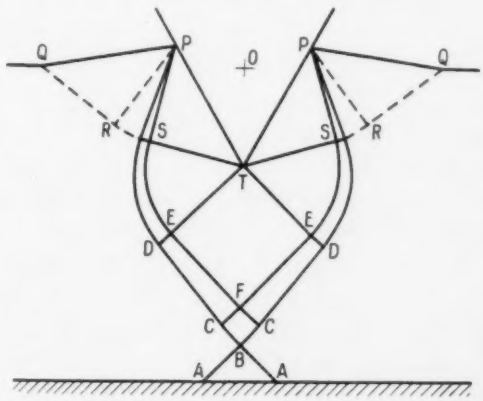

Fig. 2. Deformation zone at instant when separation begins. Wedge angle > 44°20′.

The value c_1 of the penetration at this instant is given in Table 1.† If θ is

* I am indebted to Mr. A. P. Green for checking these values and certain others in Table 1.

† The solution previously proposed by the writer (1950a) applies only to the case when a strip of double thickness is indented on opposite sides by a pair of wedges. In that solution the tension stress σ in the lower surface exceeds $2k$ by a factor $\pi/2$ when $\theta \to 0°$, 1·005 when $\theta = 30°$, 1·03 when $\theta = 60°$, and 1·13 when $\theta = 90°$. The necessary tension $\sigma - 2k$ normal to the surface could not of course be exerted by a separate foundation, but is perfectly possible in the centre of a solid block, so long as fracture is not caused by the triaxial tension.

Similar remarks apply to the indenting of a strip of thickness d by a flat die of width $2h$. The solution previously proposed (Hill 1950b) is valid when $d/h \leqslant 4{\cdot}755$, but must be modified when d/h is greater than this and less than 8·766 (Table 1). For example, when $d/h = 7{\cdot}514$, the height of B (Fig. 2) is $0{\cdot}63\,h$. The difference between the yield point pressures in the two solutions for a given value of d/h is quite negligible (less than 0·35 per cent).

small, friction on the wedge decreases c_1 by approximately $\mu(d - c_1)$; friction on the base increases c_1 but only by a negligible amount if μ is less than about 0·1; equation (4) is also very slightly modified.

4. Second Period: Separation

As the penetration is further increased, the rigid ends move apart and the contact pressure falls. If the wedge is more acute than (4) the entire zone $PQRST$ is partially unloaded; if it is more obtuse, deformation continues for a while in the material between PD and PT (Fig. 2), and a portion of the surface PQ is drawn down the wedge face. A depression appears in the base surface along UU in Fig. 1 (a) and AA in Fig. 2. Discussion of the subsequent deformation and stress state in Fig. 2 is rather complicated, and attention is now restricted to wedges satisfying (4); this is, indeed, the case of practical importance.

A later instant during the period of separation is depicted in Fig. 1 (b), where the wedge has descended an additional distance $c - c_1$ and the height of the depression is $(c - c_1)\tan\theta$. Triangle $U'T'U'$ is stressed plastically under a uniform tension $2k$; elsewhere the stress does not attain the yield point. Deformation is momentarily confined to shearing along the lines $T'U'$, as elements pass from the triangle to the separating halves. The final distortion in region $UTT'U'$ is a simple shear of amount

$$\gamma_2 = \frac{2\tan\theta}{1 + \tan\theta} \tag{5}$$

parallel to UT (Table 2). This may be seen by noting that the perpendicular distance between UT and $U'T'$ is $(c - c_1)(1 + \tan\theta)/\sqrt{2}$, while the displacement of U' parallel to UT is $\sqrt{2}(c - c_1)\tan\theta$. It is curious that γ_1 and γ_2 should be so nearly equal. It may be remarked also that the inclination of UU' to the horizontal is

$$\tan^{-1}\frac{\tan\theta}{1 + 2\tan\theta}. \tag{6}$$

Separation is complete when U' and T' meet, which happens when c reaches the value c_2 (Table 2) where

$$\frac{c_2 - c_1}{d - c_1} = \frac{1}{1 + \tan\theta}. \tag{7}$$

Table 2

2θ	0°	10°	20°	30°	40°
γ_2	0	0·161	0·300	0·423	0·534
$(c_2 - c_1)/d$	$\frac{1}{2}$	0·481	0·465	0·450	0·435
$W_1/kd^2\tan\theta$	$\frac{1}{2}$	0·498	0·494	0·489	0·483
$W_2/kd^2\tan\theta$	$\frac{1}{2}$	0·504	0·508	0·512	0·516
$(W_1 + W_2)/kd^2\tan\theta$	1	1·002	1·002	1·001	0·999

Vol. 1 1952/

In practice, fracture would intervene before this point was reached, depending on the ductility of the metal.

The farthest point to which deformation extends in the cut halves is on the upper surface at Q. The original length of strip affected is thus $h_1 (\sin\theta + \cos\phi)$ in each half, which varies from 0·5 d when $\theta \to 0°$ to 0·72 d for a 40° wedge.

The vertical load is

$$L = \begin{cases} 4k \tan\theta \,(d/c_1 - 1)\, c, & 0 \leqslant c \leqslant c_1 ; \\ 4k \tan\theta \,(1 + \tan\theta)\,(c_2 - c), & c_1 \leqslant c \leqslant c_2. \end{cases} \tag{8}$$

The load varies linearly with penetration in each period and is greatest at the moment when separation begins. If friction is present, the load is multiplied by a factor $(1 + \mu \cot\theta)$ approximately when θ is small. The total work done during the second period is $W_2 = k\gamma_2 (d - c_1)^2$ per unit width of strip, while that done during the first period is $W_1 = pc_1 h_1 \sin\theta$ (neglecting friction). From (3) and (5), or directly by integrating (8),

$$\left.\begin{aligned} &W_1 = 2kc_1 (d - c_1) \tan\theta, \quad W_2 = 2k (d - c_1)^2 \tan\theta/(1 + \tan\theta), \\ &\text{and so} \quad W_1 + W_2 = 2kd^2 \tan\theta \left(1 - \frac{c_1}{d}\right)\left(\frac{1 + c_1 \tan\theta/d}{1 + \tan\theta}\right). \end{aligned}\right\} \tag{9}$$

These quantities are given in Table 2, from which it will be seen that $W_1 + W_2 = kd^2 \tan\theta$, very nearly.

5. Qualitative Influence of Work-Hardening

If the material work-hardens at a moderate rate after the assumed sharp yield point, the surface of the lip still remains straight over most of its length except near Q where the corner is rounded off. According to the experimental investigation by Dugdale (1953) the slope and height of the lip are both decreased, while the length is correspondingly greater. The material below the wedge tip, though stressed to the yield point, is rigidly constrained during the first period and unable to harden (in actuality, the elasticity of the material permits plastic strains of elastic order of magnitude). Since work-hardening enhances the lateral load on the contact face for a given penetration. it follows that the c_1/d ratio is reduced. In the second period, work-hardening broadens the planes of instantaneous shear into layers of continuous shear, and rounds off the corners U and U'.

6. Experimental Confirmation

As the prediction that a depression should form in the rear surface of a strip during cutting is somewhat at variance with *a priori* intuitive feelings (the writer's at least) the actual experiment was briefly tried. A long bar of bright-drawn mild steel, in section 1 in. x $\frac{3}{8}$ in. was cut by a 32° wedge. This steel had a sharp yield point ($k \sim 20$ tons/in.^{2}) and hardened comparatively slowly ($k \sim 22$ tons/in.^{2} after a shear of 1·0). Despite the small width/thickness ratio, observable edge effects were confined to about 0·1 in. from either side. The bar was afterwards sectioned through its longitudinal plane of symmetry, and this section photo-

graphed (Fig. 3). The general agreement with theory is apparent. The operation was terminated by fracture along one of the two shear planes through the wedge tip.

REFERENCES

DUGDALE, D. S.	1953	To be published.
HILL, R.	1950a	*Phil. Mag.*, **41**, 745.
	1950b	*Mathematical Theory of Plasticity*, p. 256 (Clarendon Press, Oxford).
HILL, R., LEE, E. H. and TUPPER, S. J.	1947	*Proc. Roy. Soc.* A, **188**, 273.
LONGMAN, I. M.	1952	*British Iron and Steel Research Association Report*, MW/B/5/52.

Vol.
1
1952/

ol.
1
2/53

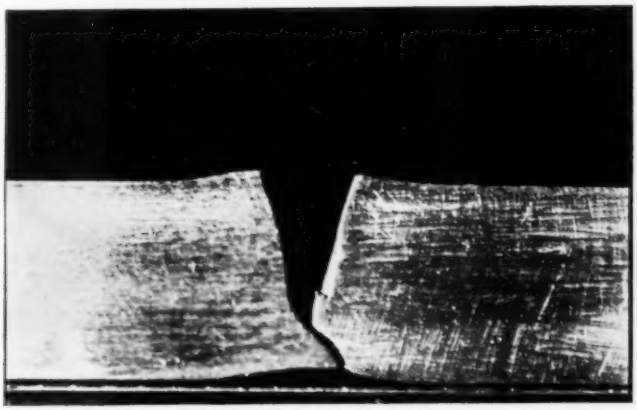

Fig. 3

Vol.
1
1952/5

Journal of the Mechanics and Physics of Soidis, 1953, Vol. 1, pp. 271 to 276. Pergamon Press Ltd., London.

A NEW METHOD FOR DETERMINING THE YIELD CRITERION AND PLASTIC POTENTIAL OF DUCTILE METALS

By R. Hill
Department of Theoretical Mechanics, University of Bristol

(*Received 14th May*, 1953)

ol.
1
2/53

Summary

The use of obliquely notched or grooved strips to obtain a long narrow zone of distortion is suggested. If such a strip is pulled in tension, the relative displacement of the unstrained parts on either side of the distortion zone makes a certain angle with the axis. The plastic potential may be derived solely from the measured dependence of this angle on the orientation of the distortion zone. If the load is measured as well, the yield criterion under any state of combined stress can be deduced. This method has several advantages over ones adopted previously.

1. Introduction

Hitherto, two methods have been used to determine the condition of yielding of a metal under arbitrary combinations of stresses, and to find the plastic potential (the function that governs the ratios of the components of the ensuing increment of permanent strain). Thin-walled tubes of circular section have been subjected to internal pressure and axial load in one method (Lode 1926; Davis 1943; Fraenkel 1948), and to torsion and tension in the other (Taylor and Quinney 1931; Schmidt 1932). During such experiments four quantities must be measured, viz. two applied loads and two components of strain. This requires complicated and costly apparatus and a lengthy period of investigation. Furthermore, to ensure that the distribution of stress and strain across the section is virtually uniform, the thickness/diameter ratio of the tube should be small, say less than 1/20, otherwise correction-factors of uncertain accuracy have to be applied. Such thin-walled tubes are not easy to produce to close tolerances. Finally, the tube material should be sufficiently isotropic; it is, however, extremely difficult to check whether this is so, as Pugh has recently emphasized (1953).

It is desirable, therefore, to consider whether an arbitrary uniform state of combined stress can be produced by some different method. This should involve (i) inexpensive apparatus, (ii) easily and accurately made specimens, (iii) relatively simple technique, and (iv) it should permit an adequate test for isotropy.

2. Description of Proposed Method

(a) *Grooved strip.*

In a uniform rectangular strip the thickness is locally reduced by cutting, on the wide faces, two opposed grooves in an oblique direction across the strip (Fig. 1.) The grooves are deep enough to ensure that plastic flow is localized there when the ends of the strip are loaded; the required depth depends on the amount of hardening in the strain range investigated, but a reduction of thickness of about one third should be ample. In order to reduce edge effects to negligible proportions the width of the strip should be some twenty to thirty times the breadth of the groove, which in turn should be somewhat greater than the remaining thickness to obtain a state of plane stress (the through-thickness component being zero). These dimensions (e.g. 2ins. x 0·08ins. x 0·05ins.), together with a rounding off of the angles of the groove, should eliminate the possibility of a notch constraint-factor. We thereby obtain, in effect, a long specimen prevented from extending plastically along its length by the adjoining effectively-rigid bulk. The specimen has only to be strained by an amount allowing an accurate determination of the ratios of the plastic strain-rate components at the moment of yielding.

In the test one load only is applied, namely a longitudinal tension at the ends of the strip. These are pivoted so that they are free to rotate in their plane. The state of stress produced in the zone of deformation is biaxial, the principal axes and stress-ratio being dependent on the inclination θ of the groove and the properties of the material. The resulting plastic strain-increment is such that the sides of the grooves move apart with a relative velocity whose direction is inclined at an angle ψ to the grooves (Fig. 1). This relative movement is partly accommodated by a rotation of the rigid ends, if the pivots can only move along the line joining them. The length of the strip must accordingly be such that this rotation is small enough not to affect the stress state significantly.

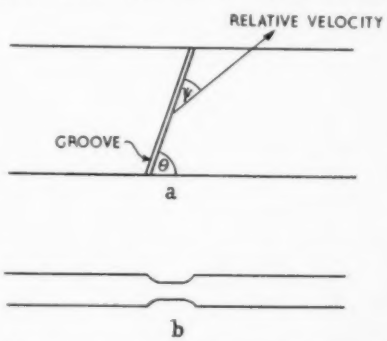

Fig. 1. (a) Plan view of obliquely grooved strip. (b) Side view of grooves.

The angle ψ will probably vary slightly over the imposed range of strain and a backward extrapolation must be used to obtain its yield-point value. ψ is to be measured for a number of inclinations θ, which, as we shall see, need only be assigned values between 55° and 90°. The plastic potential is derived directly from the $\psi(\theta)$ relation (Section 3); no load measurement is required. This is needed only for the yield criterion. It will usually be necessary to extrapolate the load/extension curve back to zero strain, in the manner described by Taylor and Quinney (1931).

It is clear that this method fulfils requirements (i) and (ii), while (iii) turns upon the possibility of measuring ψ to the necessary accuracy (Section 4). Requirement (iv) can be met much more adequately than in previous methods (Section 5).

Vol 1 1952/

(b) *Notched strip.*

The same constraint on the distortion can alternatively be secured by notching the strip unsymmetrically (Fig. 2). If the notches are deep and sharp, and the strip is sufficiently thin compared with their distance apart, plastic distortion is localized in a narrow neck joining the roots of the notches, provided the rate of hardening is not too great (HILL 1952). The breadth of the neck is comparable with, though somewhat greater than, the strip thickness. Initially, before the neck is far developed, the deformation and stress are similar to those in the grooved strip.

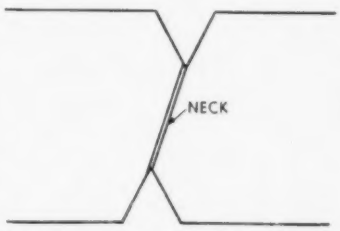

Fig. 2. Plan view of obliquely notched strip, with eventual neck.

This alternative method cannot be used with a metal such as annealed copper since the rate of hardening is so great that the distortion is not localized, but diffuse. It can, however, be used to examine the behaviour of such a metal after a sufficient degree of pre-strain, provided it is still isotropic.

These methods are at present being tried in the Sheffield Laboratories of the British Iron and Steel Research Association. It is hoped to publish the results shortly.

3. THEORY OF THE METHOD

The directions of zero strain-rate in the distortion zone are along its length and perpendicular to the direction of relative velocity. The principal axes of strain-rate bisect these directions and are therefore inclined at angles of $\frac{1}{4}\pi \pm \frac{1}{2}\psi$ to the zone. Hence, if $\dot{\epsilon}_1$ and $\dot{\epsilon}_2$ are the principal strain-rates in the plane of the strip ($\dot{\epsilon}_1 > \dot{\epsilon}_2$), and $\dot{\epsilon}_3$ is the through-thickness strain-rate,

$$\frac{\dot{\epsilon}_1}{1+\sin\psi} = \frac{\dot{\epsilon}_2}{-(1-\sin\psi)} = \frac{\dot{\epsilon}_3}{-2\sin\psi}.$$

Lode's strain variable is therefore

$$v = \frac{2\dot{\epsilon}_2 - \dot{\epsilon}_1 - \dot{\epsilon}_3}{\dot{\epsilon}_1 - \dot{\epsilon}_3} = -\frac{3(1-\sin\psi)}{1+3\sin\psi} \tag{1}$$

and takes values between 0 (pure shear) and -1 (uniaxial tension) as ψ varies between 90° and $\sin^{-1}\frac{1}{3} = 19°\ 28'$. $\dot{\epsilon}_2$ is the intermediate component in this interval.

Let σ_1 and σ_2 denote the principal stresses in the zone ($\sigma_1 > \sigma_2$, $\sigma_3 = 0$); if the material is isotropic the axes of stress coincide with those of plastic strain-rate. Then, if L is the tension load, l the length of the zone and h its thickness,

$$\left.\begin{aligned} L\sin\theta/hl &= \tfrac{1}{2}(\sigma_1+\sigma_2) + \tfrac{1}{2}(\sigma_1-\sigma_2)\sin\psi, \\ L\cos\theta/hl &= \tfrac{1}{2}(\sigma_1-\sigma_2)\cos\psi, \end{aligned}\right\} \tag{2}$$

by considering the normal and shear components of the force acting on the bounding surfaces of the zone. Hence

$$\frac{\sigma_1}{\sin(\theta-\psi)+\cos\theta}=\frac{\sigma_2}{\sin(\theta-\psi)-\cos\theta}=\frac{L}{hl\cos\psi}. \tag{3}$$

The length of the deviatoric stress vector in stress space (HILL 1950, p. 18) is

$$\sqrt{(\tfrac{2}{3})}\,(\sigma_1^2-\sigma_1\sigma_2+\sigma_2^2)^{\frac{1}{2}}=\sqrt{(\tfrac{2}{3})}\,\frac{L}{hl\cos\psi}\,[\sin^2(\theta-\psi)+3\cos^2\theta]^{\frac{1}{2}}. \tag{4}$$

Lode's stress variable is

$$\mu=\frac{2\sigma_2-\sigma_1-\sigma_3}{\sigma_1-\sigma_3}=-\frac{3\cos\theta-\sin(\theta-\psi)}{\cos\theta+\sin(\theta-\psi)}, \tag{5}$$

and the inclination of the stress vector to the direction representing pure shear is $\tan^{-1}(-\mu/\sqrt{3})$.

If the yield locus and plastic potential both have six-fold symmetry (i.e. if the metal is isotropic and if neither the strain-rate ratios nor the length of the stress vector at yielding are altered when the stresses are all reversed in sign), it is only necessary to cover a 30° segment of the deviatoric plane between pure shear ($\mu=0$) and uniaxial tension ($\mu=-1$). Correspondingly, θ need only be varied between 90° and $\tan^{-1}\sqrt{2}=54°\,44'$.

4. REQUIRED ACCURACY

Consider, now, the accuracy with which it is desirable to measure θ and ψ. It is helpful to refer to Fig. 3 where the loci of constant θ and ψ are superimposed on LODE's diagram. Inspection of this yields the following data, when the observed (μ, v) relation is in the neighbourhood of the MISES potential ($\mu=v$, $\tan\psi=\frac{1}{4}\tan\theta$).

(i) The error in the estimated μ due to an error of $\frac{1}{4}°$ in the measured ψ is 0·005 when $\theta=55°$ and 0·007 when $\theta=80°$.

(ii) The error is the estimated μ due to an error of $\frac{1}{4}°$ in the measured θ is 0·015 when $\theta=55°$ and 0·030 when $\theta=80°$.

(iii) The error in μ increases appreciably for given errors in θ or ψ as θ approaches 90°. However, since we know that the (μ, v) curve passes through (0, 0) it is unnecessary to take θ larger than about 80°. We know also that the curve passes through (-1, -1).

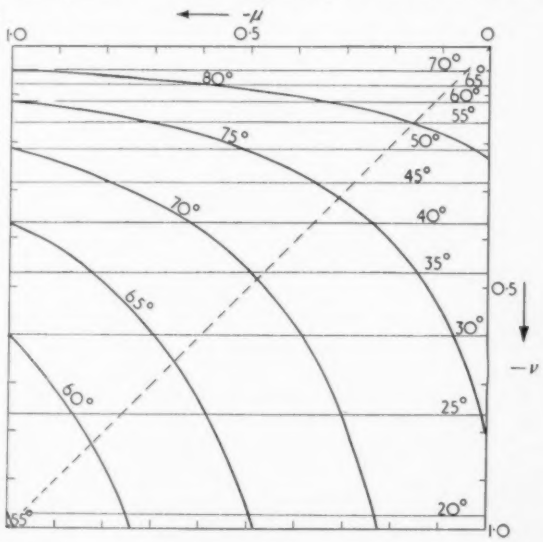

Fig. 3.

(iv) The error in the estimated v due to an error of $\frac{1}{4}°$ in the measured ψ is 0·010 when $\theta=55°$ and 0·002 when $\theta=90°$.

In short, it is necessary to measure θ to $\frac{1}{4}°$ and ψ to $\frac{1}{2}°$ to ensure that any estimated

(μ, ν) point is not farther from its true position than about 0·035 when θ is taken between 55° and 80°. The corresponding error in the orientations of the deviatoric stress and strain-rate vectors is about 1°, while the error in the length of the stress vector is about 0·5% (this is almost entirely due to the error in σ_2). A further error in the stress arises, of course, in the measurement of L/hl.

If the observed (μ, ν) relation should be in the neighbourhood of the TRESCA potential ($\mu = -1$ when $-1 \leqslant \nu < 0$; $\psi = 2\theta - \frac{1}{2}\pi$ when $\theta \geqslant \frac{1}{4}\pi$, $\psi = 0$ when $\theta \leqslant \frac{1}{4}\pi$) it is desirable to measure ψ, as well as θ, to $\frac{1}{4}°$.

5. TESTS FOR ISOTROPY

It is, of course, impossible to determine whether a metal is completely isotropic: its properties can only be compared for a finite number of directions of the axes of stress. With metal formed as sheet there is, however, the opportunity to make the comparison more extensive than with metal formed as tube. The obvious course is to test tensile specimens cut from the main sheet at, say, half a dozen different angles to the direction of rolling between 0° and 90° (provided that the rolling schedule has been such that the four quadrants should have identical properties). The load and the two transverse strain components are measured over a suitable range of distortion. If the material is isotropic the two transverse strains in any one test are equal, while the load/extension relations for the different directions are identical. These tests may be supplemented by similar observations on a cylindrical compression specimen cut with its axis normal to the sheet. Again, a circular lamina cut from the sheet may be deep-drawn and examined for earing.

Even if these criteria are not strictly satisfied, the material may still be sufficiently nearly isotropic for the present purpose. To see whether this is so, we can estimate the probable order of magnitude of the disturbing effect of the anisotropy on the (μ, ν) relation in the following way. Suppose that the anisotropy can be adequately represented by the modified Mises potential (HILL 1950, p. 321)

$$(G + H)\,\sigma_x^2 - 2H\sigma_x\,\sigma_y + (H + F)\,\sigma_y^2 + 2N\tau_{xy}^2 = 1 \qquad (6)$$

where x is the rolling direction, and the ratios of F, G, H, N are derived from the measured plastic strain-ratios in tension tests at, say, 0°, 45°, and 90° (c.f. BOURNE and HILL 1950). It may be shown that the relation between ψ and θ for such a material is

$$\tan\psi = \tfrac{1}{2}\tan\theta.\left[\frac{(FG + GH + HF)\tan^2\theta + (2NG - FG - GH - HF)}{(FG + GH + HF + NH)\tan^2\theta + N(G + H)}\right] \qquad (7)$$

if the axis of the grooved or notched specimen is in the direction of rolling. (The equation $\tan\psi = \frac{1}{4}\tan\theta$ for the isotropic MISES potential is recovered on putting $F = G = H = N/3$.)

From (1), (5) and (7) the apparent (μ, ν) relation can now be calculated. If this does not differ negligibly from $\mu = \nu$ it is not safe to disregard the anisotropy. This may also be concluded even though the actual (μ, ν) relation of this material, when fully isotropic, is different from $\mu = \nu$, and even though more tension tests might show that its actual potential, when in the anisotropic state, differs somewhat

from (6). Conversely, if the difference of the apparent (μ, ν) relation, derived from (1), (5) and (7), is negligibly different from $\mu = \nu$, it is probably safe to use the material in this state in the experiments for the actual (μ, ν) relation.

REFERENCES

BOURNE, L. and HILL, R.	1950	*Phil. Mag.* **41**, 671.
DAVIS, E. A.	1943	*Trans. Am. Soc. Mech. Eng.* **65**, A-187.
FRAENKEL, S. J.	1948	*J. Appl. Mech.* **15**, 193.
HILL, R.	1950	*Mathematical Theory of Plasticity* (Clarendon Press, Oxford).
	1952	*J. Mech. Phys. Solids*, **1**, 19.
LODE, W.	1926	*Z. Phys.* **36**, 913.
PUGH, H. Ll. D.	1953	*J. Mech. Phys. Solids*, **1**, 284
SCHMIDT, R.	1932	*Ingenieur-Archiv*, **3**, 215.
TAYLOR, G. I. and QUINNEY, H.	1931	*Phil. Trans. Roy. Soc.* A, **230**, 323.

Vol.
1
1952/

Journal of the Mechanics and Physics of Solids, 1953, Vol. 1, pp. 277 to 283. Pergamon Press Ltd., London.

EXPERIMENTS WITH A LABORATORY EXTRUSION APPARATUS UNDER CONDITIONS OF PLANE STRAIN

By N. W. Purchase and S. J. Tupper
Armament Research Establishment, Sevenoaks

(*Received 16th March*, 1953)

Summary

Experiments with a small-scale extrusion apparatus are described. The results are compared with the theory of extrusion due to Hill (1948). Excellent agreement is found between the measured pressures of extrusion and those predicted by the theory; the flow patterns also are in general agreement. In minor details, such as the extent and shape of the "dead" metal region, and the behaviour of material along the longitudinal plane of symmetry, there are some divergences.

ol.
1
2/53

1. Introduction

In an earlier paper Hill has discussed the theory of the process of extrusion (1948). It was felt at the time that there were several matters on which experimental evidence would be a valuable check on the theoretical approach. It has now been possible to carry out some small-scale extrusion experiments designed specifically to verify and amplify the two-dimensional theory. Generally speaking, it may be said that the experimental programme yields results in satisfactory agreement with the theoretical predictions. The purpose of this present paper is to describe the experiments carried out and to present the results obtained, and to take note of some of the more obvious modifications required to align theory and practice more completely.

Hill's analysis is strictly valid only when the plastic flow occurs in parallel planes, so that the metal to be extruded is a rectangular block. However, previous small-scale extrusion experiments designed to study the forces and deformations have concerned cylindrical billets only, and, although the cylindrical and plane-strain operations resemble each other in the large, it is not possible to use the axi-symmetric experiments as a reliable check on the detailed predictions of the plane-strain theory. Certainly, general agreement is found in the variation of the plastic region with die aperture and with the mode of lubrication employed; also it is found, perhaps fortuitously, that the theoretical extrusion pressures are roughly equal to those observed for cylindrical billets with the same reduction of area. The present series of experiments is therefore desirable in order that the dependence of pressure on reduction, the precise nature of the plastic straining, and the shape and extent of the "dead" metal regions may be more exactly determined in the plane-strain case.

2. Extrusion Apparatus

The essential design of the apparatus is shown in Fig. 1*. The chamber of the press is rectangular, and the material is extruded through an aperture situated symmetrically lengthwise at the bottom of the chamber. The apparatus is designed for direct extrusion under a loaded vertical plunger. The plunger itself fits the chamber closely, the clearance between plunger and chamber walls being a few thousandths of an inch only. For the purpose of removing the partially extruded billets the chamber is made in portions, lengthwise, bolted together. The width of the aperture is adjustable at will by means of dies of various thicknesses which

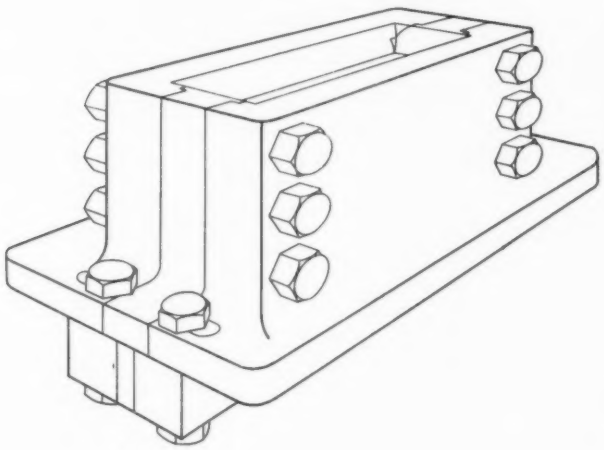

Fig. 1.

can be securely fastened into position in the base of the apparatus. The whole apparatus is substantially constructed of mild steel, being designed for a maximum load on the plunger of about twenty tons. Preliminary testing showed the necessity of replacing the mild steel bolts holding the chamber together by specially hardened steel bolts, as the threads showed a tendency to shear through at the higher loads. No special provisions were incorporated for temperature control within the apparatus or for observing the temperatures actually occurring during the extrusion process.

In use, the interior of the chamber is thoroughly lubricated to minimize friction effects between the material and the sides of the chamber. The readings taken in the course of the experiments show that nearly perfect lubrication was obtained with petroleum jelly as lubricant, under steady straining, with lead as the extruded material. With perfect lubrication the experimental results apply both to indirect extrusion, in which the bulk of the material is at rest relatively to the chamber wall (friction between chamber and material being necessarily absent), and to direct extrusion, in which the bulk of the material moves relatively to the chamber walls (so that friction occurs).

* The authors wish to acknowledge the work of Dr. E. H. Lee in connection with this design.

Vol. 1 1952/5

3. Material

This was a grade of commercial lead possessing a yield point of 0·355 tons/sq. in., in compression. The engineering stress, and the true stress in compression, for this lead are both plotted against strain in Fig. 2. The great advantage in the use of lead is its softness, though there is the added disadvantage that its large grain size tends to disturb the uniformity of straining.

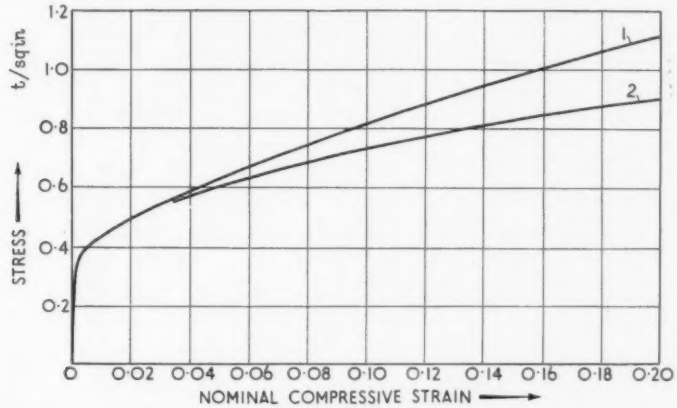

Fig. 2. Stress-strain curves for lead in compression. 1. Engineering stress. 2. True stress.

The specimen to be extruded had the form of a rectangular block 3 in. by $\frac{3}{4}$ in. by $1\frac{1}{2}$ in. deep, carefully milled to size, and just fitting into the chamber. For the purpose of following the plastic distortion in passing through the die-aperture, each block was halved and grids of lines were accurately scribed on the contacting faces with a dividing machine.

4. Description of Tests

Extrusion was carried out by placing the whole apparatus between the plates of a hydraulic testing machine. The plunger was made to move vertically downwards into the chamber, which remained at rest. The rate of travel of the plunger was uniform and the same over the whole series of experiments : approximately 0·2 in. per minute. Extrusion was continued until roughly a half of the lead originally in the chamber had been forced through the dies. As the interest is in the steady state process of extrusion, it is clear that the billet must not be extruded so far as to interfere with the stagnant, or " dead " metal, regions, in the lower corners of the chamber. Extrusion began at a load in excess of the mean extruding load by a few tenths of a ton, but the load readings fell almost immediately and then remained sensibly constant (although falling slightly, less than 0·1 ton) as the extrusion proceeded. If friction were present the load would fall since the remaining length of unextruded material decreases. The readings are given in Table I and indicate that friction had been almost entirely eliminated. The extrusion pressure for perfect lubrication can be calculated to a sufficient approximation from the minimum load at the end of travel of the plunger.

ol.
1
2/53

The thickness, d, of the extruded material was variable over a range from 0·5 in. to 0·075 in., dependent upon the dimensions of the dies inserted in the base of the apparatus (see Fig. 1). The original thickness D of the billet is 0·75 in., the extrusion ratios D/d are tabulated. The extrusion pressure P is obtained by dividing the final load by the area, 3 in. by $\frac{3}{4}$ in., of the cross-section of the chamber. The values of P are shown plotted against the percentage reduction in Fig. 3 (full line).

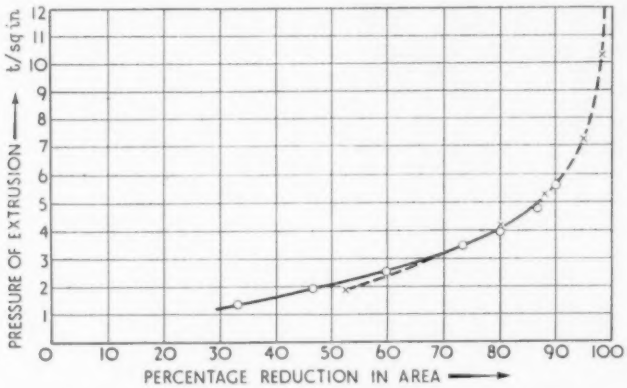

Fig. 3. Actual extrusion pressures. Rectangular billets (present experiments) are shown on the full line, with circles. Cylindrical billets (PEARSON) are shown on the broken line, with crosses.

TABLE I

Extrusion ratio D/d	*Reduction per cent*	*Initial load (tons)*	*Final load (tons)*	P *(tons/sq. in.)*	*Theoretical* P/k	k *(tons/sq. in.)*
1·5	33·3	3·5	3·2	1·42	1·78	0·80
1·875	46·7	4·6	4·35	1·93	2·36	0·82
2·5	60	6·1	5·7	2·53	3·13	0·81
3·75	73·3	8·1	7·8	3·47	4·20	0·83
5	80	8·9	8·7	3·87	4·96	0·78
7·5	86·7	10·7	10·55	4·69	6·04	0·78
10	90	12·5	12·5	5·56	6·80	0·82

5. THE PRESSURE OF EXTRUSION

It is interesting to compare the experimental extrusion pressures with those given by PEARSON (1944) for small-scale experiments with cylindrical billets. In his Table on p. 121 PEARSON gives inverted extrusion pressures for lead at 15°C and a strain rate of 0·1 in./min. These results are plotted in Fig. 3 (broken line) to compare with the plane-strain results; the reduction is calculated on an area basis for the axi-symmetrical case. It will be seen that the two curves are in reasonably close agreement, particularly for reductions in the range 65–90 per cent. Some further discussion of these results is given below.

ol.
1
2/53

I

II

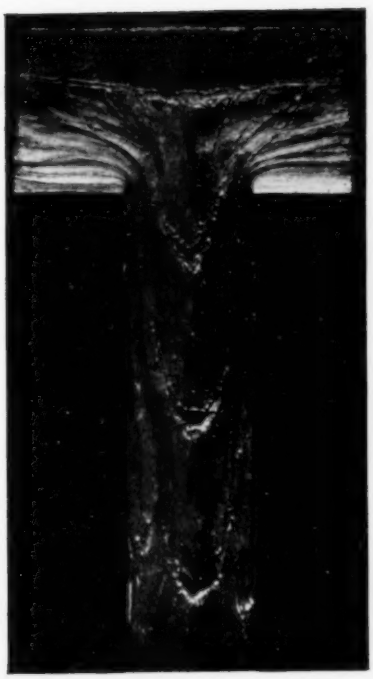

III

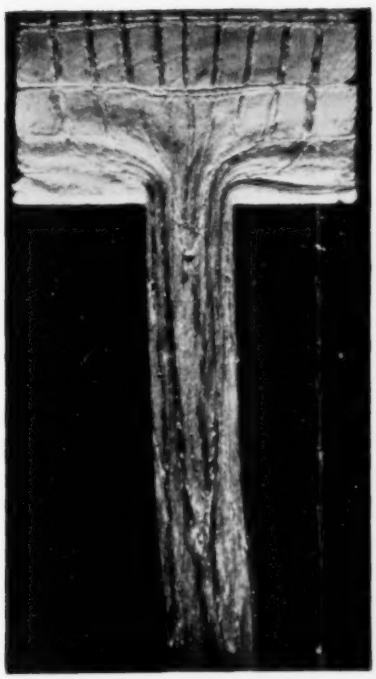

IV

Fig. 4 (a). Photographs of extruded billets.

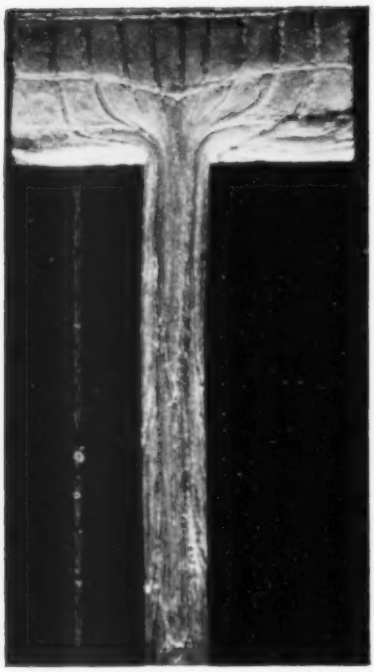

I

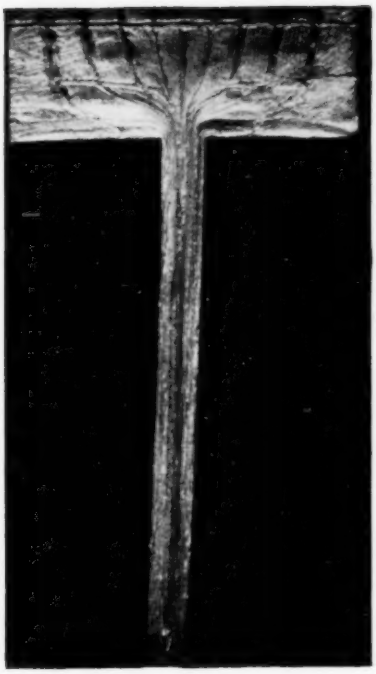

II

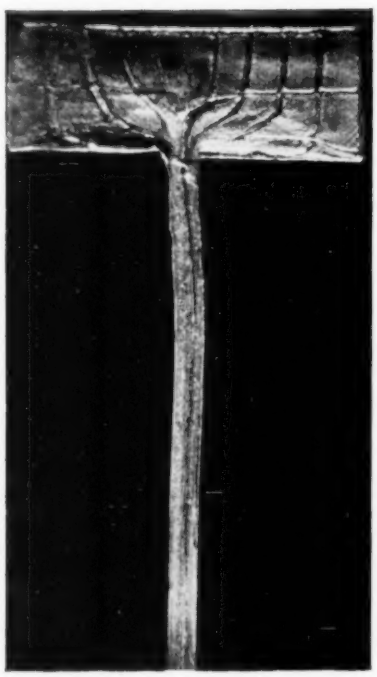

III

Fig. 4 (b). Photographs of extruded billets.

Vol.
1
1952/5

HILL (1948, 1950) has applied the slip-line theory of plastic flow to analyse plane-strain flow in extrusion. In Fig. 5 HILL's theoretical values are graphed against the percentage reduction. For reductions less than about 8 per cent it has been shown theoretically that there is a possibility of plastic flow extending round the corners of the dies to the free surface of the extruded billet. Unfortunately, the extrusion ratios employed in the experimental programme were not such as to permit any check on this particular prediction. For reductions greater than 90 per cent the pressure must rise rapidly but has not been calculated. Accordingly, the theoretical pressure in Fig. 5 is only given over a range of percentage reductions between 10 per cent and 90 per cent. It will be noted that the pressure is expressed non-dimensionally in terms of k, the constant maximum shearing stress in plastic flow. If the VON MISES criterion of flow is adopted, $k = Y/\sqrt{3}$ where Y is the yield stress in uniaxial tension.

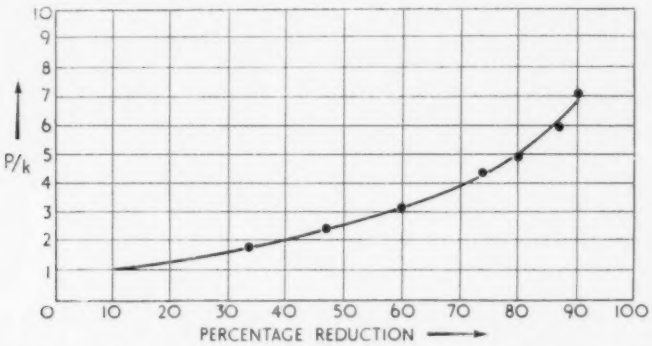

Fig. 5. Comparison of theory and experiment. — Theory. ● Present experiments, with $k = 0{\cdot}80$ tons/sq. in.

Table I also compares the theoretical and experimental extrusion pressures. A value for k has been deduced for each experiment, and is shown in the last column of the Table. The values indicate a remarkable consistency between theory and experiment, irrespective of the degree of straining. A value of $k = 0{\cdot}80$ tons/sq. in. gives $Y = 3{,}100$ lb./sq. in., using the VON MISES criterion, which may be compared with the minimum figure of 3,000 lb./sq. in., for commercially annealed lead (KENT's *Mechanical Engineers' Handbook*). If the TRESCA yield criterion is used, $k = Y/2$, and the resulting value of Y would appear to be rather high. Fig. 5 also shows the experimental values of P/k based on $k = 0{\cdot}8$ tons/sq. in.

6. THE FLOW PATTERN

An examination of Fig. 4 shows immediately the general flow pattern that occurs in frictionless extrusion operations. The main features are as follows. In all cases the billet has undergone no deformation until fairly close to the die-opening (approximately one third of the width). Also, conditions of undeformed flow are quickly attained after passing between the dies. Thus, the plastic deformation is restricted to a fairly localized region in the neighbourhood of the dies. This is in agreement with the theoretical treatment.

Secondly, the material is severely dragged back along the chamber walls, and a " dead " metal region forms under the shoulders of the dies. Only in the vicinity of the centre lines does the deformation approximate to a simple elongation corresponding to the particular amount of reduction. The distances between successive transverse lines after extrusion can be immediately calculated from the appropriate reduction ratio, under constant volume conditions, and agree with measurements of the photographs. It is clear, too, that the severe shears which occur towards the outside of the billet are the main reason for the redundant work in excess of that to cause homogeneous deformation.

The longitudinal lines of the network remain approximately equidistant after extrusion (except for end effects in the extruded material), again in agreement with the theory. There is some evidence that the central layers of material are compressed laterally rather more than the outer layers in passing between the dies.

HILL has calculated the deformation of a network of squares ruled on a cross-section of the original billet. This is shown in Fig. 6 (a) for 50 per cent reduction at the moment when a transverse line of the network is just making contact with the theoretical plastic region. For other than 50 per cent reductions it may be assumed that the pattern of the distorted network is qualitatively the same. In order to compare this deformed network with the experimental one, the grid for the reduction of 46·7 per cent (the second in the experimental series) has been drawn to the same scale and is shown in Fig. 6 (b). The general similarity is at once evident. The actual region of plastic deformation is of rather greater extent; this is only to be expected as the theoretical solution requires a definite plastic-rigid boundary which must be replaced by a more or less extensive transition region in practice. The region occupied by the dead, or stagnant, metal is not quite so extensive as predicted by the theory. The pronounced kinks (cusps) along the longitudinal plane of symmetry as required by the theoretical treatment have not been produced.

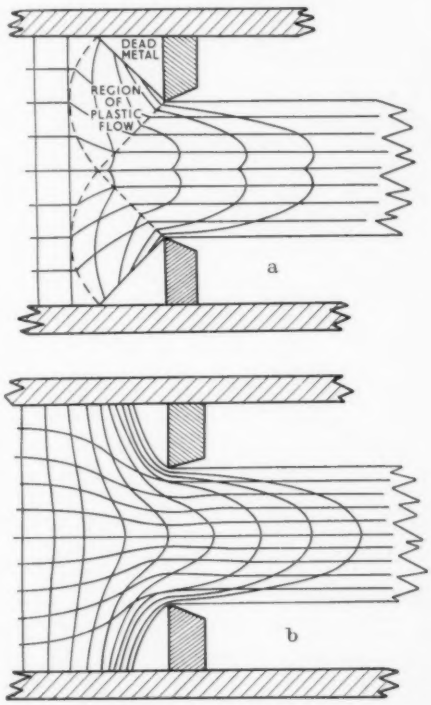

Fig. 6. Comparison of flow patterns. (a) Theoretical solution – 50% reduction. (b) Present experiments – 46·7% reduction.

For reductions in excess of 50 per cent HILL has indicated that two quite different theoretical solutions can be found, depending on the frictional conditions. In one of these the dead metal region appears as a right-angled isosceles triangle at all reductions. The present experiments seem definitely to disfavour this

Vol. 1 1952/5

solution. In the other the dead metal region extends from the chamber walls (which it meets at an angle of 45°), and the boundary between dead metal and metal in flow is a concave arc, shrinking with increasing reduction. This is very similar to the shrinking of the dead metal region shown in the series of photographs.

It may be noted, incidentally, that the theoretical pressures of extrusion are nearly the same in these two solutions.

For reductions less than 50 per cent the theoretical dead metal region is a right-angled isosceles triangle, which is reasonably confirmed in the photograph for the smallest reduction.

Acknowledgments

The authors are indebted to the Chief Scientist, Ministry of Supply, for permission to publish this paper. Crown Copyright reserved. Reproduced with the permission of the Controller of H.M. Stationery Office.

References

Hill, R. 1948 *J. Iron and Steel Inst.*, **158**, 177.

1950 *The Mathematical Theory of Plasticity* (Clarendon Press, Oxford).

Pearson, C. E. 1944 *The Extrusion of Metals* (Chapman and Hall, London).

ol.
1
2/53

Journal of the Mechan cs and Physics of Solids, 1953, Vol. 1, pp. 284 to 286. Pergamon Press Ltd., London.

A NOTE ON A TEST OF THE PLASTIC ISOTROPY OF METALS

By H. Ll. D. Pugh
Mechanical Engineering Research Laboratory, East Kilbride

(*Received 23rd March*, 1953)

Summary

It is shown that a material with a simple type of anisotropy will satisfy both of the tests used by Taylor and Quinney to check the isotropy of the test specimens used in their work on the plastic distortion of metals.

1. Introduction

The plastic behaviour of materials has been the subject of a great deal of experimental work, the object of which was to obtain fundamental information on the onset of yield and the relations between stress and strain. Metallurgical and mechanical testing of actual metals shows that unless great care is taken in their preparation they are neither homogeneous nor isotropic. Since the behaviour of anisotropic materials can differ appreciably from that of isotropic ones, it is clear that in experimental work designed either to check theories of isotropic materials or to provide data for them, considerable care must be exercised to ensure that the test specimens are, in fact, truly isotropic. However, in nearly all the experimental work carried out prior to 1929, little or no attempt was made to check whether or not the test material was isotropic. Indeed, it is probable that, in the majority of work, materials exhibiting varying degrees of anisotropy were used. In 1926 Lode investigated the validity of the Lévy-Mises relation, and found that, owing to anisotropy, there was an appreciable scatter in his experimental results which made it impossible to arrive at a definite conclusion about the validity of this relationship. In 1929, therefore, Lode took steps to minimize anisotropy by using tubes machined from the solid.

In 1931 Taylor and Quinney carried out experiments on the plastic distortion of annealed tubes of copper, aluminium and mild steel. They realized the importance of using isotropic metals and they examined the isotropy of their specimens in two ways. The first consisted essentially of measuring the change of internal volume in a thin-walled cylindrical tube when it was plastically deformed by increasing axial tension. This was done by filling the tubular specimen with water and observing the change in level of the water column in a capillary tube. Specimens which showed appreciable changes in internal volume were rejected as anisotropic, while those which were satisfactory in this test were then used for the main experimental work in which they were subjected to various combinations of tension and torsion. However, before these specimens were finally accepted as being isotropic, they had to satisfy the second test, namely that during the main experiments the directions of the principal axes of stress and of strain-increment coincided.

2. Examination of Isotropy Tests

It is here proposed to examine whether the combination of these tests does in fact ensure that the specimens are isotropic. Consider a thin cylindrical tube, length l, mean radius r, and wall thickness t, subjected to arbitrary plastic strain increments $d\epsilon_x$, $d\epsilon_y$, and $d\epsilon_z$, in the axial,

Vol
1
1952/

circumferential and radial directions, respectively. If the elastic deformation is negligible compared with the plastic deformation (as it was in TAYLOR and QUINNEY's work) and if, as is normally assumed, there is no permanent change in density,

$$d\epsilon_x + d\epsilon_y + d\epsilon_z = 0. \tag{1}$$

With the aid of this equation it can be shown that the change in internal volume, dV, of the tube during the plastic deformation is

$$dV = \pi l\,(r^2 - t^2/4)\,(d\epsilon_y - d\epsilon_z). \tag{2}$$

Thus, the change in internal volume is zero if

$$d\epsilon_y - d\epsilon_z = 0. \tag{3}$$

Conversely, the conclusion to be drawn when there is no change in internal volume is that the two transverse strain increments $d\epsilon_y$ and $d\epsilon_z$ are equal. It will be seen, therefore, that the first of TAYLOR and QUINNEY's tests can only detect anisotropy existing in a plane perpendicular to the axis of the specimen.

Consider, now, a thin-walled cylindrical specimen which has satisfied the first test, i.e., its anisotropy is rotationally symmetrical about the axis of the tube (the x axis). As suggested by HILL (1950), a simple yield criterion for such a material may be written

$$F\,(\sigma_y - \sigma_z)^2 + H\,(\sigma_z - \sigma_x)^2 + H\,(\sigma_x - \sigma_y)^2 + 2\,(H + 2F)\,\tau_{yz}^2 + 2N\tau_{zx}^2 + 2N\tau_{xy}^2 = 1, \tag{4}$$

where F, H and N are parameters characteristic of the current state of anisotropy and σ_x, σ_y, σ_z, τ_{yz}, τ_{xz}, τ_{xy} are the components of stress. It should be noted that this yield criterion reduces to VON MISES' law when the anisotropy is vanishingly small. The components of the strain increment, $d\epsilon_x$, $d\epsilon_y$, $d\epsilon_z$, $d\gamma_{yz}$, $d\gamma_{zx}$, $d\gamma_{xy}$, resulting from the following applied stresses, are

$$\left.\begin{array}{llllll} \sigma_x = P & ; & \tau_{yz} = 0 & : & d\epsilon_x = 2\,HPd\lambda & ; \quad d\gamma_{yz} = 0 \\ \sigma_y = 0 & ; & \tau_{zx} = 0 & : & d\epsilon_y = -\,HPd\lambda & ; \quad d\gamma_{zx} = 0 \\ \sigma_z = 0 & ; & \tau_{xy} = S & ; & d\epsilon_z = -\,HPd\lambda & ; \quad d\gamma_{xy} = NSd\lambda \end{array}\right\} \tag{5}$$

where $d\lambda$ is a factor of proportionality, which varies during the deformation and is not a material constant.

If θ is the inclination of a principal stress axis to the tube axis,

$$\tan 2\theta = \frac{2S}{P}. \tag{6}$$

Similarly, if ϕ is the inclination of a principal axis of strain-increment,

$$\tan 2\phi = \frac{2NS}{3HP}. \tag{7}$$

If this specimen satisfies the requirements of the second test, then $\theta = \phi$ and

$$N = 3H. \tag{8}$$

Substituting this value of N, (4) becomes

$$F\,(\sigma_y - \sigma_z)^2 + H\,(\sigma_z - \sigma_x)^2 + H\,(\sigma_x - \sigma_y)^2 + 2\,(H + 2F)\,\tau_{yz}^2 + 6H\tau_{zx}^2 + 6H\tau_{xy}^2 = 1. \tag{9}$$

For a fully isotropic material $H = F$. If may be seen, therefore, that a material can satisfy both TAYLOR and QUINNEY's tests for isotropy and yet have one degree of anisotropy remaining. Now the type of anisotropy which would remain undetected is an especially simple type, namely rotationally symmetric, i.e. ,one axis of anisotropy parallel to the axis of the tube and perfect isotropy in a plane perpendicular to this axis. This is, indeed, the type of anisotropy that might be expected to occur in tubular specimens if any anisotropy remained after annealing.

3. Relation Between Lode Variables

Since specimens with this simple type of anisotropy can satisfy both the tests for isotropy used by Taylor and Quinney, it may be thought that this is a possible explanation of their observation that the Lode variables are unequal; i.e. $\mu \neq \nu$, where $\mu = (2\sigma_2 - \sigma_3 - \sigma_1)/(\sigma_1 - \sigma_3)$; σ_1, etc., are the principal stresses; and ν is a corresponding expression in principal strain-increments. However, it can be readily shown that specimens with this type of anisotropy would also give $\mu = \nu$. If a thin tubular specimen of this material is subjected to tension and torsion, then the applied stresses and corresponding strain increments are given by (5) and (9), where $N = 3H$, as in (8). It can easily be deduced that the principal stresses and strain-increments are

$$\sigma_1 = \tfrac{1}{2}(P + \sqrt{P^2 + 4S^2}) \quad , \quad d\epsilon_1 = \tfrac{1}{2} Hd\lambda\,(P + 3\sqrt{P^2 + 4S^2}) \quad ,$$

$$\sigma_2 = 0 \quad , \quad d\epsilon_2 = -HPd\lambda \quad ,$$

$$\sigma_3 = \tfrac{1}{2}(P - \sqrt{P^2 + 4S^2}) \quad , \quad d\epsilon_3 = -\tfrac{1}{2}Hd\lambda\,(3\sqrt{P^2 + 4S^2} - P).$$

It follows that $\mu = \nu$.

It should be pointed out that in order to demonstrate the fact that an anisotropic material can satisfy both of the isotropy tests used by Taylor and Quinney, a special form of anisotropy has been visualized by the use of the yield criterion (4). A material with a more general form of anisotropy could of course also satisfy both isotropy tests and it is possible that it would involve a non-linear relation between μ and ν.

The present conclusions do not, of course, imply that the materials used by Taylor and Quinney were necessarily anisotropic, although even the possibility of its occurrence in such a classical series of experiments is disturbing.

Vol. 1 1952/

Acknowledgments

I wish to acknowledge the encouragement and helpful advice received from Professor Sir Geoffrey Taylor, and to thank Dr. J. F. W. Bishop for many valuable discussions.

The work described in this report was carried out in the Plasticity Division of the Mechanical Engineering Research Laboratory as part of the research programme of the Mechanical Engineering Research Board. It is published by permission of the Director of the Laboratory.

References

Taylor, G. I. and Quinney, H. 1931 *Phil. Trans. Roy. Soc.* A, **230**, 323.

Hill, R. 1950 *The Mathematical Theory of Plasticity*, pp. 318-20 (Clarendon Press, Oxford).

BOOK REVIEWS

E. BRANDENBERGER : **Grundriss der Allgemeinen Metallkunde.** Ernst Reinhardt Verlag. Basel 1952. 333 pp. 168 illus. DM. 15.85.

THIS little book represents a remarkable effort at compression. In little over 300 small pages Professor BRANDENBERGER gives a systematic resumé of metal science, including the micro-, macro-, and crystal structures of metals and alloys, the physical properties associated with them, phase diagrams and transformations, mechanical behaviour, recovery and recrystallization, and corrosion. References are not included, a select book list apart. Characteristics of the book which should make it profitable reading even for the expert metallographer (to whom it is not primarily addressed) are the frequent collection of experimental facts in Tables arranged in unusual ways, and the author's gift for pointing out striking connections between properties and structure. Instances are the tables classifying the homogeneity ranges of intermetallic compounds, and the graphs in many places in the book in which properties are plotted as a function of composition in binary systems. The treatment of constitution in terms of interatomic spacings is also illuminating.

The author's determination to pack as much specific information as possible into the book sometimes makes for indigestibility, notably in the five pages devoted to the phase composition of common binary systems, which are devoid of any diagrams, or the three pages on heats of formation. This complaint nowhere applies to the section on mechanical behaviour, including fracture, which is most clearly presented. On the other hand it does apply with especial force to the few pages on electron theory. For instance, the reader needs to have a good prior knowledge of atomic structure. He will be faced without preparation with the remark that the electronic structure of sodium is $(1)s^2\,(2s)^2\,(2p)^6\,(3s)^1$, and he will have to deal with a version of the Periodic Classification (Table I) which, in default of elucidation, remains incomprehensible. In the structural part, Miller indices and space group symbols are assumed to be understood. These observations are not at all intended to convey the impression that the book is too compressed to be readable, but it does follow that this is a book for the graduate who wishes to gain a bird's-eye view of the subject and that it cannot be recommended for undergraduate reading. For the more experienced reader, however (not least for the metallographer in search of occasional flashes of illumination) it is a thoroughly good book.

A few criticisms of individual points can be made. Face-centred cubic metals do not form mechanical twins (Table IV). In tin it is the grain boundaries, not the surface, which melts at a temperature 0·14°C lower than the interior of the grains (p. 51). It is unfortunate to adduce the $\alpha - \beta$ transformation in tin as " the typical instance of a polymorphic transformation." The volume change is here so great that the low-temperature phase (α) is liable to crumble into powder ; moreover, the difficulty of effecting the transformation is such that the very existence of α-tin was long doubted by some. Finally, the reviewer would like to enter a plea against the use of the old German classification of internal stresses into those of 1st, 2nd and 3rd kinds (p. 91). The extremely fine-scale stresses of the 3rd kind are divided from those of the 2nd kind by a boundary line which is so shadowy as to border on non-existence. OROWAN's classification into body-stresses and textural stresses has the advantage of being clear-cut.

R. W. CAHN.

Fatigue and Fracture of Metals : Edited by WILLIAM M. MURRAY. The Technology Press of the Massachusetts Institute of Technology and John Wiley and Sons, Inc., New York : Chapman and Hall, Ltd., London, 1952, viii + 313 pp, $6.00 and 48s.

THIS book is a collection of fourteen papers presented at a special conference on the Fatigue and Fracture of Metals given in June of 1950 at the Massachusetts Institute of Technology.

Although fatigue is given stellar billing in the title of this compendium some of the authors are errant : indeed the opening chapter by M. GENSAMER (" General Survey of the Problem of Fatigue and Fracture ") has but two pages outlining the known features of fatigue and then proceeds to a fourteen page discussion of the low temperature brittleness problem in steels and some rather specific attempts at devising lower impact strength limits for steels suitable for welded ship construction.

This ordinarily would not be a severe criticism, but as a keynote address it seems out-of-step with the great majority of papers which follow that do confine themselves directly to fatigue or the fundamental aspects of fracture applicable to fatigue. The excellent article by P. A. JACQUET and A. R. WEILL on temper brittleness and the chapter by F. JONASSEN on the problem of welded ships' failures (in which fatigue is dismissed as not being "an important factor") contribute to the *pot-pourri* character of the book. Indeed this is less a criticism of the book than the original organization of the conference.

The remaining eleven papers treat virtually every facet of fatigue that faces the research worker or engineer in this field today. The fatigue problems in aircraft structures are specifically set forth by the N.A.C.A. workers and a clear picture of the research programmes underway to cope with these problems is described. Half of R. E. PETERSON's article is devoted to the relationship between fatigue and machine design and the other half to describing the general relations between maximum and minimum limiting stresses and number of cycles, state of stress, and stress concentration in a manner developed by the Germans some years ago. O. J. HORGER and H. R. NEIFERT describe some interesting experimental results in their field of specialty : the effect of residual stresses on fatigue. TEMPLIN's article on designing is general and somewhat disappointing in a book of this type. OROWAN's chapter on the fundamentals of brittle behaviour is imaginative. A stronger indication of its applicability to the fatigue problem would have counteracted the book's meandering character. Both W. WEIBULL and N. M. NEWMARK do justice to their important specialties : the statistical aspects of fatigue and the cumulative damage developed in fatigue. C. W. MACGREGOR reports some experimental data showing transition temperature to be a sensitive indicator of damage developed during fatigue, while J. T. NORTON summarizes various other methods for assessing fatigue damage. N. J. GRANT reports data on the high temperature fatigue of a wide range of heat-resistant alloys. P. L. TEED's discussion of the effect of metallography on fatigue is rewarding.

W. M. BALDWIN.

Vol. 1 1952/5

END OF VOL.

ol.
1
2/53